Title

Estimation of ground motion characteristics of the El-Asnam, Algeria Earthquake of October 10, 1980, through analyses of the performance of school canopies

Author
Cartin, Javier

Publication Date
1984-05-01

DIVISION OF STRUCTURAL ENGINEERING AND STRUCTURAL MECHANICS

DEPARTMENT OF CIVIL ENGINEERING

UNIVERSITY OF CALIFORNIA, BERKELEY

ESTIMATION OF GROUND MOTION CHARACTERISTICS OF THE EL-ASNAM, ALGERIA EARTHQUAKE OF OCTOBER 10, 1980, THROUGH ANALYSES OF THE PERFORMANCE OF SCHOOL CANOPIES

BY

JAVIER F. CARTIN

Submitted in partial fulfillment of the requirements for the degree of Master of Engineering, University of California, Berkeley.

May 1984

Filippou

ABSTRACT

This report is concerned with the analytical studies conducted to investigate the possibility of estimating the ground motion (and particularly its effective peak acceleration EPA) capable of producing the observed building damage in the city of El-Asnam during the earthquake of October 10, 1980. For this purpose the performance of canopies in a school near the city is analyzed using different mathematical models, two different time histories of possible ground motions, and different dynamic analysis techniques. Although a small range of values for EPA (i.e. from 0.28g to 0.35g) is determined for the two ground motions considered, many uncertainties exist in the determination and use of EPA. It is concluded that the use of EPA as the sole parameter by which the damaging potential of an earthquake is judged can be misleading. Based on the canopy's performance to the El-Asnam earthquake, an inelastic design response spectrum is proposed. Finally, conclusions are drawn and recommendations for future research are formulated.

ACKNOWLEDGEMENTS

The research reported herein has been conducted by J.F. Cartin, under the supervision of Professor V.V. Bertero, in partial fulfillment of the requirements for the degree of Master of Engineering, Structural Engineering and Structural Mechanics Division, at the University of California at Berkeley.

Funding for this project was provided by the National Science Foundation under Grant No. CEE-81-10050. Any opinions, findings, conclusions, and recommendations expressed in this publication are those of the author and do not necessarily reflect the view of the National Science Foundation.

Very useful comments were offered by Professor F.C.Filippou in the proofreading of the report. The assistance of Mary Edmunds and Richard Steele in producing some of the illustrations is greatly appreciated. Other illustrations presented were obtained from various sources. This report was typed by J.F. Cartin.

ESTIMATION OF GROUND MOTION CHARACTERISTICS OF THE EL-ASNAM, ALGERIA EARTHQUAKE OF OCTOBER 10, 1980, THROUGH ANALYSES OF THE PERFORMANCE OF SCHOOL CANOPIES

TABLE OF CONTENTS

I. INTRODUCTION

1.1 General

On October 10, 1980, a destructive earthquake of Richter magnitude (M) 7.2 occurred near the city of El-Asnam, Algeria (Ref.1). The epicenter was about 6 miles (10 km) east of El-Asnam, with a focal depth of 6 miles. The duration of the earthquake was between 35 and 40 seconds. No strong motion records of the main shock were obtained.

The effect of the earthquake in the city can be summarized as follows (Ref.1):

- In downtown El-Asnam, approximately 80 percent of the buildings collapsed or were so significantly damaged that they had to be demolished. Many deaths were caused due to the collapsed structures.

- Nearly all damage observed in buildings resulted from their response to ground shaking. The effect of surface faulting, liquefaction, landslides, fire, flooding, etc. was small but did affect some buildings, aqueducts, irrigation distribution systems, highways, and railroads.

- Most of the city's adobe or masonry buildings collapsed. Reinforced concrete buildings did not behave well, either, mainly due to defects in building design and/or construction. Even the

R/C structures that remained standing suffered partial damages, with masonry panel walls blown out of frame structures. Furniture, equipment, and building contents shifted and overturned.

One question that was raised by many researchers and professional engineers concerned the kind of ground motion that could have induced the observed damage. According to the performance of different types of structures in this city, the value of the peak ground acceleration (PGA) was estimated at more than 0.40g.

It is already well accepted that PGA is not a good index to measure damage potential. Recently the new parameter EPA (effective peak acceleration) was introduced. Even though EPA has several definitions (Ref.2), it will be defined herein as follows: "the EPA of a given earthquake ground motion is the maximum acceleration of this motion which is fully effective in causing a structure to respond: a higher acceleration will not increase the response of the structure and a lower acceleration will decrease it."

Studies were conducted to determine EPA and answer the question of whether EPA is a good index of the damaging potential of an earthquake ground motion. These studies consisted of detailed analyses of the performance of some school canopies located about 3 miles (5 km) east of El-Asnam. These canopies, which covered the corridors between one-story classrooms, had a very simple structural system and suffered severe damage. Some of the R/C canopies collapsed during the earthquake, while most of them remained standing but with severe structural damage to the columns. It therefore appeared that the earthquake performance of this simple structural system offered an excellent opportunity to estimate the main characteristics of the ground motion and particularly the EPA required to induce such damage.

Furthermore, if it was possible to determine the EPA, it was of interest to try to formulate design earthquakes, based on the computed EPA, that could be used for retrofitting existing structures as well as for the design of new structures in the rebuilding of the city of El-Asnam. According to present state of the art in specifying design earthquakes, it was decided to formulate them in the form of a design spectrum (Ref.3).

The investigation reported herein was initiated with the following main objectives.

1.2 Objectives

The main objectives of the studies reported herein were: 1) to use the observed R/C school canopy performance as a transducer, if possible, to obtain an estimate of the EPA of the ground motion that could induce such performance ; and 2) to propose design response spectra that can be used in the design of new buildings and in the repair and retrofitting of the buildings that did not collapse, in order to prevent serious damage in case of future earthquake ground motions.

1.3 Scope and Layout of Report

In Chapter 2, an overall description of the R/C canopy's structural system is given. The performance of the canopies to the El-Asnam, Algeria earthquake and their most adequate analytical modeling are also discussed in this chapter.

In Chapter 3, the mechanical characteristics of the canopy are estimated. First the mechanical characteristics of the structural materials (concrete and reinforcing steel) are selected. Using these material properties the probable moment-curvature (M-Ø) relationships of the canopy's column cross section are obtained. The influence of several parameters that affect these M-Ø relationships, such as axial load, concrete cover thickness, and buckling of longitudinal compressive steel bars, are studied.

An analysis of the adequacy of the canopy's design in relation to the 1982 UBC Code Provisions is made in Chapter 4.

The dynamic characteristics of the canopy are estimated in Chapter 5, both assuming a generalized SDOF model and a 2DOF model. Different damping ratios are considered.

The analyses conducted to estimate the EPA are presented in Chapter 6. The types of ground motion considered are discussed first. The idealization of the lateral resistance function, as well as the determination of the displacement ductility are then described. The EPA determination is done in three stages: (1) using the Bertero, et al. charts (Ref.4) to estimate the peak ground acceleration PGA; (2) verifying the value of PGA with the use of the nonlinear analysis program DRAIN-2D (Ref.5); and (3) estimating the EPA by the "Clipping Method" which basically consists of clipping the acceleration peaks of a given earthquake previously normalized to a PGA found in (2), in order to study the effect of clipping on response. The effects of several parameters on EPA are also discussed in this chapter.

In Chapter 7, inelastic design response spectra are suggested based on the analyses conducted previously for estimating the EPA.

Finally, in Chapter 8, the results of the preceding chapters are summarized and general conclusions are drawn. The chapter ends with suggestions for future research.

II. DESCRIPTION OF R/C CANOPY STRUCTURAL SYSTEM, ITS EARTHQUAKE PERFORMANCE AND ITS ANALYTICAL MODELING

2.1 Introductory Remarks

Each of the school canopies covering the corridors along and between the classrooms were completely free of so called "nonstructural components" (Fig.2.1), which facilitated considerably the mathematical modeling of this particular structure. In other words, the seismic response of the canopies depended solely on its bare structural system.

2.2 Structural System

The structural system of each of the school canopies consisted of a row of four cylindrical columns supporting a very massive slab, 138 x 766 inches (3.50 x 19.45 meters) in plan, at the top (Fig.2.2). The canopy tributary weight to each of the columns was estimated as 26 kips (116 kN). The columns had 13.8 in. (350 mm) in diameter and their reinforcement consisted of 10 #6 longitudinal bars with circular ties #2 @ 7.2 in. (183 mm) used as transverse steel.

Although it was not possible to obtain information regarding the columns' foundation, from the inspection of the performance it was clear that the foundation had not suffered significant movement, i.e., it acted practically as a rigid foundation. From the way the canopy collapsed, as well as from the damage and permanent deformation observed in the canopies that remained standing, and from preliminary estimations, it became clear that the only significant response occurred in the transverse direction of the canopies. Therefore, only the response under a horizontal ground motion acting in the direction perpendicular to the longitudinal axis of the canopy will be considered herein.

It is important to mention that, since only some canopies collapsed while others were only thrown out of plumb, the maximum inertia forces of the structure were at the level of the yield capacity of the structure. Moreover, the canopies that were only thrown out of plumb did not collapse perhaps because of adjacent buildings that held them up.

As may be seen from Fig.2.1, the structural failure of the canopies was triggered by the failure of the columns at their base in the transverse direction. This failure was, in turn, triggered by flexural yielding of the main reinforcement followed by crushing of the concrete and buckling of the longitudinal compressive steel bars. Some damage occurred throughout the columns, especially at the top. The roof of the canopy sustained no damage.

Before the modeling of the canopy is discussed, it needs to be said that conceptually, the canopy's structural system in the transverse direction is not adequate for resisting earthquake loadings. The large value of concentrated mass at the top, together with the fact that the canopy was statically determinate, made it a very inefficient structure to resist earthquake excitations.

2.3 Mathematical Modeling of the Canopy

The actual structural system has been idealized as shown in Fig.2.3. Although this idealized system has infinite degrees of freedom, because of the relatively small value of the distributed mass along the column ($\bar{m}$) compared with the concentrated mass at the top of the canopy (M), it can adequately be represented by an equivalent two-degree-of-freedom system (2DOF), v_1 and v_2, in which the translational and rotational masses are considered to be concentrated at the top of the column of the canopy (Fig.2.3). To study the importance of each of these two degrees of freedom in the overall response, studies were also conducted in which the system shown in Fig.2.3 was reduced to just a single degree of freedom (SDOF) by neglecting v_2, i.e. the rotational degree of freedom.

A summary of the most important characteristics of the canopy is presented below. Detailed computations are included in Appendix A.

L = 105 in. (=2.67m) (: height of the column)

M = 0.065 k-sec^2/in. (=11 kN-sec^2/m) (: concentrated mass at the roof)

$\bar{m}$ = 3.3×10^{-5} (k-sec^2/in.)/in. (= 0.23 (kN-sec^2/m)/m) (: distributed mass of the columns)

I_o = 107 k-sec^2-in. (=12.1 kN-sec^2-m) (: mass moment of inertia of the roof)

EI_{uc} = 6.28×10^6 k-in.^{2} (=18000 kN-m^2) (: flexural stiffness of uncracked, transformed cross section of column)

$EI_{cr} = 2.62 \ X \ 10^6$ k-in.^{2} (= 7520 kN-m^2) (: flexural stiffness of cracked, transformed cross section of column)

III. ESTIMATION OF MECHANICAL CHARACTERISTICS OF CANOPY

3.1 Mechanical Characteristics of the Structural Materials

Each canopy was constructed of reinforced concrete. Unfortunately, no testing data or design values were available regarding the mechanical characteristics of the concrete and reinforcing steel. However, based on visual inspections of these materials and on conversations with people who were involved in the construction, the following probable mechanical characteristics of these materials were assumed.

3.1.1 Concrete Stress-Strain Relationships. The following upper and lower bound values for 28-day cylinder strength of the concrete, f'_c, were assumed:

Case M1 : f'_c = 3.0 ksi (21 MPa)

Case M2 : f'_c = 2.5 ksi (17 MPa)

For the two cases of concrete described above, stress-strain relationships for both the unconfined and confined concrete were considered, corresponding to the concrete outside and inside the ties of the column, respectively (Figs.3.1 and 3.2).

Both the Park & Kent (Refs.6 and 7) and the Blume et al. (Ref.8) stress-strain relationships for concrete were used to investigate the effect they had on the moment curvature diagrams. The Blume et al. relationship gave values for moments approximately 10% to 15% higher. However, since the column ties were not spaced too close, #2 @ 7.2 in. (183 mm), and therefore did not confine too well, it was concluded that the Park & Kent relationship was more suitable.

The Modified Park & Kent curve (Ref.6) was also considered but the additional sophistication was not justified for two reasons: 1) the amplification factor for f'_c turned out to be small (K=1.04) and 2) the uncertainties in the value of f'_c itself were large. Therefore, the Park & Kent concrete stress-strain curve was used, assuming different relationships for the confined and unconfined concrete (Figs.3.1 and 3.2).

3.1.2 Reinforcing Steel Stress-Strain Relationships. The following upper and lower bounds for the yield stress, f_y, were assumed:

Case M1 : f_y = 50 ksi (350 MPa)

Case M2 : f_y = 40 ksi (280 MPa)

The assumed stress-strain curves, corresponding to the two cases mentioned above, are shown in Figs. 3.3 and 3.4.

Although analyses were conducted for different combinations of the values of the mechanical characteristics of the materials, the values reported in this paper correspond to the following combinations, which are upper and lower bounds of the values of f'_c and f_y : combination 1 which corresponds to case M1 of concrete and steel; and combination 2 which corresponds to case M2 of concrete and steel. Furthermore, special attention is given to the combination 2, considered to be more realistic than combination 1. These two combinations will be designated from now on as case M1 and case M2.

3.2 Computed and Idealized Moment-Curvature (M-Ø) Relationships of Column Cross Sections

3.2.1 Variables Considered. Numerical computations of the M-Ø relationships were conducted using the RCCOLA computer program (Ref.9). In these the variation of the mechanical characteristics stated above and the effect of the following parameters were considered:

1) Different Level of Axial Loads P. Different levels of axial load were considered in order to study the possible effect of vertical acceleration, estimated to be as high as 1.0 g (Refs.1 and 10), on moment-curvature relationships.

The total tributary weight to each of the columns of the canopy was approximately 26 kips (116 kN) at the critical section (bottom of the column). Moment-curvature curves for axial loads of 0, 26, and 52 kips (0, 116, and 231 kN) were obtained using RCCOLA. The results obtained were very similar for each of these loads (Figs.3.5 and 3.6). Therefore, a value of 26 kips was used in subsequent analyses. In these curves, the maximum value of the curvature, $Ø_{max}$, was controlled by a given maximum value of the concrete compressive strain at the outer fiber of the column cross section, which was selected as 0.06 in./in. A larger value could have been chosen for this strain but, as described below, buckling of the longitudinal compressive steel bars did not permit the use of such high values of strain.

2) Different Cover Thicknesses. Field measurements of the cover

thickness showed some variations. Since the section was so small (with a practically constant total diameter of 13.8 in. = 350 mm), any deviation from the specified cover thickness could affect the M-Ø relationship. Therefore, it was considered of interest to study the effect of the measured upper and lower bounds of the cover thickness on the behavior of the column section. As Fig.3.7 indicates, the two bounds used for the cover were 1.1 in. (27 mm) and 1.6 in., (40 mm). This gives as a result, values of d′ varying from 1.7 in. (43 mm) to 2.2 in. (56 mm), where d′ is the distance from the center of the longitudinal reinforcing bars to the outside edge of the concrete on the same side of the section.

As shown in Figs. 3.8 and 3.9, the main effect of an increase in cover is a decrease of the yield and maximum flexural strength by less than 10%.

3.2.2 Estimation of Behavior of Critical Regions of Columns. Possibility of Buckling of Main Bars. The moment-rotation capacity, rather than the moment-curvature relation of critical regions of reinforced concrete structures is important in determining seismic response. The spacing of the circular hoops, 7.2 in. (183 mm), was larger than the maximum spacing, 4 in. (102 mm), permitted by the 1982 UBC (Ref.11) for seismic zones 3 and 4 [2625 (f) 4B]. It was also larger than the eight-bar diameter which is required to prevent buckling, which for #6 bars implied a distance of 6 in. (152 mm). Thus, the possibility of premature buckling, after the unconfined concrete of the cover shell had spalled, had to be considered. In some of the columns of the canopy that remained standing, there was evidence that the bars had just begun to buckle. To study the effect of buckling of main reinforcing bars on the behavior of the structure, it is necessary to study the behavior of the critical region in the area where the bar may buckle. The logical method is to find the Moment,M,-Rotation,θ, relationship along a region of length equal to the buckling length of the bar. To simplify the analysis it was assumed that the moment and curvature were constant along this critical region. Therefore, it is possible to interpret the M-Ø of the critical column cross section as the M-θ of the critical region by multiplying the curvature Ø by the buckling length of the bar, in this case 7.2 in.

Based on this assumption, the curvature at which buckling would start has been computed and is indicated in Figs. 3.8 and 3.9. It is not uniquely determined; instead a range of curvature values was obtained which defined the uncertainty of initiation of buckling. The determination of this range is discussed below.

It was assumed that, although crushing of the concrete might have started at a strain of 0.004, the actual spalling started to occur when the strain in the concrete (at the level of the compression steel) was approximately 0.007 (Figs. 3.1 and 3.2).

The value of ε_s = 0.007 (> ε_y) is in the yield plateau of the steel stress-strain curve (see Figs. 3.3 and 3.4). Therefore, the compressive force of the longitudinal steel bar is:

$$P_y = f_y A_s \quad \text{(Eq.3.1)}$$

Buckling of the longitudinal compressive bars will start at a buckling load P_b equal to:

$$P_b = (\pi^2 E_t I)/(KL)^2 \qquad \text{(Eq.3.2)}$$

where : E_t = tangential modulus of elasticity of the longitudinal reinforcing steel bar

I = moment of inertia of longitudinal reinforcing steel bar

KL = effective buckling length

By noting that L=s (spacing of stirrups) and $f_{cr}=P_b/A$ (where A is the area of the longitudinal bar), the following relationship is obtained :

$$s \leq (\pi D/4K) \times \sqrt{(E_{t,fcr}/f_{cr})} \qquad \text{(Eq.3.3)}$$

where : D = diameter of longitudinal bar

f_{cr} = stress at which buckling occurs

$E_{t,fcr}$ = tangential modulus of elasticity at f_{cr}

A value of K=0.5 was initially assumed because it was observed during the inspection of damage that the contact of the circular hoops with the reinforcing bars was good. The validity of this assumption is discussed later.

Considering the E_t corresponding to the onset of strain hardening, it was determined that the corresponding P_b was smaller than the value P_y computed on the basis of the yield strength of the steel bar. This indicates that buckling of the outermost layer of longitudinal bars will start to occur at a strain, along the entire buckling length of these bars, that is larger than the yielding strain but smaller than the strain at initiation of hardening. Consequently, the use of the strain hardening value leads to an upper bound for the initiation of buckling.

Therefore, in terms of average strain along the length needed for buckling, the initiation of buckling occurred somewhere in the interval $0.007 < \varepsilon_s < \varepsilon_{sh}$ (i.e., between the start of spalling of the concrete shell and the initiation of steel strain hardening). However, it is believed that buckling initially occured at a point closer to the first value.

Figures 3.10 and 3.11 illustrate the M-Ø diagrams for the cases with and without considering the buckling effect. These figures illustrate the sharp decrease in moment capacity once buckling starts to occur. It was therefore concluded that initiation of buckling was a controlling factor in the determination of ultimate rotation capacity, θ_u (represented by the average ultimate curvature ϕ_u) and therefore of ultimate displacement v_u and displacement ductility μ_δ.

3.2.3 Idealization of Moment-Curvature (M-Ø) Relationship. The M-Ø relationship was idealized in order to use it as input data for the DRAIN-2D computer program (Ref.5). The elastic/perfectly plastic idealization seemed reasonable for the range of curvatures investigated. No increase in moment due to strain hardening was considered since buckling of the longitudinal compressive steel bars occurs at an average strain which is smaller than the strain at the onset of strain hardening. Also, the tensile steel bars just reach the initial stages of the strain hardening range. The idealized curves are presented in

Figs. 3.12 and 3.13, corresponding to the material property cases M1 and M2, respectively (Section 3.1).

3.2.4 Estimation of Interaction Diagram M vs N. It has already been mentioned that the effect of axial load on the moment-curvature diagrams is small and can be neglected. However, it seemed appropriate to compute the interaction curve, M vs N, in order to graphically show the level of axial load being investigated. The values of moments M correspond to the maximum moment obtained from the M-Ø relationship under a given load N. The curve, which corresponds to material properties case M2, is presented in Fig. 3.14. It shows that the range of axial loads to which the canopy column could be subjected to, 26 ± 26 kips (116 ± 116 kN), is much lower than the balanced load (approximately 145 kips = 645 kN).

3.2.5 Estimation of Column Shear Strength. Shear strength evaluation becomes very important when investigation of the structure's failure mode is undertaken. The amount of shear that can be developed in the critical region of a R/C member depends upon the end moments and the loading conditions of the member. In the case of the canopy column, except for the inertia forces developed along its length (which were negligible as the distributed mass throughout the column was very small), no other load was applied between the ends. Therefore, this member is subjected to a constant shear V along its length (Fig. 3.15). The value of this constant V can be computed from $V = (M_a+M_b)/(L)$, where M_a and M_b are the moments at the two ends of the member. Note that the canopy behaves as a cantilever with concentrated lateral force and moment at its top. The applied moment is due to the rotational inertia of the roof and cannot be neglected.

The shear capacity V of the circular cross section was computed using the RCCOLA computer program, which follows recommendations by Capon & Diaz de Cossio (Ref.12). The shear resistance, V, depends on the shear strength provided by the concrete, V_c, and on that provided by the shear reinforcement, V_s. Assuming the shear resistance of concrete to be effective, the available shear strength was found to be considerably higher than the shear resulting from the lateral force required to induce flexural failure. However, based on the 1982 UBC specification 2625 (f) 5, which requires that V_c shall be considered equal to zero when $P_e/A_g < 0.12 f'_c$, the column will fail in shear before it starts yielding. As already pointed out, inspection of the damage in the standing canopies and the type of failure observed in the collapsed canopies, revealed that the failure was of the flexural type. It was concluded that shear strength was not a problem, even though according to present UBC recommendations, it should have been the controlling failure mode.

IV. COMPLIANCE OF CANOPY DESIGN WITH THE 1982 UBC SEISMIC PROVISIONS

4.1 Introduction

This chapter is mainly concerned with analyses conducted to investigate if the canopy design satisfied the minimum requirements for seismic resistant design of the present Uniform Building Code (UBC 1982). The requirements corresponding to seismic zones 3 and 4 will be used, since they are considered to represent the actual situation in El-Asnam during the October 10, 1980 earthquake.

Some of the detailing requirements cannot be examined since information regarding the canopy's design and/or construction details was not available; for example: anchorage of steel bars at the base of the column, splices, tolerances, stirrup bends, etc. Also, other important parameters (such as material properties) were not available (not even the specified value).

4.2 Material Properties

According to 1982 UBC, [2625 (d) 1 & 2], the minimum value of f'_c to be used in seismic zones 3 & 4 is: $f'_c = 3.0$ ksi (21 MPa).

Although values of $f'_c = 3.0$ ksi (21 MPa) and $f'_c = 2.5$ ksi (17 MPa) were used in this study, the latter seemed to be more realistic. Concrete of this low resistance is not permitted by

UBC.

The values of f_y used in this report, 50 ksi (350 MPa) and 40 ksi (280 MPa) are permitted by UBC.

It is important to mention again that neither the specified values of f'_c and f_y nor the actual ones were available. Therefore, the values used were estimated according to visual inspection and personal information.

4.3 Concrete Cover

A minimum concrete cover of 1.5 in. (38 mm) has to be provided for main reinforcement, ties, stirrups, or spirals in the case that the reinforcement is not exposed to weather or in contact with the ground [UBC, 2607 (o)]. Although the specified cover is not exactly known, the measured covers (which were the assumed covers in this report) varied between 1.1 in. (27 mm) and 1.6 in. (40 mm). Thus some of the measured covers do not satisfy UBC requirements.

4.4 Longitudinal Reinforcement

The UBC 1982 edition requires that at least six bars should be used for columns of circular cross section. In this case ten bars were provided; thus, the main reinforcement complied with the UBC.

UBC, [2625 (f) 2], specifies that the vertical reinforcement ratio ρ in tied columns shall be not less than 0.01 nor greater than 0.06.

For the canopy column : $A_s = 4.42\ in^2$ (10 # 6)

$$A_c = (\pi/4)(13.8)^2 = 150\ in^2$$

$$\rho = 0.03$$

$$0.01 \leqslant \rho \leqslant 0.06$$

Therefore, the longitudinal reinforcement ratio satisfied the minimum and maximum UBC requirements.

The minimum spacing of longitudinal reinforcement is limited to the smallest of the following values: bar diameter, 1.0 in, or 4/3 times the maximum size of the aggregate (not known), [2607 (e)] and [2603 (d)]. These requirements were satisfied.

4.5 Transverse Reinforcement

According to UBC [2607 (m) 3.], all bars in tied columns shall be enclosed by stirrups or transverse ties which are at least No. 3 in diameter for longitudinal bars smaller than No.11. In the columns of the canopy, # 2 ties were used (reinforcing 10 # 6 longitudinal bars); therefore, the UBC requirement was not satisfied in this case.

According to UBC, stirrups shall be spaced at no more than d/2 (= 11.8/2 = 5.9 in. = 150 mm) throughout the length of the member [2626 (e) 5B]. In addition, at critical regions, [2625 (e) 5C], along a length of at least 2D = 2(13.8)= 27.6 in. (700 mm) from the base of the column, the spacing s of the ties should satisfy the following requirements:

a) $s \leqslant d/4 = 3.0$ in. (75 mm)

b) $s \leqslant 8\ \phi_{long} = 8\ (6/8) = 6$ in. (152 mm)

c) $s \leqslant 24\ \phi_{ties} = 24\ (2/8) = 6$ in. (152 mm)

d) $s \leqslant 12$ in. (305 mm)

These UBC requirements are meant to ensure ductile flexural behavior. Note that the canopy's columns are subjected to extremely low axial forces; therefore, they are basically flexural members. If the columns of the canopy are considered under UBC [2625 (f)], as members subjected to both axial and bending stresses, the center-to-center spacing of the hoops shall not exceed 4 in. (102 mm) [2625 (f) 4B].

The transverse ties used were # 2 @ 7.2 in (183 mm); obviously, UBC is not satisfied whether the column of the canopy is considered as a flexural member or as a column.

The shear design of columns has to satisfy section [2625 (f) 5] of UBC; i.e.:

$$A_v\ f_y\ d_c\ /\ s = (V_u/\phi) - V_c \qquad \text{(Eq.4.1)}$$

where V_c should be neglected if $P_e/A_g < 0.12\ f'_c$

In this case : $P_e/A_g = 0.18$ ksi (1.2 MPa) $< 0.12\ f'_c = 0.30$ ksi (2.1 MPa). Therefore, $V_c = 0$ and the previous equation becomes:

$$A_v = (V_u)(s)/(\phi)(f_y)(d_c) \qquad \text{(Eq.4.2)}$$

From Fig. 3.15, $V_u = (M_a + M_b)/L = 2(800)(1.25)/(105) =$ 19.0 kips (84.6 kN).

Substituting the appropriate values, the required A_v becomes 0.41 in.^{2} (270 mm^2). The available A_v is equal to 0.067 in.^{2} (970 mm^2). Therefore, the columns considered here should fail in shear even before yielding begins. Damage in the standing canopies and the type of failure observed in the collapsed canopies revealed that the failure was due to flexural yielding and not to shear. Therefore, although according to present UBC recommendations the shear strength should have controlled the failure, shear was not considered to be a problem.

Although not required by UBC, it has been discussed in Chapter 3 (Section 3.2.2), that the theoretical spacing of hoops at which buckling will start to occur is given by:

$$s \leqslant (\pi D/4K) \times \sqrt{(E_{t,fcr}/f_{cr})} \qquad \text{(Eq.3.3)}$$

For the case of K=0.50 (which implies perfect workmanship) and for Grade 40 steel (and further assuming $f_{cr} = f_y$ and $E_{t,fcr} = E_{sh}$, i.e. the tangential modulus of strain hardening) : $s \leqslant 6D = 6\ (6/8) = 4.5$ in. (114 mm). Even for this case, it is seen that the minimum spacing s for initiation of buckling is smaller than the spacing used (7.2 in. = 183 mm) , which indicates the importance of considering buckling effects in the analysis of the canopy. In fact, as will be seen later, buckling controls the response, i.e. it determines the maximum displacement v_u and therefore the displacement ductility μ_δ.

It is interesting to note that if K is chosen equal to 1.0 (and if Eq.3.3 is used), buckling is determined to occur at a strain in the steel somewhere between ε_y and ε_{sh}, as obtained for the previous case with K=0.50. Therefore, the selection of the value for K is not too important for the case at hand.

4.6 Concluding Remarks

The canopy design and detailing did not satisfy many of the minimum UBC requirements for ductile moment resistant space frames.

V. ESTIMATION OF DYNAMIC CHARACTERISTICS OF CANOPY

5.1 Determination of Periods

5.1.1 Generalized SDOF Model. As a first approach, the period of the structure was computed using Raleigh's Method (Ref.13), by assuming a first mode shape $\Psi(x)=(1-\cos(\pi x/2L))a$, where a is the top nodal displacement (Fig.5.1 and Appendix B).

In terms of the frequency of vibration:

$$w^2 = \frac{k^*}{m^*} = \frac{\int_0^L EI\ (v''(x))^2 dx}{\int_c^L m\ (v(x))^2 dx + M\ (v(L))^2 + I_0\ (v'(L))^2} \qquad \text{(Eq.5.1)}$$

The period of the structure ($T=2\pi/w$) was initially obtained for three cases:

1) Using a constant column stiffness corresponding to the uncracked transformed section, EI_{uc}: T = 0.46 sec.

2) Using a constant column stiffness corresponding to the cracked transformed section, EI_{cr}: T = 0.72 sec.

3) Using EI_{uc} constant for the top half of the member and EI_{cr} constant for the lower half : T = 0.64 sec.

The influence of the geometric stiffness on the period was investigated and it was concluded that it hardly had any influence on it (Appendix B).

5.1.2 Two DOF Model. Considering the inertia forces shown in Fig.2.3 (see also Appendix B), and using elementary beam theory to determine the influence coefficients, the characteristic frequency equation is easily obtained from which the following different values of T are estimated:

1) Using a constant column stiffness corresponding to the uncracked transformed section, EI_{uc}: T_1 = 0.46 sec., T_2 = 0.11 sec.

2) Using a constant column stiffness corresponding to the cracked transformed section, EI_{cr}: T_1 = 0.72 sec., T_2 = 0.18 sec.

Since concentrated small cracks decrease the stiffness EI of the member only at regions immediately adjacent to the cracked section, the overall stiffness of the entire structure will not be greatly affected by these small cracks and the period will be close to the one corresponding to the uncracked section stiffness. Thus it is expected that initially (actually, before or at the beginning of the earthquake), the period of the first mode of vibration is closer to 0.46 sec than to 0.72 sec (unless it is assumed that the canopy was significantly cracked before the earthquake).

Based on the previous considerations, it was decided to use a value of 0.50 sec for the first mode period in estimating the peak ground acceleration (PGA) in the first stage of the analysis (Chapter VI.). The above values were obtained assuming a fixed foundation, which according to the actual type of construction and performance of the structure, appears to be a good approximation. Any rocking of the foundation would have resulted in an increase of the period T.

It is interesting to note that the first mode period of the 2DOF and 5DOF models (for both the uncracked and cracked cases) are equal. This is the case because both models have the same first mode shape.

5.2 Damping Ratios

Considering that this is a very clean building consisting of only the bare structural system, the damping ratio ξ, for the first mode of vibration has been selected as 2 percent. However, in order to study the effect of damping on the effective peak acceleration, a value of ξ = 5% has also been considered.

VI. ANALYSES TO ESTIMATE THE EFFECTIVE PEAK ACCELERATION (EPA)

6.1 Introductory Remarks

Different approaches can be followed in order to estimate the effective peak acceleration, EPA. The approach presented in this report consists of three steps.

In the first step use is made of the charts developed by Bertero, Mahin, and Herrera (Ref.4), for a one-degree-of freedom system. This procedure estimates the peak or maximum ground acceleration PGA necessary to excite the structure in such a way that it just reaches failure (collapse limit state). Although different types of hysteretic behavior can be used in the derivation of these charts, the ones used herein are based on a linear elastic/perfectly plastic response of the system. For any selected dynamic characteristics (time history) of the ground motion and any damping ratio, ξ , the charts can be constructed. In using them, an estimate of the yield strength R_y and period T, as well as an estimate of the available maximum displacement ductility, μ_δ , is required.

It should be noted that the parameter which best defines when the canopy reaches its collapse limit state is the rotation at the critical region at the base of the column, since the collapse of the canopy is due to the buckling of the main flexural reinforcement in this region. Whereas the maximum rotation at the base of the SDOF cantilever directly relates to the maximum displacement ductility ratio μ_δ at the top of the cantilever, this may not be so for the 2DOF case. However, as the results indicate, even for the 2DOF model, the maximum rotation at the base is related to the maximum displacement at the top of the canopy.

In the second stage of the approach, after obtaining an estimate of the peak ground acceleration PGA in the previous step, inelastic time history analyses were conducted using the computer program DRAIN-2D. These analyses were carried out with ground motions normalized to values of PGA close to the ones found in the first step of the studies, and using both SDOF and 2DOF models of the canopy. From these series of time history analyses it was concluded that the inclusion of the second degree of freedom significantly affected the dynamic response.

In the third stage of the studies, analyses were conducted to find out the effect of "clipping" the acceleration ground motion records used in the second stage. For each of the selected earthquake records, the variation of the response of the canopy introduced by "clipping" the peaks of the ground acceleration record above a certain level was analyzed using DRAIN-2D. The level of ground acceleration above which the peaks were clipped was decreased until it was noted that the maximum response started to decrease. This permitted the determination of the effective peak acceleration, EPA.

Generally, EPA is less than the recorded peak acceleration, PGA, because acceleration pulses of high value but short duration have little effect on the response of most structures. In addition, for structures strained into the inelastic range, the number and order of the acceleration peaks, as well as the duration of these pulses and of the entire ground motion, rather than the peak itself, greatly influence the response (Ref.14).

6.2 Problems in Estimating EPA

Besides estimating the period and the damping ratio of the canopy, it was necessary to decide on a number of parameters in order to be able to estimate the EPA which gives rise to the observed response. These are:

6.2.1 Type of Ground Motion. This is probably the main uncertainty in the determination of EPA. Since no earthquake record was obtained, it was decided to conduct this study, using two types of earthquakes considered to give an upper and a lower bound on the inelastic deformation demands. The two records were El Centro 1940 S00E and Derived Pacoima Dam 1971 S16E (Base Rock Record). From the point of view of inelastic deformation demands, and for structures with T > 0.4 sec., the El Centro record can be considered as a record with relatively very short acceleration pulses and consequently as one which will result in a lower bound of inelastic demands. On the other hand, the Derived Pacoima record is of the impulsive type (intense and long-duration acceleration pulses) and therefore will result in an upper bound of inelastic demands.

6.2.2 Idelization of the Lateral Resistance Function, R vs. v_1. The derived M-Ø diagrams shown in Figs. 3.12 and 3.13 have been used to determine idealized lateral resistance functions, R vs. v_1, of the canopy. The linear elastic/perfectly plastic idealization of the lateral resistance function, used in the estimation of EPA, is shown in Figs. 6.1 and 6.2. The figures correspond to a constant axial load of N = 26 kips (116 kN) and to the concrete cover values given in the figures. In these figures a range of possible values for v_u is indicated: (3.5 in.- 4.3 in.) = (88 mm - 110 mm) for material properties case M1, Fig.6.1; and (3.5 in. - 6.3 in.) = (88 mm - 160 mm) for material properties case M2, Fig.6.2. This range is limited by the value of $Ø_u$, which is controlled by buckling of the longitudinal reinforcing bars, as indicated in Figs. 3.8 - 3.11.

It should be recognized that a decrease in the lateral resistance R will significantly affect the response of the canopy. For example, the relative acceleration $\ddot{v}_r$ will increase as R decreases, since for the case without damping:

$$m\,\ddot{v}_r + R = m\,\ddot{v}_g \Rightarrow \ddot{v}_r = \ddot{v}_g - R/m \qquad \text{(Eq.6.1)}$$

Therefore, as buckling of the longitudinal compressive steel bars takes place, the resistance R is expected to decrease with a consequent increase in the relative acceleration $\ddot{v}_r$ and therefore an increase in displacement. Thus the initiation of buckling of the main flexural reinforcement can be considered as the point where the failure of the canopy will occur and as a limit for the maximum displacement of the canopy. It was decided to consider that buckling started at a v_u equal to 3.5 in. (90 mm) and 3.9

in. (100 mm) for the cases M1 and M2, respectively.

6.2.3 Determination of Displacement Ductility. According to the procedure suggested by Bertero, et al (Ref.4), in order to estimate PGA it is necessary to determine the value of the maximum displacement ductility ratio, μ_δ, and of the idealized linear elastic/perfectly plastic seismic resistance, R, vs. displacement, v_1, relationship. This has been accomplished using two different approaches, which are summarized below.

1) First Approach: Park and Paulay (1975) (Ref.7). These authors offered an approximate solution for the relation between curvature ductility and displacement ductility ratios in the case of a cantilever column with a lateral load at the free end (Fig.6.3a). Based on the assumed curvature distribution shown in this figure, the following relation is derived:

$$\mu_\delta = \left[1\right] + \left[\frac{(\phi_u - \phi_y)}{\phi_y}\right]\left[\frac{(L-0.5L_p)(3L_p)}{(L)^2}\right] \qquad \text{(Eq.6.2)}$$

where : μ_δ = displacement ductility

ϕ_y = curvature at yield

ϕ_u = curvature at ultimate

L = length of cantilever

L_p = length of plastic region

As may be seen from Eq.6.2, this approach depends on several parameters whose determination involves a large degree of uncertainty. Among these are the following :

A) Curvatures ϕ_y and ϕ_u. As Figs. 3.5 to 3.13 show, these values depend on the material properties, concrete cover, level of axial load, M-Ø idealization, moment distribution along the columns of the canopy, initiation of buckling, etc.

B)_Length_of_plastic_region_and_moment_distribution_along_the columns_of_the_canopy. Several formulas exist for the determination of the value of the plastic length L_p (Ref.7). However, it is considered more realistic to determine this value from an assumed moment distribution.

It can be shown that in the case that a moment is acting at the top of a cantilever beam, Fig.6.3b, it is possible to estimate μ_δ by modifying Eq.6.2 as follows:

$$\mu_\delta = 1 + \left[\frac{(\phi_u - \phi_y)}{\phi_y}\right] \left[\frac{(L-0.5L_p)(6L_p)}{(L)^2(2+c)}\right] \qquad \text{(Eq.6.3)}$$

where : $c = \phi_{top}/\phi_y$; $-1 < c < 1$

By using this equation (see Appendix C), it is shown that the influence of the top moment on the value of μ_δ is small if the value of c is small (e.g. c = 0.33). Furthermore, if c < 0, then the value of μ_δ remains fairly stable even for very large values of c . In other words, when the top and bottom moments have different signs, the plastic length L_p remains small and therefore the influence of the value of c on the μ_δ may be neglected.

Although in most of the inelastic computer analyses performed the value of the top moment was small, there were some cases in which its value was significant. In spite of this, it will be assumed in the first stage of the method that the influence of the top moment on the displacement ductility can be neglected.

A summary of the data used in the determination of μ_δ, and eventually in the estimation of PGA, is presented below:

CASE M1 : f'_c = 3.0 ksi (21 MPa)

f_y = 50 ksi (350 MPa)

N = 26 kips (116 kN)

d' = 1.7 in. (43 mm)

M_y = 785 k-in. (88.7 kN-m) = moment at first yield

ϕ_y = 0.34 X 10^{-3} rad/in. (13.4 X 10^{-3} rad/m) = curvature at yield

M_u = 974 k-in. (110 kN-m) = moment capacity

EI_{cr} = 2.62 X 10^6 k-in.^{2} (7520 kN-m^2)

c = 0.00

a) Initiation of Buckling Range :

ϕ_u = 2.27 X 10^{-3} rad/in. (89 X 10^{-3} rad/m) $\Rightarrow \mu_\delta$ = 4.0

b) End of Buckling Range :

ϕ_u = 3.00 X 10^{-3} rad/in. (118 X 10^{-3} rad/m) $\Rightarrow \mu_\delta$ = 5.1

CASE M2 : f'_c = 2.5 ksi (17 MPa)

f_y = 40 ksi (280 MPa)

N = 26 kips (116 kN)

d' = 2.2 in. (56 mm)

M_y = 612 k-in. (69.2 kN-m) = moment at first yield

ϕ_y = 0.28 X 10^{-3} rad/in. (11.0 X 10^{-3} rad/m) = curvature at yield

M_u = 800 k-in. (90.4 kN-m) = moment capacity

EI_{cr} = 2.62 X 10^6 k-in^2 (7520 kN-m^2)

c = 0.00

a) Initiation of Buckling Range :

$\varnothing_u$ = 2.28 X 10^{-3}rad/in. (90 X 10^{-3}rad/m) $\Longrightarrow \mu_\delta$ = 5.3

b) End of Buckling Range :

$\varnothing_u$ = 4.47 X 10^{-3} rad/in. (176 X10^{-3}rad/m) $\Longrightarrow \mu_\delta$ = 10.1

This approach, even though it contains several uncertainties (especially regarding the material properties) and simplifications (the influence of the top moment on the displacement ductility was neglected), seems appropriate for the case at hand. Note that Eqs.6.2 and 6.3 assume constant curvature along the plastic length L_p. Actually, cracks will develop throughout the column and a detailed study of the bond stress distribution between cracks as well as at the foundation is necessary. An approximate analysis of the effects of bond slippage at the foundation and in the column region adjacent to the main crack has been conducted (Appendix F). More refined studies are underway.

The initiation of buckling will be close to the first value of $\varnothing_u$ given above (2.28 X 10^{-3}rad/in. = 90 X10^{-3} rad/m), which gives a displacement ductility μ_δ in the range of 4 to 5 depending on which material property case is considered.

2) Second Approach. The canopies were able to undergo lateral displacement of at least 6 in (15.2 cm) without failure. This is the distance that separated the canopies from the adjacent

classrooms. Assuming that this displacement is an upper bound for v_u, and using for v_y the value of 1.2 in. (30 mm), $\mu_\delta = 5$ has been estimated. Figs. 6.1 and 6.2 show an equivalent displacement at yield that varies from 1.1 in. (29 mm) to 1.3 in. (33 mm) in the case of the linear elastic/perfectly plastic resistance function.

6.3 Estimation of EPA

6.3.1 First Stage : Estimation of PGA by Procedure Proposed by V.V.Bertero, S.A.Mahin, and R.A.Herrera (Ref.4). The procedure consists of first determining the value of η based on estimated values for the period, damping, and displacement ductility of the structure (refer to graphs in Figs. 6.4 and 6.5). A value of T = 0.50 sec was used for all cases in the first stage of the analysis; damping ratios equal to 2% and 5% were considered. Once η is determined, the value of the maximum ground acceleration PGA can be computed using the following equation :

$$\eta = (C_y)(g)/(PGA) = (R_y)/(m)(PGA) \qquad \textbf{(Eq.6.4)}$$

The value of the mass m associated with the horizontal component of the ground motion (for the equivalent one-degree-of-freedom system of Fig.2.3, where v_2 is neglected) is :

$$m = M + \bar{m}\ L/2 = 0.065 + (3.3 \times 10^{-5})(105/2) =$$
$$= 0.067 \text{ kips-sec}^2/\text{in.} \ (12 \text{ kN-sec}^2/\text{m})$$

The value of R_y was determined previously (Figs. 6.1 and 6.2). Thus, the value of the yielding seismic coefficient C_y can be determined for the two material property cases under consideration:

CASE M1 : $R_y = M_y / L = 974/105 = 9.28$ kips (41.3 kN)

$C_y = R_y / W = 9.28/26 = 0.35$

CASE M2 : $R_y = M_y / L = 800/105 = 7.62$ kips (33.9 kN)

$C_y = R_y / W = 7.62/26 = 0.29$

The required PGA's for the two normalized records considered in this study, El Centro and Derived Pacoima Dam, are summarized in Table 6.1 for the different cases considered.

A damping ratio of ξ = 2%, as well as the material properties of case M2 were considered to be more realistic than the other possible combinations. Using μ_δ = 5 (as determined previously), and rounding to the nearest 0.05g, the following values of PGA were obtained in the first stage of the studies:

- For El Centro Record: PGA = 0.55g
- For Derived Pacoima Dam Record: PGA = 0.35g

6.3.2 Second Stage: Verification of PGA Using DRAIN-2D.

6.3.2.1 Introduction. Inelastic dynamic analyses were necessary in order to accomplish the following main goals:

1) Study the variation of the response of the canopy using different types and intensity scaling of earthquakes (both the El Centro and the Derived Pacoima Dam type of records were used, normalizing the acceleration intensities as required).

2) Determine the influence of the rotational degree of freedom (v_2 in Fig.2.3) on the canopy's response. For this purpose, both SDOF and 2 DOF models were used.

3) Verify the results obtained in Section 6.3.1 referring to the determination of PGA.

4) Determine EPA by the "Clipping Method" described in Section 6.3.3.

5) Determine the influence of several parameters on the canopy's response. Among these parameters are:

a) Column stiffness EI (uncracked, cracked, etc.)

b) Material properties, concrete cover and axial load. These affect mainly the value of R_y and thus influence the inelastic response.

6.3.2.2 DRAIN-2D Computer Program. DRAIN-2D is an inelastic dynamic analysis computer program for two dimensional structural systems (Ref.5). The program uses the direct stiffness method; also, a step-by-step dynamic analysis for inelastic structures is performed.

The program can handle different types of structural elements; in this case, a beam-column element was used. This type of element may be briefly described as having variable cross section and strength and the ability of yielding through the formation of concentrated plastic hinges at its ends. Variable flexural yielding, as affected by axial force, can be incorporated by using an interaction axial force-moment diagram. In this case, however, an elastic/perfectly-plastic curve for the moment rotation relationship under a constant axial load of P = 26 kips = 116 kN was used.

The sign convention for displacements and forces used in the DRAIN-2D analyses is illustrated in Fig. 6.6.

6.3.2.3 Summary of Response Results. Tables 6.2 to 6.5 summarize the main results obtained from the analysis conducted to determine the effect of using SDOF and 2 DOF models. Analyses of these results permit to judge the validity or degree of approximation on the value of PGA as derived in 6.3.1, considering SDOF systems only . Time history responses obtained are given in Appendix G.

As was pointed out before, since failure was due to the buckling of the main flexural reinforcement at the base of the column, the parameter which best defines failure of the canopy is the rotation at the critical region at the base of the column, rather than the displacement at the top of the canopy. However, as Tables 6.3 to 6.5 indicate, the maximum value of the plastic rotation at the base of the column and the maximum top nodal displacement are related. Either these two maxima occured at the same time or the value of the top nodal displacement was close to the overall maximum displacement value (within 5%) at the time when the maximum rotation occurred.

Table 6.2 summarizes the results obtained for material properties Case M1. For a 2 DOF model and EI = 5.4×10^6 k-in^2 (15500 kN-m^2), i.e. close to the uncracked transformed section, several analyses of both El Centro and Derived Pacoima Dam ground motions were performed using different intensities to obtain an estimate of the PGA. Assuming a value of v_u = 3.5 in. (90 mm) as the displacement which caused the failure, (see Section 6.2.2), the resulting values of maximum ground acceleration were (interpolating from Table 6.2):

PGA = 0.45 g , for Derived Pacoima Dam Record

PGA = 0.70 g , for El Centro Record

Because it is believed that the actual material properties are better represented by Case M2 (f'_c = 2.5 ksi = 17 MPa; f_y = 40 ksi = 280 MPa), further investigations concentrated on this case.

6.3.2.4 Comparison of SDOF and 2DOF Models. Tables 6.3 to 6.5 give a summary of the main response results considering SDOF and 2DOF models with material properties classified as case M2. (The corresponding time history responses are given in Appendix G).

Table 6.3 summarizes the main results obtained when the influence of using a SDOF or a 2DOF on response was investigated for different stiffnesses EI and using the Derived Pacoima Dam ground motion record (scaled to a PGA of 0.35g). As far as maximum displacement is concerned, the results indicate that the maximum difference between the results of the two models is on the order of 25%. Larger values were obtained for the SDOF model than for the 2DOF model (except for one case in which the 2DOF model's maximum displacement was larger than the SDOF one by less than 5%). Time history response studies indicate that the mass moment of inertia not only affects the maximum displacement but also influences the displacement pattern and the moment at the top of the columns of the canopy. This moment reaches a value of 460 k-in (52.0 kN-m), close to the moment at first yielding of steel: 612 k-in (69.2 kN-m).

Tables 6.4 and 6.5 show the results obtained using the El Centro ground motion scaled to a PGA of 0.50g and 0.55g, respectively. It is observed, from these tables that the maximum displacement for the SDOF and 2DOF models differ by about 20%, giving larger values for the SDOF model. However, a much larger discrepancy in maximum displacement, namely 51%, is observed in the case that the canopy is subjected to the El Centro ground motion normalized to a PGA of 0.55g and EI is assumed cracked (Table 6.5). There is also a considerable variation in the displacement pattern of both models. The values of the top moment are very high (745 k-in = 84.2 kN-m for the 0.50 g case and 800 k-in = 90.4 kN-m for the 0.55 g case). This not only indicates that the rotary moment of inertia is important, but it also shows that it can induce yielding at the top of the column forcing it to its maximum capacity. The shear considering the 2DOF model was as much as 68% higher than the one from the SDOF model. These results indicate once again, at least conceptually, the importance of a capacity design for shear purposes even though in this case shear did not seem to be a problem.

Tables 6.6 and 6.7 list the maximum displacements obtained.

From the studies conducted during the second stage, the following conclusions are drawn:

1) The value of the stiffness EI is an important parameter.

The actual EI seems to be closer to the value of the cracked section, i.e. 2.62×10^6 k-in^2 (7520 kN-m^2). This is due to the fact that after the first seconds of the earthquake the section cracks on both sides.

2) For the SDOF model and for EI approximately equal to the stiffness of the cracked section, a maximum displacement of approximately 4 in. (102 mm) was obtained for both the El Centro ground motion normalized to 0.55g and the Derived Pacoima Dam ground motion normalized to 0.35g. For the 2DOF model, the Derived Pacoima Dam record normalized to 0.35g yields the same value, whereas the El Centro record normalized to 0.55g only yields 2.8 in. (71 mm). These results indicate that the charts proposed by Bertero et al., which were developed for a SDOF model, do not work well for 2DOF systems, particularly for earthquake motions such as the El Centro ground motion. It is therefore important for future research to study the possibility of finding a generalized SDOF system that gives the same results as the ones given by the 2DOF system. This might be achieved by proper selection of the SDOF shape function.

3) The contribution of the second mode of vibration is important, particularly if the predominant frequency of the ground motion is close to the canopy's second mode frequency. This mode affects the following response parameters:

a) The maximum value of v_1, which can be affected by as much as 51%, the value of the SDOF model being larger. Both positive and negative values and the time of occurrence are affected.

b) The value of permanent displacements at the end of the earthquake excitation: significantly different values were obtained for the two models (Figs.6.7 and 6.8), being the values for the SDOF larger.

c) Time history response of shear and moments: both patterns and maximum values are affected. Note that the maximum possible shear for the SDOF model is M_{max}/L, while for the 2DOF it is $2M_{max}/L$.

4) Since the results which are based on a SDOF model will give reliable results only for certain types of earthquakes, particularly those whose frequency content will not excite the canopy's second mode of vibration, it is considered that the assumption of a SDOF model is not correct as it depends significantly on the type of earthquake ground motion exciting the model. Therefore, it is NECESSARY to use a 2 DOF model for further inelastic analyses. Except for the shear, the SDOF model in general resulted in larger response. Only in one of the cases studied did the maximum values for displacement and plastic hinge rotation at the base for the 2DOF model exceeded those for the SDOF model, but the difference was less than 5%.

5) The results of the analyses show that in order to attain a v_u of 4 in. (102 mm), the PGA required should be close to 0.35g for the normalized Derived Pacoima Dam record and 0.65g for the normalized El Centro 1940 record.

6.3.3 Third Stage: Estimation of EPA by the "Clipping Method"

6.3.3.1 Introduction. In the third stage of the studies, DRAIN-2D was used to carry out time history analyses of the response of the 2DOF model when subjected to the two earthquake ground motions discussed above. The peak accelerations of these motions were clipped in order to study the influence that such clipping has on the response of the canopy models.

In analyzing the variations of the time-history of the ground motions and the displacement response, the time at which the maximum displacement occurred can be determined and the peak of the ground acceleration which coincides with this displacement can be identified. It is then possible to estimate how much the ground acceleration record can be clipped without significantly decreasing the maximum response of the canopy.

It should be noted that clipping the recorded peak ground accelerations will not necessarily result in a decrease in the response of the structure. Clipping may well result in an increase in response! When the clipped peak ground accelerations occur earlier than the critical pulse(s) of the unclipped record which induce the maximum v_u, the clipping operation might modify the response of the structure in such a way that the response values, at the time the critical pulse begins, favor a further increase in displacement due to this critical pulse. The clipping process should continue until the maximum displacement begins to decrease. The peak acceleration of the clipped (or unclipped) accelerogram for which the maximum displacement occurred is considered to be the EPA for the case (structural model) and earthquake under consideration.

6.3.3.2 DRAIN-2D Results. Tables 6.8 and 6.9 give a summary of the most important displacement peaks obtained during the time history response of the 2DOF canopy model to both the El Centro ground motion (scaled to a PGA of 0.55 g) and the Derived Pacoima Dam ground motion (scaled to a PGA of 0.35 g) and for two values of stiffnesses EI (uncracked and cracked).

Table 6.10 is similar to Table 6.9 but applies to the case of the canopy being subjected to the actual El Centro Record (PGA = 0.35g), rather than to the normalized El Centro (PGA = 0.55g). Time history responses are plotted in figures included in Appendix H.

Tables 6.8, 6.9, and 6.10 define six main cases, each of which will be considered separately in order to gain a better understanding of the behavior of the canopy. These cases should not be confused with the material property cases M1 and M2 referred to previously. The six cases are based on material properties case M2.

Fig.6.9 shows the time history earthquake ground motions used for cases 1 to 6. A numbering of the significant peaks has been made; reference to the peak numbers will be done in the description of each of the cases.

(1) Cases 1 (Canopy's 2DOF response to El Centro Record, normalized to a PGA of 0.55g, Fig.6.9a, considering:

$EI = 6.28 \times 10^6$ k-in^2 = 18000 kN-m^2 ;

M_y = 800 k-in = 90.4 kN-m ;

T_1 = 0.46 sec ; T_2 = 0.11 sec)

As may be seen from Table 6.8 and Fig.6.10, the maximum displacement occurs at a time t = 12.21 sec. Looking at the El

Centro earthquake record normalized to a PGA of 0.55g (Fig.6.9a), it is seen that peak No.17, which has a relative maximum peak acceleration of approximately 0.20g, is the one that gives rise to the maximum displacement of 2.2 in. (55mm) in the case without clipping (Fig.6.10). It would seem logical, at first, to expect that clipping the earthquake record up to the maximum value of peak No.17 (0.20g) would give approximately the same result. However, from an analysis of the obtained displacement time histories (Figs.6.10 and H.1A to H.1E), the importance of peaks No.2 and 3 (Fig.6.9a) is apparent. The first clipping (down to 0.36g, case 1B) does not affect peaks No.1 and 2; however, as peak No.3 is "clipped", the displacement response is significantly affected. The new clipped pulse No.3 induces a significantly smaller incremental (change in) displacement than the unclipped pulse.

From Fig.6.10 it can be seen that the displacement at the end of pulse No.2 (Fig.6.9a) is 1.9 in. (49 mm). Due to the unclipped pulse No.3, the displacement reversed to a value of -1.3 in. (-33 mm); on the other hand, due to the clipped pulse No.3 it reversed to only -0.7 in. (-17 mm). Even though the peaks following peak No.3 are only slightly changed, and thus the relative response does not change much (i.e. the curves are practically the same except for a shift from -1.3 in. to -0.7 in. from this point on), the total displacement now differs by about 0.6 in. (16 mm), yielding larger positive displacements for the case with clipping. Looking at it from another point of view, the initial conditions of the canopy model, when pulse No.17 started, were significantly affected by the clipping process. These initial conditions, when the acceleration record was clipped, favored an increase in displacement during pulse No.17. Therefore, it is not surprising that up to a clipping value of 0.32g, the response is increased.

Further clipping (say to 0.28g or less) results in smaller displacements as other peaks are also affected (in particular, the fact that peak No.2 is clipped causes a decrease in the response). It should be clearly noted that the clipping process has increased the peak displacement response but it has not increased the maximum total incremental displacement or cyclic displacement.

(2) Cases 2 (Canopy's response to El Centro Record, normalized to a PGA of 0.55g, Fig. 6.9a, considering:

$EI = 2.62 \times 10^6$ k-in^2 = 7520 kN-m^2 ;

M_y = 800 k-in = 90.4 kN-m ;

T_1 = 0.72 sec ; T_2 = 0.18 sec)

For the unclipped case, the maximum displacement is controlled by peak No.2 (which occurred at a time just short of 2 seconds). However, the displacement due to peak No.13 is just a little smaller than the maximum displacement (Figs.6.11b and H.2A).

Clipping peak No.3 introduces significant changes in the subsequent response since it forces the negative displacement due to peak No.2 to remain smaller than that in the unclipped case (for example, for a clipped acceleration of 0.28g, the displacement is -0.4 in. = -9 mm after peak No.3, rather than

-1.3 in. = -34 mm for the unclipped case, Fig.6.11b). As a result, the displacement curve is shifted upward and peak No.13 forces the canopy to displace 4.1 in. (104 mm), which is the maximum response value. It is thus seen that clipping can cause the maximum displacement to occur at a different instant and to be larger than in the unclipped case (in this case, by almost 50% !).

From analysis of the time history response (Figs. H.2A to H.2D) it has been observed that:

A) The rotation at the top node of the canopy is not small (almost 0.05 radians). Also, the pattern of the rotation time history response is similar to that of the displacement response which was described above. Therefore, the difference between rotation time history patterns in the unclipped and clipped cases can be explained in a similar way to that presented for the displacements.

B) The bottom moment reaches (or is close to reaching) yielding at almost every cycle.

C) The value of the top moment reaches its maximum capacity (800 k-in = 90.4 kN-m) at a time close to 5 seconds. At a time equal to about 2 seconds, the top moment is also very large.

D) The shear also attains high values (of approximately 12.1 kips = 53.8 kN), higher than the maximum capacity of the SDOF model (M_{max}/L = 7.61 kips = 33.9 kN), and close to the maximum capacity of the 2DOF model ($2M_{max}/L$ = 15.2 kips = 67.6 kN).

It should be noted that the predominant frequency of the El

Centro ground motion is approximately 1.4 cps (Fig.6.12, Ref.15), which results in a period of 0.71 sec. This value is very close to the period of the first mode of the canopy (0.72 sec).

(3) Cases 3 and 4 (Canopy's Response to the Derived Pacoima Dam Record, normalized to a PGA of 0.35g, Fig.6.9b, considering:

M_y = 800 k-in = 90.4 kN-m ;

Case 3: EI = 6.28 X 10^6 k-in^2 = 18000 kN-m^2 ;

T_1= 0.46 sec ; T_2= 0.11 sec

Case 4: EI = 2.62 X 10^6 k-in^2 = 7520 kN-m^2 ;

T_1= 0.72 sec ; T_2= 0.18 sec)

For the Derived Pacoima Dam Record normalized to 0.35g (Fig.6.9b), it was not possible to do any "clipping" since a smaller displacement value was obtained for just a small amount of clipping. This was the case because the long duration pulses of the ground motion, particularly the pulse corresponding to peak No.2, controlled the response. This pulse induced the maximum displacement of the canopy and therefore any clipping of the peak affected the response (see Fig.6.11d).

Because case 3 considers a much more rigid structure than case 4, it resulted in a much smaller maximum displacement. Also, the displacement patterns for cases 3 and 4 are different (as expected) and the maximum displacement occurs at different instants (see figures Appendix H, cases 3 and 4). It should be noted that although the maximum displacements for cases 4 are larger than those of cases 3, the maximum displacement ductility ratios are somewhat smaller. This emphasizes that deformations should not be confused with ductility ratio.

The resulting rotations have approximately the same magnitude as those obtained in the El Centro 0.55g case.

Yielding at the bottom of the canopy is mainly a consequence of peaks No.1 and 2. Note that soon after these peaks occur, the canopy yields continuously (i.e. the bottom moment is constant and equal to the moment at yield) for approximately 0.35 seconds. After a time equal to 5 seconds, almost no continuous yielding is obtained, i.e. as soon as yielding occurs, the value of the moment starts to decrease.

The values obtained for the top moment are not very large (they reach approximately 430 k-in = 48.6 kN-m, i.e. about half its moment capacity). This is due to the fact that the Derived Pacoima Dam ground motion does not excite the second mode of vibration very much. As a consequence, the maximum shear reaches a value of about 9.9 kips = 44.1 kN, barely exceeding the SDOF maximum of 7.61 kips = 33.9 kN, and is well below the 2DOF maximum of 15.2 kips = 67.6 kN.

<u>(4) Cases 5 and 6</u> (Canopy's Response to Actual El Centro Record, PGA equal to 0.35g, Fig.6.9c, considering:

M_y = 800 k-in = 90.4 kN-m ;

Case 5: EI = 6.28 X 10^6 k-in^2 = 18000 kN-m^2 ;

T_1= 0.46 sec ; T_2= 0.11 sec

Case 6: EI = 2.62 X 10^6 k-in^2 = 7520 kN-m^2 ;

T_1= 0.72 sec ; T_2= 0.18 sec)

It was initially found that in order to attain the observed performance of the canopy it was necessary to normalize the actual El Centro record (with PGA=0.35g) to a PGA of 0.55g. Furthermore, it was found that by applying the clipping process the EPA could be reduced from a PGA value of 0.55g to 0.32g, which is smaller than the actual recorded PGA of 0.35g. Because of these reasons, it was decided to perform additional analyses by clipping the actual El Centro ground motion.

Since the value of PGA was reduced (from 0.55g to 0.35g), but the R_y was not (i.e. the ratio R_y/PGA was increased), it is of interest to study what the effect of the increase of this factor is on the amount of clipping that is possible. Would the ratio of EPA to unclipped PGA be maintained if the ground motion record is initially normalized to different acceleration intensities or if different values of EI's are used?

Case_5: This is similar to Case 1 in that the maximum displacement occurs at approximately the same time and in that the clipping process is controlled by peak No.3, Figs.6.9, 6.10 and 6.13. However, once clipping was applied at a level of 0.20g in the case 5, it was noticed that further clipping (to 0.15g) started to reduce the peak No.13, and this affected significantly the response at later times. From the performed analyses it appeared that a value of 0.16g is a good estimate of the EPA (see Figs. H.5A to H.5D). Furthermore, it should be noted that for a large range of clipping (0.25g to 0.16g) the value for the maximum v_1 remains the same, 1.7 in. (43.2 mm). It should be noted that the EPA of 0.16g is obtained on the assumption that the parameter controlling damage is the peak displacement v_1. If what is important is the maximum total cyclic displacement then the EPA is actually 0.35g.

Note that the ratio (EPA/PGA) for the actual recorded El Centro accelerogram is 0.16/0.35 = 0.46, while for the El Centro ground motion normalized to 0.55g this value is 0.32/0.55 = 0.58. This fact gives additional ideas on the complexity of estimating seismic risk by a parameter such as EPA. In other words, the amount of clipping depends not only on the type of earthquake but also on the way that the acceleration record is scaled or normalized. Furthermore, as pointed out before, it also depends on how the damage is measured, i.e. in terms of peak displacement, cyclic deformation, accumulated deformation, or energy dissipation.

Case 6: Up to about 2 seconds, the displacement response is almost the same as for the uncracked case 5 (Figs.6.13 and 6.14). Peaks No.2 and 3 (Fig.6.9c) are again the controlling ones: while peak No.2 makes the structure just reach yielding in Case 6, it makes it yield for a longer time in case 5. The result is to obtain very different negative displacements just after peak No.3: -2.4 in. (-60 mm) for case 6 and only -1.0 in. (-26 mm) for case 5. After this, the response is also very different for these two cases, the main reason being the difference of period of vibration of the structure (0.46 sec for Case 5, 0.72 sec for Case 6) vs. the predominant period of the earthquake (approximately 0.71 sec, Fig.6.12).

Maximum displacement values v_u (2.6 in. = 67 mm), occur at a time t = 12 seconds. This maximum displacement is mainly due to the inelastic deformations triggered by the pulses corresponding to peaks No.2 and 3, even though the maximum occurs after the pulse corresponding to peak No.16. It was not possible to do any clipping of the record as peak No.3 (the largest) is the most important one. Therefore, the ratio (EPA/PGA) = 0.35/0.35 = 1.00.

Even though the top nodal rotation, top moment, and shear values are not too large, they cannot be neglected as they have maxima close to 0.035 rads., 606 k-in. = 68.5 kN-m, and 11 kips = 49 kN, respectively. Again, the importance of the rotational degree of freedom is emphasized.

Another interesting comparison is relative to Cases 2 and 6, Figs.6.11b and 6.14. This refers to the effect of clipping on finding the EPA for the El Centro ground motion normalized to 0.55g and for the same record without any normalization (i.e. as recorded, with a PGA of 0.35g).

First of all, note that while the El Centro normalized to a PGA of 0.55g could be clipped to an EPA of 0.28g, no clipping of the actual (recorded) El Centro ground motion is possible without decreasing the canopy's response. Therefore, while the EPA for the actual recorded accelerogram is 0.35g, which is somewhat larger than the EPA of 0.28g corresponding to case 2, it induces a much lower displacement (2.6 in. = 67 mm vs. 3.9 in. = 100 mm). The displacement pattern is also different. Three substantial reversals are obtained for Case 2 (at approximately seconds No. 2, 5, and 12) while only one large reversal is observed in Case 6. This may be one reason for not being able to clip Case 6 since the only peak that significantly affected the canopy's response was that at a time t = 2 seconds. Note also that the maximum displacement for Case 6 occurred in the negative direction, while for Case 2 it was positive. It is also important to note that the values of the top and bottom moments were higher for Case 2 (Appendix H, cases 2 and 6). These results point out the serious distortions in damage potential that can be introduced by the very common practice of normalizing recorded accelerograms to a quite different PGA.

The main results of Tables 6.8 and 6.9 are summarized in Table 6.11. From the values presented in this table, it is clear that the response obtained for both the El Centro ground motion normalized to 0.55g, and then clipped to its corresponding EPA (i.e. to the value that gave maximum displacement response), and the response to the Derived Pacoima Dam ground motion normalized to 0.35g, is similar. This happened for both EI's considered. Specifically, for EI = 6.28×10^6 k-in^2 = 18000 kN-m^2 (uncracked), both the El Centro ground motion normalized to 0.55g and then clipped to 0.32g and the Derived Pacoima Dam ground motion normalized to 0.35g and unclipped gave maximum displacement values of approximately 2.8 in. (70 mm). Therefore, the EPA is approximately 0.32g for the El Centro normalized to 0.55g and 0.35g for the Derived Pacoima Dam to 0.35g, i.e. very close. The same comments apply for EI = 2.62×10^6 k-in^2 = 7520 kN-m^2 (cracked). The EPA is approximately 0.28g for the El Centro normalized to 0.55g and 0.35g for the Derived Pacoima Dam normalized to 0.35g. Of course, the maximum displacements obtained , 3.9 in. (100 mm), were larger than those of the uncracked member.

Two important observations can be made at this time:

1) Independently of the EI's and the type of earthquakes used, similar EPA's were obtained. They range from 0.28g to 0.35g.

2) The displacement response patterns (not only the peaks) of the 2DOF canopy model were very different for the two values of EI considered.

It is believed that as far as the study of the maximum displacements is concerned, an EI value of 2.62×10^6 k-in^2 = 7520 kN-m^2 (cracked) is closer to the actual one. This being the case, the obtained maximum lateral displacement response (: 3.9 in. = 100 mm) matches very well the maximum given by the lateral resistance function estimated in Fig.6.2, which has an EI close to the stiffness of the cracked section also. Fig.6.11 summarizes the results for Cases 2 and 4 (corresponding to the El Centro ground motion normalized to 0.55g and the Derived Pacoima Dam normalized to 0.35g for clipped and unclipped cases).

6.3.4 Elastic vs. Inelastic Analyses. The main purpose of performing dynamic elastic analyses of the canopy was to investigate the effect of clipping on the limit state under consideration.

The studies concentrated on the 2DOF model of the canopy, using the material properties case M2, EI cracked, and a damping ratio of 2%. Only the El Centro earthquake record was used in these studies.

Elastic analyses were performed using the computer program SAP IV (Ref.16).

6.3.4.1 Canopy's Response to El Centro Ground Motion Normalized to 0.55g (Unclipped). The first case considered was that of the canopy subjected to the El Centro ground motion with a PGA of 0.55g, unclipped (Fig.6.15). This has to be compared with the results obtained from the inelastic analyses (Case 2A, Fig.6.11 and Table 6.8).

The first difference lies in the maximum displacement response. The elastic case gives a larger maximum displacement, both in the positive direction: 4.3 in. (110 mm) vs. 2.8 in. (70 mm) and in the negative direction: 3.5 in. (90 mm) vs. 1.6 in. (40 mm).

The displacement pattern obtained from the elastic analysis is quite different from that obtained in the inelastic behavior. In the elastic case many displacement reversals (of the order of 4.5 in. = 114 mm on the average) are observed throughout the response of the canopy with one extremely large full reversal of 7.8 in. (200 mm) at a time shortly after 2 seconds. (Recall that in the inelastic case only three significant reversals occurred with values of approximately 3.9 in. = 100 mm). The elastic response is of the harmonic type and El Centro's predominant period (approximately 0.71 sec) is very close to the period of the canopy's first mode (0.72 sec.), indicating proximity to the resonance phenomenon.

6.3.4.2 Canopy's Response to El Centro Ground Motion Normalized to 0.55g (Clipped Cases). Fig.6.16 illustrates the effect of clipping the El Centro ground motion normalized to 0.55g on the elastic response of the canopy. As it is seen from this figure, no clipping was possible without decreasing the maximum response (i.e. the EPA for the elastic case is the same as the PGA; in this case: 0.55g).

It has been pointed out previously that clipping from 0.55g to 0.28g was possible in the inelastic case and this last value increased the maximum displacement response from 2.8 in. (70 mm) to 4.1 in. (104 mm), Fig.6.11. Note that the latter value is close to the maximum value obtained for the unclipped elastic case, i.e. 4.3 in. (109 mm).

Table 6.12 summarizes these results and indicates that if a displacement value in the range (3.9 in. - 4.7 in.) (100 mm - 120 mm) is to be obtained, the EPA in the elastic case is 0.55g and in the inelastic case it is 0.28g. These quite different results stress the fact that use of elastic linear analysis cannot give a good representation of the actual inelastic behavior.

6.3.4.3 Canopy's Response to Actual (or Recorded) El Centro Ground Motion. The elastic response to the actual (unnormalized) El Centro ground motion, with a PGA of 0.35g, can be obtained from Fig.6.15 with the appropriate proportionality factor (0.35/0.55) = 0.64.

Comparing the inelastic case (Case 6, Fig.6.14) with the elastic case, the following observations are made:

1) The displacement pattern is quite different. In the case

of inelastic behavior the displacements are completely shifted to the negative side.

2) The maximum displacements in the two cases are: in the elastic case: 4.3 X 0.64 = 2.7 in. (69 mm), positive value; and in the inelastic case: 2.6 in. (66 mm), negative value.

3) It was not possible to clip the recorded PGA without decreasing the elastic displacement response. Therefore, the EPA is equal to 0.35g in both cases (elastic and inelastic case 6) yielding approximately the same maximum displacement v_u (in absolute value).

6.4 An Alternative Approach to Estimate EPA.

Rather than first finding the PGA that will produce the observed damage (deformation) , normalizing the recorded or selected ground motion to the found PGA, and then clipping the normalized record, as discussed and used above, the following alternative approach is suggested:

1) Clip the selected recorded ground motion (accelerogram) in order to find the EPA for such accelerogram corresponding to the model (structure) under consideration.

2) Normalize the clipped ground motion to an intensity that is capable of producing the observed damage (deformation). The maximum value of this normalized and clipped ground motion is the final EPA for the accelerogram and structure under consideration.

It is important to mention that this procedure may not give the same results as those given by the procedure used in this report. Since the clipping process depends on the level of accelerations of the earthquake, it may very well be that once clipping is done for the unscaled earthquake ground motion, it is distorted in such a way that its normalization to obtain a specified deformation may be different than the EPA as obtained previously. Furthermore, even after clipping and normalization is done, it may also be possible that by clipping this normalized ground motion the response might increase or remain the same. Thus a new process of clipping should be tried.

VII. SUGGESTED INELASTIC DESIGN RESPONSE SPECTRA

7.1 Introduction

The second main objective of the research reported herein has been to attempt to formulate a design earthquake, in terms of design response spectra, that can be used for adequately retrofitting existing building structures and/or design of new buildings. This is a complex problem and only an approximate solution is offered herein.

In proposing the design spectra, it was initially intended to use the method proposed by Newmark and Hall (Ref.17). However, due to the following uncertainties and deficiencies of this method, it was decided to use another one.

1) Damping and Displacement Ductility. The Newmark-Hall Method becomes in general less conservative as the values of the specified ductility and viscous damping are increased (Ref.18). Veletsos, et al. (Ref.19) indicate that the method does not work well for damping ratios in excess of 5%. The effect of displacement ductility and damping ratio on the design response spectrum is accounted for in a better way by the statistical approach suggested by Riddell and Newmark (Ref.20).

2) Elastic/Perfectly Plastic Idealization. Studies indicate that "stiffness deterioration and moderate amounts of deformation

hardening generally appear to have small effects on ductility demands of SDOF systems. Moderate amounts of deformation softening, however, were found to substantially increase ductility demands in several cases" (Ref.18).

3) Ground Motion Characteristics. The effective peak acceleration, EPA, was estimated to be in the range of 0.28g to 0.35g. The influence of the ratio V/A (maximum velocity/maximum acceleration) on the determination of the response spectrum is very important (Ref.18). For near-fault ground motion records, as is the case of El-Asnam during the 1980 Algeria earthquake, severe long-duration acceleration pulses and high values of maximum velocity frequently occur. For example, for the Derived Pacoima Dam record the maximum velocity is 42.1 in/sec. This yields a value for V/A of 42.1/.40 (105 (in/sec)/g), which is more than twice the value for the El Centro earthquake, with V/A = 48 (in/sec)/g.

7.2 Elastic Design Response Spectra (EDRS)

Rather than directly obtaining the peak velocity and displacement from an earthquake and then using the Newmark & Hall coefficients to obtain the elastic design response spectrum (EDRS), it was decided to directly obtain the EDRS from the earthquake ground motion. The EDRS for the El Centro ground motion normalized to 0.55g and clipped to 0.28g was computed for two different damping ratios (2% and 5%). This is shown in Fig.7.1. The linearization of these spectra is performed by drawing the lines "by eye" and is not based on any regression analysis or other formal procedure. The latter are not justified by the degree of uncertainty in the data. The linearized EDRS for this earthquake is defined by a maximum displacement, velocity, and acceleration of 20 in. (510 mm), 60 in./sec (1520 mm/sec), and 1.60g, respectively, for 2% damping and 16 in. (410 mm), 45 in./sec (1140 mm/sec), and 1.2g, respectively, for 5% damping.

These values are reasonable for the El Centro type of motion (normalized to 0.55g and clipped to 0.28g). The Derived Pacoima Dam ground motion normalized to 0.35g gives approximately the same values for acceleration and displacement but larger values of velocity: 88in./sec (2240 mm/sec) and 70 in./sec (1780 mm/sec), for damping ratios equal to 2% and 5%, respectively. (This values were obtained from normalizing the maximum values given in Ref.21 by the factor 0.35g/0.40g). With these values, the EDRS becomes:

A) For ξ = 2% :

- constant displacement : 20 in. (510 mm)
- constant velocity : 88 in./sec (2240 mm/sec)
- constant acceleration : 1.60g

B) For ξ = 5% :

- constant displacement : 16 in. (410 mm)
- constant velocity : 70 in./sec (1780 mm/sec)
- constant acceleration : 1.20g

Fig.7.2 shows a comparison of the EDRS obtained using the previous values and the EDRS obtained using the Newmark and Hall Method (Ref.17). In the latter, a peak ground acceleration of 0.28g has been used and the maximum values for ground velocity and displacement are obtained to be 13.4 in./sec and 10 in., based on the assumption that the peak acceleration, velocity and displacement are in the ratio 1.0g, 48 in./sec, and 36 in. With these values, the EDRS is defined by maximum displacement, velocity, and acceleration of 18 in., 38 in./sec, and 1.20g for 2% damping and 14 in., 25 in./sec, and 0.73g for 5% damping.

From Fig.7.2 the following conclusions can be drawn on the EDRS:

1) The use of the Newmark & Hall procedure leads to results which are different (and on the unconservative side) to the ones given by the method proposed in this study.

2) In the low period zone (up to about 0.1 seconds), the difference in these spectra is large but not important for practical purposes.

3) The difference in the values for maximum acceleration for both EDRS methods is substantial, giving lower values for the Newmark & Hall method. For periods between 0.1 and 0.5 seconds, the difference is on the order of 50%; for higher periods, the difference may be as high as 400%.

4) In particular, the high values of the maximum velocity in the EDRS (as given often for near-fault type of earthquakes) is not accounted for in the Newmark & Hall method.

5) The values of maximum displacement given by the two methods is similar.

6) Due to the previous reasons, the EDRS proposed herein

corresponds to the one obtained in this study (and not to the Newmark and Hall approach) and will be referred to simply as EDRS in the parragraphs that follow.

7.3 Inelastic Design Response Spectra (IDRS)

The IDRS is derived based on the approach by Riddell and Newmark (Ref.20). It is obtained by applying "deamplification factors ϕ_u" to the EDRS. For the two values of damping ratios chosen (2% and 5%), and assuming an elastoplastic model with μ_δ = 5, the following factors ϕ_u are obtained from Figs.7.3, 7.4, and 7.5.

A) For ξ = 2% :

ϕ_u = 0.165, 0.18, and 0.29 corresponding to the displacement, velocity, and acceleration regions, respectively. Also, for the low period range, the acceleration deamplification is given by $\mu_\delta^{-0.13}$ = 0.81. Therefore:

- constant displacement : 0.165 x 20 = 3.3 in. (84 mm)
- constant velocity : 0.18 x 88 = 16 in./sec (280 mm)
- constant acceleration (amplified region) : 0.29 x 1.60g = 0.46g
- constant acceleration (controlled region): 0.81 x 0.28g = 0.23g

B) For ξ = 5% :

ϕ_u = 0.17, 0.23, and 0.34 corresponding to the displacement, velocity, and acceleration regions, respectively.

Therefore:

- constant displacement : 0.17 x 16 = 2.7 in. (69 mm)
- constant velocity : 0.23 x 70 = 16 in./sec (250 mm)

- constant acceleration (amplified region) : 0.34 x 1.20g = 0.41g
- constant acceleration (controlled region): 0.81 x 0.28g = 0.23g

Both the elastic and inelastic response spectra are presented in Figs.7.6 for damping values of 2% and 5%. The EDRS corresponds to the one obtained in the present study (Figs.7.2). The IDRS corresponds to the Newmark & Riddell approach applied to the EDRS previously obtained.

If the IDRS is obtained following the procedure adopted in the present study, it can be observed that this IDRS is different (on the conservative side) to the IDRS obtained with the Newmark & Hall approach. This is because the latter IDRS is based on the EDRS of Newmark & Hall. Therefore, the same comments done in Section 7.2 can be made when comparing the two IDRS methods.

7.4 Remarks

It is important to mention that the EDRS proposed are based on two earthquake ground motions, namely: El Centro 1940 normalized to 0.55g and clipped to 0.28g and Derived Pacoima Dam normalized to 0.35g. Obviously, more information on the seismicity of Algeria (i.e. larger number of earthquakes as well as the main characteristics of earthquake ground shaking that actually may occur in El-Asnam) is needed to adequately propose a design spectrum. At present, however, since not enough earthquake ground motions are available, these spectra may serve as design guidelines.

The values of maximum acceleration, velocity, and displacement in the EDRS and IDRS are high but before more information is available it seems necessary to respect these conservative estimates based on the response of the canopies to the two earthquake ground motions mentioned above.

VIII. SUMMARY, CONCLUSIONS, AND RECOMMENDATIONS

8.1 Summary

The analytical studies which were conducted in order to determine the EPA and to propose the inelastic design response spectra were described in the previous chapters.

First, an overall description of the R/C structural system, as well as of its performance during the Algeria earthquake, was given. The analytical model used in the analysis, as well as the estimation of the main mechanical and dynamic characteristics were described. The influence of different parameters on the M-Ø relationships and on the dynamic characteristics is then investigated. It was concluded that buckling of the longitudinal compressive steel bars plays an important role in estimating the maximum response of the canopy. This is due to the large spacing of stirrup ties, which did not satisfy the 1982 UBC requirements.

Two different types of earthquake ground motions were considered: El Centro 1940 SOOE and Derived Pacoima Dam 1971 S16E, considered to be able to give upper and lower bounds on the inelastic deformation demands. After idealizing the lateral resistance function, the estimation of EPA was discussed. The studies were subdivided in three steps: (1) using the Bertero, et al. charts to estimate the PGA, (2) verifying the value of PGA found in (1) with the aid of the computer program DRAIN-2D, and

(3) using the "Clipping Method", which consists of clipping a given earthquake normalized to the PGA found in (2), in order to study how clipping affects the response.

The values of EPA obtained for the two earthquakes were given and the most important parameters affecting the EPA were discussed. Although the determined values of EPA fall within a small range (0.28g to 0.35g) for the two ground motions considered, many uncertainties exist in the determination and use of EPA.

Finally an inelastic design response spectrum was proposed based on the results of the previous chapters.

The following conclusions and recommendations are drawn:

8.2 Conclusions

1. Adequacy of the Canopy Structural System. The structural system of the canopy was conceptually inadequate for resisting earthquake excitations. Not only was the mass of the system large and concentrated at the top, but the structural system had no degree of indeterminacy in the transverse direction. The detailing of reinforcement was also poor, the tie spacing being the main weakness. The ties did not provide sufficient confinement to the concrete and therefore did not ensure that the column of the canopy had enough energy dissipation capacity. Even more important than the lack of good concrete confinement was the fact that the ties were separated so much that buckling of the longitudinal compressive steel bars occurred before strain

hardening of steel was initiated. Therefore, the moment capacity of the column of the canopy could not develop any increase in resistance due to this strain hardening of the reinforcement. Neither did it give sufficient range of plastic deformation under the constant yielding moment nor a stable hysteretic behavior.

2. Stiffness EI of the Canopy. The value of the stiffness EI is an important parameter. Both the displacement response maxima and the displacement pattern are different for the values of EI considered. The actual EI seems to be closer to the value of the cracked section since after the first seconds of the earthquake, the section cracks on both sides.

3. Modelling of the Canopy. A 2DOF model, rather than a SDOF system must be considered in the analysis in order to obtain adequate approximations of the canopy's actual behavior. A SDOF model gave very conservative values of maximum lateral displacement (up to 51% higher than a 2DOF model) in all but one of the cases considered. This case corresponds to the uncracked canopy subjected to the normalized to 0.35g Derived Pacoima Dam, in which the maximum displacements obtained for the SDOF and the 2DOF models were very close (2.5 in. and 2.6 in., respectively). On the other hand, the SDOF model gave very unconservative values of the maximum response for shear and no estimate of the moment at the top of the column. This study confirms once more the importance of a design against shear based on a capacity method considering realistic models of the actual structure.

4. Estimation of EPA. (1) Among the main parameters that affect EPA are: a) the idealization of the lateral resistance

function, which in turn depends on assumed material properties, concrete cover, axial load, buckling of longitudinal compressive steel bars and fixed-end rotation, among other factors; b) idealization of structural system: SDOF vs. 2DOF model; c) period and damping; d) ground motion characteristics, e) limit state being considered, which involves deciding what constitutes failure or unacceptable damge and what response parameter is used to measure such failure or damage; and f) the approach used in estimating the EPA.

(2) Because the assumed recorded ground motions (horizontal components of El Centro 1940 S00E and Derived Pacoima Dam 1971 S16E) did not produce the observed response, it was decided to use the following approach to estimate EPA: these ground motions had to be normalized to values of PGA as required to induce the assumed maximum displacement. Values of PGA of 0.55g and 0.35g, respectively were determined in the first two stages of the these studies. The values of EPA determined in the present investigation (i.e., 0.28g and 0.35g for the El Centro and Derived Pacoima Dam earthquake motions) were therefore derived from clipping distorted records, due to the normalization of the recorded PGA, from 0.35g and 0.40g to 0.55g and 0.35g, respectively. In other words, the original El Centro record with PGA equal to 0.35g produces low values of canopy displacement and therefore would not have resulted in the observed damage, i.e. collapse of the canopy. Also, the stiffness EI used in the analyses (and thus the period), had a significant effect on the (EPA/PGA) ratio. Thus the amount of clipping depends on the normalization of an earthquake, as well as on the mechanical

(dynamic) characteristics of the model.

(3) The results indicate that for the two types of ground motion used in this study, the EPA necessary to induce the observed damage is in the range of 0.28g to 0.35g, provided that the El Centro and the Derived Pacoima Dam records are first normalized to 0.55g and 0.35g, respectively. This small range is apparently fortuitous given the wide range of parameters that affect the result. Generally, the EPA depends on: a) the type of earthquake ground motion under consideration; b) the interaction of the dynamic characteristics of the ground motion and the entire soil-foundation-structure system; c) the method used for estimating the EPA even in the case that the clipping procedure is used; and d) the acceptable ductility as concluded below.

(4) The EPA will depend on the type of structural behavior, i.e. elastic or inelastic, and in particular on the acceptable ductility level. Although the use of EPA can provide an idea of the relative damaging potential of a given ground motion, its use as the sole parameter to define this damaging potential can be very misleading, particularly if the original recorded ground motions are normalized to higher PGA's.

5. Miscellaneous Conclusions. (1) The use of the charts suggested by Bertero et al. (Figs.6.4 and 6.5), developed for SDOF, can lead to misleading results when used for multidegree of freedom systems. (2) Clipping peak accelerations of an accelerogram does not necessarily reduce the peak response.

6. Inelastic Design Response Spectrum. An inelastic design response spectrum is proposed for the zone where the canopy was

located (near the fault). Due to the data available, as well as the many assumptions introduced in the studies presented herein, the proposed design spectrum should be viewed merely as a guideline to the solution of the design problem in Algeria.

8.3 Recommendations

1. Experimental studies on the dynamic response of the canopy based on known material properties, detailing, and earthquake ground motion should be conducted to obtain more accurate data on the mechanical (static and dynamic) characteristics of the canopy, as well as a better understanding of the important parameters affecting the damaging potential of an earthquake. While the influence of bond slippage (at the foundation and in regions adjacent to the main cracks of the column) on the canopy's top nodal displacement is qualitatively recognized, it still remains to be quantitatively determined. Experimental studies on this subject are necessary as the top nodal displacement is an extremely important quantity. Reliable analytical modeling of the bond slippage also needs to be developed.

2. To establish the different parameters that can be used to measure the damage observed in the canopy and to establish which are most important to investigate in the experimental studies.

3. To investigate the sensitivity of the estimate of the EPA on the different parameters used to measure damage. (It is believed that the rotation along the critical region at the base

of the column of the canopy is a better parameter than the roof displacement).

4. To investigate alternative methods of applying the clipping procedure, such as first finding the EPA of the selected ground motion by directly clipping the selected accelerogram, and then (after the EPA has been found) normalizing the clipped accelerogram to an intensity sufficient to produce the desired damage.

5. To study the effect that other types of earthquake ground motion have on the value of EPA as well as on the damage to the canopy.

6. To develop more reliable methods for formulating design earthquakes.

REFERENCES

1) Bertero,V.V., et al., "El-Asnam, Algeria Earthquake October 10,1980, A Reconnaissance and Engineering Report", National Research Council, Committee on National Disasters, Commission of Engineering and Technical Systems/ Earthquake Engineering Research Institute, Berkeley, California, January, 1983.

2) Blume,J.A., "On Instrumental Versus Effective Acceleration and Design Coefficients", Proceedings of the 2nd U.S. National Conference on Earthquake Engineering, Stanford University, Stanford, California, August 22-24, 1979, pp.868-882.

3) Newmark,N.M., Blume,J.A., and Kapur,K.K., "Seismic Design Spectra for Nuclear Power Plants", Journal of the Power Division, ASCE, Vol.99, No.PO2, Proceedings Paper 10142, November, 1973.

4) Bertero,V.V., Mahin,S.A., and Herrera,R.A., "Aseismic Design Implications of Near-Fault San Fernando Earthquake Records", Earthquake Engineering and Structural Dynamics, Vol.6,31-42 , Department of Civil Engineering, University of California, Berkeley, 1973, (Revised November 1976).

5) Kannan,A.E. and Powell,G.H., "DRAIN-2D - A General Purpose Computer Program for Dynamic Analysis of Inelastic Plane Structures with User's Guide", Earthquake Engineering Research Center, Reports No.EERC 73-6 and EERC 73-22, University of California, Berkeley, April, 1973 (Revised September, 1973 and August, 1975).

6) Park,R., Priestley,N.M.J., and Gill,W.D. , "Ductility of Square-Confined Concrete Columns", Journal of the Structural Division of ASCE, Vol.108, No.ST4, April, 1982.

7) Park,R. and Paulay,T., "Reinforced Concrete Structures", Department of Civil Engineering, University of Canterbury, Christchurch, New Zealand, 1975.

8) Blume,J.A., Newmark,N.M., and Corning,L.H., "Design of Multistorey Reinforced Concrete Buildings for Earthquake Motions", Portland Cement Association, Illinois, Skokie, 1961.

9) Mahin,S.A. and Bertero,V.V., "RCCOLA - A Computer Program for Reinforced Concrete Column Analysis - User's Manual and Documentation", Department of Civil Engineering, University of California, Berkeley, August, 1977.

10) Papastamatiou,D., " El-Asnam, Algeria Earthquake of October 10, 1980: Field Evidence of Ground Motion in the Epicentral Region", Geognosis, Ltd., London, December, 1980.

11) Uniform Building Code, International Conference of Building Officials, Whittier, CA, 1979.

12) Faradji Capon,M.J. and Diaz de Cossio, "Tension Diagonal en Miembros de Concreto de Seccion Circular", Ingenieria, April, 1965.

13) Clough,R.W. and Penzien,J., "Dynamics of Structures", McGraw-Hill, Inc., 1975.

14) Bertero,V.V., "Implications of Recent Research Results on Present Methods for Seismic Resistant Design of R/C Frame-Wall Building Structures", Proceedings, 51st Annual Convention, SEAOC, California, Sacramento, 1982.

15) "Analyses of Strong Motion Earthquake Accelerograms", Vol.IV - Fourier Amplitude Spectra, Part A - Accelerograms IIA001 through IIA020, Earthquake Engineering Research Laboratory, Report No.EERL 72-100, California Institue of Technology, Pasadena, California, August, 1972.

16) Bathe,K.J., Wilson,E.L., and Peterson,F.E., "SAP IV - A Structural Analysis Program for Static and Dynamic Response of Linear Systems", Earthquake Engineering Research Center, Report No.EERC 73-11, University of California, Berkeley, June, 1973 (Revised April, 1974).

17) Newmark,N.M. and Hall,W.J., "Procedure and Criteria for Earthquake Resistant Design", Building Practice for Disaster Mitigation, Building Science Series 45, National Bureau of Standards, Washington, D.C., February, 1973, pp.209-236.

18) Mahin,S.A. and Bertero,V.V., "An Evaluation of Inelastic Seismic Design Spectra", Journal of the Structural Division, ASCE, Vol.107, No.ST9, Proceedings Paper 16501, September, 1981, pp.1777-1795.

19) Veletsos,A.S., Newmark,N.M., and Chelapati,C.V., "Deformation Spectra for Elastic and Elastoplastic Systems to Ground Shock and Earthquake Motions", Proceedings, Third World Conference on Earthquake Engineering, 1965, pp.663-682.

20) Riddell,R. and Newmark,N.M., "Statistical Analysis of the Response of Nonlinear Systems Subjected to Earthquakes", Civil Engineering Studies, Structural Research Series, University of Illinois, Urbana, August, 1979.

21) Mahin,S.A., Bertero,V.V., Chopra,A.K., and Collins,R.G., "Response of the Olive View Hospital Main Building During the San Fernando Earthquake", Earthquake Engineering Research Center, Report No.EERC 76-22, University of California, Berkeley, October, 1976.

Earthquake Ground Motion	Displacement Ductility, μ_δ	4		5		6	
	Damping Ratio ξ	2%	5%	2%	5%	2%	5%
Normalized El Centro Record	$\eta = \frac{C_y}{\lvert PGA \rvert / g}$	0.65	0.59	0.56	0.50	0.50	0.42
	PGA Case M1	0.52g	0.57g	0.60g	0.67g	0.67g	0.80g
	PGA Case M2	0.45g	0.50g	0.53g	0.59g	0.59g	0.70g
Normalized Derived Pacoima Dam Record	$\eta = \frac{C_y}{\lvert PGA \rvert / g}$	0.92	0.87	0.83	0.76	0.75	0.69
	PGA Case M1	0.37g	0.39g	0.41g	0.44g	0.45g	0.49g
	PGA Case M2	0.32g	0.34g	0.35g	0.39g	0.39g	0.43g

Table 6.1 Determination of PGA Required for the El Centro and Derived Pacoima Dam Records to Attain Assumed Responses of the Canopy

TABLE 6.2 TIME HISTORY ANALYSES: SUMMARY OF MAIN RESPONSES OF 2DOF MODEL OF CANOPY

$M_y = 974^{\,k\text{-}in} = 110^{\,kN\text{-}m}$
$f'_c = 3.0\,ksi = 21\,MPa$ } Material Properties
$f_y = 50\,ksi = 350\,MPa$ } Case M1
$EI = 5.4 \times 10^6\,k\text{-}in^2 = 15,500\,kN\text{-}m^2$

1 in. = 25.4 mm
1 k = 4.45 kN
1 k-in = 0.113 kN-m

DESCRIPTION OF EARTHQUAKE AND MODEL USED	VALUES OF RESPONSE PARAMETERS				
	TIME OF MAXIMUM RESPONSE (SEC)	TOP NODAL DISPLACEMENT (IN)	MOMENT AT BASE (K-IN)	MOMENT AT TOP (K-IN)	SHEAR AT BASE (K)
DERIVED PACOIMA DAM (0.30g) 2 DOF MODEL	2.65 3.45 6.60 8.40	-0.6 1.6 1.6 -0.8	-870 974 974 -814	52 -147 -91 216	-7.8 7.9 8.4 -5.7
DERIVED PACOIMA DAM (0.40g) 2 DOF MODEL	2.66 3.53 7.71	-0.9 2.7 2.8	-974 974 974	22 -95 -502	-9.1 8.4 4.5
DERIVED PACOIMA DAM (0.50g) 2 DOF MODEL	2.94 3.63 7.70	-2.0 4.8 4.4	-974 974 974	-52 -65 -506	-9.8 8.7 4.4
EL CENTRO 1940 S00E (0.55g) 2DOF MODEL	1.61 1.96 2.25 12.21	-1.1 2.0 -1.8 2.7	-974 974 -974 974	-43 -329 519 87	-9.7 6.1 -4.3 10.1
EL CENTRO 1940 S00E (0.70g) 2DOF MODEL	1.63 1.98 2.29 5.33 8.70 9.22 12.25	-1.7 2.3 -2.1 3.2 3.3 3.3 3.5	-974 974 -974 974 974 974 974	130 -173 433 216 -43 -312 -130	-8.0 7.6 -5.1 11.3 8.9 6.3 8.0

Table 6.3 Time History Analyses: Summary of Main Responses of 2DOF & SDOF

Models of Canopy Subjected to Derived Pacoima Dam Normalized to 0.35g

$M_y = 800^{k\text{-}in} = 90.4^{kN\cdot m}$
$f'_c = 2.5$ ksi $= 17$ MPa
$f_y = 40$ ksi $= 280$ MPa
Material Properties Case M2

1 in. = 25.4 mm
1 k = 4.45 kN
1 k-in. = 0.113 kN-m

Description of Earthquake and Model Used	Values of Response Parameters					
	Time of Maximum Response (sec)	Top Nodal Displacement (in)	Moment at Base (k-in)	Moment at Top (k-in)	Shear at Base (k)	Plastic Rotation at Base (rad)
Derived Pacoima	3.01	-3.4	-800	52	-7.1	-0.0222
Dam (0.35g)	3.65	3.9	800	13	7.7	0.0268
	7.97	0.2	-800	442	-3.4	0.0094
2DOF Model	6.23	2.5	520	-294	2.1	0.0146
$EI = 2.62 \times 10^6$ k-in^2	4.43	2.2	554	325	8.4	0.0121
(Cracked)	7.82	-2.7	-800	-159	-9.1	-0.0166
	2.92	-2.4	-800	-52	-8.1	-0.0159
Derived Pacoima	3.60	2.8	771	-251	5.0	0.0183
Dam (0.35g)	8.62	1.3	800	-359	4.2	0.0051
2 DOF Model	8.45	-0.2	-589	329	-2.5	0.0045
$EI = 3.78 \times 10^6$ k-in^2	2.72	-1.8	-800	-171	-9.2	-0.0111
	3.33	0.6	800	171	9.2	0.0005
	2.62	-0.6	-800	13	-7.5	-0.0013
Derived Pacoima	3.56	2.6	800	-52	7.1	0.0204
Dam (0.35g)	5.04	2.6	771	-173	5.7	0.0203
2DOF Model	5.50	2.6	740	-225	4.9	0.0203
	8.01	0.6	-346	459	1.1	0.0080
$EI = 6.28 \times 10^6$ k-in^2	8.19	1.0	-173	-372	-5.2	0.0079
(Uncracked)	3.28	1.0	800	229	9.8	0.0070
	5.78	1.0	-800	-205	-9.6	0.0137
Derived Pacoima Dam (0.35g) SDOF Model	2.98	-3.6	-800	0	-7.6	-0.0239
$EI = 2.62 \times 10^6$ k-in^2 (Cracked)	3.63	4.1	800	0	7.6	+0.0288
Derived Pacoima Dam (0.35g)	2.77	-1.4	-800	0	-7.6	-0.0058
SDOF Model	3.56	2.8	800	0	7.6	0.0196
$EI = 3.78 \times 10^6$ k-in^2	7.74	3.5	800	0	7.6	0.0253
Derived Pacoima Dam (0.35g)	3.50	2.0	800	0	7.6	0.0149
SDOF Model	5.05	2.5	800	0	7.6	0.0193
$EI = 6.28 \times 10^6$ k-in^2	5.44	2.5	800	0	7.6	0.0195
(Uncracked)	8.38	-0.8	-800	0	-7.6	-0.0032

TABLE 6.4 TIME HISTORY ANALYSES: SUMMARY OF MAIN RESPONSES OF 2DOF & SDOF MODELS OF CANOPY SUBJECTED TO EL CENTRO 1940 NORMALIZED TO 0.50g

$M_y = 800^{k\text{-}in} = 90.4^{kN\text{-}m}$
$f'_c = 2.5\ ksi = 17\ MPa$ } Material Properties
$f_y = 40\ ksi = 280\ MPa$ } Case M2

1 in. = 25.4 mm
1 k = 4.45 kN
1 k-in. = 0.113 kN-m

DESCRIPTION OF EARTHQUAKE AND MODEL USED	VALUES OF RESPONSE PARAMETERS					
	TIME OF MAXIMUM RESPONSE (SEC)	TOP NODAL DISPLACEMENT (IN)	MOMENT AT BASE (K-IN)	MOMENT AT TOP (K-IN)	SHEAR AT BASE (K)	PLASTIC ROTATION AT BASE (RAD)
EL CENTRO 1940	2.00	2.4	800	208	9.6	0.0107
S00E (0.50g)	2.33	-1.7	-800	-433	-11.7	-0.0078
	2.24	-1.7	-800	710	-0.9	0.0041
2 DOF MODEL	5.36	2.6	800	268	10.2	0.0153
	12.00	-1.6	-800	87	-6.8	-0.0040
$EI = 2.62 \times 10^6\ k\text{-}in^2$	4.92	-1.3	-693	745	0.5	0.0267
(CRACKED)	5.42	2.5	416	528	9.0	-0.0328
	5.32	2.4	800	356	11.0	0.0153
	2.35	-1.7	-800	-443	-11.8	-0.0078
EL CENTRO 1940 S00E (0.50g)	1.66	-1.1	-800	217	-5.5	-0.0032
2 DOF MODEL	1.99	2.4	800	-303	4.7	0.0149
$EI = 3.78 \times 10^6\ k\text{-}in^2$	2.30	-1.1	-800	-67	-8.3	-0.0031
	12.25	2.7	800	-49	7.2	0.0132
EL CENTRO 1940 S00E (0.50g)	1.96	1.8	800	-139	6.3	0.0121
	2.27	-1.4	-800	381	-4.0	-0.0085
2 DOF MODEL	4.39	-1.5	-800	126	-6.4	-0.0089
	2.25	-1.3	-800	745	-0.5	-0.0063
$EI = 6.28 \times 10^6\ k\text{-}in^2$	2.55	-0.4	277	-606	-3.1	-0.0075
(UNCRACKED)	2.48	-0.5	693	614	12.4	-0.0075
	2.18	-0.8	-800	-391	-11.3	-0.0061
EL CENTRO 1940 S00E (0.50g)	1.98	2.4	800	0	7.6	0.0154
SDOF MODEL	2.28	-1.8	-800	0	-7.6	-0.0097
$EI = 3.78 \times 10^6\ k\text{-}in^2$	12.25	2.6	800	0	7.6	0.0178
EL CENTRO 1940 S00E (0.50g)	1.95	2.1	794	0	7.5	0.0157
SDOF MODEL	2.25	-1.5	-800	0	-7.6	-0.0096
$EI = 6.28 \times 10^6\ k\text{-}in^2$ (UNCRACKED)	12.15	2.2	800	0	7.6	0.0163

TABLE 6.5 TIME HISTORY ANALYSES : SUMMARY OF MAIN RESPONSES OF 2DOF & SDOF MODELS OF CANOPY SUBJECTED TO EL CENTRO NORMALIZED TO 0.55g

$M_y = 800^{k\text{-}in} = 90.4^{kN\text{-}m}$

$f'_c = 2.5\,ksi = 17\,MPa$ } Material Properties

$f_y = 40\,ksi = 280\,MPa$ } Case M2

1 in. = 25.4 mm

1 k = 4.45 kN

1 k-in. = 0.113 kN-m

DESCRIPTION OF EARTHQUAKE AND MODEL USED	VALUES OF RESPONSE PARAMETERS					
	TIME OF MAXIMUM RESPONSE (SEC)	TOP NODAL DISPLACEMENT (IN)	MOMENT AT BASE (K-IN)	MOMENT AT TOP (K-IN)	SHEAR AT BASE (K)	PLASTIC ROTATION AT BASE (RAD.)
EL CENTRO 1940 SOOE (0.55g)	2.01	2.8	800	-208	5.6	0.0142
	2.34	-1.3	-800	-472	-12.1	-0.0050
2DOF MODEL	4.98	-1.4	-800	173	-6.0	-0.0016
	5.37	2.7	800	173	9.3	0.0172
$EI = 2.62 \times 10^6\,k\text{-}in^2$	12.00	-1.7	-800	26	-7.4	-0.0049
(CRACKED)	5.42	2.6	381	597	9.3	0.0172
	4.92	-1.1	-800	800	0	0.0027
	5.32	2.4	-800	425	11.7	0.0129
EL CENTRO 1940 SOOE (0.55g)	1.98	2.0	800	104	8.6	0.0141
	12.20	2.2	800	-156	6.1	0.0160
	2.28	-1.3	-800	173	-6.0	-0.0081
2 DOF MODEL	4.40	-1.3	-800	87	-6.8	-0.0077
	2.25	-1.3	-800	766	-0.3	-0.0056
$EI = 6.28 \times 10^6\,k\text{-}in^2$	2.55	-0.4	312	-645	-3.2	-0.0074
(UNCRACKED)	2.32	-1.3	-800	-414	-11.6	-0.0084
	2.48	-0.6	800	541	12.8	-0.0074
EL CENTRO 1940 SOOE (0.55g)	1.66	-1.7	-800	0	-7.6	-0.0054
SDOF MODEL	2.00	3.1	800	0	7.6	0.0190
$EI = 2.62 \times 10^6\,k\text{-}in^2$ (CRACKED)	5.38	4.2	800	0	7.6	0.0289
EL CENTRO 1940 SOOE (0.55g)	1.96	2.5	800	0	7.6	0.0195
SDOF MODEL	2.27	-1.4	-800	0	-7.6	-0.0087
	3.26	-1.4	-800	0	-7.6	-0.0089
$EI = 6.28 \times 10^6\,k\text{-}in^2$ (UNCRACKED)	12.17	2.6	800	0	7.6	0.0201

TABLE 6.6 DISPLACEMENT RESPONSE OF CANOPY TO EL CENTRO NORMALIZED TO 0.55g FOR SDOF AND 2DOF MODELS

MODEL DESCRIPTION	EI ($\times 10^6$ K-IN^2)	v_μ (DRAIN-2D OUTPUT) (IN)
SDOF	2.62	4.2
	6.28	2.6
2DOF	2.62	2.8
	6.28	2.2

1 IN. = 25.4 mm
1 K-IN.^{2} = 0.00287 KN-m^2

TABLE 6.7 DISPLACEMENT RESPONSE OF CANOPY TO DERIVED PACOIMA DAM NORMALIZED TO 0.35g FOR SDOF AND 2DOF MODELS

MODEL DESCRIPTION	EI ($\times 10^6$ K-IN^2)	v_μ (DRAIN-2D OUTPUT) (IN)
SDOF	2.62	4.1
	3.78	3.5
	6.28	2.5
2DOF	2.62	3.9
	3.78	2.8
	6.28	2.6

1 IN. = 25.4 mm
1 K-IN.^{2} = 0.00287 KN-m^2

TABLE 6.8 SUMMARY OF DISPLACEMENT RESPONSE OF THE 2DOF CANOPY MODEL WHEN SUBJECTED TO EL CENTRO NORMALIZED TO 0.55g

a) CASES 1:

$EI = 6.28 \times 10^6$ k-in^2
$T_1 = 0.46$ sec ; $T_2 = 0.11$ sec
$M_y = 800$ k-in

1 in. = 25.4 mm
1 k-in. = 0.113 kN-m
1 k-in.^{2} = 0.00287 kN-m^2

Clipped Acceleration		Point a (*)		Point b (*)		Point c (*)		Point d (*)		Point e (*)	
Cases	Peak Value	Time (sec)	Displ. (in)	Time (sec)	Displ. (in)	Time (sec)	Displ. (in)	Time (sec)	Displ. (in)	Time (sec)	Displ. (in)
1A	0.55g	1.60	-1.1	1.95	1.9	2.28	-1.3	5.25	1.6	12.21	2.2
1B	0.36g	1.62	-1.1	1.95	1.9	2.25	-0.7	5.25	2.2	12.21	2.8
1C	0.32g	1.62	-1.1	1.95	1.9	2.25	-0.5	5.25	2.3	12.21	2.9
1D	0.28g	1.62	-1.1	1.95	1.8	2.25	-0.5	5.25	2.1	12.20	2.7
1E	0.22g	1.60	-1.0	1.95	1.3	2.25	-0.9	5.25	1.4	12.19	1.9

b) CASES 2:

$EI = 2.62 \times 10^6$ k-in^2
$T_1 = 0.72$ sec ; $T_2 = 0.18$ sec
$M_y = 800$ k-in

1 in. = 25.4 mm
1 k-in. = 0.113 kN-m
1 k-in.^{2} = 0.00287 kN-m^2

Clipped Acceleration		Point a (*)		Point b (*)		Point c (*)		Point d (*)		Point e (*)	
Cases	Peak Value	Time (sec)	Displ. (in)	Time (sec)	Displ. (in)	Time (sec)	Displ. (in)	Time (sec)	Displ. (in)	Time (sec)	Displ. (in)
2A	0.55g	1.65	-1.0	2.01	2.8	2.35	-1.3	5.38	2.7	12.01	-1.7
2B	0.32g	1.67	-1.0	2.00	2.7	2.30	-0.4	5.38	3.9	12.00	-0.6
2C	0.28g	1.67	-1.0	2.00	2.6	2.30	-0.4	5.38	4.1	12.00	-0.2
2D	0.22g	1.67	-1.0	2.00	2.2	2.30	-0.7	5.37	4.0	12.00	-0.1

(*) Note: Points a to e correspond to important relative maxima as given by Figs. H.1A - H.1E and H.2A - H.2D. See also Figs. 6.8 and 6.9.

Table 6.9 Summary of Displacement Response of the 2DOF Canopy Model when Subjected to Derived Pacoima Dam Normalized to 0.35g

a) Cases 3:

$EI = 6.28 \times 10^6$ k-in^2
$T_1 = 0.46$ sec ; $T_2 = 0.11$ sec
$M_y = 800$ k-in

1 in. = 25.4 mm
1 k-in. = 0.113 kN-m
1 k-in.^{2} = 0.00287 kN-m^2

Clipped Acceleration		Point a (*)		Point b (*)		Point c (*)		Point d (*)	
Cases	Peak Value	Time (sec)	Displ (in)	Time (sec)	Displ. (in)	Time (sec)	Displ. (in)	Time (sec)	Displ. (in)
3A	0.35g	2.62	-0.6	3.55	2.6	5.05	2.6	5.50	2.6
3B	0.30g	2.62	-0.6	3.55	2.3	5.04	2.3	5.50	2.2

b) Cases 4:

$EI = 2.62 \times 10^6$ k-in^2
$T_1 = 0.72$ sec ; $T_2 = 0.18$ sec
$M_y = 800$ k-in

1 in. = 25.4 mm
1 k-in. = 0.113 kN-m
1 k-in.^{2} = 0.00287 kN-m^2

Clipped Acceleration		Point a (*)		Point b (*)		Point c (*)		Point d (*)	
Cases	Peak Value	Time (sec)	Displ. (in)	Time (sec)	Displ. (in)	Time (sec)	Displ. (in)	Time (sec)	Displ. (in)
4A	0.35g	3.01	-3.4	3.65	3.9	5.20	2.7	6.15	2.6
4B	0.30g	3.01	-3.4	3.65	3.5	5.20	2.3	6.15	2.2

(*) Note: Points a to d correspond to important relative maxima as given by Figs. H.3A, H.3B, H.4A, and H.4B. See also Fig. 6.9.

TABLE 6.10 SUMMARY OF DISPLACEMENT RESPONSE OF THE 2DOF CANOPY MODEL WHEN SUBJECTED TO THE UNNORMALIZED EL CENTRO (PGA = 0.35g)

a) CASES 5

$EI = 6.28 \times 10^6$ k-in.^{2}
$T_1 = 0.46$ sec ; $T_2 = 0.11$ sec
$M_y = 800$ k-in

1 in. = 25.4 mm
1 k-in. = 0.113 kN-m
1 k-in.^{2} = 0.00287 kN-m^2

Clipped Acceleration		Point a (*)		Point b (*)		Point c (*)		Point d (*)		Point e (*)	
Cases	Peak Value	Time (sec)	Displ. (in)	Time (sec)	Displ. (in)	Time (sec)	Displ. (in)	Time (sec)	Displ. (in)	Time (sec)	Displ. (in)
5A	0.35g	1.90	1.3	2.24	-1.0	4.35	-0.9	5.15	1.4	12.10	1.5
5B	0.25g	1.90	1.3	2.20	-0.8	4.37	-0.8	5.15	1.5	12.09	1.7
5C	0.20g	1.90	1.3	2.20	-0.6	4.38	-0.7	5.15	1.5	12.09	1.7
5D	0.15g	1.90	1.1	2.25	-0.4	4.38	-0.6	5.15	1.5	12.09	1.6

b) CASES 6

$EI = 2.62 \times 10^6$ k-in^2
$T_1 = 0.72$ sec ; $T_2 = 0.18$ sec
$M_y = 800$ k-in

1 in. = 25.4 mm
1 k-in. = 0.113 kN-m
1 k-in.^{2} = 0.00287 kN-m^2

Clipped Acceleration		Point a (*)		Point b (*)		Point c (*)		Point d (*)		Point e (*)	
Cases	Peak Value	Time (sec)	Displ. (in)	Time (sec)	Displ. (in)	Time (sec)	Displ. (in)	Time (sec)	Displ. (in)	Time (sec)	Displ. (in)
6A	0.35g	1.98	1.4	2.35	-2.4	4.00	-2.2	5.70	-2.3	12.00	-2.6
6B	0.30g	1.98	1.4	2.30	-2.2	4.00	-2.0	5.60	-1.7	12.00	-2.5
6C	0.25g	1.98	1.4	2.30	-2.0	4.00	-1.7	5.70	-1.8	12.00	-2.1

(*) Note: Points a to e correspond to important relative maxima as given by Figs. H.5A - H.5D and H.6A - H.6C. See also Figs. 6.11 and 6.12

DESCRIPTION OF EARTHQUAKE	EI	PEAK CLIPPED ACCELERATION	MAXIMUM v_μ	
			TIME (SEC)	v_μ (in)
EL CENTRO 1940 NORMALIZED TO 0.55g	$EI = 6.28 \times 10^6 k\text{-}in^2$ (UNCRACKED) $T_1 = 0.46$ sec $T_2 = 0.11$ sec	0.55g 0.36g 0.32g 0.28g	12.21 12.21 12.21 12.20	2.2 2.8 2.9 2.7
	$EI = 2.62 \times 10^6 k\text{-}in^2$ (CRACKED) $T_1 = 0.72$ sec $T_2 = 0.18$ sec	0.55g 0.32g 0.26g 0.22g	2.01 5.38 5.38 5.37	2.8 3.9 4.1 4.0
DERIVED PACOIMA DAM NORMALIZED TO 0.35g	$EI = 6.28 \times 10^6 k\text{-}in^2$ (UNCRACKED) $T_1 = 0.46$ sec $T_2 = 0.11$ sec	0.35g 0.30g	5.05 5.04	2.6 2.3
	$EI = 2.62 \times 10^6 k\text{-}in^2$ (CRACKED) $T_1 = 0.72$ sec $T_2 = 0.18$ sec	0.35g 0.30g	3.65 3.65	3.9 3.5

TABLE 6.11 EFFECT OF CLIPPING EL CENTRO NORMALIZED TO 0.55g AND DERIVED PACOIMA DAM NORMALIZED TO 0.35g ON DISPLACEMENT RESPONSE OF A 2DOF MODEL OF THE CANOPY

CASE CONSIDERED	PEAK CLIPPED ACCELERATION	MAXIMUM v_u OBTAINED (in)	EPA
ELASTIC CASE $EI = 2.62 \times 10^6$ k-in^2 $\xi = 2\%$	0.55g 0.35g	4.3 3.5	0.55g
INELASTIC CASE $EI = 2.62 \times 10^6$ k-in^2 $\xi = 2\%$	0.55g 0.28g	2.8 4.1	0.28g

TABLE 6.12 INFLUENCE OF TYPE OF BEHAVIOR (ELASTIC OR ELASTIC / PERFECTLY PLASTIC ON THE DETERMINATION OF EPA FOR A 2DOF MODEL OF THE CANOPY SUBJECTED TO EL CENTRO NORMALIZED TO 0.55g

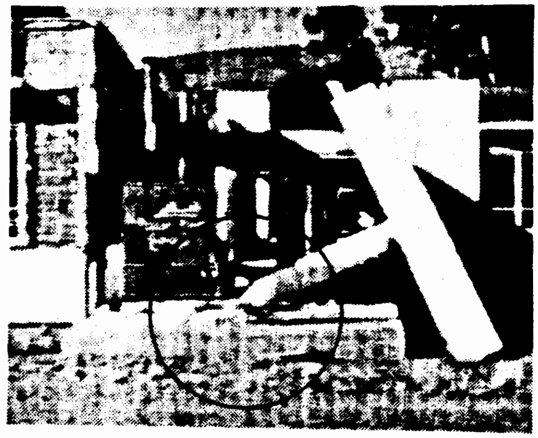

(a) Collapsed Canopy

(b) Canopy that Remained Standing

Fig.2.1 Primary School Canopies--El-Asnam, Algeria

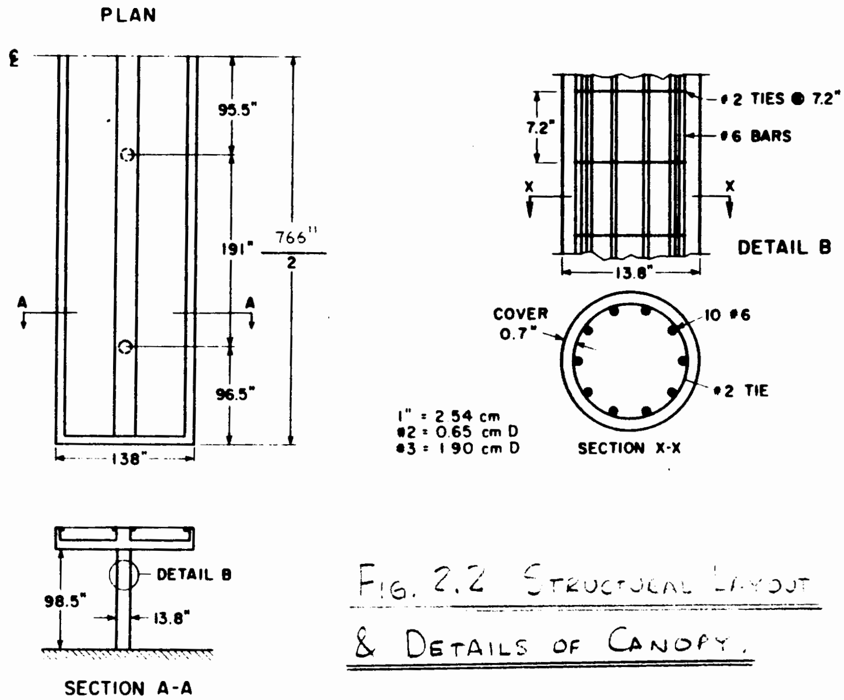

Fig. 2.2 Structural Layout & Details of Canopy.

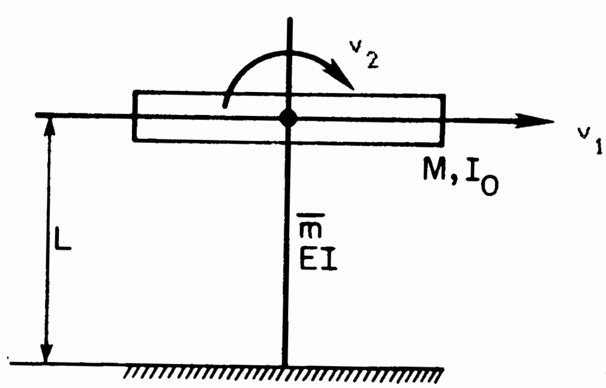

Fig. 2.3 Analytical Model of Canopy

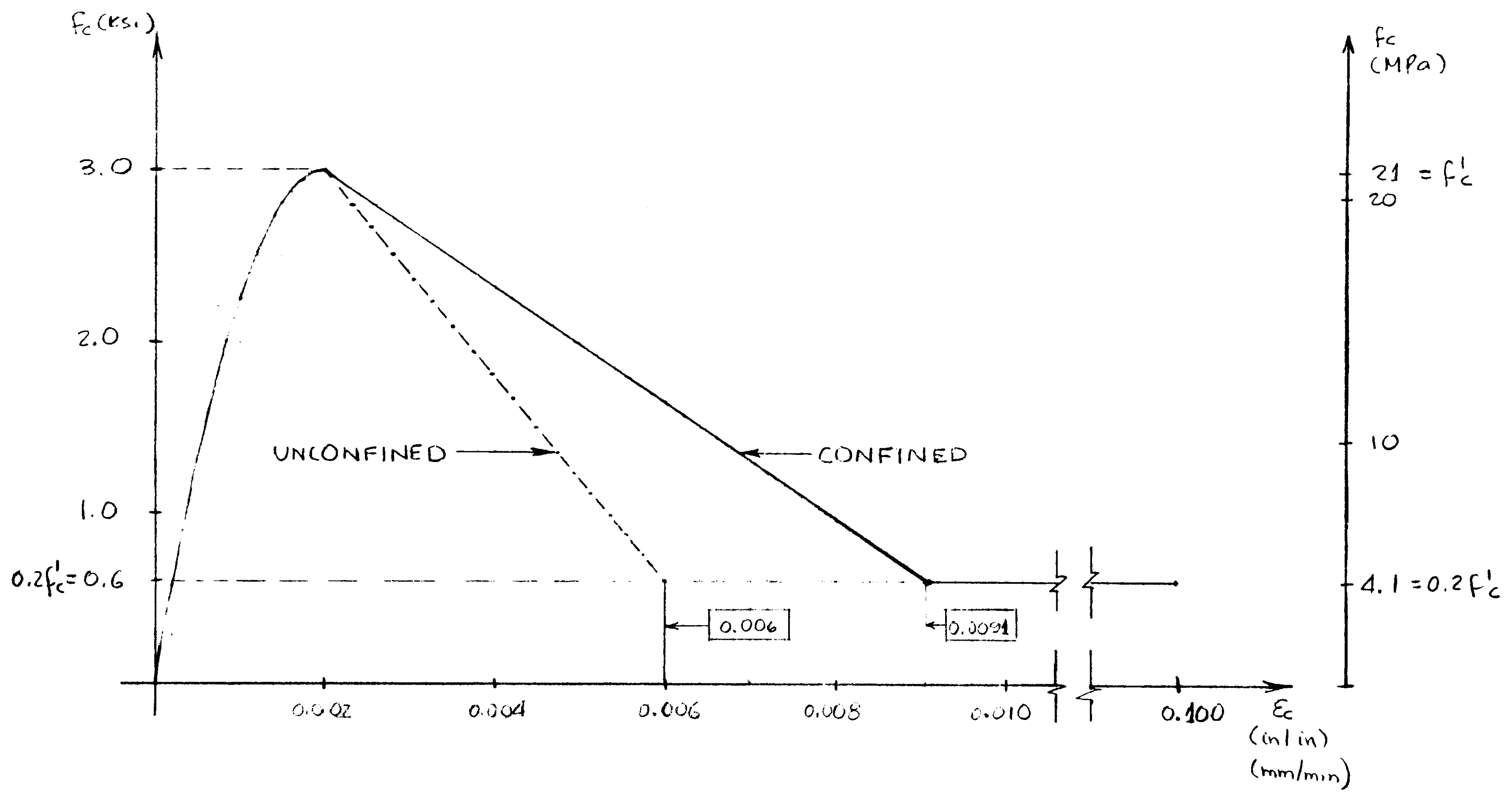

FIG. 3.1 CONCRETE STRESS-STRAIN RELATIONSHIP FOR CASE M1 : $f'_c = 3.0$ ksi (21 MPa)

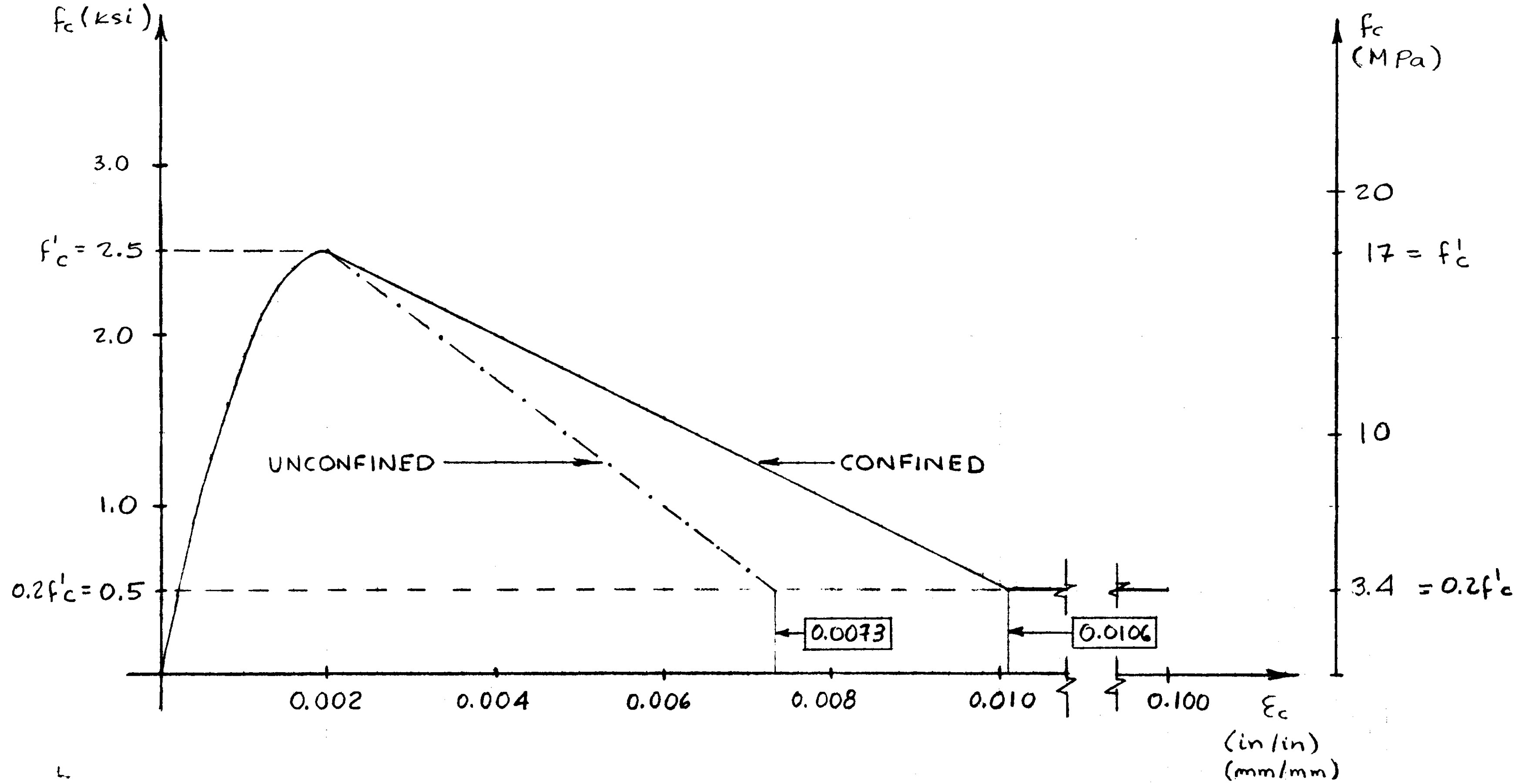

Fig. 3.2 Concrete Stress-Strain Relationship for Case M2 : f'_c = 2.5 ksi (17 MPa)

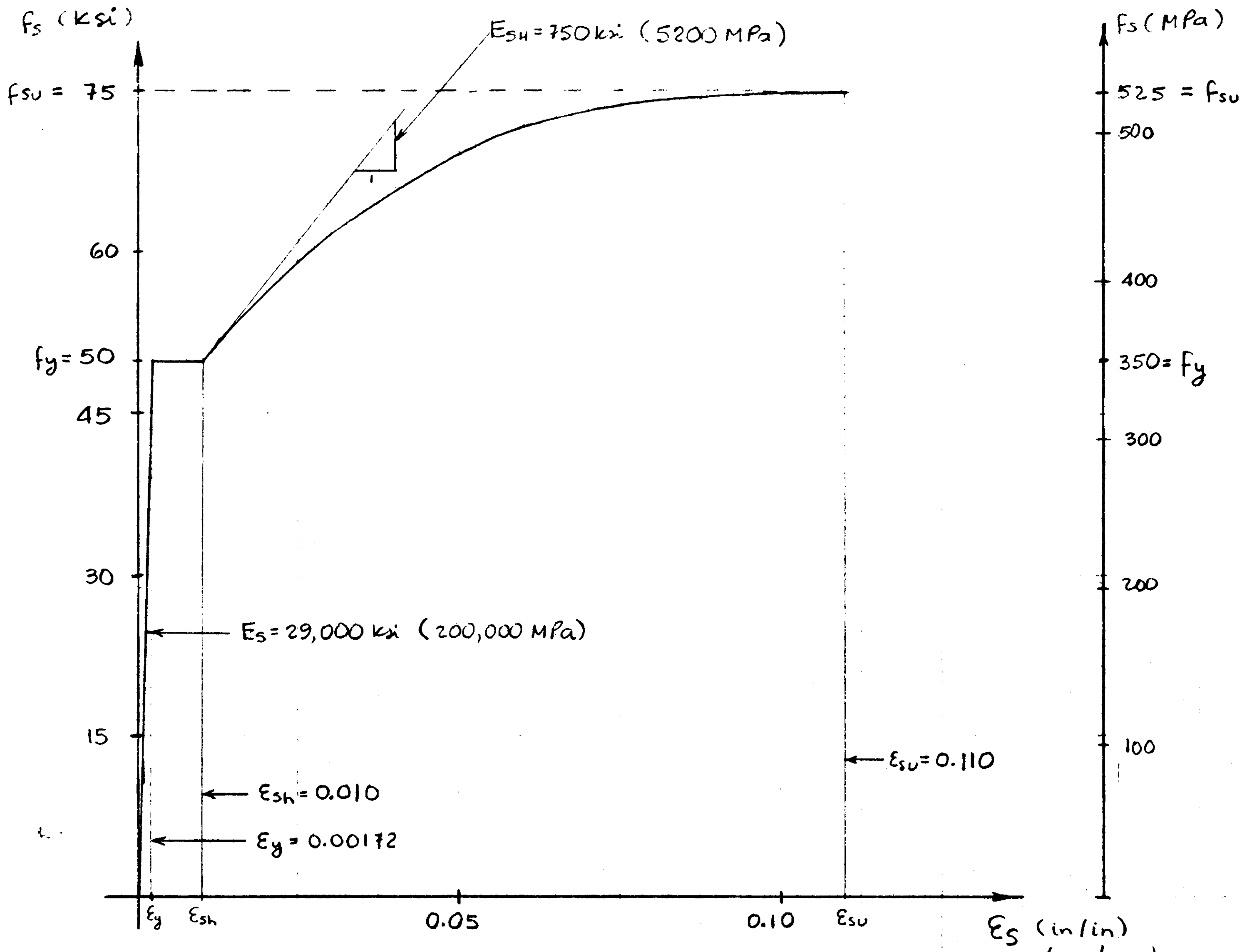

FIG. 3.3 REINFORCING STEEL STRESS-STRAIN RELATIONSHIP FOR CASE M1: $f_y = 50$ ksi (350 MPa)

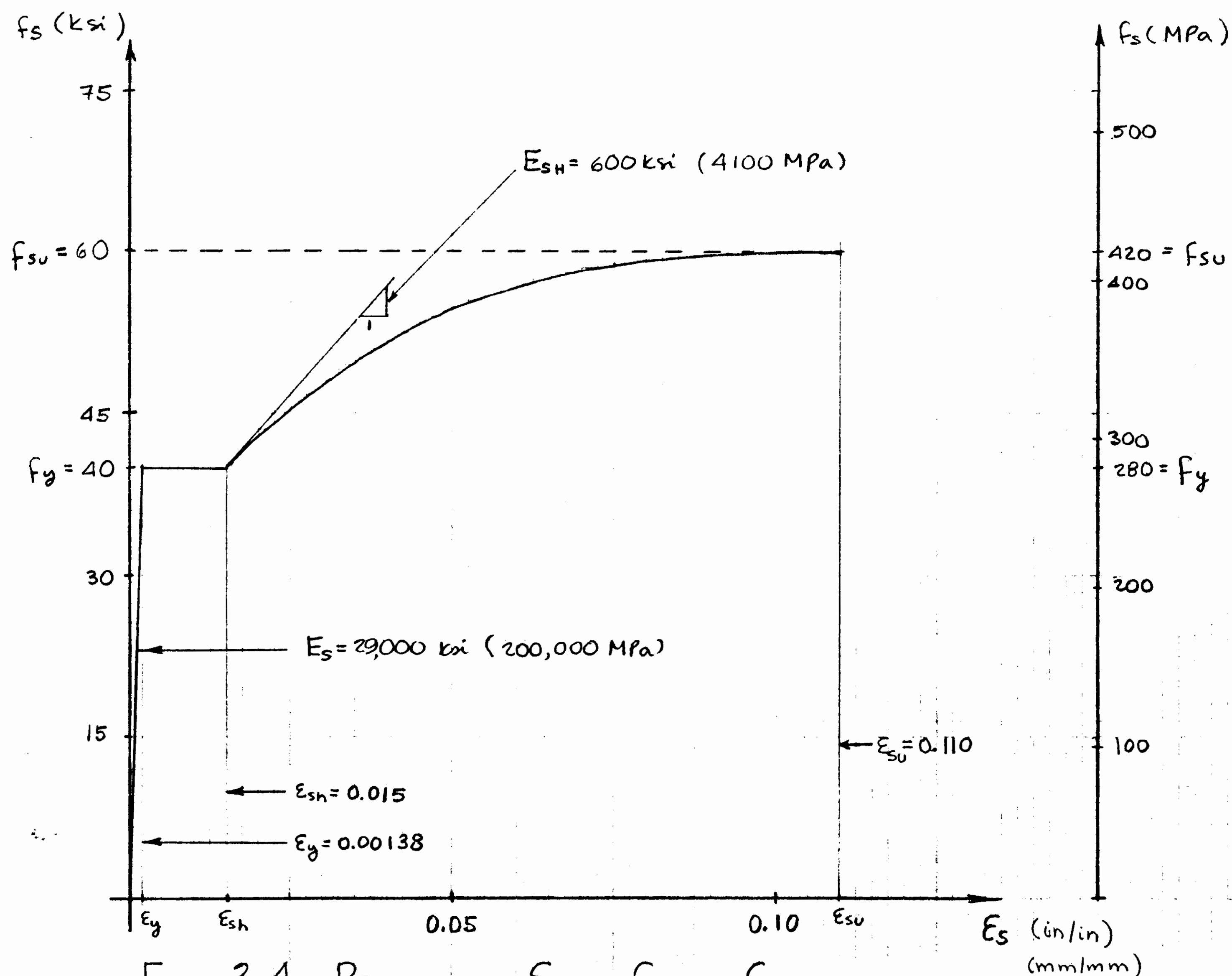

Fig. 3.4 Reinforcing Steel Stress-Strain Relationship for Case M2: $f_y = 40$ ksi (280 MPa).

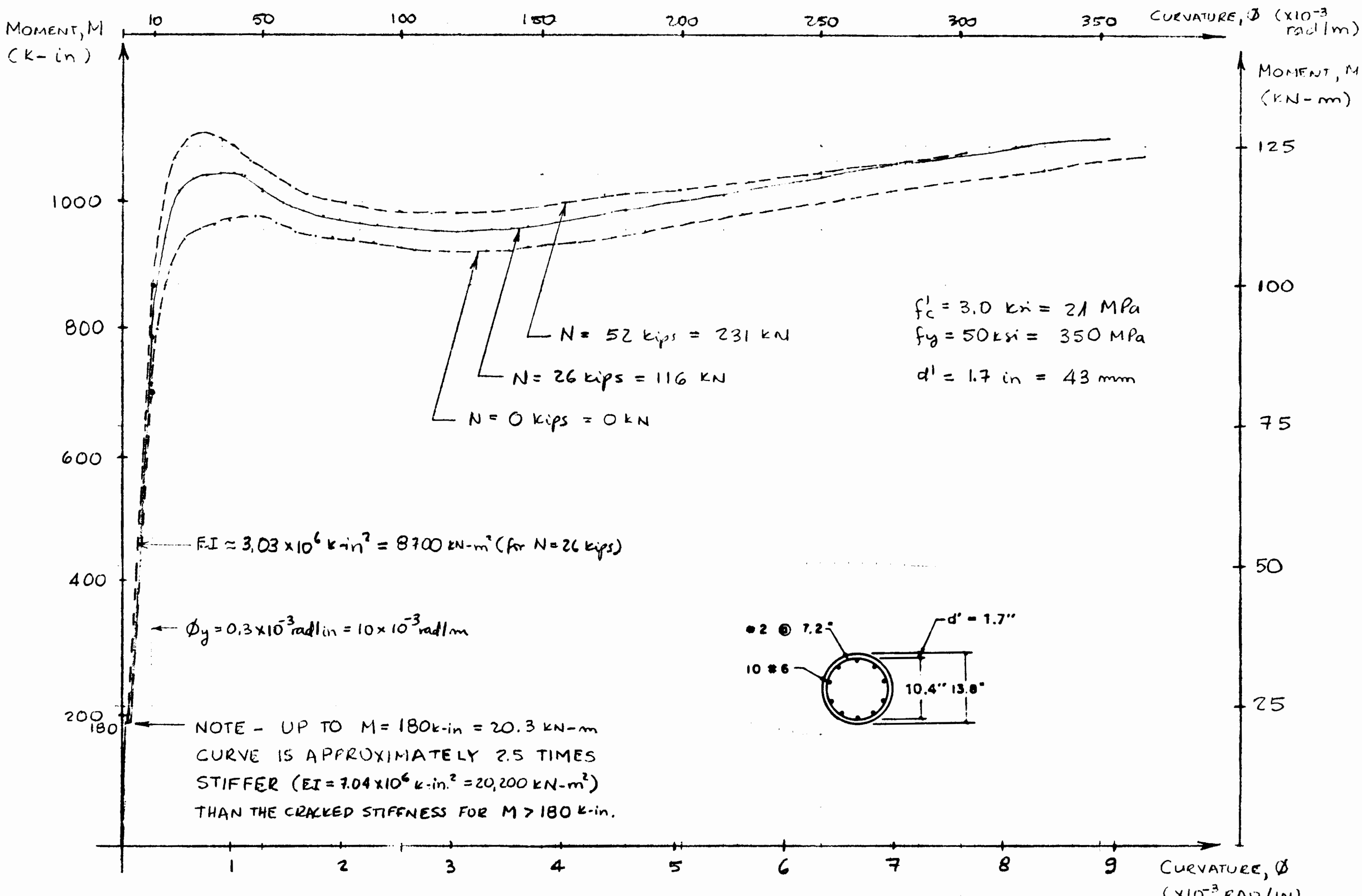

FIG. 3.5 EFFECT OF DIFFERENT AXIAL LOADS ON M-Ø RELATION OF COLUMN CROSS SECTION FOR MATERIAL PROPERTIES CASE M1

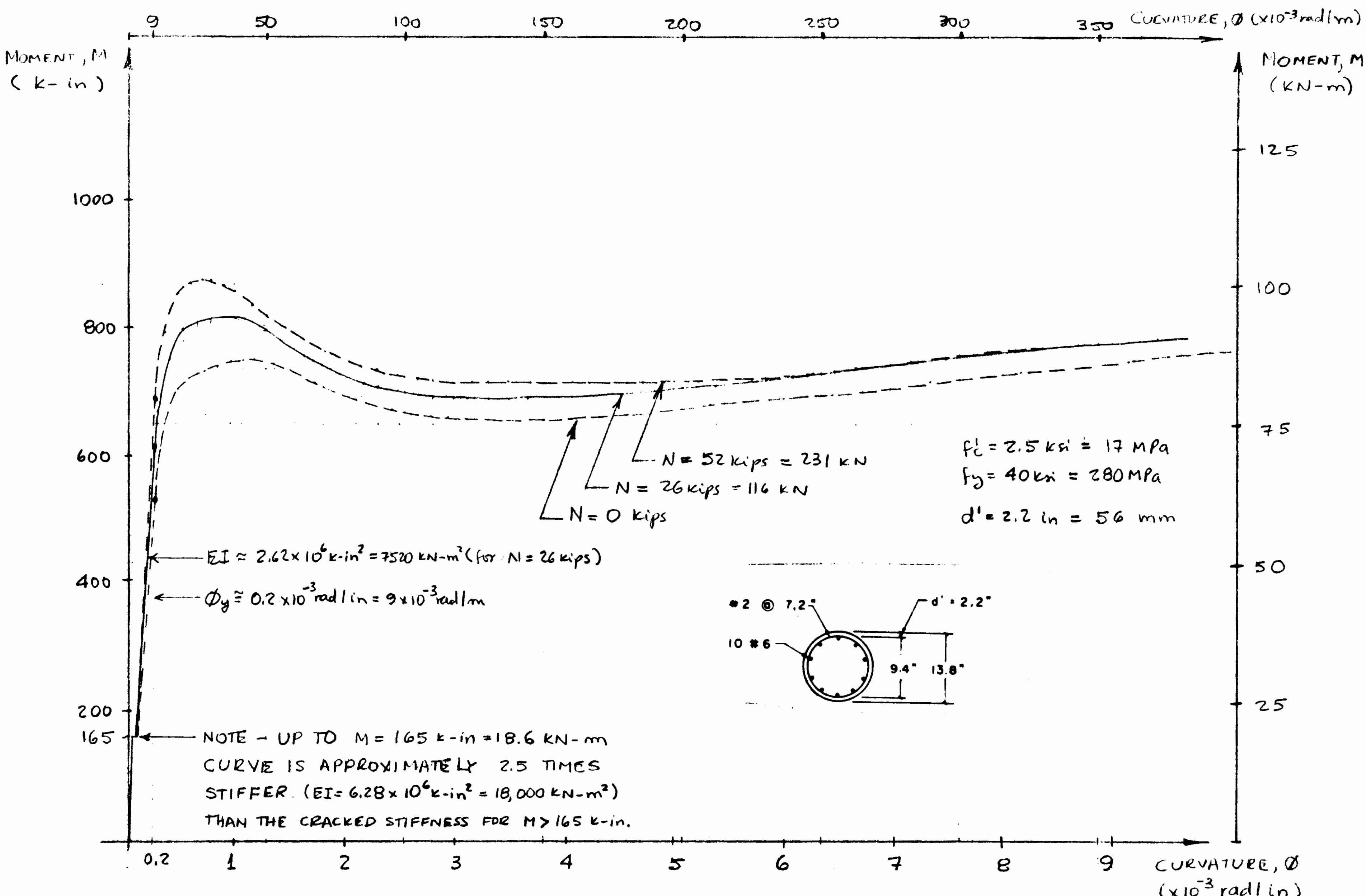

Fig. 3.6 Effect of Different Axial Loads on M-Ø Relation of Column Cross Section for Material Properties Case M2.

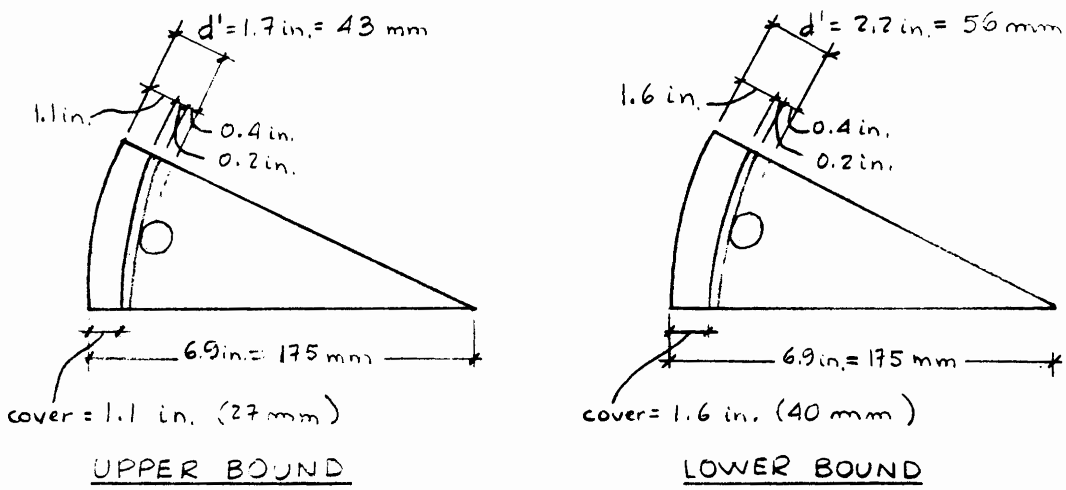

FIG. 3.7 DIFFERENT COVERS CONSIDERED IN THE ANALYSIS

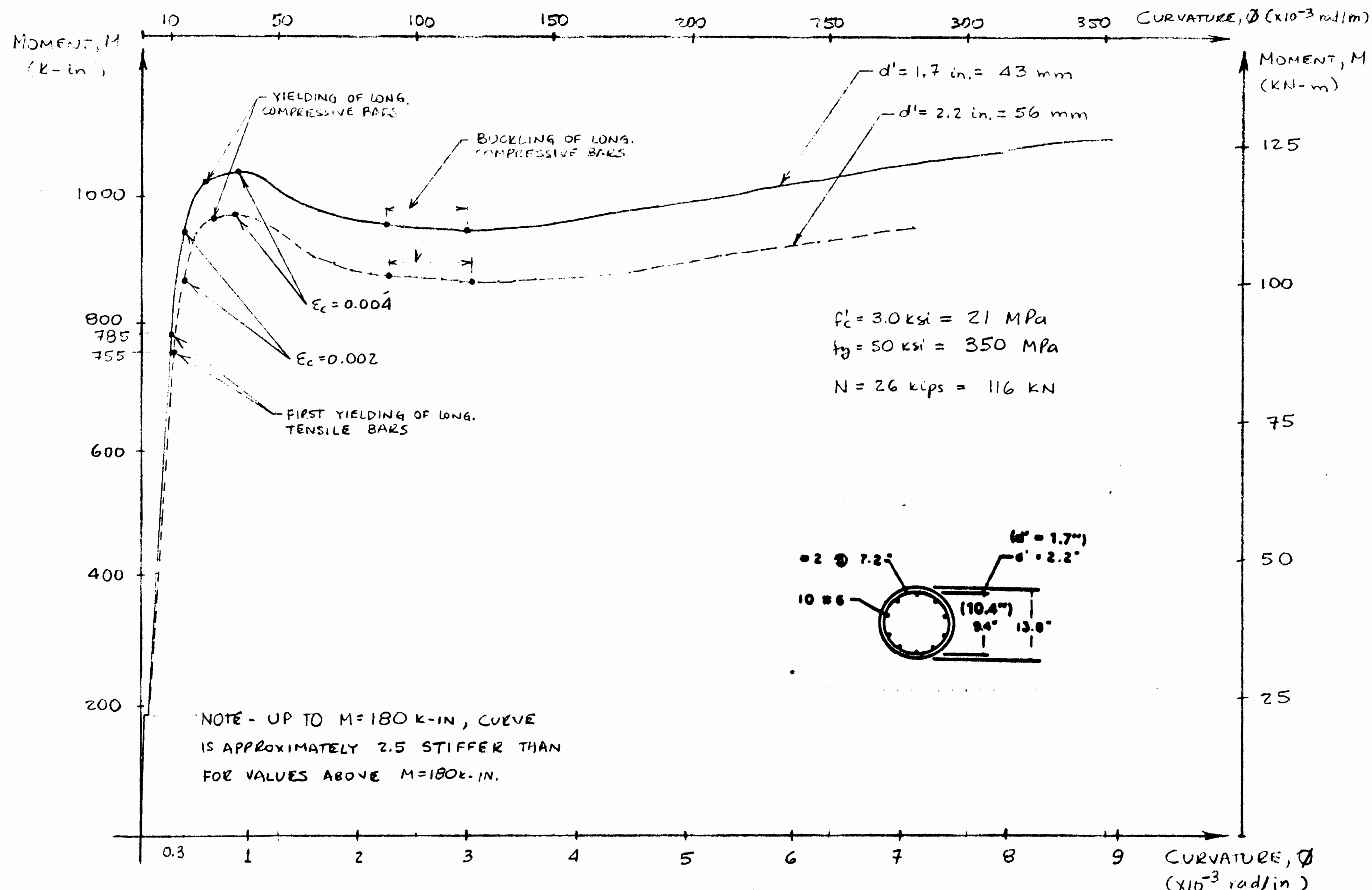

Fig. 3.8 Effect of Cover Thickness on M-Ø Relation of Column Cross Section under N=26[k] for Material Properties Case M1

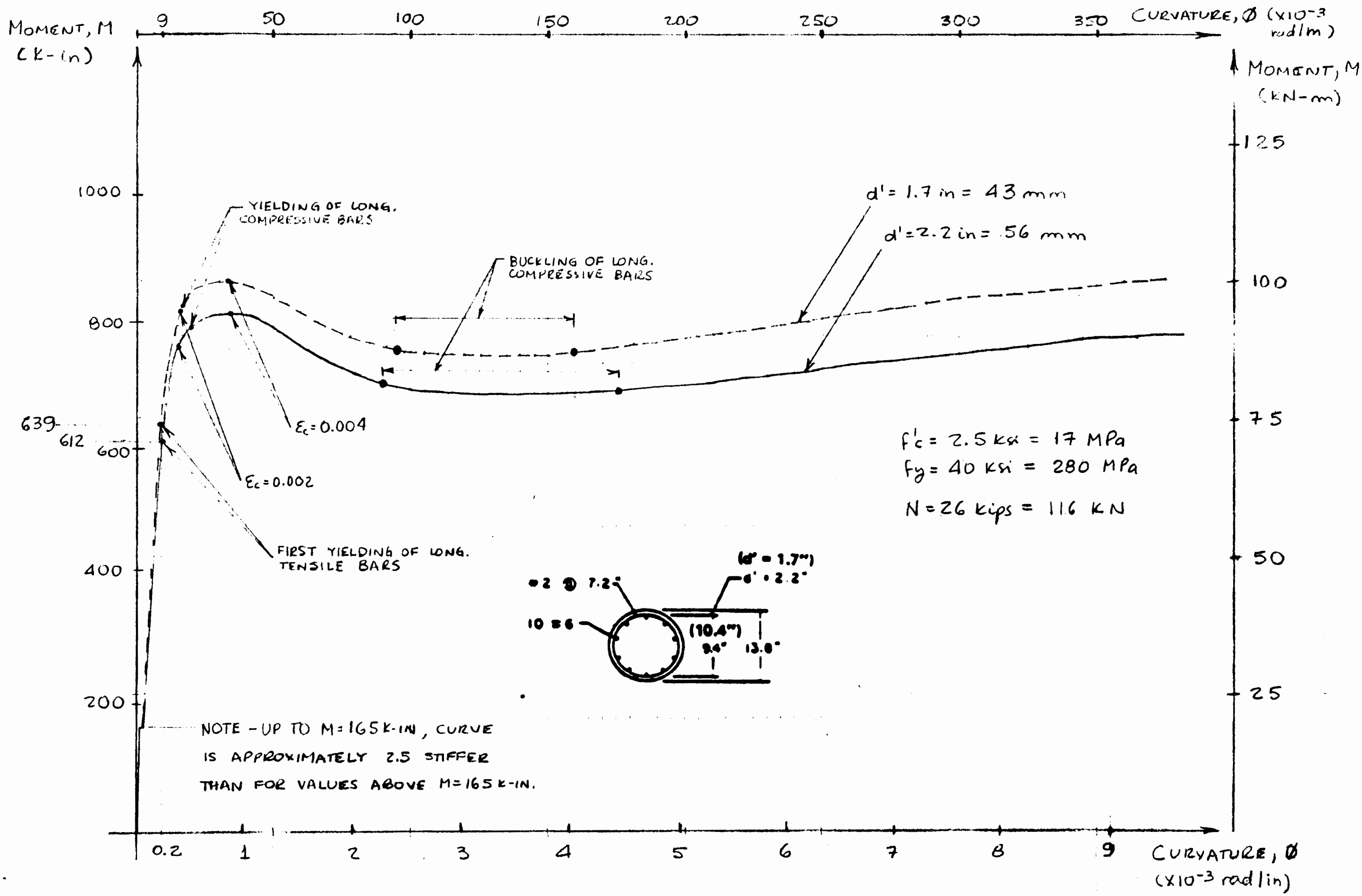

FIG. 3.9 EFFECT OF COVER THICKNESS ON M-Ø RELATION OF COLUMN CROSS SECTION UNDER $N=26^k$ FOR MATERIAL PROPERTIES CASE M2

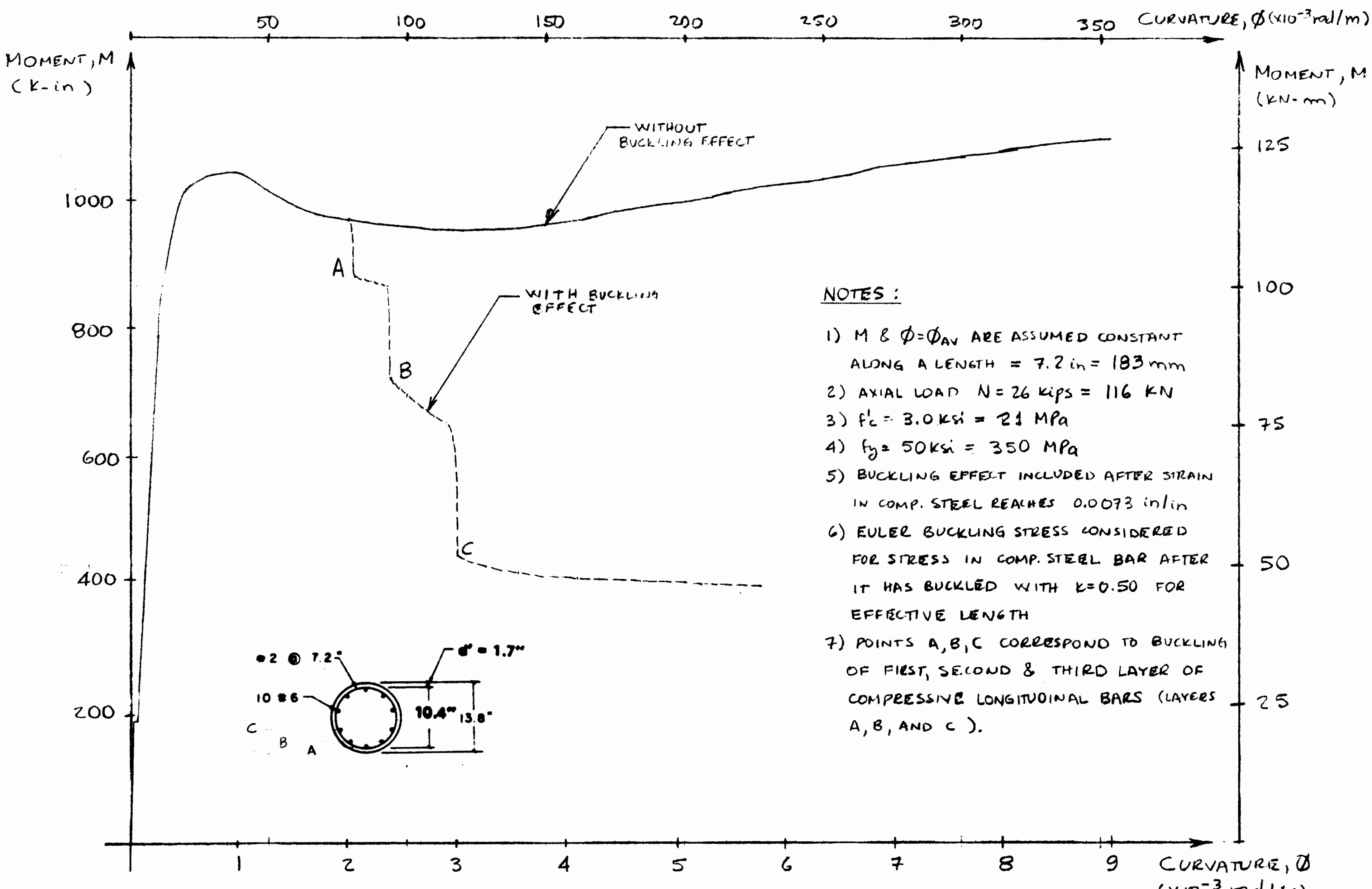

Fig. 3.10 Effect of Compression Reinforcement Buckling on M-Ø Relation of Column Cross Section for Material Properties Case M1

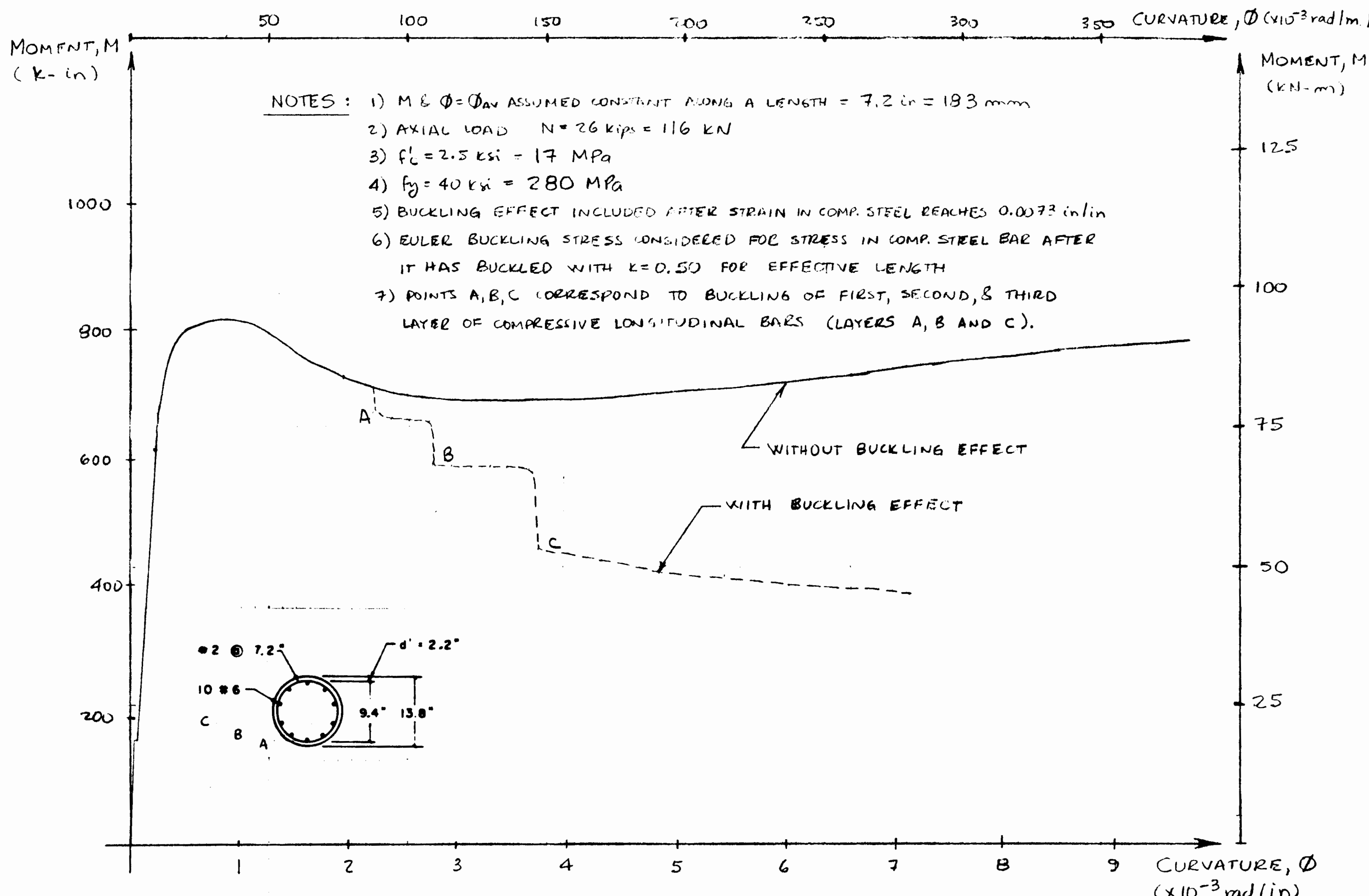

Fig. 3.11 Effect of Compression Reinforcement Buckling on M-Ø Relation of Column Cross Section for Material Properties Case M2

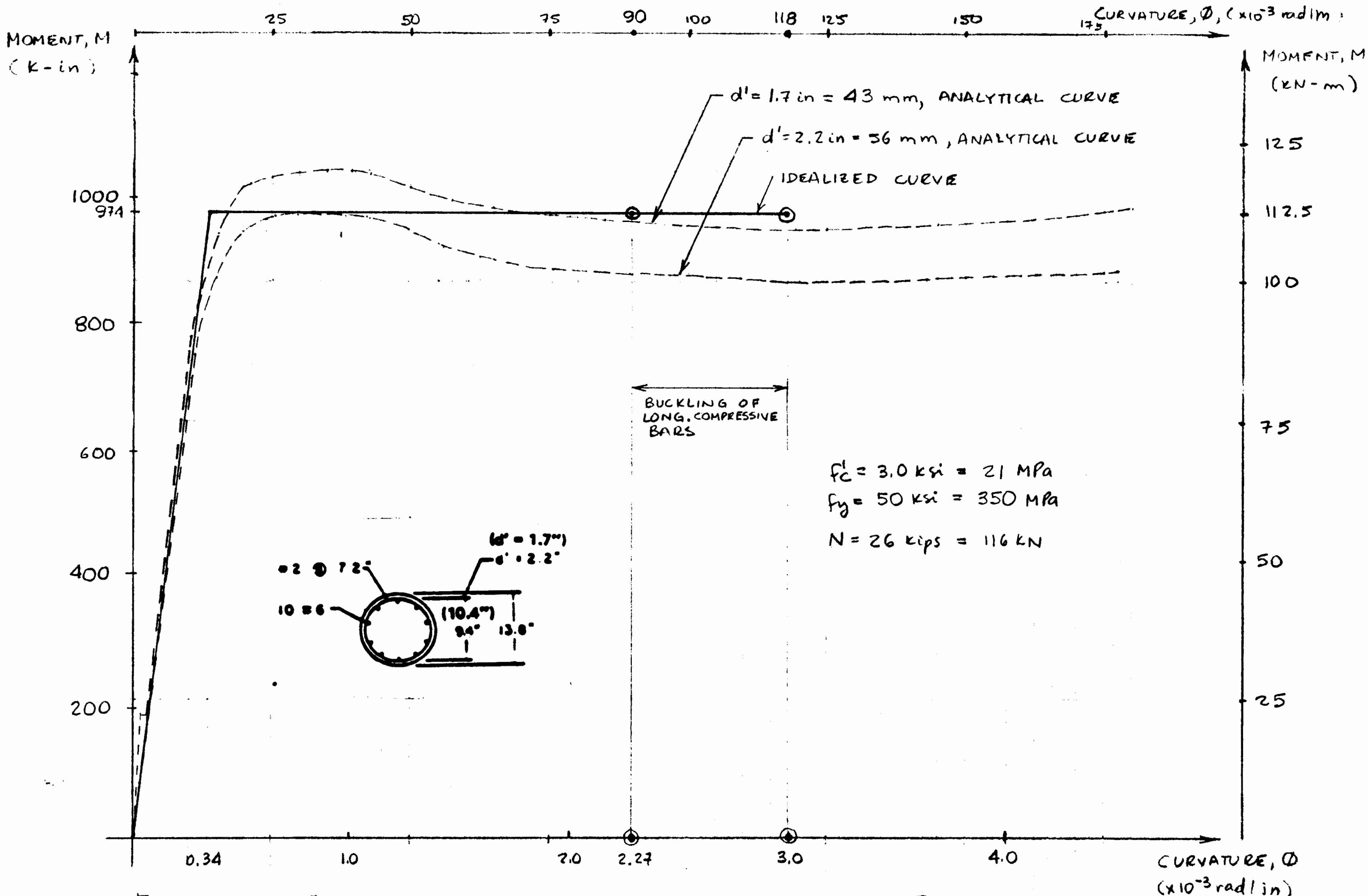

FIG. 3.12 IDEALIZED M-Ø RELATIONSHIP OF COLUMN CROSS SECTION FOR MATERIAL PROPERTIES CASE M1

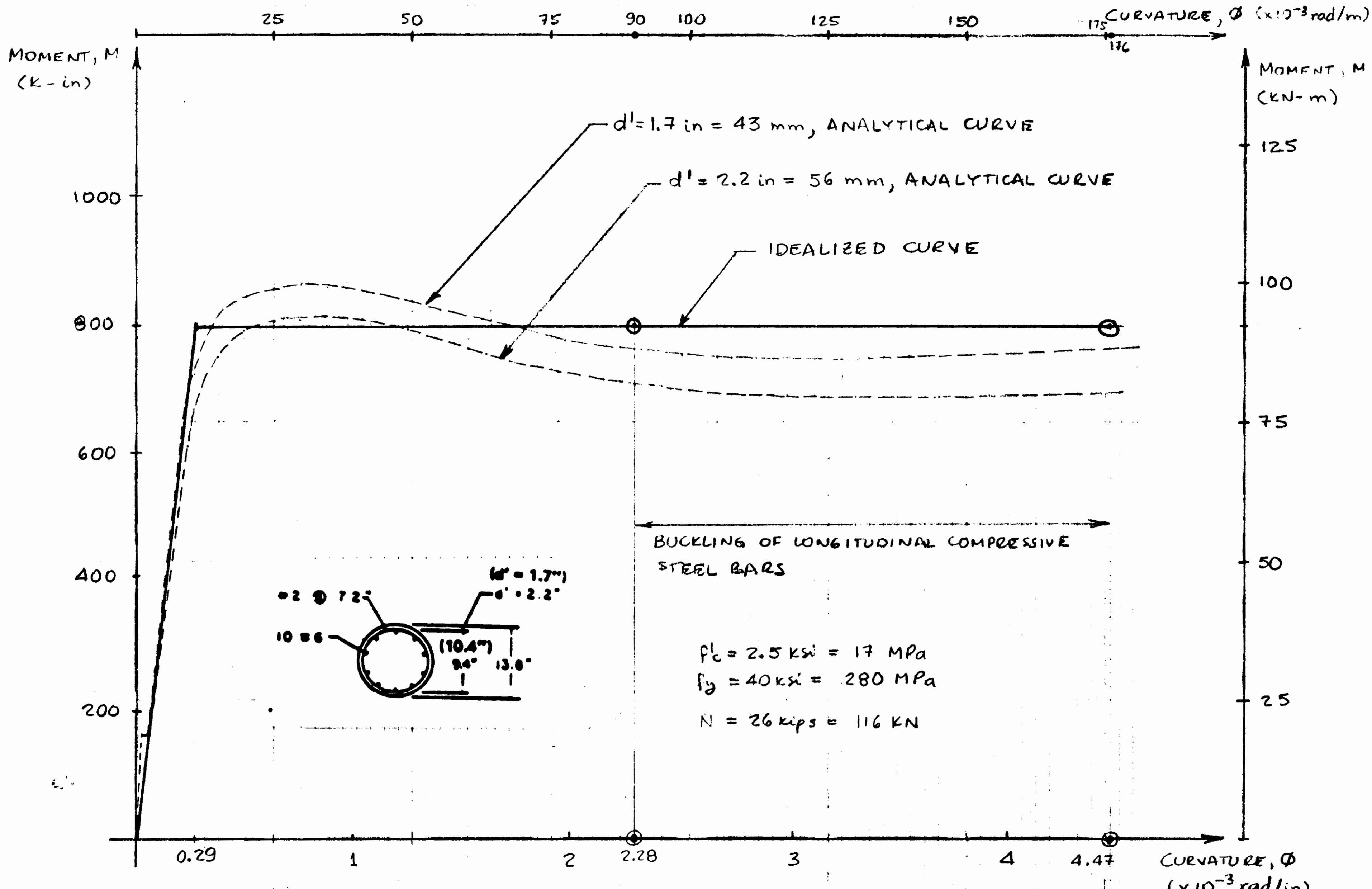

Fig. 3.13 Idealized M-Ø Relationship of Column Cross Section for Material Properties Case M2

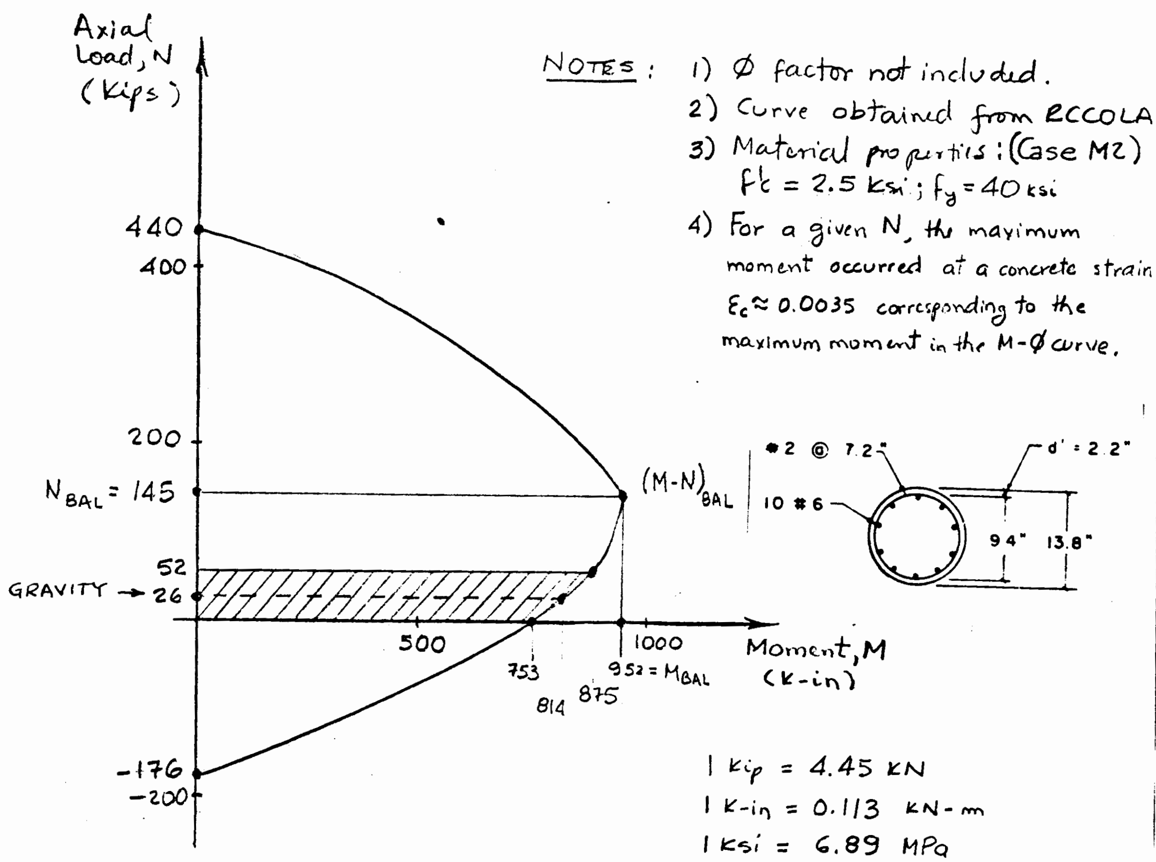

Fig. 3.14 CANOPY COLUMN: M-N INTERACTION CURVE AND EXPECTED RANGE OF AXIAL FORCE VARIATION

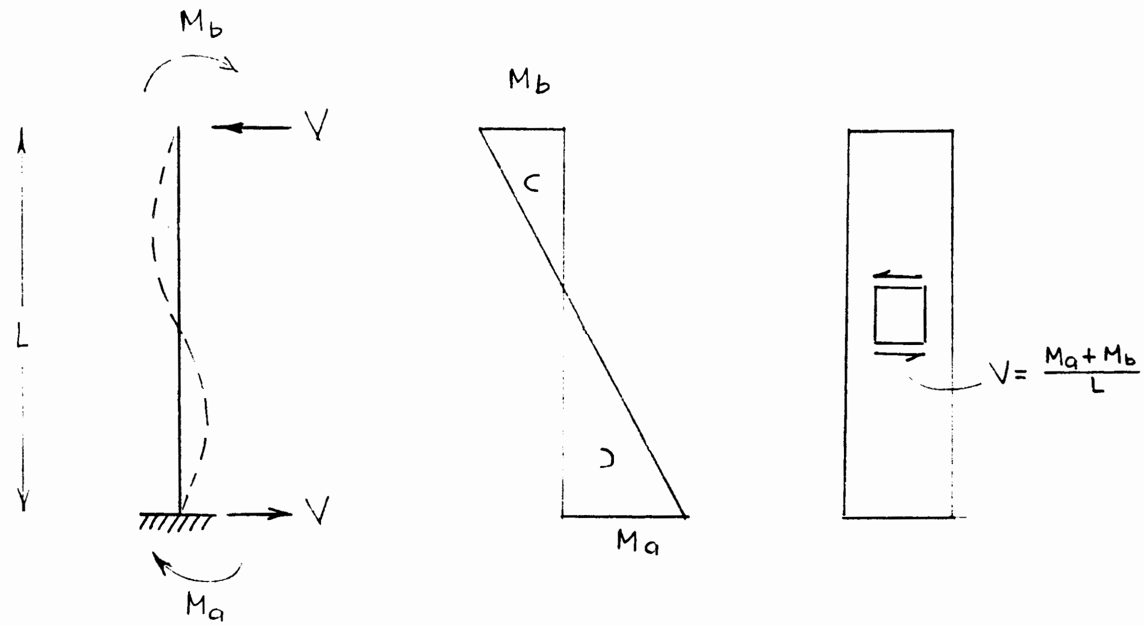

FIG. 3.15 MEMBER WITH CONSTANT SHEAR

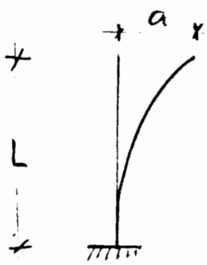

$$v(x) = \left(1 - \cos\frac{\pi x}{2L}\right)a$$

$$v'(x) = \left(\sin\frac{\pi x}{2L}\right)\left(\frac{\pi}{2L}\right)a$$

$$v''(x) = \left(\cos\frac{\pi x}{2L}\right)\left(\frac{\pi}{2L}\right)^2 a$$

FIG. 5.1 MODE SHAPE ASSUMED FOR ESTIMATION OF PERIOD USING RAYLEIGH'S METHOD

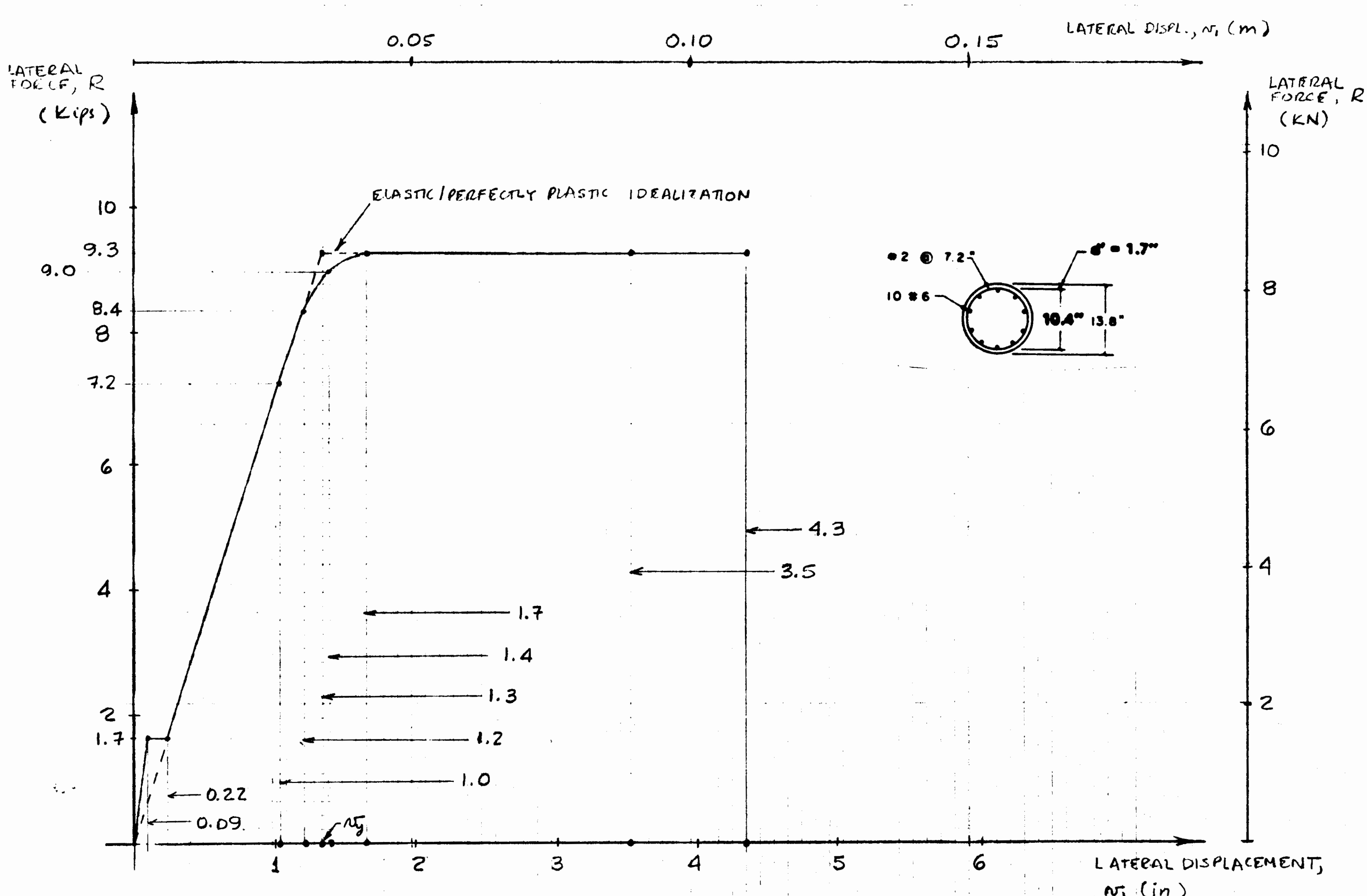

FIG. 6.1 LATERAL RESISTANCE FUNCTION, R VS. v_1 FOR MATERIAL PROPERTIES CASE M1

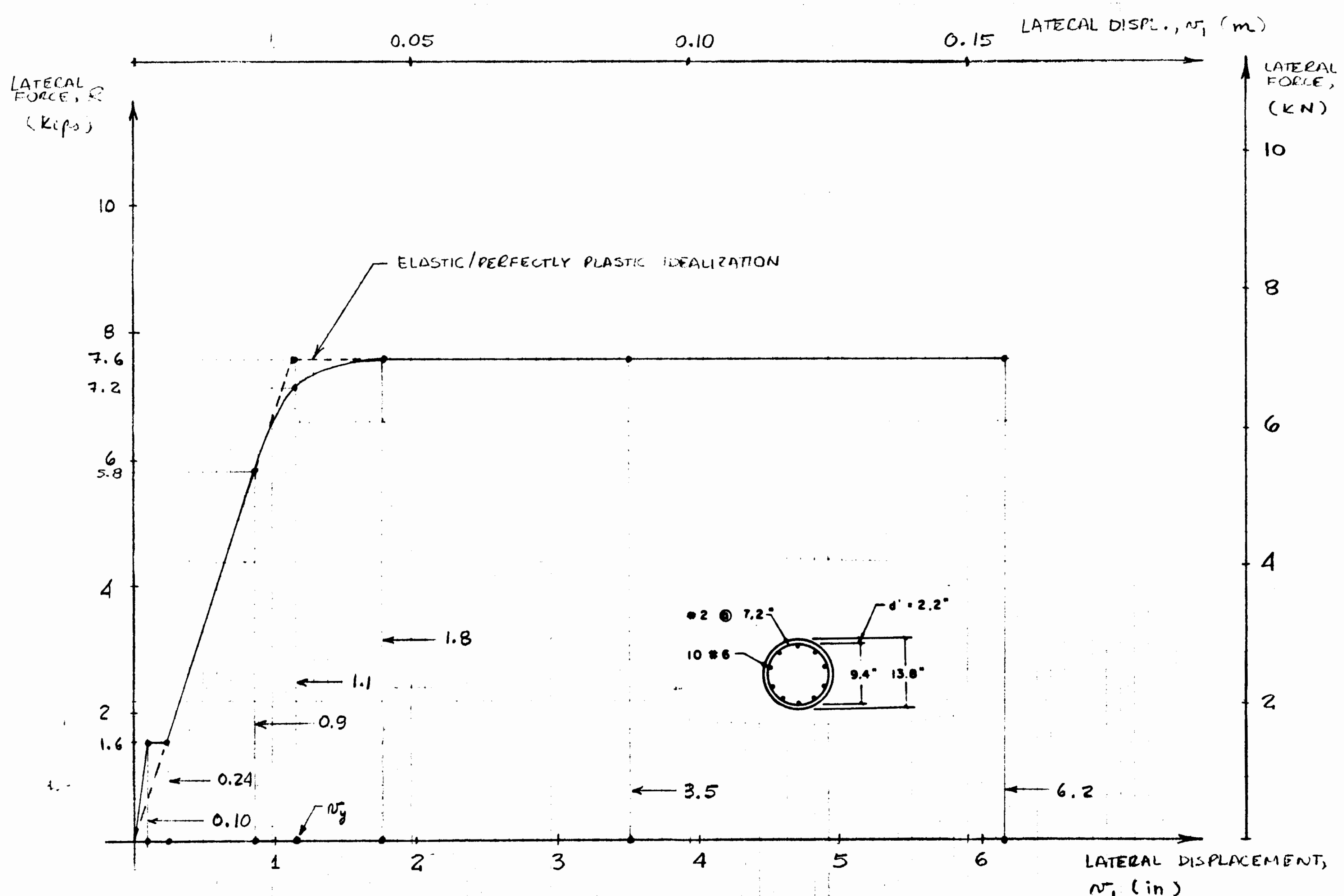

Fig. 6.2. Lateral Resistance Function, R vs. v_1 for Material Properties Case M2

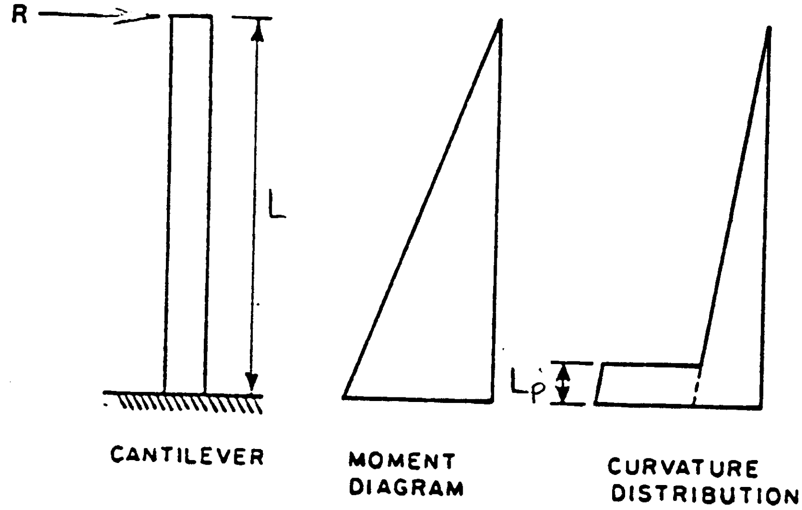

a) Curvature Distribution of a Cantilever Column Subjected to a Lateral Force R at the Top.

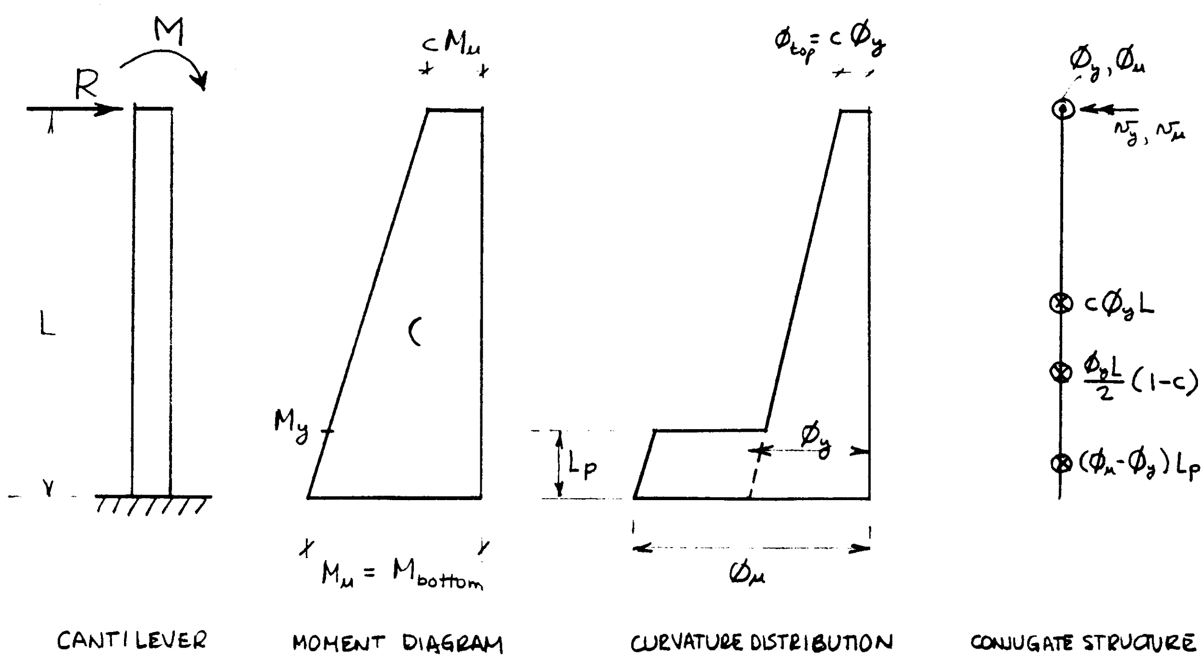

b) Curvature Distribution of a Cantilever Column Subjected to a Lateral Force R and a Moment M at the Top

Fig. 6.3 Curvature Distribution of a Cantilever Column

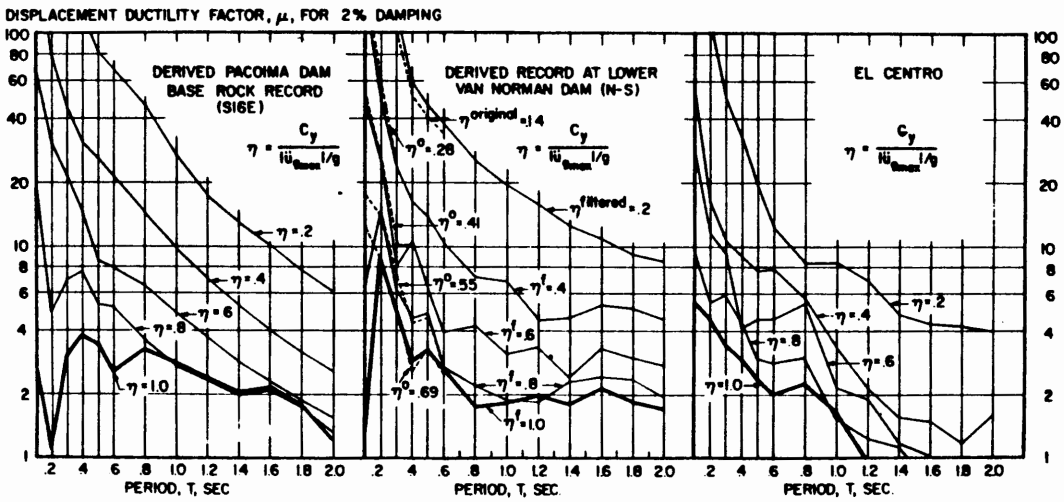

Fig. 6.4 Inelastic Response Spectra for 2% Damping

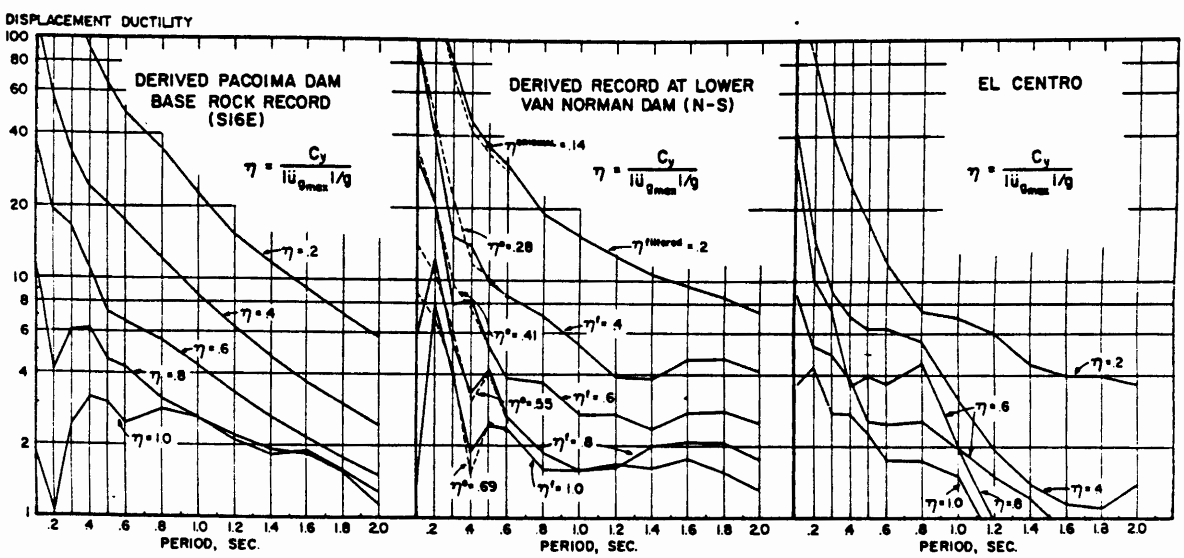

Fig. 6.5 Inelastic Response Spectra for 5% Damping

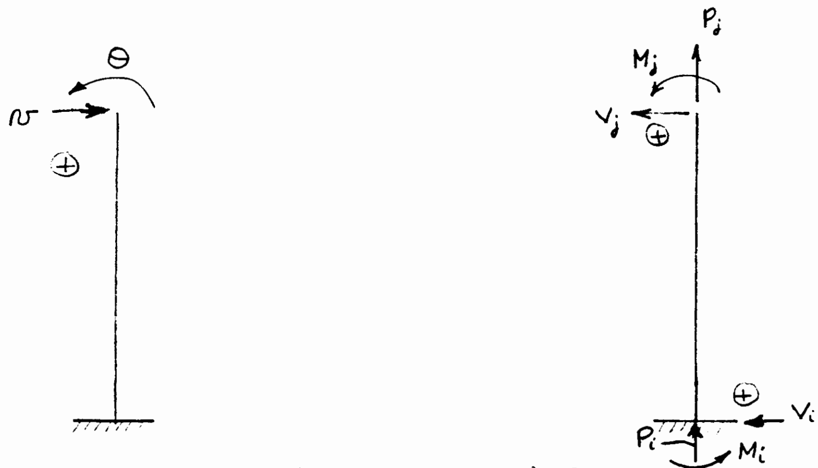

a) Positive sense for nodal displacements & rotations

b) Positive sense for forces and moments

FIG. 6.6 SIGN CONVENTION FOR DRAIN-2D OUTPUT

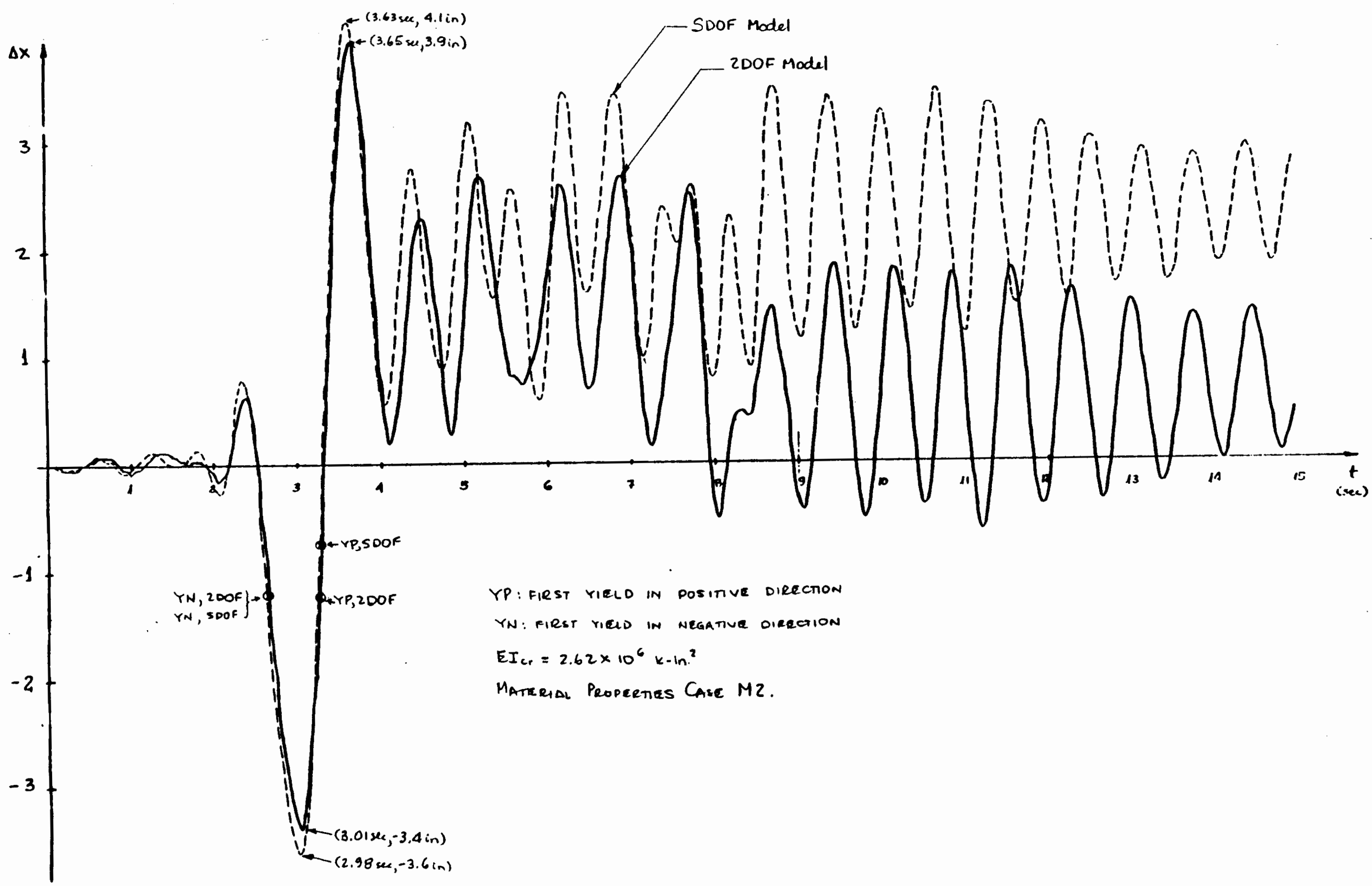

FIG. 6.7 EFFECT OF USING SDOF OR 2DOF MODEL ON DISPLACEMENT RESPONSE OF CANOPY WHEN SUBJECTED TO DERIVED PACOIMA DAM NORMALIZED TO 0.35g

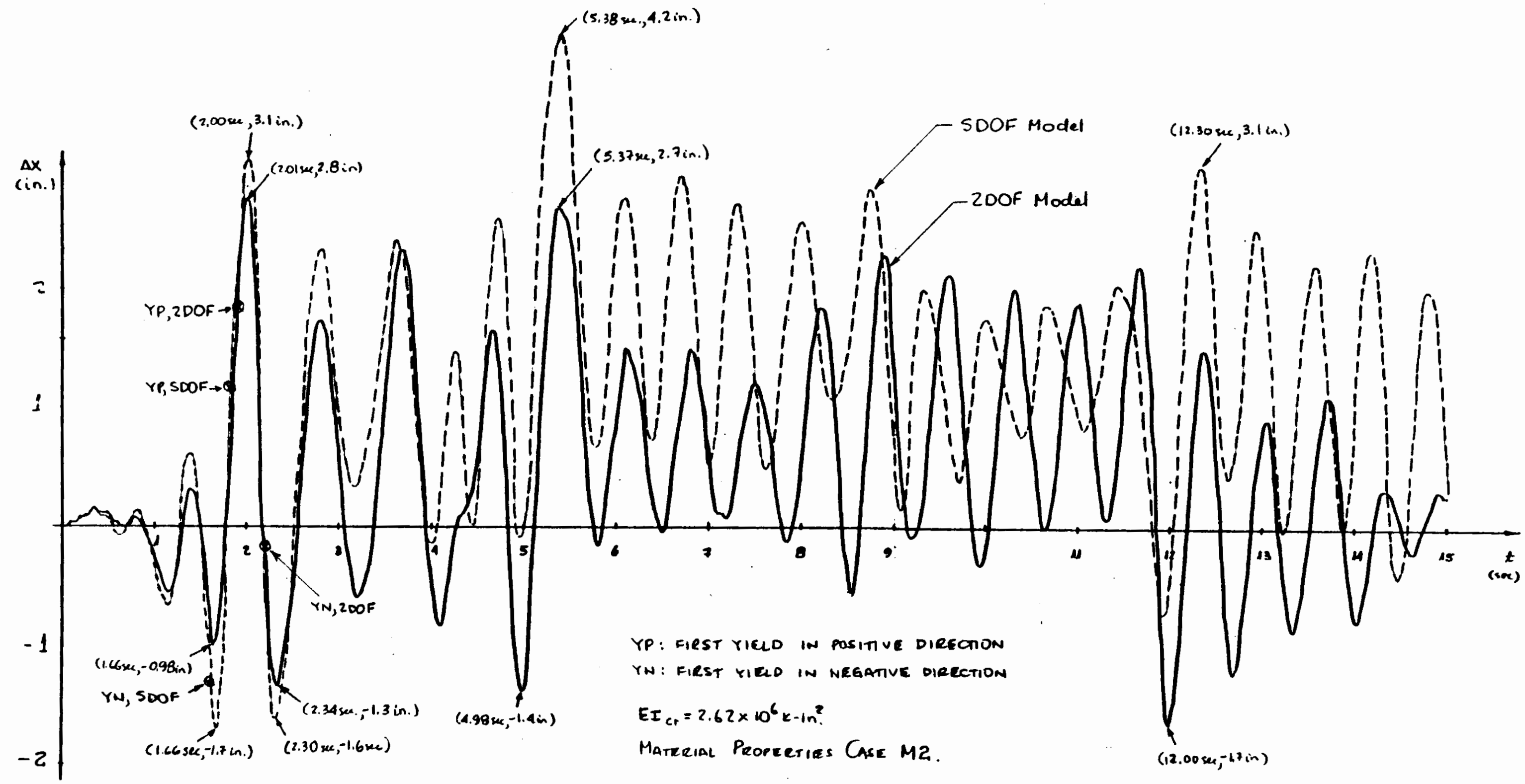

FIG. 6.8 EFFECT OF USING SDOF OR 2DOF MODEL ON DISPLACEMENT RESPONSE OF CANOPY WHEN SUBJECTED TO EL CENTRO NORMALIZED TO 0.55g

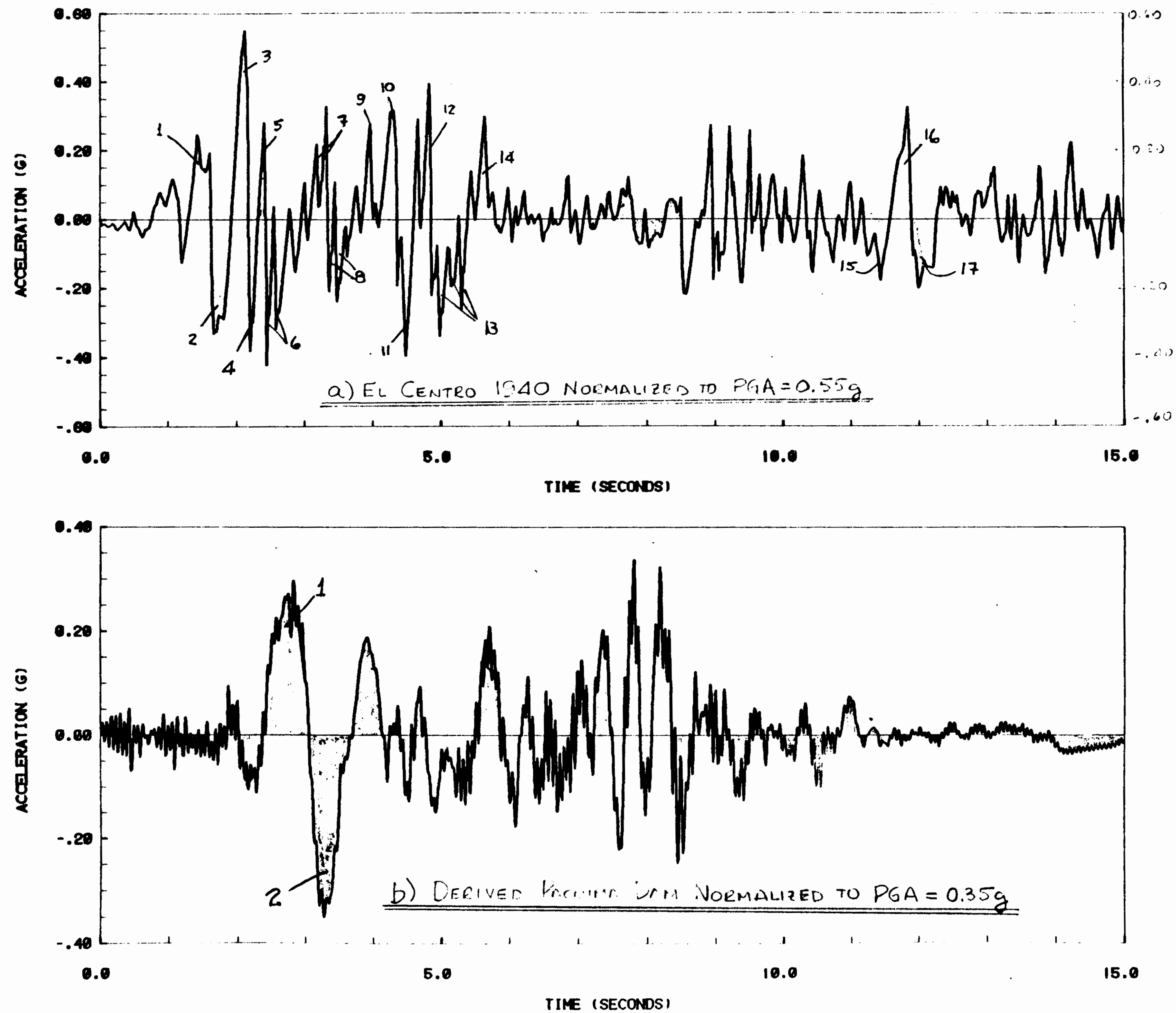

FIG. 6.9 GROUND MOTIONS CONSIDERED

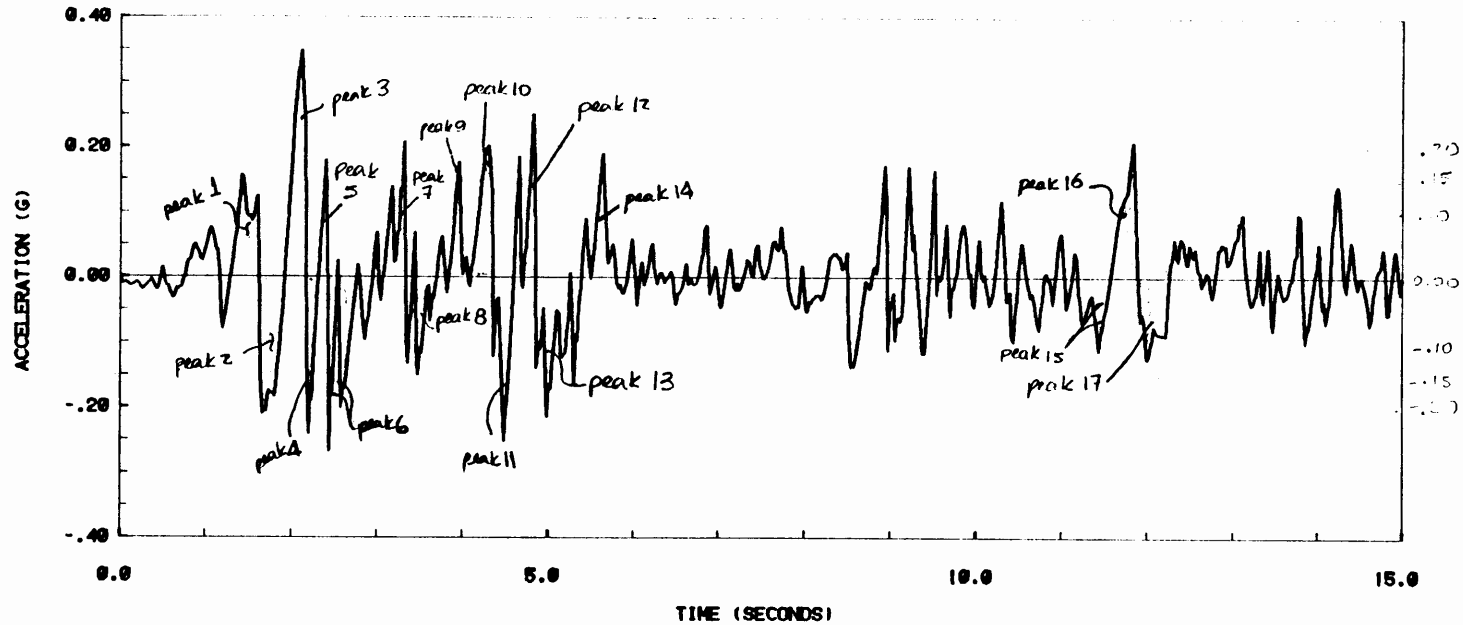

c) ACTUAL (OR RECORDED) EL CENTRO 1940, SOOE

(UNNORMALIZED, PGA = 0.3485g

FIG. 6.9 GROUND MOTIONS CONSIDERED

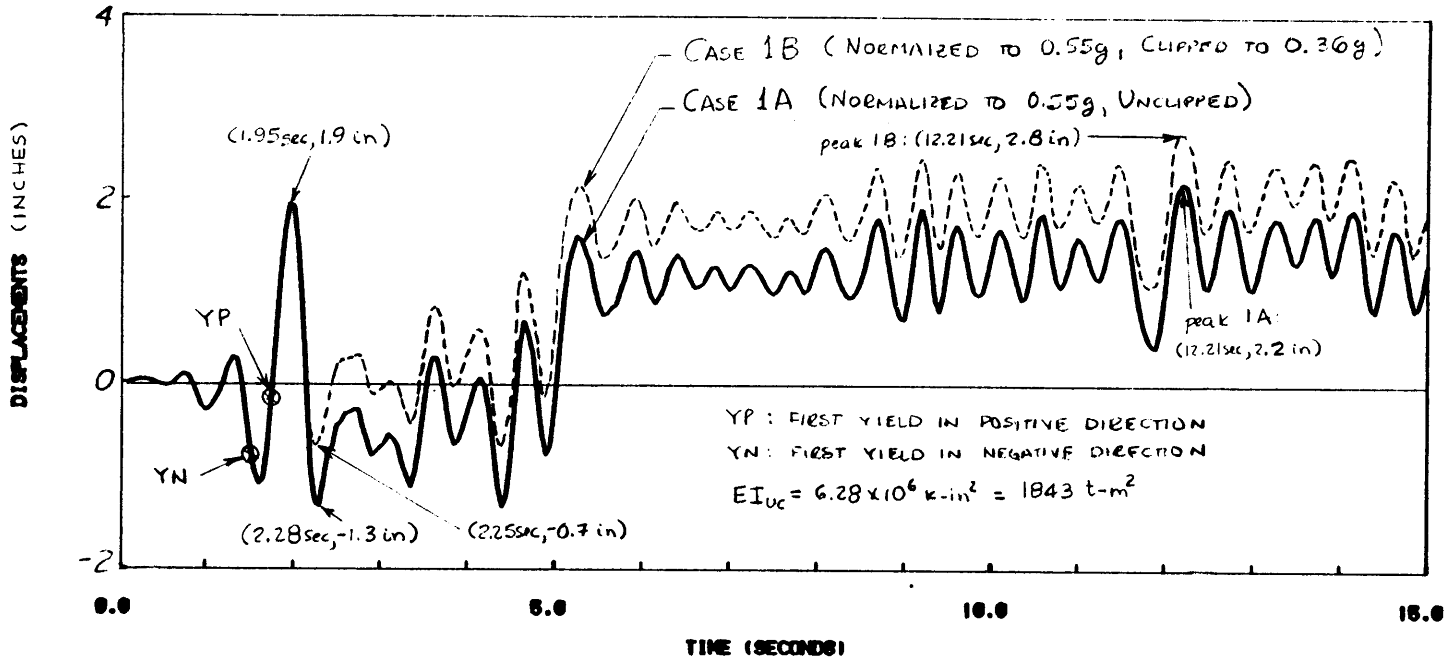

FIG. 6.10 EFFECT OF CLIPPING EL CENTRO NORMALIZED TO 0.55g ON DISPLACEMENT RESPONSE OF A 2DOF CANOPY MODEL (CASES 1A & 1B).

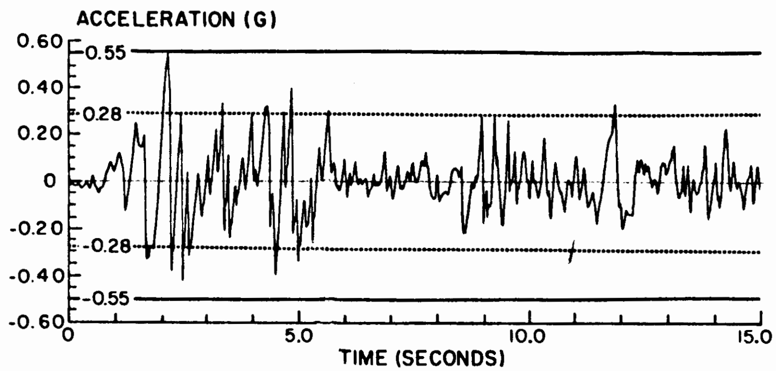

(a) EL CENTRO 1940 NORMALIZED TO 0.55g

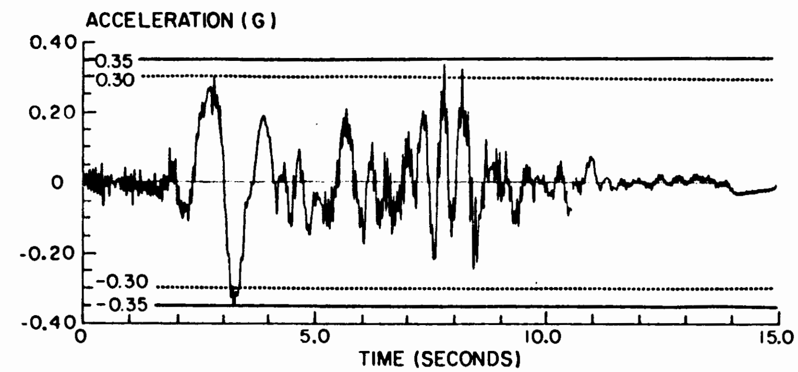

(c) DERIVED PACOIMA DAM NORMALIZED TO 0.35g

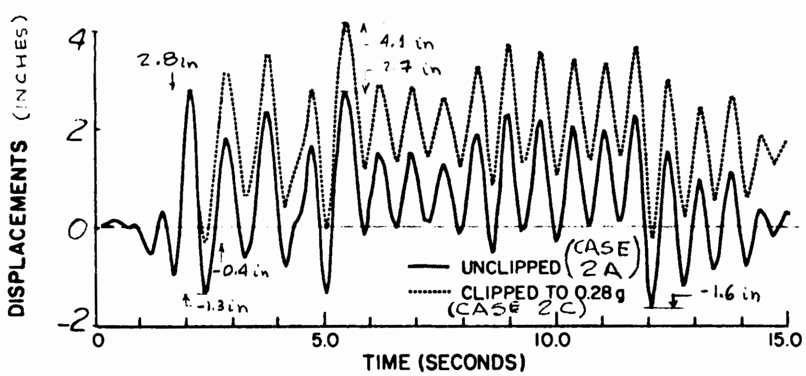

(b) DISPLACEMENT RESPONSE OF CANOPY TO EL CENTRO NORMALIZED TO 0.55g: UNCLIPPED & CLIPPED TO 0.28g

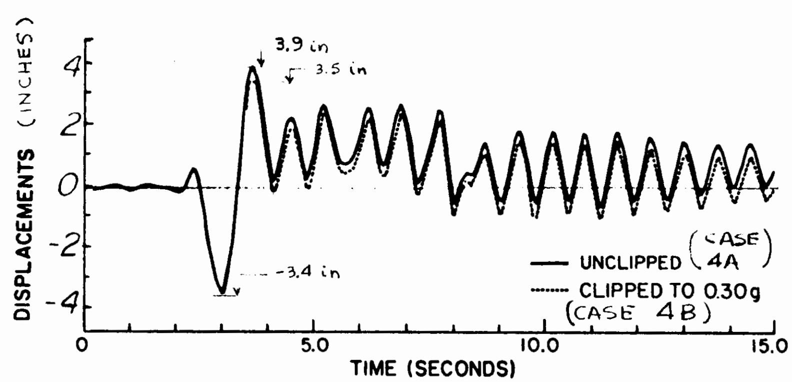

(d) DISPLACEMENT RESPONSE OF CANOPY TO DERIVED PACOIMA DAM NORMALIZED TO 0.35g: UNCLIPPED & CLIPPED TO 0.30g

FIG. 6.11 EFFECT OF CLIPPING EL CENTRO NORMALIZED TO 0.55g & DERIVED PACOIMA DAM NORMALIZED TO 0.35g ON DISPLACEMENT RESPONSE OF A 2DOF CANOPY MODEL

Fig. 6.12

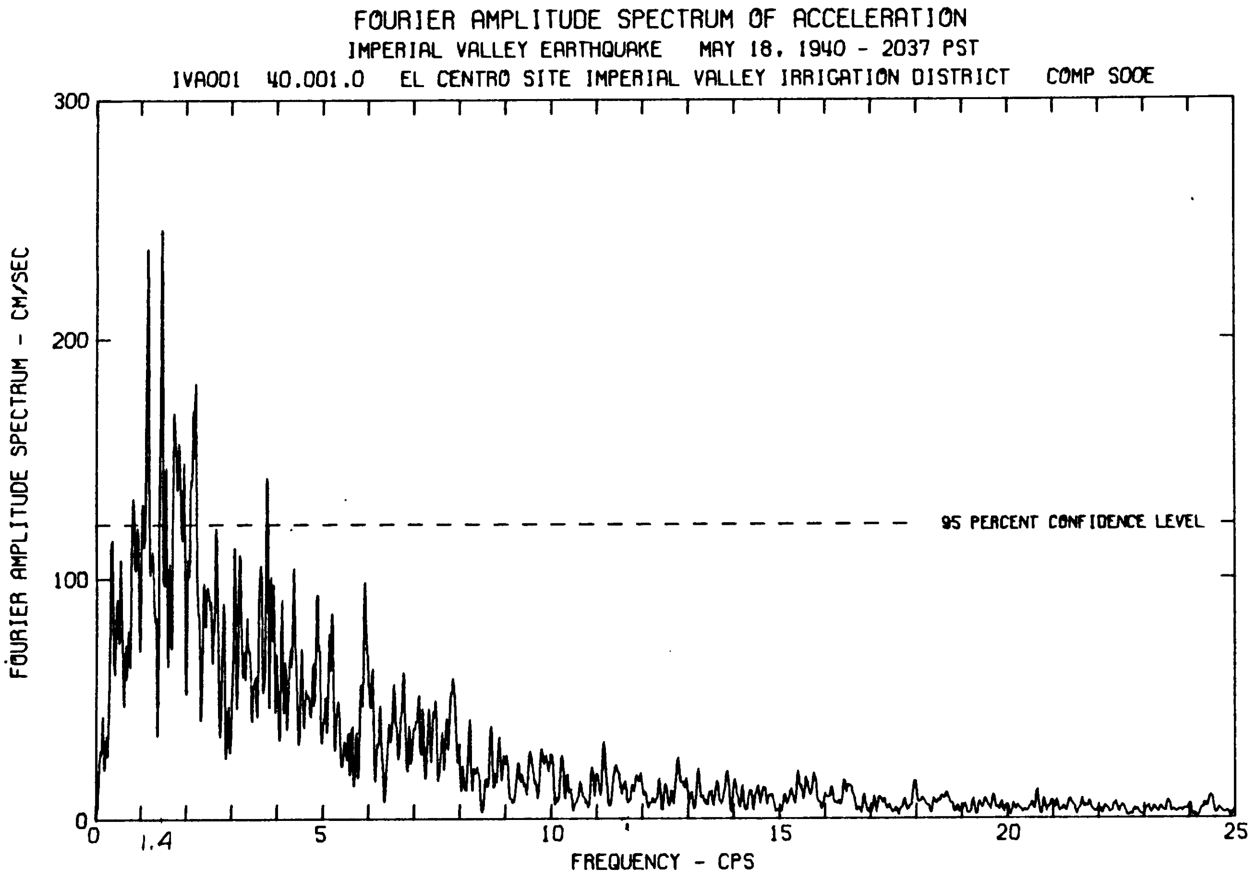

FOURIER AMPLITUDE SPECTRUM OF ACCELERATION
IMPERIAL VALLEY EARTHQUAKE MAY 18, 1940 - 2037 PST
IVA001 40.001.0 EL CENTRO SITE IMPERIAL VALLEY IRRIGATION DISTRICT COMP SOOE
FOURIER AMPLITUDE SPECTRUM - CM/SEC
300
200
100
0
95 PERCENT CONFIDENCE LEVEL
0
1.4
5
10
15
20
25
FREQUENCY - CPS

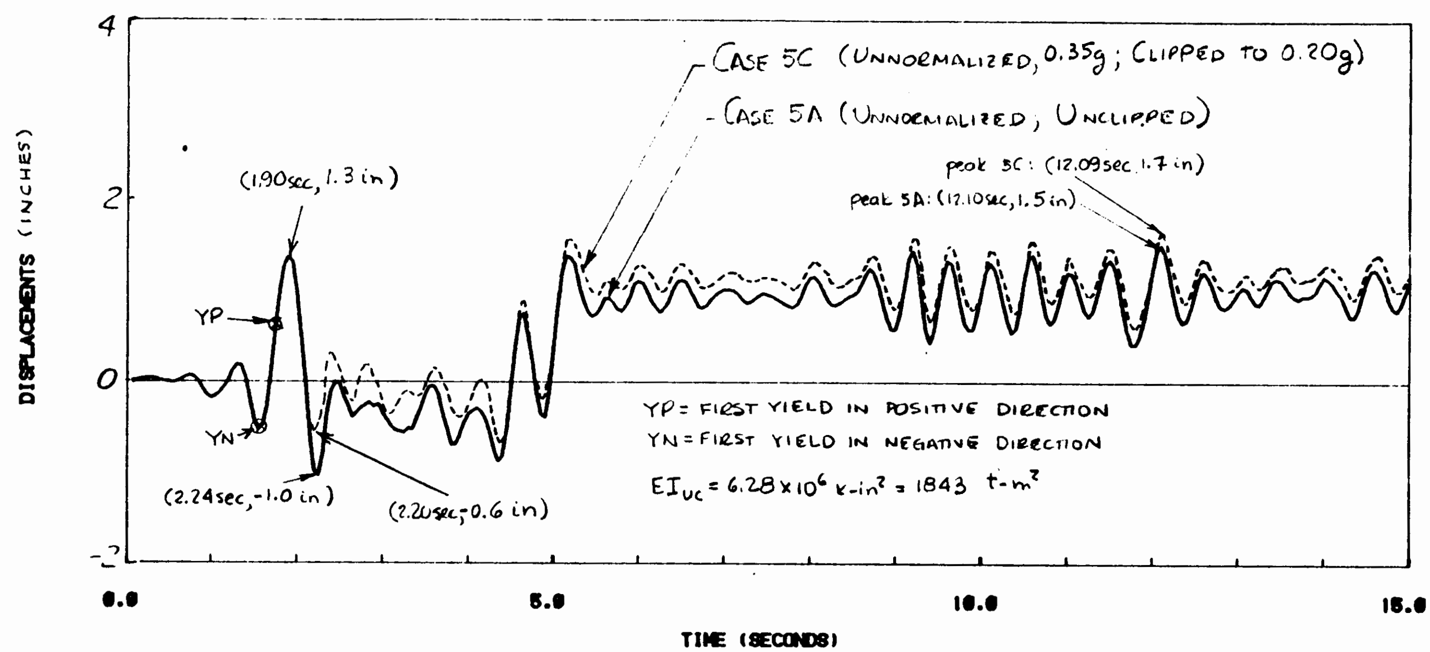

Fig. 6.13 Effect of Clipping El Centro Unnormalized (Recorded) on Displacement Response of a 2DOF Canopy Model (Cases 5A & 5C)

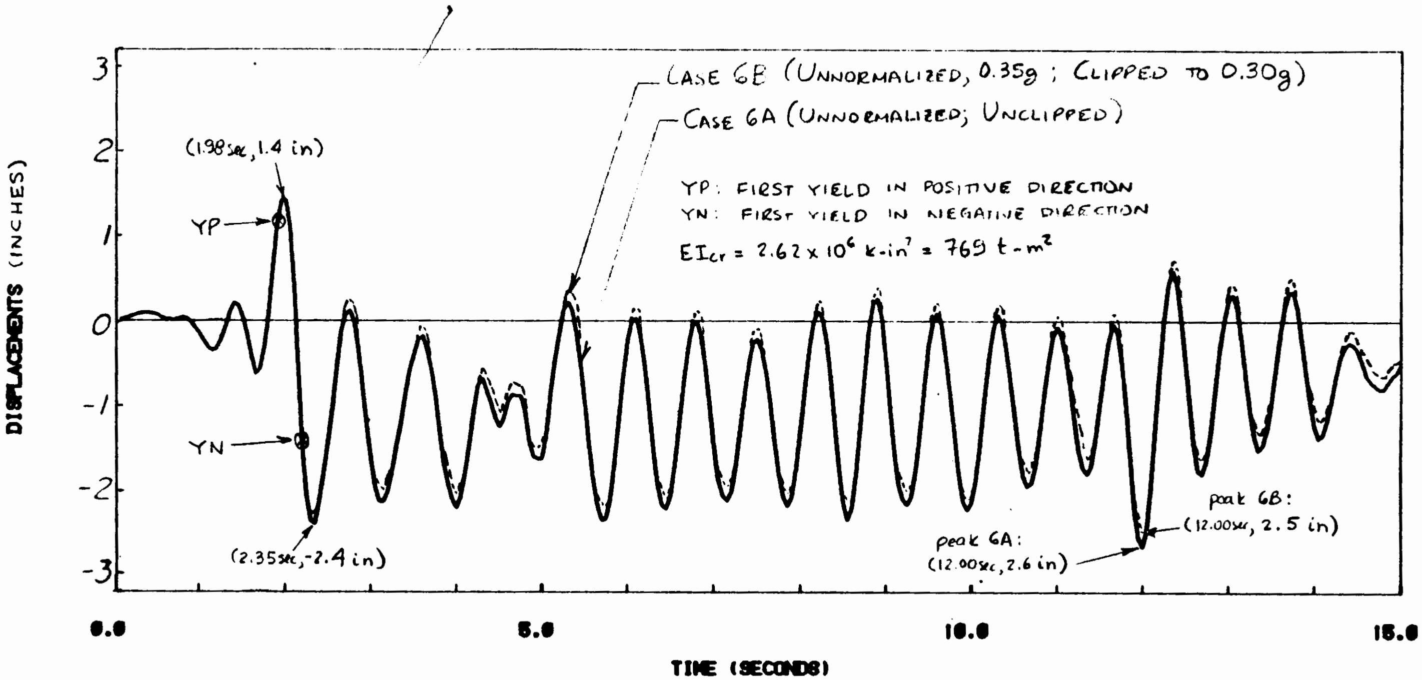

Fig. 6.14 Effect of Clipping El Centro Unnormalized (Recorded) on Displacement Response of a 2DOF Canopy Model (Cases 6A & 6B)

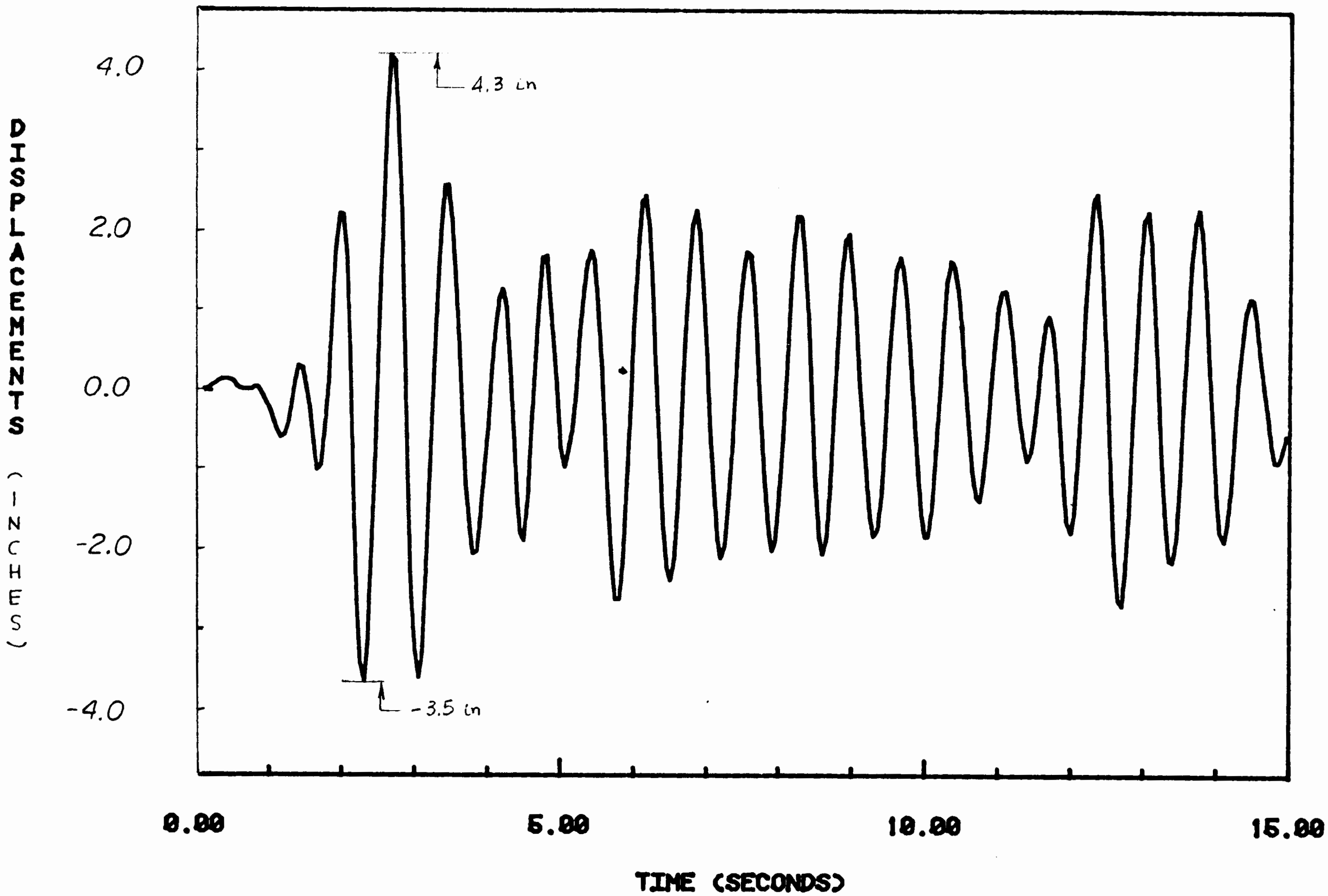

FIG. 6.15 ELASTIC RESPONSE OF CANOPY SUBJECT TO EL CENTRO NORMALIZED TO 0.55g.

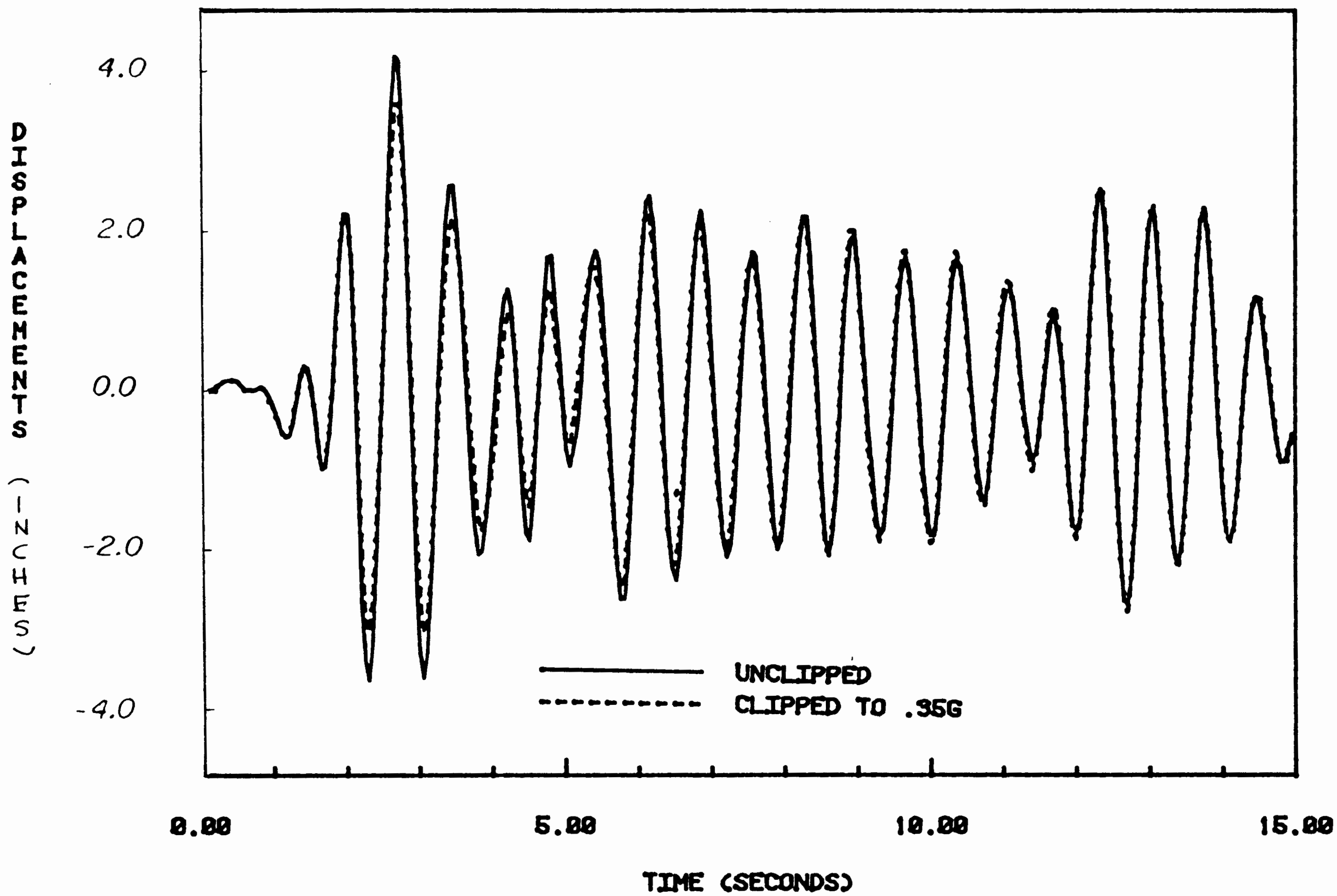

Fig. 6.16 Effect of Clipping El Centro Normalized to 0.55g on Elastic Displacement Response of the Canopy

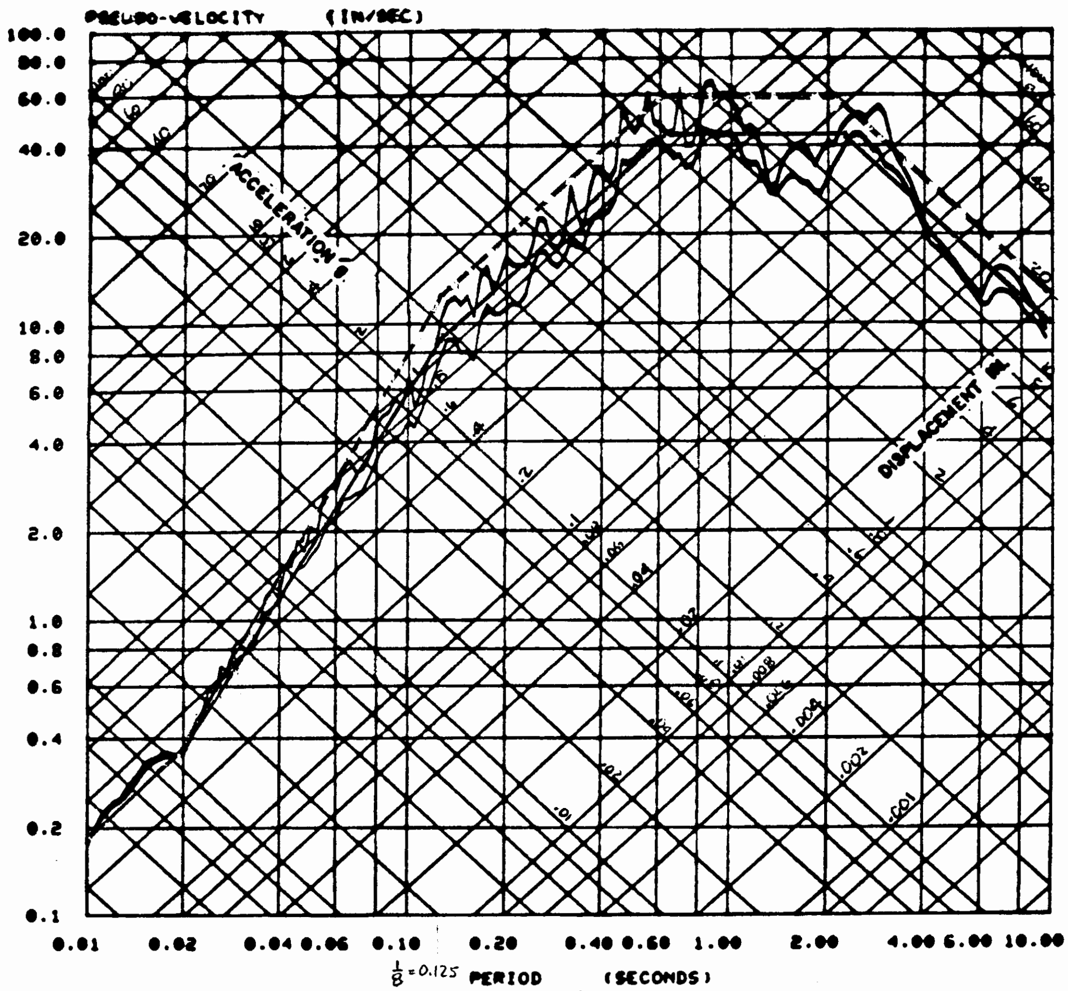

FIG. 7.1 ELASTIC RESPONSE SPECTRA FOR EL CENTRO 1940 NORMALIZED TO 0.55g AND CLIPPED TO 0.28g FOR DAMPING = ξ = 2%, 5%.

Note: Straight lines correspond to the elastic design response spectra simplifications for:

ξ = 2% — — — — — —

ξ = 5% ————————

Fig. 7.2 a) Comparison of Elastic Design Response Spectra (EDRS) Based on Method Used in This Study vs. Newmark & Hall Method ($\xi = 2\%$)

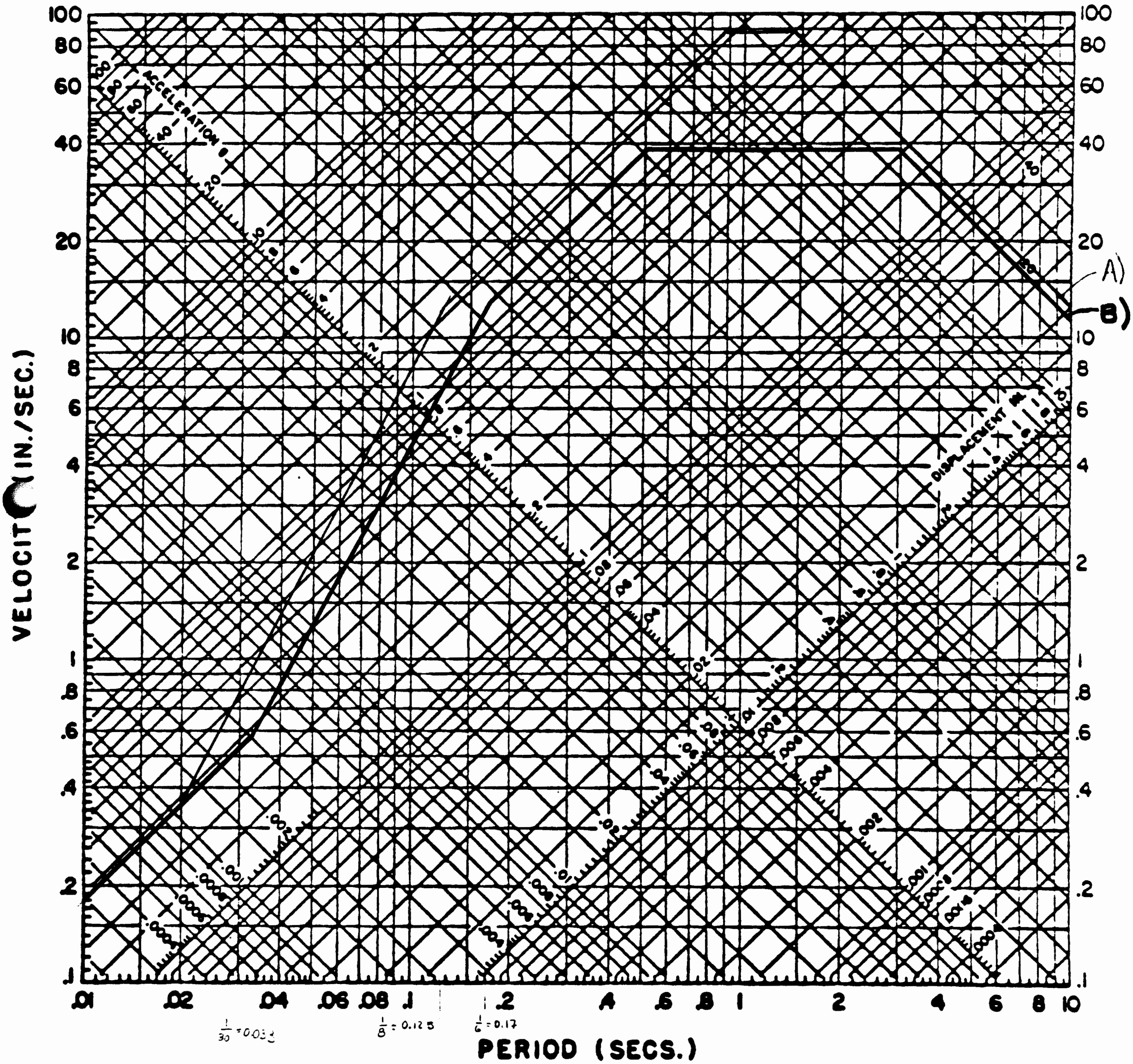

A) EDRS Based on Method Used in this Study

B) EDRS Based on Newmark & Hall Method

Fig. 7.2 b) Comparison of Elastic Design Response Spectra (EDRS) Based on Method Used in This Study vs. Newmark & Hall Method ($\xi = 5\%$)

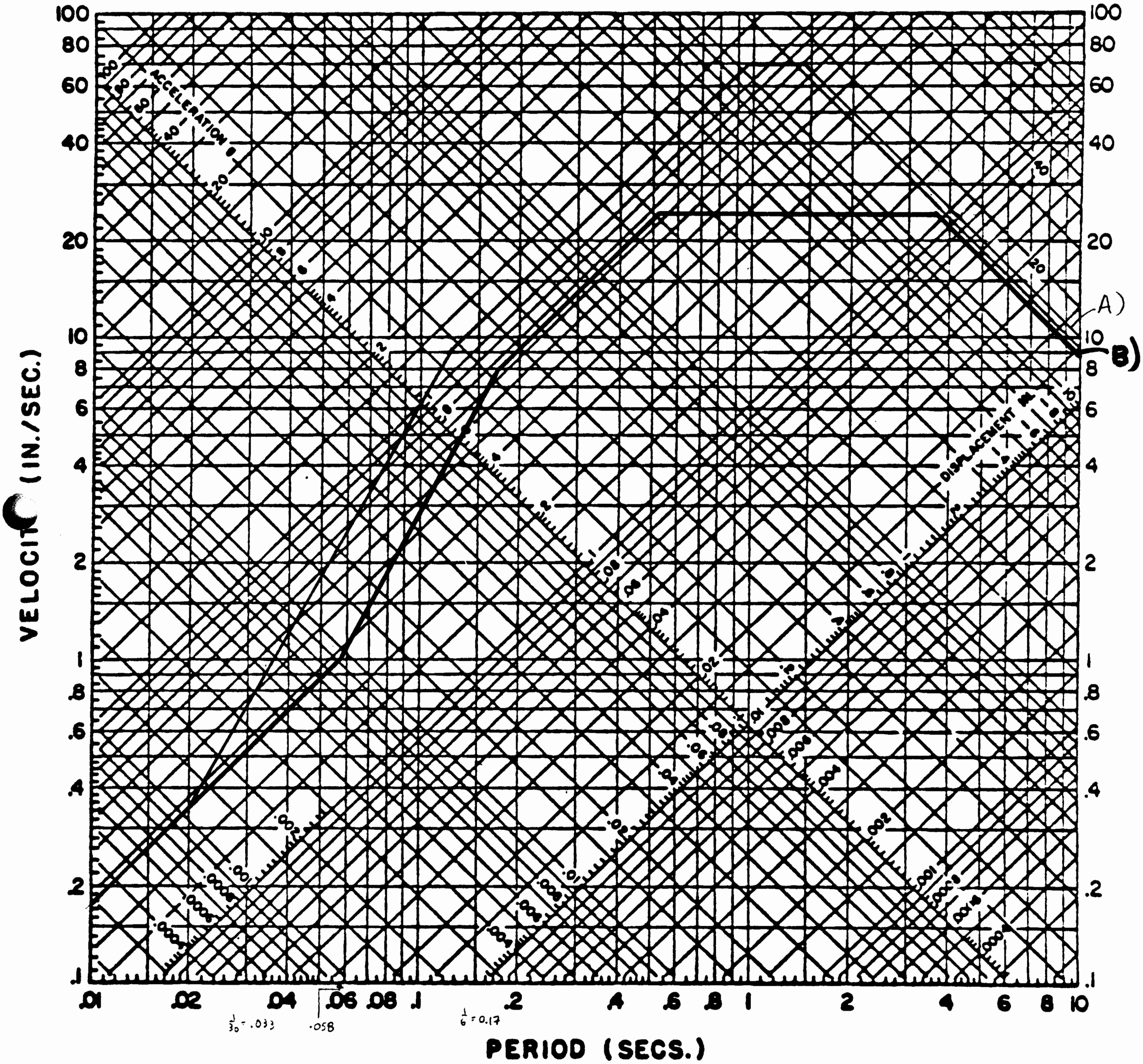

A) EDRS Based on Method Used in This Study

B) EDRS Based on Newmark & Hall Method

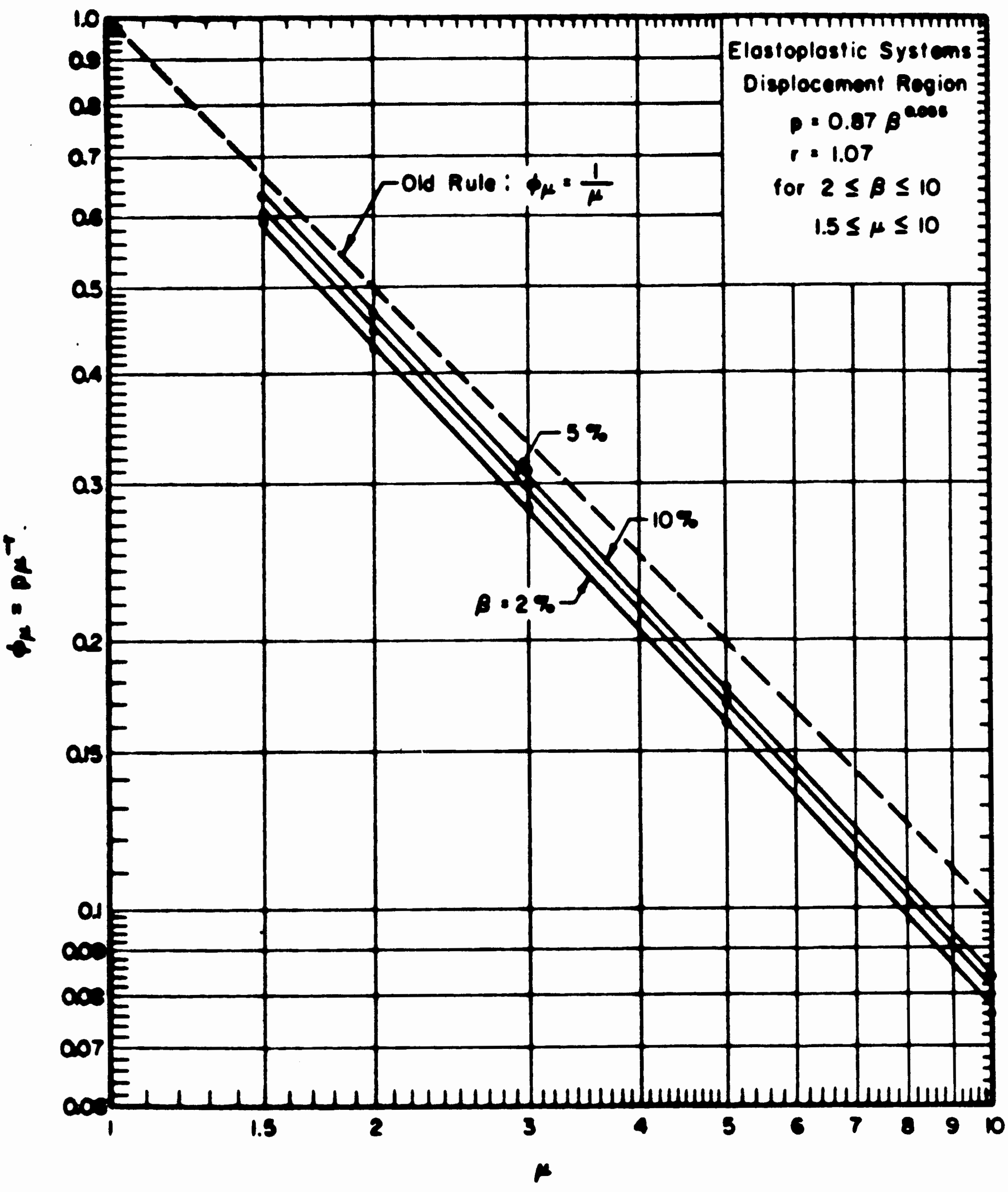

FIG. 7.3 DEAMPLIFICATION FACTORS DERIVED BY RIDDELL AND AND NEWMARK (REF. 20), DISPLACEMENT REGION

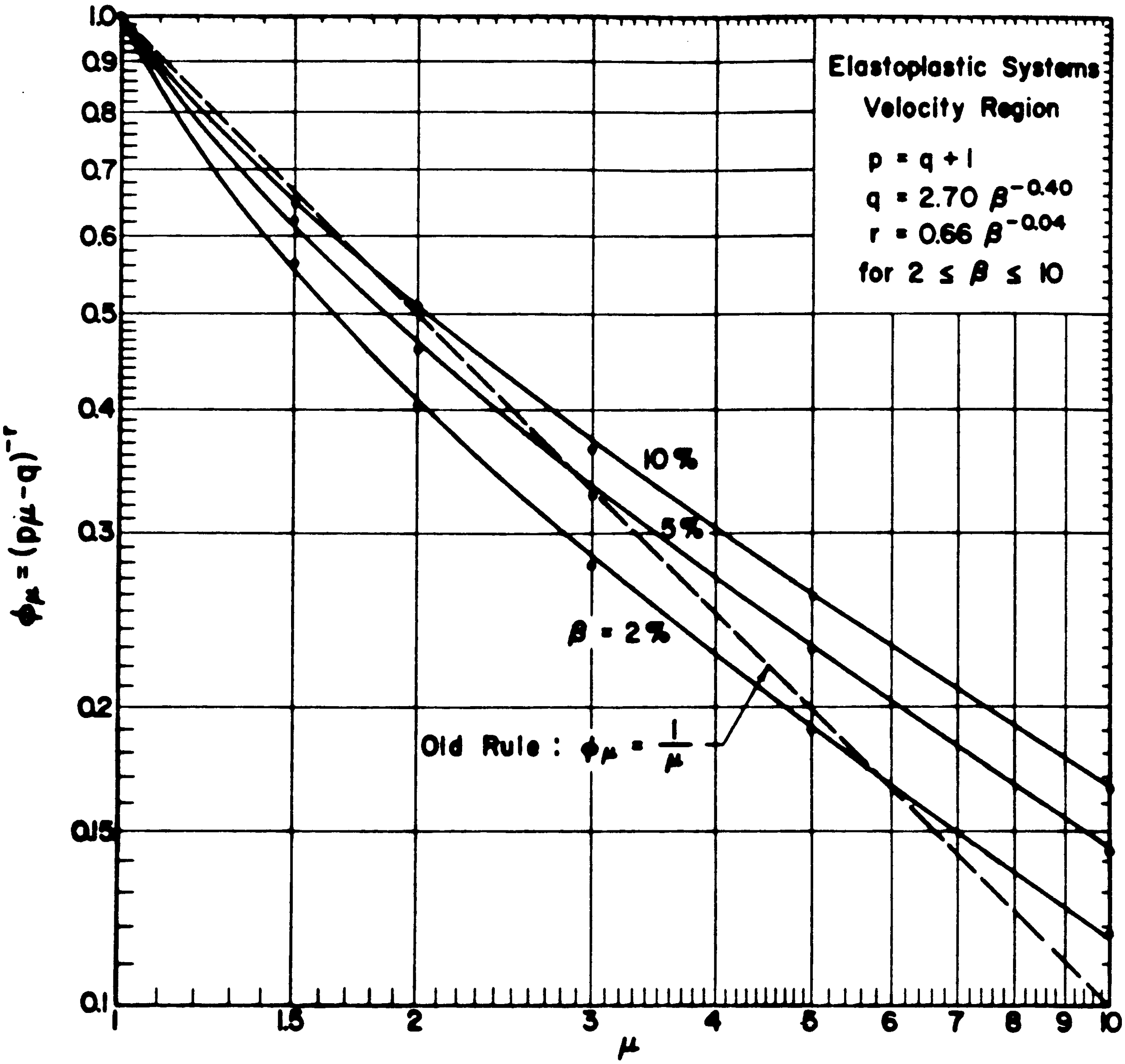

FIG. 7.4 DEAMPLIFICATION FACTORS DERIVED BY RIDDELL AND NEWMARK (REF. 20), VELOCITY REGION

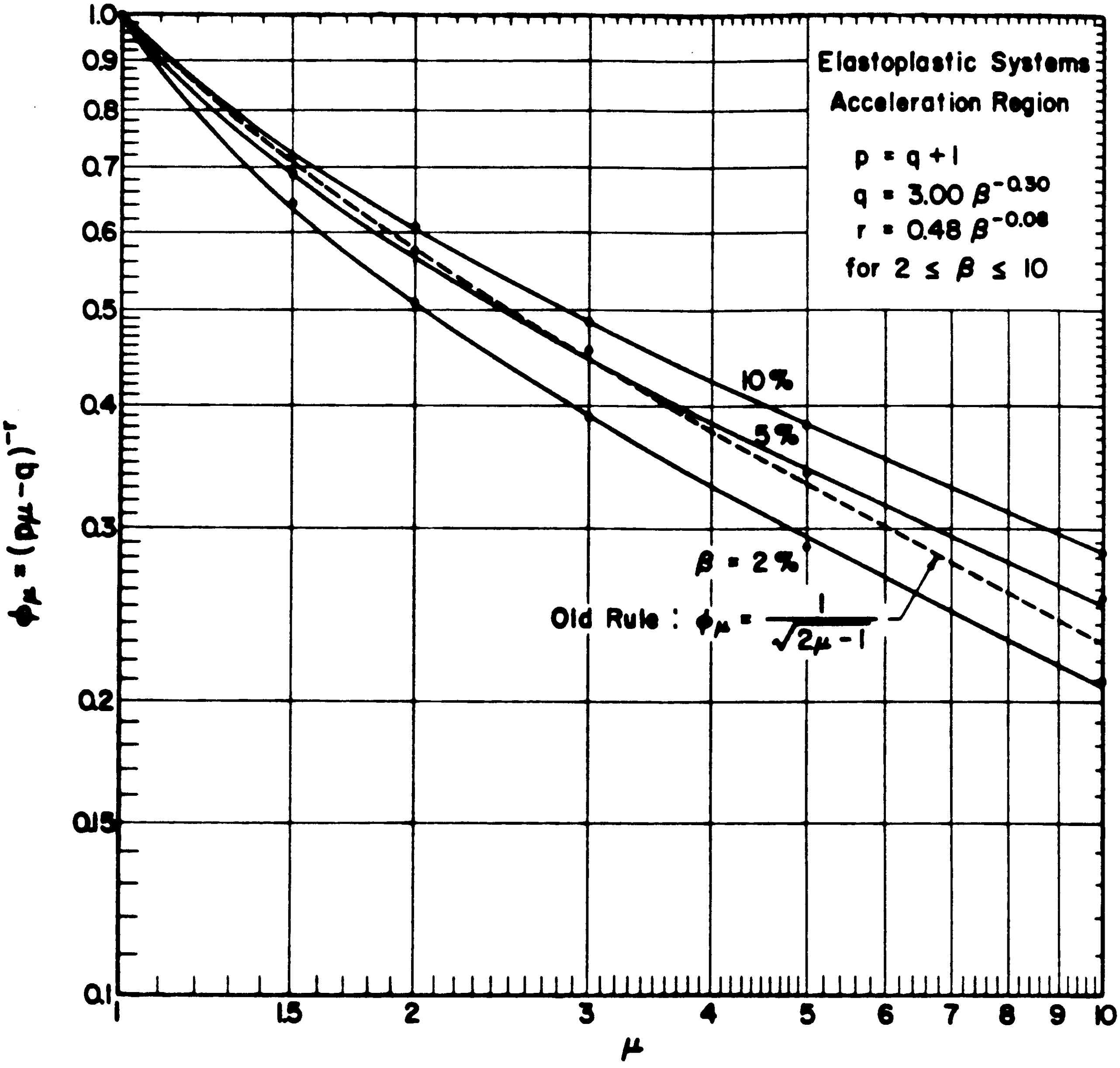

Fig. 7.5 Deamplification Factors Derived by Riddell and Newmark (Ref. 20), Acceleration Region

FIG. 7.6a) SUGGESTED DESIGN RESPONSE SPECTRA ($\xi = 2\%$, $\mu_s = 5$)

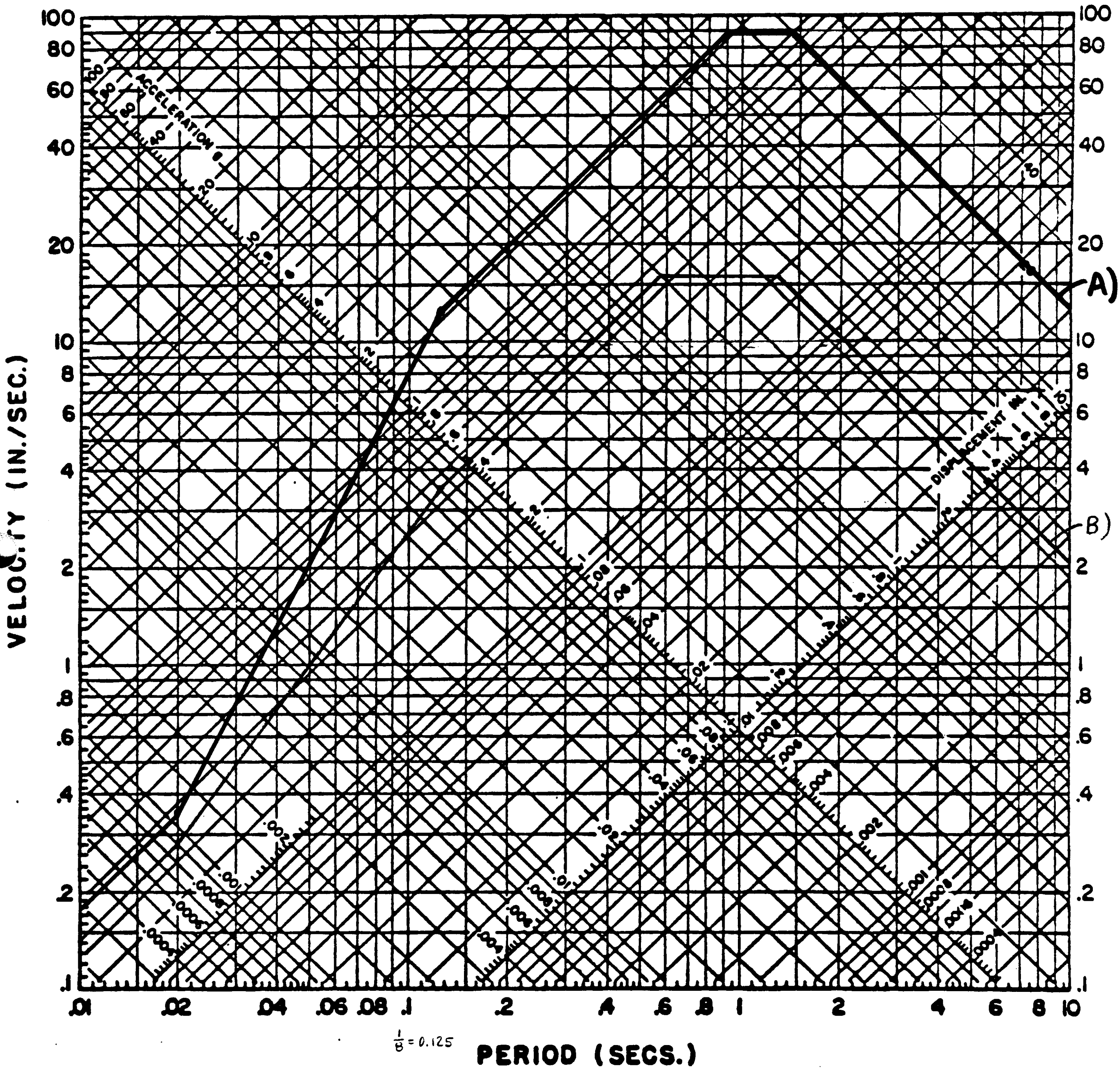

A) ELASTIC DESIGN RESPONSE SPECTRUM

B) INELASTIC DESIGN RESPONSE SPECTRUM

FIG. 7.6 b) SUGGESTED DESIGN RESPONSE SPECTRA ($\xi = 5\%$, $\mu_s = 5$).

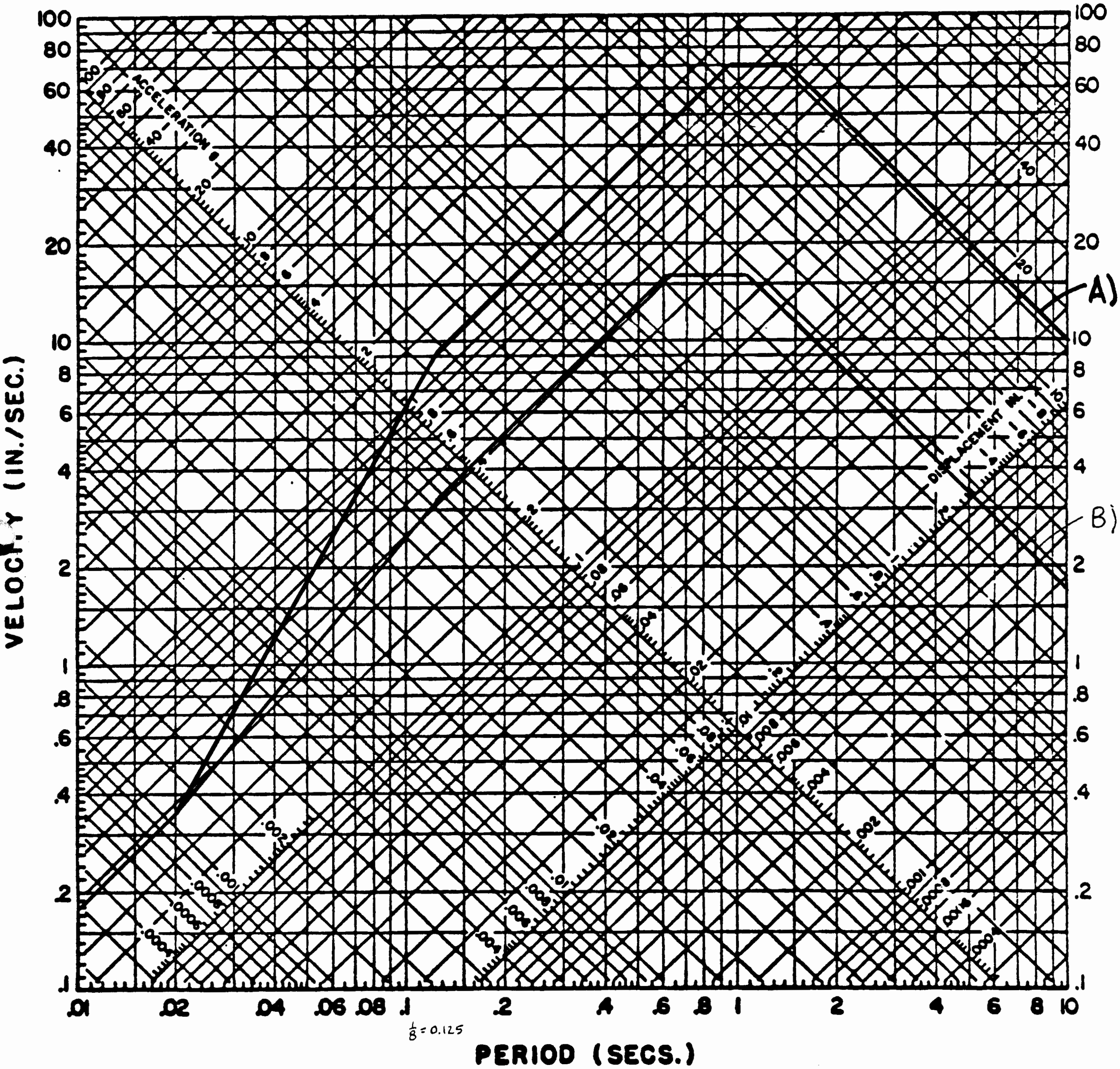

A) ELASTIC DESIGN RESPONSE SPECTRUM

B) INELASTIC DESIGN RESPONSE SPECTRUM

APPENDIX A

EVALUATION OF PROPERTIES OF STRUCTURAL SYSTEM

A.1 System Idealization

For computation of properties of system, the system will be idealized as follows:

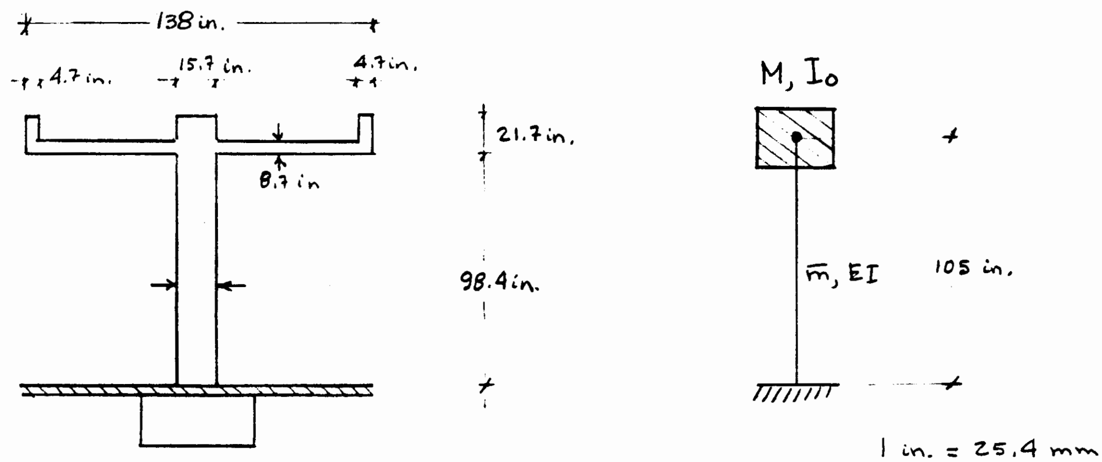

A.2 Calculation of M and $\bar{m}$

The concentrated mass tributary to each of the columns of the canopy, due to its roof is given by:

$$M = [8.65\times10^{-5}][(21.7\times138)-(138-9.4-15.7)(13)]\times[766/4][1/386] = 0.0655 \ \text{k-sec}^2/\text{in}$$

the distributed mass $\bar{m}$ throughout the canopy's column is:

$$\bar{m} = [8.65\times10^{-5}][(\tfrac{\pi}{4})(13.8)^2][1/386] = 3.35\times10^{-5} \ (\text{k-sec}^2/\text{in.})/(\text{in.})$$

A.3 Calculation of I_o

the polar moment of inertia is : $\bar{I}_\theta = I_x + I_y$

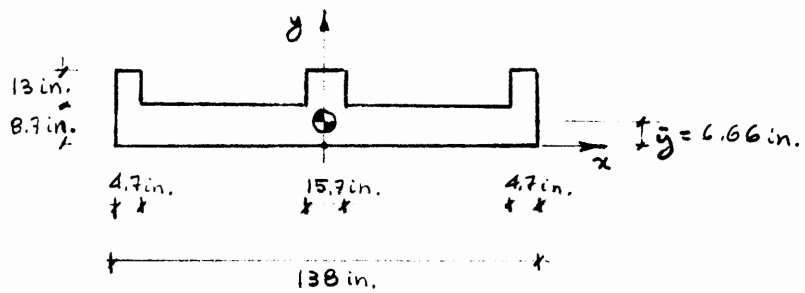

$y_i A_i = (25.1)(13)(15.2) + (138)(8.7)(4.35) = 10,180 \text{ in}^3$

$A_i = (138)(8.7) + (25.1)(13) = 1,527 \text{ in}^2$

$\bar{y} = y_i A_i / A_i = 6.66$ in

$I_x = \left[\frac{1}{12} \times 25.1 \times (21.7)^3\right] + \left[(25.1 \times 21.7)\left(\frac{21.7}{2} - 6.66\right)^2\right] + \left[\frac{1}{12} \times 112.9 \times (8.7)^3\right] + \left[(112.9)(8.7)\left(6.66 - \frac{8.7}{2}\right)^2\right] =$

$= 42,370 \text{ in.}^4$

$I_y = \left[\frac{1}{12} \times 8.7 \times (138)^3\right] + \left[\frac{1}{12} \times 13 \times (15.7)^3\right] + \left[\frac{2}{12} \times 13 \times (4.7)^3\right] + \left[2 \times (13 \times 4.7)(66.7)^2\right] =$

$= 2.453 \times 10^6 \text{ in.}^4$

$\bar{I}_\theta = I_x + I_y = 2.495 \times 10^6 \text{ in.}^4$

Total mass moment of inertia :

$I_o' = \rho \cdot L \cdot \bar{I}_\theta / g = (8.65 \times 10^{-5} \text{ k/in}^3)(766 \text{ in.})(2.495 \times 10^6 \text{ in.}^4)/(386 \text{ in./sec}^2)$

$I_o' = 428$ k-in.-sec^2

At each column : $I_o = I_o'/4 = 107$ k-sec^2-in

A.4 Computation of EI_{uc} (uncracked transformed stiffness)

A.4.1 Case $d' = 2.2$ in.

f'_c		E_c		$\eta = \frac{E_s}{E_c}$	A	I	EI_{uc}	
MPa	ksi	MPa	ksi		(in.^{2})	(in.^{4})	kN-in.^{2}	$\times 10^6$ k-in^2
17 21	2.5 3.0	19,600 21,500	2850 3120	10.2 9.3	189 186	2,230 2,190	18,000 19,400	6.28 6.75

Notes: $E_c = 57\sqrt{1000 f'_c}$, ksi
$E_s = 29{,}000$ ksi $= 200{,}000$ MPa
$A = \pi(6.9)^2 + (n-1)(4.42)$, in.^{2}
$I = [\pi(6.9)^4/4] + [(n-1)(0.442)][2(4.69)^2 + 4(3.80)^2 + 4(1.50)^2]$, in.^{4}

f'_c		f_r		M_{cr}		ϕ_{cr}		Axial Load
MPa	ksi	MPa	ksi	kN-m	k-in	$\times 10^{-3}$ rad/m	$\times 10^{-3}$ rad/in	P, kips
17 21	2.5 3.0	2.6 2.8	0.375 0.411	13.6 14.6	120 129	0.753 0.753	0.0191 0.0191	0
17 21	2.5 3.0	2.6 2.8	0.375 0.411	18.6 19.7	165 174	1.04 1.02	0.0263 0.0258	26

Notes: $f_r = 0.0075\sqrt{1000 f'_c}$, ksi
For axial load $P = 0^k$: $M_{cr} = \frac{f_r I}{y_l}$; $\phi_{cr} = \frac{(f_r/E_c)}{y_b}$

For axial load $P = 26^k$: $M_{cr} = \left(f_r + \frac{P}{A}\right)\left(\frac{I}{y_b}\right)$; $\phi_{cr} = M_{cr}/E_c I$

A.4.2 Case $d' = 1.7$ in.

f'_c		E_c		$n = \frac{E_s}{E_c}$	A	I	EI_{uc}	
MPa	ksi	MPa	ksi		(in.^{2})	(in.^{4})	kN-m^2	$\times 10^6$ k-in^2
17 21	2.5 3.0	19,600 21,500	2850 3120	10.2 9.3	189 186	2320 2270	18,800 20,200	6.56 7.04

Notes: $E_c = 57\sqrt{1000 f'_c}$, ksi
$E_s = 29{,}000$ ksi $= 200{,}000$ MPa
$A = \pi(6.9)^2 + (m-1)(4.42)$
$I = [(\pi/4)(6.9)^4] + [(m-1)(0.442)][2(5.2)^2 + 4(1.62)^2 + 4(4.21)^2]$, in.^{4}

f'_c		f_r		M_{cr}		ϕ_{cr}		Axial Load
MPa	ksi	MPa	ksi	kN-m	k-in	$\times 10^{-3}$ rad/m	$\times 10^{-3}$ rad/in	P, kips
17 21	2.50 3.00	2.6 2.8	0.375 0.411	14.1 15.1	125 134	0.753 0.753	0.0191 0.0191	0
17 21	2.50 3.00	2.6 2.8	0.375 0.411	19.4 20.3	172 180	1.03 1.01	0.0263 0.0257	26

Notes: $f_r = 0.0075\sqrt{1000 f'_c}$, ksi
For axial load $P = 0^k$: $M_{cr} = \frac{f_r I}{y_b}$; $\phi_{cr} = \frac{(f_r/E_c)}{y_b}$
For axial load $P = 26^k$: $M_{cr} = \left(f_r + \frac{P}{A}\right)\left(\frac{I}{y_b}\right)$; $\phi_{cr} = \frac{M_{cr}}{E_c I}$

A.5 Computation of EI_{cr} (cracked transformed stiffness)

Results obtained from RCCOLA will be used here.

f'_c		f_y		M_y		ϕ_y		EI_{cr}		d'
				VALUES GIVEN BY RCCOLA FOR						
MPa	ksi	MPa	ksi	KN-m	k-in	$\times 10^{-3}$ rad/m	$\times 10^{-3}$ rad/in	KN-m^2	$\times 10^{6}$ k-in^2	(in.)
17 21	2.5 3.0	280 350	40 50	69.2 85.3	612 755	9.2 11.0	0.233 0.280	7,520 7,750	2.62 2.70	2.2
17 21	2.5 3.0	280 350	40 50	72.2 88.7	639 785	8.5 10.2	0.216 0.259	8,500 8,700	2.96 3.03	1.7

APPENDIX B

NUMERICAL COMPUTATION OF PERIOD OF CANOPY

B.1 Generalized SDOF Model

The period of the structure will be computed using Raleigh's method assuming a first mode shape:

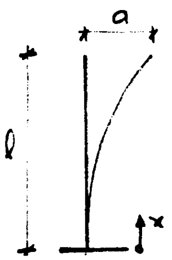

Fig. B.1

$$v(x) = \left(1 - \cos\frac{\pi x}{2\ell}\right)a$$

$$v'(x) = \left(\sin\frac{\pi x}{2\ell}\right)\left(\frac{\pi a}{2\ell}\right)$$

$$v''(x) = \left(\cos\frac{\pi x}{2\ell}\right)\left(\frac{\pi}{2\ell}\right)^2 a$$

$$w^2 = \frac{\int_0^\ell EI\, v''^2\, dx}{\int_0^\ell \bar{m}\, v^2 dx + M v^2(\ell) + I_0\, v'(\ell)^2} = \frac{k^*}{m^*}$$

- Evaluation of terms: [Ref.]

$$\int_0^\ell v^2 dx = a^2 \int_0^\ell \left(1 - \cos\frac{\pi x}{2\ell}\right)^2 = 0.228\, L a^2$$

$$v'(\ell) = \frac{\pi a}{2\ell} \quad ; \quad v(\ell) = a$$

$$EI \int_0^\ell v''^2 dx = \frac{\pi^4}{32} \cdot \frac{EI}{\ell^3} \cdot a^2$$

$$\therefore\ w^2 = \frac{\frac{\pi^4}{32} \cdot \frac{EI}{\ell^3} \cdot a^2}{(\bar{m})(0.228 \ell \cdot a^2) + M a^2 + I_0 \left(\frac{\pi}{2\ell}\right)^2 (a^2)}$$

$$w^2 = \frac{\frac{\pi^4}{32} \cdot \frac{EI}{(105)^3}}{\underbrace{(3.35\times10^{-5})(0.228\times105)}_{0.000802} + (0.0655) + \underbrace{(107)\left(\frac{\pi}{2\times105}\right)^2}_{0.0239}} = \frac{0.0000026\ EI}{0.0902} = \frac{k^*}{m^*}$$

$$w^2 = 0.0000291\ EI$$

- With $EI_{uc} = 6.28\times10^6$ k-in^2 (uncracked, see Appendix A)

$$w_1^2 = 184 \left(\frac{rad}{sec}\right)^2 \Rightarrow w_1 = 13.6 \frac{rad}{sec} \Rightarrow T_1 = \frac{2\pi}{w_1} = 0.464 \text{ sec}$$

- With $EI_{cr} = 2.62\times10^6$ k-in^2 (cracked, see Appendix A)

$$w_1^2 = 76.6 \left(\frac{rad}{sec}\right)^2 \Rightarrow w_1^2 = 8.75 \frac{rad}{sec} \Rightarrow T_1 = \frac{2\pi}{w_1} = 0.72 \text{ sec}$$

Actually, the column has different EI's along its length, due to the fact that the moments vary and are large enough to force certain sections of the columns into the non-linear range.

An approximate procedure will be followed in order to calculate the period considering that the value of EI will not be constant throughout the column's length.

The upper half of the cantilever will be assumed uncracked and the lower half will be cracked.

It is hard to find the variation of EI's along the lower half of the column. However, since the moments that caused the failure were close to yielding, a constant value of EI_{cr} will be used in order to approximate the period of the canopy.

$$k^* = EI_{cr}\int_0^{\ell/2} \frac{\pi^4}{16\ell^4}\cdot a^2 \cdot \cos^2\frac{\pi x}{2\ell}\,dx + EI_{uc}\int_{\ell/2}^{\ell} \frac{\pi^4}{16\ell^4}\cdot a^2\cdot \cos^2\frac{\pi x}{2\ell}\,dx$$

$$= \frac{EI_{cr}\pi^4 a^2}{16\ell^4}\left\{\left[\frac{1}{2}x + \frac{\ell}{2\pi}\sin\frac{\pi x}{\ell}\right]_0^{\ell/2} + \left[\frac{EI_{uc}}{EI_{cr}}\right]\left[\frac{1}{2}x + \frac{\ell}{2\pi}\sin\frac{\pi x}{\ell}\right]_{\ell/2}^{\ell}\right\}$$

$$= \frac{EI_{cr}\pi^4 a^2}{16\ell^4}\left\{\left[\frac{\ell}{4} + \frac{\ell}{2\pi}\right] + \left[\frac{\ell}{4} + \frac{\ell}{2\pi}(0-1)\right]\left[\frac{EI_{uc}}{EI_{cr}}\right]\right\}$$

$$= \frac{(2.62\times10^6)\pi^4 a^2}{16(105)^3}\left\{\left[\frac{1}{4} + \frac{1}{2\pi}\right] + \left[\frac{1}{4} - \frac{1}{2\pi}\right]\left[\frac{6.28}{2.62}\right]\right\}$$

$$k^* = 8.64$$

Using this value of k^*:

$$\therefore\ \omega_1^2 = \frac{8.64}{0.0902} = 96.0\left(\frac{rad}{sec}\right)^2 \Rightarrow \omega_1 = 9.80\ rad/sec$$

$$\Rightarrow T_1 = \frac{2\pi}{\omega_1} = 0.64\ sec$$

It is concluded in Chapter V that the initial period is closer to 0.44 sec and it is decided that a period of T=0.50 sec will be used in the first stage of the analyses.

Therefore: $\omega = \frac{2\pi}{0.50} = 12.57\ rad/sec \Rightarrow \omega^2 = 158\ (rad/sec)^2$

$$\omega^2 = \frac{k^*}{m^*} = \frac{2.6\times10^{-6}\,EI}{0.0902} = 158 \Rightarrow EI = 5.5\times10^6\ k\text{-}in^2$$

that is: $k^* = (2.6\times10^{-6})(5.5\times10^6) = 14.3\ k/in$

Another way to consider the inelastic displacements would be to assume a function of the type (Fig. B.2)

$$\psi_T = (1 - \cos\frac{\pi x}{2L})\, a_y + (\mu_\delta - 1)(x/L)\, a_y$$

Since k^* involves a second derivative ($\because k^* = \int_0^L EI(\psi_T'')^2 dx$), then the second term in the above expression will not contribute to the stiffness and therefore: $k^* = (2.6\times10^{-6})(EI)(a_y)^2$, as before.

For the determination of m^*, it will be assumed that the contribution of the distributed mass $\bar{m}$ is negligible. Note that:

$\psi_T(L) = \mu_\delta\, a_y$; $\psi_T'(L) = (\mu_\delta + 0.57)\frac{a_y}{L}$

$$m^* = \int_0^L \bar{m}\,[\psi(x)]^2 dx + M[\psi(L)]^2 + I_o\,[\psi'(L)]^2$$

$$= 0 + M(\mu_\delta a_y)^2 + I_o\left[(\mu_\delta + 0.57)\frac{a_y}{L}\right]^2 = \left\{M\mu_\delta^2 + \frac{I_o}{L^2}\left[\mu_\delta^2 + 1.14\mu_\delta + 0.325\right]\right\}a_y^2$$

$$= \left[\left(M + \frac{I_o}{L^2}\right)\mu_\delta^2 + \frac{1.14 I_o}{L^2}\mu_\delta + \frac{0.325 I_o}{L^2}\right]a_y^2$$

$$= \left[0.0752\,\mu_\delta^2 + 0.0111\,\mu_\delta + 0.00315\right]a_y^2$$

$$\therefore\ \omega^2 = \frac{k^*}{m^*} = \frac{2.6\times10^{-6}\,EI}{(0.0752\,\mu_\delta^2 + 0.0111\,\mu_\delta + 0.00315)}$$

The following Table summarizes the results obtained:

EI (k-$in.^2$)	Displ. Duct. μ_δ	ω^2 $(rad/sec)^2$	ω (rad/sec)	T (sec)
6.28×10^6 (Uncracked)	1	183	13.5	0.46
	2	50.1	7.08	0.89
	3	22.9	4.78	1.31
	4	13.1	3.61	1.74
	5	8.42	2.90	2.17
2.67×10^6 (cracked)	1	76	8.7	0.72
	2	20.9	4.57	1.37
	3	9.55	3.09	2.03
	4	5.45	2.33	2.69
	5	3.51	1.87	3.35

From the previous table it can be seen that the inclusion of the inelastic shape function $\Psi(x)$ described above leads to the conclusion that once inelastic displacements occur, the value of μ_s becomes extremely important in the determination of the period. (The relationship between μ_s and T is close to a linear one).

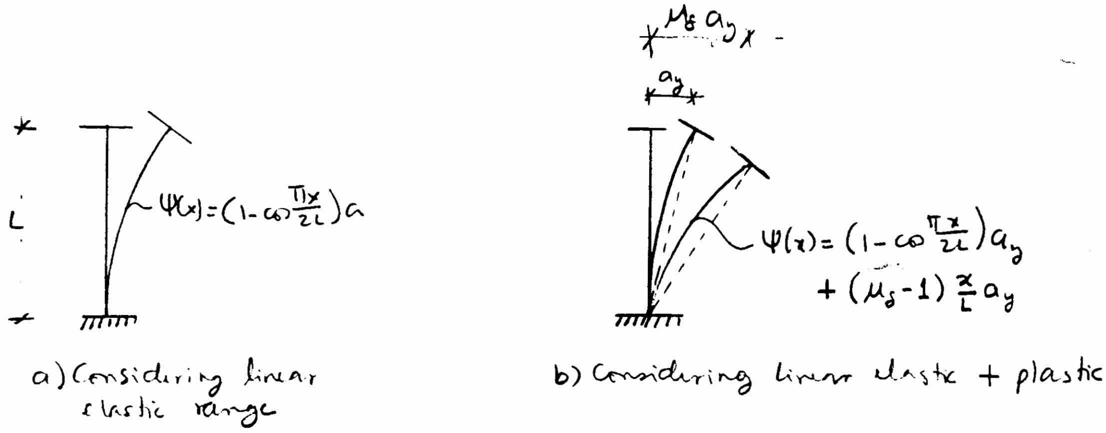

FIG. B.2 MODE SHAPE ASSUMED FOR ESTIMATION OF PERIOD IN INELASTIC RANGE

Geometric Stiffness

The influence of the geometric stiffness on the combined stiffness is to be evaluated.

$$k_G = N \int_0^L (\psi'(x))^2\, dx = N \int_0^L \left(\frac{\pi a}{2L} \sin \frac{\pi x}{2L} \right)^2 dx = N \left(\frac{\pi a}{2L}\right)^2 \left\{\frac{2L}{\pi}\right\} \left\{ \frac{\pi x}{4L} - \frac{1}{4} \sin \frac{\pi x}{L} \Big|_0^L \right\}$$

$$= \left\{ \frac{N\pi}{2L} a^2 \right\} \left\{ \frac{\pi}{4} \right\} = \frac{N\pi^2}{8L} a^2 = \frac{(26)\pi^2 a^2}{8(105)} = 0.305\ a^2$$

$$k_{elastic} = (2.6 \times 10^{-6}\ EI)\, a^2 = (2.6 \times 10^{-6})(5.5 \times 10^{6}) = 14.3\ a^2$$

$$\bar{k} = k_{elastic} - k_G \doteq 14\ a^2$$

$(k_G / \bar{k}) \times 100 \doteq 2.2\%$ $\longrightarrow$ not too much !

Therefore it may be ignored.

B.2 2DOF Model

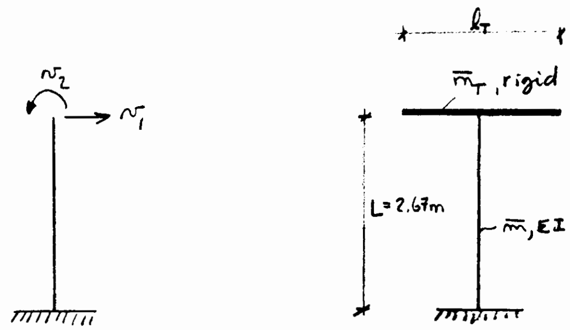

B.2.1 Dynamic Properties

i) Stiffness

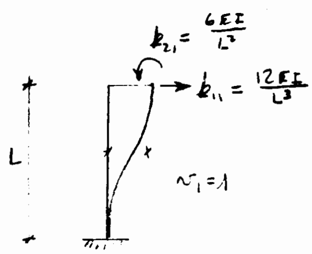

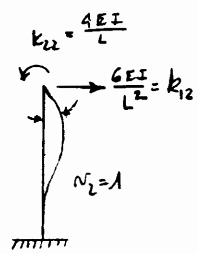

$$\underline{k} = \frac{2EI}{L^3}\begin{bmatrix} 6 & 3L \\ 3L & 2L^2 \end{bmatrix}$$

ii) Mass

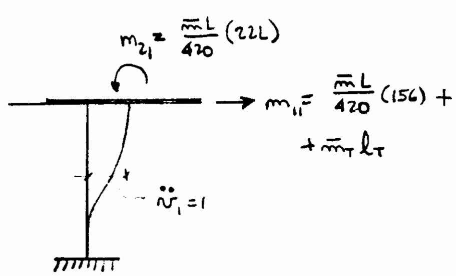

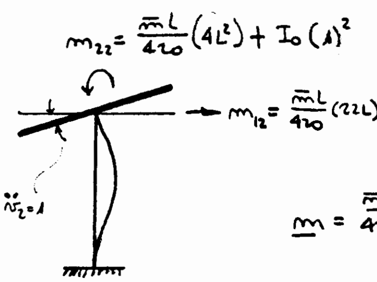

$$\underline{m} = \frac{\bar{m}L}{420}\begin{bmatrix} 156 + \frac{420}{\bar{m}L}\bar{m}_T l_T & 22L \\ 22L & 4L^2 + \frac{420}{\bar{m}L} I_0 \end{bmatrix}$$

For this case: $L = 105$ in. ; $l_T = 138$ in.
$\bar{m} = 3.35 \times 10^{-5}$ (k-sec²/in.)/in. ; $\bar{m}_T = \frac{0.0655}{138} = 0.000475$ (k-sec²/in)/in
$I_0 = 107$ k-sec² - in.

$$m^* = \begin{bmatrix} (0.00131 + 0.0655) & (0.0193) \\ (0.0193) & (0.369 + 107) \end{bmatrix} \approx \begin{bmatrix} 0.0655 & 0 \\ 0 & 107 \end{bmatrix}$$

$$k^* = \frac{EI}{10^4}\begin{bmatrix} 0.104 & 5.442 \\ 5.442 & 381 \end{bmatrix}$$

B.2.2 Frequencies and Periods of Modes

$$\underline{k} - \omega^2 \underline{m} = \frac{EI}{10{,}000}\begin{bmatrix} 0.104 - 0.0655B & 5.442 \\ 5.442 & 381 - 107B \end{bmatrix} \quad ; \quad B = \frac{10000}{EI}\omega^2$$

Set $\Delta = 0$: $(0.104 - 0.0655B)(381 - 107B) - (5.442)^2 = 0$

$\Rightarrow 7.009B^2 - 36.08B + 10.01 = 0$

$B_1 = 0.2942 \Rightarrow \omega_1 = 0.00542\sqrt{EI} \Rightarrow T_1 = 1158/\sqrt{EI}$

$B_2 = 4.854 \Rightarrow \omega_2 = 0.0220\sqrt{EI} \Rightarrow T_2 = 285/\sqrt{EI}$

For $EI = 6.28 \times 10^6$ k-in² (uncracked) : $T_1 = 0.46$ sec ; $T_2 = 0.11$ sec

For $EI = 2.62 \times 10^6$ k-in² (cracked) : $T_1 = 0.72$ sec ; $T_2 = 0.18$ sec

B.2.3 Modes Φ

$$\phi_{2n} = -[381 - 107B_n]^{-1}[5.442]$$

First Mode: $B_1 = 0.2942 \Rightarrow \phi_{21} = -0.0156$

Second Mode: $B_2 = 4.854 \Rightarrow \phi_{22} = 0.0396$

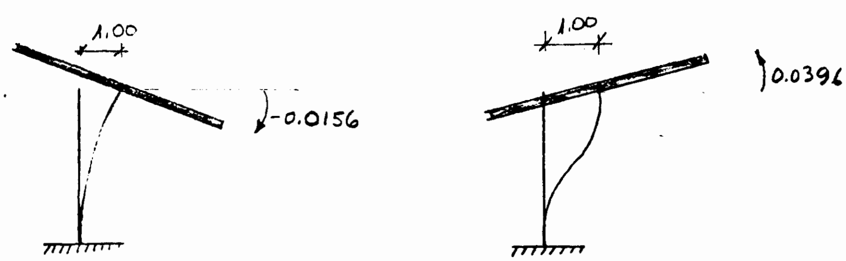

MODE 1

$T_1 = 0.46$ sec
(0.72 sec)

MODE 2

$T_2 = 0.11$ sec
(0.18 sec)

$$\Phi = \begin{array}{cc} \text{mode 1} & \text{mode 2} \\ \downarrow & \downarrow \end{array}$$
$$\Phi = \begin{bmatrix} 1.00 & 1.00 \\ -0.0156 & 0.0396 \end{bmatrix}$$

B.2.4 Mode Normalization

First Mode:
$$\begin{bmatrix} 1.00 & -0.0156 \end{bmatrix} \begin{bmatrix} 0.0655 & 0 \\ 0 & 107 \end{bmatrix} \begin{bmatrix} 1.00 \\ -0.0156 \end{bmatrix} = \begin{bmatrix} 1.00 & -0.0156 \end{bmatrix} \begin{bmatrix} 0.0655 \\ -1.669 \end{bmatrix} = 0.0915 = M_1$$

$$\hat{\underline{\phi}}_1 = \underline{\phi}_1 M_1^{-1/2} = \frac{1}{\sqrt{0.0915}} \begin{bmatrix} 1.00 \\ 0.0156 \end{bmatrix} = \begin{bmatrix} 3.305 \\ -0.0516 \end{bmatrix}$$

Second Mode:
$$\begin{bmatrix} 1.00 & 0.0396 \end{bmatrix} \begin{bmatrix} 0.0655 & 0 \\ 0 & 107 \end{bmatrix} \begin{bmatrix} 1.00 \\ 0.0396 \end{bmatrix} = \begin{bmatrix} 1.00 & 0.0396 \end{bmatrix} \begin{bmatrix} 0.0655 \\ 4.237 \end{bmatrix} = 0.233 = M_2$$

$$\hat{\underline{\phi}}_2 = \underline{\phi}_2 M_2^{-1/2} = \frac{1}{\sqrt{0.233}} \begin{bmatrix} 1.00 \\ 0.0396 \end{bmatrix} = \begin{bmatrix} 2.070 \\ 0.0820 \end{bmatrix}$$

therefore:
$$\hat{\underline{\phi}} = \begin{bmatrix} 3.305 & 2.070 \\ -0.0516 & 0.0820 \end{bmatrix}$$

Check:
$$\hat{\underline{\phi}}^T \underline{m} \hat{\underline{\phi}} = \begin{bmatrix} 3.305 & -0.0516 \\ 2.070 & 0.0820 \end{bmatrix} \begin{bmatrix} 0.0655 & 0 \\ 0 & 107 \end{bmatrix} \begin{bmatrix} 3.305 & 2.070 \\ -0.0516 & 0.0820 \end{bmatrix} =$$

$$= \begin{bmatrix} 3.305 & -0.0516 \\ 2.070 & 0.0820 \end{bmatrix} \begin{bmatrix} 0.2165 & 0.1356 \\ -5.521 & 8.774 \end{bmatrix} = \begin{bmatrix} 1.00 & 0.00 \\ 0.00 & 1.00 \end{bmatrix}$$

APPENDIX C

INFLUENCE OF TOP MOMENT AND OF LENGTH OF PLASTIC HINGE ON DISPLACEMENT DUCTILITY

Fig. C.1 shows the moment distribution when a cantilever is subjected to a force R and a moment M at its free end. It also shows the assumed curvature distribution used for the computation of lateral displacement of this cantilever (canopy). A simple conjugate structure approach was used to compute these displacements. Since curvature ductility μ_δ is the value being studied, displacements at yield (v_y) and at ultimate (v_u) were computed in order to then compute $\mu_\delta = \frac{v_u}{v_y}$.

According to this figure:

$$v_y = \left[\frac{(1-c)\,\phi_y L}{2}\right]\left[\frac{2L}{3}\right] + \left[c\,\phi_y L\right]\left[\frac{L}{2}\right] = \frac{(1-c)\phi_y L^2}{3} + \frac{c\,\phi_y L^2}{2}$$

$$\Rightarrow \quad v_y = \phi_y L^2 \left[\frac{2+c}{6}\right]$$

$$v_u = \phi_y L^2\left[\frac{2+c}{6}\right] + \left[(\phi_u - \phi_y)L_p\right]\left[L - \frac{L_p}{2}\right]$$

$$\Rightarrow \mu_\delta = \frac{v_u}{v_y} = 1 + \left[\frac{(\phi_u - \phi_y)}{\phi_y}\right]\left[\frac{6\,(L - 0.5\,L_p)\,L_p}{(2+c)\,L^2}\right]$$

$$\Rightarrow \mu_\delta = 1 + \left[\frac{\phi_u - \phi_y}{\phi_y}\right]\left[\frac{(L-0.5\,L_p)\,L_p}{(2+c)\,(L^2/6)}\right] \qquad \text{(Eq. C.1)}$$

According to Fig. C.1 b, the value of L_p can be determined by direct proportionality:

$$L_p = \frac{(M_u - M_y)L}{M_u(1-c)} \qquad \text{(Eq. C.2)}$$

where:

M_y = moment at first yield

M_u = moment at ultimate

$c = \frac{M_{top}}{M_y} = \frac{\phi_{top}}{\phi_y}$

The computation of μ_s was done for several cases:

1) For Material Properties Case M1 $\quad f'_c = 3.0$ ksi, $f_y = 50$ ksi

A) $\phi_u = 2.27 \times 10^{-3}$ rad/in (initiation of buckling range)

From Figs. 3.8 and 3.12: (using $d' = 1.7$ in.)

$M_y = 785^{\text{k-in}}$ $\qquad M_u = 974^{\text{k-in}}$

$\phi_y = 0.34 \times 10^{-3}$ rad/in $\qquad \phi_u = 2.27 \times 10^{-3}$ rad/in

B) $\phi_u = 3.0 \times 10^{-3}$ rad/in (end of buckling range)

Same values M_y, M_u, ϕ_y as above. $\phi_u = 3.0 \times 10^{-3}$ rad/in

2) For Material Properties Case M2 $\quad f'_c = 2.5$ ksi, $f_y = 40$ ksi

A) $\phi_u = 2.28 \times 10^{-3}$ rad/in (initiation of buckling range)

From Figs. 3.9 and 3.13: (using $d' = 2.2$ in.)

$M_y = 612^{\text{k-in}}$ $\qquad M_u = 800^{\text{k-in}}$

$\phi_y = 0.29 \times 10^{-3}$ rad/in $\qquad \phi_u = 2.28 \times 10^{-3}$ rad/in.

B) $\phi_u = 4.47 \times 10^{-3}$ rad/in (end of buckling range)

Same values M_y, M_u, ϕ_y as above. $\phi_u = 4.47 \times 10^{-3}$ rad/in

For each of these cases, values of μ_s were obtained using equations C.1 and C.2 for different values of moment at the top (i.e. of $c = M_{top}/M_y$). Tables C.1 and C.2 summarize the results obtained.

$C = \frac{M_{top}}{M_y}$	L_p, (in) (Eq. C.2)	$\mu_\delta = \frac{v_y}{v_u}$ (Eq. C.1)	
		Case 1A	Case 1B
-1.00	10.2	4.12	5.32
-0.90	10.7	3.98	5.12
-0.80	11.3	3.87	4.98
-0.70	12.0	3.80	4.87
-0.60	12.7	3.75	4.81
-0.50	13.6	3.73	4.77
-0.40	14.6	3.73	4.77
-0.30	15.7	3.75	4.80
-0.20	17.0	3.79	4.86
-0.10	18.5	3.86	4.96
0.00	20.4	3.96	5.10
0.10	19.5	4.10	5.29
0.20	25.5	4.28	5.53
0.30	26.5	4.51	5.86
0.40	30.9	4.82	6.28
0.50	37.0	5.23	6.85
0.60	46.3	5.78	7.61
0.70	61.7	6.48	8.59
0.80	92.6	7.04	9.36
0.90	> 105	——	——
1.00	> 105	——	——

TABLE C.1 INFLUENCE OF TOP MOMENT ON DISPLACEMENT DUCTILITY FOR MATERIAL PROPERTIES CASE M1

$C = \frac{M_{top}}{M_y}$	L_p, (in) (Eq. C.2)	$\mu_\delta = \frac{\nu_y}{\nu_u}$ (Eq. C.1) Case 2A	Case 2B
-1.00	12.3	5.61	10.7
-0.90	13.0	5.39	10.2
-0.80	13.7	5.24	9.89
-0.70	14.5	5.12	9.65
-0.60	15.4	5.05	9.50
-0.50	16.5	5.01	9.41
-0.40	17.6	5.00	9.40
-0.30	19.0	5.03	9.45
-0.20	20.6	5.09	9.58
-0.10	22.4	5.18	9.78
0.00	24.7	5.32	10.1
0.10	27.4	5.50	10.4
0.20	30.8	5.75	11.0
0.30	35.3	6.06	11.6
0.40	41.1	6.47	12.5
0.50	49.4	6.99	13.6
0.60	61.7	7.65	15.0
0.70	82.3	8.35	16.4
0.80	>105	—	—
0.90	>105	—	—
1.00	>105	—	—

TABLE C.2 INFLUENCE OF TOP MOMENT ON DISPLACEMENT DUCTILITY FOR MATERIAL PROPERTIES CASE M2

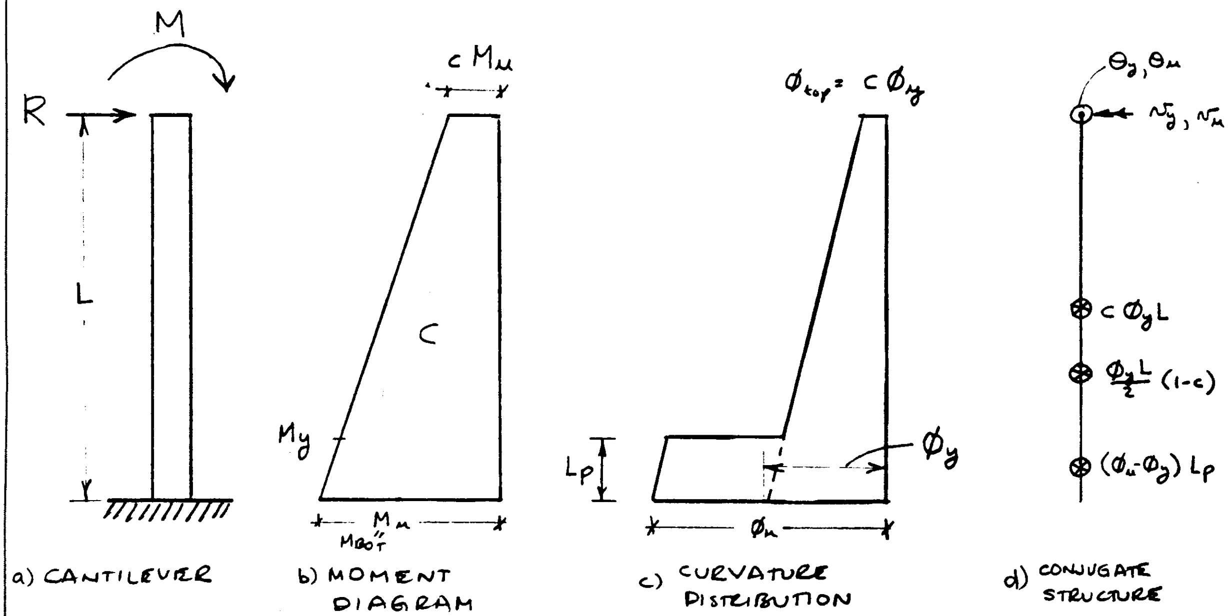

Fig. C.1 Curvature Distribution of a Cantilever Column Subjected to a Lateral Force R and a Moment M at the Top.

APPENDIX D

Computation of Lateral Resistance Function $\dot{R}$ vs N_1

D.1 Case M1: $f'_c = 3.0$ ksi $= 21$ MPa
$f_y = 50$ ksi $= 350$ MPa
$d' = (1.7" - 2.2") = (43\text{mm} - 56\text{ mm})$

The following M-Ø curve will be assumed, based on Fig. 3.12

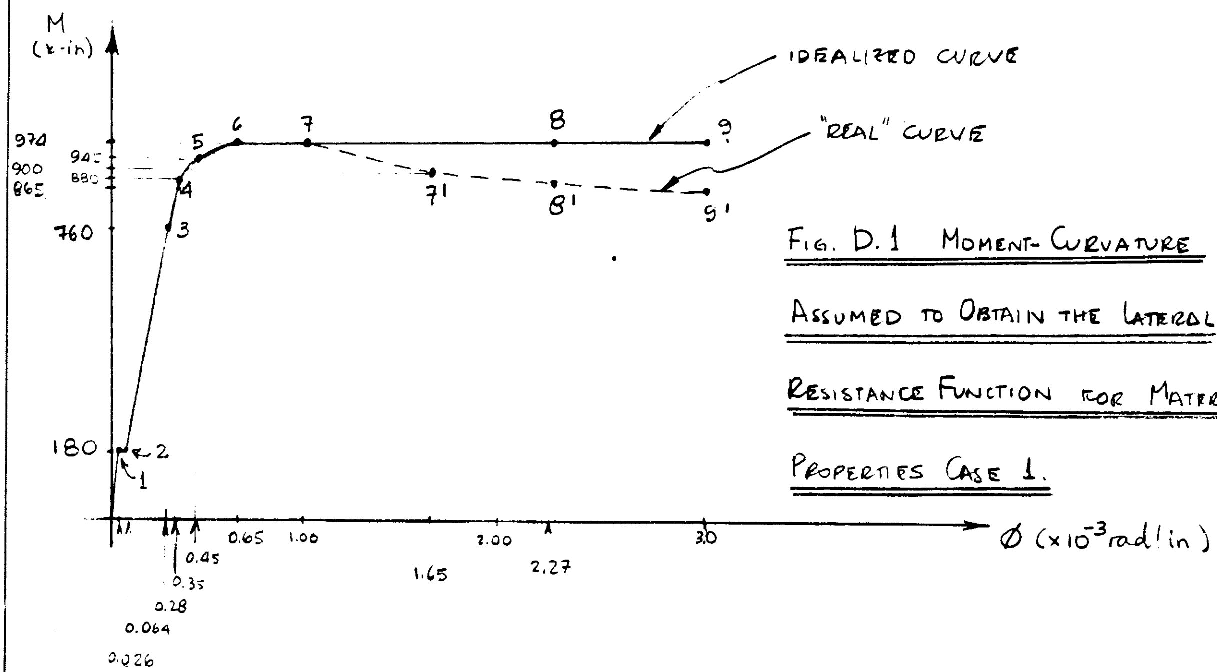

FIG. D.1 MOMENT-CURVATURE ASSUMED TO OBTAIN THE LATERAL RESISTANCE FUNCTION FOR MATERIAL PROPERTIES CASE 1.

$EI_{uc} = 7.04 \times 10^6$ k-in^2 $= 20{,}200$ kN-m
$EI_{cr} = 3.03 \times 10^6$ k-in^2 $= 8{,}700$ kN-m

Point	Moment (k-in)	Curvature ($\times 10^{-3}$ rad/in)	
1	180	0.026	(Cracking Moment)
2	180	0.064	
3	760	0.28	(First yield)
4	880	0.35	
5	945	0.45	
6	974	0.65	(Max. moment first reached)
7	974	1.00	
7'	900	1.65	
8	974	2.27	
8'	880	2.27	
9	974	3.00	(Max. curvature)
9'	865	3.00	

1) Idealized Curve (See Fig. D.1)

a) Point 1

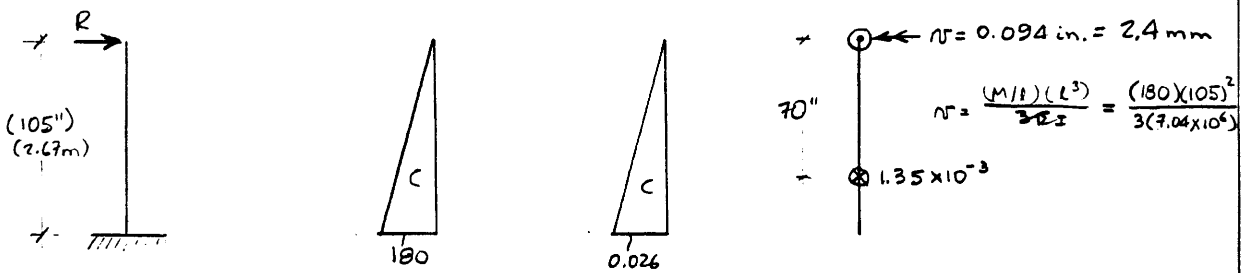

$R = \frac{180}{105} = 1.71^k$ (7.61 kN)

Moment Distrib. (K-in)

Curvature Distrib. ($\times10^{-3}$ rad/in)

Conjugate Structure.

b) Point 2

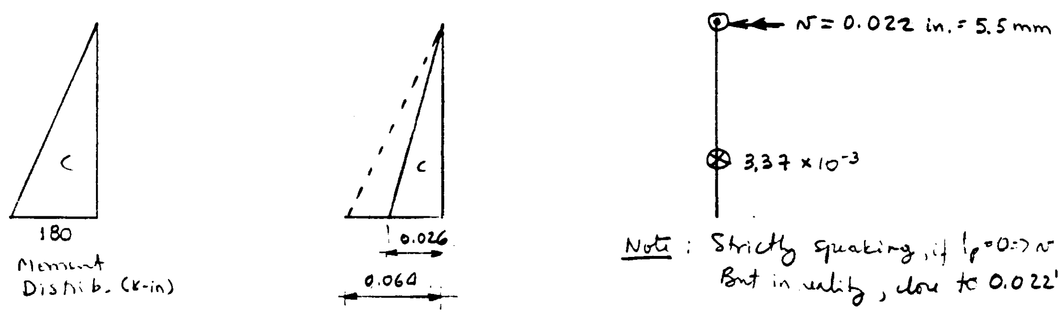

Moment Distrib. (K-in)

$R = 1.71^k$ (7.61 kN)

Curvature Distr. ($\times10^{-3}$ rad/in)

Note: Strictly speaking, if $l_p = 0 \Rightarrow v = 0.094$ "
But in reality, close to 0.022"

Conjugate Structure

c) Point 3

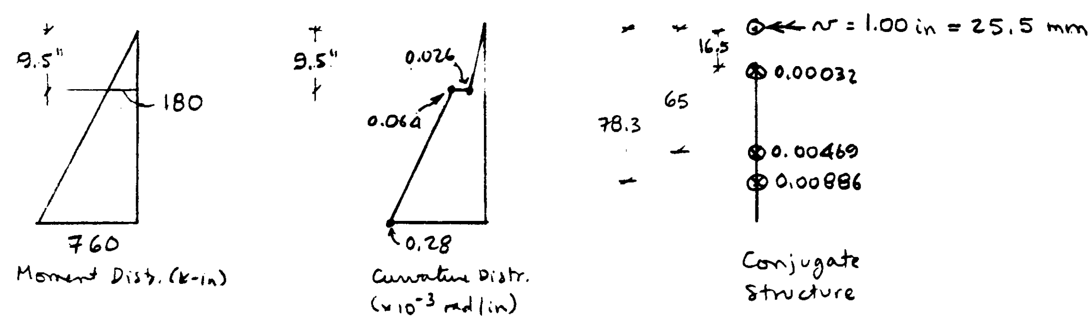

Moment Dist. (K-in)

Curvature Distr. ($\times10^{-3}$ rad/in)

Conjugate Structure

$R = 7.24^k$ (32.2 kN)

d) Point 4

$R = 8.38^k$ (37.3 kN)

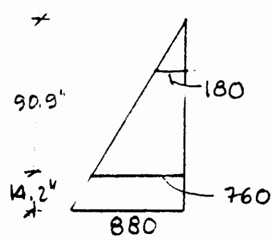

Moment Dist.
(k-in)

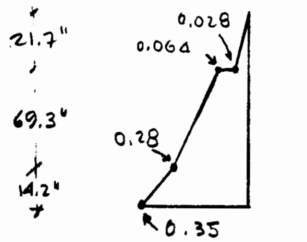

Curvature Distrib.
($\times 10^{-3}$ rad/in)

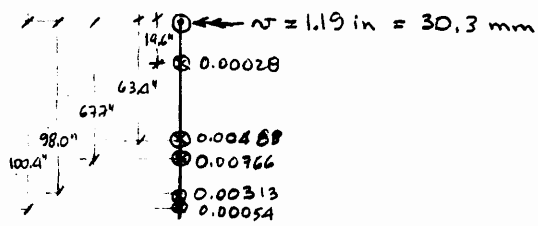

Conjugate
Structure

e) Point 5

$R = 8.99^k$ (40.0 kN)

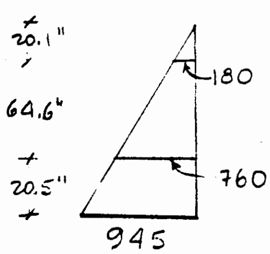

Moment Distribution
(k-in)

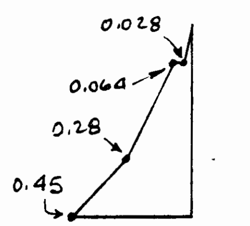

Curvature Distrib
($\times 10^{-3}$ rad/in)

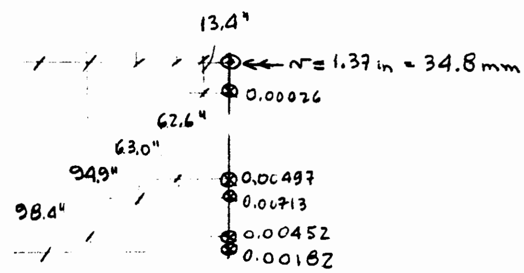

Conjugate
Structure

f) Points 6,7,8,9

$R = 9.27^k$ (41.3 kN)

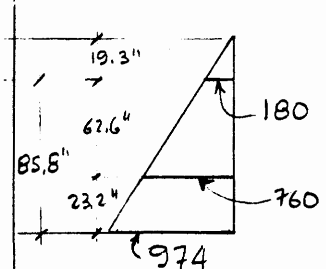

Moment Distr. (k-in)

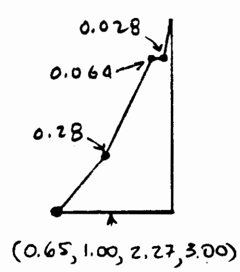

Curvature
($\times 10^{-3}$ rad/in)

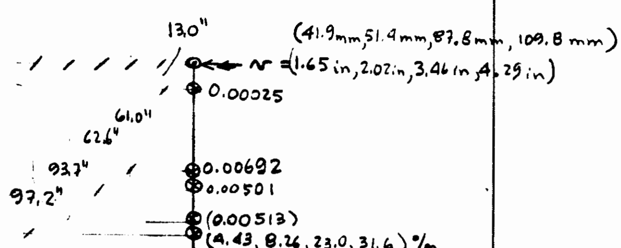

Conjugate
Structure

2) "Real" Curve (See Fig. D.1)

a) Point 7'

$R = 8.57^k$ (38.1 kN)

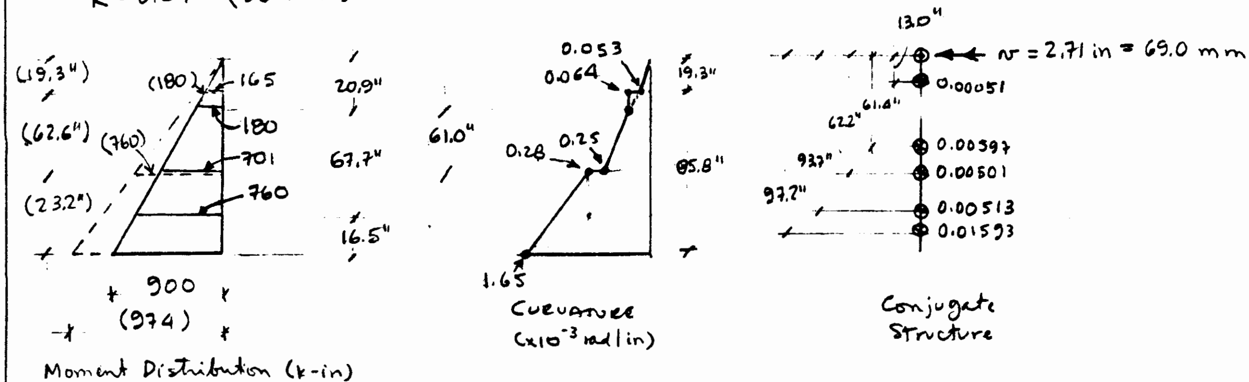

b) Point 8'

$R = 8.38^k$ (37.3 kN)

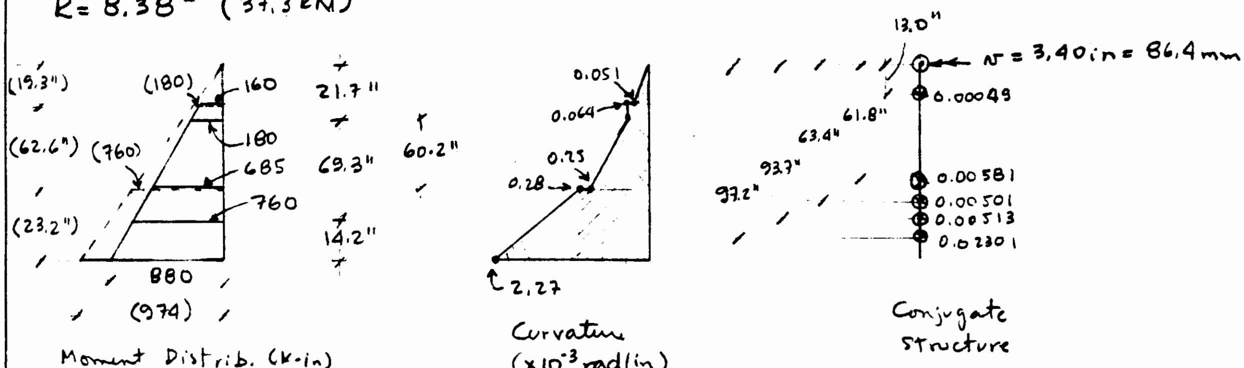

c) Point 9'

$R = 8.23^k$ (36.6 kN)

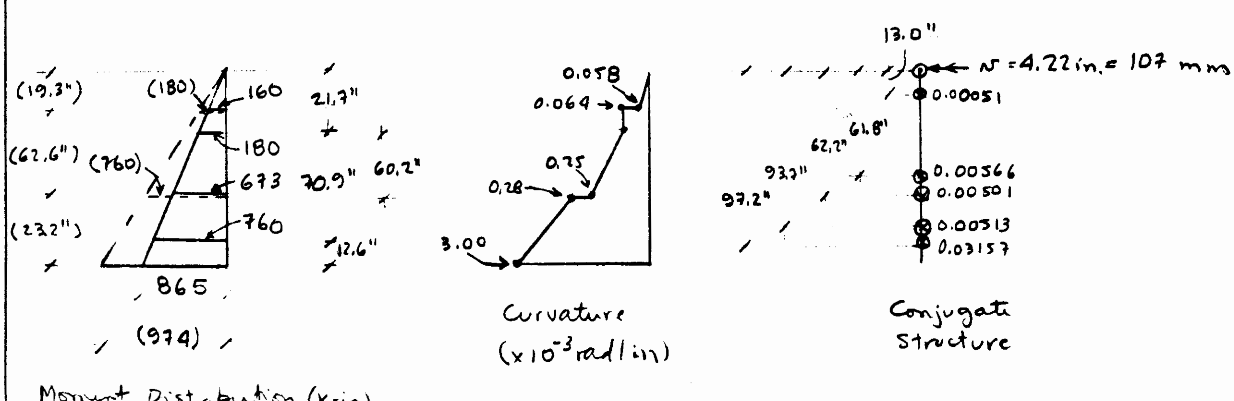

The results obtained are summarized in the following table.

Point Number	Lateral Displacement v		Lateral Force R	
	in	mm	k	kN
1	0.094	2.4	1.71	7.61
2	0.22	5.5	1.71	7.61
3	1.00	25.5	7.24	32.2
4	1.19	30.3	8.38	37.3
5	1.37	34.8	8.99	40.0
6	1.65	41.9	9.27	41.3
7	2.02	51.4	9.27	41.3
7'	2.71	69.0	8.57	38.1
8	3.46	87.8	9.27	41.3
8'	3.40	86.4	8.38	37.3
9	4.29	109.8	9.27	41.3
9'	4.22	107	8.23	36.6

Fig. 6.1 is obtained from these results.

D.2 Case M2: $f'_c = 2.5$ ksi $= 17$ MPa
$f_y = 40$ ksi $= 280$ MPa
$d' = 2.2$ in $= 56$ mm

The following M-ϕ curve will be assumed, based on Fig. 3.13 (not drawn to scale):

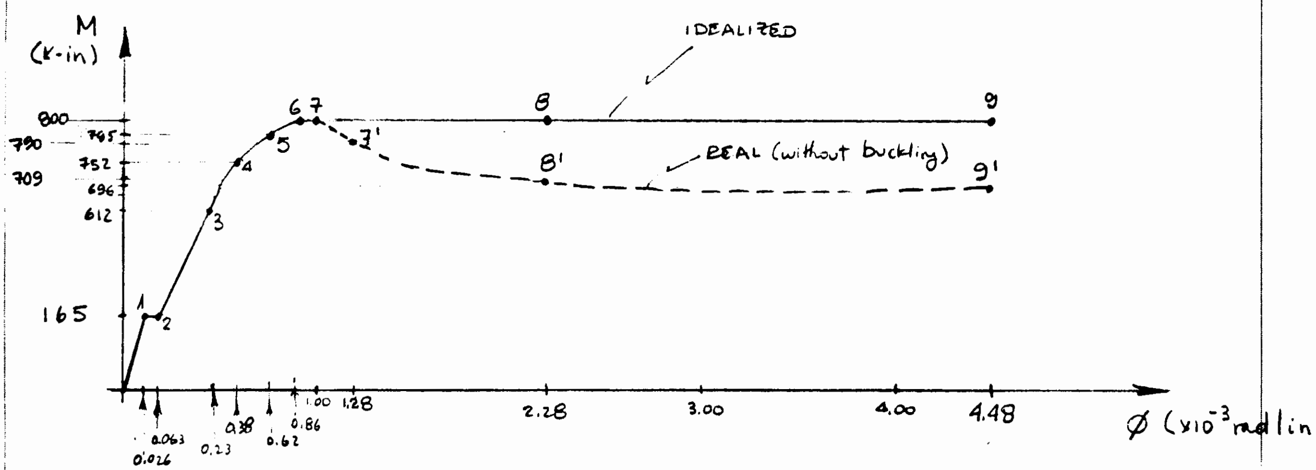

FIG. D.2 MOMENT-CURVATURE ASSUMED TO OBTAIN THE LATERAL RESISTANCE FUNCTION FOR MATERIAL PROPERTIES CASE M2.

$EI_{uc} = 6.28 \times 10^6$ k-in^2 $=$ 18,000 kN-m^2
$EI_{cr} = 2.62 \times 10^6$ k-in^2 $=$ 7,520 kN-m^2

Point	Moment (k-in)	Curvature ($\times 10^{-3}$ rad/in)	
1	165	0.026	(Cracking Moment)
2	165	0.063	
3	612	0.23	(First yield)
4	752	0.38	
5	795	0.62	
6	800	0.86	(Max. moment 1st reached)
7	800	1.00	
7'	790	1.28	
8	800	2.28	
8'	709	2.28	
9	800	4.48	(Max. curvature)
9'	696	4.48	

1) Idealized Curve (see Fig. D.2)

a) Point 1

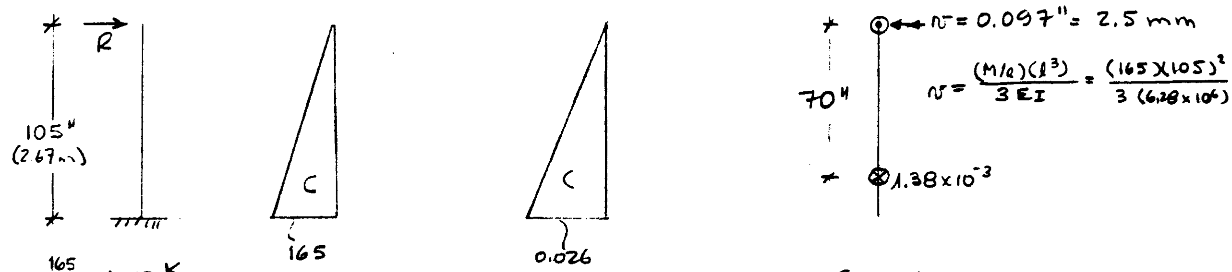

$R = \frac{165}{105} = 1.57^k$ (6.99 kN)

Moment Distribution (k-in)

Curvature Distribution ($\times 10^{-3}$ rad/in)

Conjugate Structure

b) Point 2

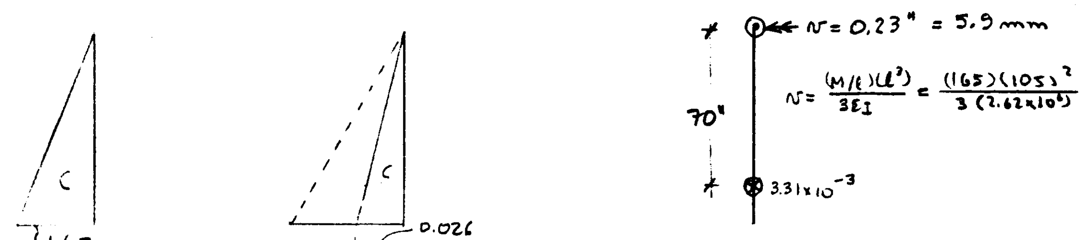

Moment Distribution (k-in)

Curvature Distribution ($\times 10^{-3}$ rad/in)

Note. Strictly speaking, if $t_p = 0 \Rightarrow v = 0.097"$
But in reality, close to 0.23"

$R = 1.57^k$ (6.99 kN)

c) Point 3

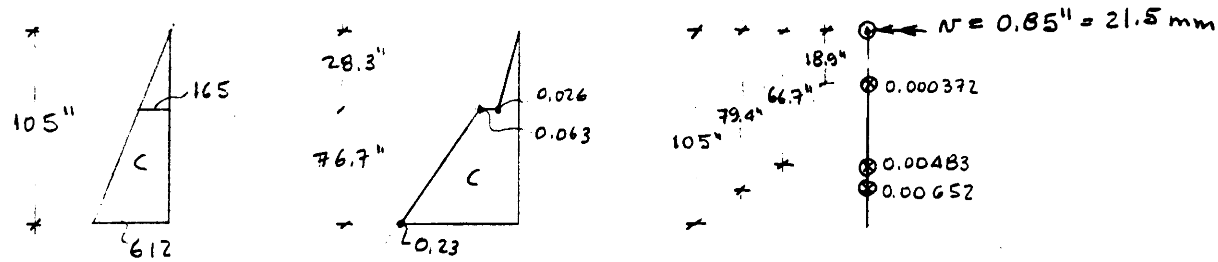

Moment Distribution (k-in)

Curvature Distribution ($\times 10^{-3}$ rad/in)

Conjugate Structure

$R = 5.83^k$ (25.9 kN)

d) Point 4

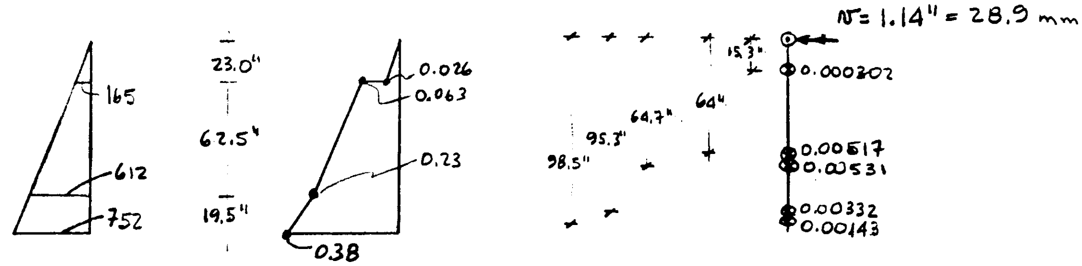

Moment Distribution (k-in)

Curvature Distribution ($\times 10^{-3}$ rad/in)

Conjugate Structure

$R = 7.16^k$ (31.9 kN)

e) Point 5

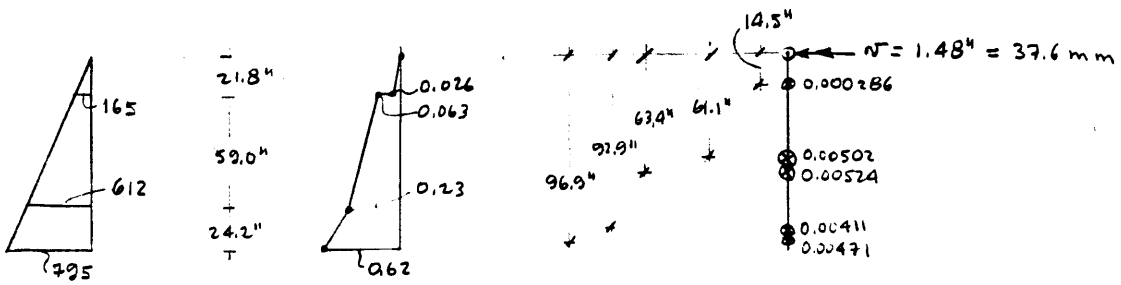

Moment Distribution (k-in)

Curvature Distribution ($\times 10^{-3}$ rad/in)

Conjugate Structure

$R = 7.57^k$ (33.7 kN)

f) Points 6, 7, 8, 9

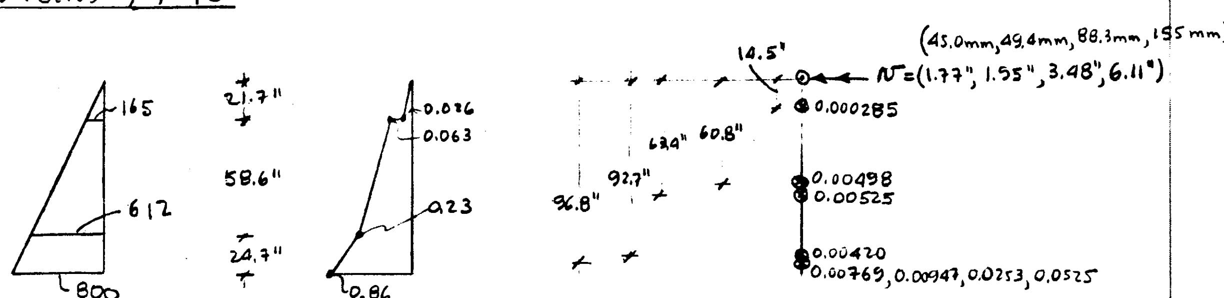

Moment Distribution (k-in)

Curvature Distrib. ($\times 10^{-3}$ rad/in)

Conjugate Structure

$R = 7.61^k$ (33.9 kN)

2) "Real Curve"

(See Fig. D.2)

a) Point 7'

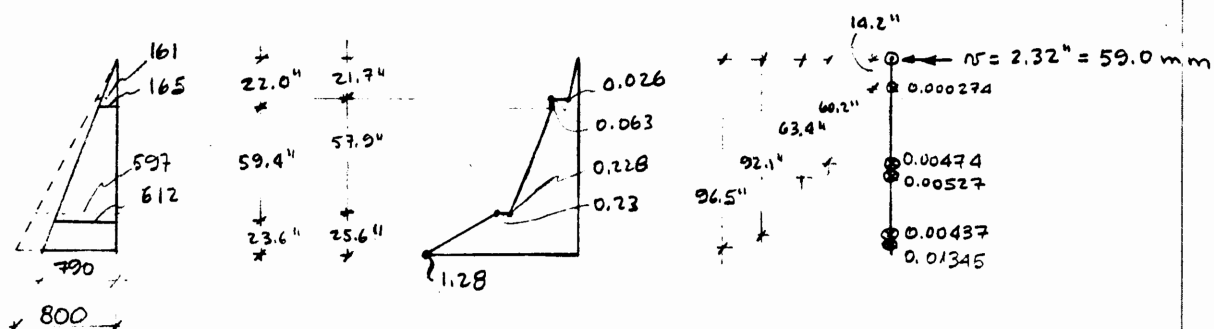

Moment Distribution (k-in)

Curvature Distribution ($\times 10^{-3}$ rad/in)

Conjugate Structure

$R = 7.52^k$ (33.5 kN)

b) Point 8'

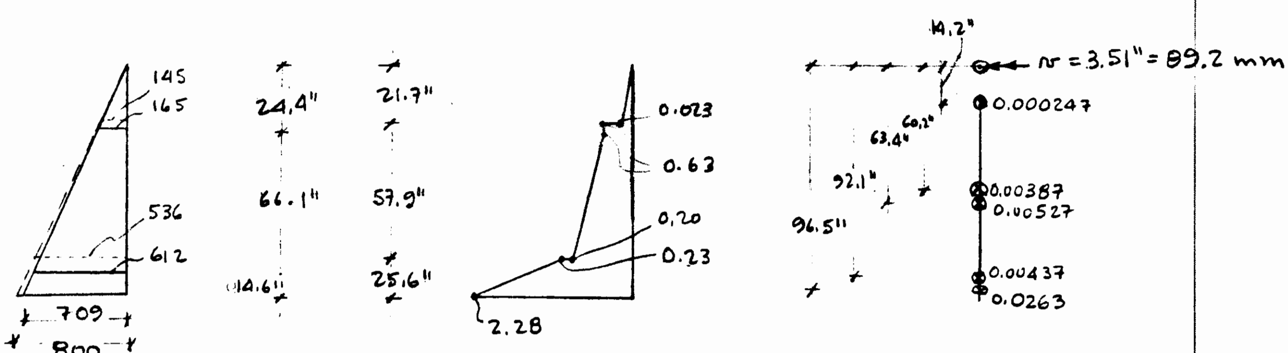

Moment Distribution (k-in)

Curvature Distribution ($\times 10^{-3}$ rad/in)

Conjugate Structure

$R = 6.75^k$ (30.0 kN)

c) Point 9'

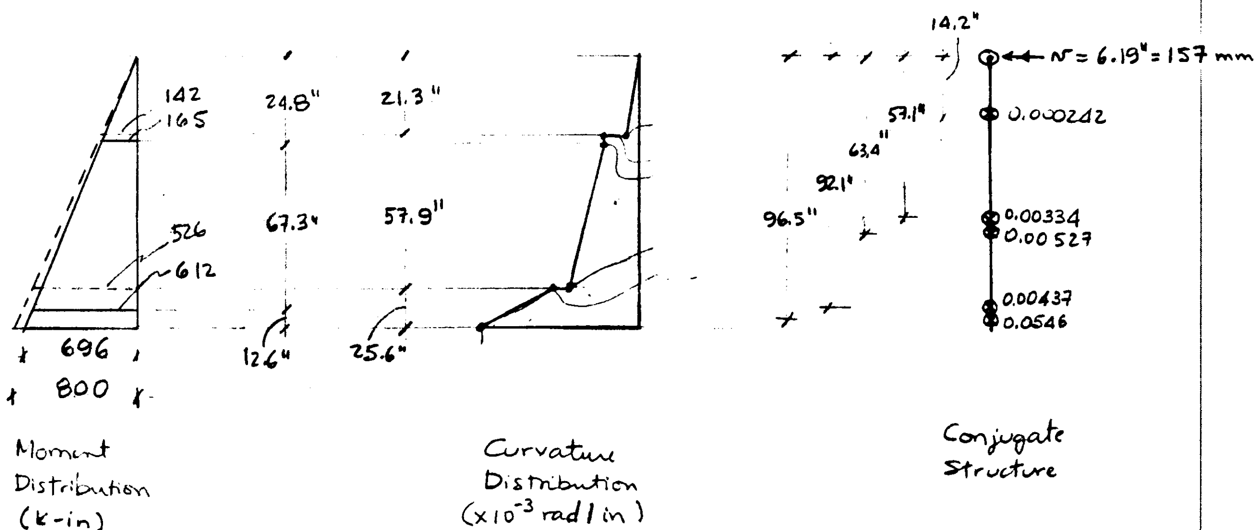

$R = 6.63^k$ (29.5 kN)

The results obtained are summarized in the following table:

POINT NUMBER	LATERAL DISPLACEMENT v		LATERAL FORCE R	
	in.	mm	k	kN
1	0.097	2.5	1.57	6.99
2	0.23	5.9	1.57	6.99
3	0.85	21.5	5.83	25.9
4	1.14	28.9	7.16	31.9
5	1.48	37.6	7.57	33.7
6	1.77	45.0	7.61	33.9
7	1.95	49.4	7.61	33.9
7'	2.32	59.0	7.52	33.5
8	3.48	88.3	7.61	33.9
8'	3.51	89.2	6.75	30.0
9	6.11	155	7.61	33.9
9'	6.19	157	6.63	29.5

Fig. 6.2 is obtained from these results.

APPENDIX E - BUCKLING OF LONGITUDINAL BARS.

As said earlier, the compressive longitudinal steel bars may buckle if there is enough axial compression force acting upon them.

According to the discussion in Sections 3.2.2 and 6.2.3 (see also Figs. 3.5 to 3.13), spalling starts to occur at ε_c (concrete strain) of approximately 0.007 in/in (see Figs. 3.1 and 3.2). Since buckling of longitudinal bars might occur when this strain value is reached at its position (i.e. $\varepsilon'_s \doteq 0.007$ in/in), a value of ε_c and ε_s will be taken from the output of the program in order to compute the value ε'_s.

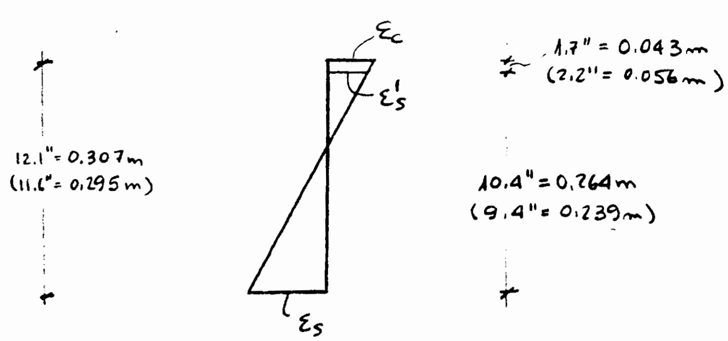

Actually, as presented in Section 3.2.2, buckling will occur somewhere in the range:

$$0.007 \text{ in/in} < \varepsilon'_s < 0.010 \text{ in/in} = \varepsilon_{SH}, \quad \text{for } f_y = 50 \text{ ksi} = 350 \text{ MPa}$$
$$0.015 \text{ in/in} = \varepsilon_{SH}, \quad \text{for } f_y = 40 \text{ ksi} = 280 \text{ MPa}$$

In the following pages, the corresponding range of curvatures is computed interpolating from the output of the program. This is done for an axial load $N = 26^k = 12^t$, for both types of covers ($d' = 1.7" = 43$ mm and $d' = 2.2" = 56$ mm), and for $f_y = 50$ ksi $= 350$ MPa and $f_y = 40$ ksi $= 280$ MPa.

Range of Curvatures at which Buckling occurs (FROM OUTPUT OF RCCOLA)
(FOR AXIAL LOAD OF $N = 26^k = 12^t$

1) CASE M1
$f'_c = 3.0\,ksi = 21\,MPa$, $f_y = 50\,ksi = 350\,MPa$

A) $d' = 1.7''$ (43 mm)

NOTE: $\varepsilon'_s = \left[\frac{(\varepsilon_s + \varepsilon_c)\,(10.4)}{(12.1)}\right] - [\varepsilon_s]$

From output of RCCOLA:

$\varepsilon_s = 0.01556$, $\varepsilon_c = 0.0100$ } $\varepsilon'_s = 0.00641$ ($\phi = 2.11‰ \frac{rad}{in}$)

$\varepsilon_s = 0.01666$, $\varepsilon_c = 0.0110$ } $\varepsilon'_s = 0.00711$ ($\phi = 2.29‰ \frac{rad}{in}$)

For $\varepsilon'_s = 0.007 \Rightarrow \phi \approx 2.26‰$ rad/in (0.0890 rad/m)

$\varepsilon_s = 0.02099$, $\varepsilon_c = 0.0150$ } $\varepsilon'_s = 0.00994$ ($\phi = 2.97‰ \frac{rad}{in}$)

$\varepsilon_s = 0.02219$, $\varepsilon_c = 0.0160$ } $\varepsilon'_s = 0.01063$ ($\phi = 3.16‰ \frac{rad}{in}$)

For $\varepsilon'_s = 0.01 \Rightarrow \phi \approx 2.99‰$ rad/in (0.1177 rad/m)

B) $d' = 2.2''$ (56 mm)

NOTE: $\varepsilon'_s = \left[\frac{(\varepsilon_s + \varepsilon_c)(9.4)}{(11.6)}\right] - [\varepsilon_s]$

From output of RCCOLZ:

$\varepsilon_s = 0.01444$, $\varepsilon_c = 0.0120$ } $\varepsilon'_s = 0.00699$ ($\phi = 2.28‰ \frac{rad}{in}$) = 0.0898 rad/m

$\varepsilon_s = 0.01825$, $\varepsilon_c = 0.0160$ } $\varepsilon'_s = 0.00972$ ($\phi = 2.95‰ \frac{rad}{in}$)

$\varepsilon_s = 0.01914$, $\varepsilon_c = 0.0170$ } $\varepsilon'_s = 0.01015$ ($\phi = 3.12‰ \frac{rad}{in}$)

For $\varepsilon'_s = 0.0100 \Rightarrow \phi \approx 3.06‰$ rad/in (0.1205 rad/m)

2) CASE 2:

$f'_c = 2.5$ ksi $= 17$ MPa , $f_y = 40$ ksi $= 280$ MPa

A) $d' = 1.7''$ (43 mm)

NOTE : $\varepsilon'_s = \left[\frac{(\varepsilon_s + \varepsilon_c)(10.4)}{(12.1)}\right] - [\varepsilon_s]$

From output of RCCOL2:

$\left.\begin{array}{l}\varepsilon_s = 0.01604 \\ \varepsilon_c = 0.0120\end{array}\right\} \Rightarrow \varepsilon'_s = 0.00668$ ($\phi = 2.32‰ \frac{rad}{in}$)

$\left.\begin{array}{l}\varepsilon_s = 0.01722 \\ \varepsilon_c = 0.0130\end{array}\right\} \Rightarrow \varepsilon'_s = 0.00727$ ($\phi = 2.50‰ \frac{rad}{in}$)

For $\varepsilon'_s = 0.007 \Rightarrow \phi = 2.42‰ \frac{rad}{in}$ (0.0953 rad/m)

$\left.\begin{array}{l}\varepsilon_s = 0.02495 \\ \varepsilon_c = 0.0200\end{array}\right\} \Rightarrow \varepsilon'_s = 0.0137$ ($\phi = 3.71‰ \frac{rad}{in}$)

$\left.\begin{array}{l}\varepsilon_s = 0.03065 \\ \varepsilon_c = 0.0250\end{array}\right\} \Rightarrow \varepsilon'_s = 0.0172$ ($\phi = 4.60‰ \frac{rad}{in}$)

For $\varepsilon'_s = 0.0150 \Rightarrow \phi = 4.04‰ \frac{rad}{in}$ (0.1591 rad/m)

B) $d' = 2.2''$ (56 mm)

NOTE : $\varepsilon'_s = \left[\frac{(\varepsilon_s + \varepsilon_c)(9.4)}{(11.6)}\right] - [\varepsilon_s]$

From output of RCCOL2:

$\left.\begin{array}{l}\varepsilon_s = 0.01444 \\ \varepsilon_c = 0.0120\end{array}\right\} \Rightarrow \varepsilon'_s = 0.00699$ ($\phi = 2.28‰ \frac{rad}{in}$)

$\left.\begin{array}{l}\varepsilon_s = 0.01551 \\ \varepsilon_c = 0.0130\end{array}\right\} \Rightarrow \varepsilon'_s = 0.00759$ ($\phi = 2.46‰ \frac{rad}{in}$)

For $\varepsilon'_s = 0.007 \Rightarrow \phi = 2.28‰ \frac{rad}{in}$ (0.0898 rad/m)

$\left.\begin{array}{l}\varepsilon_s = 0.02232 \\ \varepsilon_c = 0.0200\end{array}\right\} \Rightarrow \varepsilon'_s = 0.0120$ ($\phi = 3.65‰ \frac{rad}{in}$)

$\left.\begin{array}{l}\varepsilon_s = 0.02729 \\ \varepsilon_c = 0.0250\end{array}\right\} \Rightarrow \varepsilon'_s = 0.0151$ ($\phi = 4.51‰ \frac{rad}{in}$)

For $\varepsilon'_s = 0.0150 \Rightarrow \phi = 4.48‰ \frac{rad}{in}$ (0.1764 rad/m)

Table E.1 summarizes the results obtained.

Material Property Case Number	d'		Definition of Buckling Range in terms of Curvature Ø. Initiation of Buckling Range (Spalling of Unconf. Concrete Shell)		End of Buckling Range (Initiation of Strain-Hardening in Steel)	
	in	mm	Ø $\times 10^{-3}$ rad/in	Ø $\times 10^{-3}$ rad/m	Ø $\times 10^{-3}$ rad/in	Ø $\times 10^{-3}$ rad/m
CASE M1 $f'_c = 3.0$ ksi (21 MPa) $f_y = 50$ ksi (350 MPa)	1.7	43	2.26	89	2.99	118
	2.2	56	2.28	90	3.06	121
CASE M2 $f'_c = 2.5$ ksi (17 MPa) $f_y = 40$ ksi (280 MPa)	1.7	43	2.42	95	4.04	159
	2.2	56	2.28	90	4.48	176

TABLE E.1 SUMMARY OF CURVATURE VALUES Ø OBTAINED DEFINING THE RANGE IN WHICH BUCKLING MAY OCCUR.

APPENDIX F

COMPUTATION OF CANOPY'S TOP NODAL DISPLACEMENT WITH ACCOUNT OF CRACKING

I) COMPUTATION OF CANOPY'S TOP NODAL DISPLACEMENT DUE TO ROTATION OF THE FIXED END Θ_{FE}.

From RCCOLA and RCCOL2 it was obtained that the canopy's cross section started to lose its capacity very sharply due to buckling of the longitudinal compressive steel bars. This effect started to occur at curvatures on the order of 0.002 rad/in (0.0787 rad/m) or 0.0025 rad/in (0.0984 rad/m), which correspond to a tensile strain (at the level of the tensile steel bar) in the range 0.012 - 0.015 (i.e. in plateau of steel's stress-strain relationship).

Therefore, the value of Θ_{FE} is to be computed at start of yield ($\varepsilon_s = \varepsilon_y = \frac{40\ ksi}{29000\ ksi} = 0.00138$), at the plateau ($\varepsilon_s = 0.005000$, $\varepsilon_s = 0.010000$), and at the start of strain hardening ($\varepsilon_s = \varepsilon_{SH} = 0.015000$).

Important Data:

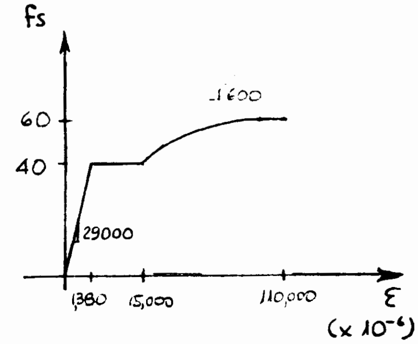

Stress-Strain for Steel

#6 Bars:

$\Sigma_o = \pi\,(6/8) = 2.36''$

$A_s = \pi/4\,(6/8)^2 = 0.442\ in^2$

$(E_{tx})_{initially} = 29000$ ksi

$(E_{tx})_{strain\ hard.} = 600$ ksi

a) $\varepsilon_{sA} = \varepsilon_y = 1{,}380\,\mu\varepsilon$ (Region 2)

(Start of yield)

$$C_1 = \frac{\Sigma_0}{A_s E_{tx}} = \frac{(2.36)}{(0.442)(29000)} = 1.84 \times 10^{-4}$$

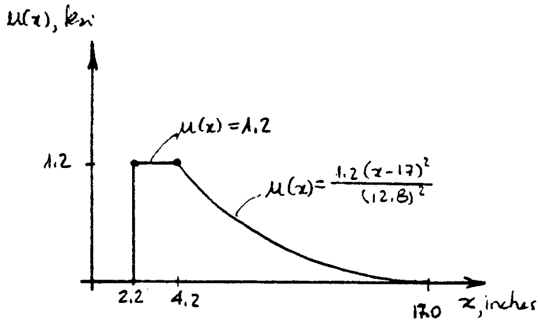

$0 \le x \le 2.2''$: $\varepsilon_{sA} - \varepsilon_s(x) = 0$; $\delta'_{A2} = 0$

$2.2'' \le x \le 4.2''$: $\varepsilon_{sA} - \varepsilon_s(x) = 1.2C_1(x-2.2)$

at $x = 4.2''$: $\varepsilon_{sA} - \varepsilon_s(x) = 2.4C_1 = 442\,\mu\varepsilon$

$$\delta''_{A2} = \left.\frac{1.2C_1(x-2.2)^2}{2}\right|_{2.2}^{4.2} = 0.000442''$$

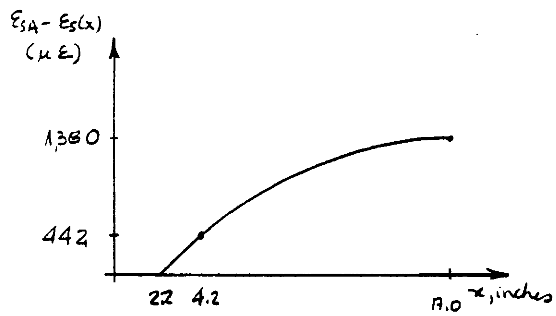

$4.2'' \le x \le 17.0''$: $\varepsilon_{sA} - \varepsilon_s(x) = (442\mu\varepsilon) + \left.\frac{1.2C_1(x-17)^3}{3(12.8)^2}\right|_{4.2}^{x}$

$= (442\mu\varepsilon) + (4.49\times10^{-7})\{(x-17)^3 + (12.8)^3\}$

at $x = 17''$: $\varepsilon_{sA} - \varepsilon_s(x) = 1{,}380\,\mu\varepsilon$

$$\delta'''_{A2} = \left.\{(442\mu\varepsilon)x\} + (4.49\times10^{-7})\left\{\frac{(x-17)^4}{4} + (12.8)^3 x\right\}\right|_{4.2}^{17}$$

$= 0.0147''$

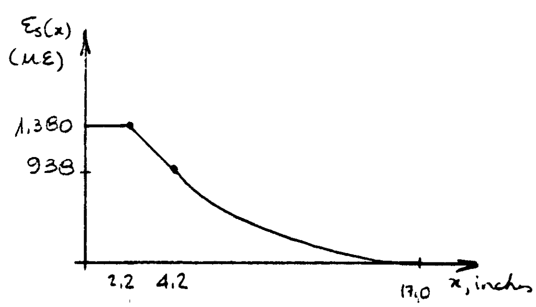

$$\delta_{A2} = \sum_{i=1}^{3} \delta^{i}_{A2} = 0.0151''$$

$$\delta_{A1} = (1{,}380\mu\varepsilon)(17.0) = 0.0235''$$

$$\delta_A = \delta_{A1} - \delta_{A2} = 0.00840'' = 0.213\text{ mm}$$

Equilibrium check :

$$F_{BOND} = \Sigma_0^{2.36''} \{(1.2)(2) + (\tfrac{1}{3})(1.2)(12.8)\} = 17.7^k = 8.05^t$$

$f_y = 40$

$$F_s = E_s\,\varepsilon_s\,A_s = (29000)(1380\mu\varepsilon)(0.442) = 17.7^k = 8.05^t$$ O.K.

From RCCOLA, neutral axis location = 5.69" from top compressive fiber

$$\theta_{FE} = \frac{(0.00840)}{(13.8 - 2.2 - 5.69)} = 0.00142\text{ rad}$$

$$\Delta X_{\theta_{FE}} = (0.00142)(105'') = 0.149'' = 0.00379\text{ m}$$

b) $\varepsilon_{SA} = 5{,}000\ \mu\varepsilon$ (Region 3)

(On plateau)

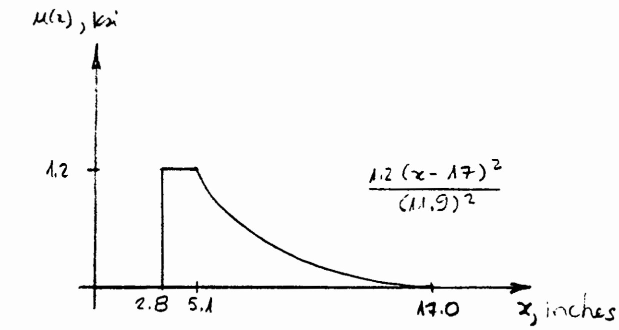

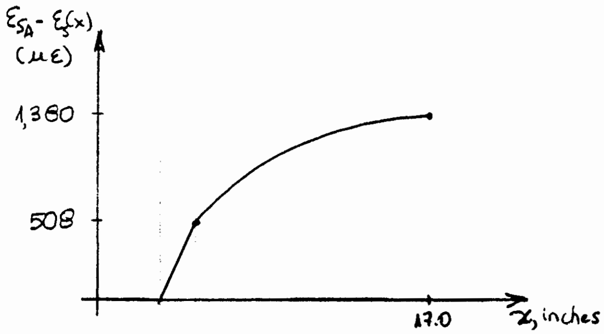

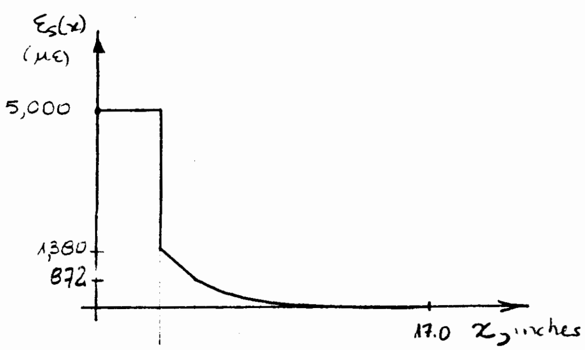

$$C_1 = \frac{\varepsilon_0}{A_s E_{tx}} = \frac{2.36}{(0.442)(29000)} = 1.84 \times 10^{-4}$$

$0 \le x \le 2.8''$: $\varepsilon_{SA} - \varepsilon_s(x) = 0$; $\delta'_{A2} = 0$

$2.8'' \le x \le 5.10''$: $\varepsilon_{SA} - \varepsilon_s(x) = 1.2 C_1 (x - 2.8)$

at $x = 5.10''$: $\varepsilon_{SA} - \varepsilon_s(x) = 2.76 C_1 = 508\ \mu\varepsilon$

$$\delta''_{A2} = \frac{1.2 C_1}{2}(x-2.8)^2 \Big|_{2.8}^{5.1} = 5.84 \times 10^{-4}$$

$5.10'' \le x \le 17.0''$:

$$\varepsilon_{SA} - \varepsilon_s(x) = 2.76\, C_1 + \frac{1.2 C_1 (x-17)^3}{3(11.9)^2}\Big|_{5.10}^{x} =$$

$$= 2.76 C_1 + 5.20 \times 10^{-7} \left\{ (x-17)^3 + (11.9)^3 \right\}$$

at $x = 17.0''$: $\varepsilon_{SA} - \varepsilon_s(x) = 1380\ \mu\varepsilon$

$$\delta'''_{A2} = \left\{ 2.76 C_1 x + 5.20 \times 10^{-7} \left\{ \frac{(x-17)^4}{4} + (11.9)^3 x \right\} \right\} \Big|_{5.1}^{17.0}$$

$$= 0.0139''$$

$$\delta_{A2} = \sum_{i=1}^{3} \delta^i_{A2} = 0.0144''$$

$$\delta_{A1} = (1380\mu\varepsilon)(17.0) + (5{,}000\mu\varepsilon - 1{,}380\mu\varepsilon)(2.8)$$
$$= 0.0235'' + 0.0101'' = 0.0336''$$

$$\delta_A = \delta_{A1} - \delta_{A2} = 0.0197'' = 0.500\ mm$$

Equilibrium check:

$$F_{BOND} = \overset{2.36}{\Sigma_0} \left\{ 1.2(2.30) + \left(\tfrac{1.2}{3}\right)(11.90) \right\} = 17.7^k = 8.05^t$$

$$F_S = f_y A_s = (40)(0.442) = 17.7^k = 8.05^t \qquad \text{o.k.}$$

From ECCOLA, neutral axis location = 4.72" from top compressive fiber.

$$\theta_{FE} = \frac{(0.0197)}{(11.6 - 4.72)} = 0.00286\ rad$$

$$\Delta X_{\theta_{FE}} = (0.00286)(105'') = 0.301'' = 0.00765\ m$$

c) $\varepsilon_{SA} = 10{,}000\,\mu\varepsilon$ (Region 2)

(On plateau)

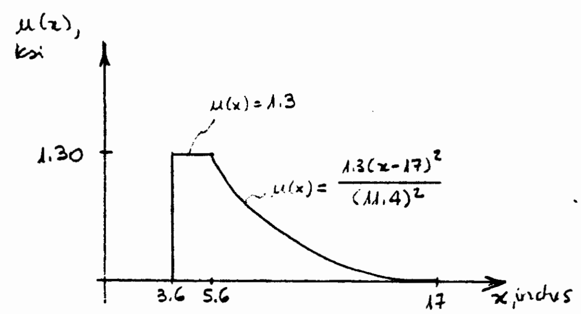

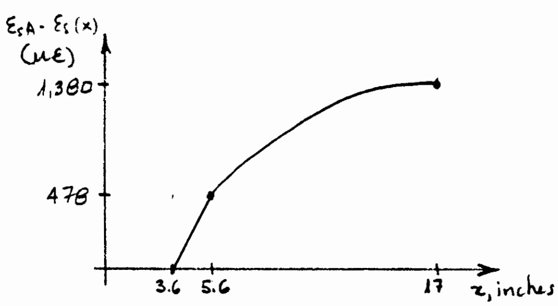

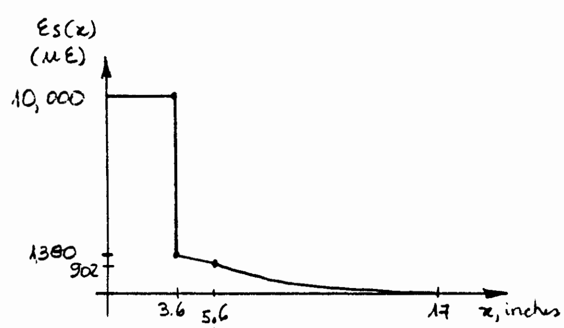

$$C_1 = \frac{\Sigma_0}{A_s E_{tx}} = \frac{(2.36)}{(0.442)(29000)} = 1.84\times10^{-4}$$

$0 \le x \le 3.6''$: $\varepsilon_{SA} - \varepsilon_s(x) = 0$; $\delta'_{A2} = 0$

$3.6 \le x \le 5.6''$: $\varepsilon_{SA} - \varepsilon_s(x) = 1.3C_1(x-3.6)$

at $x = 5.6''$: $\varepsilon_{SA} - \varepsilon_s(x) = 2.6C_1 = 478\,\mu\varepsilon$

$$\delta''_{A2} = \left.\frac{1.3C_1(x-3.6)^2}{2}\right|_{3.6}^{5.6} = 0.000478''$$

$$5.6'' \le x \le 17'':\ \varepsilon_{SA} - \varepsilon_s(x) = \{2.6C_1\} + \left.\left\{\frac{1.3C_1(x-17)^3}{3(11.4)^2}\right\}\right|_{5.6}^{x}$$

$$= 2.6C_1 + 6.14\times10^{-7}\{(x-17)^3 + (11.4)^3\}$$

at $x = 17''$: $\varepsilon_{SA} - \varepsilon_s(x) = 1{,}380\,\mu\varepsilon$

$$\delta'''_{A2} = 2.6C_1x + 6.14\times10^{-7}\left[\frac{(x-17)^4}{4} + (11.4)^3x\right]\Big|_{5.6}^{17}$$

$$= 0.0132''$$

$$\delta_{A2} = \sum_{i=1}^{3}\delta^i_{A2} = 0.0137''$$

$$\delta_{A1} = (1{,}380\mu\varepsilon)(17'') + (10{,}000\mu\varepsilon - 1{,}380\mu\varepsilon)(3.6'') =$$
$$= 0.0235'' + 0.0310'' = 0.0545''$$

$$\delta_A = \delta_{A1} - \delta_{A2} = 0.0408'' = 1.04\text{ mm}$$

Equilibrium check:

$$F_{BOND} = \overset{2.36}{\overset{\shortparallel}{\Sigma_0}}\left\{1.3(2.0) + \left(\tfrac{1}{3}\right)(1.30)(11.4)\right\} = 17.8^k = 8.09^t$$

$$F_s = f_y A_s = (40)(0.442) = 17.7^k = 8.04^t \qquad \underline{\text{o.k.}}$$

From ECCOLA, neutral axis location = 5.00" from top compressive fiber

$$\Theta_{FE} = \frac{(0.0408)}{(11.6-5.0)} = 0.00618\text{ rad}$$

$$\Delta X_{\Theta_{FE}} = (0.00618)(105'') = 0.649'' = 0.0165\,m$$

d) $\varepsilon_{SA} = 15{,}000\ \mu\varepsilon$ (Region 3)

(On plateau)

$$C_1 = \frac{\Sigma_o}{A_s E_{tx}} = \frac{(2.36)}{(0.442)(29000)} = 1.84 \times 10^{-4}$$

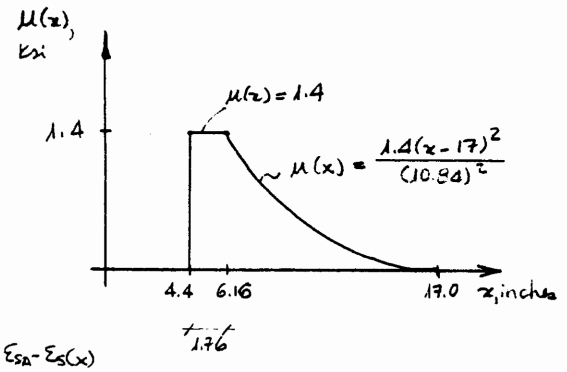

$0 \le x \le 4.4''$: $\varepsilon_{SA} - \varepsilon_S(x) = 0$; $\delta_{A2}' = 0$

$4.4'' \le x \le 6.16''$: $\varepsilon_{SA} - \varepsilon_S(x) = 1.4\,C_1\,(x - 4.4)$

at $x = 6.16''$: $\varepsilon_{SA} - \varepsilon_S(x) = 453\ \mu\varepsilon$

$$\delta_{A2}'' = \left.\frac{1.4\,C_1\,(x-4.4)^2}{2}\right|_{4.4}^{6.16} = 0.000399''$$

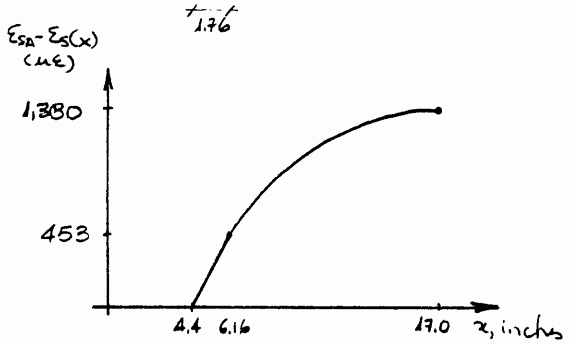

$6.16'' \le x < 17''$: $\varepsilon_{SA} - \varepsilon_S(x) = (453\ \mu\varepsilon) + \left.\frac{1.4\,C_1(x-17)^3}{3(10.84)^2}\right|_{6.16}^{x}$

$$= (453\ \mu\varepsilon) + 7.31\times 10^{-7}\left\{(x-17)^3 + (10.84)^3\right\}$$

at $x = 17''$: $\varepsilon_{SA} - \varepsilon_S(x) = 1{,}380\ \mu\varepsilon$

$$\delta_{A2}''' = (453\mu\varepsilon)\,x + 7.31\times10^{-7}\left.\left\{\frac{(x-17)^4}{4} + (10.84)^3 x\right\}\right|_{6.16}^{17.0}$$

$$= 0.0125''$$

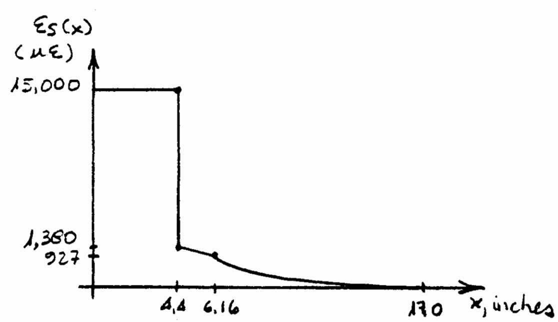

$$\delta_{A2} = \sum_{i=1}^{3} \delta_{A2}^{i} = 0.0129''$$

$$\delta_{A1} = (1{,}380\mu\varepsilon)(17.0'') + (15{,}000\mu\varepsilon - 1{,}380\mu\varepsilon)(4.4'')$$
$$= 0.0235'' + 0.0599'' = 0.0834''$$

$$\delta_A = \delta_{A1} - \delta_{A2} = 0.0705'' = 1.79\ \text{mm}$$

Equilibrium check:

$$F_{BOND} = \overset{2.36}{\Sigma_o}\left\{(1.4)(1.76) + (\tfrac{1}{3})(1.4)(10.84)\right\} = 17.7^{k} = 8.05^{t}$$

$$F_s = E_s\,\varepsilon_s\,A_s = f_y\,A_s = (40)(0.442) = 17.7^{k} = 8.05^{t}$$ o.k.

From ECCOLA, neutral axis location = 5.28" from top compressive fiber.

$$\Theta_{FE} = \frac{(0.0705)}{(11.6 - 5.28)} = 0.0112\ \text{rad}$$

$$\Delta X_{\Theta_{FE}} = (0.0112)(105'') = 1.17'' = 0.0298\ \text{m}$$

Summary of Canopy's Top Nodal Displacement Due to Rotation of the Fixed End

	$\Delta X_{\theta_{FE}}$
$\varepsilon_{SA} = \varepsilon_y = 1{,}380\,\mu\varepsilon$ (Start of yield)	0.149" (0.00379 m)
$\varepsilon_{SA} = 5{,}000\,\mu\varepsilon$ (On Plateau)	0.301" (0.00765 m)
$\varepsilon_{SA} = 10{,}000\,\mu\varepsilon$ (On plateau)	0.649" (0.0165 m)
$\varepsilon_{SA} = 15{,}000\,\mu\varepsilon$ (Start of Strain Hardening)	1.17" (0.0298 m)

II) COMPUTATION OF TOP NODAL DISPLACEMENT DUE TO ROTATION OF CANOPY'S CROSS SECTION AT CRACKS

Assumed Moment Distributions:

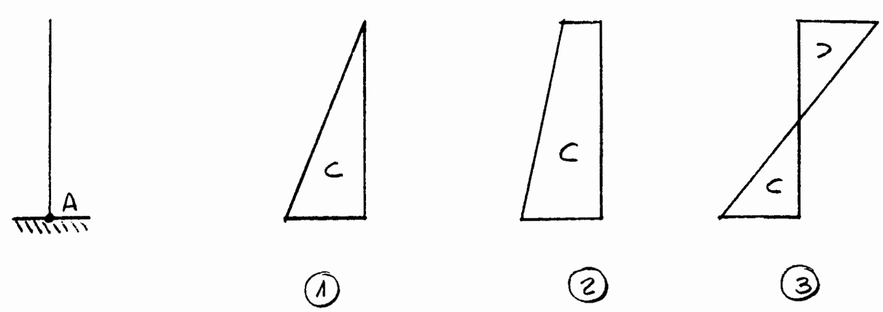

F) Moment Distribution (1)

a) $\varepsilon_{SA} = \varepsilon_y$ (FIRST YIELDING OF TENSILE STEEL BARS AT SUPPORT)

$\varepsilon_y = 1380 \mu\varepsilon \Rightarrow M_y = 612^{k\text{-}in}$

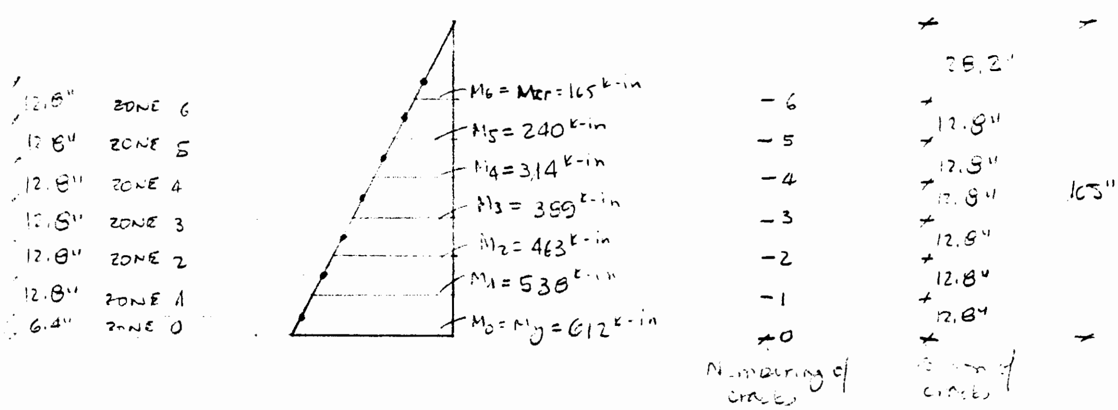

Assume constant average moment throughout each of the zones 1-6. Each of these moments corresponds to moment at level of crack. Zones 1 to 6 are defined to go from mid-distances between cracks. Zone 0 goes from crack at "fixed end" to mid-distance between this crack and the following one.

Using results from RCCOLA:

ZONE	MAV (k-in)	Curvature ($\times 10^{-3}$ rad/in)	Tensile Steel Strain ($\mu\varepsilon$)	Neutral Axis depth (in)
0	612	0.233	1380	5.69
1	538	0.205	1210	5.83
2	463	0.177	1040	5.96
3	389	0.146	877	6.10
4	314	0.120	708	6.24
5	240	0.091	541	6.37
6	165	0.063	372	6.51

$\varepsilon_{SA} = \varepsilon_y = 1{,}380\,\mu\varepsilon$

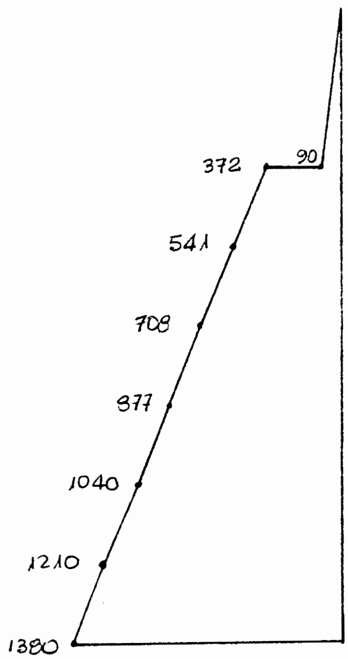

Tensile Steel Strain Distribution ε_s ($\mu\varepsilon$)
(AS GIVEN BY RCCOLA)
(linear interpolation)

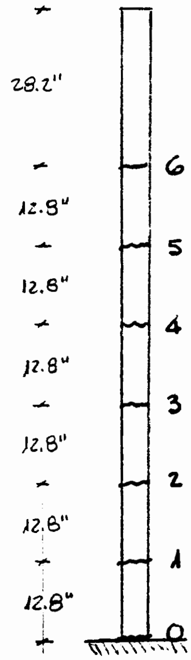

Position & Numbering of Cracks

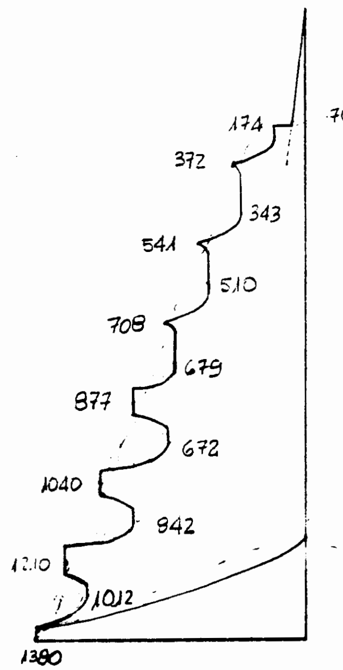

Tensile Steel Strain Distribution ε_s ($\mu\varepsilon$)
a) at cracks : as given by RCCOLA
b) other points : as given by assumed bond distribution.

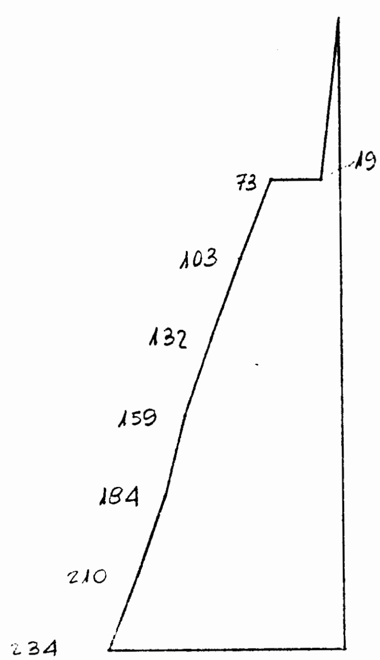

Curvature distribution ϕ ($\times 10^{-6}$ rad/in)
(as given by RCCOLA)
(linear interpolation)

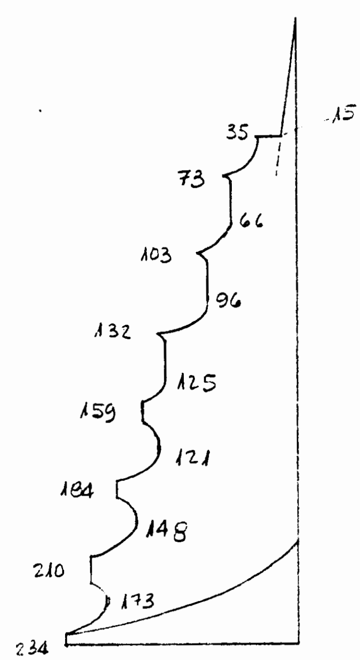

Curvature Distribution ϕ ($\times 10^{-6}$ rad/in)
a) at cracks : as given by RCCOLA
b) other pts : as given by assumed bond

i) Zone O

$$C_1 = \frac{\Sigma_o}{A_s E_{tx}} = \frac{(2.36)}{(0.442)(29000)} = 1.84 \times 10^{-4}$$

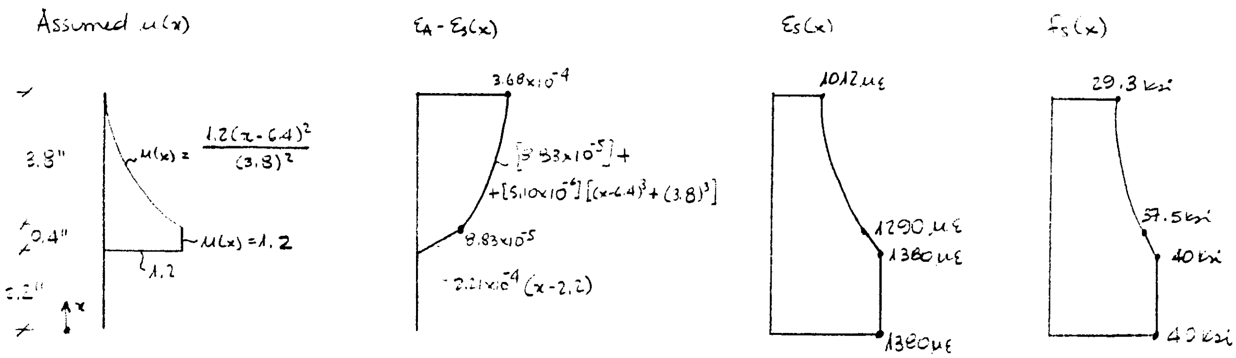

$$F_{BOND} = \underset{3\,bars}{3}\, \Sigma_o \int u(x)\,dx = (3)(2.36)(1.2)\left[(0.4) + \tfrac{1}{3}(3.8)\right] = 14.2^k$$

Tensile force required to crack the concrete:

$A_c f'_t = (41.1)(0.350) = 14.4^k > 14.2^k$

$\Rightarrow$ no cracks in between assumed cracks

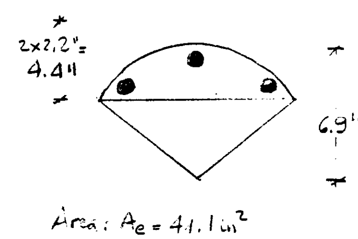

$0 \leq x \leq 2.2"$: $\varepsilon_A - \varepsilon_s(x) = 0$; $\delta'_{A2} = 0$

$2.2" \leq x \leq 2.6"$: $\varepsilon_A - \varepsilon_s(x) = \int_{2.2}^{x} C_1 u(x)\,dx = (C_1)(1.2)(x-2.2) = 2.21\times10^{-4}(x-2.2)$

at $x = 2.6$: $\varepsilon_A - \varepsilon_s(x) = 8.83\times10^{-5}$

$$\delta''_{A2} = \int_{2.2}^{2.6} (\varepsilon_A - \varepsilon_s(x))\,dx = (1.2\,C_1)\left.\frac{(x-2.2)^2}{2}\right|_{2.2}^{2.6} = 1.77\times10^{-5}$$

$2.6" \leq x \leq 6.4"$: $\varepsilon_A - \varepsilon_s(x) = [8.83\times10^{-5}] + \frac{1.2\,C_1}{(3.8)^2}\left.\frac{(x-6.4)^3}{3}\right|_{2.6}^{x}$

$$= [8.83\times10^{-5}] + [5.10\times10^{-6}][(x-6.4)^3 + (3.8)^3]$$

at $x = 6.4$: $\varepsilon_A - \varepsilon_s(x) = 3.65\times10^{-4}$

$$\delta'''_{A2} = \int_{2.6}^{6.4} (\varepsilon_A - \varepsilon_s(x))\,dx = 8.83\times10^{-5}x + 5.10\times10^{-6}\left[\frac{(x-6.4)^4}{4} + (3.8)^3 x\right]_{2.6}^{6.4} = 0.00113"$$

$\delta_{A1} = [1380\,\mu\varepsilon][6.4"] = 0.00883"$

$\delta_{A2} = \Sigma\, \delta^i_{A2} = 0.001150"$

$\delta_A = \delta_{A1} - \delta_{A2} = 0.00768" = 0.195$ mm

$\theta_{cr_o} = \frac{(0.007680)}{(13.8 - 2.2 - 5.69)} = 0.00130$ rad

$\Delta X_{\theta_{cr}} = (0.00130)(105") = 0.136" = 0.00347$ m

ii. Zone 1

– Below Crack

Assumed $\mu(x)$
BELOW CRACK

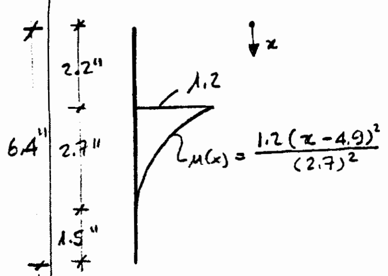

$\varepsilon_A - \varepsilon_s(x)$

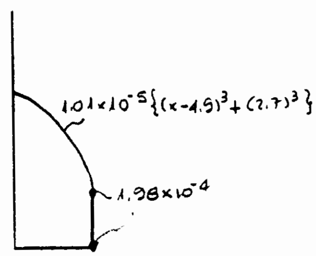

$\varepsilon_s(x)$

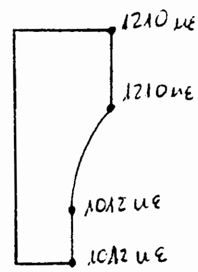

$f_s(x)$

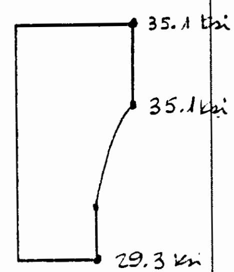

$F_{BOND} = 3\Sigma_0 \int \mu(x)\,dx = (3)(2.36)(1.2)(2.7)(\frac{1}{3}) = 7.6^k < A_e f'_t = 14.4^k$ o.k.

$0 \le x \le 2.2"$: $\varepsilon_A - \varepsilon_s(x) = 0$ $\qquad \delta'_{A2} = 0$

$2.2" \le x \le 4.9"$: $\varepsilon_A - \varepsilon_s(x) = \int_{2.2}^{x} C_1\,\mu(x)\,dx = \frac{1.2C_1}{3(2.7)^2}(x-4.9)^3\Big|_{2.2}^{x} = 1.01\times10^{-5}\{(x-4.9)^3+(2.7)^3\}$

$$\delta''_{A2} = \int_{2.2}^{4.9}(\varepsilon_A - \varepsilon_s(x))\,dx = 1.01\times10^{-5}\left\{\tfrac{1}{4}(x-4.9)^4+(2.7)^3 x\right\}\Big|_{2.2}^{4.9} = 0.000402"$$

$4.9" \le x \le 6.4"$: $\varepsilon_A - \varepsilon_s(x) = 1.98\times10^{-4}$

$$\delta'''_{A2} = (198\,\mu\varepsilon)(1.5") = 0.000297"$$

$\delta_{A1} = (1210\,\mu\varepsilon)(6.4") = 0.00774"$

$\delta_{A2} = \Sigma\,\delta^i_{A2} = 0.000699"$

$\left.\right\}\ \delta_{A\,\text{BELOW CRACK}} = \delta_{A1} - \delta_{A2} = 0.00704"$

– Above Crack

Assume $\mu(x)$ distribution as in zone 0. $\Rightarrow \delta_{A2} = 0.001150"$

$\delta_{A1} = (1210\,\mu\varepsilon)(6.4") = 0.007740"$

$\Rightarrow \delta_{A\,\text{ABOVE CRACK}} = \delta_{A1} - \delta_{A2} = 0.006590"$

$\delta_A = \delta_{A\,\text{BELOW CRACK}} + \delta_{A\,\text{ABOVE CRACK}} = 0.0136"$
(0.346 mm)

$\varepsilon_s(x)$

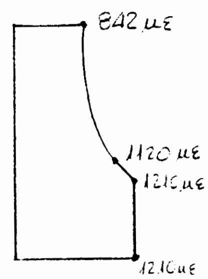

$f_s(x)$

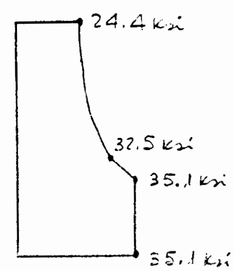

$\theta_{cr1} = \frac{(0.0136)}{(11.6-5.83)} = 0.00236$ rad

$\Delta X_{\theta_{cr1}} = (0.00236)(92.2") = 0.218"$
$= 0.00553$ m

iii) Zone 2

Assume same $u(x)$ distribution as in zone 1.

$$\left.\begin{array}{l} \delta_{A1} = (1040\,\mu\varepsilon)(12.8") = 0.0133" \\ \left.\begin{array}{l} \delta_{A2_{\text{BELOW CRACK}}} = 0.000699" \\ \delta_{A2_{\text{ABOVE CRACK}}} = 0.001150" \end{array}\right\} \delta_{A2} = 0.00165" \end{array}\right\} \delta_A = \delta_{A1} - \delta_{A2} = 0.0115" = 0.291\text{ mm}$$

$$\theta_{cr2} = \frac{(0.0115)}{(11.6 - 5.96)} = 0.00203\text{ rad}$$

$$\Delta X_{\theta cr2} = (0.00203)(79.4") = 0.161" = 0.00410\text{ m}$$

iv) Zone 3

- Below crack

Assume same $u(x)$ distribution as in zone 1 for part below crack.

$$\left.\begin{array}{l} \delta_{A1} = (877\,\mu\varepsilon)(6.4") = 0.00561" \\ \delta_{A2} = 0.000699" \end{array}\right\} \delta_{A_{\text{BELOW CRACK}}} = \delta_{A1} - \delta_{A2} = 0.00491" = 0.125\text{ mm}$$

- Above crack:

Assume $u(x)$ distribution as in zone 1 for part below crack.

$$\left.\begin{array}{l} \delta_{A1} = (877\,\mu\varepsilon)(6.4") = 0.00561" \\ \delta_{A2} = 0.000699" \end{array}\right\} \delta_{A_{\text{ABOVE CRACK}}} = \delta_{A1} - \delta_{A2} = 0.00491" = 0.125\text{ mm}$$

$$\delta_A = \delta_{A_{\text{BELOW CRACK}}} + \delta_{A_{\text{ABOVE CRACK}}} = 0.00982" = 0.249\text{ mm}$$

$$\theta_{cr3} = \frac{(0.00982)}{(11.6 - 6.10)} = 0.00179\text{ rad}$$

$$\Delta X_{\theta cr3} = (0.00179)(66.6") = 0.119" = 0.00302\text{ m}$$

Note: At end of crack 3 (start of crack 4):
$\varepsilon_s(x) = (877\,\mu\varepsilon) - (198\,\mu\varepsilon) = 679\,\mu\varepsilon$

v) Zone 4

- Below crack

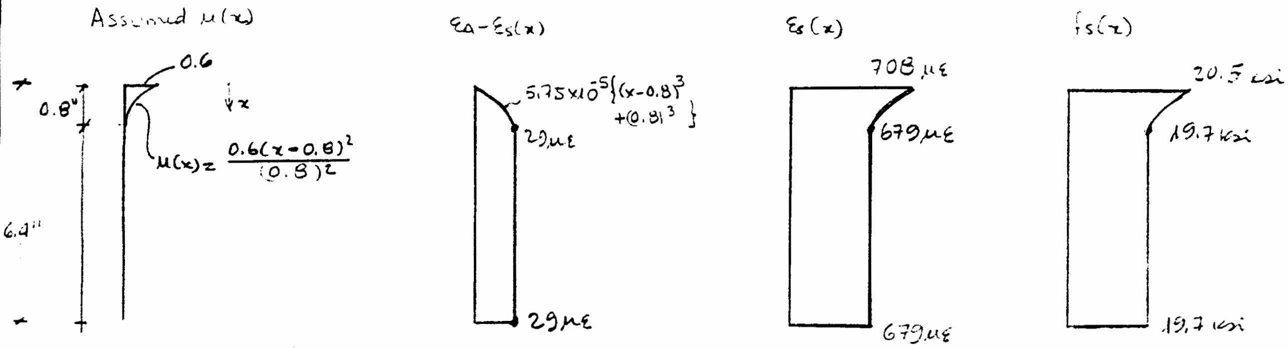

$F_{BOND} = 3\Sigma_0 \int \mu(x)\,dx = 3(2.36)(0.6)(0.8)(1/3) = 1.1^k < A_e f'_t = 14.4^k$ O.K.

$0 \le x \le 0.8"$: $\varepsilon_A - \varepsilon_s(x) = \frac{0.6\, C_1 (x-0.8)^3}{3(0.8)^2}\Big|_0^x = 5.75\times10^{-5}\{(x-0.8)^3 + (0.8)^3\}$

$\delta'_{A2} = 5.75\times10^{-5}\{\frac{1}{4}(x-0.8)^4 + (0.8)^3 x\}\Big|_0^{0.8} = 0.0000177"$

$0.8" \le x \le 6.4"$: $\varepsilon_A - \varepsilon_s(x) = 29\ \mu\varepsilon$

$\delta''_{A2} = (29\,\mu\varepsilon)(5.6") = 0.000162"$

$\left.\begin{array}{l} \delta_{A1} = (708\,\mu\varepsilon)(6.4") = 0.00453" \\ \delta_{A2} = 0.000180" \end{array}\right\}\ \delta_{A_{\text{BELOW CRACK}}} = \delta_{A1} - \delta_{A2} = 0.00435"$

- Above crack

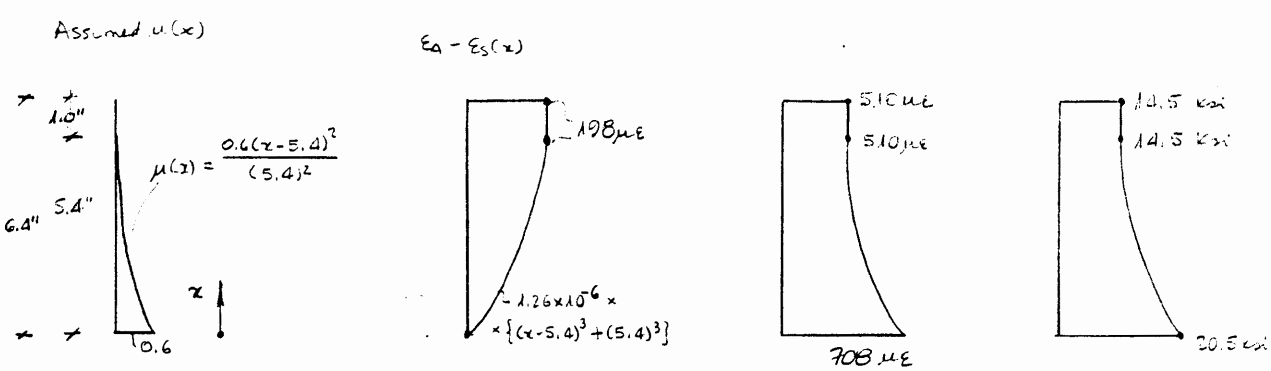

$F_{BOND} = 3\Sigma_0 \int \mu(x)\,dx = 3(2.36)(0.6)(5.4)(\frac{1}{3}) = 7.6^k < A_e f'_t = 14.4^k$ O.K.

$0 \le x \le 5.4"$: $\varepsilon_A - \varepsilon_s(x) = \frac{0.6\, C_1 (x-5.4)^3}{3(5.4)^2}\Big|_0^x = 1.26\times10^{-6}\{(x-5.4)^3 + (5.4)^3\}$

$\delta'_{A2} = 1.26\times10^{-6}\{\frac{1}{4}(x-5.4)^4 + (5.4)^3 x\}\Big|_0^{5.4} = 0.000805"$

$5.4" \leq x \leq 6.4"$: $\varepsilon_A - \varepsilon_s(x) = 198\ \mu\varepsilon$

$$\delta''_{A2} = (198\ \mu\varepsilon)(1.0") = 0.000198"$$

$$\left.\begin{array}{l}\delta_{A1} = (708\ \mu\varepsilon)(6.4") = 0.00453" \\ \delta_{A2} = 0.00100"\end{array}\right\} \delta_{A_{\text{ABOVE CRACK}}} = \delta_{A1} - \delta_{A2} = 0.00353"$$

$$\delta_A = \delta_{A_{\text{BELOW CRACK}}} + \delta_{A_{\text{ABOVE CRACK}}} = 0.00788" = 0.200\ mm$$

$$\theta_{cr_4} = \frac{(0.00788)}{(11.6 - 6.24)} = 0.00147\ rad$$

$$\Delta X_{\theta_{cr4}} = (0.00147)(53.8") = 0.0791" = 0.00201\ m$$

vi) <u>Zone 5</u>

- Below crack

Assume $\mu(x)$ as in zone 4 (below crack) $\Rightarrow \delta_{A2} = 0.000180"$
$\delta_{A1} = (541\ \mu\varepsilon)(6.4") = 0.00346"$

$$\delta_{A_{\text{BELOW CRACK}}} = \delta_{A1} - \delta_{A2} = 0.00328"$$

- Above crack

Assume $\mu(x)$ as in zone 4 (above crack) $\Rightarrow \delta_{A2} = 0.00100"$
$\delta_{A1} = (541\ \mu\varepsilon)(6.4") = 0.00346"$

$$\delta_{A_{\text{ABOVE CRACK}}} = \delta_{A1} - \delta_{A2} = 0.00246"$$

$$\delta_A = \delta_{A_{\text{BELOW CRACK}}} + \delta_{A_{\text{ABOVE CRACK}}} = 0.00574" = 0.146\ mm$$

$$\theta_{cr_5} = \frac{(0.00574)}{(11.6 - 6.37)} = 0.00110\ rad$$

$$\Delta X_{\theta_{cr5}} = (0.00110)(41.0") = 0.0450" = 0.00114\ m$$

<u>Note</u>: At end of crack 5 (start of crack 6):
$\varepsilon_s(x) = (541\ \mu\varepsilon) - (198\ \mu\varepsilon) = 343\ \mu\varepsilon$

vii) Zone 6

- Below crack

Assume $u(x)$ as in zone 4 (below crack) $\Rightarrow \delta_{A2} = 0.000180''$

$\delta_{A1} = (372\mu\varepsilon)(6.4'') = 0.00238''$

$$\delta_{A_{\substack{BELOW\\CRACK}}} = \delta_{A1} - \delta_{A2} = 0.00220''$$

- Above crack

Assume $u(x)$ as in zone 4 (above crack) $\Rightarrow \delta_{A2} = 0.00100''$

$\delta_{A1} = (372\mu\varepsilon)(6.4'') = 0.00238''$

$$\delta_{A_{\substack{ABOVE\\CRACK}}} = \delta_{A1} - \delta_{A2} = 0.00138''$$

$$\delta_A = \delta_{A_{\substack{BELOW\\CRACK}}} + \delta_{A_{\substack{ABOVE\\CRACK}}} = 0.00358'' = 0.0910\,mm$$

$$\theta_{cr6} = \frac{(0.00358)}{(11.6-6.51)} = 0.000704\ rad$$

$$\Delta X_{\theta_{cr6}} = (0.000704)(28.2'') = 0.0198'' = 0.000504\ m$$

Note: At end of crack 6:

$\varepsilon_s(x) = (372\mu\varepsilon) - (198\mu\varepsilon) = 174\mu\varepsilon$

viii) Uncracked Zone

$l = 28.2 - 6.4 = 21.8''$

$$R = \frac{M}{L} = \frac{612}{105} = 5.83^k$$

$$\Delta X_{el} = \frac{R\,l^3}{3EI_{uncr}} = \frac{(5.83)(21.8)^3}{(3)(6.28\times10^6)} = 0.00321'' = 0.0000814\ m$$

Summary: $\Delta X_{\theta FE} = 0.149'' = 0.00379\ m$

($\varepsilon_{s0} = 1{,}380\mu\varepsilon$) $\sum_{i=0}^{6} \Delta X_{\theta cr_i} = 0.778'' = 0.0198\ m$

$\Delta X_{el} = 0.00321'' = 0.0000814\ m$

$(\Delta X)_{TOTAL} = 0.930'' = 0.0236\ m$

Note that the deflections computed with assumed crack distribution ($\sum_{i=0}^{6} \Delta X_{\theta cri}$ and ΔX_{ce}) are based on a curvature distribution as given in page F'-10 (bottom right).

If now the deflections are computed based on average curvature distribution (cracked but as given by ECCOLA), as given in page F'-10 (bottom left), they will be:

$$\Delta X = \{12.8\}\{10^{-6}\}\{(210)(98.6)+(184)(85.8)+(159)(73.0)+(132)(60.2)+ + (103)(47.4)+(73)(34.6)\} +$$

$$+ \{\tfrac{12.8}{2}\}\{10^{-6}\}\{(24)(100.7)+(26)(87.9)+(25)(75.1)+(27)(62.3)+(29)(49.5)+(30)(36.7)\} +$$

$$+ \{\tfrac{28.2}{2}\}\{10^{-6}\}\{(19)(\tfrac{2}{3})(28.2)\} =$$

$$= 0.812 + 0.0691 + 0.00504 = 0.886'' = 0.0225\, m$$

c) $\varepsilon_{sA} = 5{,}000\,\mu\varepsilon$ (ON PLATEAU OF STEEL'S STRESS-STRAIN RELATIONSHIP AT BASE OF CANOPY)

$\varepsilon_s = 5{,}000\,\mu\varepsilon \Rightarrow M_s = 807^{\text{k-in}}$

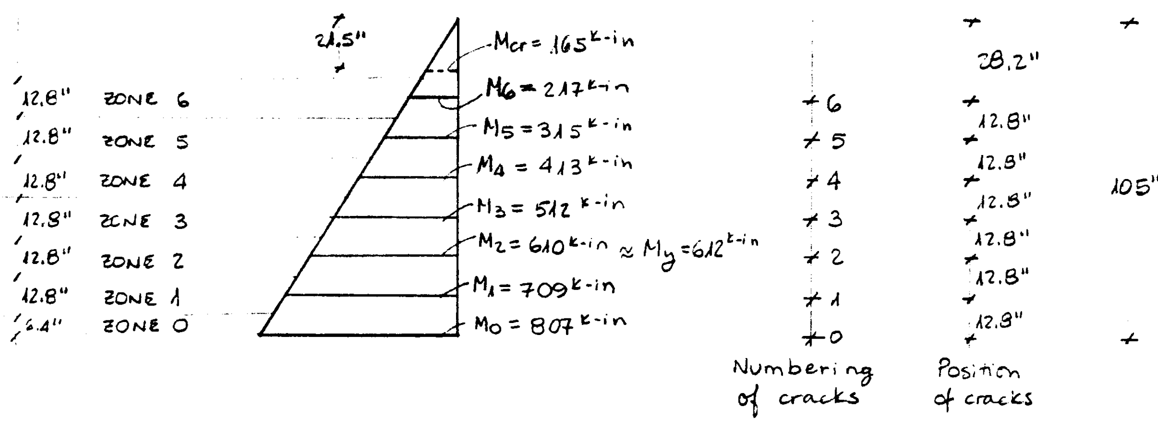

Same assumptions as for case a). (see p. F'-7)

Using results from ECCOLA:

ZONE	Mav (k-in)	Curvature ($\times 10^{-3}$ rad/in)	Tensile Steel Strain ($\mu\varepsilon$)	Neutral Axis Location (in)
0	807	0.713	5,000	4.75
1	709	0.322	1,990	5.45
2	612	0.233	1,380	5.69
3	512	0.195	1,150	5.97
4	413	0.157	931	6.06
5	315	0.119	710	6.23
6	217	0.083	489	6.41
	165	0.063	372	6.51

$\varepsilon_{SA} = 5{,}000\,\mu\varepsilon$

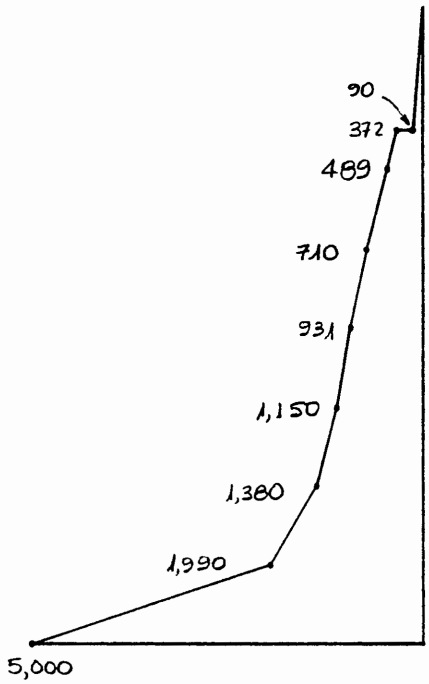

Tensile Steel Strain Distribution ε_s ($\mu\varepsilon$) (as given by RCCOLA) (linear interpolation)

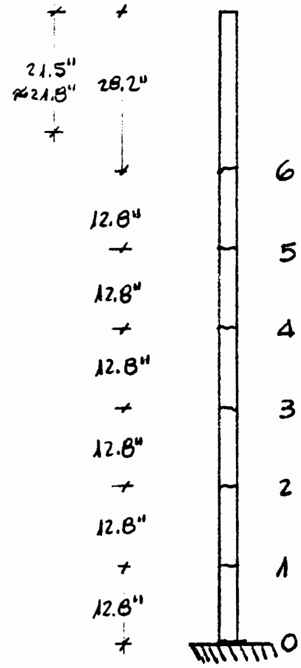

Position & Numbering of cracks

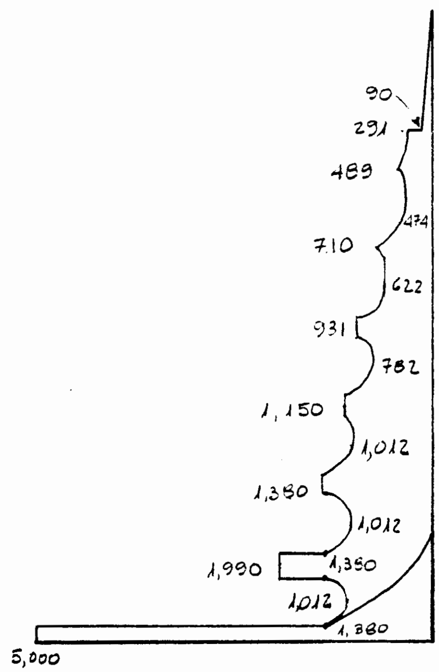

Tensile Steel Strain Distribution ε_s ($\mu\varepsilon$)
a) at cracks: as given by RCCOLA
b) other points: as given by assumed bond distribution

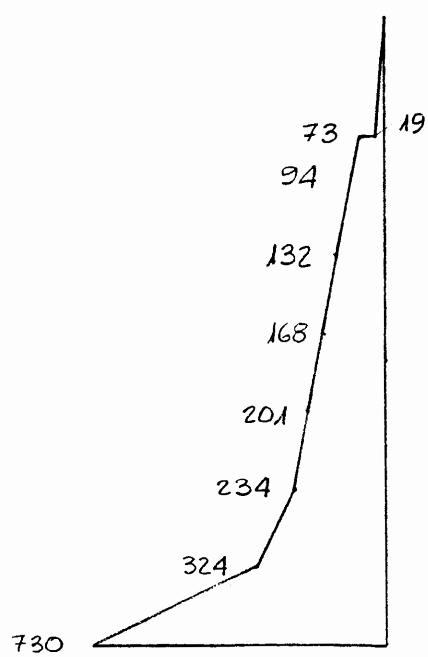

Curvature Distribution ϕ ($\times 10^{-6}$ rad/in) (as given by RCCOLA) (linear interpolation)

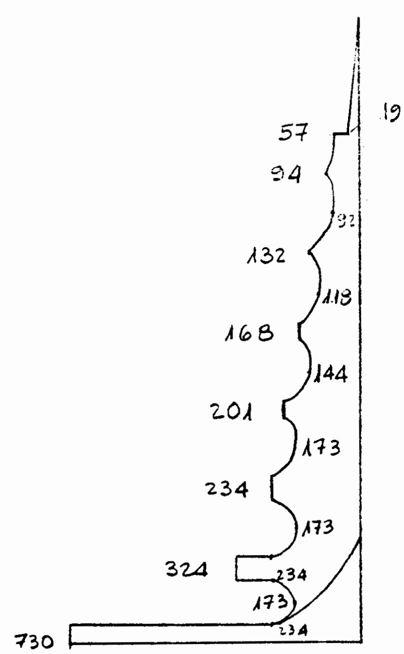

Curvature Distribution ϕ ($\times 10^{-6}$ rad/in)
a) at cracks: as given by RCCOLA
b) other pts: as given by assumed bond distribution

i) Zone 0

$$C_1 = \frac{\Sigma_o}{A_s E_{tx}} = \frac{(2.36)}{(0.442)(29000)} = 1.84 \times 10^{-4}$$

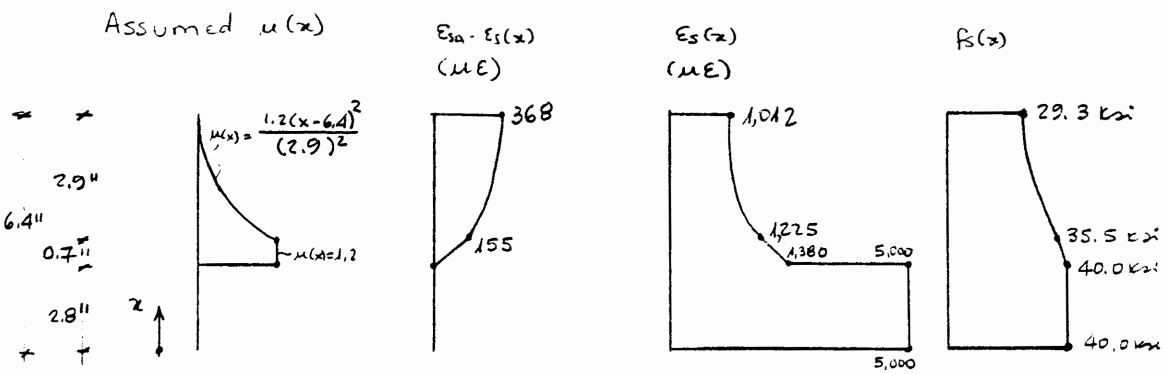

$$F_{BOND} = \overset{3\,bars}{3}\,\Sigma_o \int \mu(x)\,dx = (3)(2.36)(1.2)\left[(0.7) + (\tfrac{1}{3})(2.9)\right] = 14.2^k < A_e f'_t = 14.4^k$$

$0 \leq x \leq 2.8"$: $\varepsilon_{SA} - \varepsilon_s(x) = 0$; $\delta'_{A2} = 0$

$2.8" \leq x \leq 3.5"$: $\varepsilon_{SA} - \varepsilon_s(x) = 1.2\, C_1 (x - 2.8)$

at $x = 3.5"$: $\varepsilon_{SA} - \varepsilon_s(x) = 155\,\mu\varepsilon$

$$\delta''_{A2} = \frac{1.2\, C_1 (x-2.8)^2}{2}\Bigg|_{2.8}^{3.5} = 0.0000541"$$

$$3.5 \leq x \leq 6.4" : \varepsilon_{SA} - \varepsilon_s(x) = \frac{1.2\, C_1 (x-6.4)^3}{3\,(2.9)^2}\Bigg|_{3.5}^{x} + (155\,\mu\varepsilon) = (155\,\mu\varepsilon) + (8.75\times10^{-6})\left\{(x-6.4)^3 + (2.9)^3\right\}$$

at $x = 6.4"$: $\varepsilon_{SA} - \varepsilon_s(x) = 368\,\mu\varepsilon$

$$\delta'''_{A2} = (155\,\mu\varepsilon)\,x + (8.75\times10^{-6})\left\{\frac{(x-6.4)^4}{4} + (2.9)^3 x\right\}\Bigg|_{3.5}^{6.4} = 0.000914"$$

$$\delta_{A1} = (1{,}380\,\mu\varepsilon)(6.4") + (5{,}000\,\mu\varepsilon - 1{,}380\,\mu\varepsilon)(2.8") = 0.0190"$$

$$\delta_{A2} = \sum_{i=1}^{3} \delta^i_{A2} = 0.000968"$$

$$\delta_A = \delta_{A1} - \delta_{A2} = 0.0180" = 0.458\ mm$$

$$\theta_{cro} = \frac{(0.0180)}{(11.6 - 4.75)} = 0.00263\ rad$$

$$\Delta X_{\theta_{cro}} = (0.00263)(105") = 0.276" = 0.00702\ m$$

ii) Zone 1

- Below crack

Assume $\mu(x)$ distribution as in zone 0. $\Rightarrow \delta_{A2} = 0.000963"$
$\delta_{A1} = (1{,}380\mu\varepsilon)(6.4") + (1{,}990 - 1{,}380)(\mu\varepsilon)(2.8") = 0.00883 + 0.00171 = 0.0105"$

$$\Rightarrow \delta_{A\,\substack{BELOW\\CRACK}} = \delta_{A1} - \delta_{A2} = 0.00953" = 0.242 \text{ mm}$$

- Above crack

Assume $\mu(x)$ distribution as in zone 0 ($\varepsilon_{SA} = 1{,}350\mu\varepsilon$, p. F'-11) $\Rightarrow \delta_{A2} = 0.00115"$
$\delta_{A1} = (1{,}380\mu\varepsilon)(6.4") + (1{,}990 - 1{,}380)(\mu\varepsilon)(2.2") = 0.00883 + 0.00134 = 0.0102"$

$$\Rightarrow \delta_{A\,\substack{ABOVE\\CRACK}} = \delta_{A1} - \delta_{A2} = 0.00902" = 0.229 \text{ mm}$$

$$\delta_A = \delta_{A\,\substack{BELOW\\CRACK}} + \delta_{A\,\substack{ABOVE\\CRACK}} = 0.0186" = 0.471 \text{ mm}$$

$$\theta_{cr1} = \frac{(0.0186)}{(11.6 - 5.45)} = 0.00302 \text{ rad}$$

$$\Delta X_{\theta_{cr1}} = (0.00302)(92.2") = 0.278" = 0.00706 \text{ m}$$

Note: At end of crack 1 (start of crack 2):
$\varepsilon_s(x) = 1012\,\mu\varepsilon$ (see p. F'-11)

iii) Zone 2

For both below and above crack, assume $\mu(x)$ distribution as in zone 0 ($\varepsilon_{SA} = 1{,}350\mu\varepsilon$, p. F'-11) $\Rightarrow \delta_{A2} = 2(0.00115) = 0.00230"$
$\delta_{A1} = \{(1{,}380\,\mu\varepsilon)(6.4")\}\{2\} = 0.0177"$

$$\delta_A = \delta_{A1} - \delta_{A2} = 0.0154" = 0.390 \text{ mm}$$

$$\theta_{cr2} = \frac{(0.0154)}{(11.6 - 5.69)} = 0.00260 \text{ rad}$$

$$\Delta X_{\theta_{cr2}} = (0.00260)(79.4") = 0.206" = 0.00524 \text{ m}$$

Note: At end of crack 2 (start of crack 3):
$\varepsilon_s(x) = 1012\ \mu\varepsilon$ (see p. F'-11).

(v) Zone 3

- Below crack

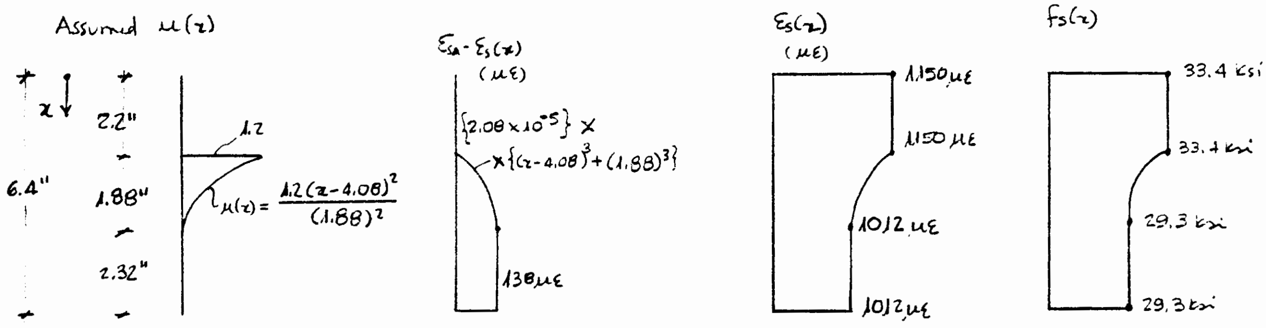

$$F_{BOND} = 3\Sigma_0 \int \mu(x)dx = (3)(2.36)(1.2)(1.88)(\tfrac{1}{3}) = 5.3^k < A_e f'_t = 14.4^k$$ o.k.

$0 \le x \le 2.2"$: $\varepsilon_{sA} - \varepsilon_s(x) = 0$; $\delta'_{A2} = 0$

$2.2" \le x \le 4.08"$: $\varepsilon_{sA} - \varepsilon_s(x) = \frac{1.2\, C_1\, (x-4.08)^3}{3\,(1.88)^2}\Big|_{2.2}^{x} = 2.08\times10^{-5}\{(x-4.08)^3 + (1.88)^3\}$

at $x = 4.08"$: $\varepsilon_{sA} - \varepsilon_s(x) = 138\ \mu\varepsilon$

$$\delta''_{A2} = 2.08\times10^{-5}\left\{\frac{(x-4.08)^4}{4} + (1.88)^3 x\right\}\Big|_{2.2}^{4.08} = 0.000195"$$

$4.08" \le x \le 6.4"$: $\varepsilon_{sA} - \varepsilon_s(x) = (138\mu\varepsilon)$

at $x = 6.4$: $\delta'''_{A2} = (138\ \mu\varepsilon)(2.32") = 0.000320"$

$\delta_{A1} = (1{,}150\ \mu\varepsilon)(6.4") = 0.00736"$

$\delta_{A2} = \sum_{i=1}^{3} \delta^i_{A2} = 0.000515"$

$\delta_{A_{\text{BELOW CRACK}}} = \delta_{A1} - \delta_{A2} = 0.00684"$

- Above crack

Assume $\mu(x)$ distribution as in zone 0 ($\varepsilon_{sA} = 1{,}380\ \mu\varepsilon$, p. F'-11) $\Rightarrow \delta_{A2} = 0.00115"$

$\delta_{A1} = (1{,}150\mu\varepsilon)(6.4") = 0.00736"$

$\delta_{A_{\text{ABOVE CRACK}}} = \delta_{A1} - \delta_{A2} = 0.00621"$

$$\delta_A = \delta_{A_{\text{BELOW CRACK}}} + \delta_{A_{\text{ABOVE CRACK}}} = 0.0131" = 0.331\ mm$$

$$\theta_{cr3} = \frac{(0.0131)}{(11.6 - 5.87)} = 0.00228\ rad$$

$\Delta X_{\theta_{cr3}} = (0.00228)(66.6") = 0.152" = 0.00386\ m$

<u>Note:</u> At end of crack 3 (start of crack 4):

$\varepsilon_s(x) = (1{,}150\,\mu\varepsilon) - (368\,\mu\varepsilon) = 782\,\mu\varepsilon$

<u>v) Zone 4</u>

- Below crack

Assumed $\mu(x)$

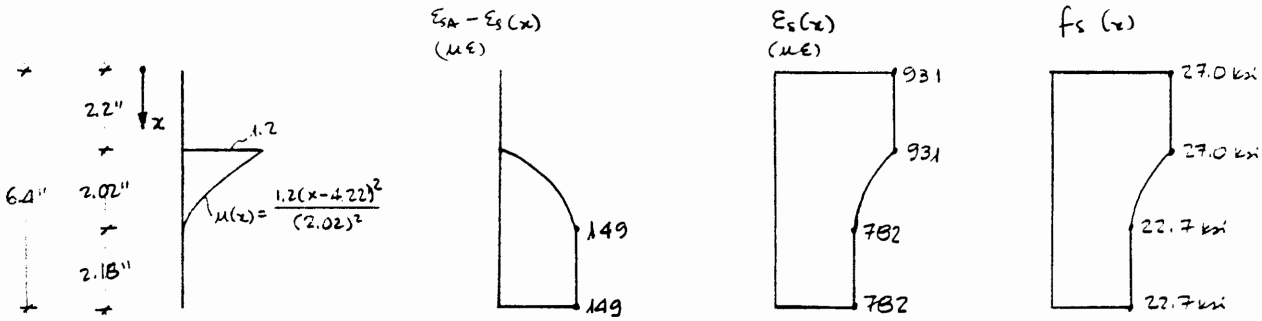

$F_{BOND} = 3\Sigma_o \int \mu(x)dx = (3)(2.36)(1.2)(2.02)(\frac{1}{3}) = 5.72^K < A_e f'_t = 14.4^K$ <u>O.K.</u>

$0 \le x \le 2.2"$: $\varepsilon_{sA} - \varepsilon_s(x) = 0$; $\delta'_{A2} = 0$

$2.2" \le x \le 4.22"$: $\varepsilon_{sA} - \varepsilon_s(x) = \frac{1.2C_1(x-4.22)^3}{3(2.02)^2}\Big|_{2.2}^{x} = 1.80\times10^{-5}\{(x-4.22)^3 + (2.02)^3\}$

$$\delta''_{A2} = 1.80\times10^{-5}\left\{\frac{(x-4.22)^4}{4} + (2.02)^3 x\right\}\Big|_{2.2}^{4.22} = 0.000225"$$

$4.22" \le x \le 6.4"$: $\varepsilon_{sA} - \varepsilon_s(x) = 149\ \mu\varepsilon$

$$\delta'''_{A2} = (149\,\mu\varepsilon)(2.18") = 0.000325"$$

$\left.\begin{array}{l} \delta_{A1} = (931\,\mu\varepsilon)(6.4") = 0.00596" \\ \delta_{A2} = \sum_{i=1}^{3} \delta^{i}_{A2} = 0.000550" \end{array}\right\} \delta_{A_{BELOW\ CRACK}} = \delta_{A1} - \delta_{A2} = 0.00541" = 0.137\,mm$

- Above crack

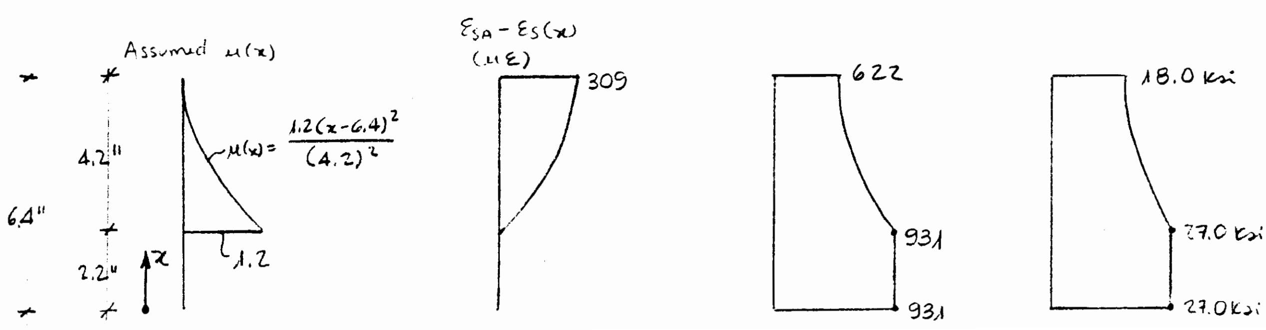

$F_{BOND} = 3\Sigma_0 \int \mu(x)dx = (3)(2.36)(1.2)(4.2)(1/3) = 11.9^k < A_e f'_t = 14.4^k$ o.k.

$0 \le x \le 2.2"$: $\varepsilon_{SA} - \varepsilon_s(x) = 0$; $\delta'_{A2} = 0$

$2.2" \le x \le 6.4"$: $\varepsilon_{SA} - \varepsilon_s(x) = \left.\frac{1.2C_1(x-6.4)^3}{3(4.2)^2}\right|_{2.2}^{x} = 4.17\times10^{-6}\{(x-6.4)^3 + (4.2)^3\}$

at $x = 6.4"$: $\varepsilon_{SA} - \varepsilon_s(x) = 309\ \mu\varepsilon$

$\delta''_{A2} = 4.17\times10^{-6}\left\{\frac{(x-6.4)^4}{4} + (4.2)^3 x\right\}\Big|_{2.2}^{6.4} = 0.000974"$

$$\left.\begin{array}{l}\delta_{A1} = (931\,\mu\varepsilon)(6.4") = 0.00596" \\ \delta_{A2} = \sum_{i=1}^{3} \delta^i_{A2} = 0.000974"\end{array}\right\} \delta_{A_{\text{ABOVE CRACK}}} = \delta_{A1} - \delta_{A2} = 0.00498" = 0.127\text{ mm}$$

$\delta_A = \delta_{A_{\text{BELOW CRACK}}} + \delta_{A_{\text{ABOVE CRACK}}} = 0.0104" = 0.264$ mm

$\theta_{cr4} = \frac{(0.0104)}{(11.6 - 6.06)} = 0.00188$ rad

$\Delta X_{\theta_{cr4}} = (0.00188)(53.8") = 0.101" = 0.00256$ m

vi) Zone 5

- Below crack

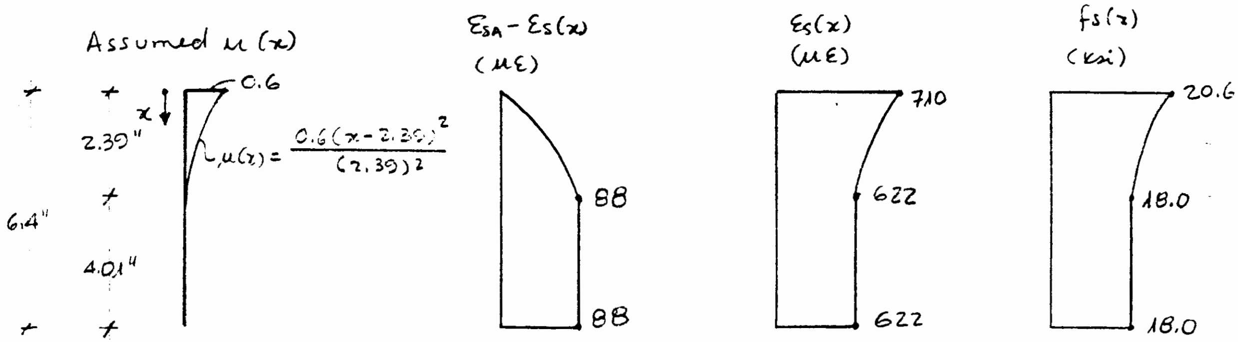

$F_{BOND} = 3\Sigma_0 \int \mu(x)dx = 3(2.36)(0.6)(2.39)(1/3) = 3.4^K < A_e f'_t = 14.4^K$ o.k.

$0 \le x \le 2.39"$: $\varepsilon_{SA} - \varepsilon_s(x) = \left.\frac{0.6C_1(x-2.39)^3}{3(2.39)^2}\right|_0^x = 6.44\times10^{-6}\{(x-2.39)^3 + (2.39)^3\}$

at $x = 2.39"$: $\varepsilon_{SA} - \varepsilon_s(x) = 88\ \mu\varepsilon$

$\delta'_{A2} = 6.44\times10^{-6}\left\{\frac{1}{4}(x-2.39)^4 + (2.39)^3 x\right\}\Big|_0^{2.39} = 0.000158"$

$2.39'' \leq x \leq 6.4''$: $\varepsilon_{SA} - \varepsilon_s(x) = 88\mu\varepsilon$

$$\delta_{A2}'' = (88\mu\varepsilon)(4.01'') = 0.000353''$$

$$\left.\begin{aligned} \delta_{A1} &= (710\,\mu\varepsilon)(6.4'') = 0.00454'' \\ \delta_{A2} &= \sum_{i=1}^{2} \delta_{A2}^{i} = 0.000511'' \end{aligned}\right\} \delta_{A_{\text{BELOW CRACK}}} = \delta_{A1} - \delta_{A2} = 0.00403''$$

– Above crack

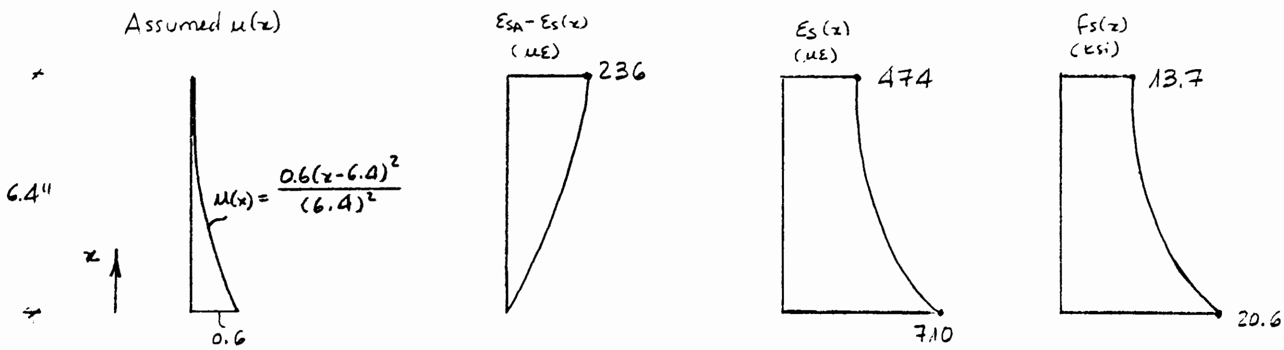

$$F_{BOND} = 3\Sigma_o \int \mu(x)\,dx = 3(2.36)(0.6)(6.4)(1/3) = 9.1^k < A_e f_t' = 14.4^k \quad \text{o.k.}$$

$$0 \leq x \leq 6.4'': \quad \varepsilon_{SA} - \varepsilon_s(x) = \frac{0.6\,C_1(x-6.4)^3}{3(6.4)^2}\Bigg|_0^x = 8.98\times10^{-7}\left\{(x-6.4)^3 + (6.4)^3\right\}$$

$$\text{At } x = 6.4'': \quad \varepsilon_{SA} - \varepsilon_s(x) = 236\,\mu\varepsilon$$

$$\delta_{A2} = 8.98\times10^{-7}\left\{\tfrac{1}{4}(x-6.4)^4 + (6.4)^3 x\right\}\Bigg|_0^{6.4} = 0.00113''$$

$$\left.\begin{aligned} \delta_{A1} &= (710\,\mu\varepsilon)(6.4'') = 0.00454'' \\ \delta_{A2} &= 0.00113'' \end{aligned}\right\} \delta_{A_{\text{ABOVE CRACK}}} = \delta_{A1} - \delta_{A2} = 0.00341'' = 0.0866\text{ mm}$$

$$\theta_{crs} = \frac{(0.00341)}{(11.6 - 6.23)} = 0.000635 \text{ rad}$$

$$\Delta X_{\theta_{crs}} = (0.000635)(41.0'') = 0.0260'' = 0.000661 \text{ m}$$

vii) Zone 6

– Below crack

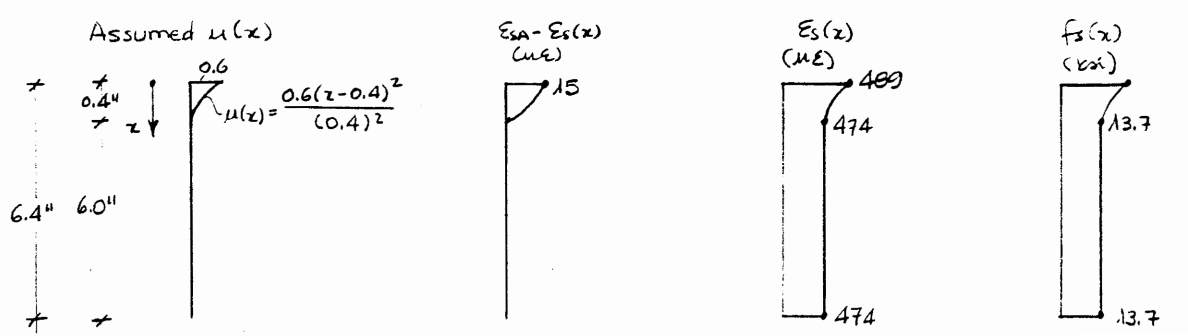

$$F_{BOND} = 3\,\Sigma_0 \int \mu(x)\,dx = 3(2.36)(0.6)(0.4)(1/3) = 0.6^{K} < A_e f'_t = 14.4^{K} \qquad \underline{O.K.}$$

$$0 \le x \le 0.4'' : \quad \varepsilon_{sA} - \varepsilon_s(x) = \frac{0.6\,C_1\,(x-0.4)^3}{3\,(0.4)^2}\Big|_0^x = 0.000230\left\{(x-0.4)^3 + (0.4)^3\right\}$$

$$\text{at } x = 0.4'' : \quad \varepsilon_{sA} - \varepsilon_s(x) = 15\,\mu\varepsilon$$

$$\delta'_{A2} = 0.000230\left\{\tfrac{1}{4}(x-0.4)^4 + (0.4)^3 x\right\}\Big|_0^{0.4} = 0.00000442''$$

$$0.4'' \le x \le 6.4'' : \quad \varepsilon_{sA} - \varepsilon_s(x) = 15\,\mu\varepsilon$$

$$\delta''_{A2} = (15\,\mu\varepsilon)(6.0'') = 0.0000900''$$

$$\left.\begin{array}{l} \delta_{A1} = (489\,\mu\varepsilon)(6.4'') = 0.00313'' \\ \\ \delta_{A2} = 0.0000944'' \end{array}\right\} \delta_{A_{\text{BELOW CRACK}}} = \delta_{A,1} - \delta_{A2} = 0.00304'' = 0.0771\text{ mm}$$

- Above crack

Assume same $\mu(x)$ as in zone 4 (above crack) ($\varepsilon_{sA} = 1{,}380\,\mu\varepsilon$) (see p. F'-14 & F'-15)

$$\Rightarrow \delta_{A2} = 0.00100''$$

$$\delta_{A1} = (489\,\mu\varepsilon)(6.4'') = 0.00313''$$

$$\delta_{A_{\text{ABOVE CRACK}}} = \delta_{A1} - \delta_{A2} = 0.00213'' = 0.0541\text{ mm}$$

$$\delta_A = \delta_{A_{\text{BELOW CRACK}}} + \delta_{A_{\text{ABOVE CRACK}}} = 0.00517'' = 0.131\text{ mm}$$

$$\theta_{cr_6} = \frac{(0.00517)}{(11.6 - 6.41)} = 0.000996\text{ rad}$$

$$\Delta X_{\theta_{cr_6}} = (0.000996)(28.2'') = 0.0281'' = 0.000714\text{ m}$$

<u>Note</u> : At end of crack 6 :
$\varepsilon_s(x) = (489\,\mu\varepsilon) - (198\,\mu\varepsilon) = 291\,\mu\varepsilon$

<u>viii) Uncracked zone</u>

$$R = \frac{M}{L} = \frac{807}{105} = 7.69^{K}$$

$$\ell = 28.2 - 6.4 = 21.8''$$

$$\Delta X_\ell = \frac{R\,\ell^3}{3\,E\,I_{uncr}} = \frac{(7.69)(21.8)^3}{3\,(6.26\times10^6)} = 0.00423'' = 0.000107\text{ m}$$

Summary: $\Delta X_{\theta_{FE}} = 0.301'' = 0.00765$ m

($\varepsilon_{sA} = 5{,}000\,\mu\varepsilon$)

$$\sum_{i=0}^{6} \Delta X_{\theta_{cri}} = 1.067'' = 0.0271 \text{ m}$$

$$\Delta X_{el} = 0.00423'' = 0.000107 \text{ m}$$

$$(\Delta X)_{TOTAL} = 1.372'' = 0.0349 \text{ m}$$

Note that the deflections computed with assumed crack distribution ($\sum_{i=0}^{6} \Delta X_{\theta_{cri}}$ and ΔX_{el}) are based on a curvature distribution as given in page F'-19 (bottom right).

If now the deflections are computed based on average curvature distribution (cracked but as given by RCCOLA), as given in page F'-19 (bottom left), they will be:

$$\Delta X = \{12.8\}\{10^{-6}\}\{(324)(98.6) + (234)(85.8) + (201)(73.0) + (168)(60.2) + (132)(47.4) + (94)(34.6)\} +$$

$$+ \left\{\tfrac{12.8}{2}\right\}\{10^{-6}\}\{(406)(100.7) + (90)(87.9) + (33)(75.1) + (33)(62.3) + (26)(49.5) + (38)(36.7)\} +$$

$$+ \left\{\tfrac{12.8}{2}\right\}\{10^{-6}\}\{(73)(25) + (21)(\tfrac{1}{2})(26.1)\} + \{(21.8)(19)(\tfrac{1}{2})(\tfrac{2}{3})(21.8)\}\{10^{-6}\}$$

$$= 1.105 + 0.362 + 0.0134 + 0.00301 = 1.483'' = 0.0377 \text{ m}$$

c) $\varepsilon_{s} = 10,000\ \mu\varepsilon$ (ON PLATEAU OF STEEL'S STRESS-STRAIN RELATIONSHIP AT SUPPORT)

$\varepsilon_s = 10,000\ \mu\varepsilon \Rightarrow M_s = 766^{k\text{-}in}$

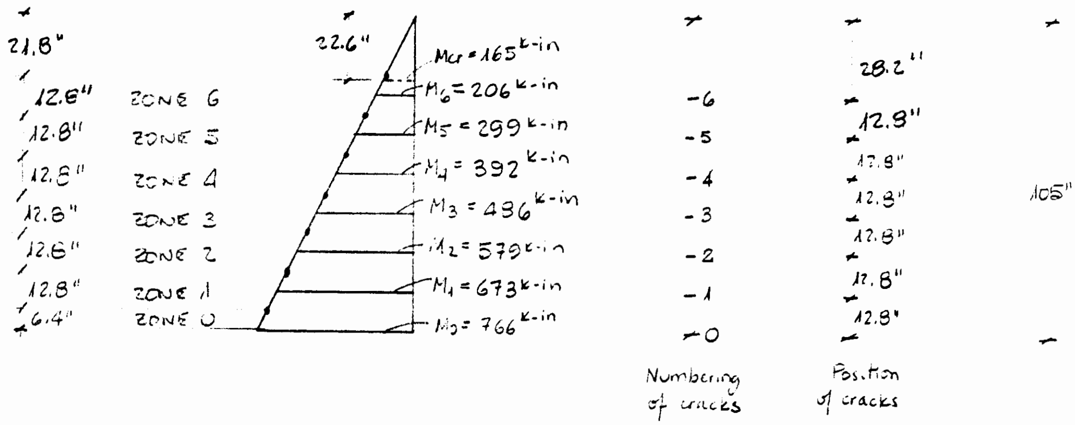

Same assumptions as for case a).

Using results from RCCOLA:

ZONE	M_{AV} (k-in)	Curvature ($\times 10^{-3}$ rad/in)	Tensile Steel Strain ($\mu\varepsilon$)	Neutral Axis Location (in)
0	766	1.50	10,000	4.96
1	673	0.276	1,660	5.59
2	579	0.221	1,310	5.75
3	486	0.185	1,100	5.92
4	392	0.149	884	6.09
5	299	0.114	674	6.27
6	206	0.079	465	6.44

$\varepsilon_{sA} = 10{,}000\ \mu\varepsilon$

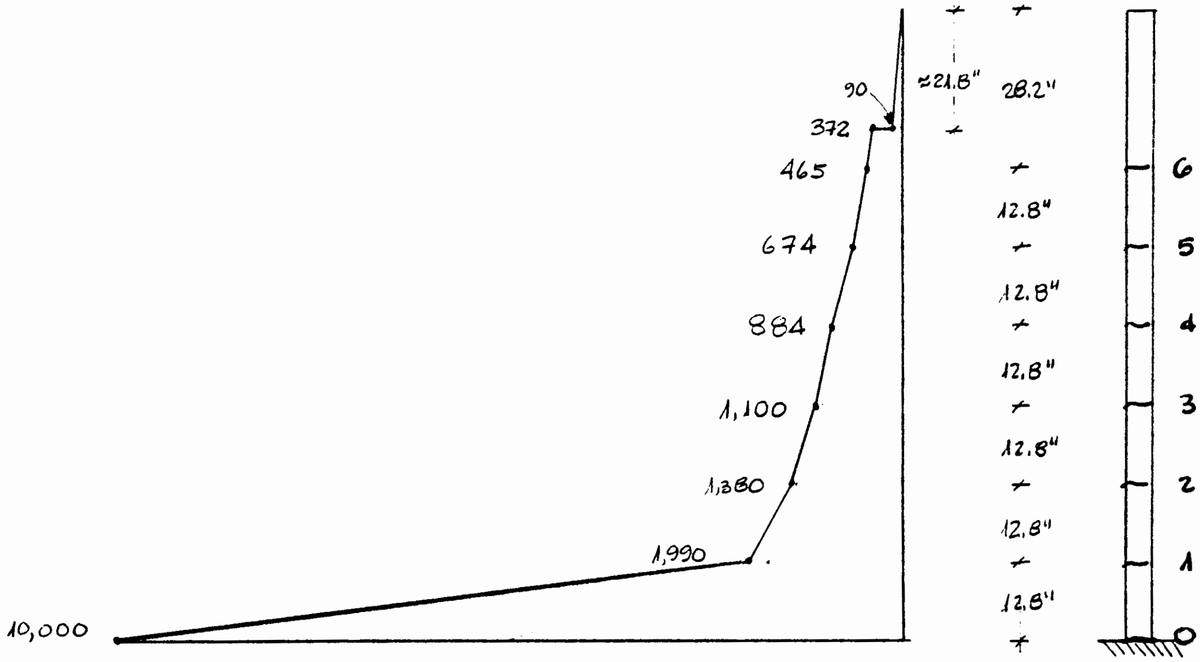

Tensile Steel Strain Distribution ε_s ($\mu\varepsilon$)
(as given by RCCOLA) (linear interpolation)
(Attention to ε_s history, see pages F'-10 & F'-19)

Position & Numbering of cracks

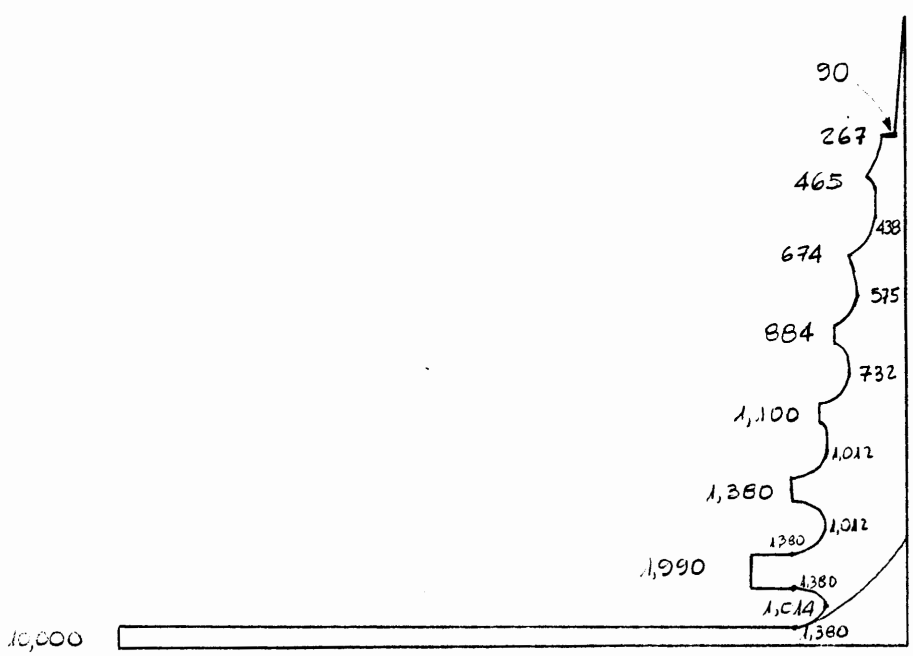

Tensile Steel Strain Distribution ε_s ($\mu\varepsilon$)
a) at cracks: as given by RCCOLA
b) at other pts: as given by assumed bond distribution

Attention to ε_s history (See pages F'-10 & F'-19)

$\varepsilon_{SA} = 10{,}000\ \mu\varepsilon$

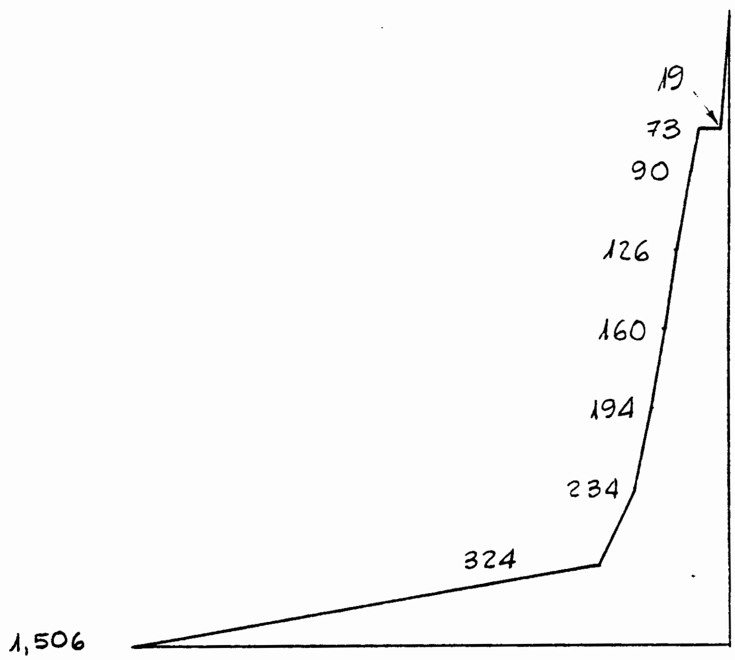

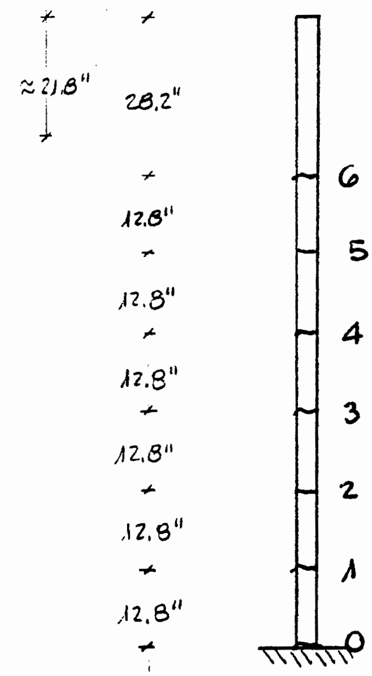

Curvature Distribution ϕ ($\times 10^{-6}$ rad/in)
(as given by RCCOLA) (linear interpolation)
(Attention to ϕ history, see p. F'-10 & F'-19)

Position & Numbering of Cracks

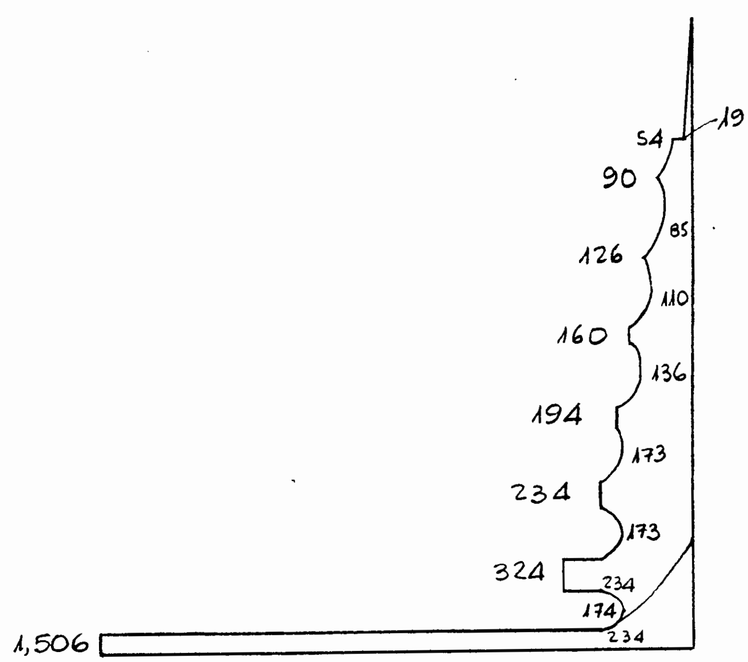

Curvature Distribution ϕ ($\times 10^{-6}$ rad/in)
a) at cracks: as given by RCCOLA
b) other points: as given by assumed bond distribution
Attention to ϕ history, see pages F'-10 & F'-19)

i) Zone 0

$$C_1 = \frac{\varepsilon_o}{A_s E_{tx}} = \frac{(2.36)}{(0.442)(29000)} = 1.84 \times 10^{-4}$$

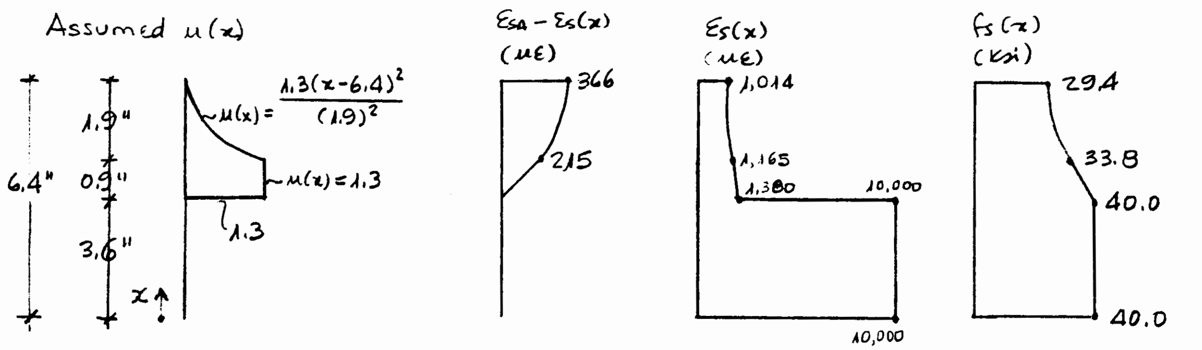

$$F_{BOND} = 3\,\Sigma_o \int \mu(x)dx = (3)(2.36)(1.3)\left[(0.9) + (\tfrac{1}{3})(1.9)\right] = 14.1^k < A_e f'_t = 14.4^k$$

$0 \le x \le 3.6"$: $\varepsilon_{SA} - \varepsilon_S(x) = 0$; $\delta'_{A2} = 0$

$3.6" \le x \le 4.5"$: $\varepsilon_{SA} - \varepsilon_S(x) = 1.3\,C_1\,(x - 3.6)$

at $x = 4.5"$: $\varepsilon_{SA} - \varepsilon_S(x) = 215\,\mu\varepsilon$

$$\delta''_{A2} = \frac{1.3C_1}{2}(x-3.6)^2\Big|_{3.6}^{4.5} = 0.0000969"$$

$4.5" \le x \le 6.4"$: $\varepsilon_{SA} - \varepsilon_S(x) = (215\mu\varepsilon) + \dfrac{1.3\,C_1\,(x-6.4)^3}{3\,(1.9)^2}\Big|_{4.5}^{x} = (215\mu\varepsilon) + 2.21\times10^{-5}\{(x-6.4)^3 + (1.9)^3\}$

at $x = 6.4"$: $\varepsilon_{SA} - \varepsilon_S(x) = 366\ \mu\varepsilon$

$$\delta'''_{A2} = (215\mu\varepsilon)x + 2.21\times10^{-5}\left\{\tfrac{1}{4}(x-6.4)^4 + (1.9)^3 x\right\}\Big|_{4.5}^{6.4} = 0.000624"$$

$$\delta_{A1} = (1{,}380\mu\varepsilon)(6.4") + (10{,}000\mu\varepsilon - 1{,}380\mu\varepsilon)(3.6") = 0.0399"$$

$$\delta_{A2} = \sum_{i=1}^{3} \delta^i_{A2} = 0.000721"$$

$$\delta_A = \delta_{A1} - \delta_{A2} = 0.0391" = 0.994\ mm$$

$$\theta_{cro} = \frac{(0.0391)}{(11.6 - 4.96)} = 0.00589\ rad$$

$$\Delta X_{\theta_{cro}} = (0.00589)(105") = 0.619" = 0.0157\ m$$

ii) Zone 1

- Below crack

Assume $\mu(x)$ distribution as in zone 0 ($\varepsilon_{SA} = 1{,}380\,\mu\varepsilon$, p. F'-1.1) $\Rightarrow \delta_{A2} = 0.00115''$
$\delta_{A1} = (1{,}380\,\mu\varepsilon)(6.4'') + (1{,}990 - 1{,}380)(\mu\varepsilon)(2.2'') = 0.0102''$

$$\Rightarrow \delta_{A_{\text{BELOW CRACK}}} = \delta_{A1} - \delta_{A2} = 0.00902'' = 0.229\ \text{mm}$$

- Above crack

Assume $\mu(x)$ distribution as in zone 0 ($\varepsilon_{SA} = 1{,}380\,\mu\varepsilon$, p. F'-1.1) $\Rightarrow \delta_{A2} = 0.00115''$
$\delta_{A1} = (1{,}380\,\mu\varepsilon)(6.4'') + (1{,}990\,\mu\varepsilon - 1{,}380\,\mu\varepsilon)(2.2'') = 0.0102''$

$$\Rightarrow \delta_{A_{\text{ABOVE CRACK}}} = \delta_{A1} - \delta_{A2} = 0.00902'' = 0.229\ \text{mm}$$

$$\delta_A = \delta_{A_{\text{BELOW CRACK}}} + \delta_{A_{\text{ABOVE CRACK}}} = 0.0180'' = 0.458\ \text{mm}$$

$$\theta_{cr1} = \frac{(0.0180)}{(11.6 - 5.45)} = 0.00293\ \text{rad}$$

$$\Delta X_{\theta cr1} = (0.00293)(92.2'') = 0.270'' = 0.00687\ \text{m}$$

<u>Note</u>: At end of crack 1 (start of crack 2):
$\varepsilon_s(x) = 1012\,\mu\varepsilon$ (see p. F'-11)

iii) Zone 2

this zone is exactly the same as zone 2 for $\varepsilon_{SA} = 5{,}000\,\mu\varepsilon$ (see p. F'-2.1).

$$\Rightarrow \Delta X_{\theta cr2} = 0.206'' = 0.00524\ \text{m}$$

<u>Note</u>: At end of crack 2 (start of crack 3):
$\varepsilon_s(x) = 1012\,\mu\varepsilon$ (see p. F'-11)

iv) Zone 3

– Below crack

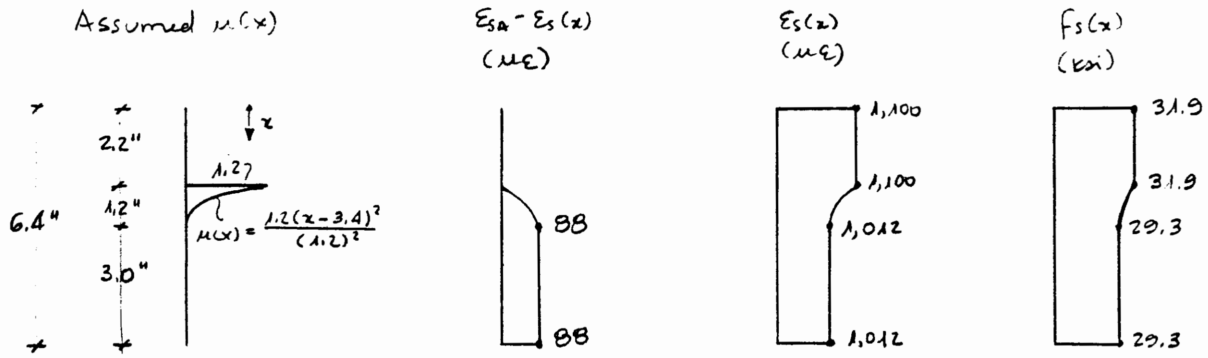

$F_{BOND} = 3\Sigma_0 \int \mu(x)\,dx = 3(2.36)(1.2)(1.2)(1/3) = 3.4^k < A_c f'_t = 14.4^k$ O.K.

$0 \leq x \leq 2.2"$: $\varepsilon_{SA} - \varepsilon_s(x) = 0$; $\delta'_{A2} = 0$

$2.2" \leq x \leq 3.4"$: $\varepsilon_{SA} - \varepsilon_s(x) = \frac{1.2\,C_1\,(x-3.4)^3}{3\,(1.2)^2}\Big|_{2.2}^{x} = 5.11\times10^{-5}\{(x-3.4)^3 + (1.2)^3\}$

at $x = 3.4"$: $\varepsilon_{SA} - \varepsilon_s(x) = 88\ \mu\varepsilon$

$\delta''_{A2} = 5.11\times10^{-5}\{\frac{1}{4}(x-3.4)^4 + (1.2)^3 x\}\Big|_{2.2}^{3.4} = 0.0000795"$

$3.4" \leq x \leq 6.4"$: $\varepsilon_{SA} - \varepsilon_s(x) = 88\ \mu\varepsilon$

$\delta'''_{A2} = (88\mu\varepsilon)\,x\Big|_{3.4}^{6.4} = 0.000264"$

$$\left.\begin{array}{l} \delta_{A1} = (1{,}100\ \mu\varepsilon)(6.4") = 0.00704" \\ \delta_{A2} = \sum_{i=1}^{3} \delta^i_{A2} = 0.000344" \end{array}\right\} \delta_{A_{\text{BELOW CRACK}}} = \delta_{A1} - \delta_{A2} = 0.00670" = 0.170\ mm$$

– Above crack

Assume $\mu(x)$ distribution as in zone 0 ($\varepsilon_{SA} = 1{,}380\ \mu\varepsilon$, p. $F'-11$) $\Rightarrow \delta_{A2} = 0.00115"$

$\delta_{A1} = (1{,}100\ \mu\varepsilon)\ (6.4") = 0.00704"$

$\delta_{A_{\text{ABOVE CRACK}}} = \delta_{A1} - \delta_{A2} = 0.00589" = 0.150\ mm$

$\delta_A = \delta_{A_{\text{BELOW CRACK}}} + \delta_{A_{\text{ABOVE CRACK}}} = 0.0126" = 0.320\ mm$

$\theta_{cr3} = \frac{(0.0126)}{(11.6 - 5.92)} = 0.00222\ rad$

$\Delta X_{\theta cr3} = (0.00222)(66.6") = 0.148" = 0.00375\ m$

Note: At end of crack 3 (start of crack 4): $\varepsilon_s(x) = (1{,}100\ \mu\varepsilon) - (368\ \mu\varepsilon) = 732\ \mu\varepsilon$

v) Zone 4

$$C_1 = \frac{\varepsilon_0}{A_s E_{tx}} = \frac{(2.36)}{(0.442)(29000)} = 1.84 \times 10^{-4}$$

– Below crack

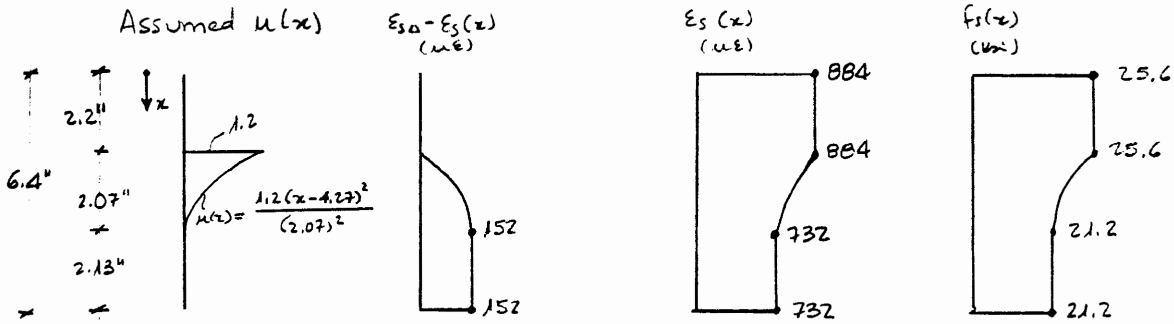

$$F_{BOND} = 3\Sigma_0 \int \mu(x)dx = 3(2.36)(1.2)(2.07)(1/3) = 5.9^k < A_e f'_t = 14.4^k \qquad \underline{\text{o.k.}}$$

$0 \le x \le 2.2''$: $\varepsilon_{sA} - \varepsilon_s(x) = 0$; $\delta'_{A2} = 0$

$2.2'' \le x \le 4.27''$: $\varepsilon_{sA} - \varepsilon_s(x) = \left.\frac{1.2 C_1 (x-4.27)^3}{3(2.07)^2}\right|_{2.2}^{x} = 1.72 \times 10^{-5}\{(x-4.27)^3 + (2.07)^3\}$

At $x = 4.27''$: $\varepsilon_{sA} - \varepsilon_s(x) = 152\ \mu\varepsilon$

$$\delta''_{A2} = 1.72\times 10^{-5}\left\{\tfrac{1}{4}(x-4.27)^4 + (2.07)^3 x\right\}\Big|_{2.2}^{4.27} = 0.000237''$$

$4.27 \le x \le 6.4''$: $\varepsilon_{sA} - \varepsilon_s(x) = 152\mu\varepsilon$

$$\delta'''_{A2} = (152\ \mu\varepsilon)(2.13'') = 0.000324''$$

$$\left.\begin{aligned} \delta_{A1} &= (884\mu\varepsilon)(6.4'') = 0.00566'' \\ \delta_{A2} &= \sum_{i=1}^{3} \delta^i_{A2} = 0.000561'' \end{aligned}\right\} \quad \delta_{A_{\substack{BELOW\\CRACK}}} = \delta_{A1} - \delta_{A2} = 0.00510'' = 0.129\text{ mm}$$

– Above crack

Assume $\mu(x)$ distribution as in zone 4 (above crack, $\varepsilon_{sA} = 5{,}000\mu\varepsilon$, p. F'-23 & F'-24)

$$\left.\begin{aligned} &\Rightarrow \delta_{A2} = 0.000974'' \\ &\delta_{A1} = (884\mu\varepsilon)(6.4'') = 0.00566'' \end{aligned}\right\} \quad \delta_{A_{\substack{ABOVE\\CRACK}}} = \delta_{A1} - \delta_{A2} = 0.00469'' = 0.119\text{ mm}$$

$$\delta_A = \delta_{A_{\substack{BELOW\\CRACK}}} + \delta_{A_{\substack{ABOVE\\CRACK}}} = 0.00979'' = 0.249\text{ mm}$$

$$\theta_{cr4} = \frac{(0.00979)}{(11.6 - 6.09)} = 0.00178\text{ rad}$$

$$\Delta X_{\theta cr_4} = (0.00178)(53.8'') = 0.0956'' = 0.00243\text{ m}$$

Note: At end of crack 4 (start of crack 5):
$\varepsilon_s(x) = (884\mu\varepsilon) - (309\mu\varepsilon) = 575\mu\varepsilon$

vi) Zone 5

$C_1 = \frac{\Sigma_0}{A_s E_{t_x}} = \frac{(2.36)}{(0.442)(29000)} = 1.84 \times 10^{-4}$

– Below crack

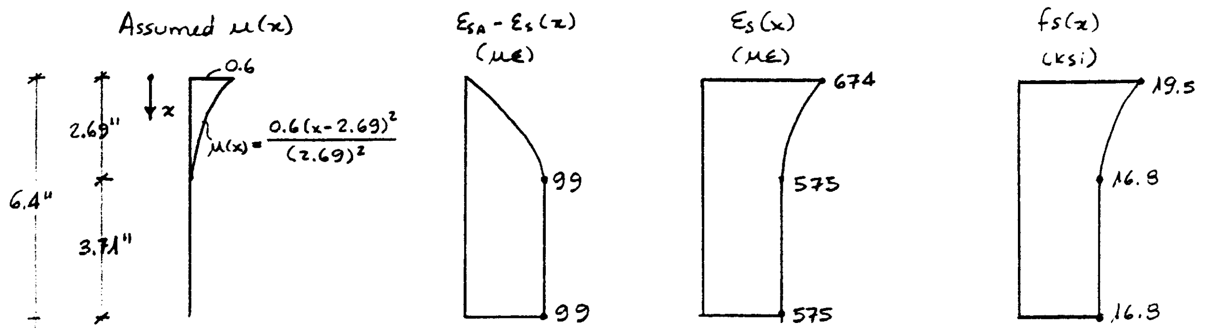

$F_{BOND} = 3\Sigma_0 \int \mu(x)\,dx = 3(2.36)(0.6)(2.69)(1/3) = 3.8^k < A_0 f_t' = 14.4^k$ o.k.

$0 \le x \le 2.69"$; $\varepsilon_{sA} - \varepsilon_s(x) = \left.\frac{0.6C_1(x-2.69)^3}{3(2.69)^2}\right|_0^x = 5.09\times10^{-6}\{(x-2.69)^3 + (2.69)^3\}$

$\delta'_{A2} = 5.09\times10^{-6}\{\frac{1}{4}(x-2.69)^4 + (2.69)^3 x\}\Big|_0^{2.69} = 0.000200"$

$2.69" \le x \le 6.4"$: $\varepsilon_{sA} - \varepsilon_s(x) = 99\,\mu\varepsilon$

$\delta''_{A2} = (99\mu\varepsilon)(3.71") = 0.000367"$

$\left.\begin{array}{l}\delta_{A1} = (674\mu\varepsilon)(6.4") = 0.00431" \\ \delta_{A2} = \sum_{i=1}^{2} \delta^i_{A2} = 0.000567"\end{array}\right\} \delta_{A_{\text{BELOW CRACK}}} = \delta_{A1} - \delta_{A2} = 0.00375" = 0.0952\,mm$

– Above crack

Assume same $\mu(x)$ distribution as in zone 5 (above crack, $\varepsilon_{sA} = 5{,}000\,\mu\varepsilon$, p. F'-25)

$\left.\begin{array}{l}\Rightarrow \delta_{A2} = 0.00113" \\ \delta_{A1} = (674\mu\varepsilon)(6.4") = 0.00431"\end{array}\right\} \delta_{A_{\text{ABOVE CRACK}}} = \delta_{A1} - \delta_{A2} = 0.00318" = 0.0808\,mm$

$\delta_A = \delta_{A_{\text{BELOW CRACK}}} + \delta_{A_{\text{ABOVE CRACK}}} = 0.00693" = 0.176\,mm$

$\theta_{cr_5} = \frac{(0.00693)}{(11.6 - 6.27)} = 0.00130$ rad

$\Delta X_{\theta_{cr_5}} = (0.00130)(41.0") = 0.0533" = 0.00135\,m$

Note: At end of crack 5 (start of crack 6):
$\varepsilon_s(x) = (674\mu\varepsilon) - (236\mu\varepsilon) = 438\,\mu\varepsilon$

vii) Zone 6

$$C_1 = \frac{\Sigma_o}{A_s E_{tx}} = \frac{(2.36)}{(0.442)(29000)} = 1.84 \times 10^{-4}$$

- Below crack

Assumed $\mu(x)$ $\qquad$ $\varepsilon_{sA} - \varepsilon_s(x)$ ($\mu\varepsilon$)

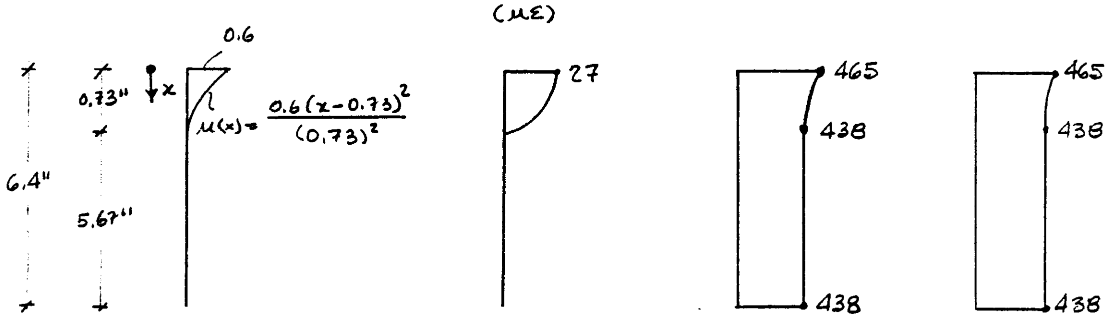

$$F_{BOND} = 3\Sigma_o \int \mu(x)dx = 3(2.36)(0.6)(0.73)(1/3) = 1.0^k < 14.4^k = A_e f_t'$$

$$0 \leq x \leq 0.73" : \quad \varepsilon_{sA} - \varepsilon_s(x) = \frac{0.6\, C_1 (x-0.73)^3}{3(0.73)^2}\Big|_0^x = 6.91 \times 10^{-5}\{(x-0.73)^3 + (0.73)^3\}$$

$$\delta_{A2}' = 6.91 \times 10^{-5}\left\{\tfrac{1}{4}(x-0.73)^4 + (0.73)^3 x\right\}\Big|_0^{0.73} = 0.0000147"$$

$$0.73 \leq x \leq 6.4" ; \quad \varepsilon_{sA} - \varepsilon_s(x) = 27\,\mu\varepsilon$$

$$\delta_{A2}'' = (27\,\mu\varepsilon)(5.67") = 0.000153"$$

$$\left.\begin{array}{l} \delta_{A1} = (465\,\mu\varepsilon)(6.4") = 0.00298" \\ \delta_{A2} = 0.000168" \end{array}\right\} \delta_{A_{\text{BELOW CRACK}}} = 0.00281"$$

- Above crack

Assume same $\mu(x)$ as in zone 4 (above crack, $\varepsilon_{sA} = 1{,}380\,\mu\varepsilon$) (see p. F'-14 & F'-15)

$$\left.\begin{array}{l} \Rightarrow \delta_{A2} = 0.00100" \\ \delta_{A1} = (465\,\mu\varepsilon)(6.4") = 0.00298" \end{array}\right\} \delta_{A_{\text{ABOVE CRACK}}} = 0.00198"$$

$$\delta_A = \delta_{A_{\text{BELOW CRACK}}} + \delta_{A_{\text{ABOVE CRACK}}} = 0.00479" = 0.122\text{ mm}$$

$$\theta_{cr6} = \frac{(0.00479)}{(11.6 - 6.44)} = 0.000929\text{ rad}$$

$$\Delta X_{\theta_{cr6}} = (0.000928)(28.2") = 0.0262" = 0.000665\text{ m}$$

Note: At end of crack 6: $\varepsilon_s(x) = (465\,\mu\varepsilon) - (198\,\mu\varepsilon) = 267\,\mu\varepsilon$

viii) Uncracked zone

$$R = \frac{M}{L} = \frac{766}{105} = 7.30^k \quad ; \quad l = 28.2 - 6.4 = 21.8"$$

$$\Delta X_l = \frac{R l^3}{3EI_{uncr}} = \frac{(7.3)(21.8)^3}{3(6.28 \times 10^6)} = 0.00401" = 0.000102\text{ m}$$

Summary:

$\varepsilon_{SA} = 10{,}000\,\mu\varepsilon$

$$\Delta X_{\theta_{FE}} = 0.649'' = 0.0165\ m$$

$$\sum_{i=0}^{6} \Delta X_{\theta_{cri}} = 1.413'' = 0.0360\ m$$

$$\Delta X_{sl} = 0.00401'' = 0.000102\ m$$

$$(\Delta X)_{TOTAL} = 2.071'' = 0.0526\ m$$

Note that the deflections computed with assumed crack distribution ($\sum_{i=0}^{6} \Delta X_{\theta_{cri}}$ and ΔX_{sl}) are based on a curvature distribution as given in page F'- 30 (bottom).

If now the deflections are computed based on an average curvature distribution (cracked but as given by RCCOLA), as given in page F'- 30 (top), they will be:

$$\Delta X = \{12.8\}\{10^{-6}\}\{(324)(98.6)+(234)(85.8)+(194)(73.0)+(160)(60.2)+(126)(47.4)+(90)(34.6)\} +$$

$$+\left\{\frac{12.8}{2}\right\}\{10^{-6}\}\{(1{,}182)(100.7)+(90)(87.9)+(40)(75.1)+(34)(62.3)+(34)(49.5)+(36)(36.7)\} +$$

$$+\left\{\frac{12.8}{2}\right\}\{10^{-6}\}\{(73)(25)+(17)(\tfrac{1}{2})(26.1)\} + \{(21.8)(19)(\tfrac{1}{2})(\tfrac{2}{3})(21.8)\}\{10^{-6}\} =$$

$$= 1.087 + 0.864 + 0.0131 + 0.00301 = 1.967'' = 0.0500\ m$$

d) $\varepsilon_{SA} = 15{,}000\ \mu\varepsilon$ (START OF STRAIN HARDENING)

$\varepsilon_s = 15{,}000\ \mu\varepsilon \Rightarrow M_s = 704^{k\text{-}in}$

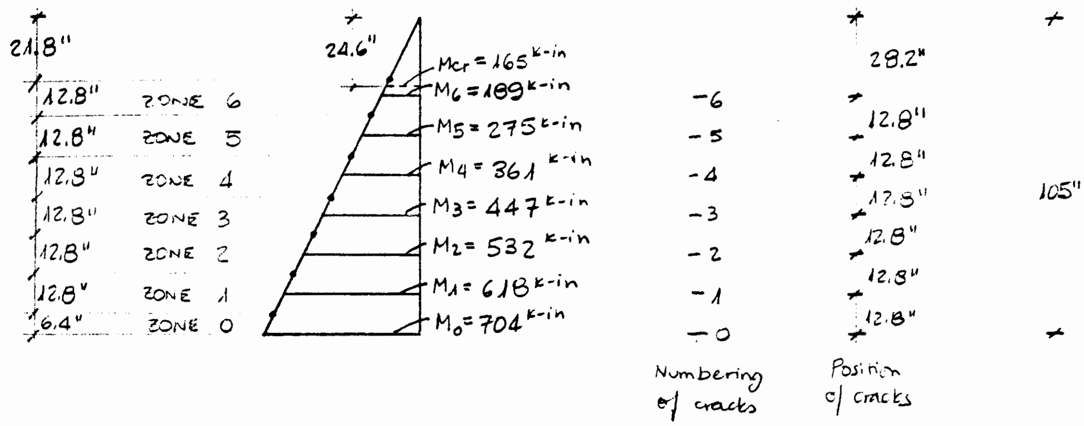

Same assumptions as for case a)

Using results from RCCOLA :

ZONE	M_{AV} (k-in)	Curvature ($\times 10^{-3}$ rad/in)	Tensile Steel Strain ($\mu\varepsilon$)	Neutral Axis Location (in)
0	704	2.38	15,000	5.28
1	618	0.236	1,390	5.68
2	532	0.203	1,200	5.84
3	447	0.170	1,012	5.99
4	361	0.138	814	6.15
5	275	0.105	620	6.30
6	189	0.072	426	6.46

$\varepsilon_{SA} = \varepsilon_{SH} = 15{,}000\,\mu\varepsilon$

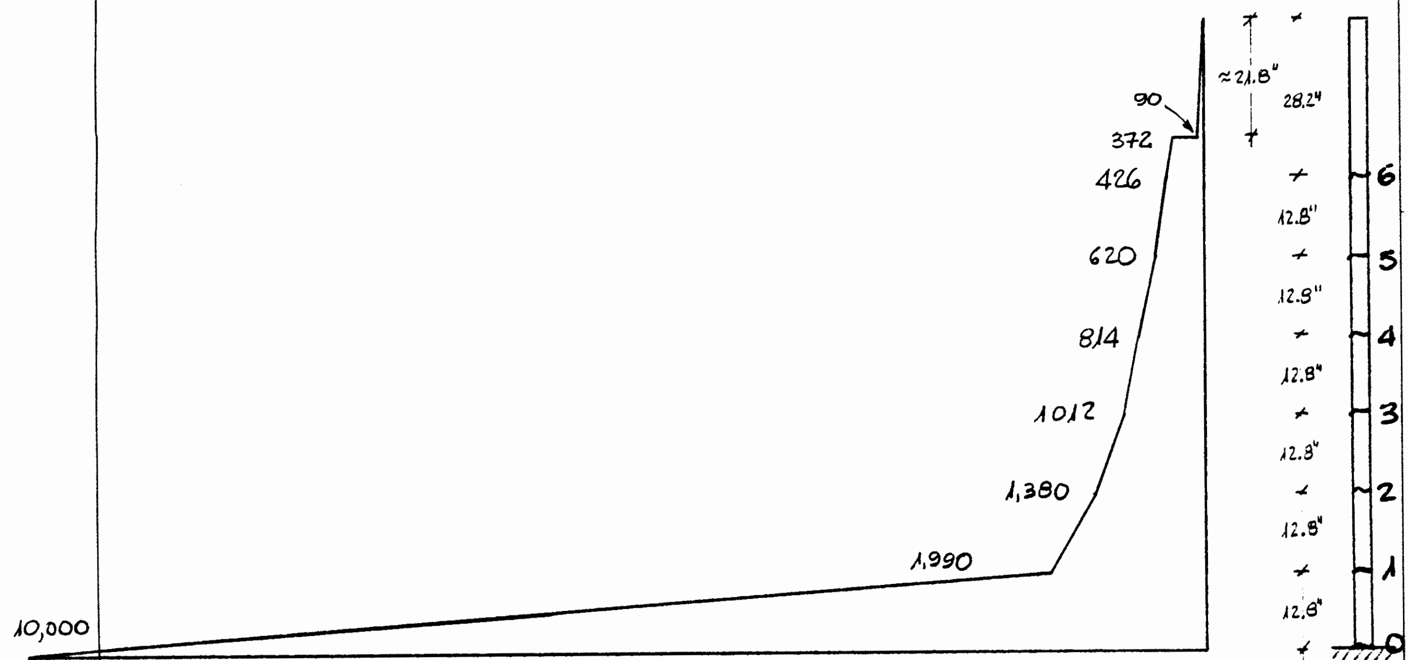

Tensile Steel Strain Distribution ε_s ($\mu\varepsilon$)
(as given by RCCOLA) (linear interpolation)
(Attention to ε_s history, see pages F'-10, F'-19 & F'-29)

Position & Numbering of Cracks

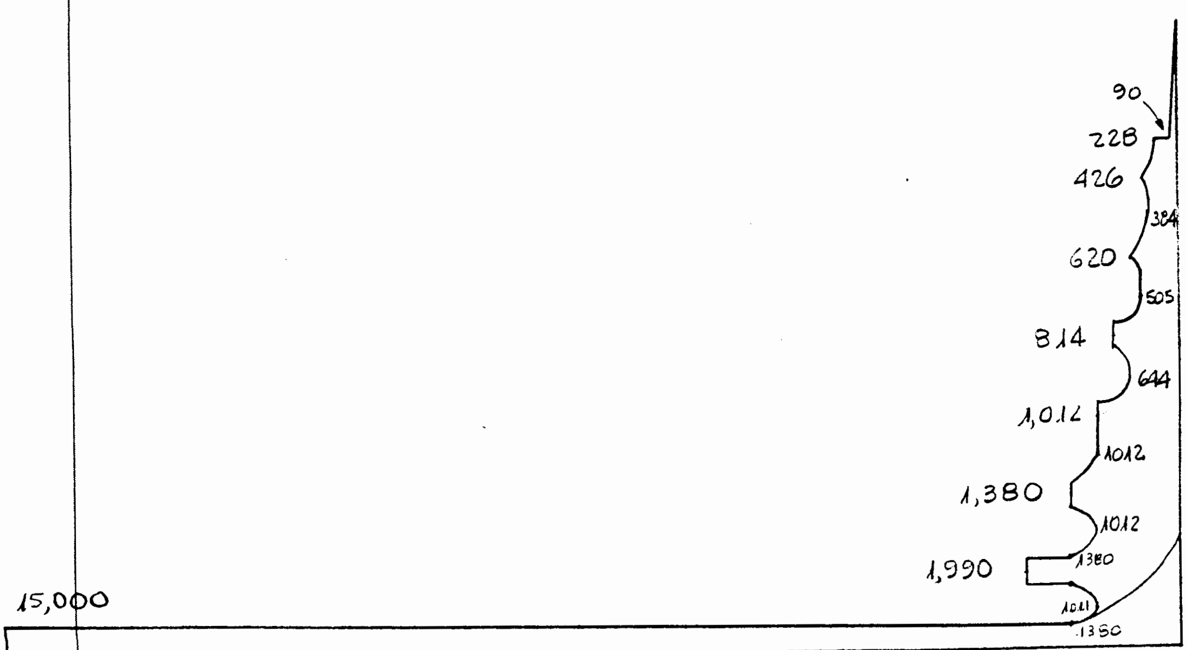

Tensile Steel Strain Distribution ε_s ($\mu\varepsilon$)
a) at cracks: as given by RCCOLA
b) at other points: as given by assumed bond distribution
(Attention to ε_s history, see pages F'-10, F'-19 & F'-29)

$\varepsilon_{SA} = \varepsilon_{SH} = 15,000\ \mu\varepsilon$

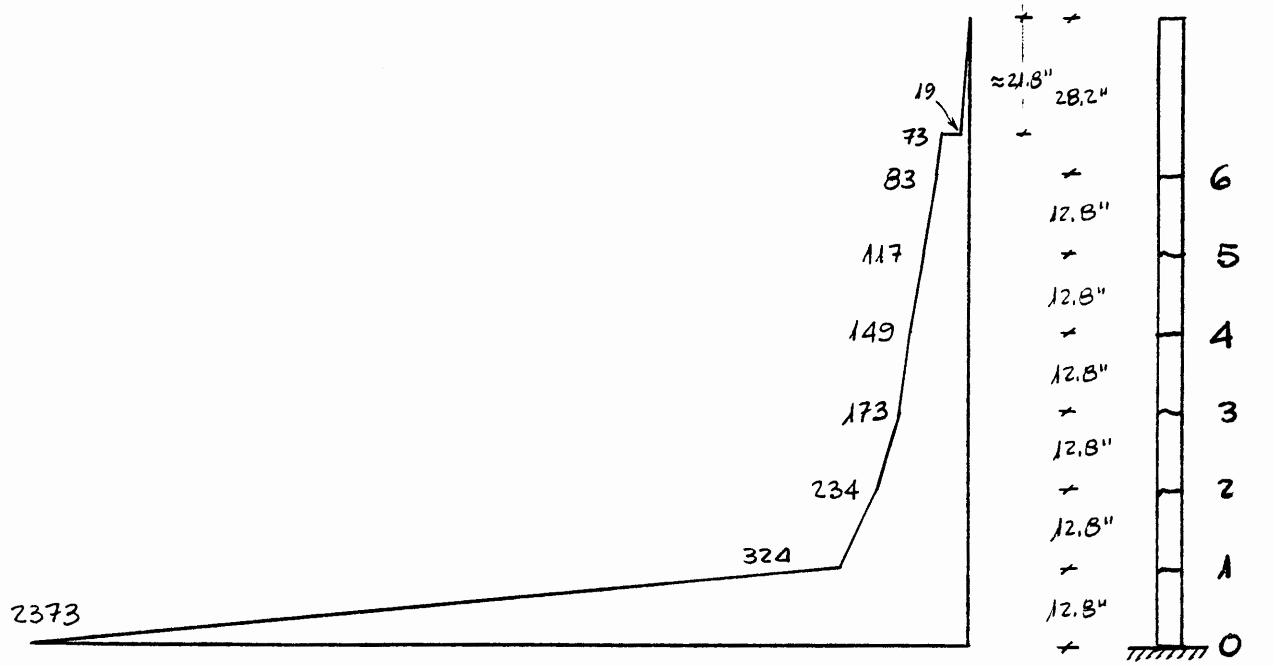

Curvature Distribution ϕ ($\times 10^{-6}$ rad/in)
(as given by RCCOLA) (linear interpolation)
(Attention to ϕ history, see p. F'-10, F'-19, & F'-30)

Position & Numbering of Cracks

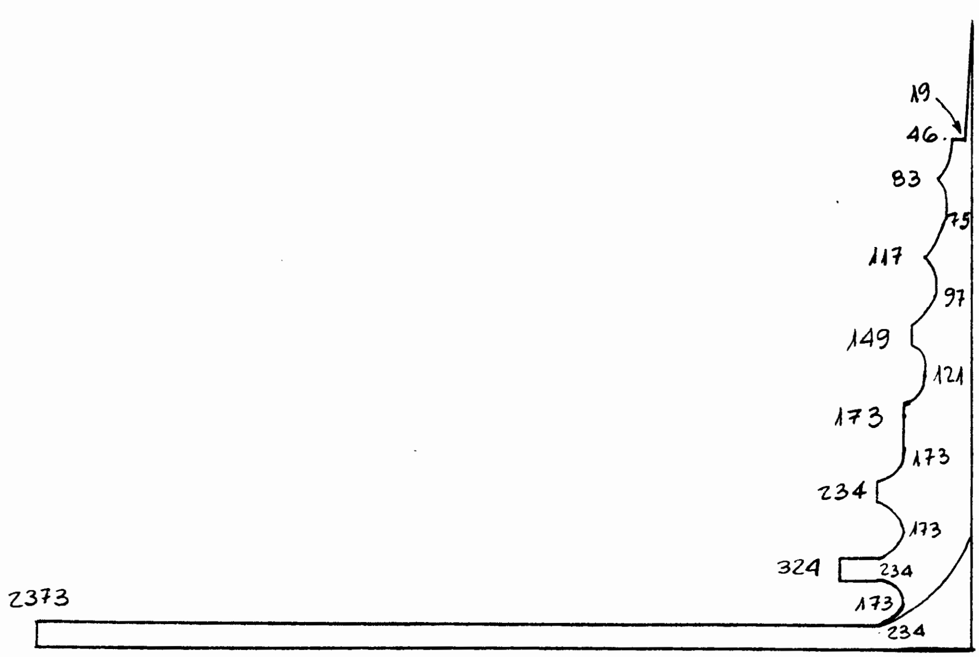

Curvature Distribution ϕ ($\times 10^{-6}$ rad/in)
a) at cracks: as given by RCCOLA
b) at other points: as given by assumed bond distribution
Attention to ϕ history, see pages F'-10, F'-19, & F'-30)

i) Zone 0

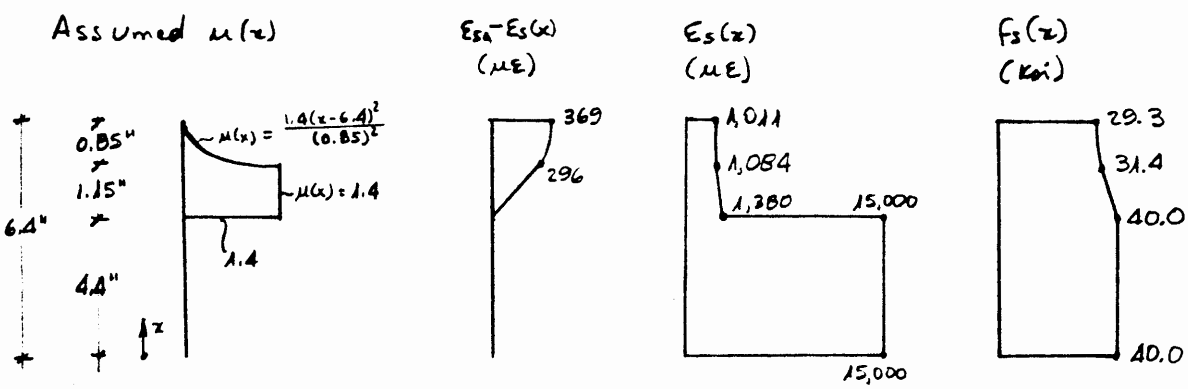

$$F_{BOND} = 3\,\Sigma_o \int \mu(x)\,dx = 3(2.36)(1.4)\left[(1.15)+(1/3)(0.85)\right] = 14.2^k < A_c f'_t = 14.4^k$$

$0 \leq x \leq 4.4"$: $\varepsilon_{sA} - \varepsilon_s(x) = 0$; $\delta'_{A2} = 0$

$4.4 \leq x \leq 5.55"$: $\varepsilon_{sA} - \varepsilon_s(x) = 1.4\,C_1\,(x-4.4)$

at $x = 5.55"$: $\varepsilon_{sA} - \varepsilon_s(x) = 296\ \mu\varepsilon$

$$\delta''_{A2} = \frac{1.4C_1}{2}(x-4.4)^2 \Big|_{4.4}^{5.55} = 0.000170"$$

$5.55" \leq x \leq 6.4"$: $\varepsilon_{sA} - \varepsilon_s(x) = (296\mu\varepsilon) + \dfrac{1.4\,C_1\,(x-6.4)^3}{3(0.85)^2}\Big|_{5.55}^{x} = (296\mu\varepsilon) + 1.19\times10^{-4}\left\{(x-6.4)^3+(0.85)^3\right\}$

at $x = 6.4"$: $\varepsilon_{sA} - \varepsilon_s(x) = 369\ \mu\varepsilon$

$$\delta'''_{A2} = (296\mu\varepsilon)x + 1.19\times10^{-4}\left\{\tfrac{1}{4}(x-6.4)^4 + (0.85)^3 x\right\}\Big|_{5.55}^{6.4} = 0.000298"$$

$$\delta_{A1} = (1{,}380\mu\varepsilon)(6.4") + (15{,}000\mu\varepsilon - 1{,}380\mu\varepsilon)(4.4") = 0.0688"$$

$$\delta_{A2} = \sum_{i=1}^{3} \delta^{i}_{A2} = 0.000468"$$

$$\delta_A = \delta_{A1} - \delta_{A2} = 0.0683" = 1.735\ \text{mm}$$

$$\theta_{cro} = \frac{(0.0683)}{(11.6-5.28)} = 0.0108\ \text{rad}$$

$$\Delta X_{\theta_{cro}} = (0.0108)(105") = 1.135" = 0.0288\ \text{m}$$

ii) Zone 1

Assume $\mu(x)$ distribution as in zone 0 ($\varepsilon_{SA} = 1{,}380\,\mu\varepsilon$, p. F'-11) for both above & below crack.

$\Rightarrow \delta_{A2} = 2\,(0.00115'') = 0.00230''$

$\delta_{A1} = \{(1380\,\mu\varepsilon)(6.4) + (1{,}990 - 1{,}380)(\mu\varepsilon)(2.2'')\}\{2\} = 0.0203''$

$\delta_A = \delta_{A1} - \delta_{A2} = 0.0180'' = 0.458$ mm

$\theta_{cr_1} = \dfrac{(0.0180)}{(11.6 - 5.45)} = 0.00293$ rad

$\Delta X_{\theta cr_1} = (0.00293)(92.2'') = 0.271'' = 0.00687$ m

Note: At end of crack 1 (start of crack 2): $\varepsilon_s(x) = 1012\,\mu\varepsilon$ (see p. F'-11)

iii) Zone 2

Assume $\mu(x)$ distribution as in zone 0 ($\varepsilon_{SA} = 1{,}380\,\mu\varepsilon$, p. F'-11) for both above & below crack.

$\Rightarrow \delta_{A2} = 2\,(0.00115'') = 0.00230''$

$\delta_{A1} = \{(1{,}380\,\mu\varepsilon)(6.4)\}\{2\} = 0.0177''$

$\delta_A = \delta_{A1} - \delta_{A2} = 0.0154'' = 0.390$ mm

$\theta_{cr_2} = \dfrac{(0.0154)}{(11.6 - 5.69)} = 0.00260$ rad

$\Delta X_{\theta cr_2} = (0.00260)(79.4'') = 0.206'' = 0.00524$ m

Note: At end of crack 2 (start of crack 3): $\varepsilon_s(x) = 1012\,\mu\varepsilon$ (see p. F'-11)

iv) Zone 3

- Below crack

Assume $\mu(x) = 0 \Rightarrow \delta_{A2} = 0 \quad \Rightarrow \varepsilon_s(x) = 1012\,\mu\varepsilon$

$\delta_{A\,\text{BELOW CRACK}} = (1012\,\mu\varepsilon)(6.4'') = 0.00648''$

- Above crack

Assume $\mu(x)$ distribution as in zone 0 ($\varepsilon_{SA} = 1{,}380\,\mu\varepsilon$, p. F'-11) $\Rightarrow \delta_{A2} = 0.00115''$

$\delta_{A1} = (1012\,\mu\varepsilon)(6.4'') = 0.00648''$

$$\delta_{A_{\substack{ABOVE\\CRACK}}} = \delta_{A1} - \delta_{A2} = 0.00533''$$

$$\delta_A = \delta_{A_{\substack{BELOW\\CRACK}}} + \delta_{A_{\substack{ABOVE\\CRACK}}} = 0.0118'' = 0.000300\ mm$$

$$\theta_{cr3} = \frac{(0.0118)}{(11.6-5.99)} = 0.00210\ rad$$

$$\Delta X_{\theta cr3} = (0.00210)(66.6'') = 0.140'' = 0.00356\,m$$

<u>Note</u>: At end of crack 3 (start of crack 4):
$\varepsilon_s(z) = (1012\,\mu\varepsilon) - (368\,\mu\varepsilon) = 644\,\mu\varepsilon$

<u>v) Zone 4</u>

- Below crack

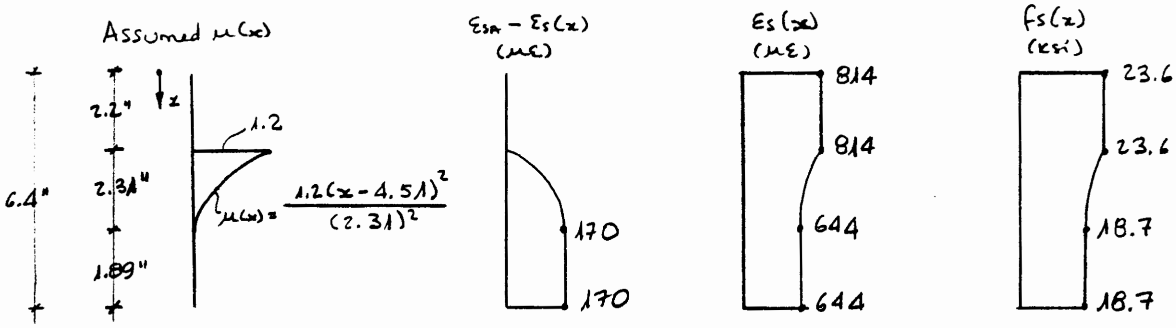

$$F_{BOND} = 3\Sigma_0 \int \mu(x)dx = 3(2.36)(1.2)(2.31)(1/3) = 6.5^K < A_e f'_t = 14.4^K \quad \underline{O.K.}$$

$0 \le x \le 2.2''$: $\varepsilon_{sA} - \varepsilon_s(x) = 0$; $\delta'_{A2} = 0$

$$2.2'' \le x \le 4.51'' : \varepsilon_{sA} - \varepsilon_s(x) = \left.\frac{1.2\,C_1\,(x-4.51)^3}{3\,(2.31)^2}\right|_{2.2}^{x} = 1.38\times10^{-5}\left\{(x-4.51)^3 + (2.31)^3\right\}$$

at $x = 4.51''$: $\varepsilon_{sA} - \varepsilon_s(x) = 170\,\mu\varepsilon$

$$\delta''_{A2} = 1.38\times10^{-5}\left.\left\{\tfrac{1}{4}(x-4.51)^4 + (2.31)^3 x\right\}\right|_{2.2}^{4.51} = 0.000295''$$

$4.51'' \le x \le 6.4''$: $\varepsilon_{sA} - \varepsilon_s(x) = 170\,\mu\varepsilon$

$$\delta'''_{A2} = (170\,\mu\varepsilon)(1.89'') = 0.000321''$$

$$\left.\begin{aligned}\delta_{A1} &= (814\,\mu\varepsilon)(6.4'') = 0.00521''\\ \delta_{A2} &= \sum_{i=1}^{3}\delta^{i}_{A2} = 0.000616''\end{aligned}\right\}\ \delta_{A_{\substack{BELOW\\CRACK}}} = 0.00459''$$

- Above crack

Assume $\mu(x)$ distribution as in zone 4 (above crack, $\varepsilon_{SA} = 5{,}000\mu\varepsilon$, p. F'-23 & F'-24)

$$\left.\begin{aligned} &\Rightarrow \delta_{A2} = 0.000974" \\ &\delta_{A1} = (814\mu\varepsilon)(6.4") = 0.00521" \end{aligned}\right\} \delta_{A_{\text{ABOVE CRACK}}} = \delta_{A1} - \delta_{A2} = 0.00424"$$

$$\delta_A = \delta_{A_{\text{BELOW CRACK}}} + \delta_{A_{\text{ABOVE CRACK}}} = 0.00883" = 0.224\,\text{mm}$$

$$\theta_{cr4} = \frac{(0.00883)}{(11.6 - 6.15)} = 0.00162 \text{ rad}$$

$$\Delta X_{\theta_{cr4}} = (0.00162)(53.8") = 0.0872" = 0.00221\text{ m}$$

Note: At end of crack 4 (start of crack 5): $\varepsilon_s(x) = (814\mu\varepsilon) - (309\mu\varepsilon) = 505\mu\varepsilon$

vi) Zone 5

- Below crack

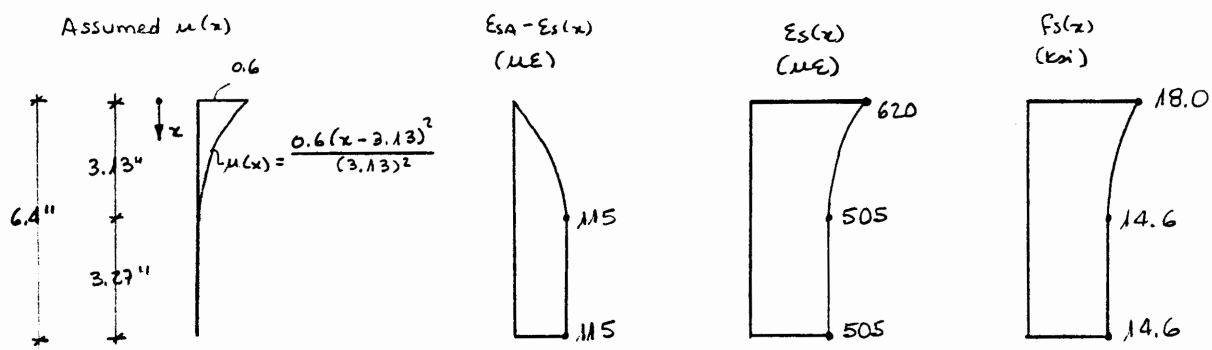

$$F_{BOND} = 3\Sigma_0 \int \mu(x)\,dx = 3(2.36)(0.6)(3.13)(1/3) =$$

$0 \le x \le 3.13"$: $\varepsilon_{SA} - \varepsilon_s(x) = \left.\frac{0.6\,C_1(x-3.13)^3}{3(3.13)^2}\right|_0^x = 3.76\times10^{-6}\{(x-3.13)^3 + (3.13)^3\}$

at $x = 3.13"$: $\varepsilon_{SA} - \varepsilon_s(x) = 115\,\mu\varepsilon$

$$\delta'_{A2} = 3.76\times10^{-6}\left\{\tfrac{1}{4}(x-3.13)^4 + (3.13)^3 x\right\}\Big|_0^{3.13} = 0.000270"$$

$3.13" \le x \le 6.4"$: $\varepsilon_{SA} - \varepsilon_s(x) = 115\mu\varepsilon$

$$\delta''_{A2} = (115\mu\varepsilon)(3.27") = 0.000376"$$

$$\left.\begin{aligned} &\delta_{A1} = (620\mu\varepsilon)(6.4") = 0.00397" \\ &\delta_{A2} = \sum_{i=1}^{2} \delta^i_{A2} = 0.000646" \end{aligned}\right\} \delta_{A_{\text{BELOW CRACK}}} = \delta_{A1} - \delta_{A2} = 0.00332"$$

- Above crack :

Assume same $\mu(x)$ distribution as in zone 5 (above crack, $\varepsilon_{SA} = 5{,}000\,\mu\varepsilon$, p. F'-25) $\Rightarrow$ $\delta_{A2} = 0.00113''$

$\delta_{A1} = (620\,\mu\varepsilon)(6.4'') = 0.00397''$ $\Big\}$ $\delta_{A_{\text{ABOVE CRACK}}} = \delta_{A1} - \delta_{A2} = 0.00284$

$$\delta_A = \delta_{A_{\text{BELOW CRACK}}} + \delta_{A_{\text{ABOVE CRACK}}} = 0.00616'' = 0.156\ \text{mm}$$

$$\Theta_{cr5} = \frac{(0.00616)}{(11.6 - 6.30)} = 0.00116\ \text{rad}$$

$$\Delta X_{\Theta_{cr5}} = (0.00116)(41.0'') = 0.0477'' = 0.00121\ \text{m}$$

Note : At end of crack 5 (start of crack 6) :
$\varepsilon_S(x) = (620\,\mu\varepsilon) - (236\,\mu\varepsilon) = 384\,\mu\varepsilon$

vii) Zone 6

- Below crack

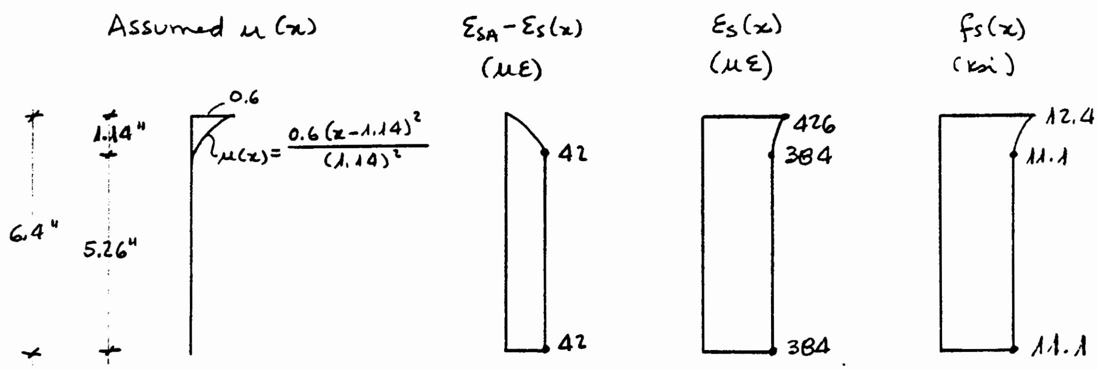

$$F_{BOND} = 3\Sigma_0 \int \mu(x)\,dx = 3\,(2.36)(0.6)(1.14)(1/3) = 1.6^k < A_e f'_t = 14.4^k$$

$0 \le x \le 1.14''$: $\varepsilon_{SA} - \varepsilon_S(x) = \left.\dfrac{0.6 C_1 (x-1.14)^3}{3\,(1.14)^2}\right|_0^x = 2.83\times10^{-5}\{(x-1.14)^3 + (1.14)^3\}$

at $x = 1.14''$; $\varepsilon_{SA} - \varepsilon_S(x) = 42\,\mu\varepsilon$

$$\delta^1_{A2} = 2.83\times10^{-5}\left\{\tfrac{1}{4}(x-1.14)^4 + (1.14)^3 x\right\}\Big|_0^{1.14} = 0.0000359''$$

$1.14'' \le x \le 6.4''$; $\varepsilon_{SA} - \varepsilon_S(x) = 42\,\mu\varepsilon$

$$\delta^{11}_{A2} = (42\,\mu\varepsilon)(5.26'') = 0.000221''$$

$\delta_{A1} = (426\,\mu\varepsilon)(6.4'') = 0.00273''$
$\delta_{A2} = \sum_{i=1}^{2} \delta^i_{A2} = 0.000257''$ $\Big\}$ $\delta_{A_{\text{BELOW CRACK}}} = \delta_{A1} - \delta_{A2} = 0.00247'' = 0.0627\ \text{mm}$

- Above crack

Assume $u(x)$ as in zone 4 (above crack, $\varepsilon_{sA} = 1{,}380\mu\varepsilon$) (see p. F'-14 & F'-15)

$\Rightarrow \delta_{A2} = 0.00100''$

$\delta_{A1} = (426\mu\varepsilon)(6.4'') = 0.00273''$

$\left.\begin{matrix} \delta_{A2} = 0.00100'' \\ \delta_{A1} = 0.00273'' \end{matrix}\right\} \delta_{A_{\text{ABOVE CRACK}}} = 0.00173''$

$$\delta_A = \delta_{A_{\text{BELOW CRACK}}} - \delta_{A_{\text{ABOVE CRACK}}} = 0.00420'' = 0.107\ mm$$

$$\theta_{cr6} = \frac{(0.00420)}{(11.6 - 6.46)} = 0.000817\ rad$$

$$\Delta X_{\theta_{cr6}} = (0.000817)(28.2'') = 0.0230'' = 0.000585\ m$$

Note: At end of crack 6 : $\varepsilon_s(x) = (426\mu\varepsilon) - (198\mu\varepsilon) = 228\ \mu\varepsilon$

viii) Uncracked zone

$$R = \frac{M}{L} = \frac{704}{105} = 6.70^k$$

$$\ell = 28.2 - 6.4 = 21.8''$$

$$\Delta X_{\ell} = \frac{R\ell^3}{3EI_{uncr}} = \frac{(6.7)(21.8)^3}{3(6.28\times10^6)} = 0.00368'' = 0.0000936\ m$$

Summary:

$\varepsilon_{SA} = \varepsilon_{SH} = 15{,}000\,\mu\varepsilon$

$$\Delta X_{\theta_{FE}} = 1.17'' = 0.0298\ m$$

$$\sum_{i=0}^{6} \Delta X_{\theta_{cri}} = 1.910'' = 0.0485\ m$$

$$\Delta X_{el} = 0.00368'' = 0.0000936\ m$$

$$(\Delta X)_{TOTAL} = 3.084'' = 0.0783\ m$$

1.35
0.371
0.306
0.140
0.0377
0.0477
0.0230
1.909

Note that the deflections computed with assumed crack distribution ($\sum_{i=0}^{6} \Delta X_{\theta_{cri}}$ and ΔX_{el}) are based on a curvature distribution as given in page F'-40 (bottom).

If now the deflections are computed based on an average curvature distribution (cracked but as given by ECCOLA), as given in page F'-40 (top), they will be:

$$\Delta X = \{12.8\}\{10^{-6}\}\{(324)(98.6)+(234)(85.8)+(173)(73.0)+(149)(60.2)+(117)(47.4)+(83)(34.6)\} +$$

$$+ \left\{\frac{12.8}{2}\right\}\{10^{-6}\}\{(2{,}049)(100.7)+(90)(87.9)+(61)(75.1)+(24)(62.3)+(32)(49.5)+(34)(36.7)\} +$$

$$+ \left\{\frac{12.8}{2}\right\}\{10^{-6}\}\{(73)(25)+(10)(\tfrac{1}{2})(26.1)\} + \{(21.8)^2(19)(\tfrac{1}{2})(\tfrac{2}{3})\}\{10^{-6}\} =$$

$$= 1.050 + 1.428 + 0.0125 + 0.00301 = 2.494'' = 0.0633\ m$$

SUMMARY FOR FIRST ASSUMED MOMENT DISTRIBUTION ON CANOPY (NO TOP MOMENT):

	CANOPY'S TOP NODAL DISPLACEMENTS DUE TO:			
	FIXED END ROTATION $\Delta X_{\theta FE}$ (1)	ROTATION AT EACH OF THE CRACKS $\sum_{i=0}^{6} \Delta X_{\theta cr i}$ (2)	ELASTIC DISPL. UNCRACKED TOP ZONE (3)	TOTAL (1)+(2)+(3)
$\varepsilon_{SE} = 1{,}380\,\mu\varepsilon$ (Start of Yield)	0.149" (0.00379 m)	0.778" (0.0198 m)	0.00321" (0.0000814 m)	0.930" (0.0236 m)
$\varepsilon_{SA} = 5{,}000\,\mu\varepsilon$ (On plateau)	0.301" (0.00765 m)	1.067" (0.0271 m)	0.00423" (0.000107 m)	1.372" (0.0349 m)
$\varepsilon_{SA} = 10{,}000\,\mu\varepsilon$ (On plateau)	0.649" (0.0165 m)	1.418" (0.0360 m)	0.00401" (0.000102 m)	2.071" (0.0526 m)
$\varepsilon_{SA} = 15{,}000\,\mu\varepsilon$ (Start of Strain Hardening)	1.170" (0.0298 m)	1.910" (0.0485 m)	0.00368" (0.0000936 m)	3.084" (0.0783 m)

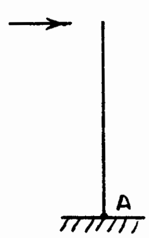

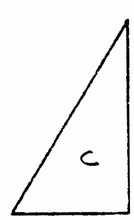

APPENDIX G

DRAIN-2D RESULTS REGARDING THE SECOND STAGE

(VERIFICATION OF PGA BY DRAIN-2D)

This appendix presents the time-history inelastic response of the canopy for the different cases considered in the second stage of the analysis. The following response plots are given :

a) time vs. lateral displacement

b) time vs. rotation

c) time vs. bottom moment

d) time vs. top moment

e) time vs. bottom shear

The sign convention is as given in Fig. 6.6.

The studies were subdivided in different groups:

GROUP NUMBER = = FIGURE NUMBER	MATERIAL PROPERTY CASE NUMBER	DESCRIPTION OF EARTHQUAKE	DESCRIPTION OF MODEL USED	EI ($\times 10^6$ K-in^2)
G. 1A	M1	DER. PAC. DAM (0.30g)	2DOF	5.4
G. 1B	M1	DER. PAC. DAM (0.40g)	2DOF	5.4
G. 1C	M1	DER. PAC. DAM (0.50g)	2DOF	5.4
G. 1D	M1	EL CENTRO (0.55g)	2DOF	5.4
G. 1E	M1	EL CENTRO (0.70g)	2DOF	5.4
G. 2A	M2	DERIVED PACOIMA DAM NORMALIZED TO 0.35g	2DOF	2.62 (cracked)
G. 2B	M2		2DOF	3.78
G. 2C	M2		2DOF	6.28 (uncracked)
G. 2D	M2		5DOF	2.62 (cracked)
G. 2E	M2		5DOF	3.78
G. 2F	M2		5DOF	6.28 (uncracked)
G. 3A	M2	EL CENTRO NORM. TO 0.50g	2DOF	2.62 (cracked)
G. 3B	M2		2DOF	3.78
G. 3C	M2		2DOF	6.28 (uncracked)
G. 3D	M2		5DOF	3.78
G. 3E	M2		5DOF	6.28 (uncracked)

GROUP NUMBER = FIGURE NUMBER	MATERIAL PROPERTY CASE NUMBER	DESCRIPTION OF EARTHQUAKE	DESCRIPTION OF MODEL USED	EI ($\times 10^6$ k-in^2)
6.4A	M2	↑	2DOF	2.62 (cracked)
6.4B	M2	EL CENTRO NORMALIZED	2DOF	6.28 (uncracked)
6.4C	M2	TO 0.35g	5DOF	2.62 (cracked)
6.4D	M2	↓	5DOF	6.28 (uncracked)

Note: Material property case M1: $f'_c = 3.0$ ksi (21 MPa)
$f_y = 50$ ksi (350 MPa)

Material property case M2: $f'_c = 2.5$ ksi (17 MPa)
$f_y = 40$ ksi (280 MPa)

ALGERIA CANOPY SUBJECT TO DERIVED PACOIMA DAM (0.30g)
TOP NODAL DISPLACEMENT (X - DIRECTION)

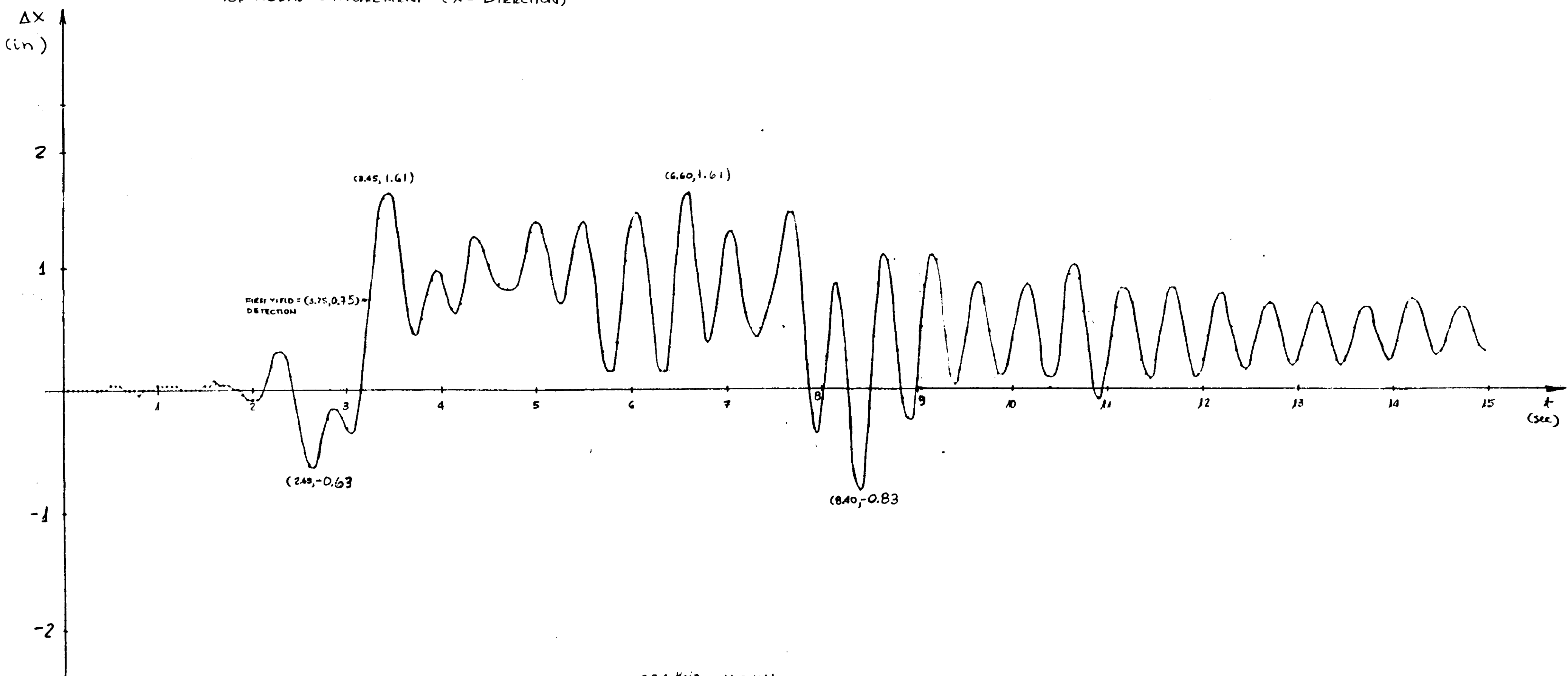

CANOPY'S MAIN FEATURES
1. f'_c = 3.0 ksi = 21 MPa
2. f_y = 50 ksi = 350 MPa
3. 2DOF model
4. M_y = 974 k-in = 110 kN-m
5. EI = 5.4×10^6 k-in^2 = 15500 kN-m^2

Fig. G.1A a)

ALGERIA CANOPY SUBJECT TO DERIVED PACOIMA DAM (0.30g)
MOMENT AT BASE OF CANOPY

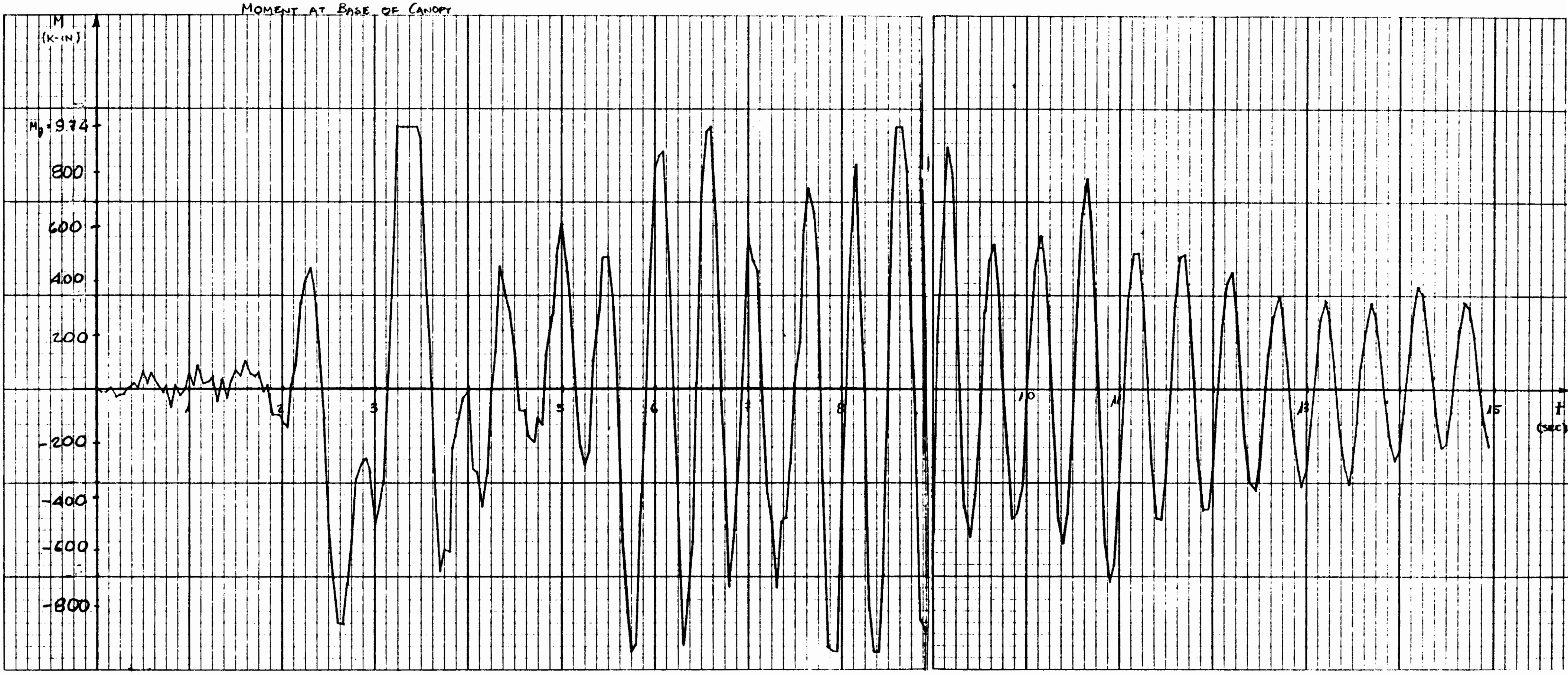

Fig. G.1A b)

ALGERIA CANOPY SUBJECT TO DERIVED PACOIMA DAM (0.30g)
MOMENT AT TOP OF CANOPY

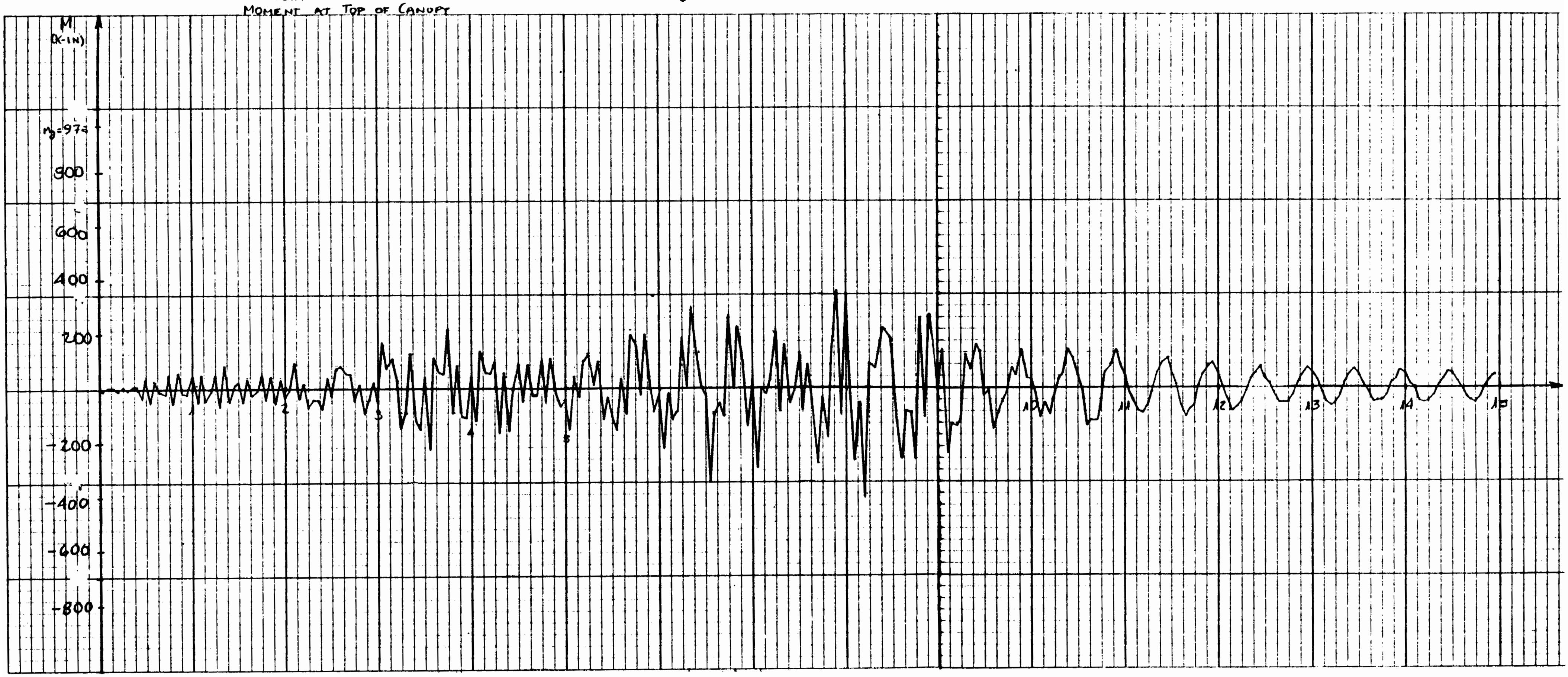

Fig. G.1A c)

ALGERIA CANOPY SUBJECT TO DERIVED PACOIMA DAM (0.40g)
TOP NODAL DISPLACEMENT (X-DIRECTION)

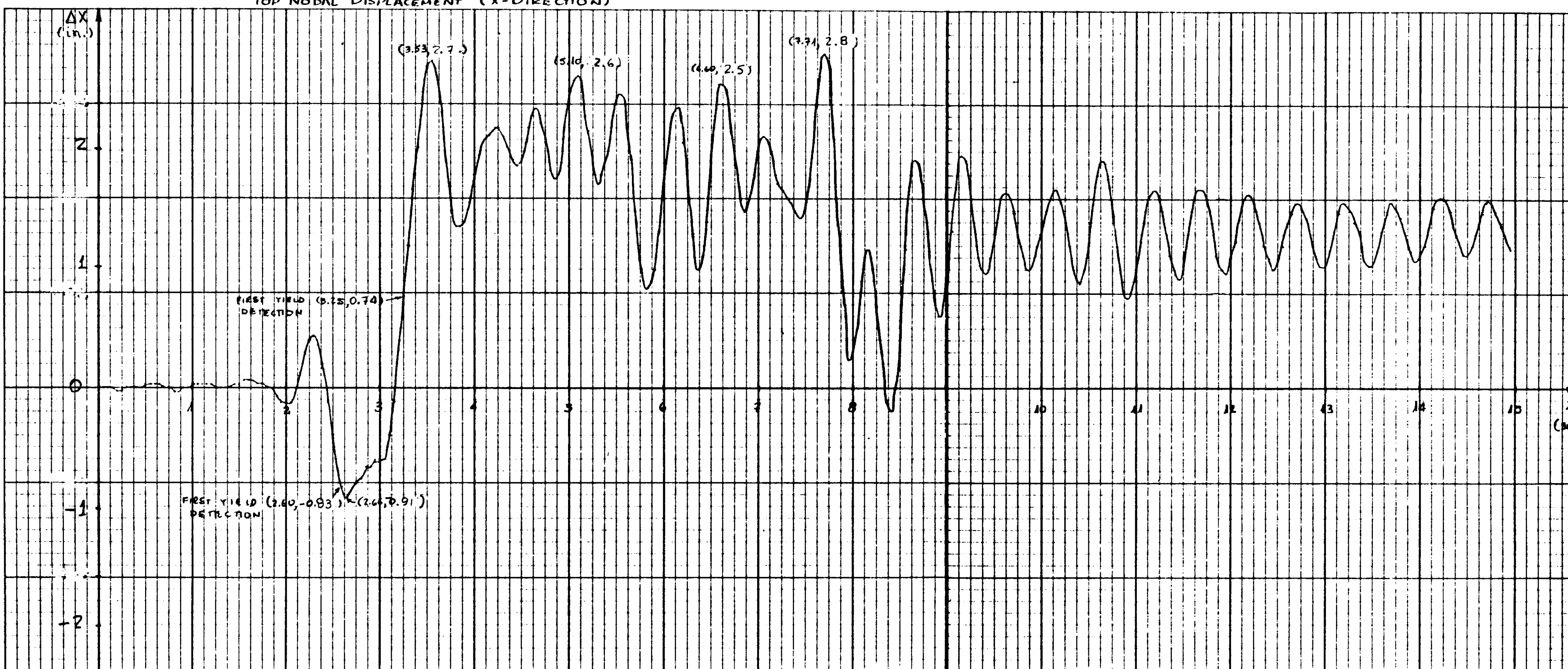

CANOPY'S MAIN FEATURES
1. f'c = 3.0 ksi = 21 MPa
2. fy = 50 ksi = 350 MPa
3. 2 DOF model
4. My = 974 k-in = 110 KN-m
5. EI = 5.4 x 10^6 k-in² = 15,500 KN-m²

Fig. 1B a)

Algeria Canopy subject to Derived Pacoima Dam (0.40g)
Moment at Base of Canopy

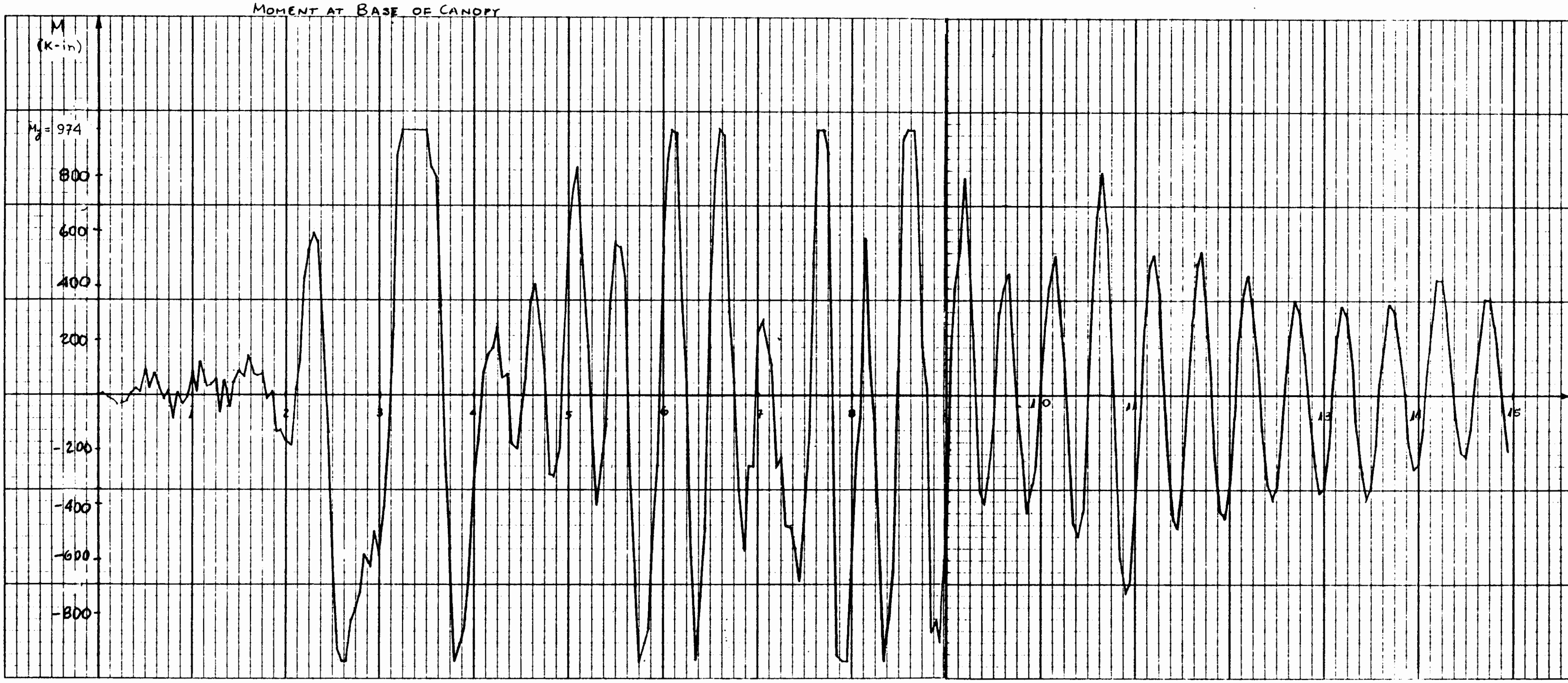

Fig. G.1B b)

Algeria Canopy subject to Derived Pacoima Dam (0.50 g)
Top Nodal Displacement (X- Direction)

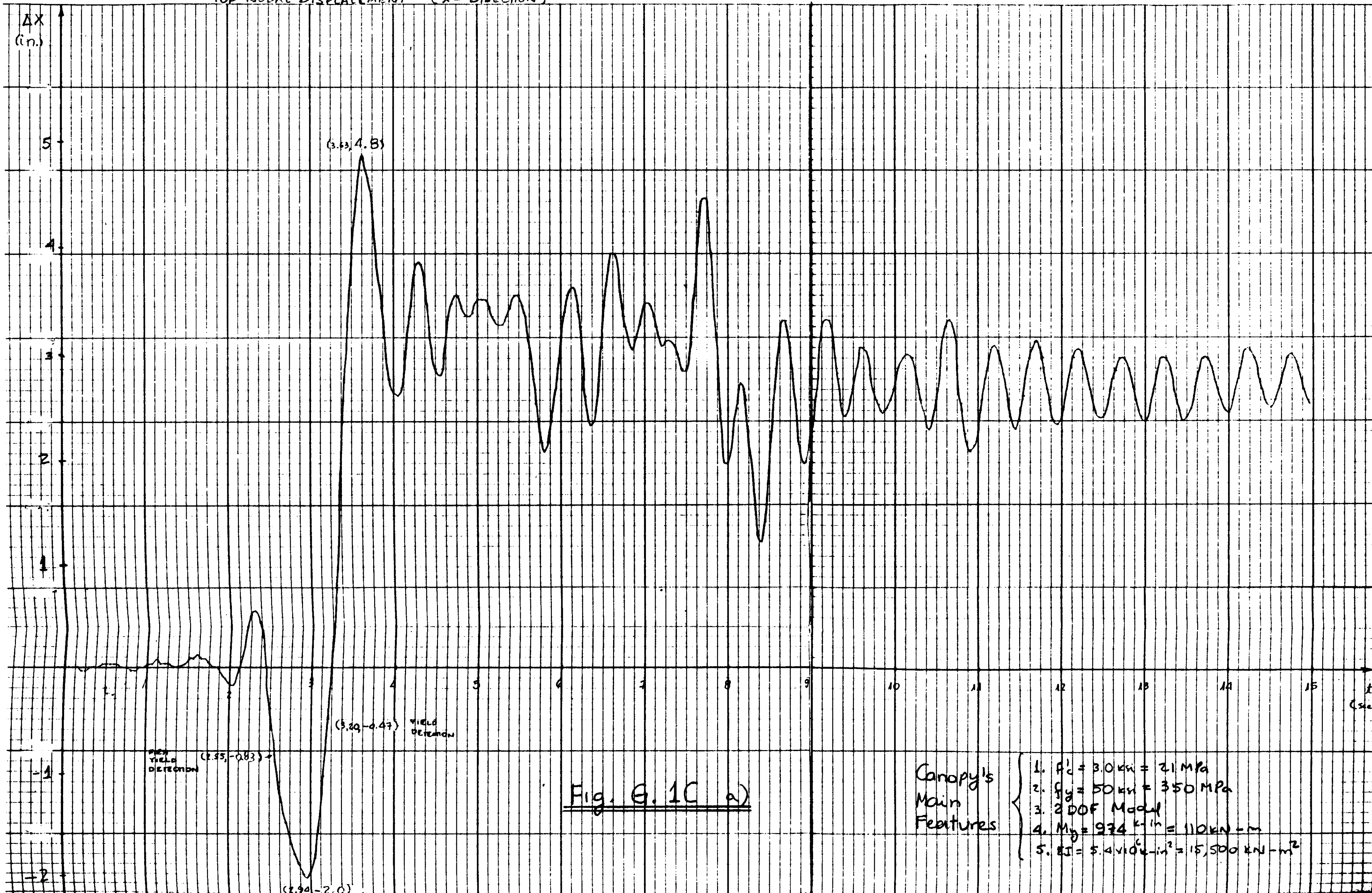

Fig. G. 1C a)

Canopy's Main Features:
1. $f'_c = 3.0$ ksi = 21 MPa
2. $f_y = 50$ ksi = 350 MPa
3. 2 DOF Model
4. $M_y = 974$ k-in = 110 kN-m
5. $EI = 5.4 \times 10^6$ k-in^2 = 15,500 kN-m^2

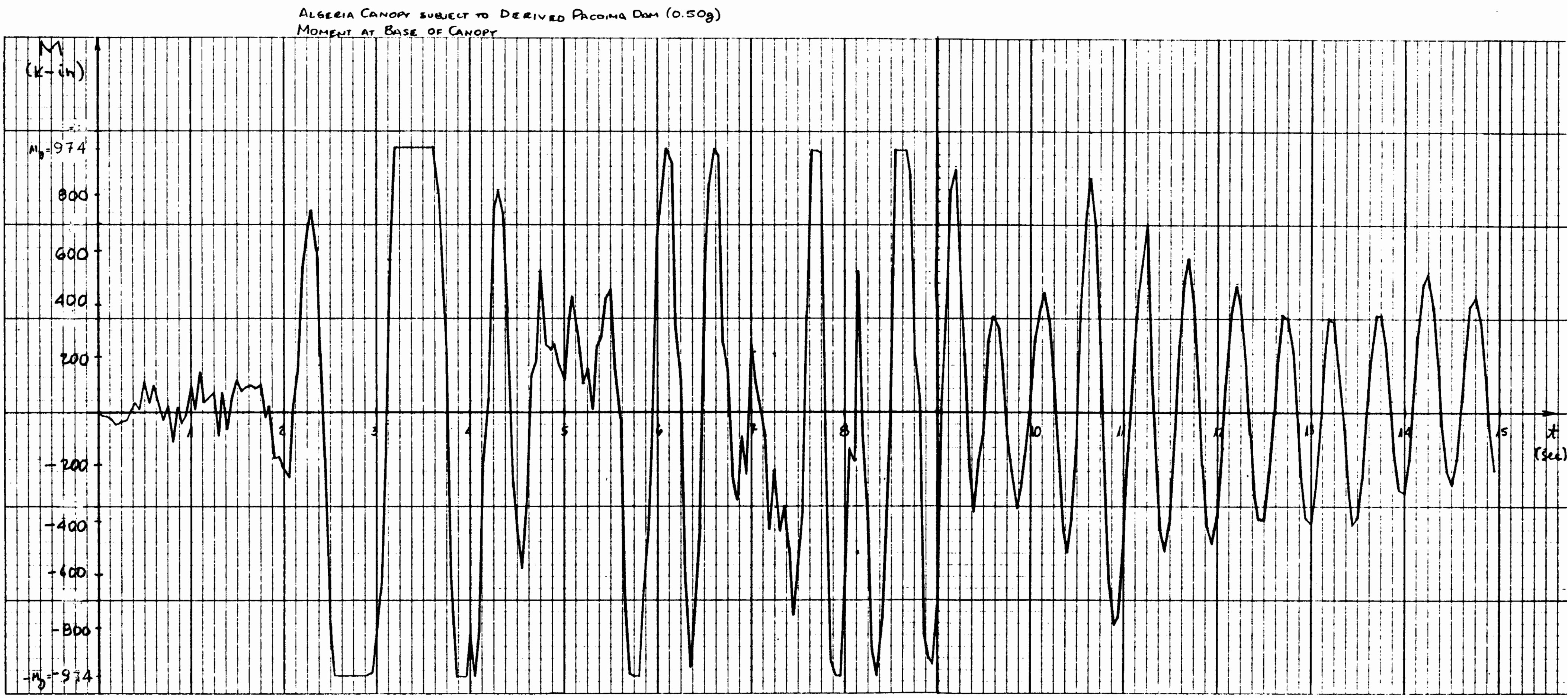
ALGERIA CANOPY SUBJECT TO DERIVED PACOIMA DAM (0.50g)
MOMENT AT BASE OF CANOPY
M (K-in)
M_y=974
800
600
400
200
-200
-400
-600
-800
$-M_y$=-974
1
2
3
4
5
6
7
8
10
11
12
13
14
15
t (sec)

Fig. G.1C b)

Algeria Canopy subject to Derived Pacoima Dam (0.50g)
Moment at Top of Canopy

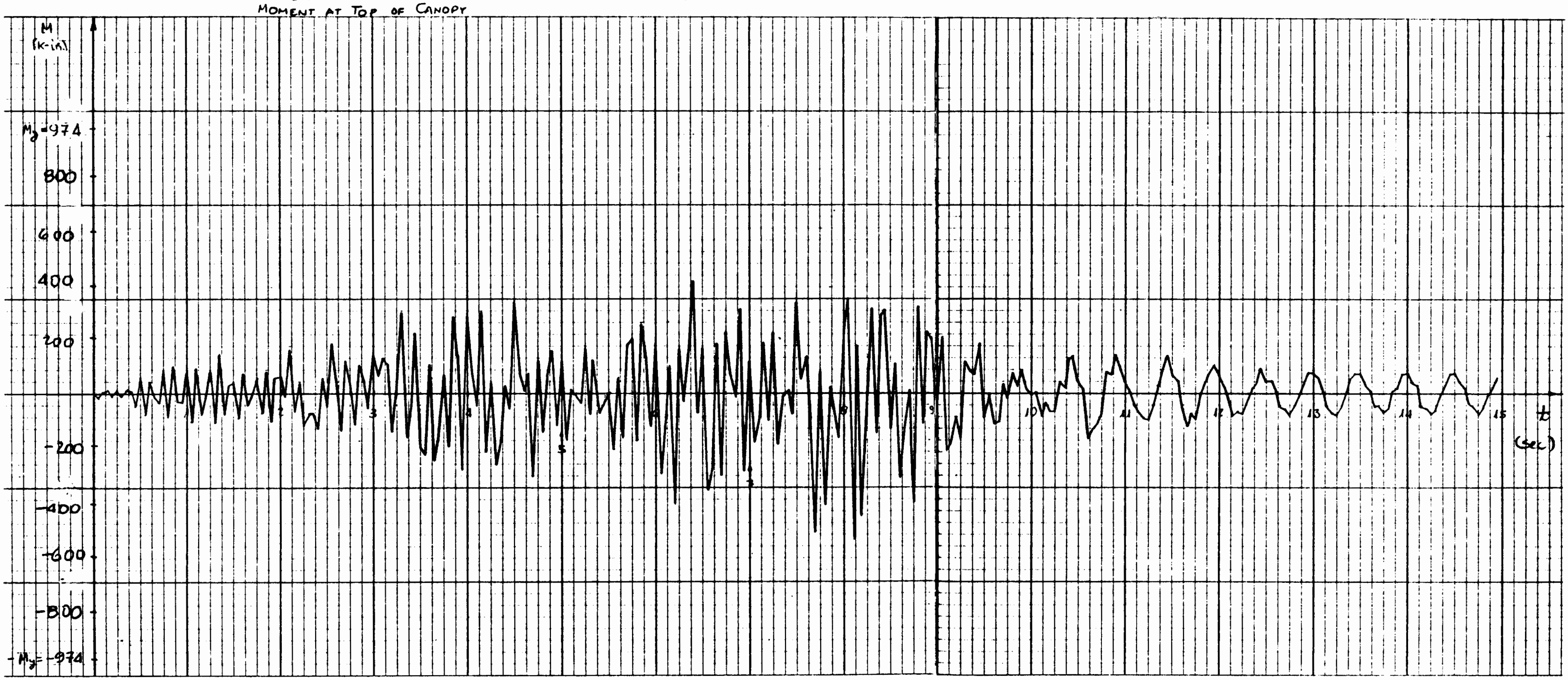

Fig. G. 1C c)

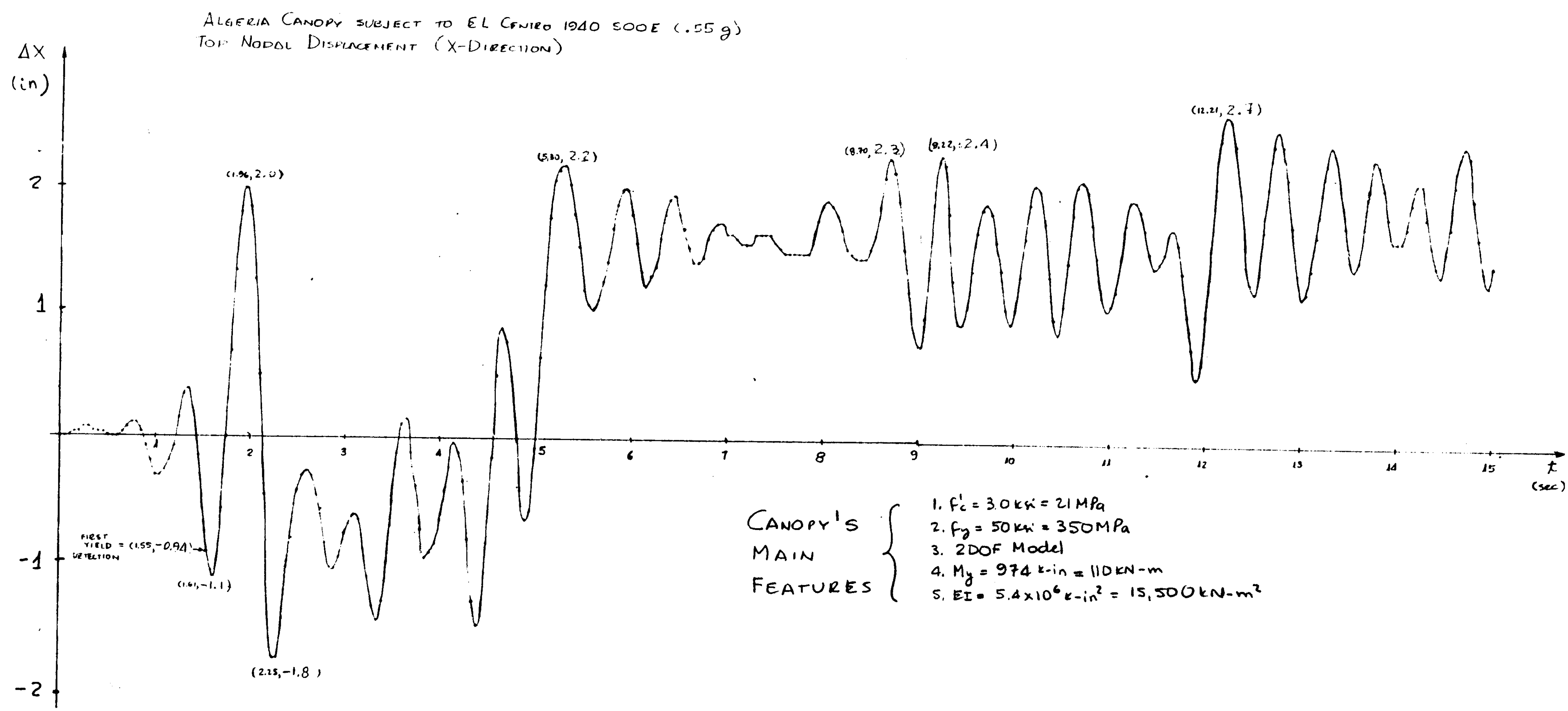

ALGERIA CANOPY SUBJECT TO EL CENTRO 1940 S00E (.55 g)
TOP NODAL DISPLACEMENT (X-DIRECTION)
ΔX (in)
2
1
-1
-2
t (sec)
1 2 3 4 5 6 7 8 9 10 11 12 13 14 15
(1.96, 2.0)
(5.30, 2.2)
(8.70, 2.3)
(9.22, 2.4)
(12.21, 2.7)
(2.25, -1.8)
(1.61, -1.1)
FIRST YIELD DETECTION = (1.55, -0.94)
CANOPY'S MAIN FEATURES
1. f'_c = 3.0 ksi = 21 MPa
2. f_y = 50 ksi = 350 MPa
3. 2DOF Model
4. M_y = 974 k-in = 110 kN-m
5. EI = 5.4×10^6 k-in^2 = 15,500 kN-m^2

Fig. G.1D a)

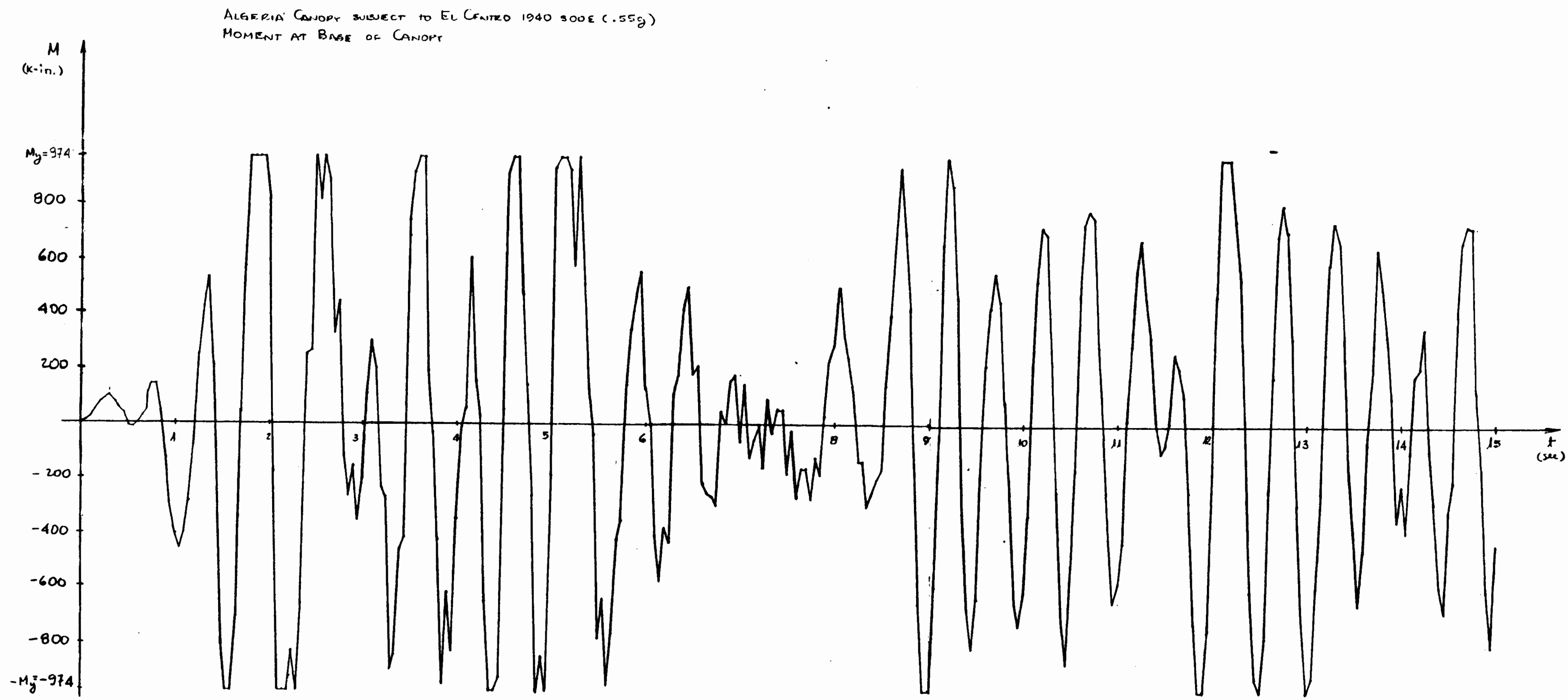

Algeria Canopy subject to El Centro 1940 sooe (.55g)
Moment at Base of Canopy
M
(k-in.)
My=974
800
600
400
200
-200
-400
-600
-800
-My=-974
1
2
3
4
5
6
8
9
10
11
12
13
14
15
t
(sec)

Fig. G.1D b)

Algeria Canopy subject to El Centro 1940 S00E (.55g)
Moment at Top of Canopy

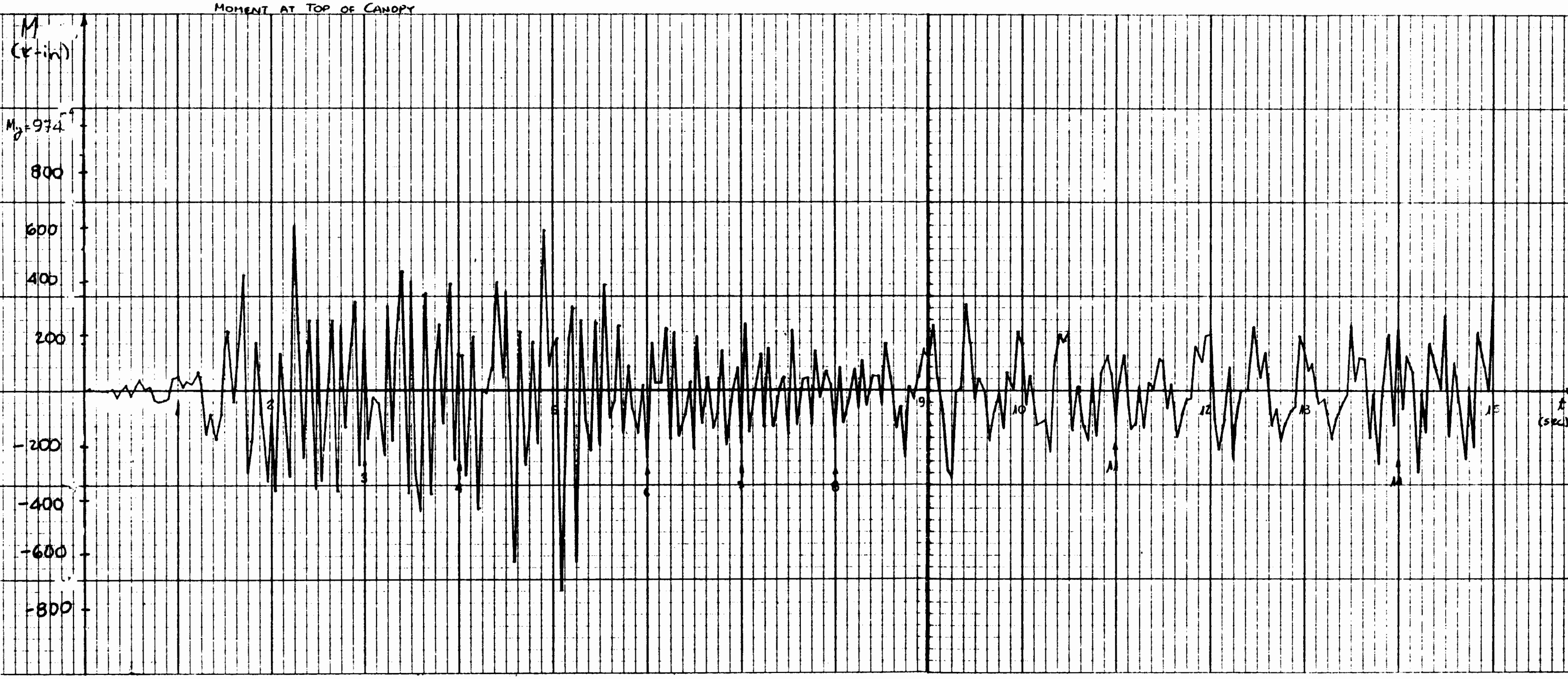

Fig. G.1D c)

Algeria Canopy subject to El Centro 1940 S00E (0.70g)
Top Nodal Displacement (X-Direction)

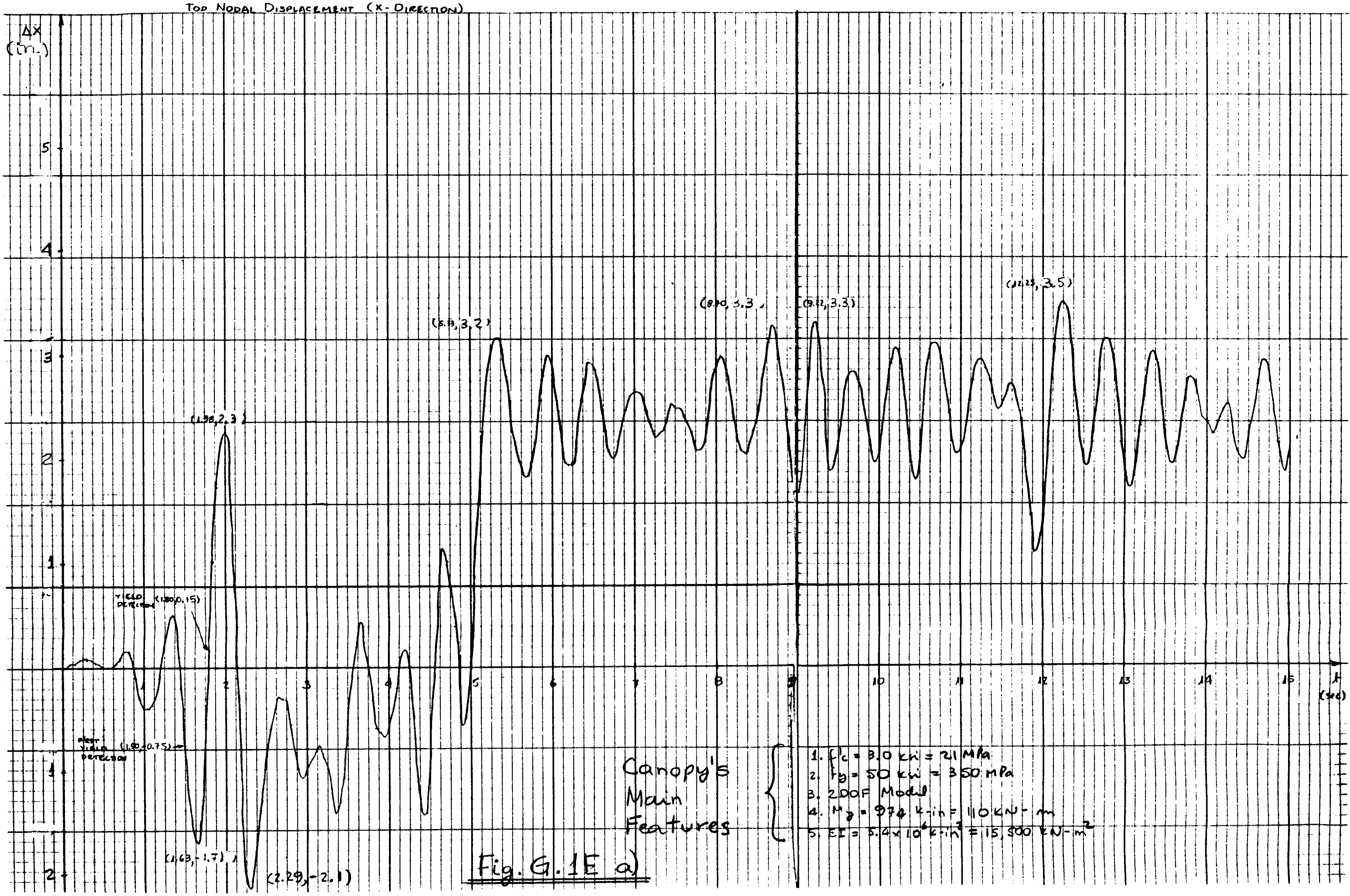

Fig. G.1E a)

Algeria Canopy subject to El Centro 1940 S00E (0.70g)
Moment at Base of Canopy

Fig. G. 1E b)

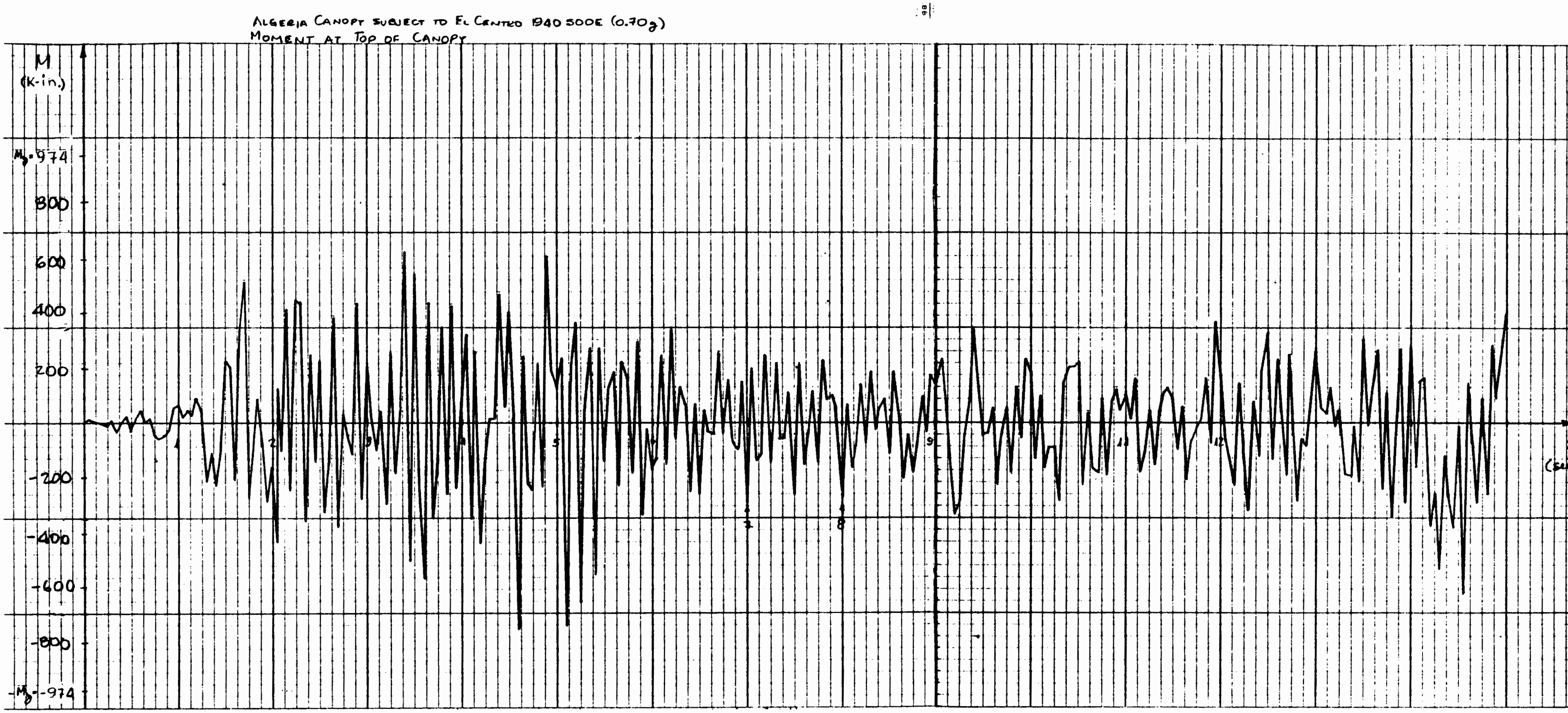

Algeria Canopy subject to El Centro 1940 S00E (0.70g)
Moment at Top of Canopy
M
(k-in.)
M_y = 974
800
600
400
200
-200
-400
-600
-800
$-M_y$ = -974
t
(sec)

Fig. G. 1E c)

Algeria Canopy subject to Derived Pacoima Dam (0.35g)
Top Nodal Displacement (X-Direction)

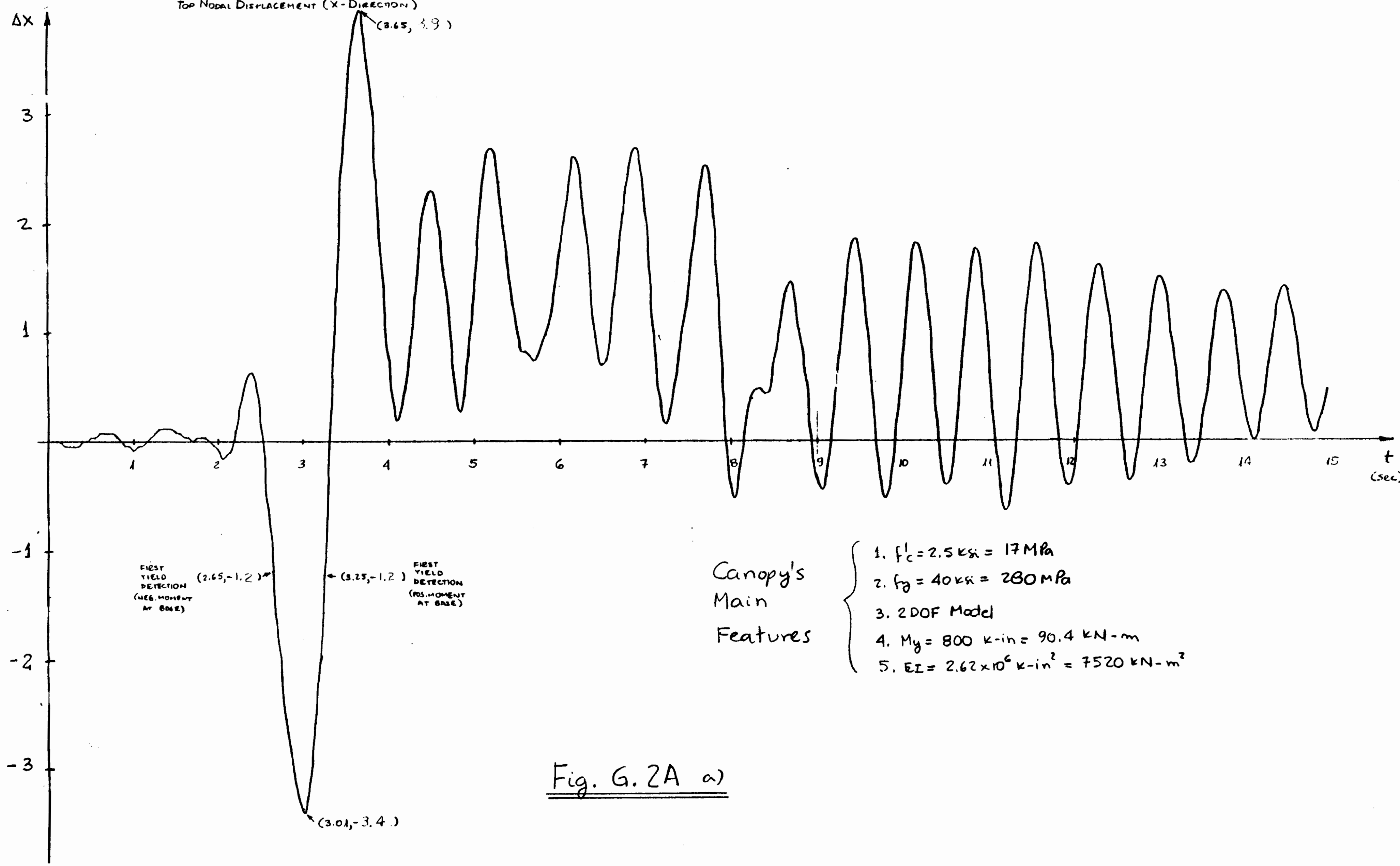

Canopy's Main Features

1. $f'_c = 2.5$ ksi = 17 MPa
2. $f_y = 40$ ksi = 280 MPa
3. 2DOF Model
4. $M_y = 800$ k-in = 90.4 kN-m
5. $EI = 2.62 \times 10^6$ k-in^2 = 7520 kN-m^2

Fig. G.2A a)

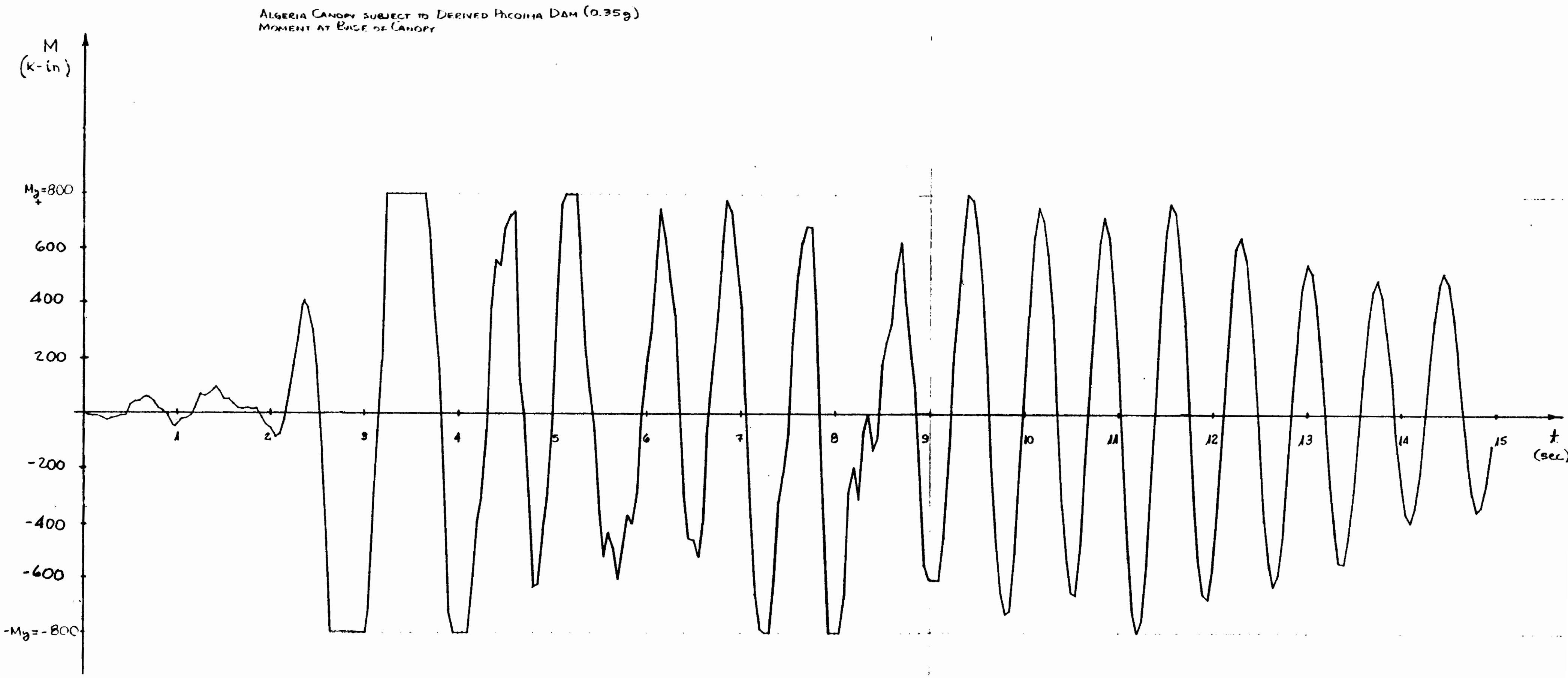
Algeria Canopy subject to Derived Pacoima Dam (0.35g)
Moment at Base of Canopy
M
(k-in)
M_y=800
600
400
200
-200
-400
-600
$-M_y$=-800
1
2
3
4
5
6
7
8
9
10
11
12
13
14
15
t
(sec)

Fig. G.2A b)

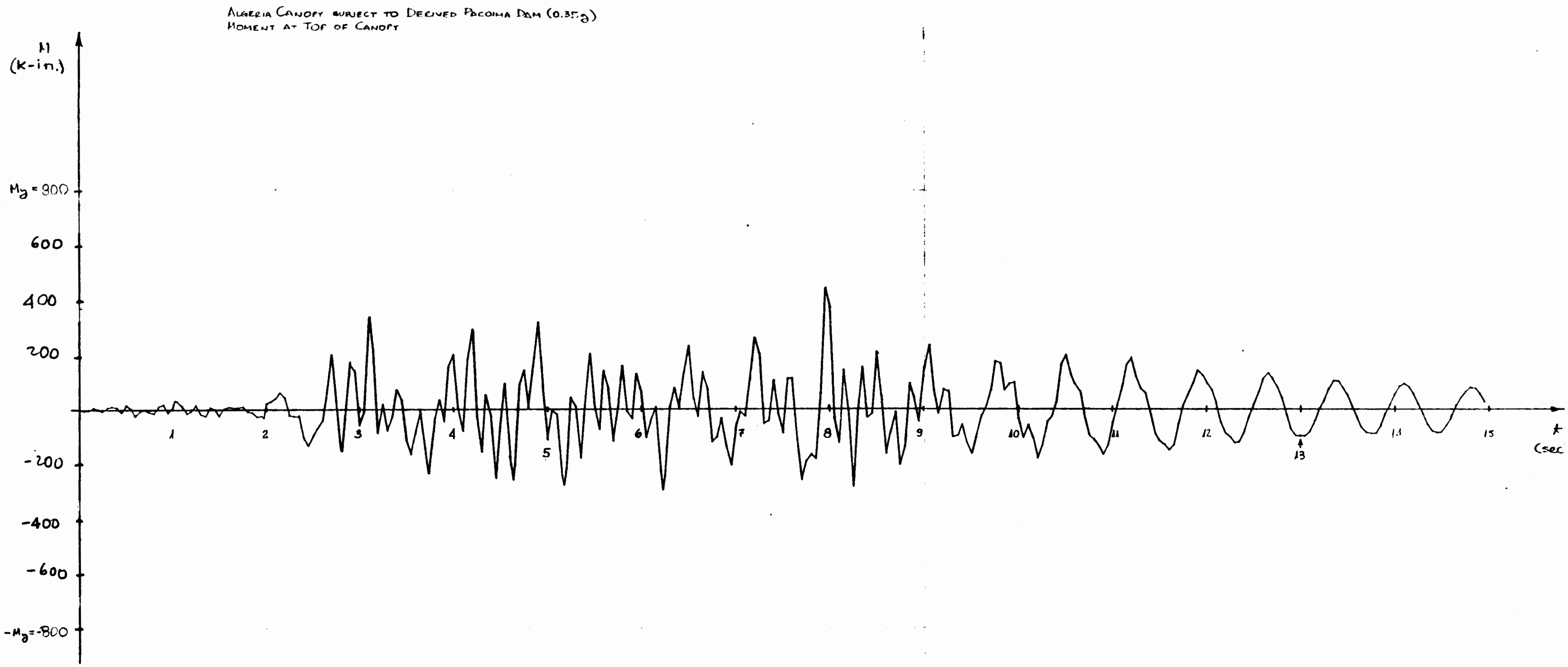
ALGERIA CANOPY SUBJECT TO DERIVED PACOIMA DAM (0.35g)
MOMENT AT TOP OF CANOPY
M
(k-in.)
My = 800
600
400
200
-200
-400
-600
-My = -800
1
2
3
4
5
6
7
8
9
10
11
12
13
14
15
t
(sec

Fig. G. 2A c)

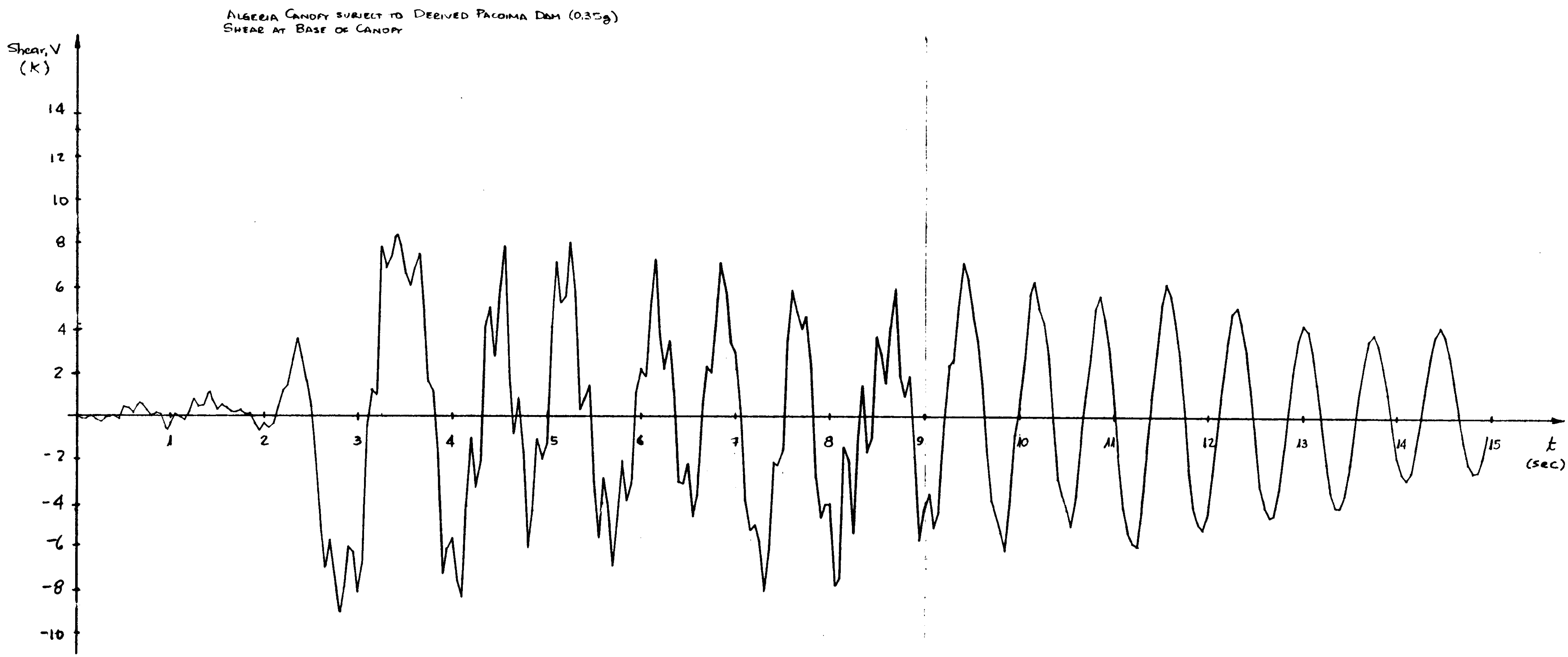
Algeria Canopy subject to Derived Pacoima Dam (0.35g)
Shear at Base of Canopy
Shear, V (k)
14
12
10
8
6
4
2
-2
-4
-6
-8
-10
1
2
3
4
5
6
7
8
9
10
11
12
13
14
15
t (sec)

Fig. G. 2A d)

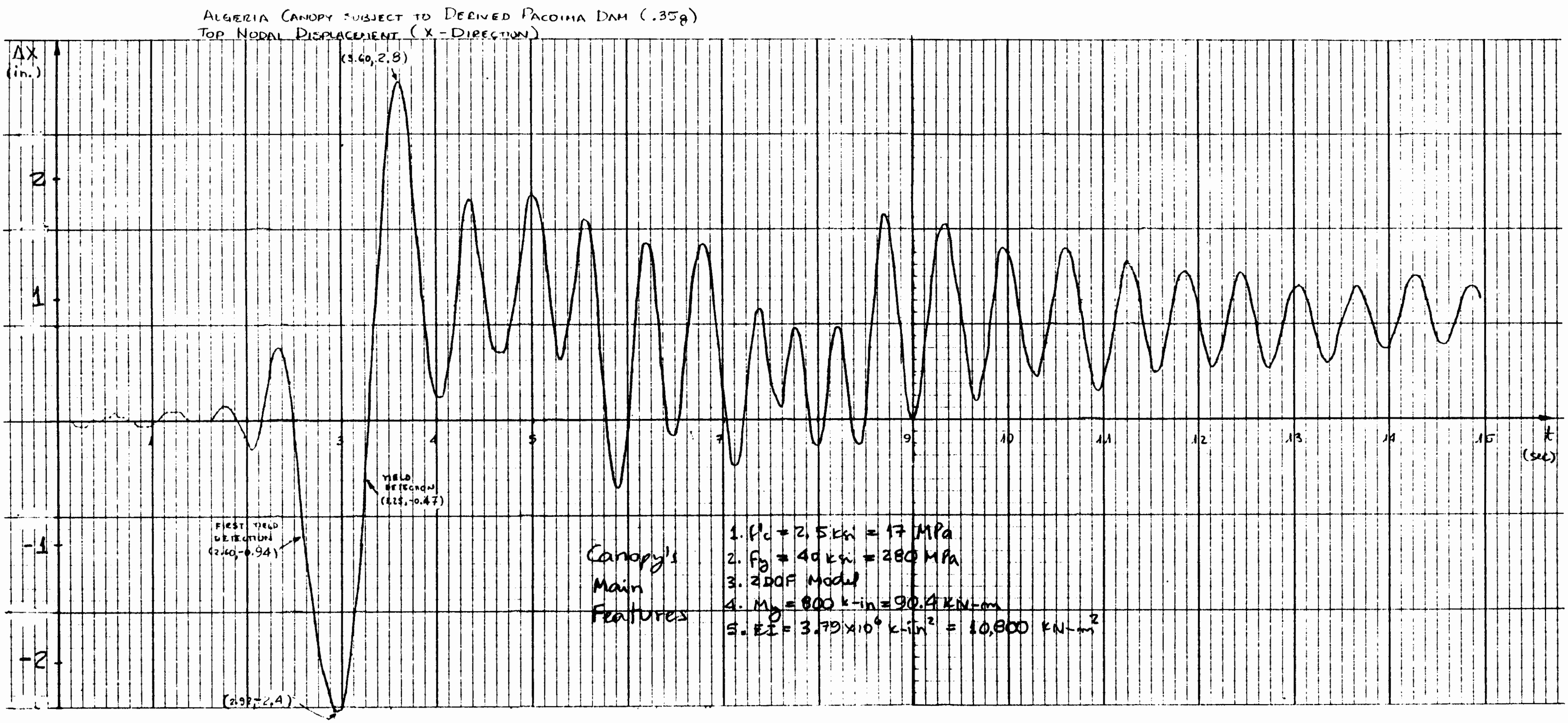

ALGERIA CANOPY SUBJECT TO DERIVED PACOIMA DAM (.35g)
TOP NODAL DISPLACEMENT (X-DIRECTION)
ΔX (in.)
t (sec)
(3.60, 2.8)
YIELD DETECTION (3.25, -0.47)
FIRST YIELD DETECTION (2.60, -0.94)
(2.97, -2.4)
Canopy's Main Features
1. f'c = 2.5 ksi = 17 MPa
2. fy = 40 ksi = 280 MPa
3. 2DOF Model
4. My = 800 k-in = 90.4 kN-m
5. EI = 3.79x10^6 k-in² = 10,800 kN-m²

Fig. G. 2B a)

ALGERIA CANOPY SUBJECT TO DERIVED PACOIMA DAM (.35g)
MOMENT AT BASE OF CANOPY

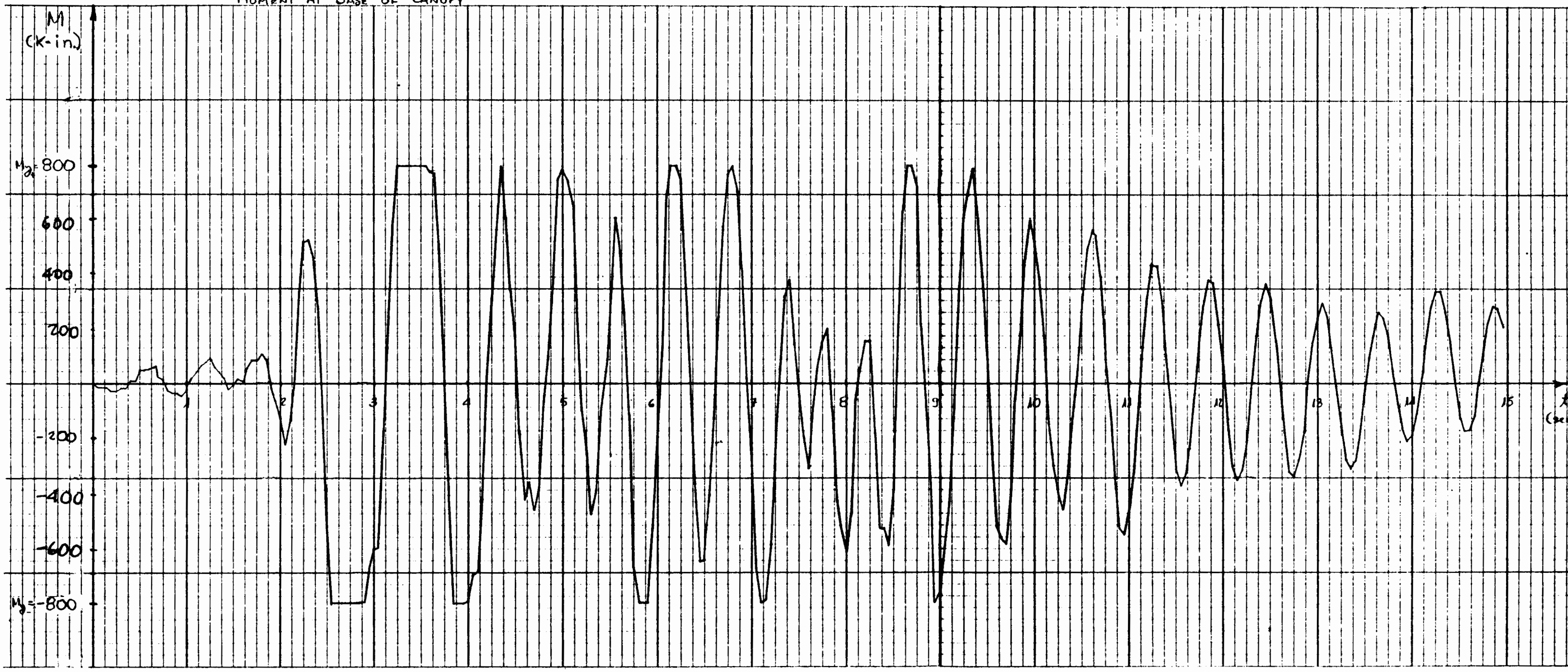

Fig. G.2B b)

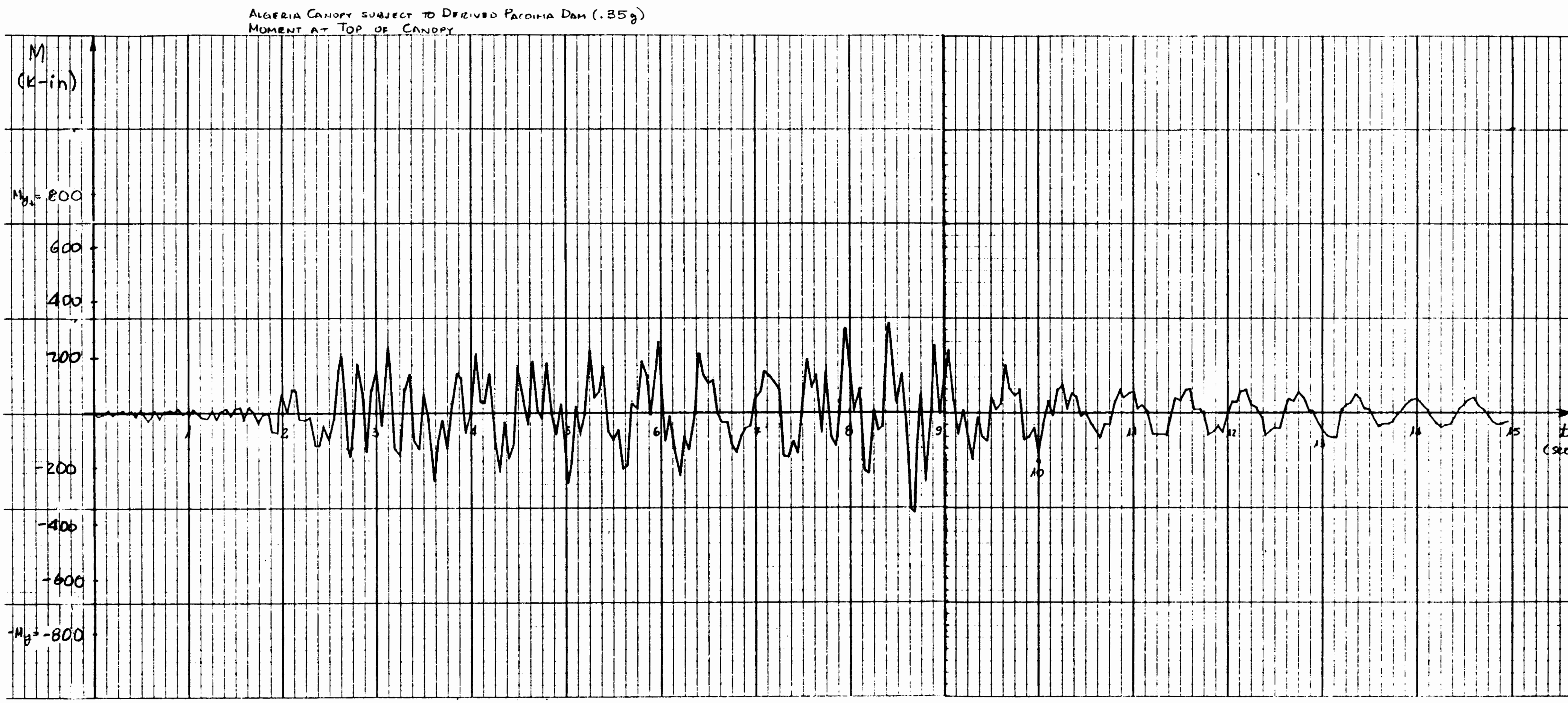

Algeria Canopy subject to Derived Pacoima Dam (.35g)
Moment at Top of Canopy
M
(k-in)
My+ = 800
600
400
200
-200
-400
-600
-My = -800
1
2
3
4
5
6
7
8
9
10
11
12
13
14
15
t
(sec)

Fig. G.2B c)

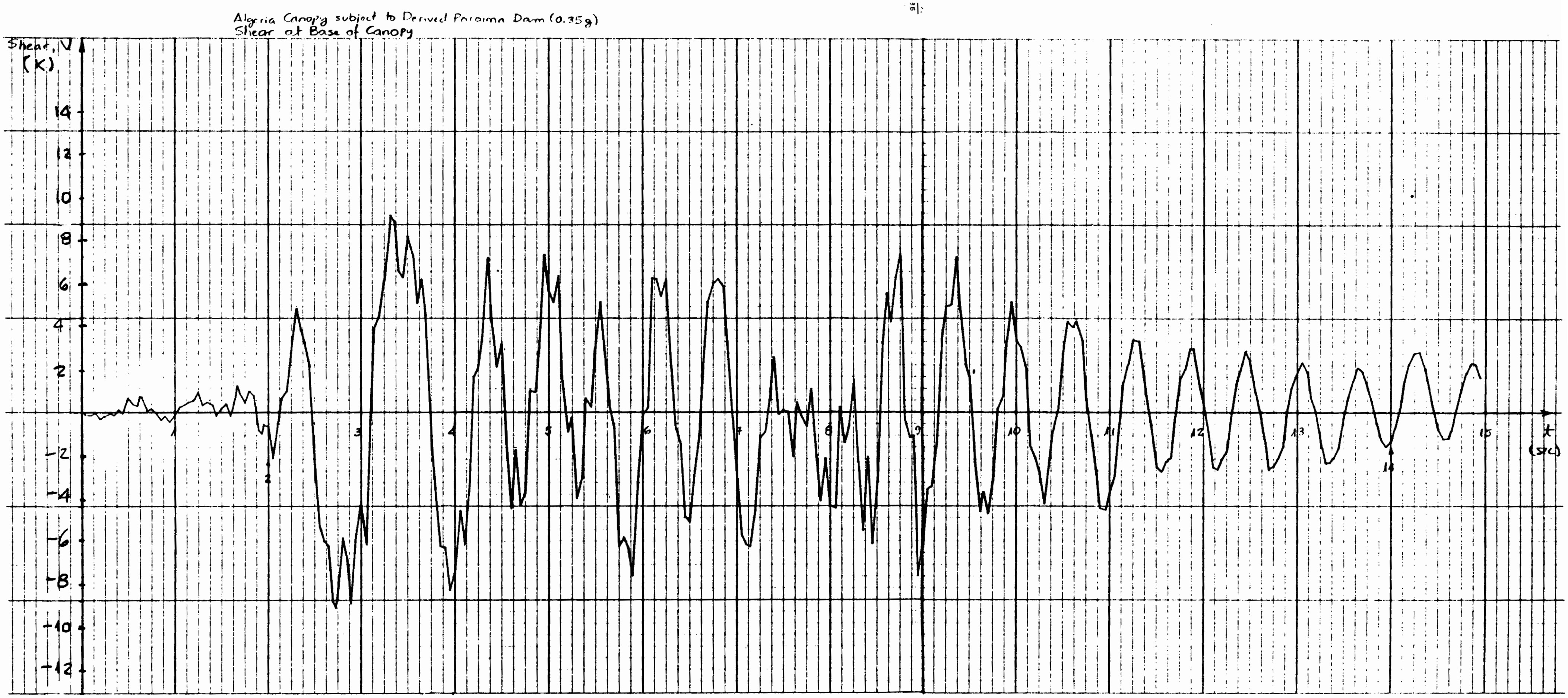

Algeria Canopy subject to Derived Pacoima Dam (0.35g)
Shear at Base of Canopy
Shear, V (K)
14
12
10
8
6
4
2
-2
-4
-6
-8
-10
-12
1
2
3
4
5
6
7
8
9
10
11
12
13
14
15
t (sec)

Fig. G.2B d)

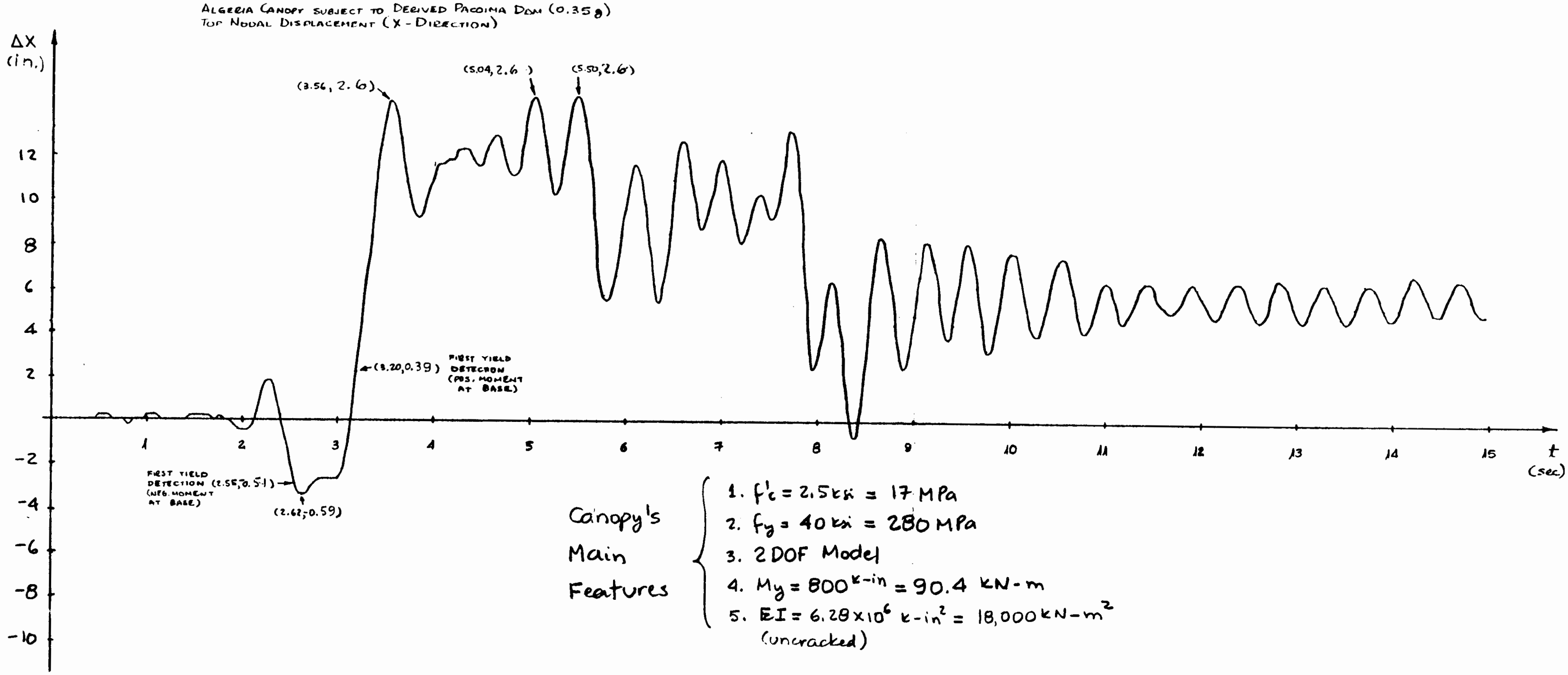

Canopy's Main Features

1. $f'_c = 2.5\,ksi = 17\,MPa$
2. $f_y = 40\,ksi = 280\,MPa$
3. 2 DOF Model
4. $M_y = 800^{k\text{-}in} = 90.4\,kN\text{-}m$
5. $EI = 6.28 \times 10^6\,k\text{-}in^2 = 18{,}000\,kN\text{-}m^2$ (uncracked)

Fig. G.2C a)

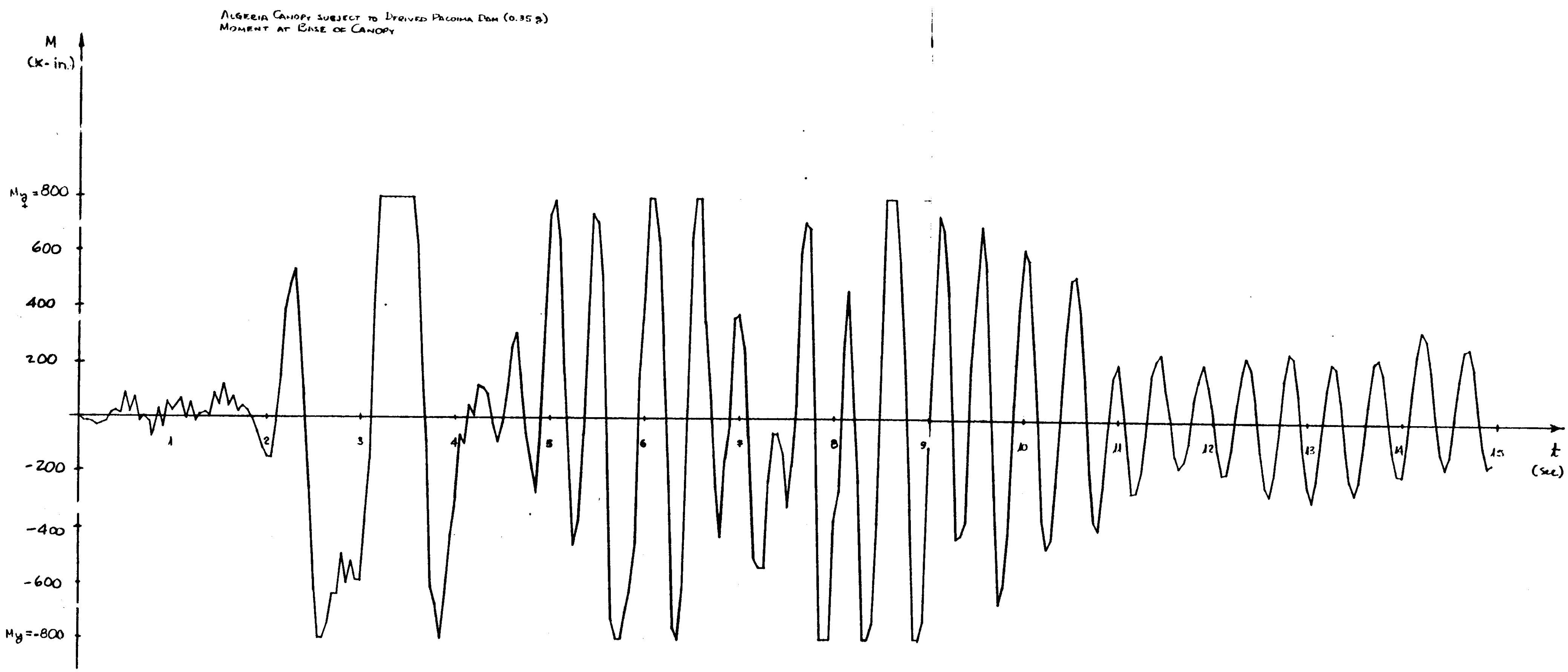

ALGERIA CANOPY SUBJECT TO DERIVED PACOIMA DAM (0.35 g)
MOMENT AT BASE OF CANOPY
M
(K-in.)
My=800
600
400
200
-200
-400
-600
My=-800
1
2
3
4
5
6
7
8
9
10
11
12
13
14
15
t
(sec)

Fig. G.2C b)

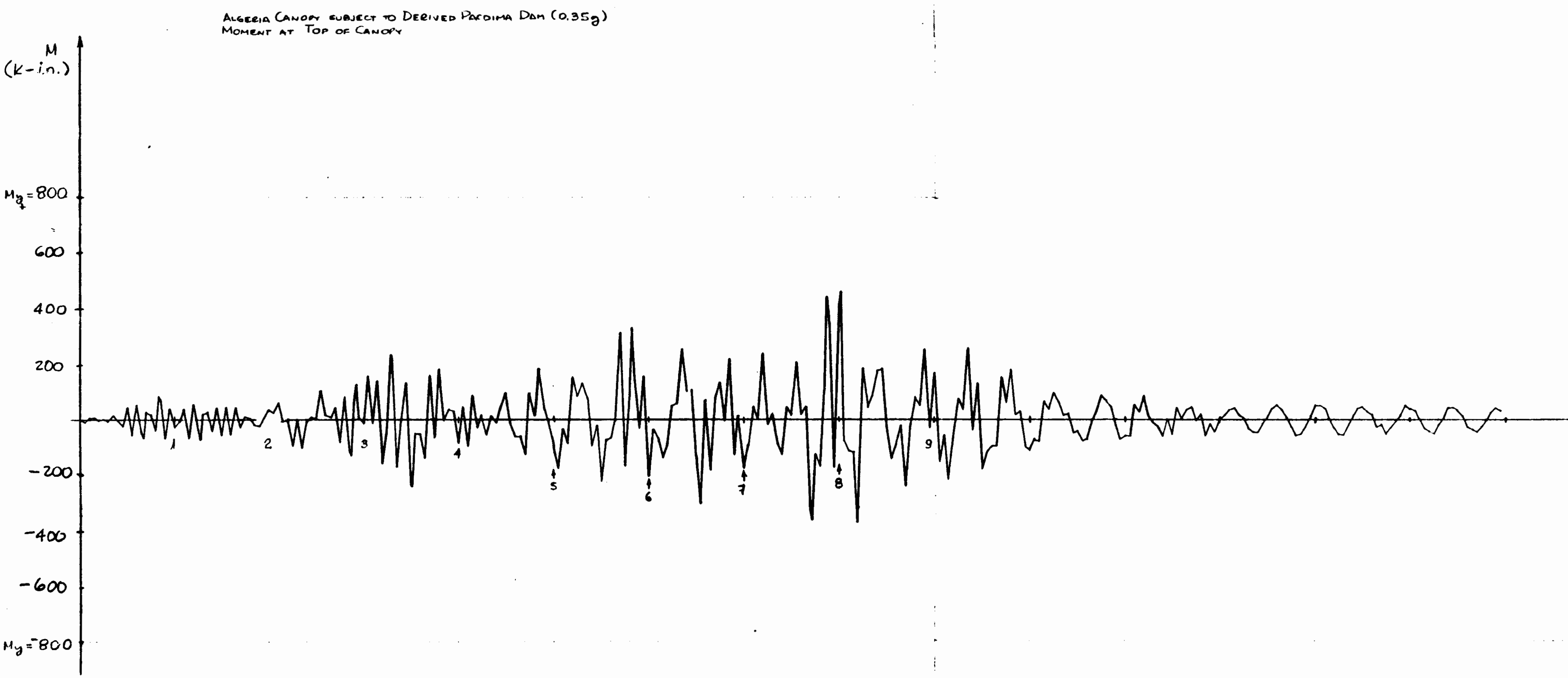
ALGERIA CANOPY SUBJECT TO DERIVED PACOIMA DAM (0.35g)
MOMENT AT TOP OF CANOPY
M
(K-in.)
My=800
600
400
200
-200
-400
-600
My=-800
1
2
3
4
5
6
7
8
9

Fig. G. 2C c)

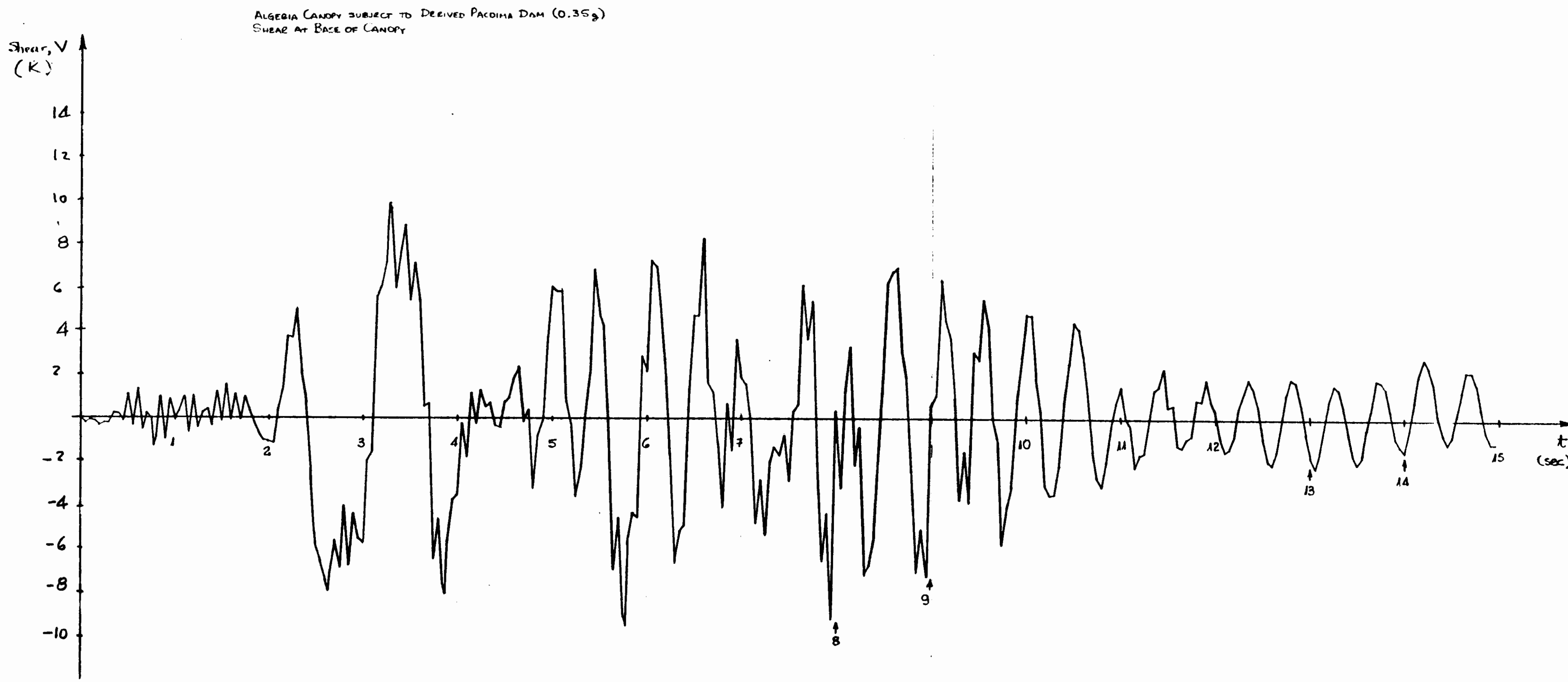

ALGERIA CANOPY SUBJECT TO DERIVED PACOIMA DAM (0.35g)
SHEAR AT BASE OF CANOPY
Shear, V
(K)
14
12
10
8
6
4
2
-2
-4
-6
-8
-10
1
2
3
4
5
6
7
8
9
10
11
12
13
14
15
t
(sec)

Fig. G. 2C d)

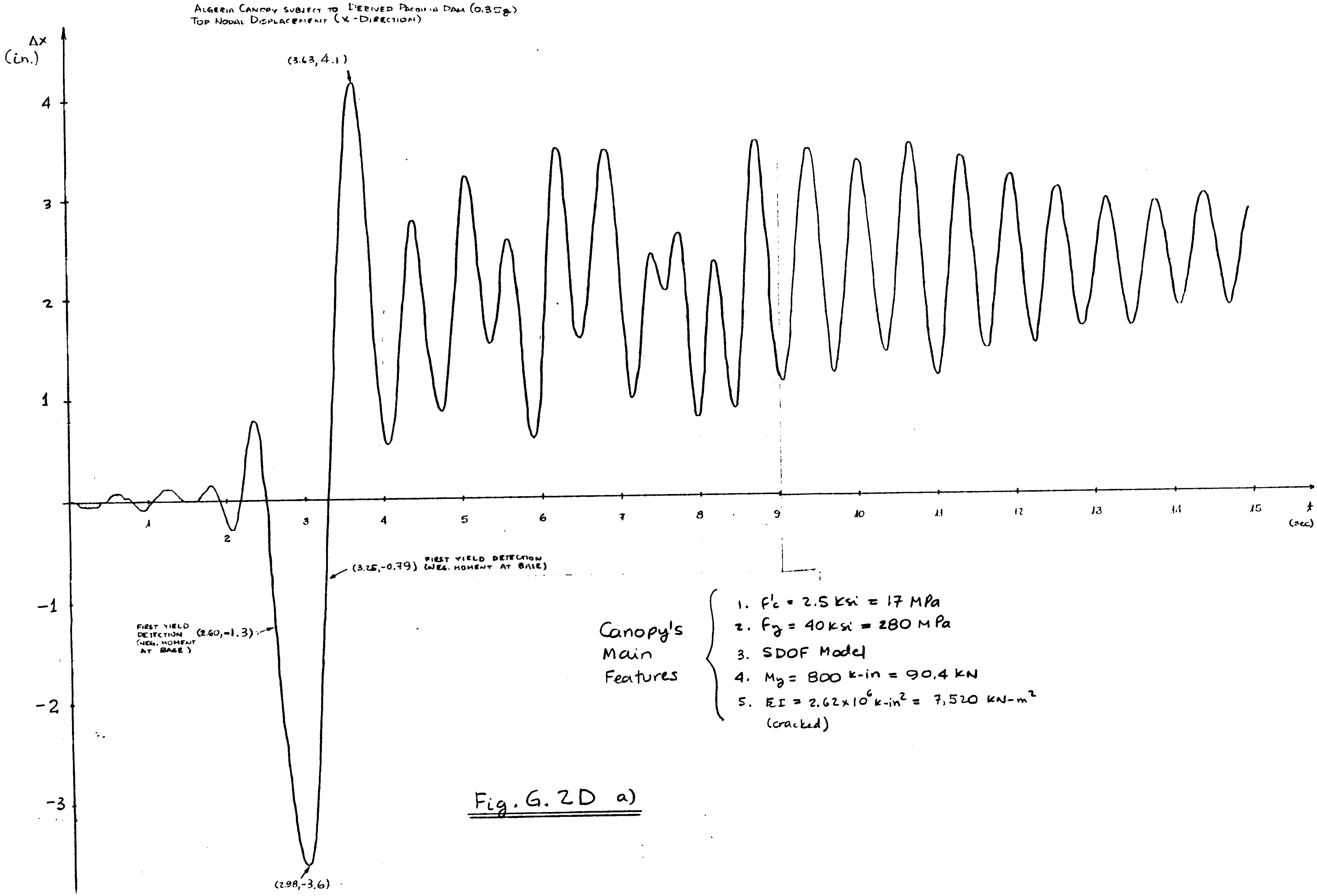

Algeria Canopy subject to Derived Pacoima Dam (0.35g)
Top Nodal Displacement (x-Direction)
Δx (in.)
4
3
2
1
-1
-2
-3
1
2
3
4
5
6
7
8
9
10
11
12
13
14
15
t (sec)
(3.63, 4.1)
(3.25, -0.79) First yield detection (Neg. moment at base)
First yield detection (Neg. moment at base) (2.60, -1.3)
(2.98, -3.6)
Canopy's Main Features
1. f'_c = 2.5 ksi = 17 MPa
2. f_y = 40 ksi = 280 MPa
3. SDOF Model
4. M_y = 800 k-in = 90.4 kN
5. $EI = 2.62 \times 10^6$ k-in^2 = 7,520 kN-m^2 (cracked)

Fig. G. 2D a)

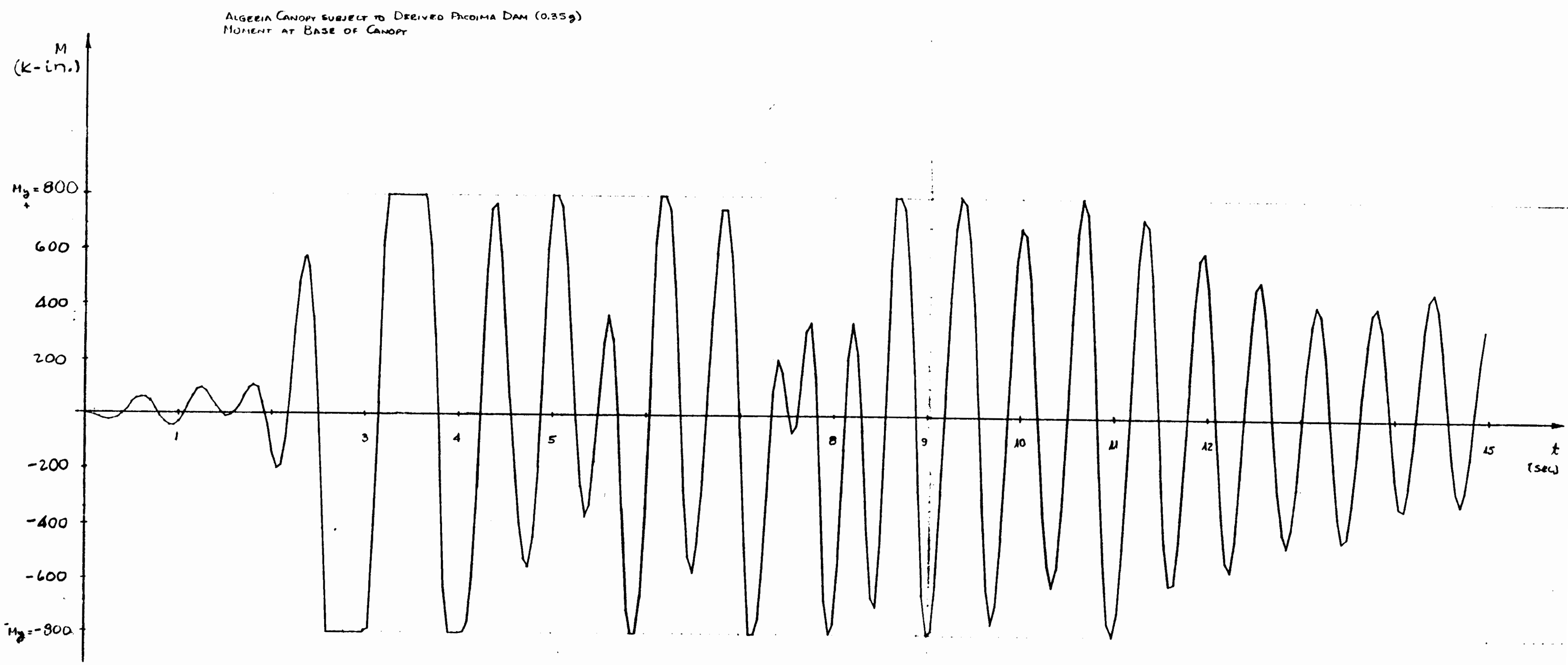

Algeria Canopy subject to Derived Pacoima Dam (0.35g)
Moment at Base of Canopy
M
(k-in.)
M_y = 800
600
400
200
-200
-400
-600
M_y = -800
1
3
4
5
8
9
10
11
12
15
t
(sec)

Fig. G.2D b)

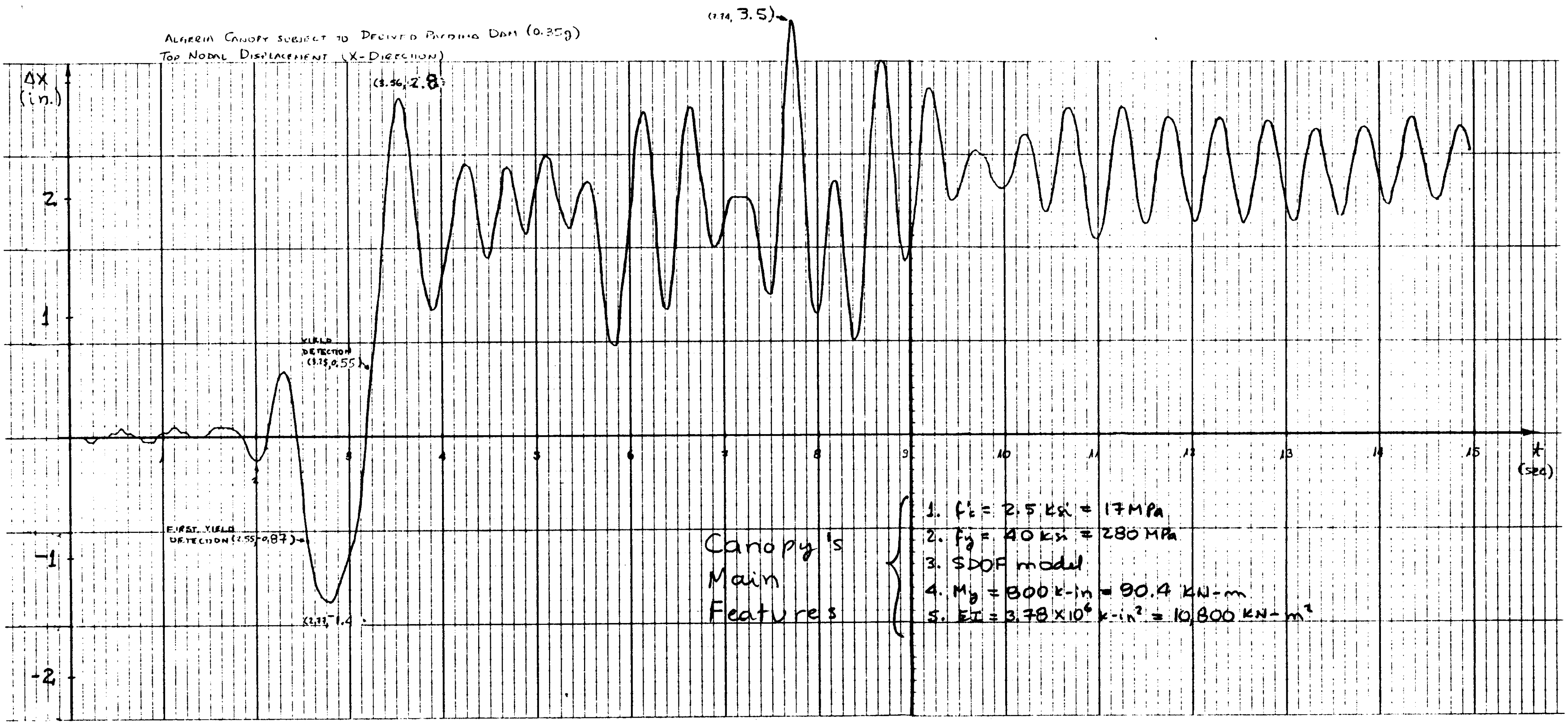

Algeria Canopy subject to Derived Parding Dam (0.35g)
Top Nodal Displacement (X-Direction)
ΔX (in.)
2
1
-1
-2
t (sec)
(7.74, 3.5)
(3.56, 2.8)
Yield Detection (3.15, 0.55)
First Yield Detection (2.55, -0.87)
(2.77, -1.4)
Canopy's Main Features
1. f'c = 2.5 ksi = 17 MPa
2. fy = 40 ksi = 280 MPa
3. SDOF model
4. My = 800 k-in = 90.4 kN-m
5. EI = 3.78 x 10^6 k-in^2 = 10,800 kN-m^2

Fig. G. 2E a)

Algeria Canopy subject to Derived Pacoima Dam (0.35g)
Moment at Base of Canopy

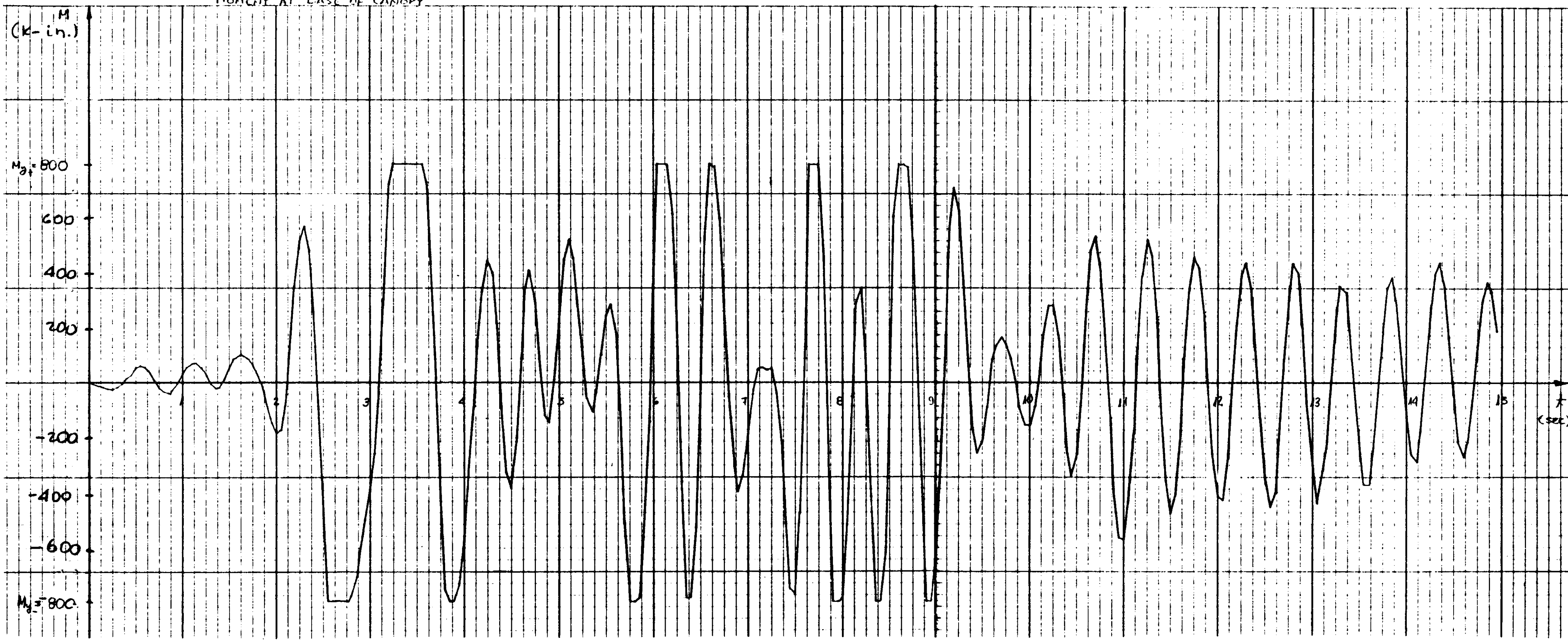

Fig. G.2E b)

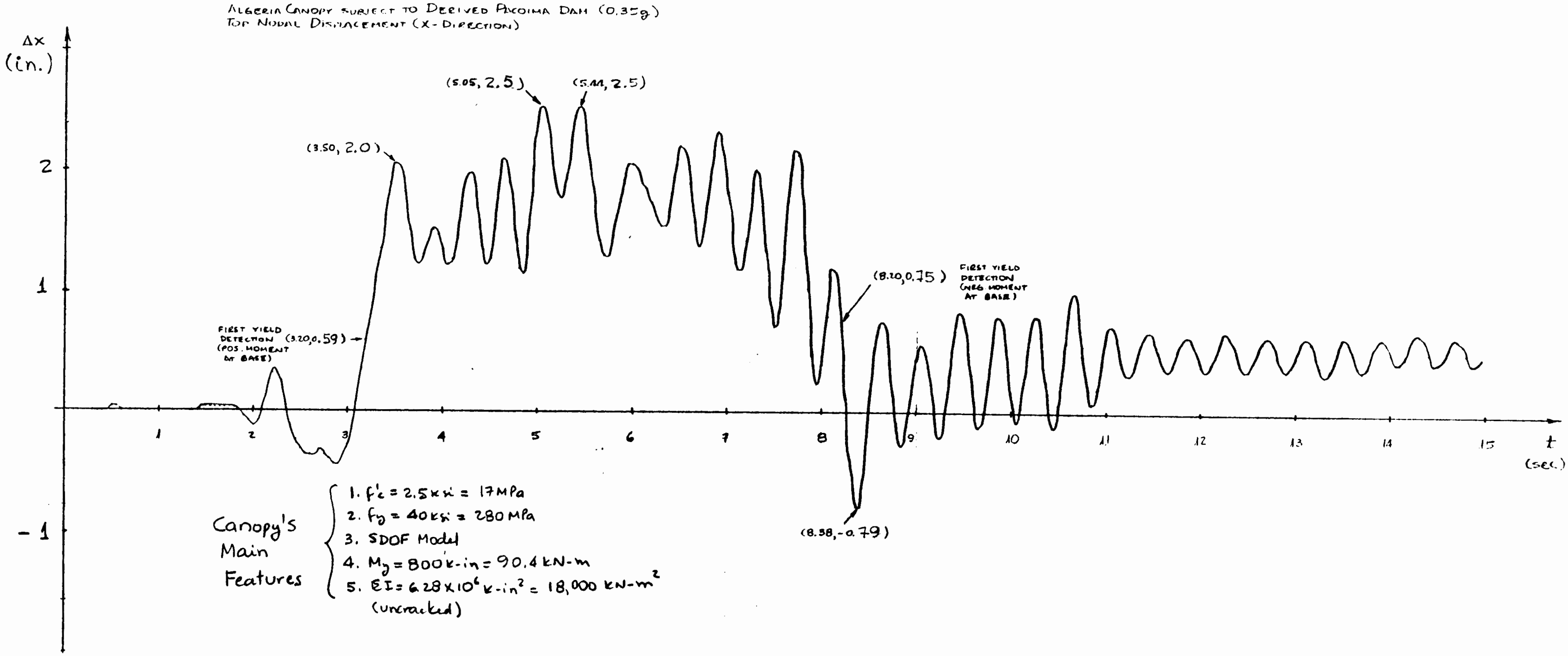

Canopy's Main Features
1. $f'_c = 2.5 ksi = 17 MPa$
2. $f_y = 40 ksi = 280 MPa$
3. SDOF Model
4. $M_y = 800 k\text{-}in = 90.4 kN\text{-}m$
5. $EI = 6.28 \times 10^6 k\text{-}in^2 = 18{,}000 kN\text{-}m^2$ (uncracked)

Fig. G.2F a)

ALGERIA CANOPY SUBJECT TO DERIVED PACOIMA DAM (0.35g)
MOMENT AT BASE OF CANOPY

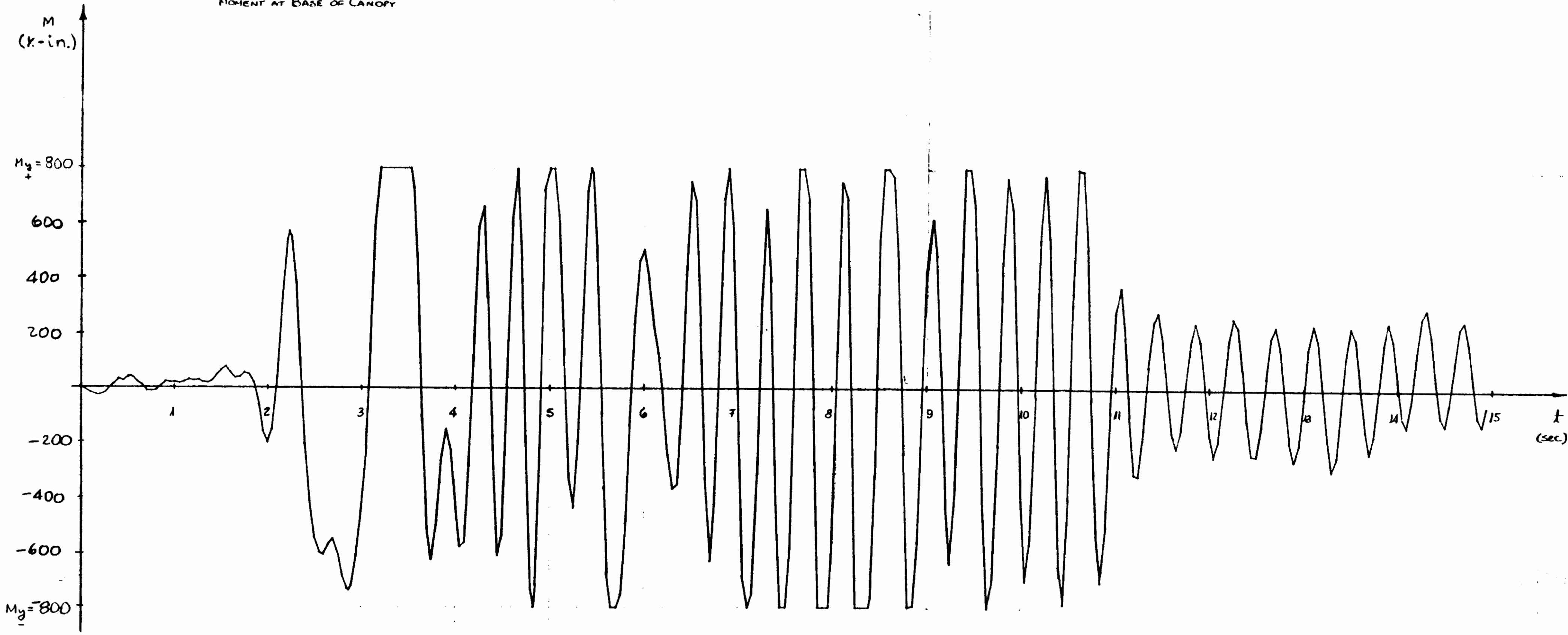

Fig. G. 2F b)

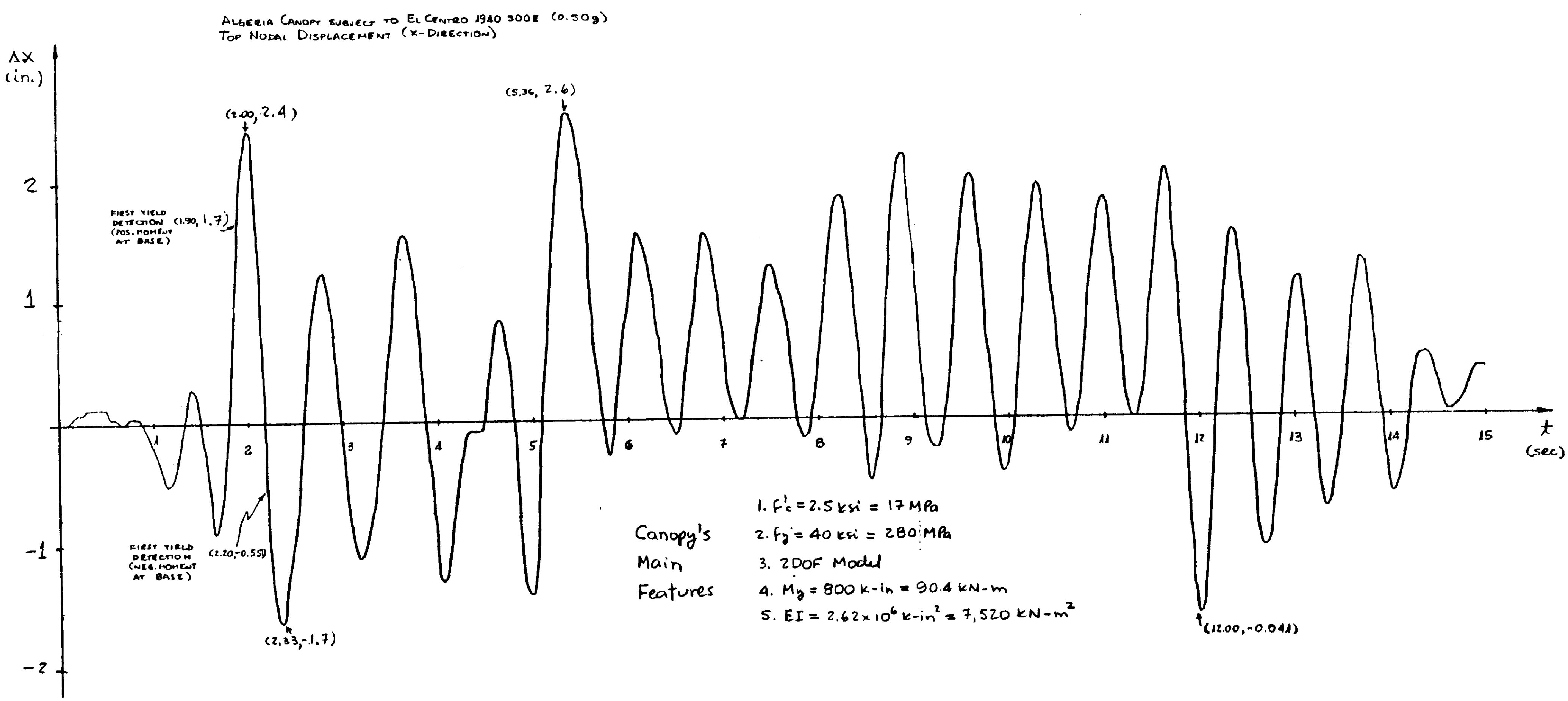
ALGERIA CANOPY SUBJECT TO EL CENTRO 1940 S00E (0.50g)
TOP NODAL DISPLACEMENT (X-DIRECTION)
ΔX (in.)
2
1
-1
-2
t (sec)
1
2
3
4
5
6
7
8
9
10
11
12
13
14
15
(2.00, 2.4)
(5.36, 2.6)
FIRST YIELD DETECTION (1.90, 1.7) (POS. MOMENT AT BASE)
FIRST YIELD DETECTION (NEG. MOMENT AT BASE)
(2.20,-0.55)
(2.33,-1.7)
(12.00,-0.041)
Canopy's Main Features
1. $f'_c = 2.5$ ksi = 17 MPa
2. $f_y = 40$ ksi = 280 MPa
3. 2DOF Model
4. $M_y = 800$ k-in = 90.4 kN-m
5. $EI = 2.62 \times 10^6$ k-in^2 = 7,520 kN-m^2

Fig. G.3A a)

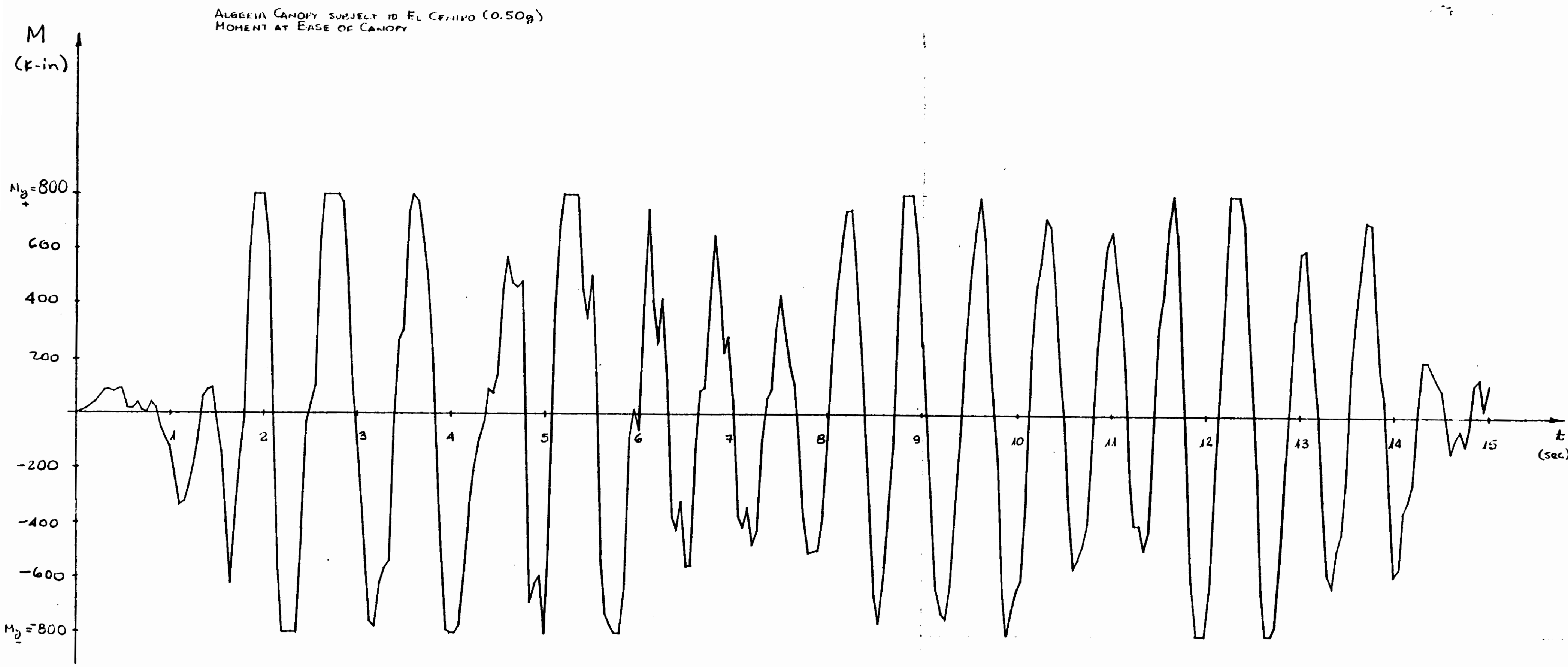

ALGERIA CANOPY SUBJECT TO EL CENTRO (0.50g)
MOMENT AT BASE OF CANOPY
M
(k-in)
$M_y^+ = 800$
600
400
200
-200
-400
-600
$M_y^- = -800$
1
2
3
4
5
6
7
8
9
10
11
12
13
14
15
t
(sec)

Fig. G.3A b)

ALGERIA CANOPY SUBJECT TO EL CENTRO 1940 S00E (0.50g)
MOMENT AT TOP OF CANOPY

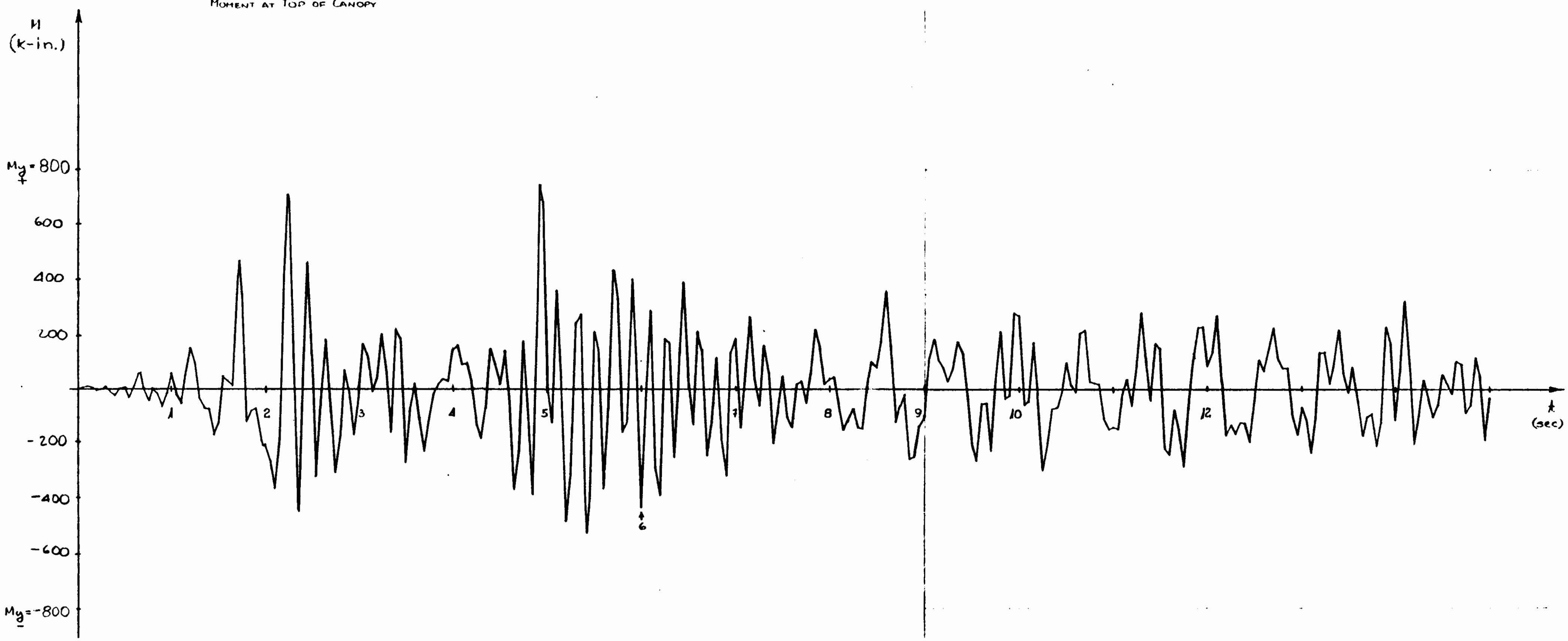

Fig. G. 3A c)

ALGERIA CANOPY SUBJECT TO EL CENTRO 1940 S00E (0.50g)
SHEAR AT BASE OF CANOPY

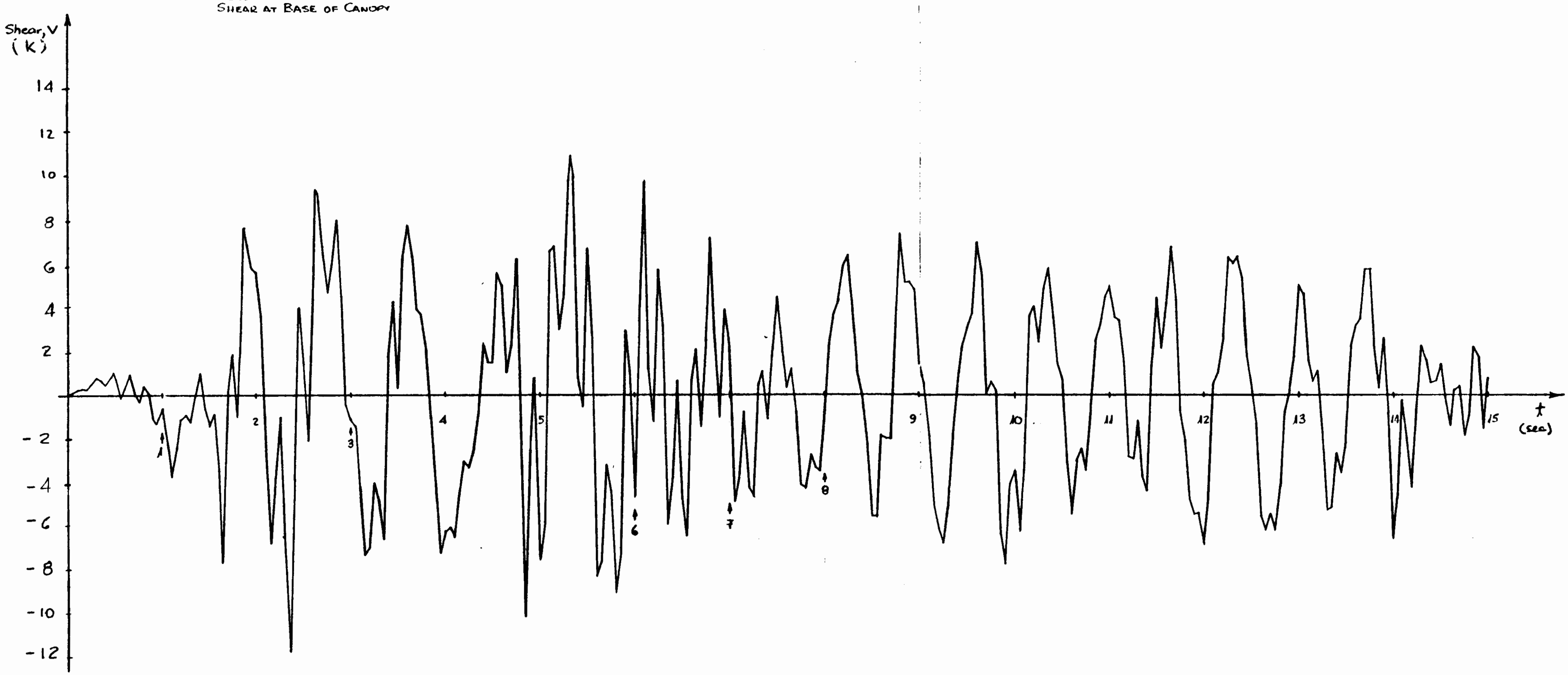

Fig. G.3A d)

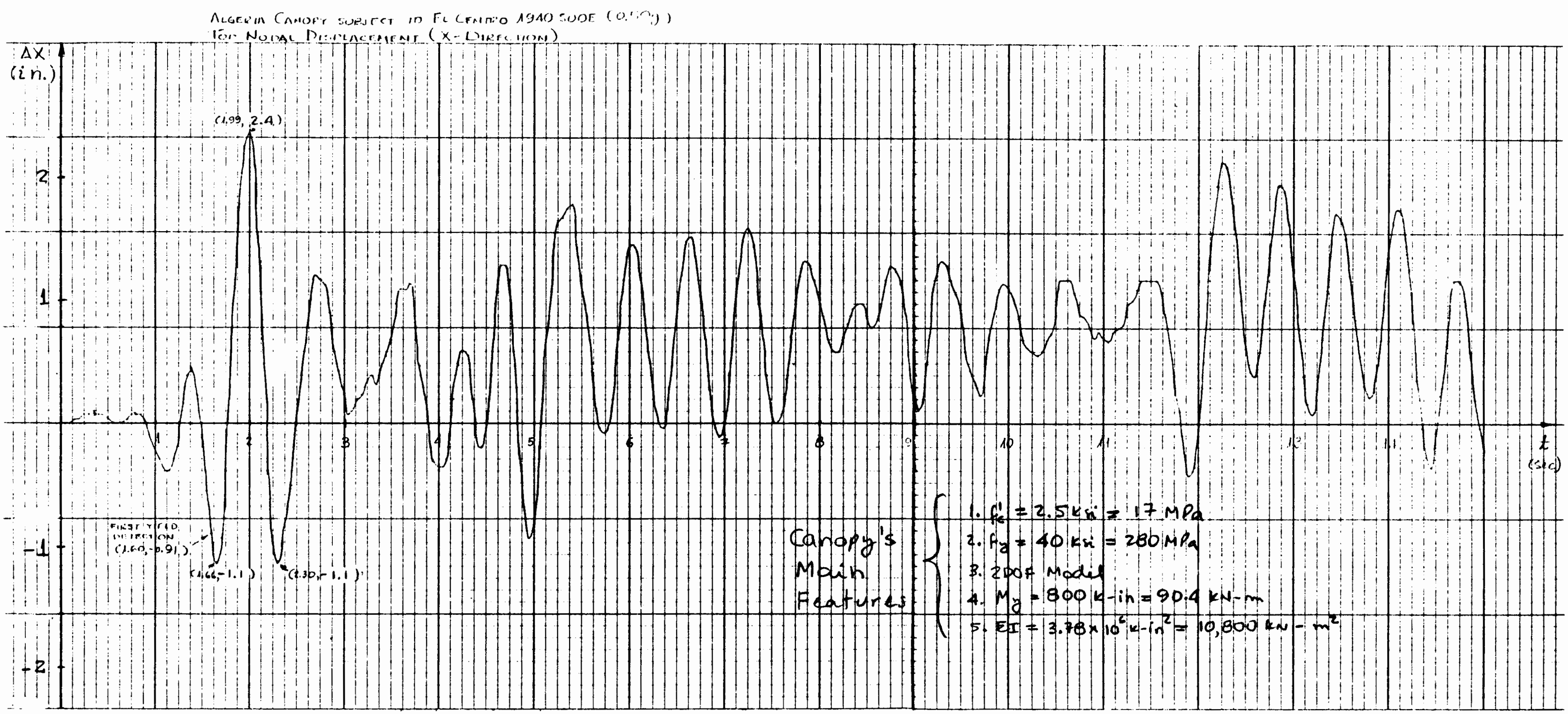
Algeria Canopy subject to El Centro 1940 S00E (0.5g)
Top Nodal Displacement (X-Direction)
ΔX (in.)
t (sec)
(1.99, 2.4)
First yield detection (1.60, -0.91)
(1.66, -1.1)
(2.30, -1.1)
Canopy's Main Features
1. f'c = 2.5 ksi = 17 MPa
2. fy = 40 ksi = 280 MPa
3. 2DOF Model
4. My = 800 k-in = 90.4 kN-m
5. EI = 3.78x10^6 k-in^2 = 10,800 kN-m^2

Fig. 6.3B a)

ALGERIA CANOPY SUBJECT TO EL CENTRO 1940 S00E (.50g)
MOMENT AT BASE OF CANOPY

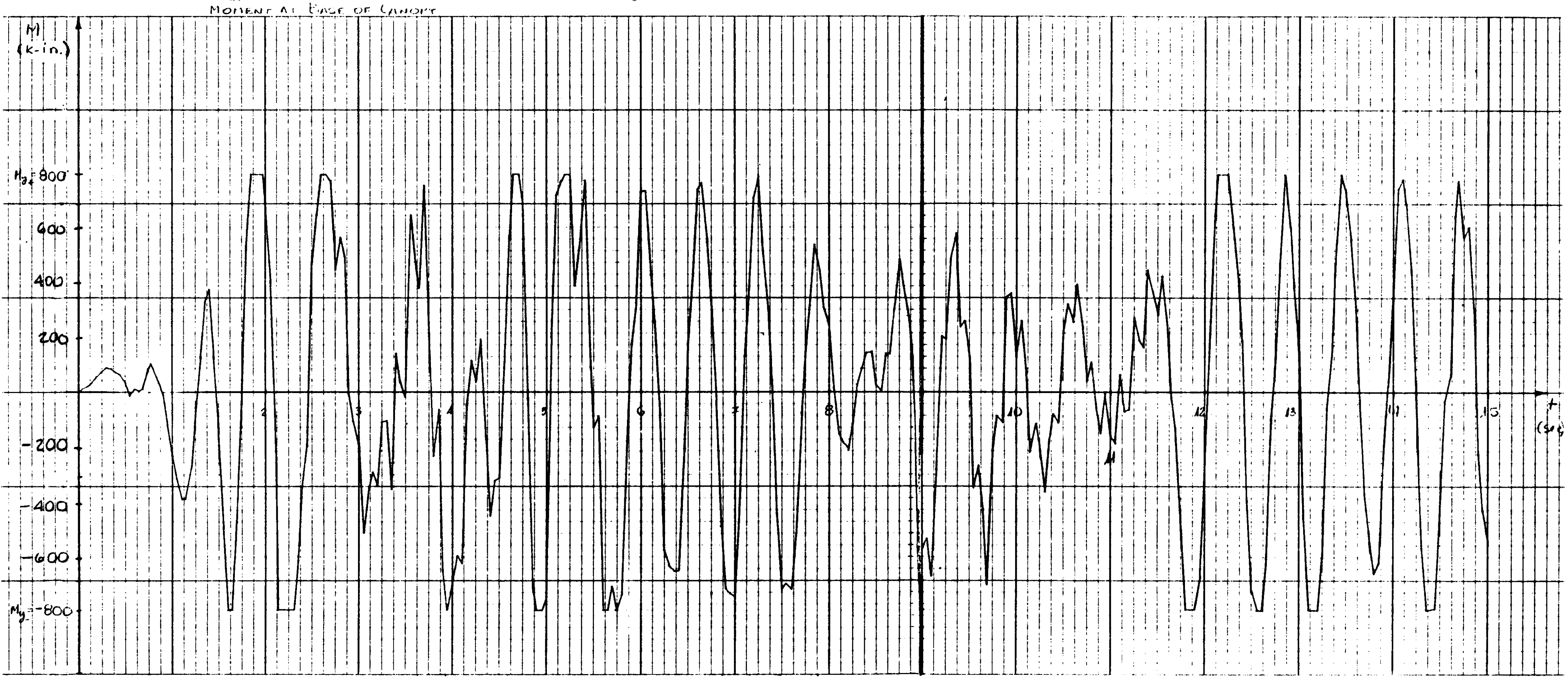

Fig. G.3B b)

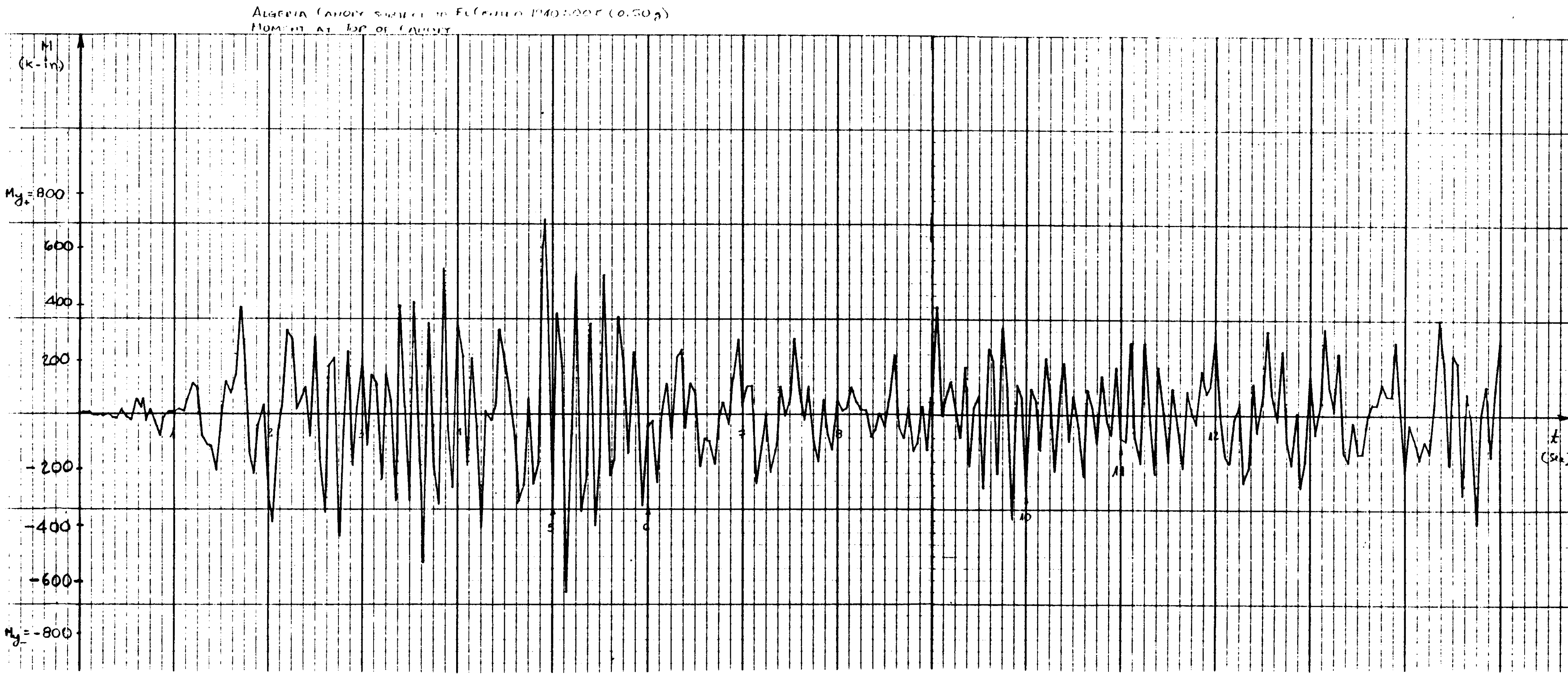

Fig. G.3B c)

Algeria Canopy subject to El Centro 1940 SOOE (0.50g)
Shear at Base of Canopy

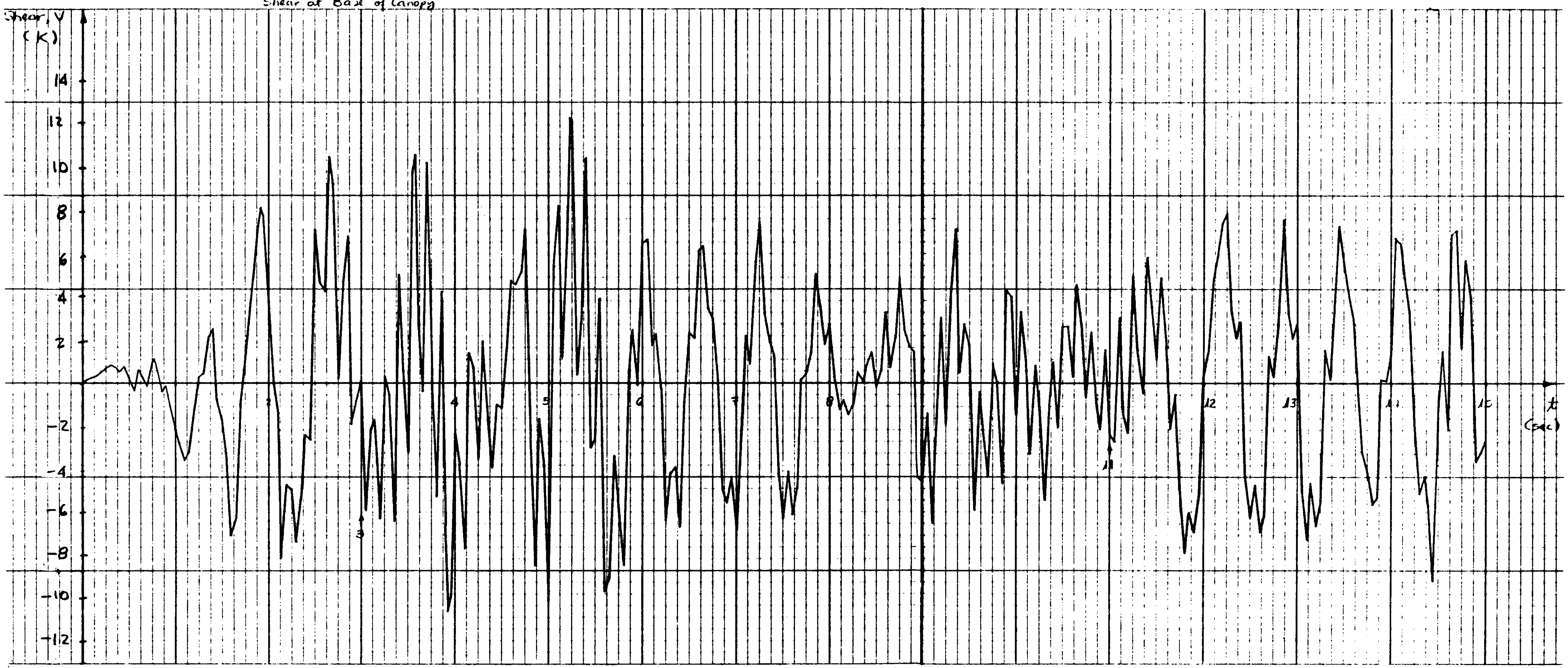

Fig. G. 3B d)

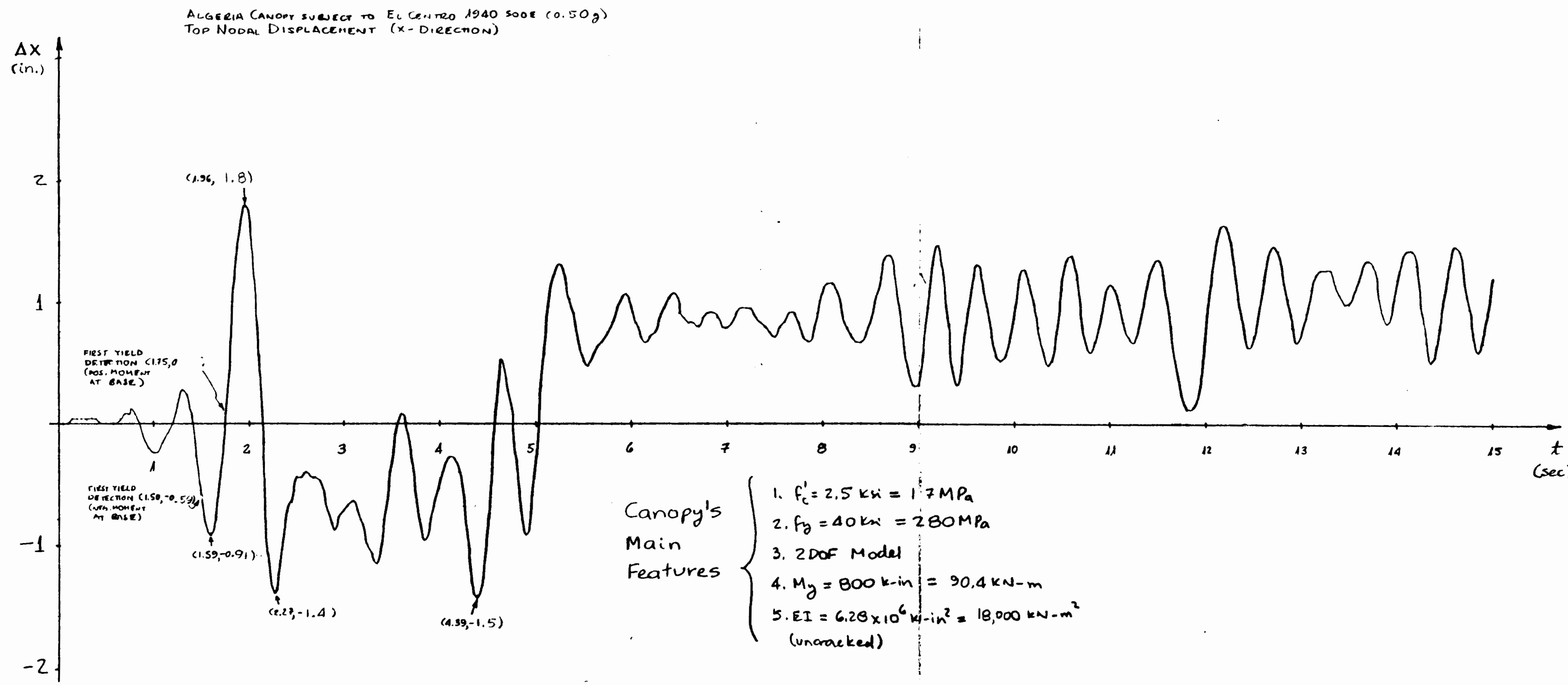
ALGERIA CANOPY SUBJECT TO EL CENTRO 1940 S00E (0.50g)
TOP NODAL DISPLACEMENT (X-DIRECTION)
ΔX (in.)
2
1
-1
-2
(1.96, 1.8)
FIRST YIELD DETECTION (1.75,0 (POS. MOMENT AT BASE)
FIRST YIELD DETECTION (1.50,-0.59) (NEG. MOMENT AT BASE)
(1.59,-0.91)
(2.27,-1.4)
(4.39,-1.5)
2
3
4
5
6
7
8
9
10
11
12
13
14
15
t (sec)
Canopy's Main Features
1. f'_c = 2.5 ksi = 17 MPa
2. f_y = 40 ksi = 280 MPa
3. 2DOF Model
4. M_y = 800 k-in = 90.4 kN-m
5. EI = 6.28×10^6 k-in^2 = 18,000 kN-m^2 (uncracked)

Fig. G. 3C a)

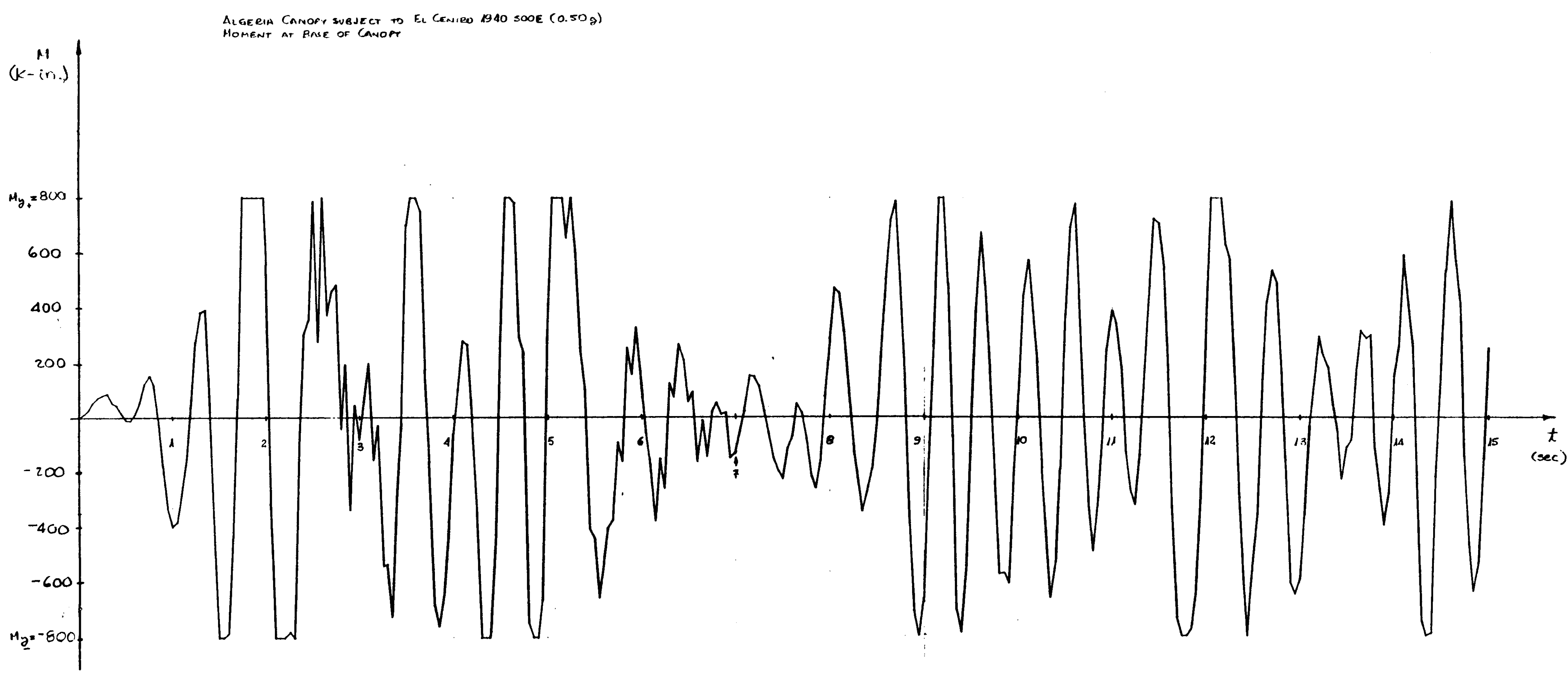
ALGERIA CANOPY SUBJECT TO EL CENTRO 1940 S00E (0.50g)
MOMENT AT BASE OF CANOPY
M
(k-in.)
M_{y+}=800
600
400
200
-200
-400
-600
M_{y-}=-800
1
2
3
4
5
6
7
8
9
10
11
12
13
14
15
t
(sec)

Fig. G.3C b)

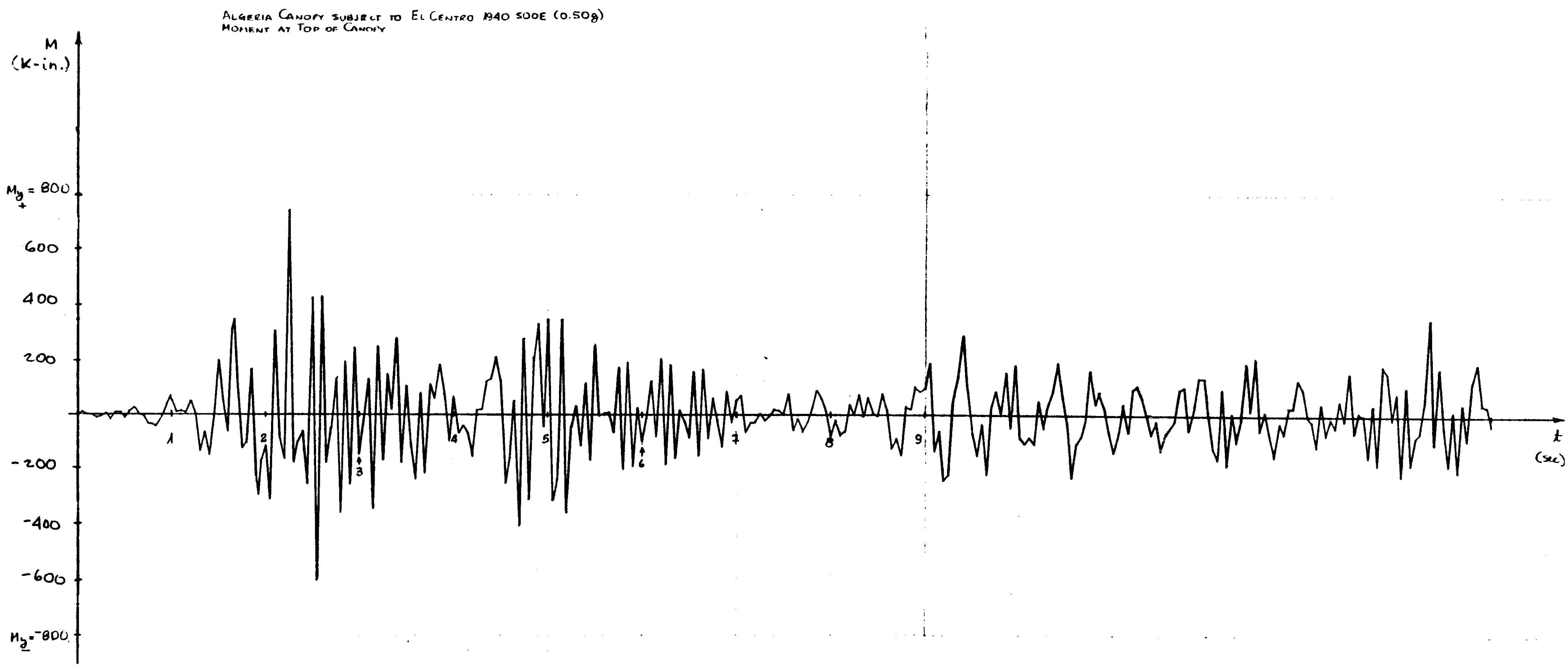
ALGERIA CANOPY SUBJECT TO EL CENTRO 1940 SOOE (0.50g)
MOMENT AT TOP OF CANOPY
M
(K-in.)
M_{y+} = 800
600
400
200
-200
-400
-600
M_{y-} = -800
1
2
3
4
5
6
7
8
9
t
(sec)

Fig. G. 3C c)

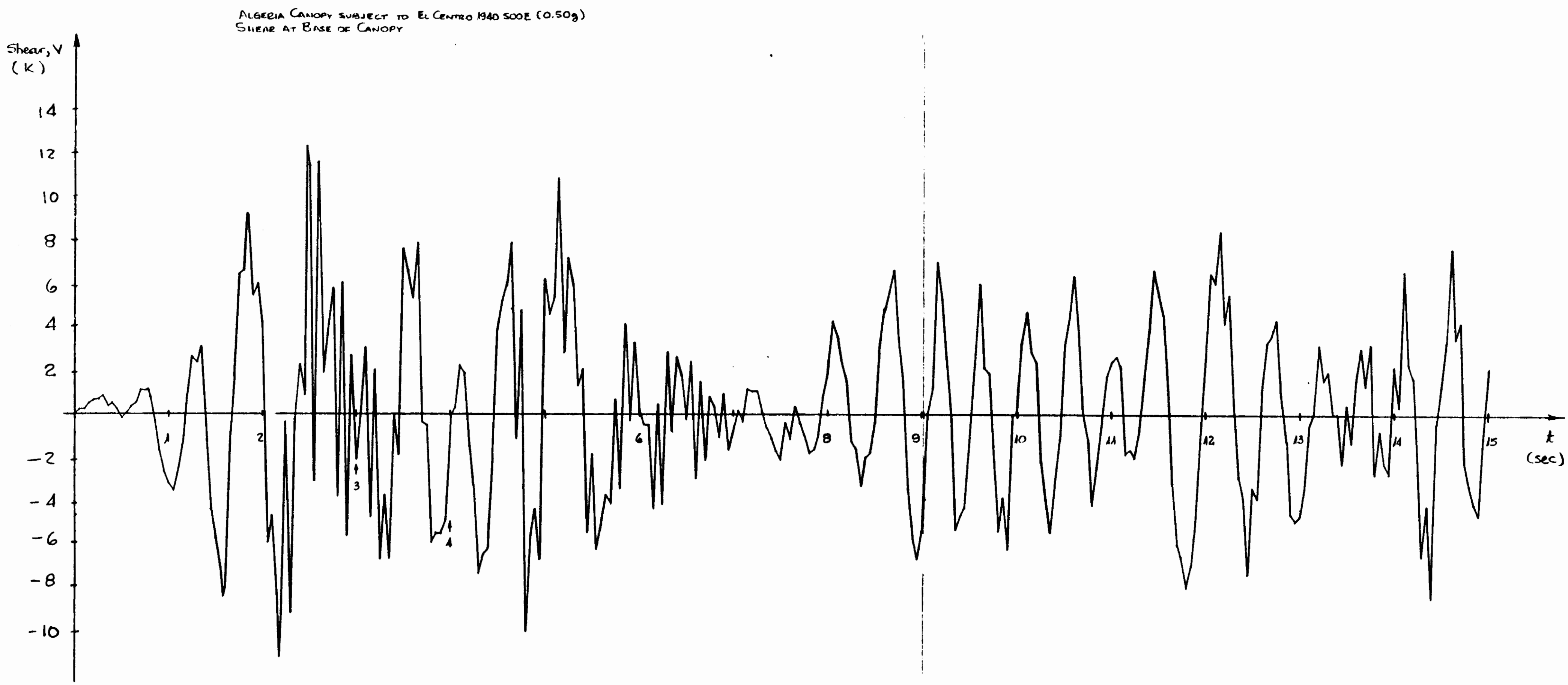

Algeria Canopy subject to El Centro 1940 S00E (0.50g)
Shear at Base of Canopy
Shear, V
(K)
14
12
10
8
6
4
2
-2
-4
-6
-8
-10
1
2
3
4
6
8
9
10
11
12
13
14
15
t
(sec)

Fig. G. 3C d)

ALGERIA CANOPY SUBJECT TO EL CENTRO 1940 S00E (0.50g)
TOP NODAL DISPLACEMENT (X-DIRECTION)

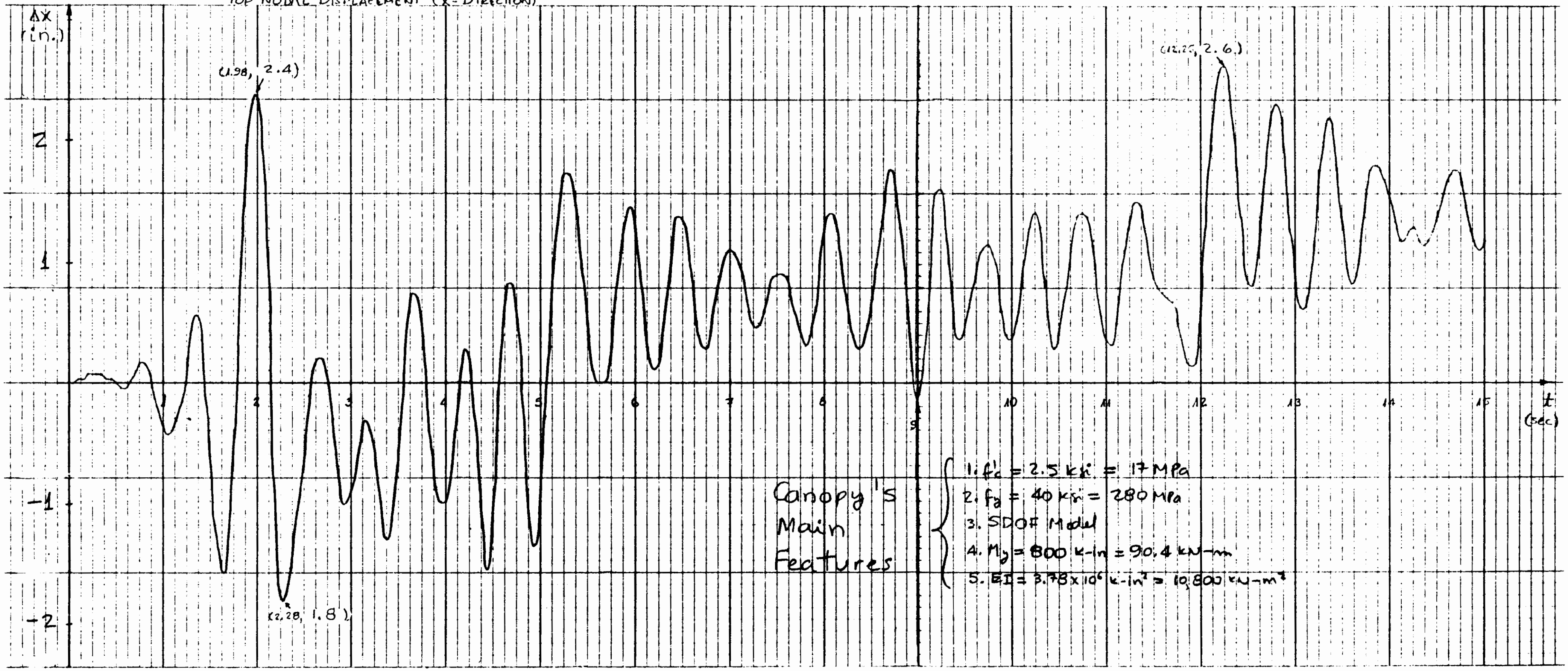

Fig. G. 3D a)

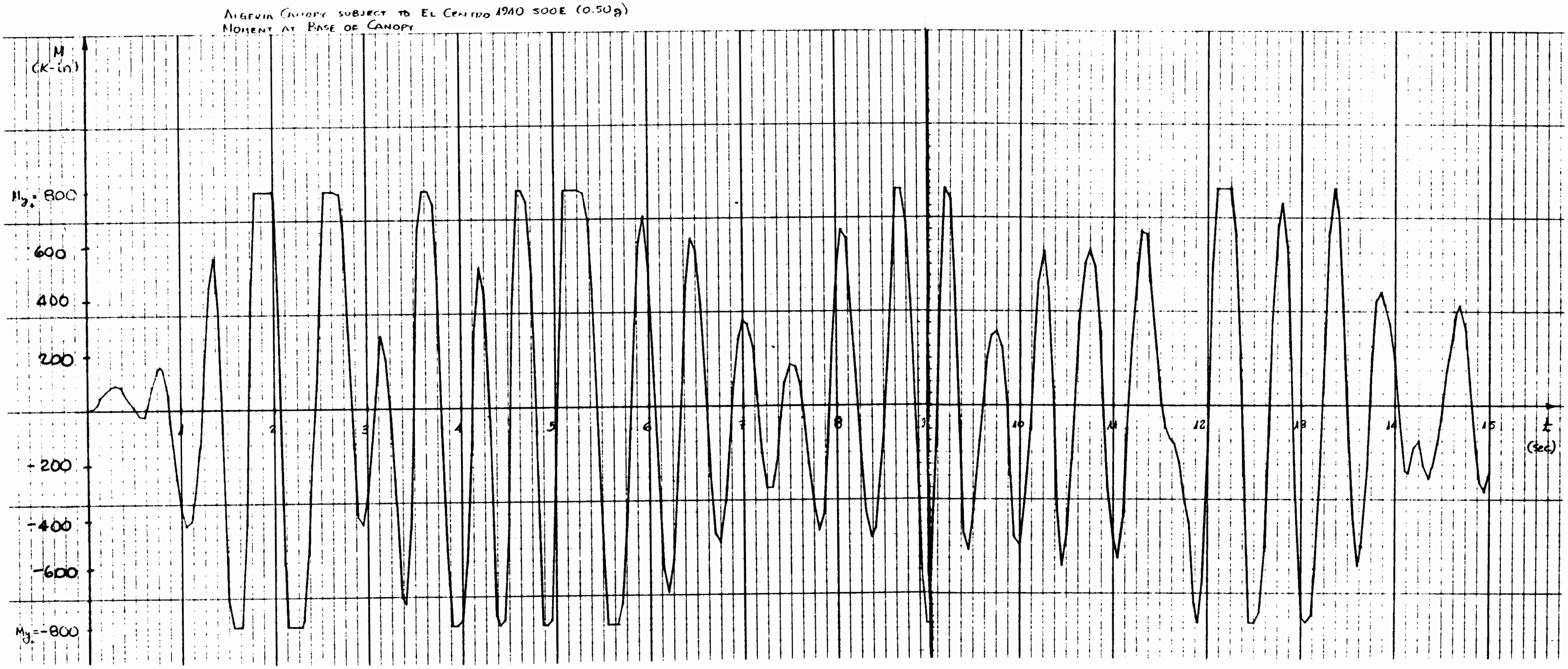
Algeria Canopy subject to El Centro 1940 S00E (0.50g)
Moment at Base of Canopy
M
(k-in)
M_{y+} = 800
600
400
200
-200
-400
-600
M_y = -800
1
2
3
4
5
6
7
8
9
10
11
12
13
14
15
t
(sec)

Fig. G.3D b)

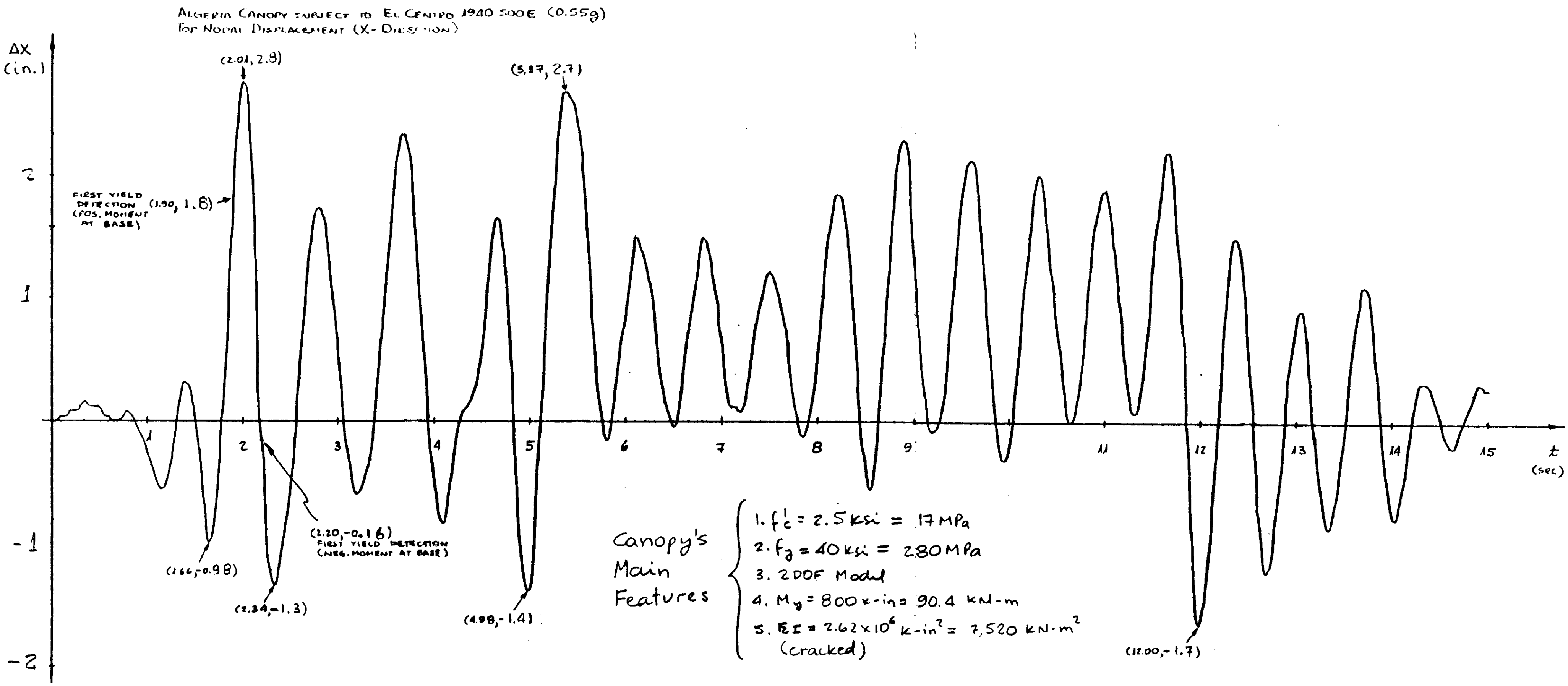
ALGERIA CANOPY SUBJECT TO EL CENTRO 1940 S00E (0.55g)
TOP NODAL DISPLACEMENT (X-DIRECTION)
ΔX (in.)
2
1
-1
-2
t (sec)
1
2
3
4
5
6
7
8
9
11
12
13
14
15
(2.01, 2.8)
(5.87, 2.7)
FIRST YIELD DETECTION (POS. MOMENT AT BASE) (1.90, 1.8)
(1.66, -0.98)
(2.34, -1.3)
(2.20, -0.16) FIRST YIELD DETECTION (NEG. MOMENT AT BASE)
(4.98, -1.4)
(12.00, -1.7)
Canopy's Main Features
1. f'_c = 2.5 ksi = 17 MPa
2. f_y = 40 ksi = 280 MPa
3. 2DOF Model
4. M_y = 800 k-in = 90.4 kN-m
5. EI = 2.62×10^6 k-in^2 = 7,520 kN-m^2 (cracked)

Fig. G.4A a)

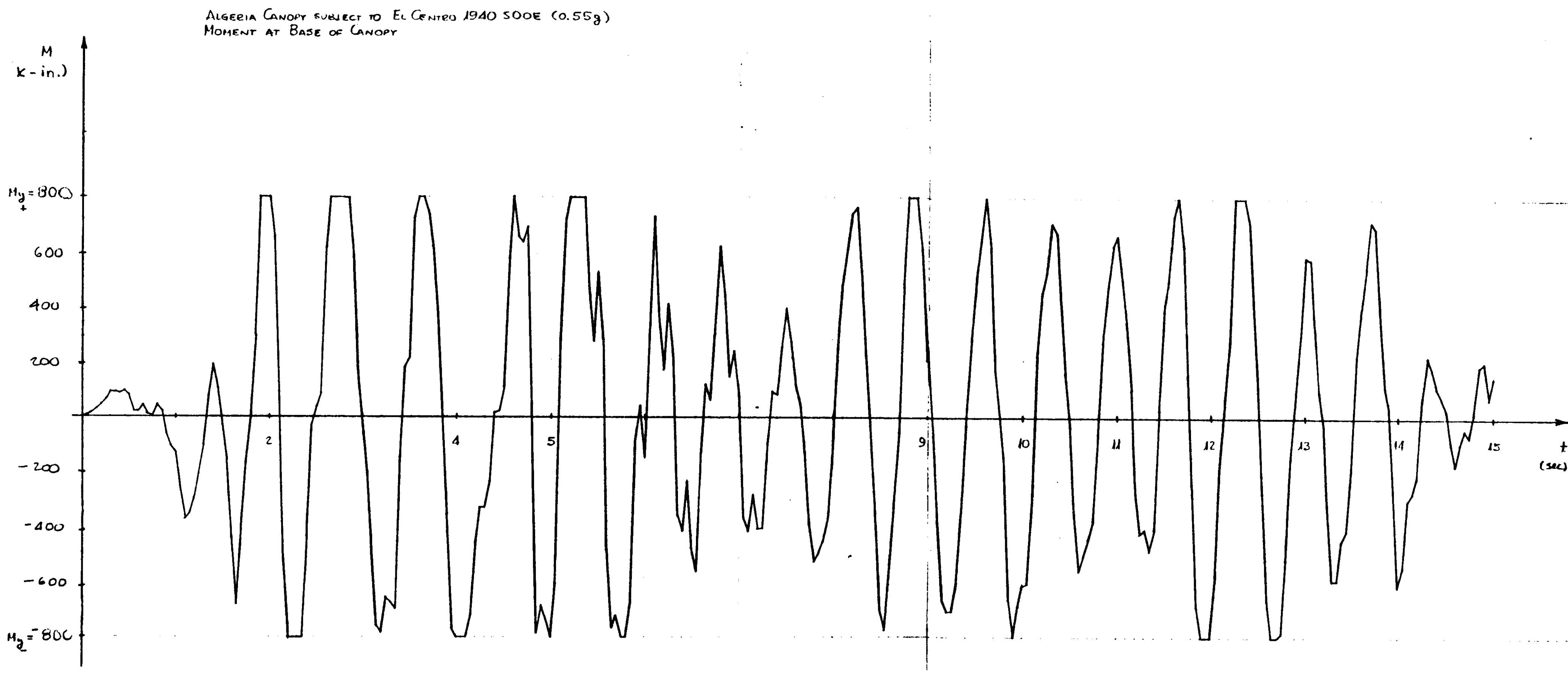
Algeria Canopy subject to El Centro 1940 S00E (0.55g)
Moment at Base of Canopy
M
k-in.)
$M_y = 800$
600
400
200
-200
-400
-600
$M_y = -800$
2
4
5
9
10
11
12
13
14
15
t
(sec)

Fig. G.4A b)

Algeria Canopy subject to El Centro 1940 S00E (0.55g)
Moment at Top of Canopy

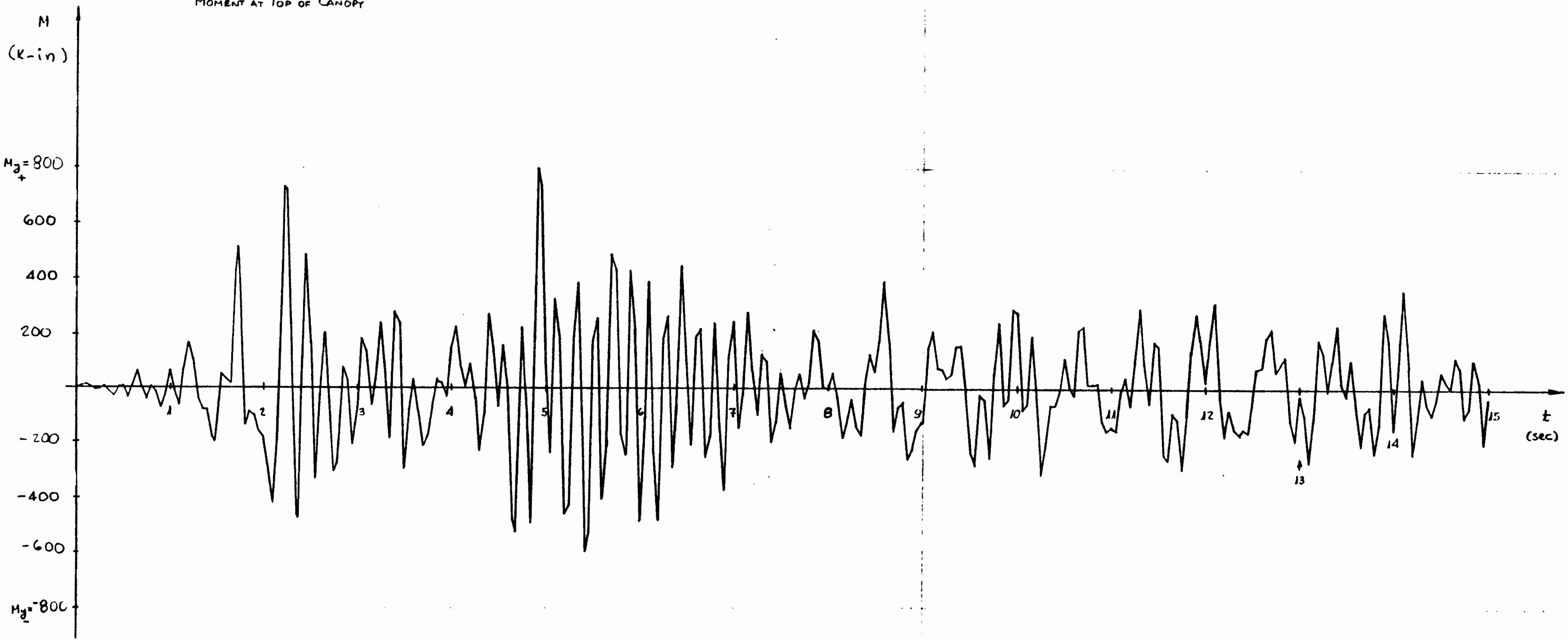

Fig. G.4A c)

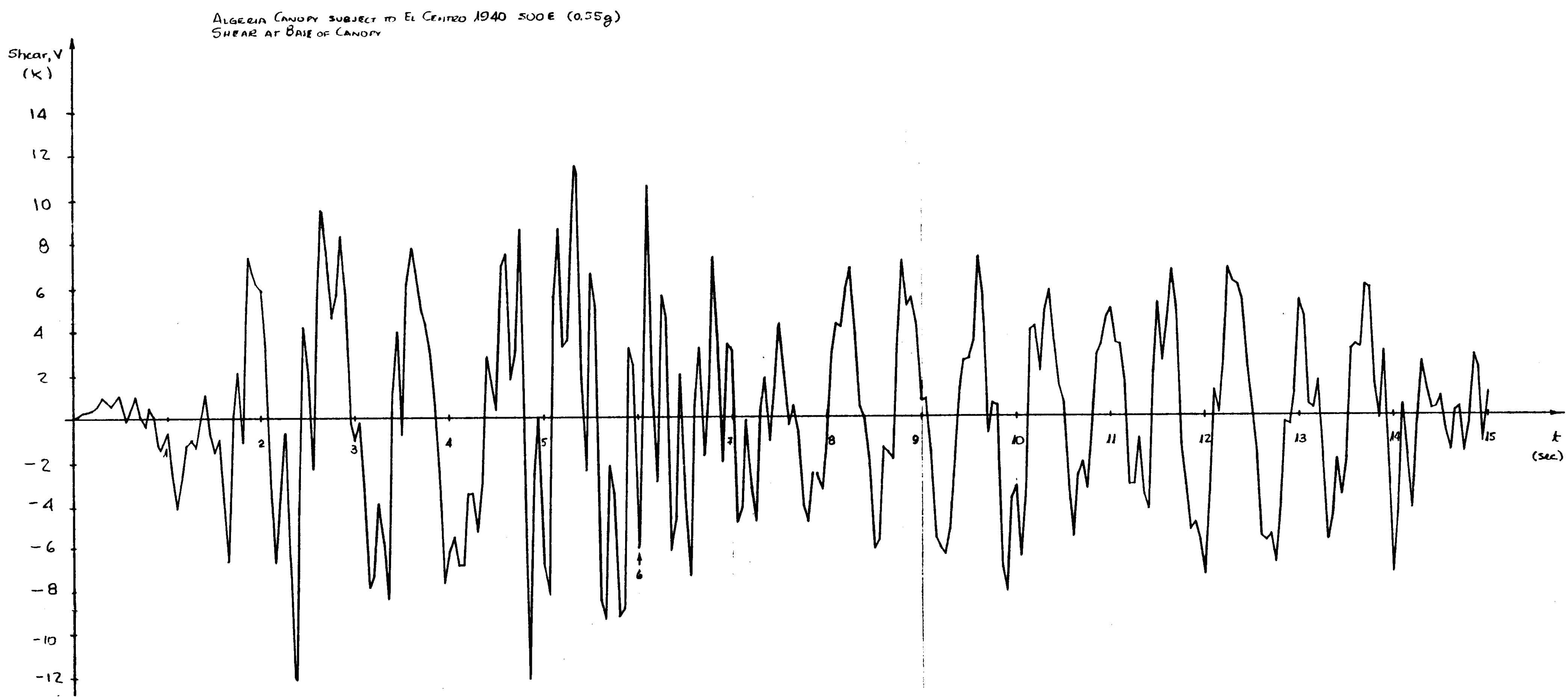

Algeria Canopy subject to El Centro 1940 S00E (0.55g)
Shear at Base of Canopy
Shear, V
(K)
14
12
10
8
6
4
2
-2
-4
-6
-8
-10
-12
1
2
3
4
5
6
7
8
9
10
11
12
13
14
15
t
(sec)

Fig. G. 4A d)

Algeria Canopy subject to El Centro 1940 S00E (0.55g)
Top Nodal Displacement (X-Direction)

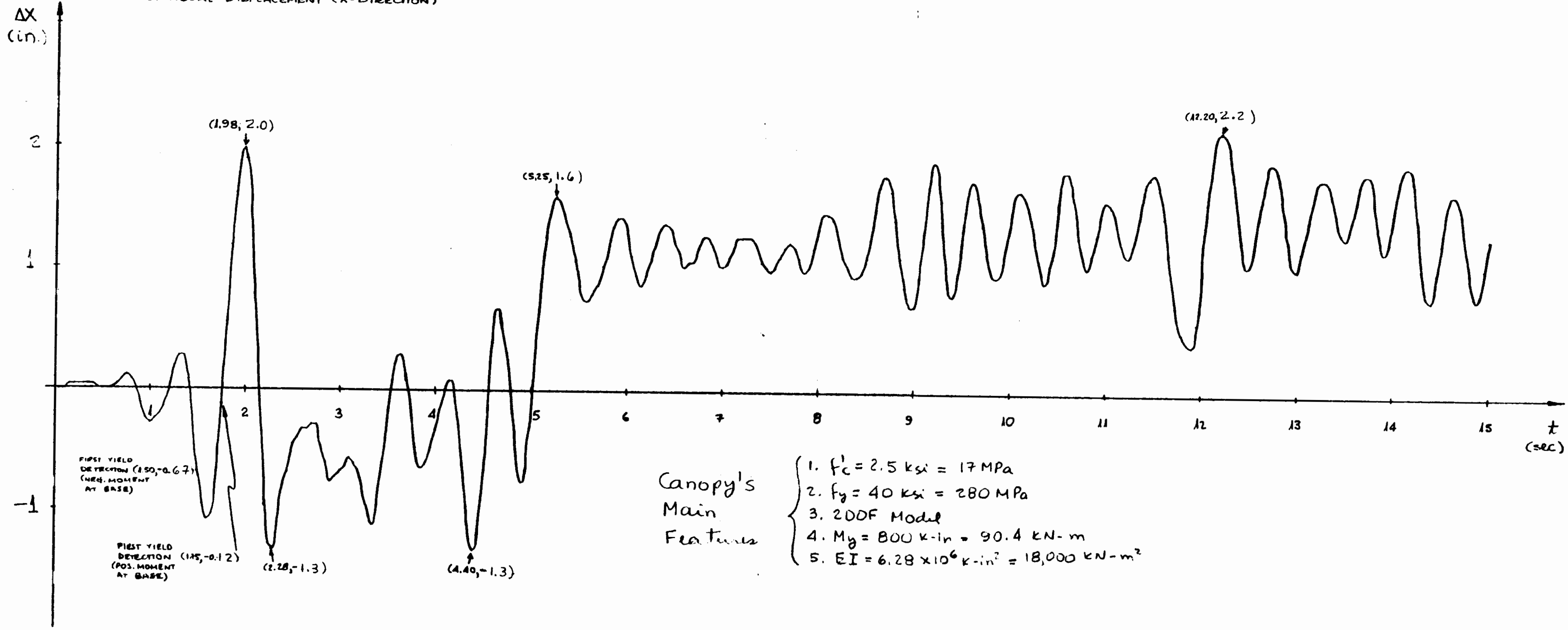

Fig. G.4B a)

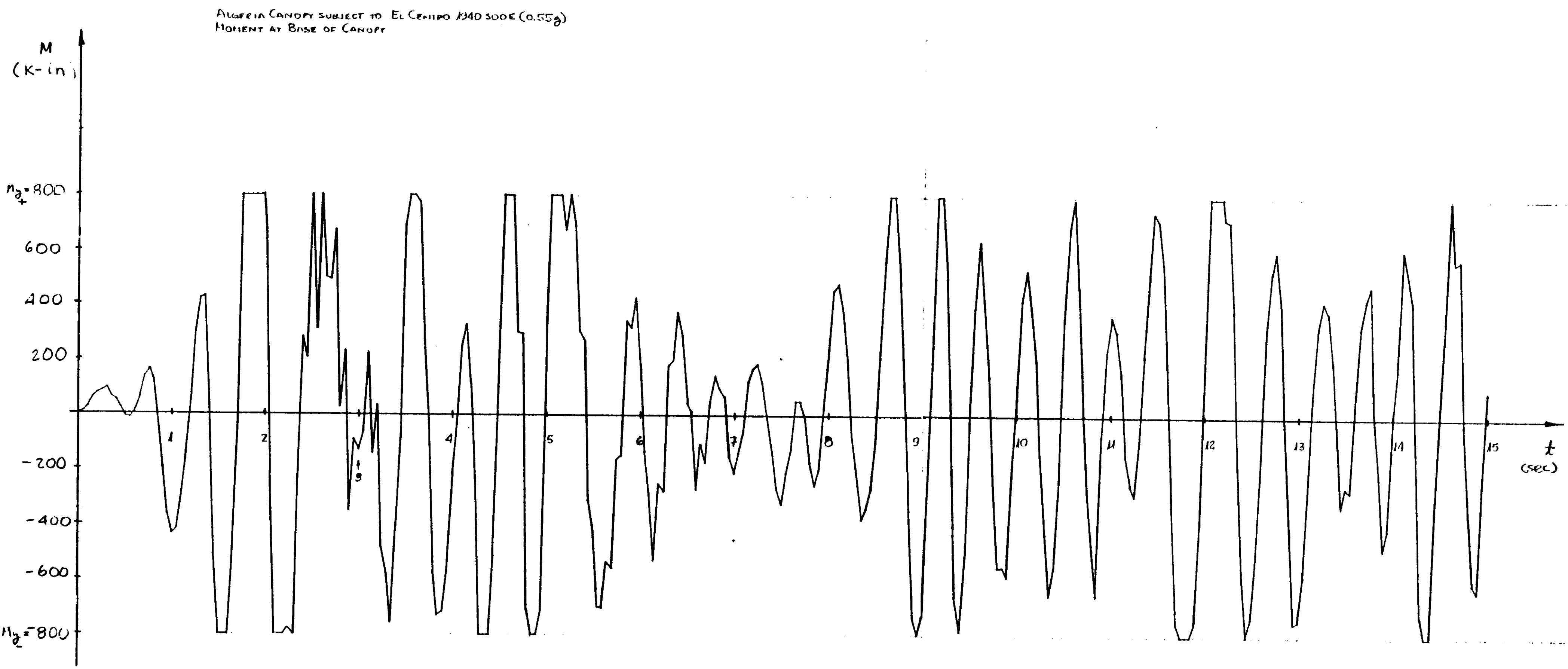
ALGERIA CANOPY SUBJECT TO EL CENTRO 1940 S00E (0.55g)
MOMENT AT BASE OF CANOPY
M
(K-in)
M_{y+}=800
600
400
200
-200
-400
-600
M_{y-}=-800
1
2
4
5
6
7
8
9
10
11
12
13
14
15
t
(sec)

Fig. G.4B b)

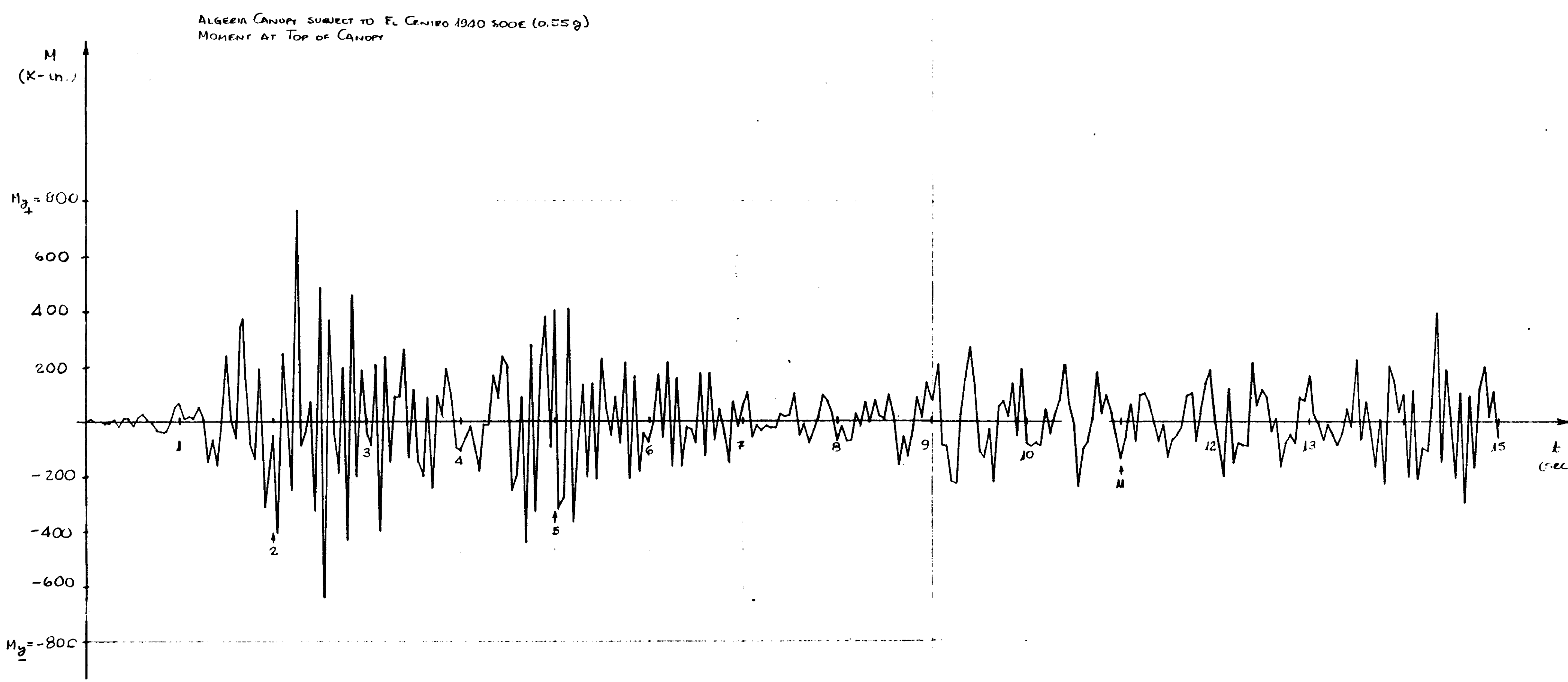

ALGERIA CANOPY SUBJECT TO EL CENTRO 1940 S00E (0.55g)
MOMENT AT TOP OF CANOPY
M
(K-in.)
My+ = 800
600
400
200
-200
-400
-600
My- = -800
1
2
3
4
5
6
7
8
9
10
11
12
13
15
t
(sec)

Fig. G.4B c)

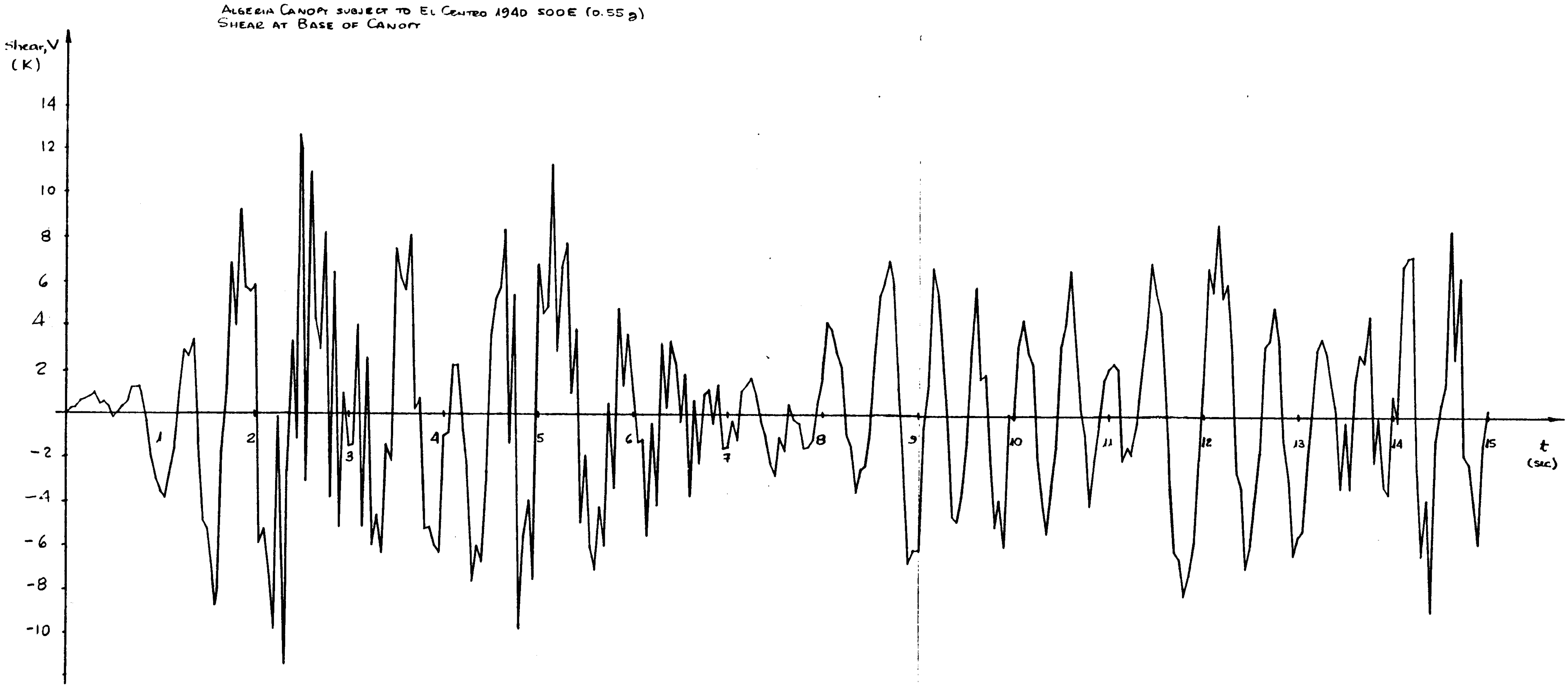
Algeria Canopy subject to El Centro 1940 S00E (0.55 g)
Shear at Base of Canopy
Shear, V
(K)
14
12
10
8
6
4
2
-2
-4
-6
-8
-10
1
2
3
4
5
6
7
8
9
10
11
12
13
14
15
t
(sec)

Fig. G.4B d)

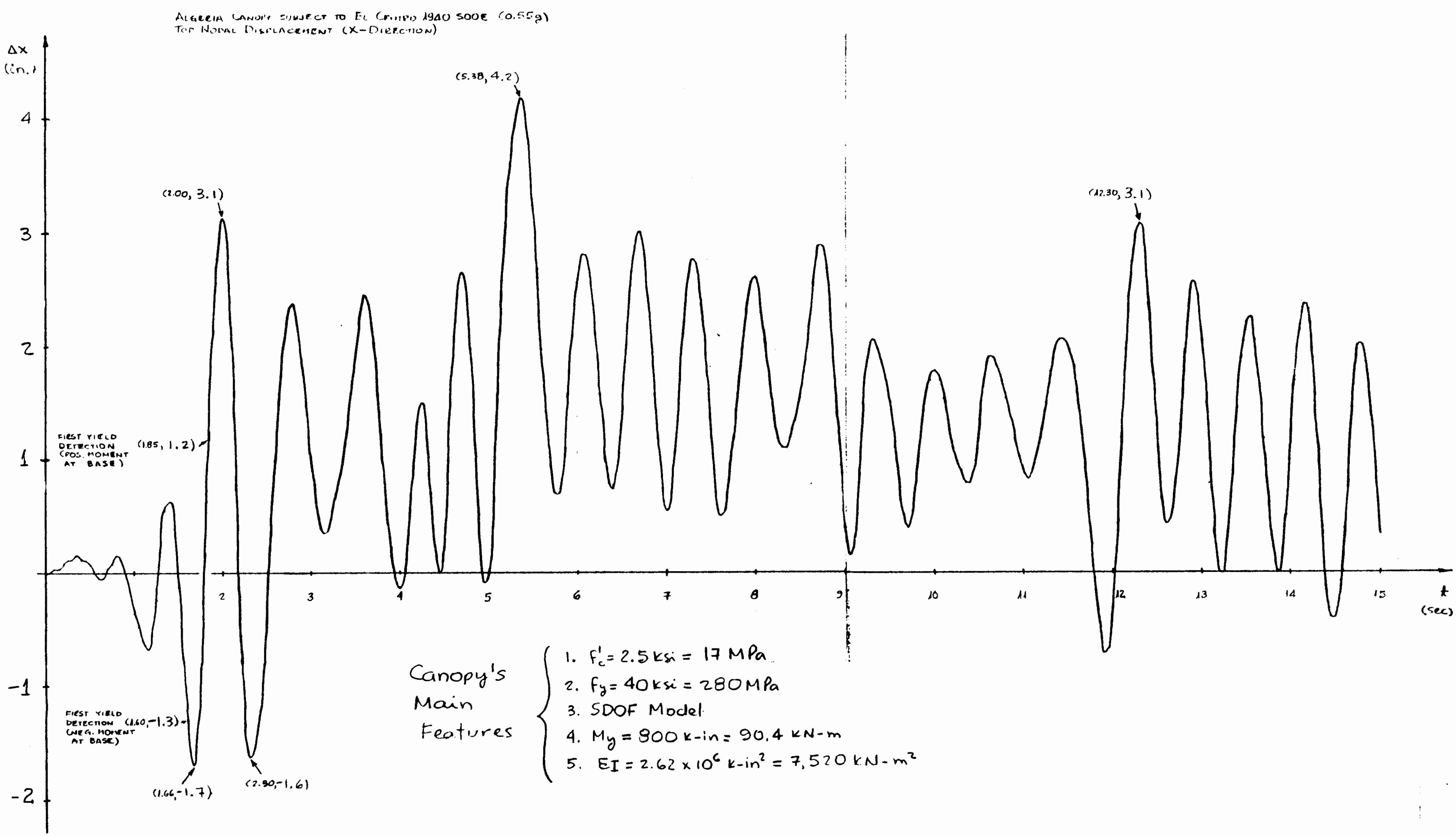
Algeria Canopy subject to El Centro 1940 S00E (0.55g)
Top Nodal Displacement (X-Direction)
Δx (in.)
4
3
2
1
-1
-2
2
3
4
5
6
7
8
9
10
11
12
13
14
15
t (sec)
(2.00, 3.1)
(5.38, 4.2)
(12.30, 3.1)
First yield detection (pos. moment at base)
(1.85, 1.2)
First yield detection (neg. moment at base)
(1.60, -1.3)
(1.66, -1.7)
(2.30, -1.6)
Canopy's Main Features
1. $f'_c = 2.5$ ksi = 17 MPa
2. $f_y = 40$ ksi = 280 MPa
3. SDOF Model
4. $M_y = 800$ k-in = 90.4 kN-m
5. $EI = 2.62 \times 10^6$ k-in^2 = 7,520 kN-m^2

Fig. G.4C a)

Algeria Canopy subject to El Centro 1940 S00E (0.55g)
Moment at Base of Canopy

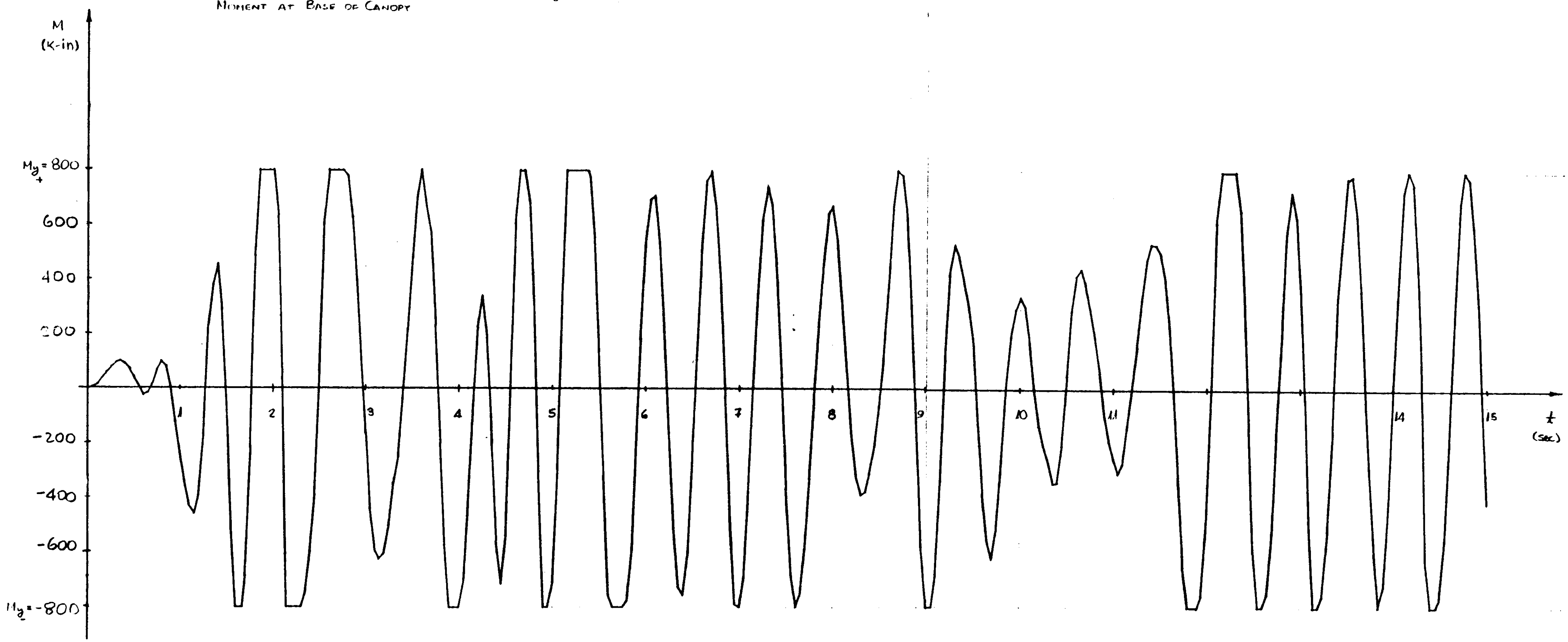

Fig. G.4C b)

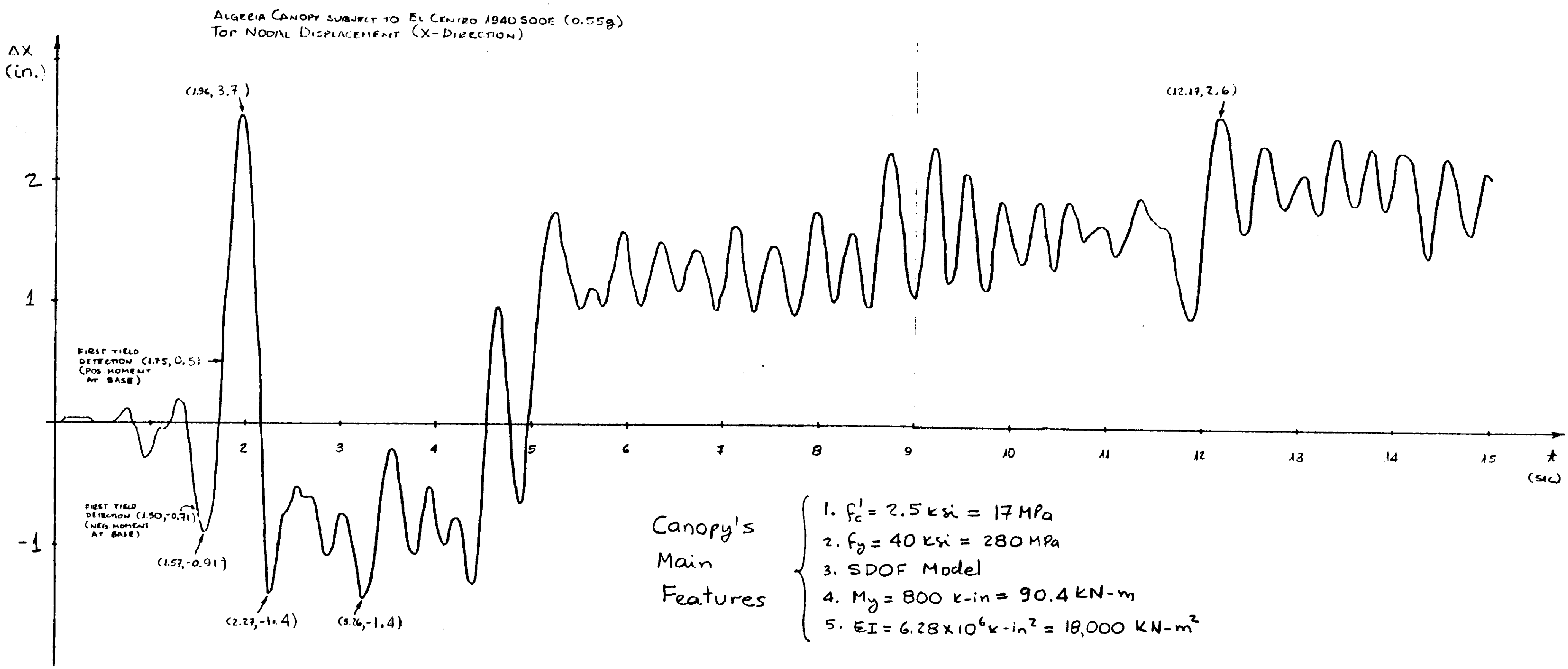

ALGERIA CANOPY SUBJECT TO EL CENTRO 1940 S00E (0.55g)
TOP NODAL DISPLACEMENT (X-DIRECTION)
ΔX (in.)
2
1
-1
(1.96, 3.7)
(12.17, 2.6)
FIRST YIELD DETECTION (1.75, 0.51) (POS. MOMENT AT BASE)
FIRST YIELD DETECTION (1.50, -0.71) (NEG. MOMENT AT BASE)
(1.57, -0.91)
(2.27, -1.4)
(3.26, -1.4)
2
3
4
5
6
7
8
9
10
11
12
13
14
15
t (sec)
Canopy's Main Features
1. f'c = 2.5 ksi = 17 MPa
2. fy = 40 ksi = 280 MPa
3. SDOF Model
4. My = 800 k-in = 90.4 KN-m
5. EI = 6.28x10^6 k-in^2 = 18,000 KN-m^2

Fig. G.4D a)

Algeria Canopy subject to El Centro 1940 S00E (0.55g)
Moment at Base of Canopy

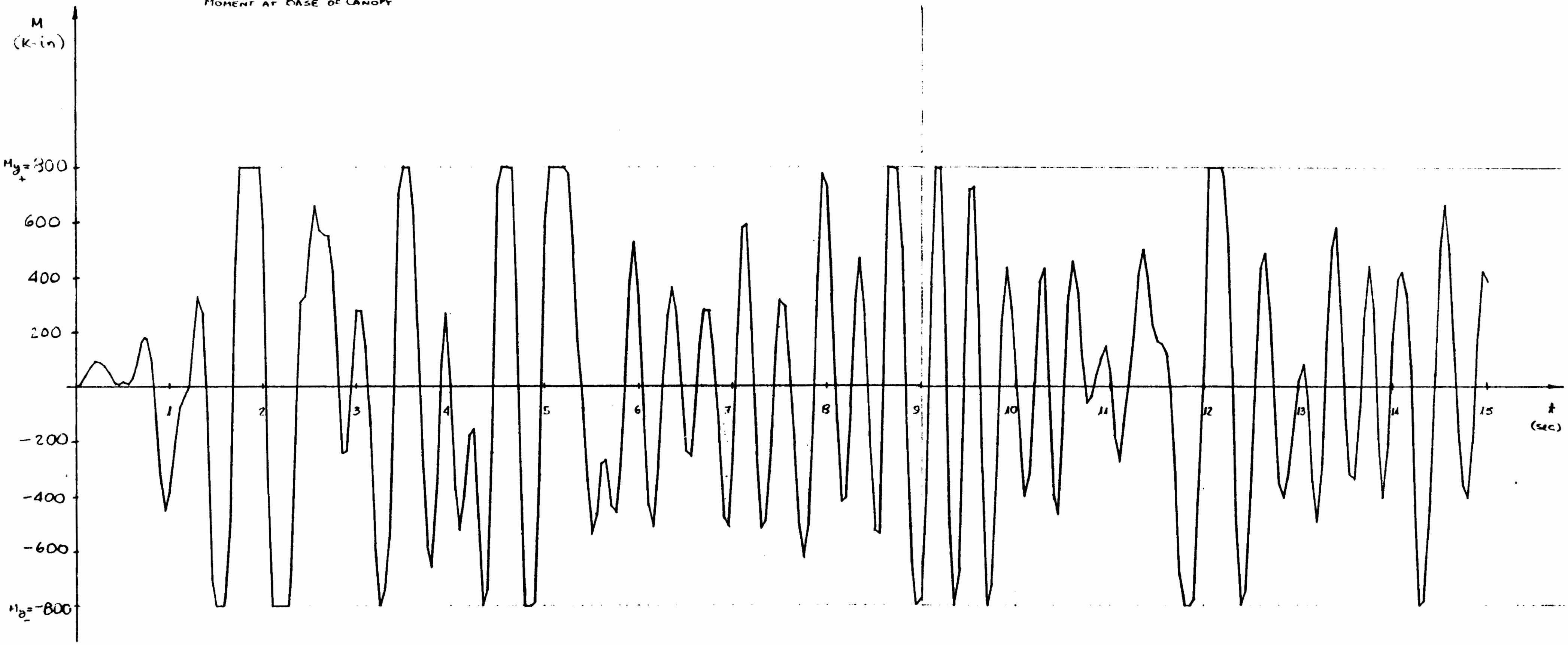

Fig. G.4D b)

APPENDIX H

DRAIN-2D RESULTS REGARDING THE THIRD STAGE (THE "CLIPPING METHOD")

This appendix presents the time-history inelastic response of the canopy for the different cases considered in the third stage of the analysis. For each of the cases, the following response plots are given:

a) time vs. lateral displacement

b) time vs. rotation

c) time vs. bottom moment

d) time vs. top moment

e) time vs. bottom shear

The sign convention is as given in Fig. 6.6.

In summary, the cases considered were:

Inelastic Response of Canopy when subjected to					
El Centro Normalized to 0.55g		Derived Pacoima Dam Normalized to 0.35g		El Centro Unnormalized (PGA = 0.3485g)	
$EI = 1843\ t/m^2$ Uncracked	$EI = 769\ t/m^2$ Cracked	$EI = 1843\ t/m^2$ Uncracked	$EI = 769\ t/m^2$ Cracked	$EI = 1843\ t/m^2$ Uncracked	$EI = 769\ t/m^2$ Cracked
CASES 1	CASES 2	CASES 3	CASES 4	CASES 5	CASES 6

Furthermore, for each of the cases 1 to 6 described above, different inelastic computer runs were made with different amounts of clipping.

For each of the time-displacement figures, the first yielding in the positive and negative directions are indicated (YP and YN, respectively).

CASES 1 : INELASTIC RESPONSE OF 2DOF CANOPY MODEL TO EL CENTRO NORMALIZED TO PGA = 0.55g

$EI = 6.28 \times 10^6$ k-in^2

$T_1 = 0.46$ sec ; $T_2 = 0.11$ sec

$M_y = 800^{\text{k-in}}$

CASE	PEAK CLIPPED ACCELERATION	Figure
1A	0.55g (unclipped)	H.1A
1B	0.36g	H.1B
1C	0.32g	H.1C
1D	0.28g	H.1D
1E	0.22g	H.1E

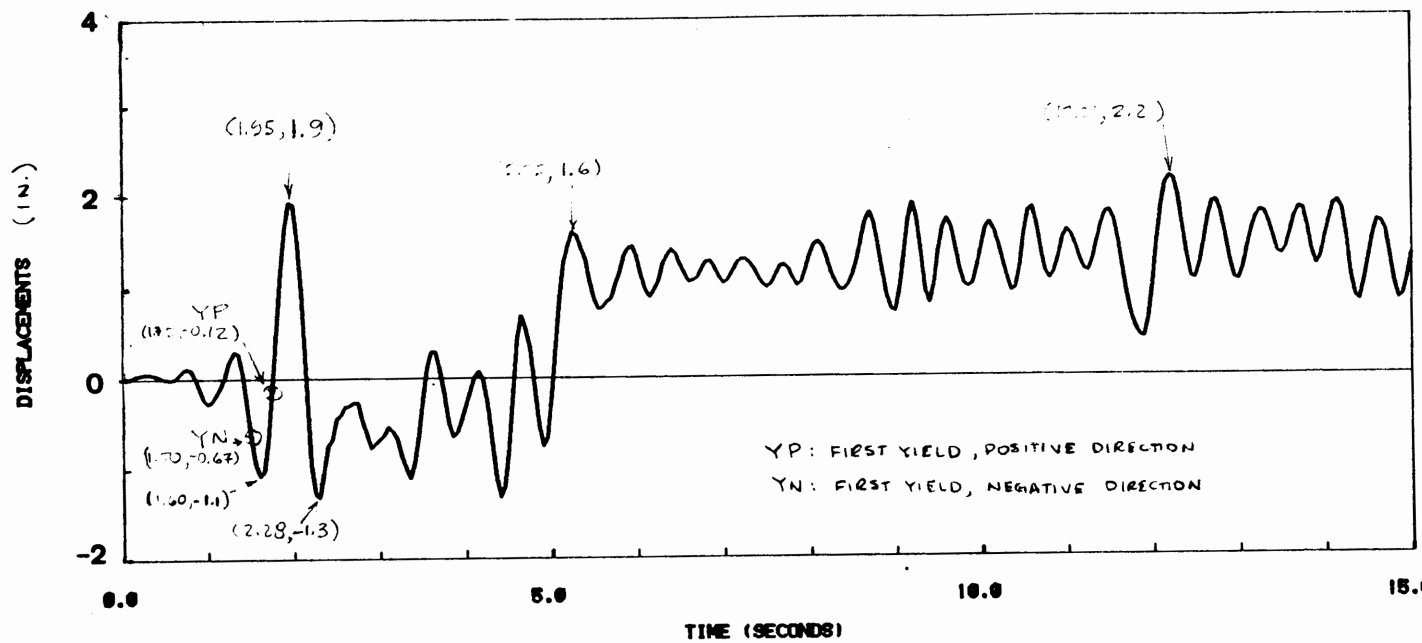

Fig. H.1A a)

CASE 1A

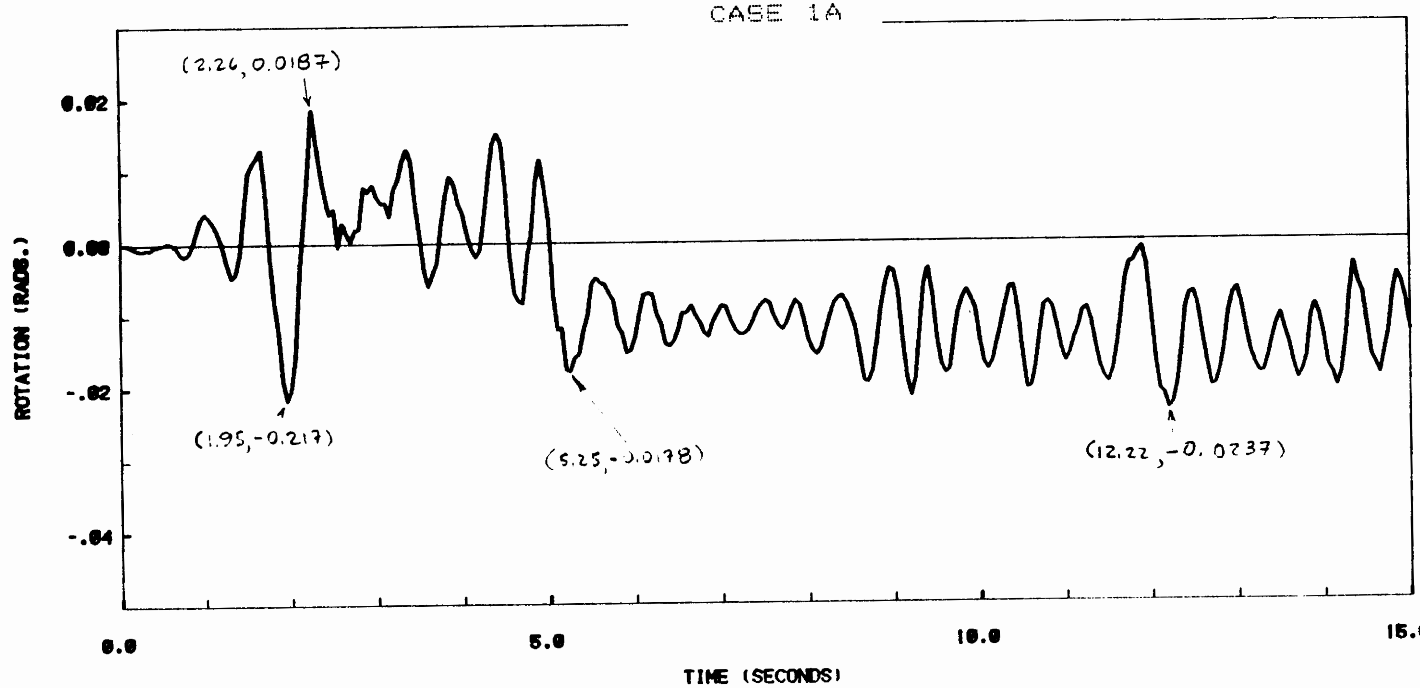

Fig. H.1A b)

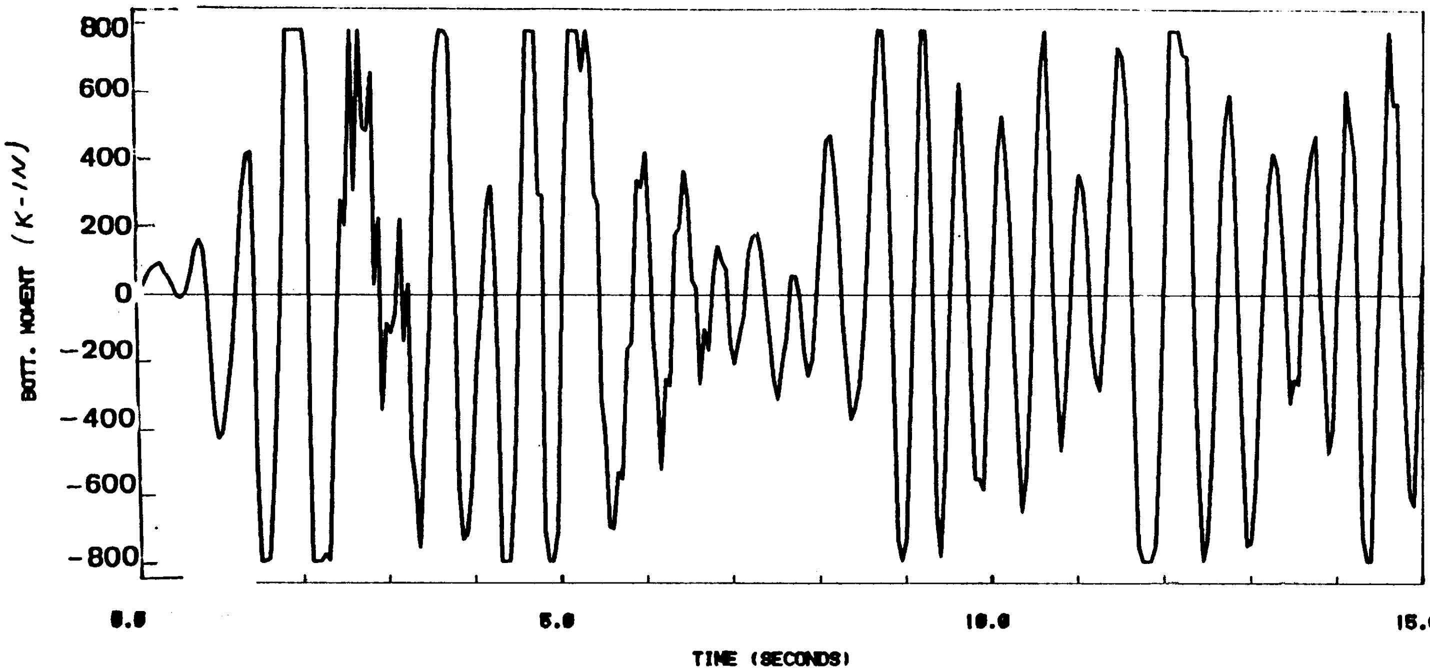

Fig. H.1A c)

CASE 1A

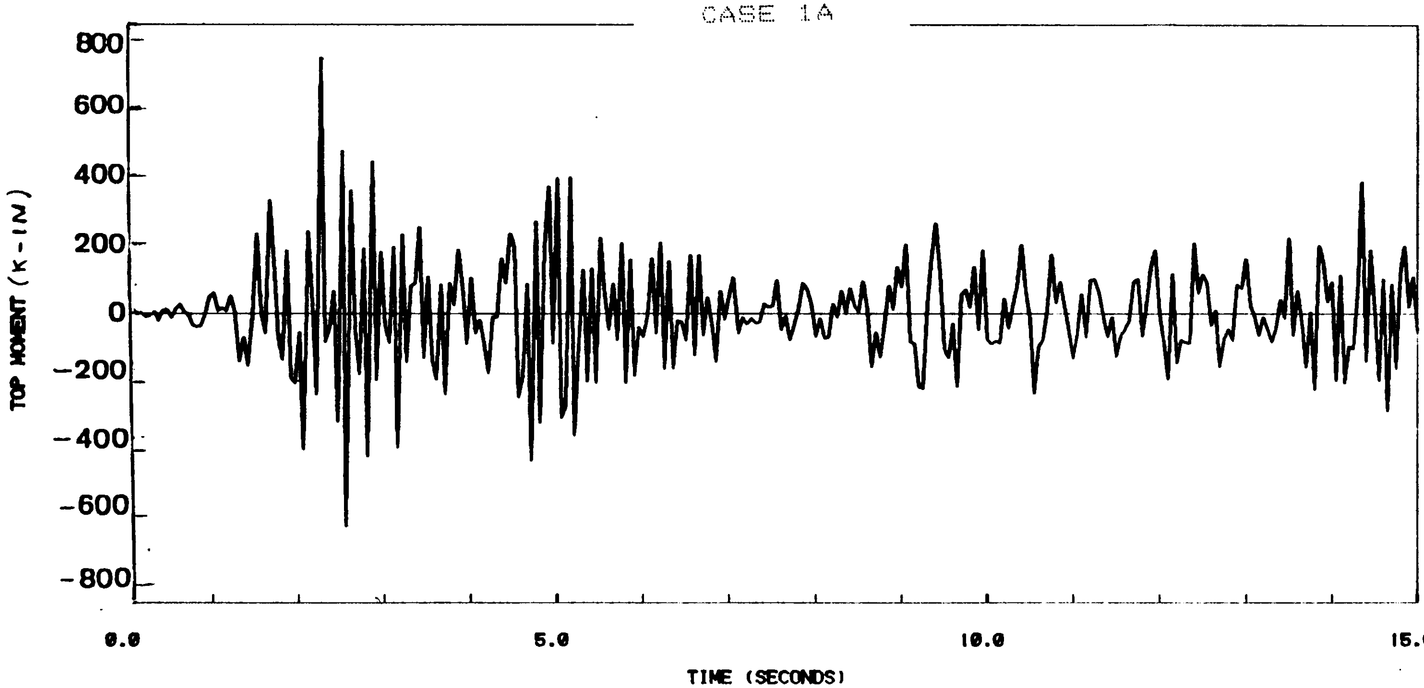

Fig. H.1A. d)

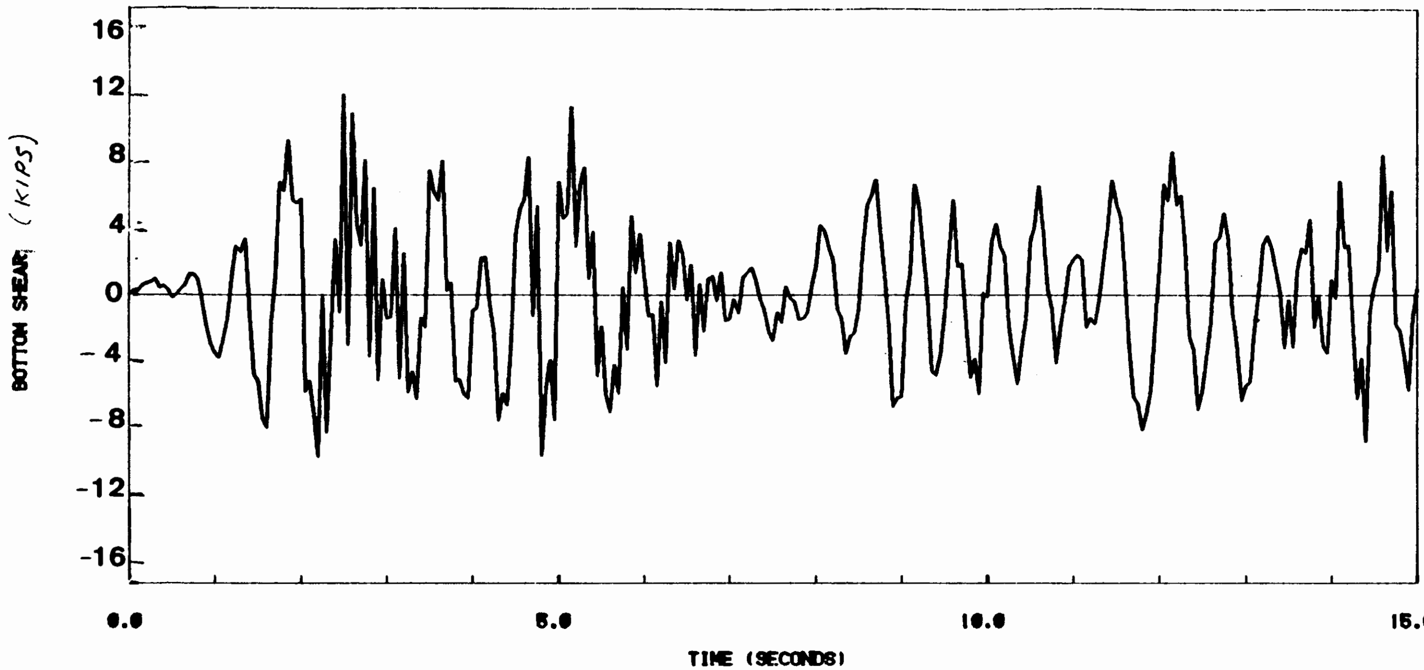

CASE 1A

Fig. H.1A e)

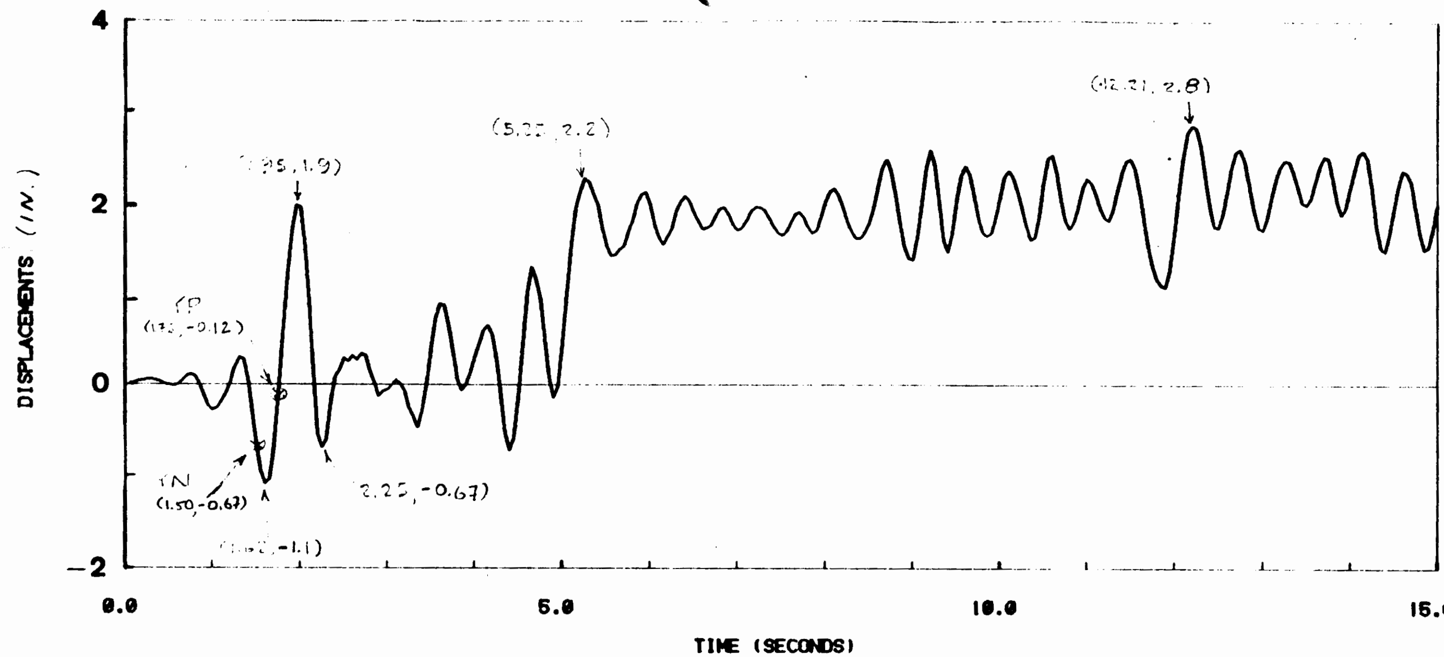

Fig. H.1B. a)

CASE 1B

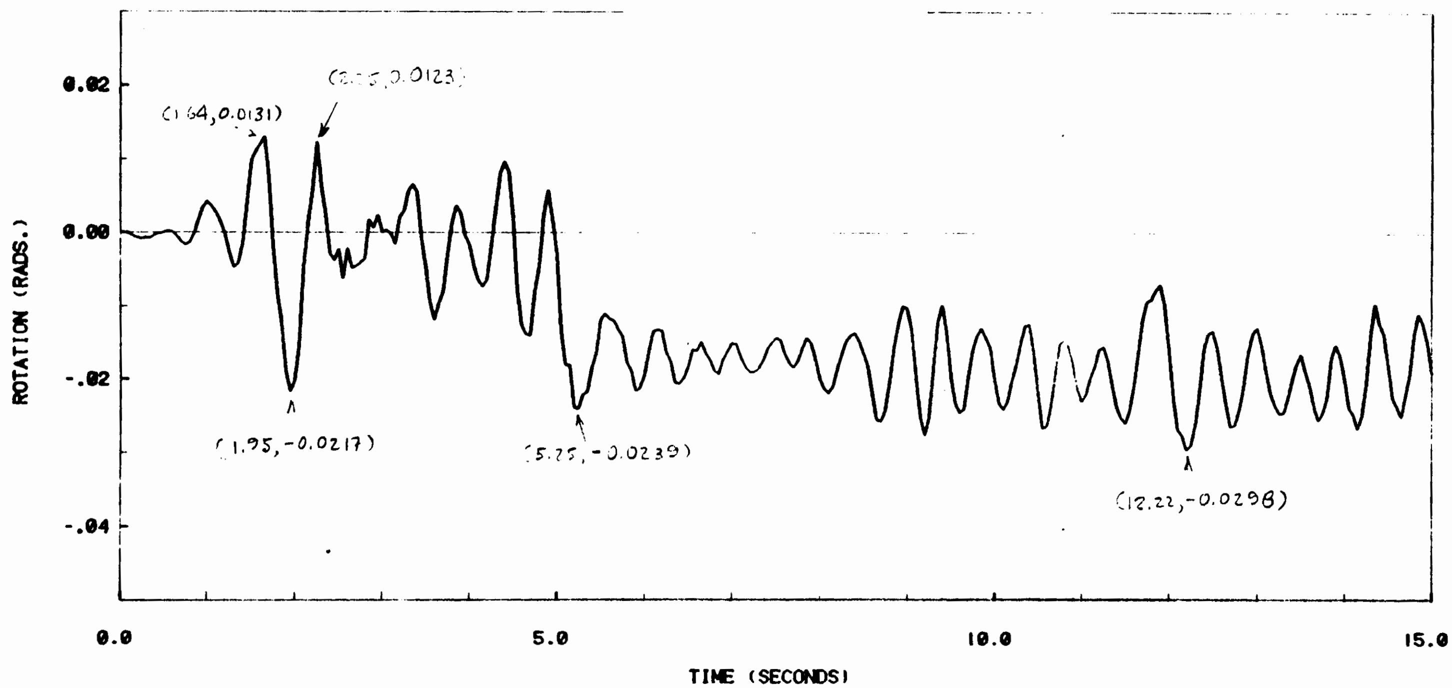

Fig. H.1B b)

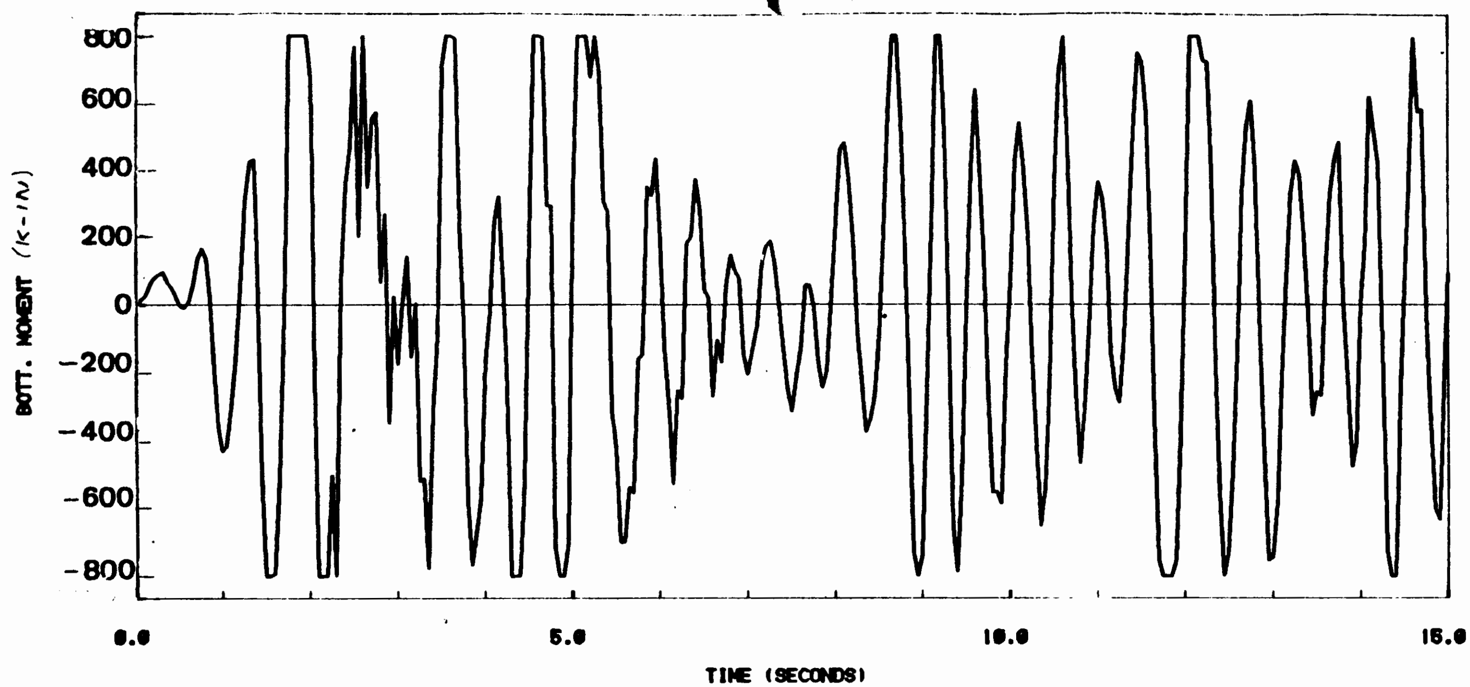

Fig. H.1B c)

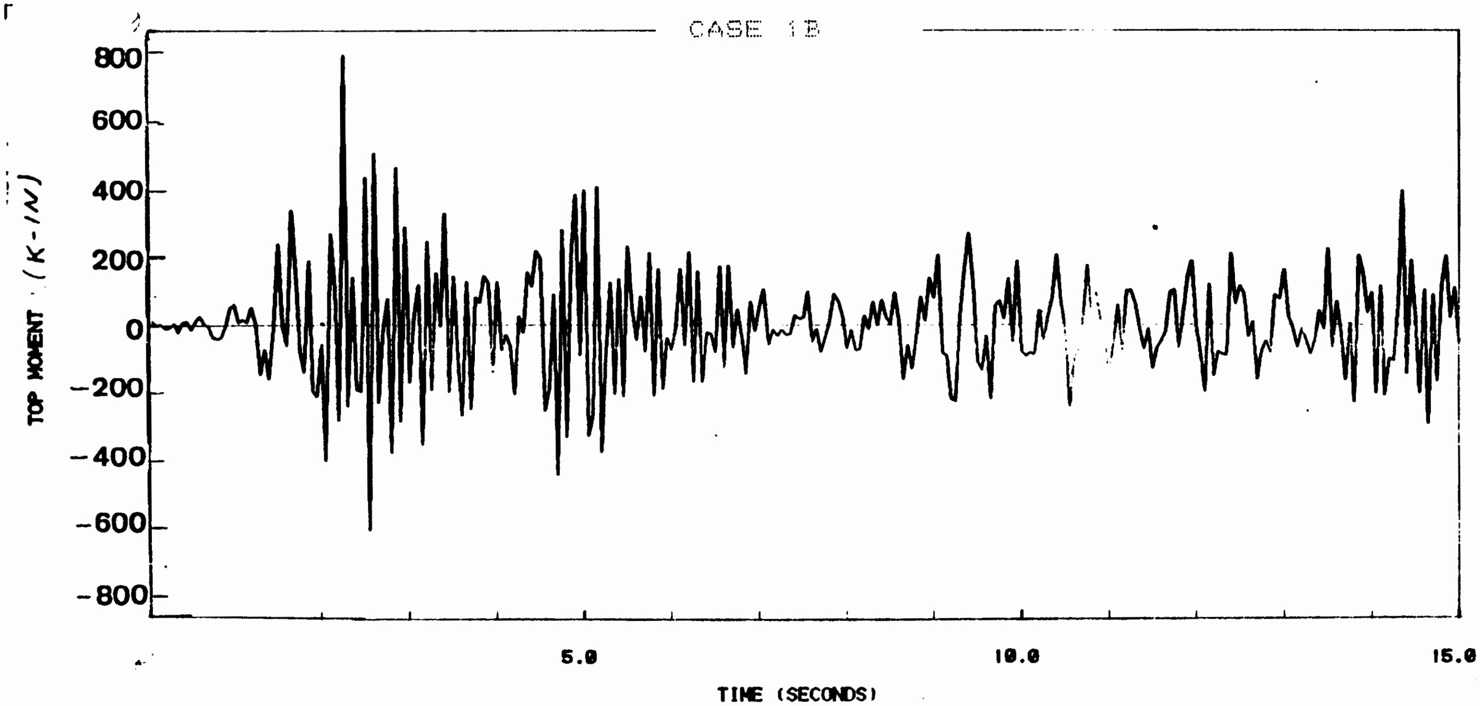

Fig. H.1B d)

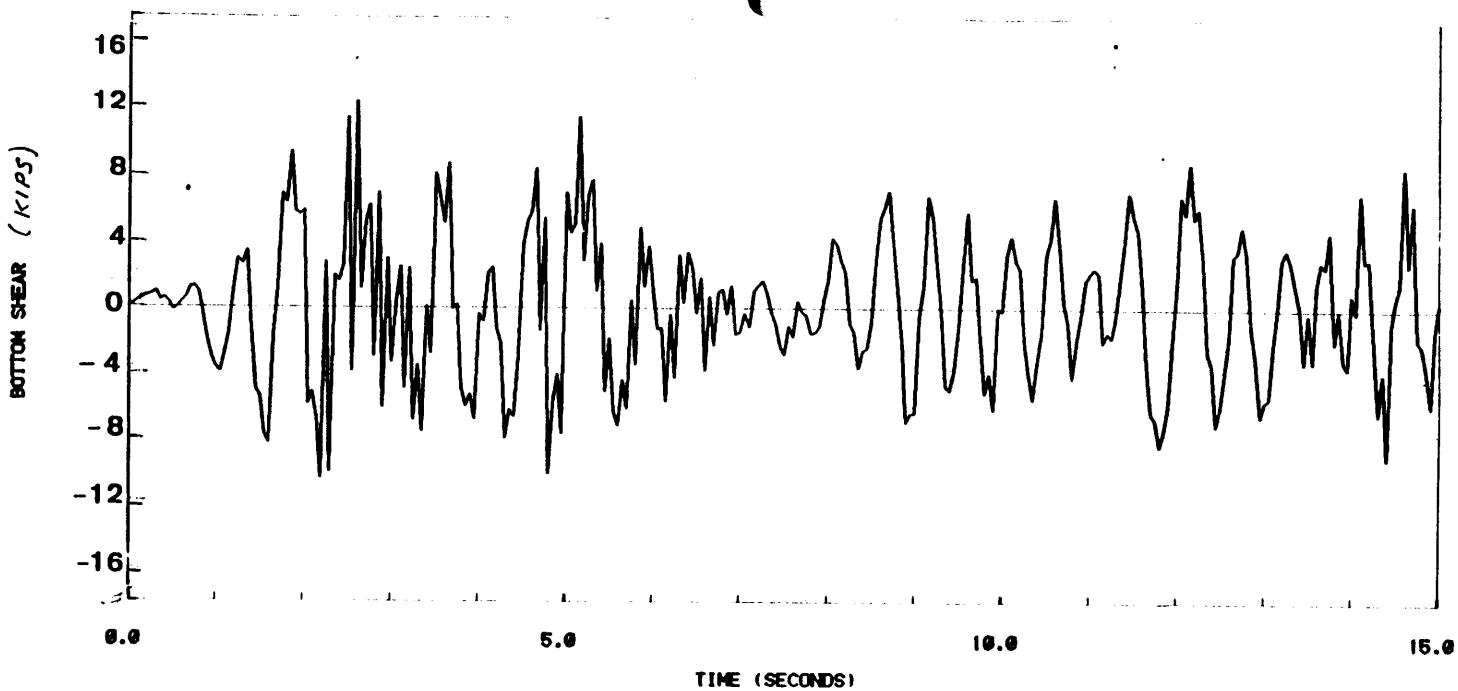

CASE 1B

Fig. H.1B e)

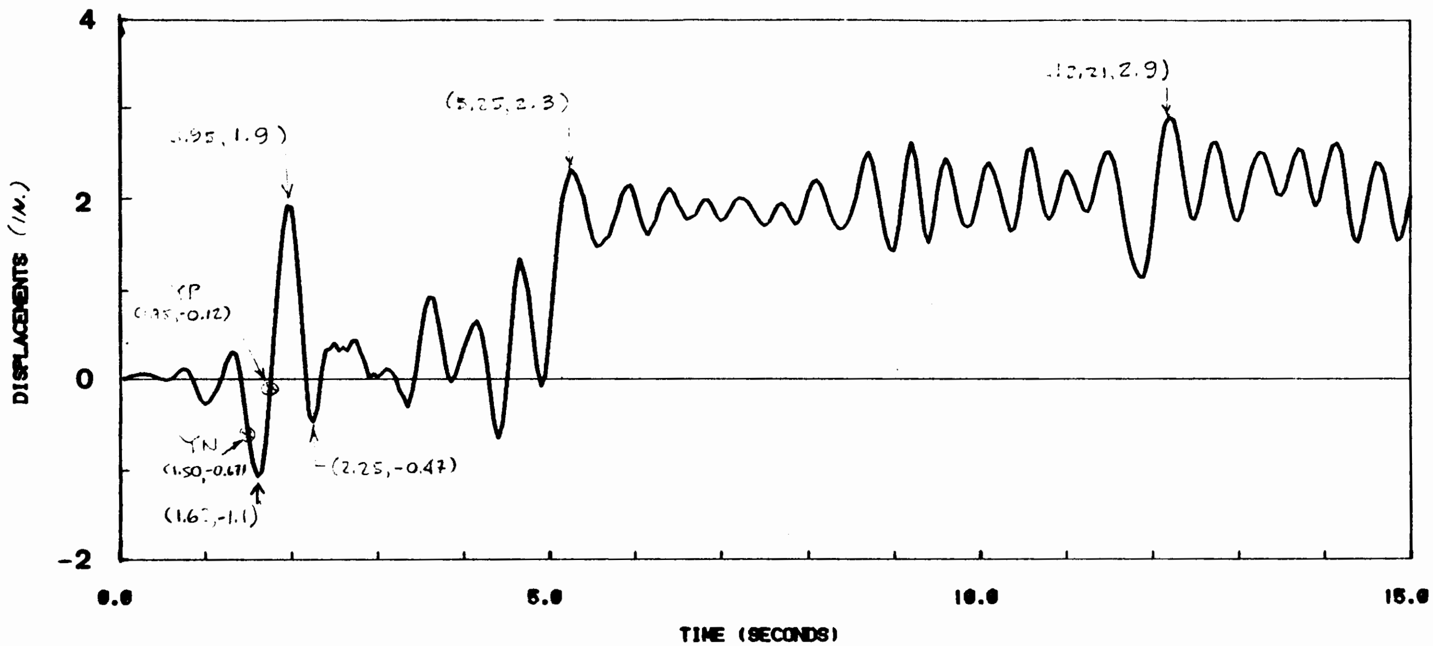

Fig. H.1C a)

CASE 1C

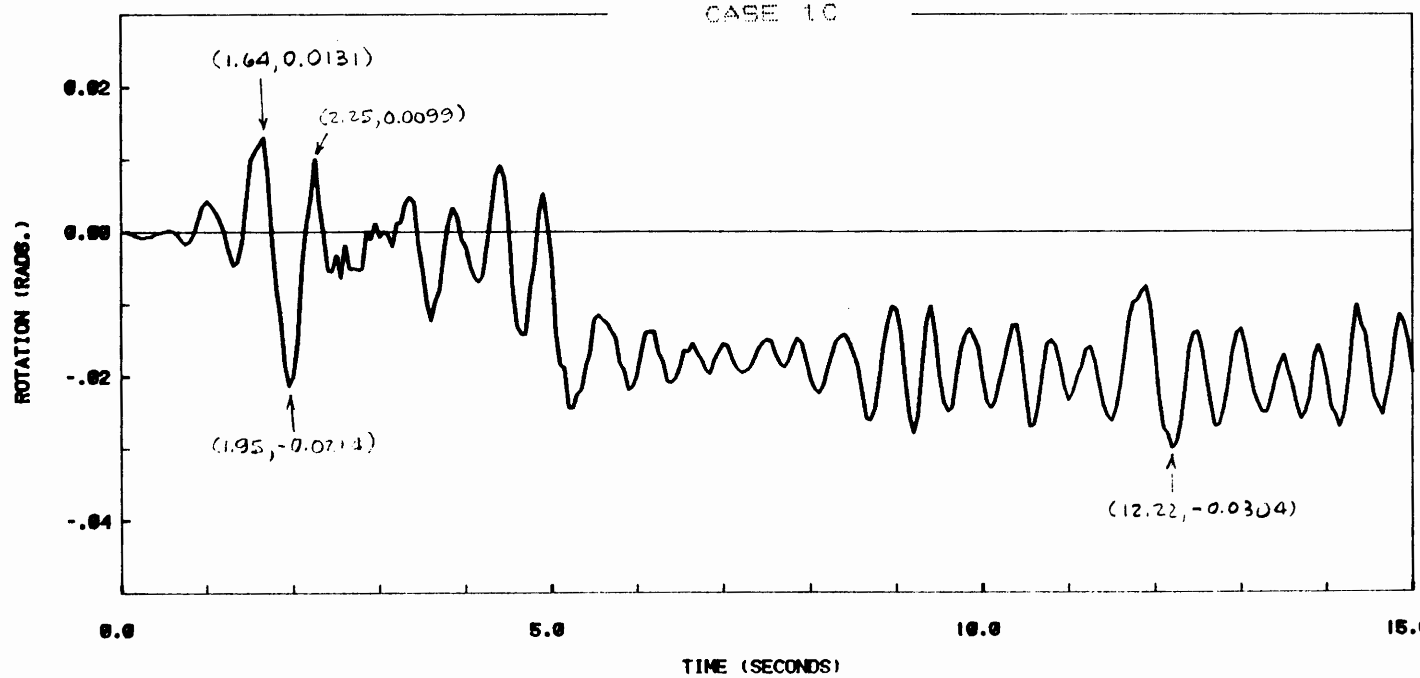

Fig. H.1C b)

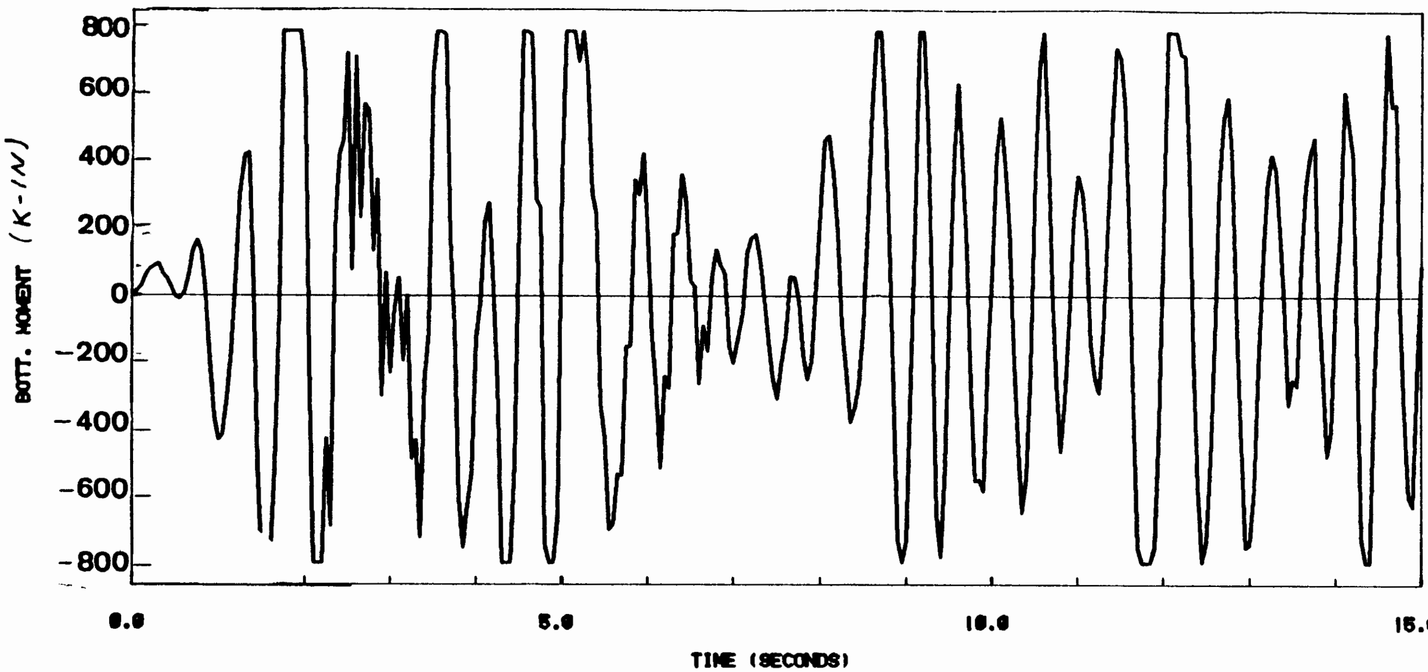

Fig. H.1C c)

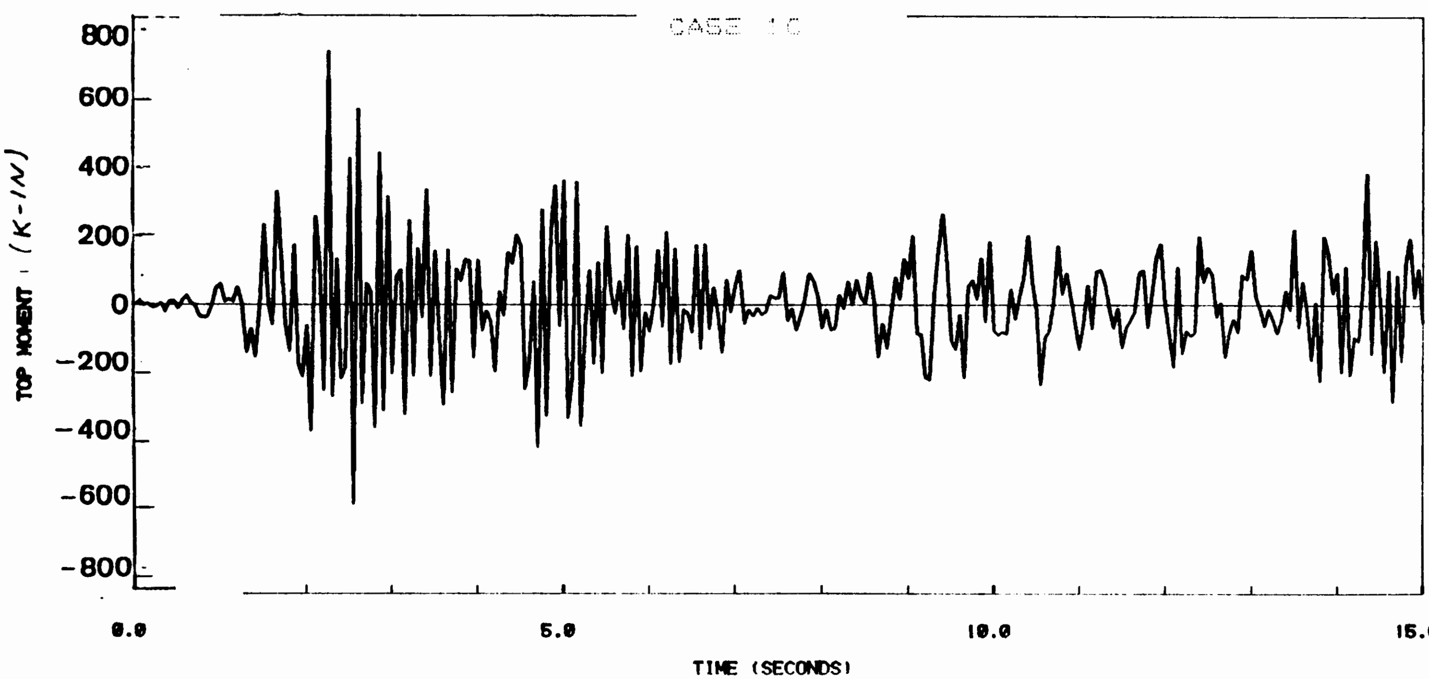

Fig. H.1C d)

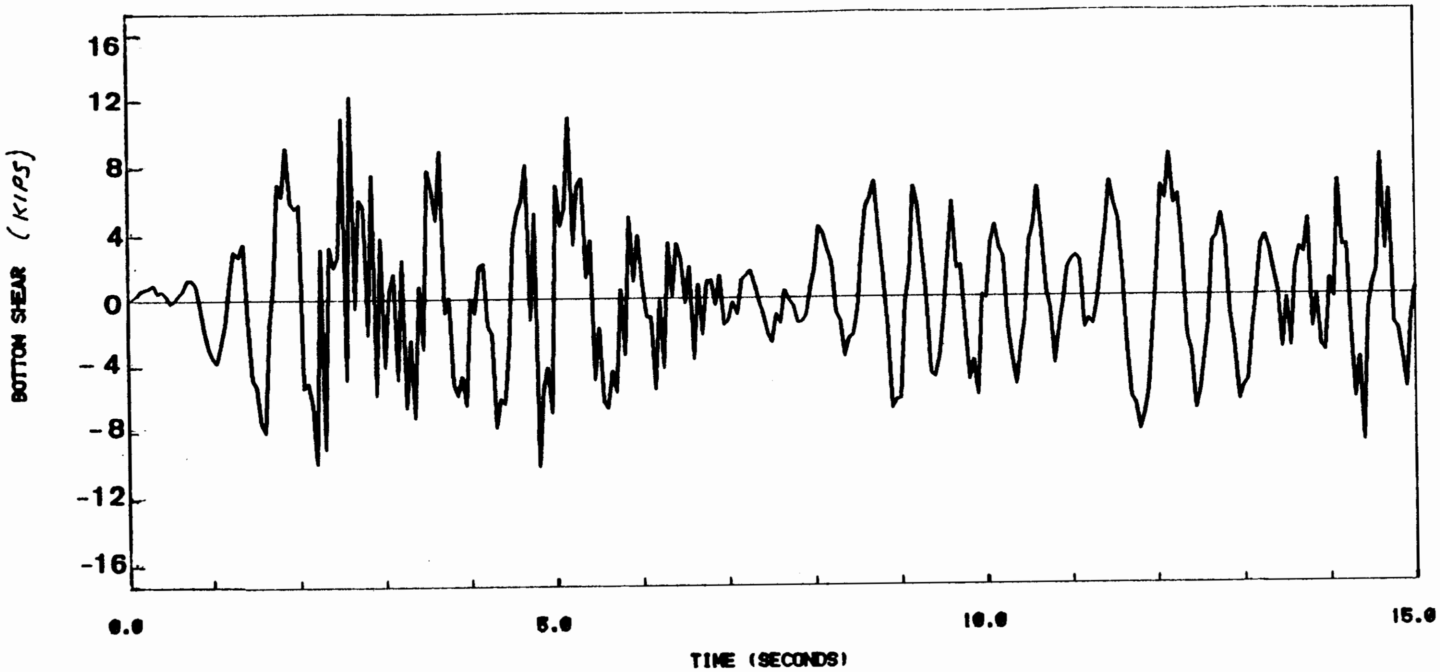

CASE 1C

Fig. H.1C e)

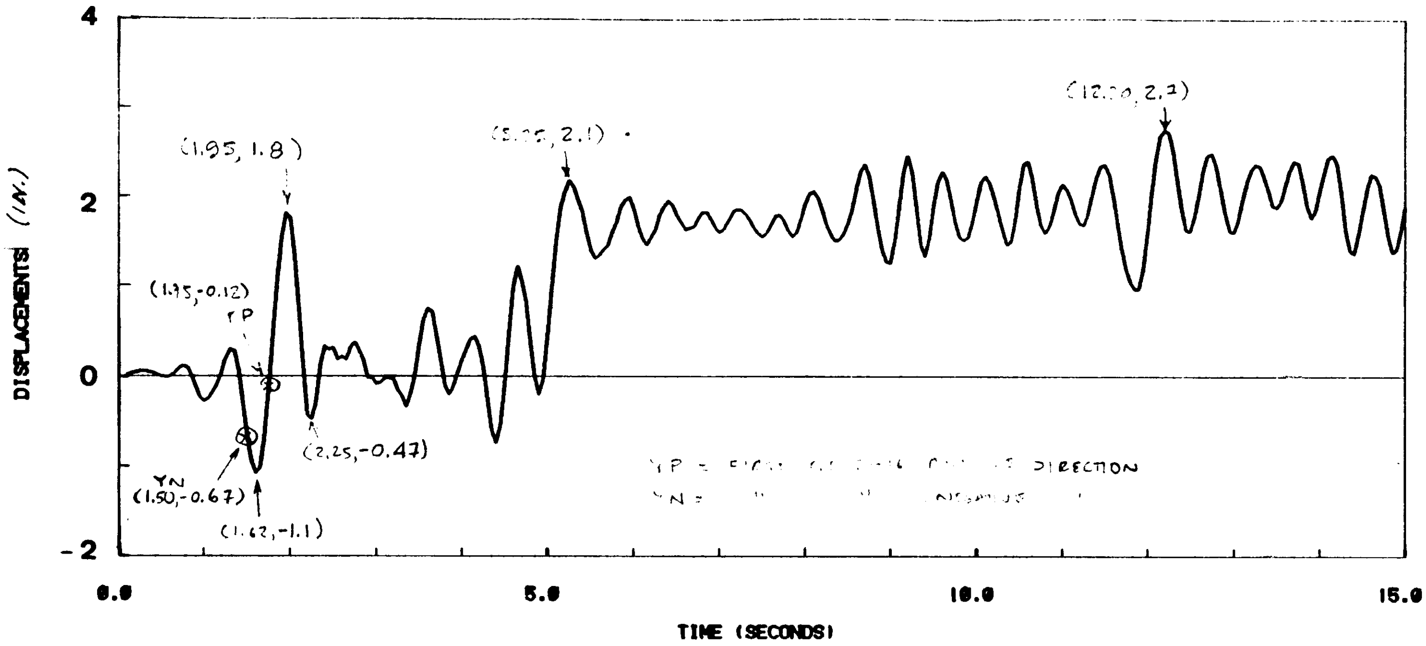

Fig. H. 1D a)

CASE 1D

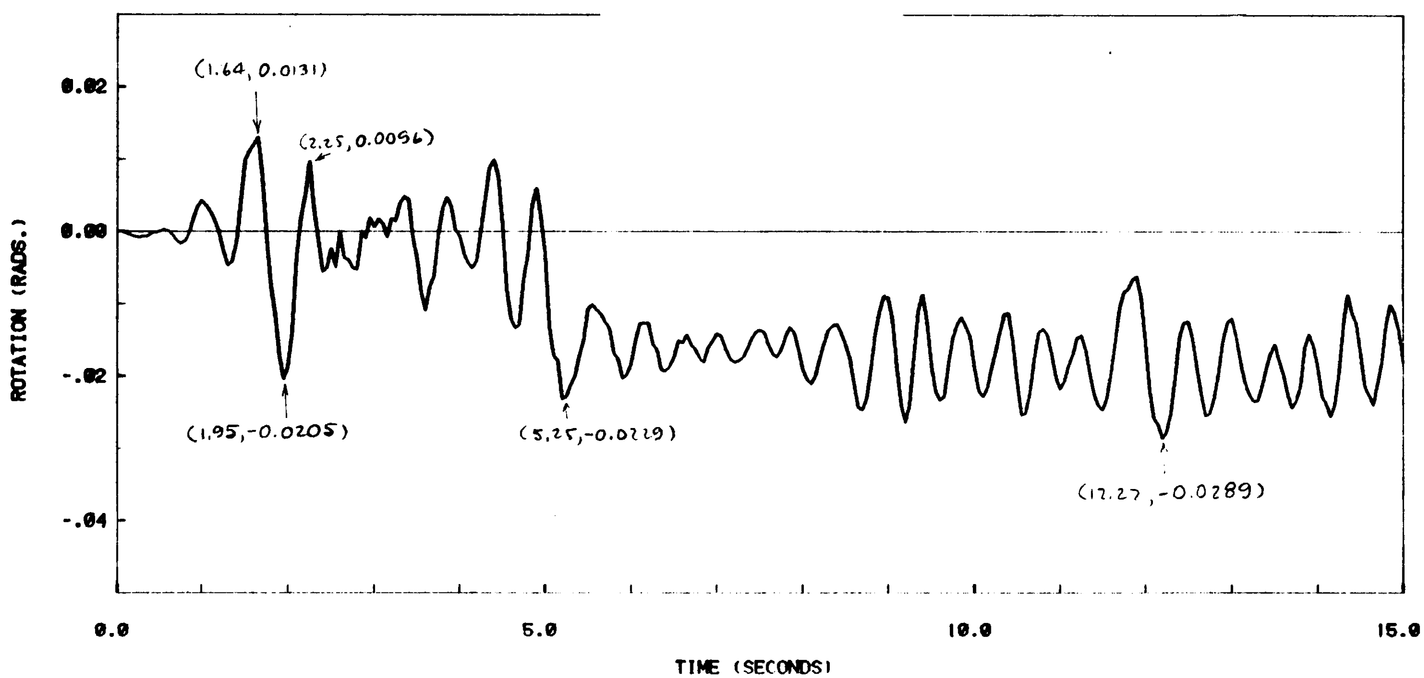

Fig. H. 1D b)

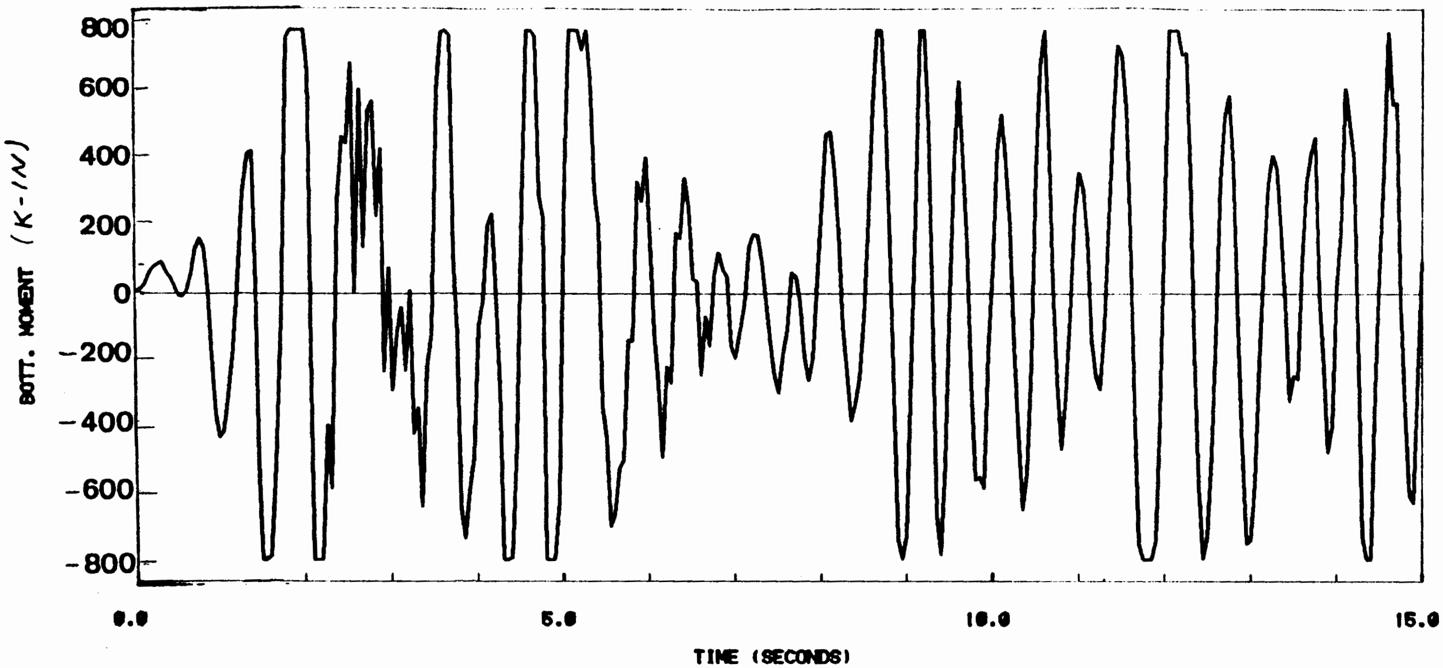

Fig. H.1D c)

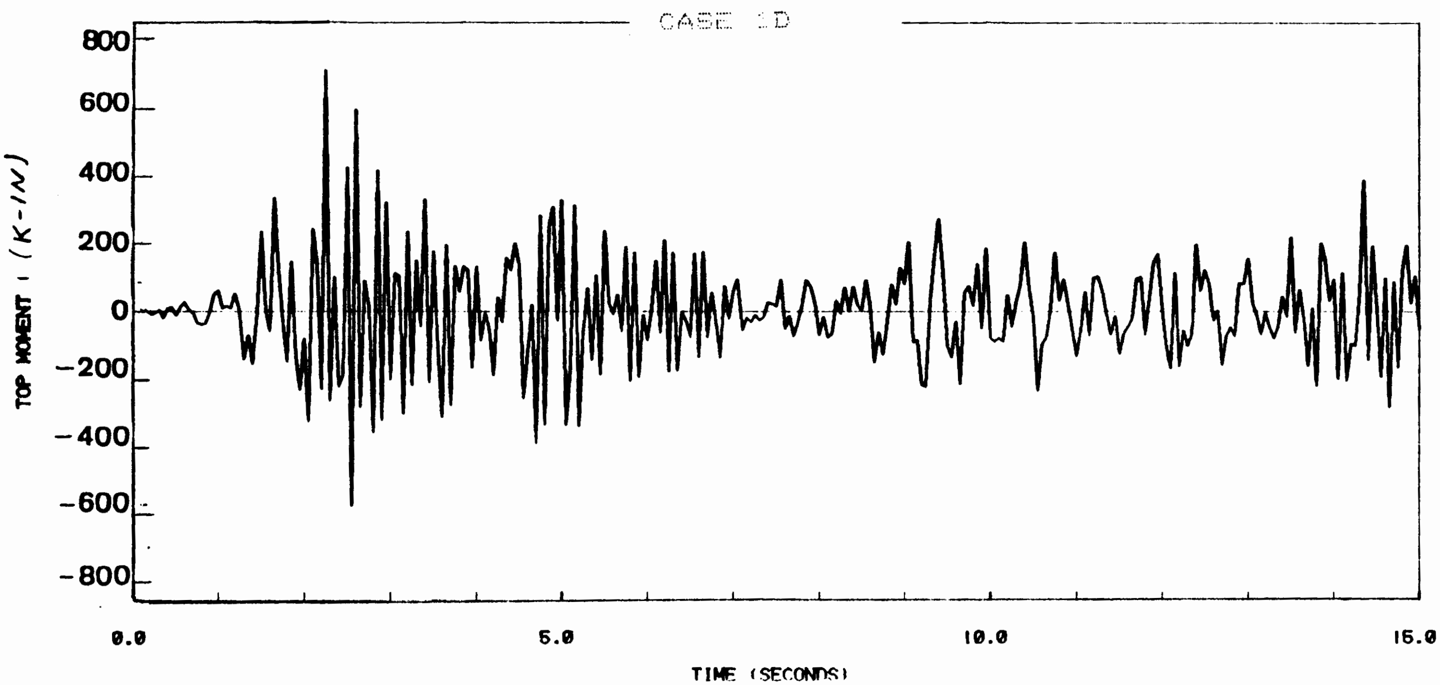

Fig. H.1D d)

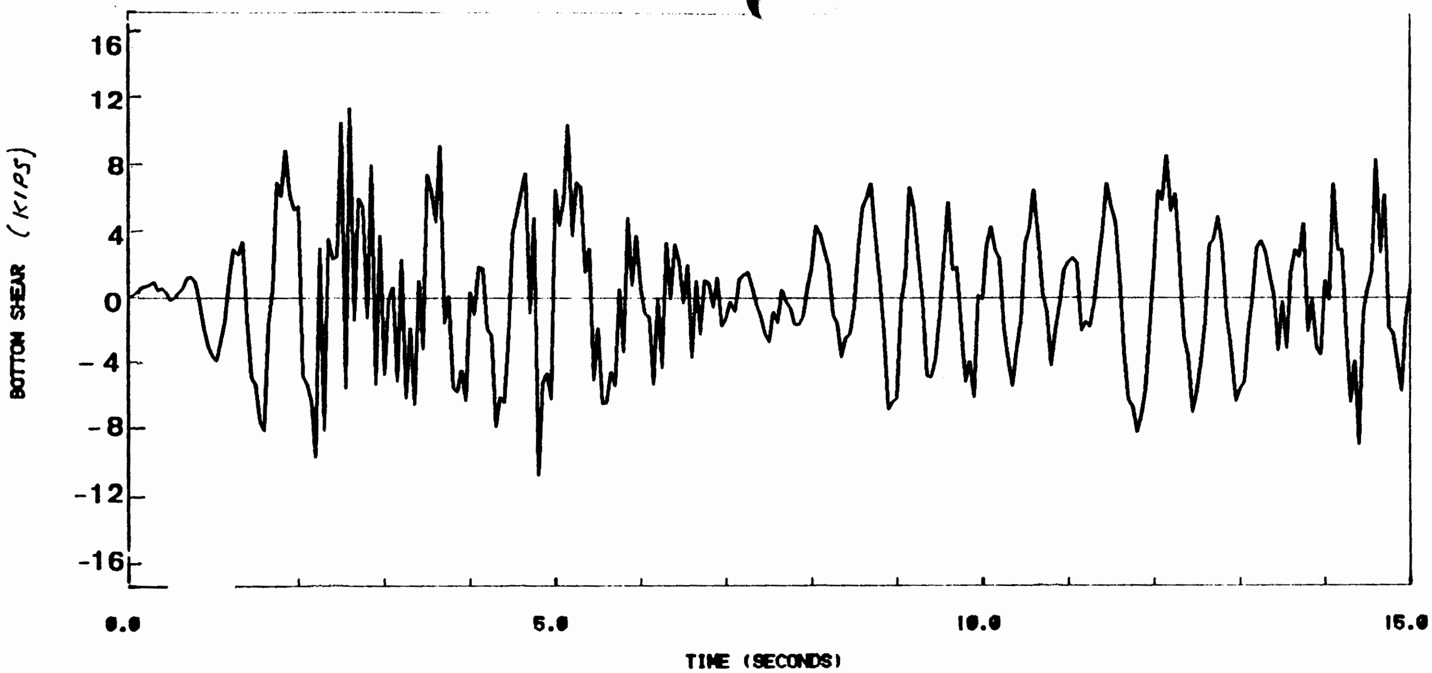

CASE 1D

Fig. H. 1D e)

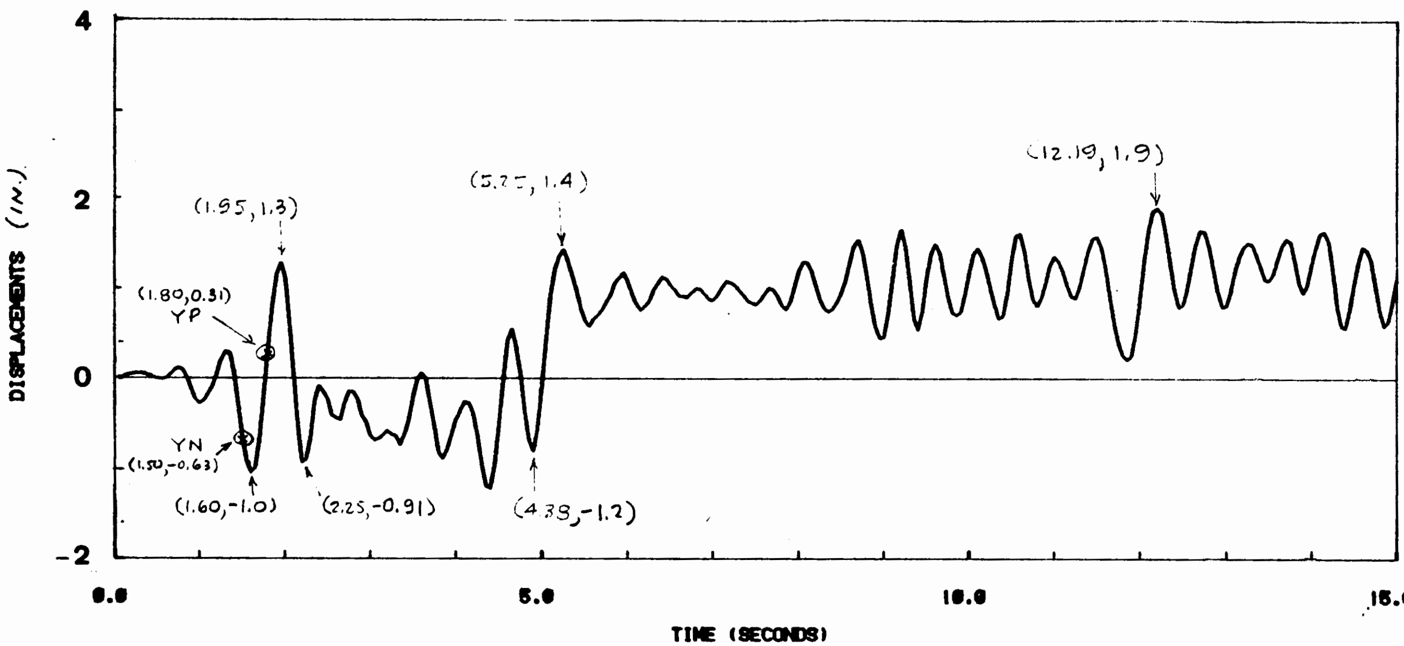

Fig. H.1E a)

CASE 1E

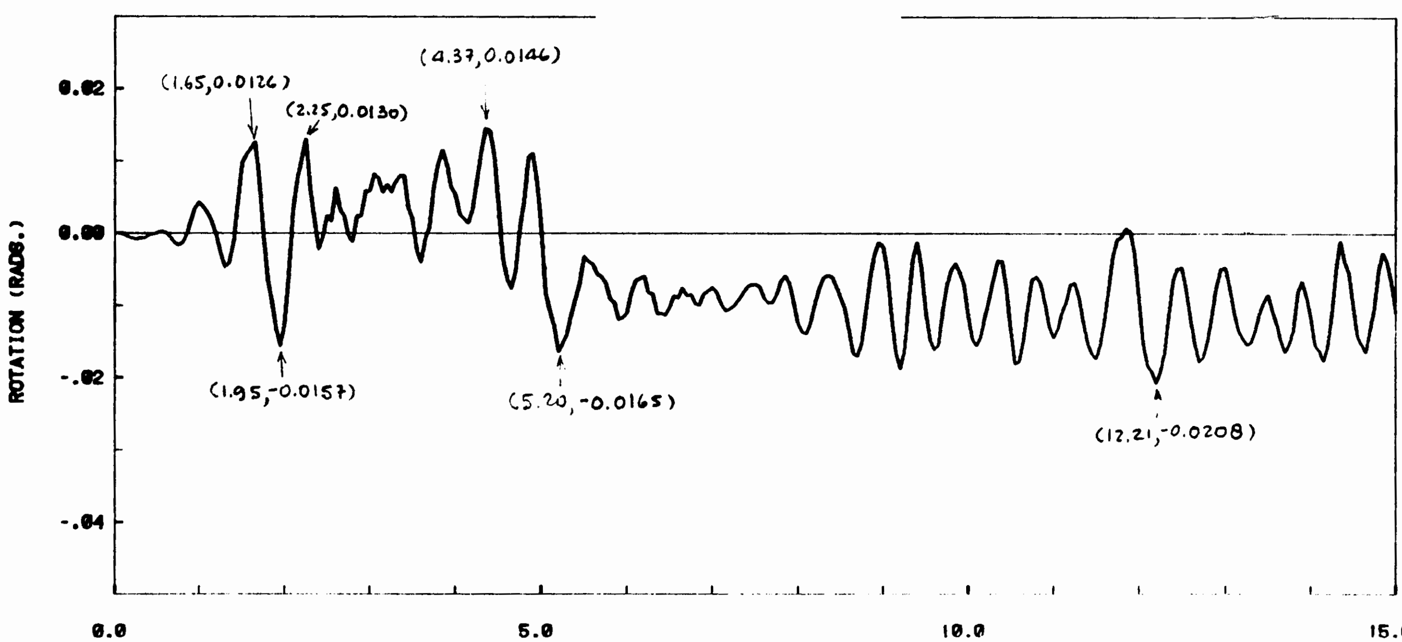

Fig. H.1E b)

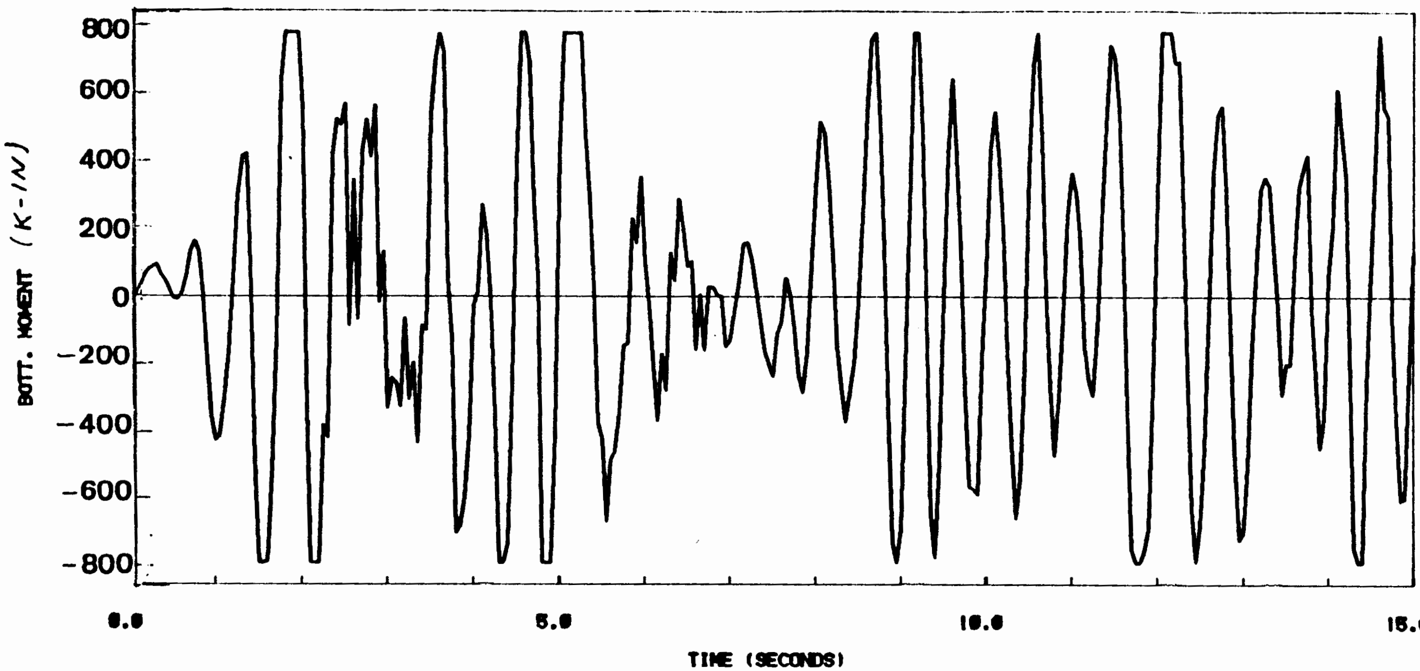

Fig. H.1E c)

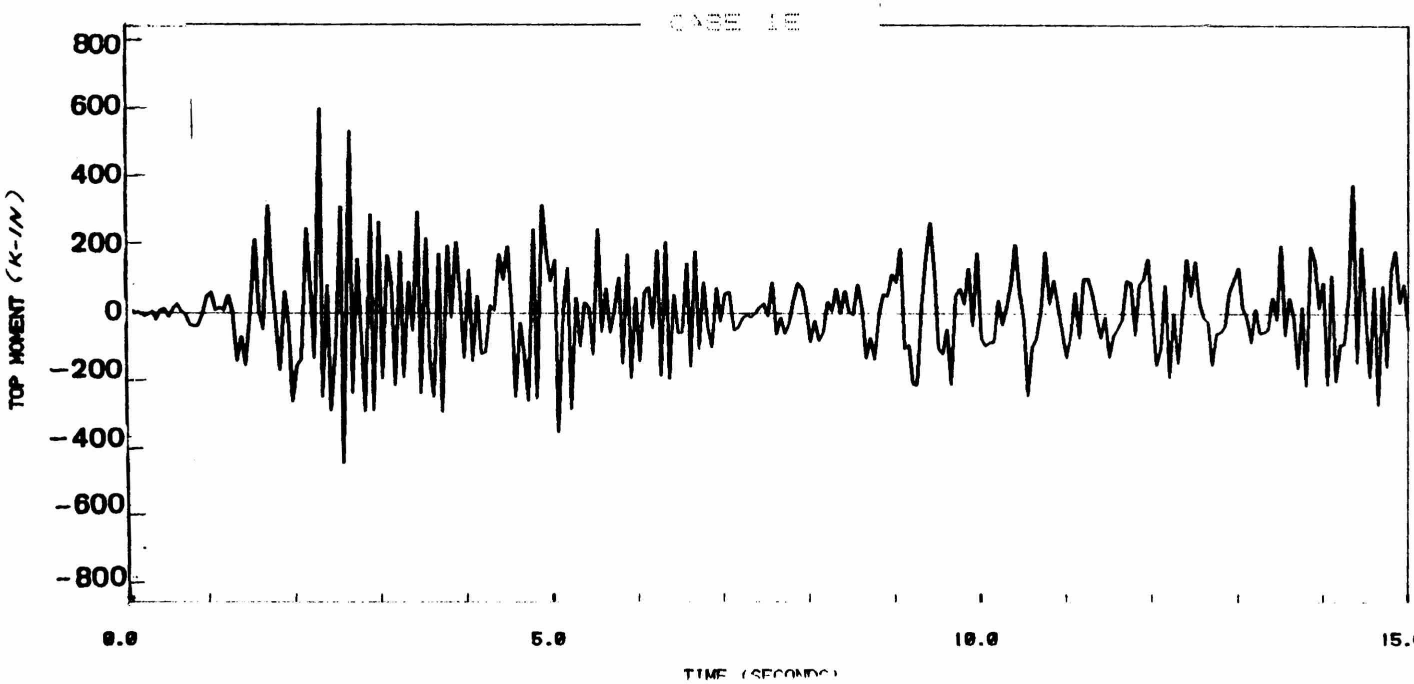

Fig. H.1E d)

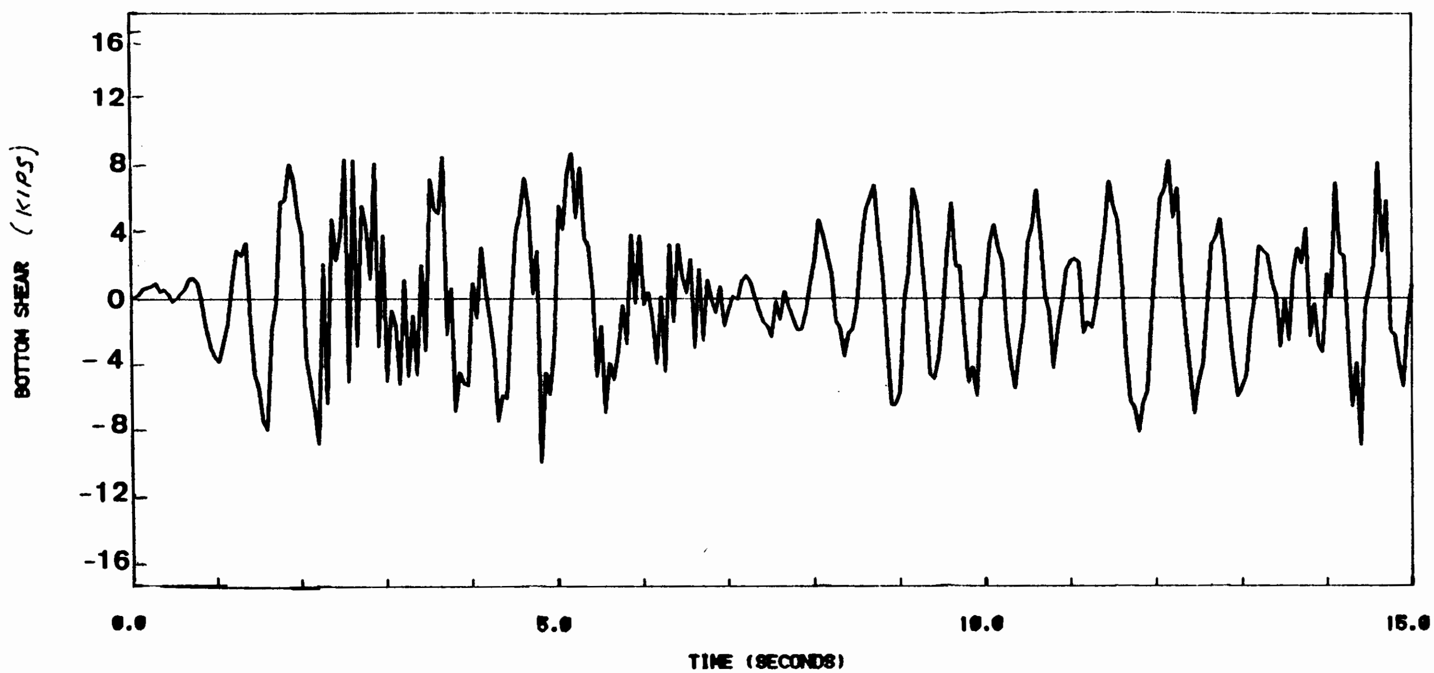

CASE 1E

Fig. H.1E e)

CASES 2 :

INELASTIC RESPONSE OF 2DOF CANOPY MODEL TO EL CENTRO NORMALIZED TO PGA = 0.55g

$EI = 2.62 \times 10^6 \text{ k-in}^2$

$T_1 = 0.72$ sec ; $T_2 = 0.18$ sec

$M_y = 800^{\text{ k-in}}$

CASE	PEAK CLIPPED ACCELERATION	FIGURE
2A	0.55g (unclipped)	H.2A
2B	0.32g	H.2B
2C	0.28g	H.2C
2D	0.22g	H.2D

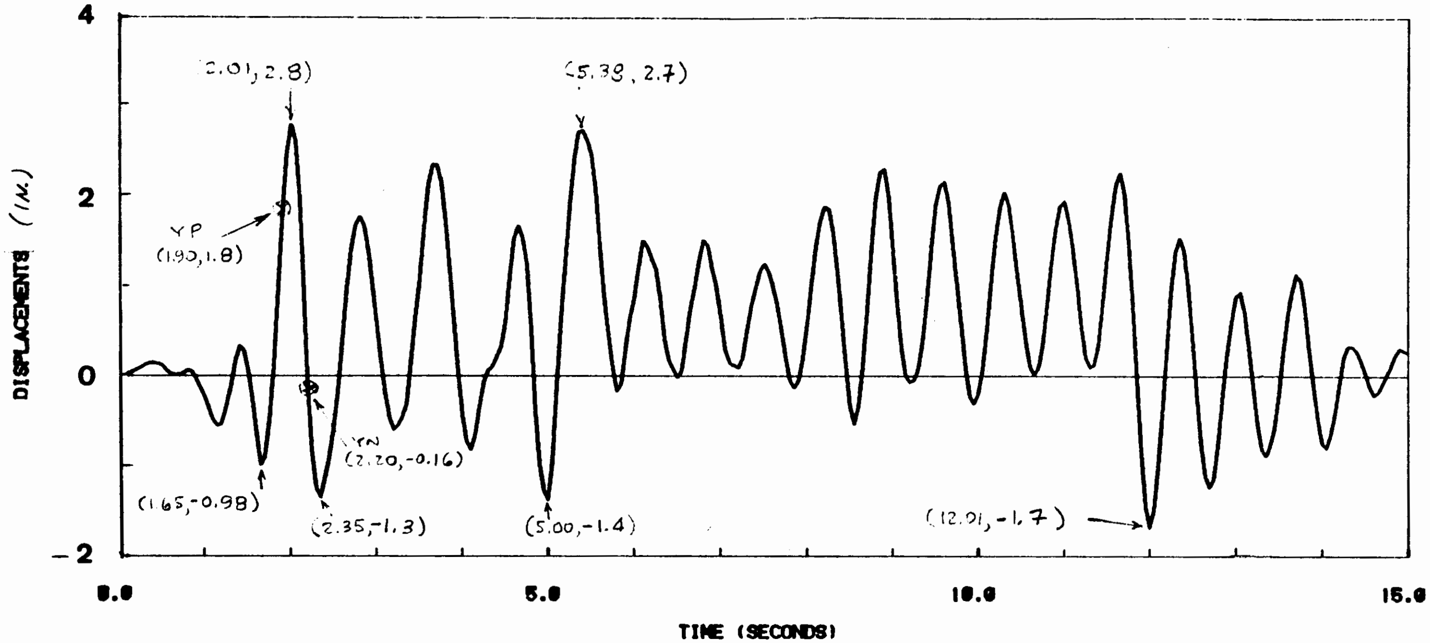

Fig. H. 2A a)

CASE 2A

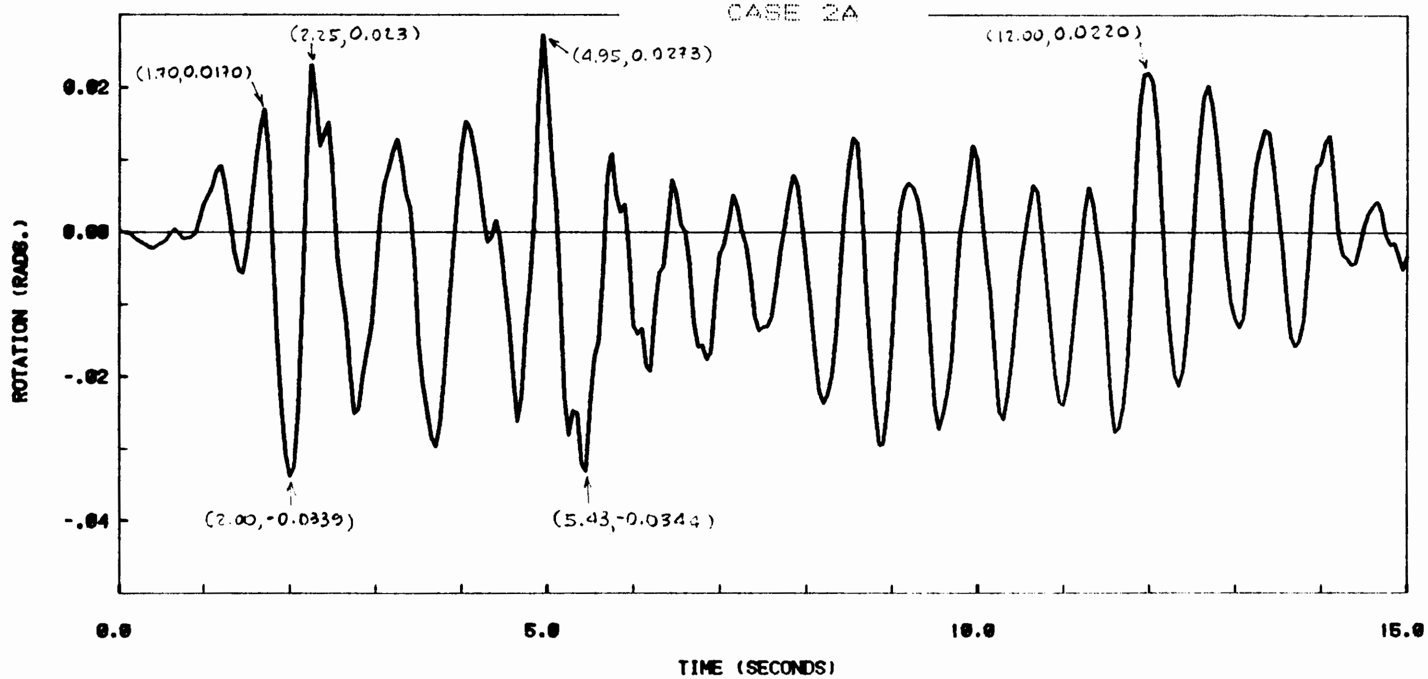

Fig. H. 2A b)

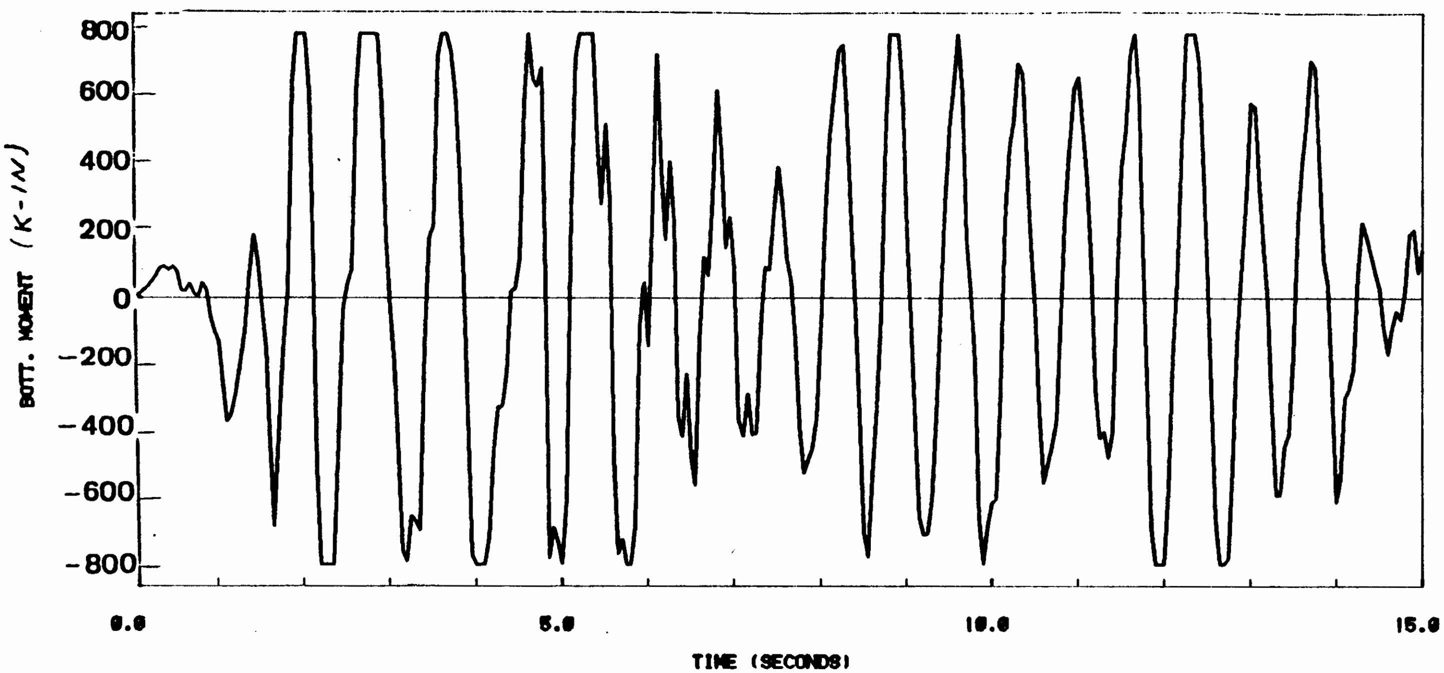

Fig. H. 2A c)

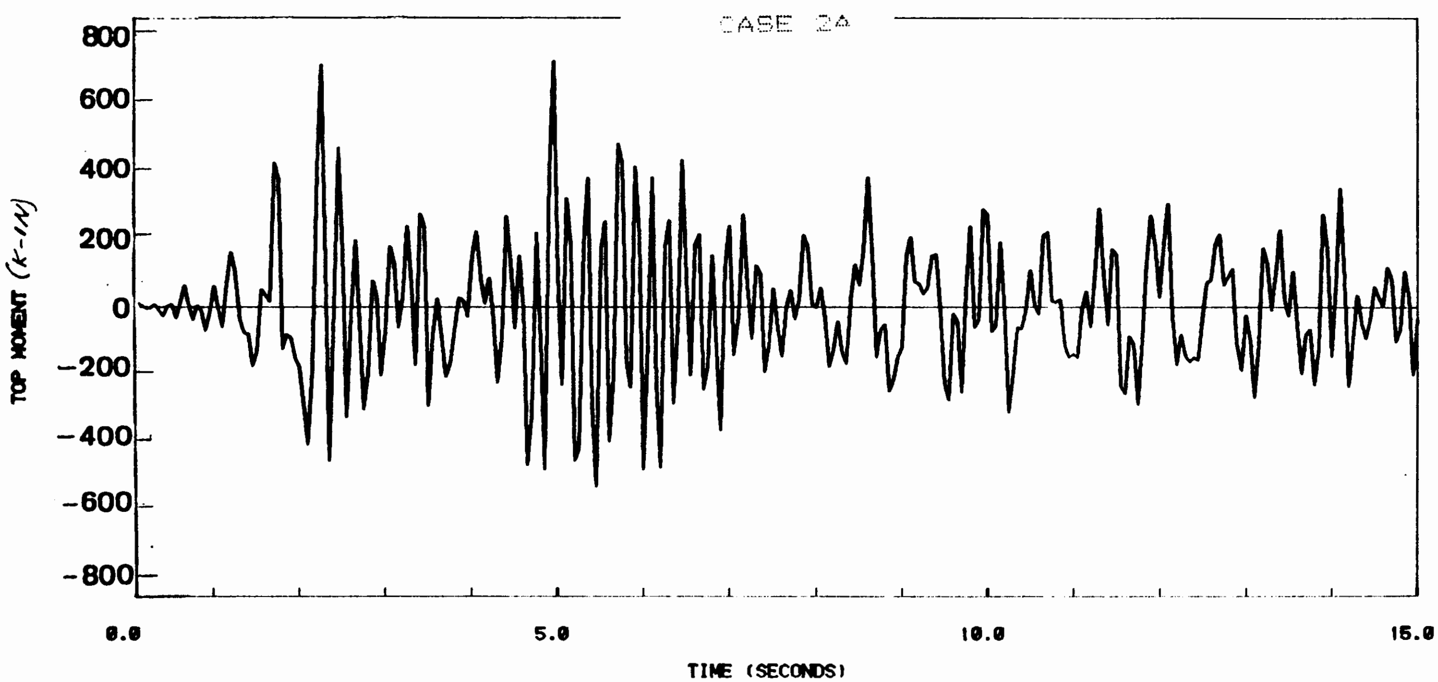

Fig. H. 2A d)

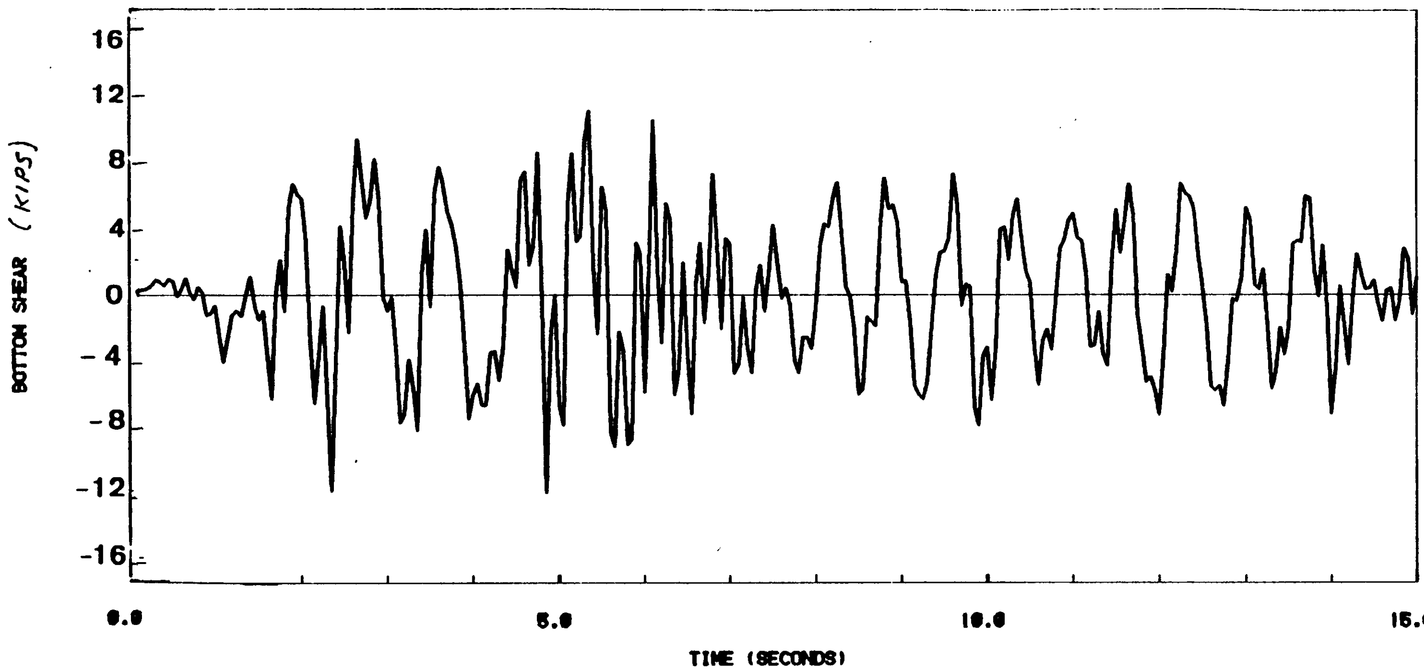

CASE 2A

Fig. H. 2A e)

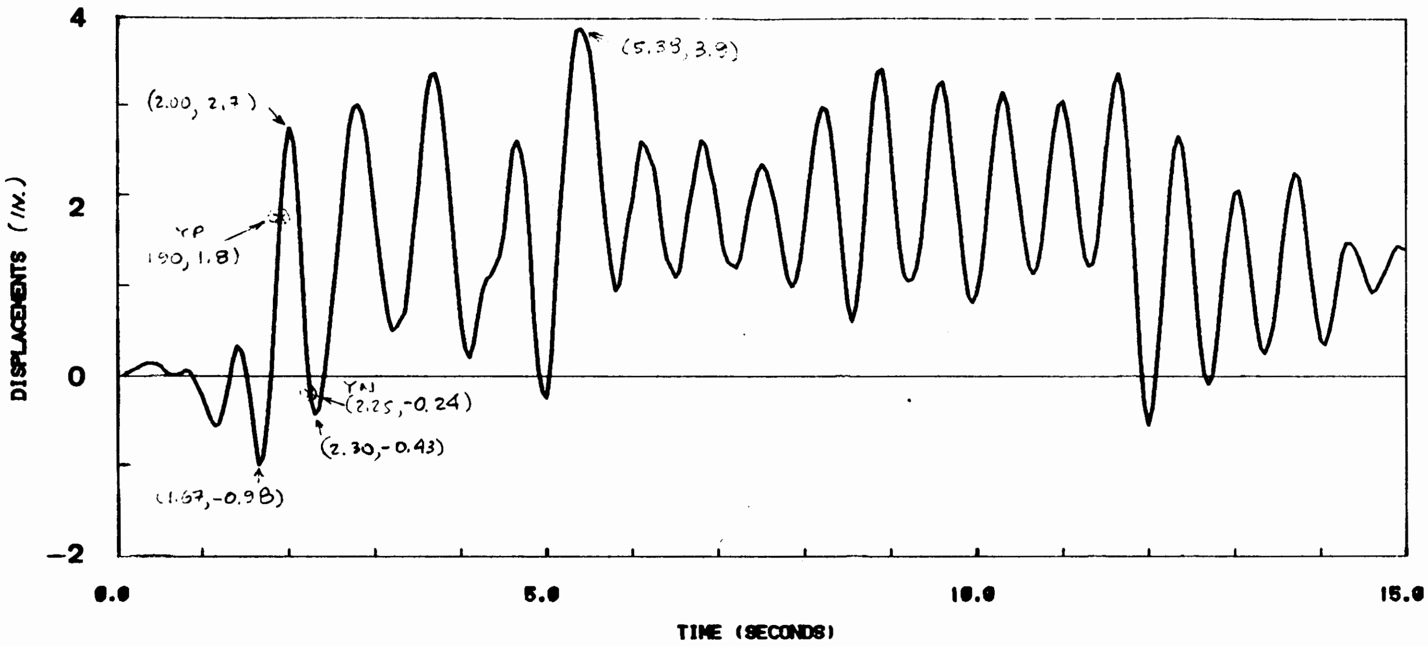

Fig. H.2B a)

CASE 2B

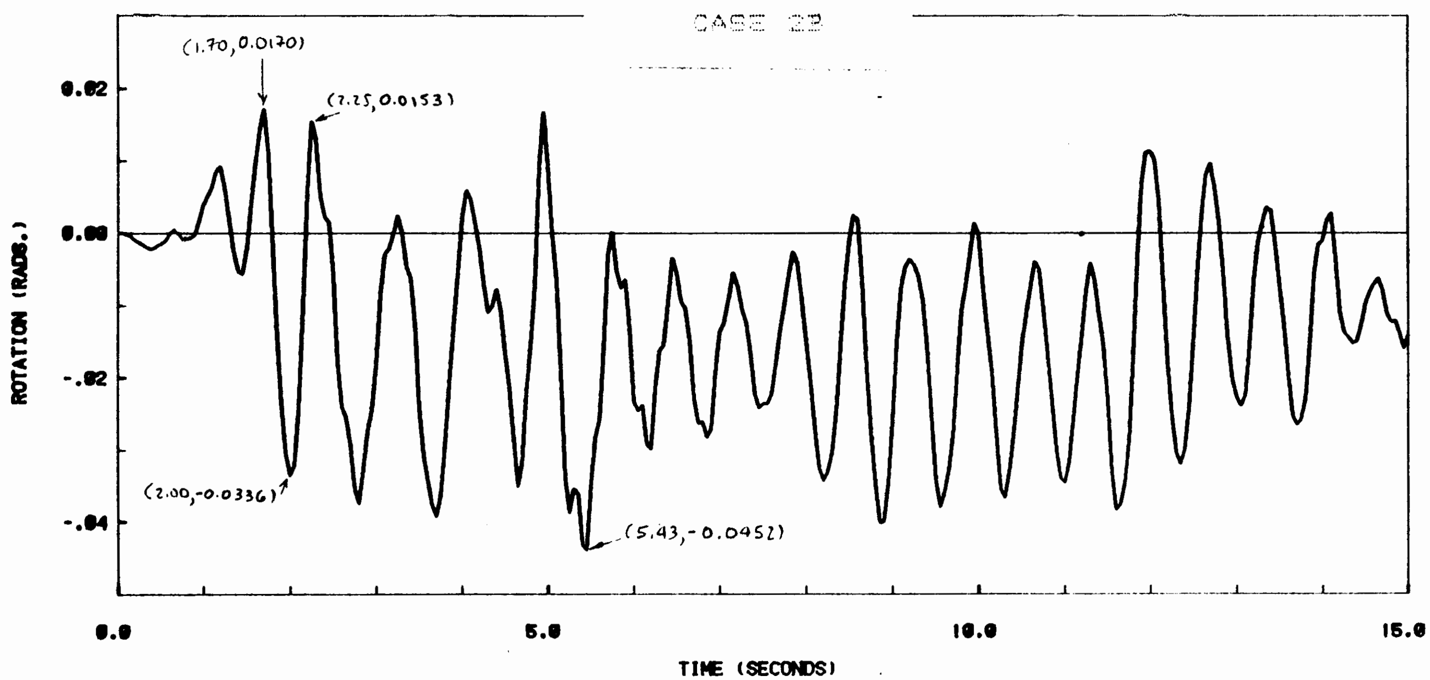

Fig. H.2B b)

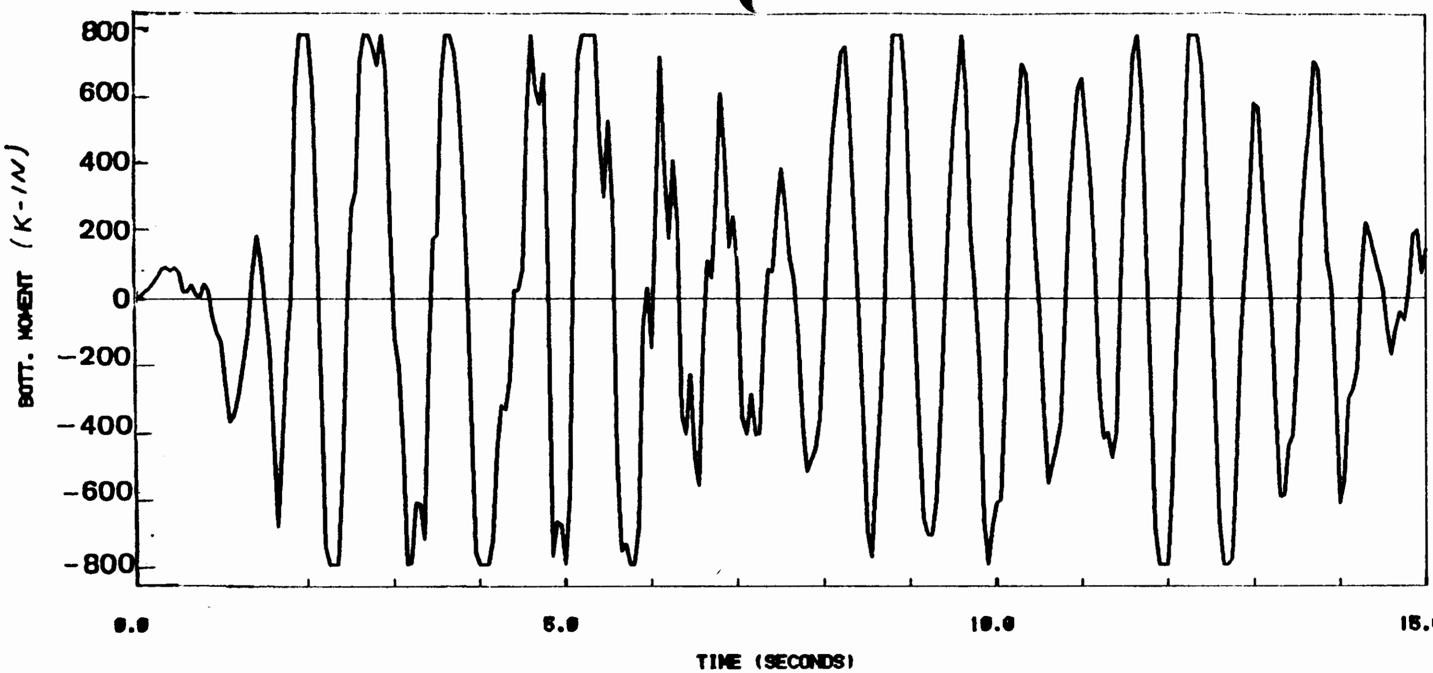

Fig. H.2B c)

CASE 2B

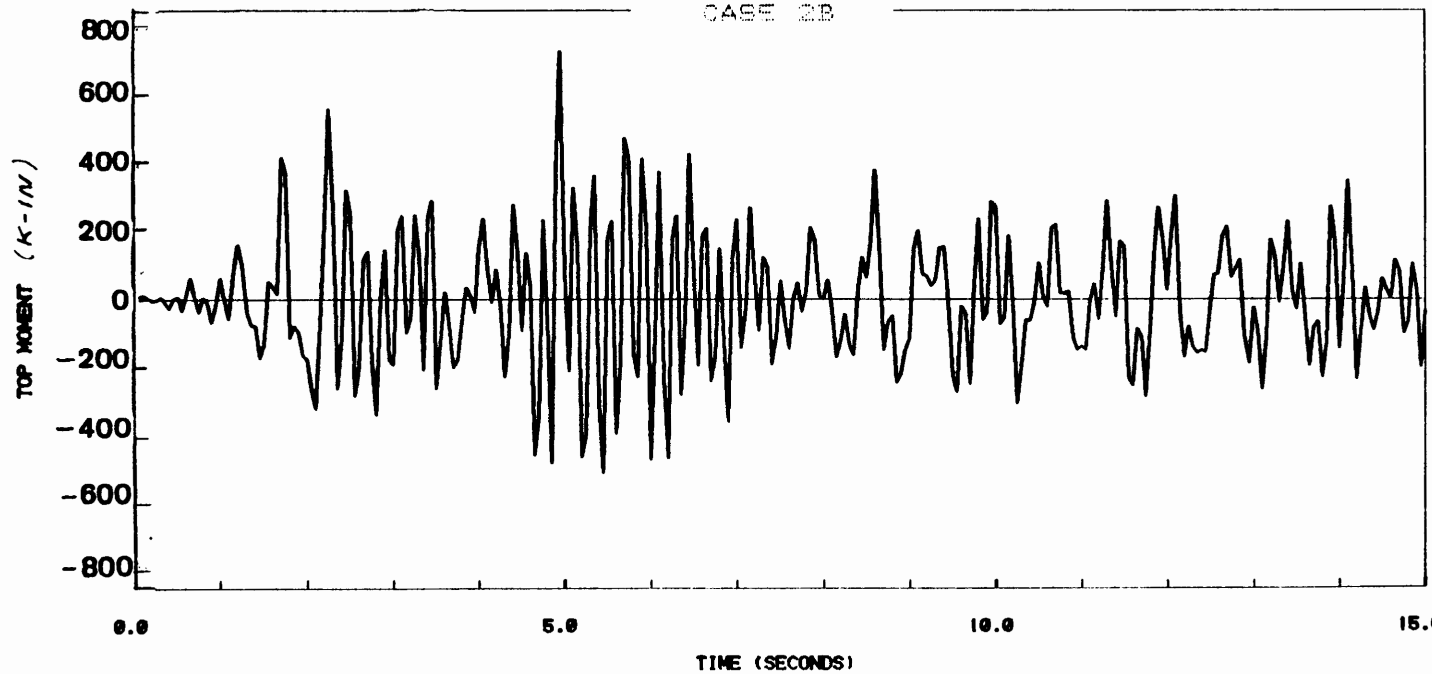

Fig. H.2B d)

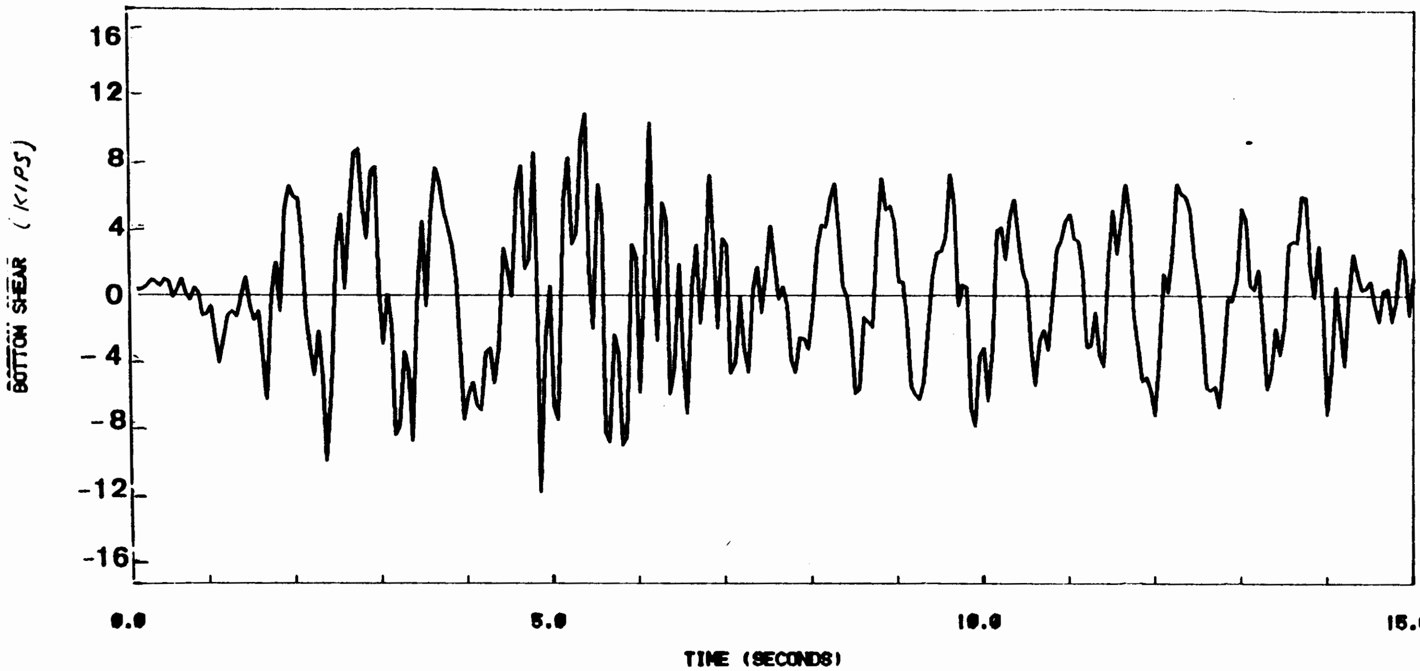

CASE 2B

Fig. H. 2B e)

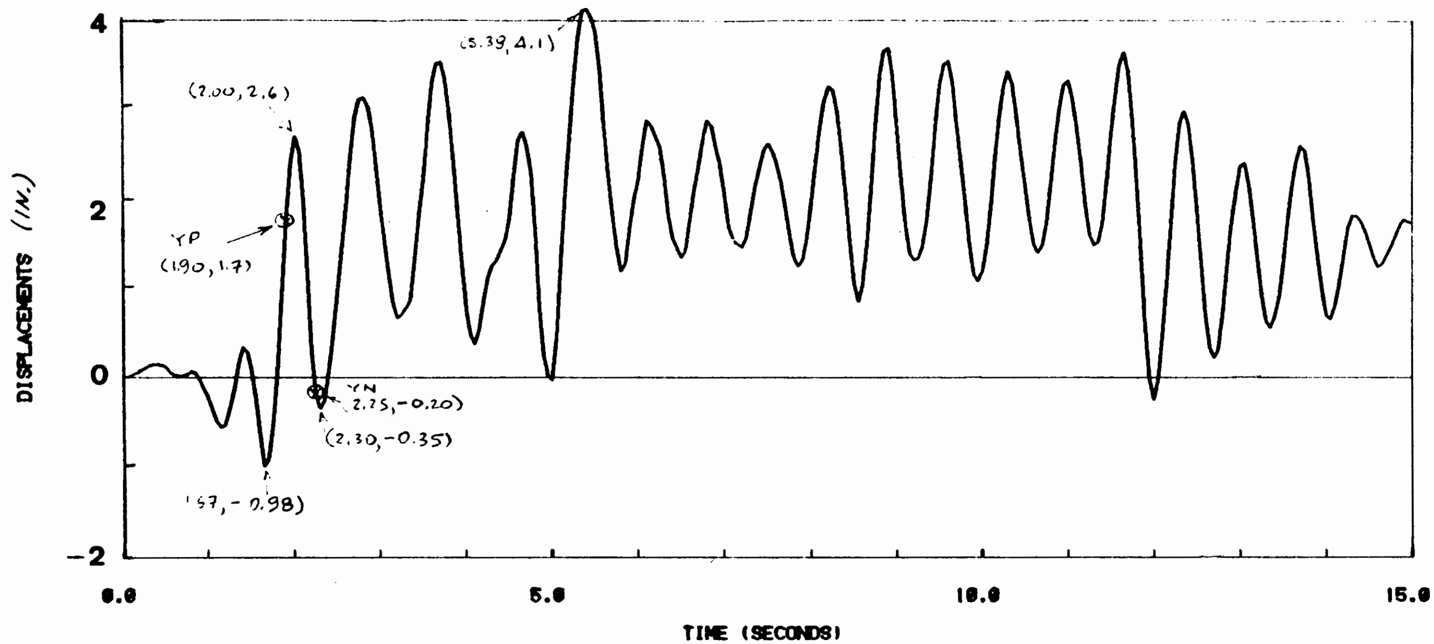

Fig. H.2C a)

CASE 2C

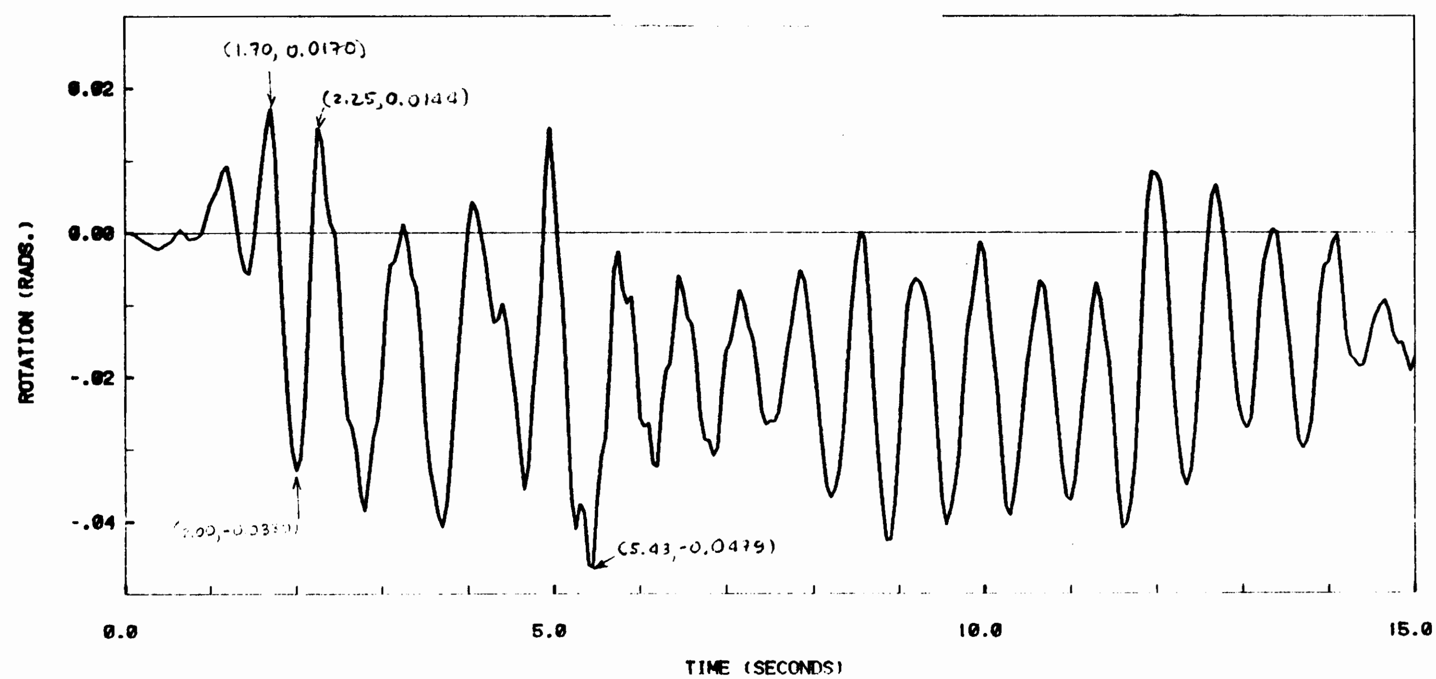

Fig. H.2C b)

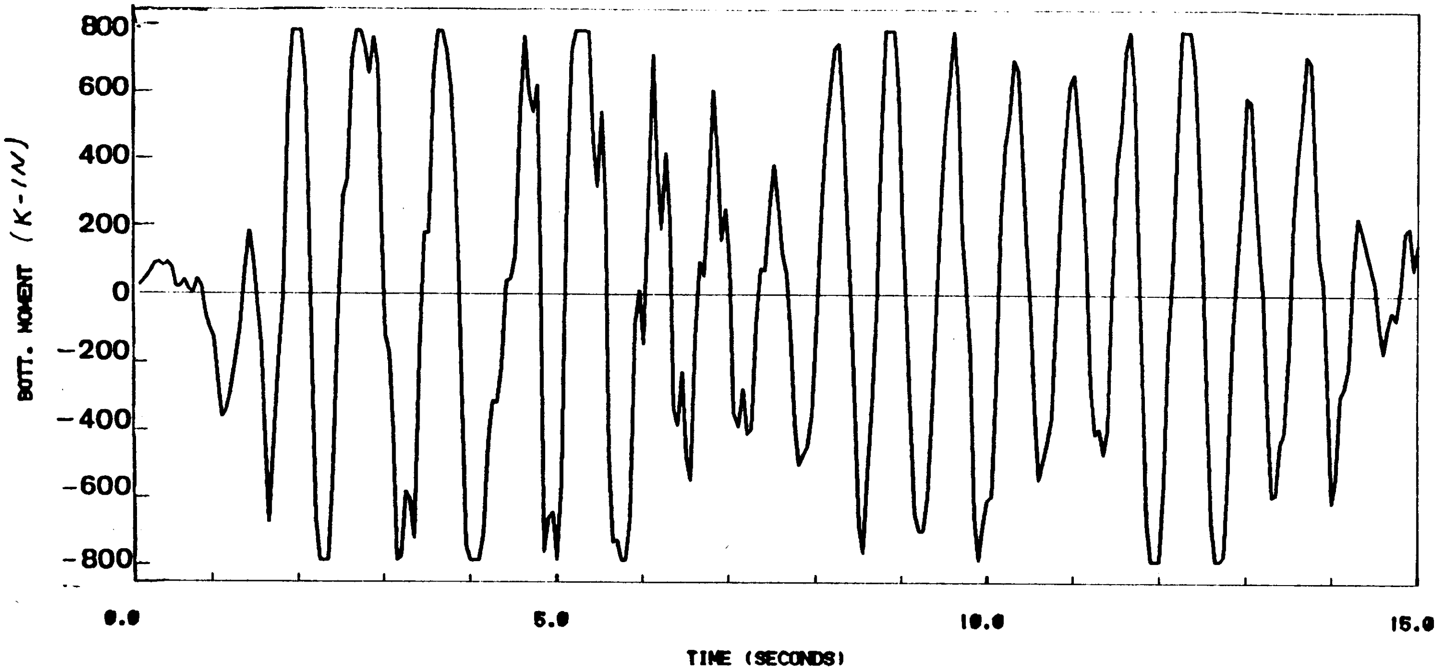

Fig. H.2C c)

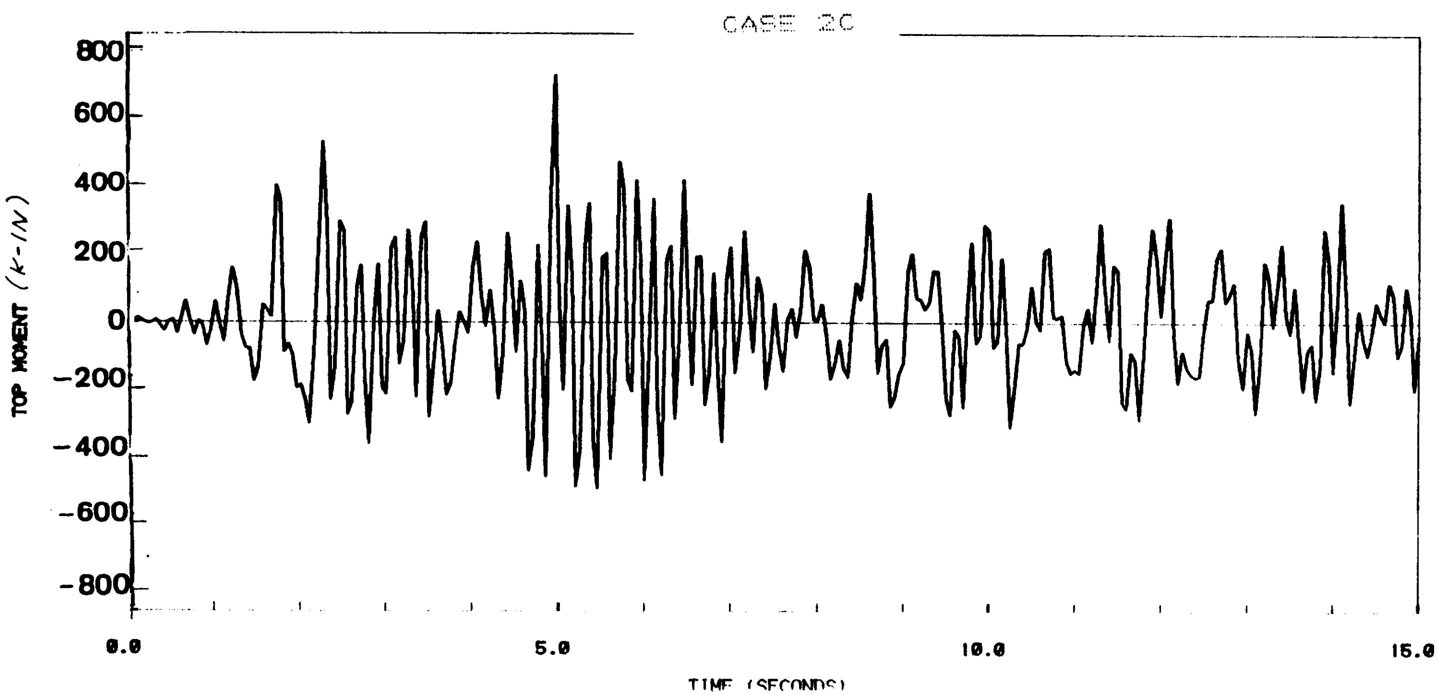

Fig. H.2C d)

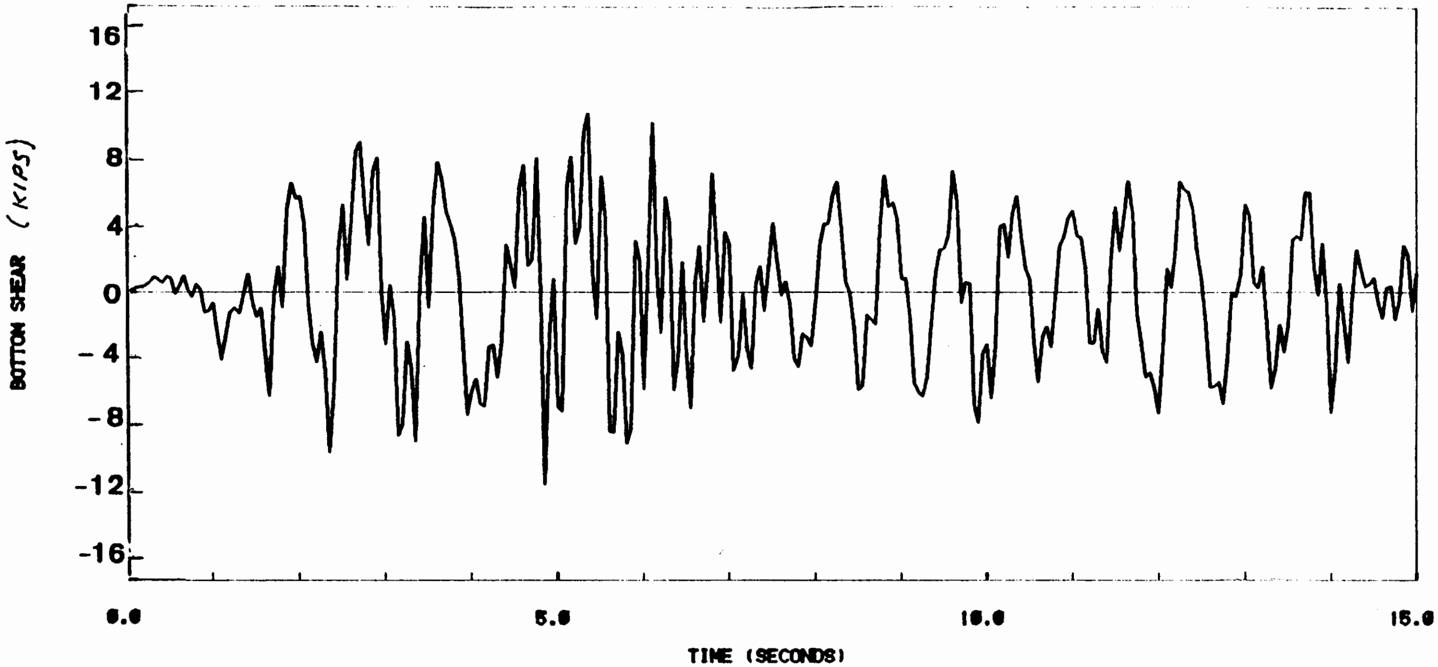

CASE 2C

Fig. H.2C e)

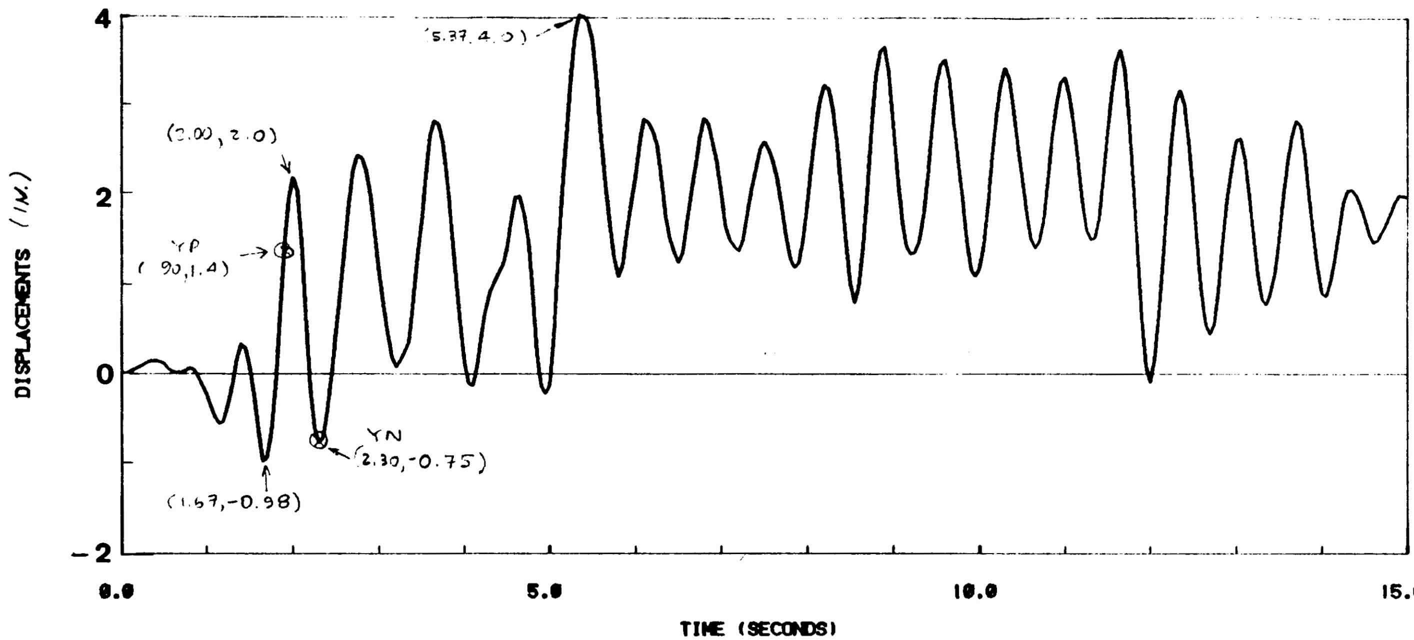

Fig. H.2D a)

CASE 2D

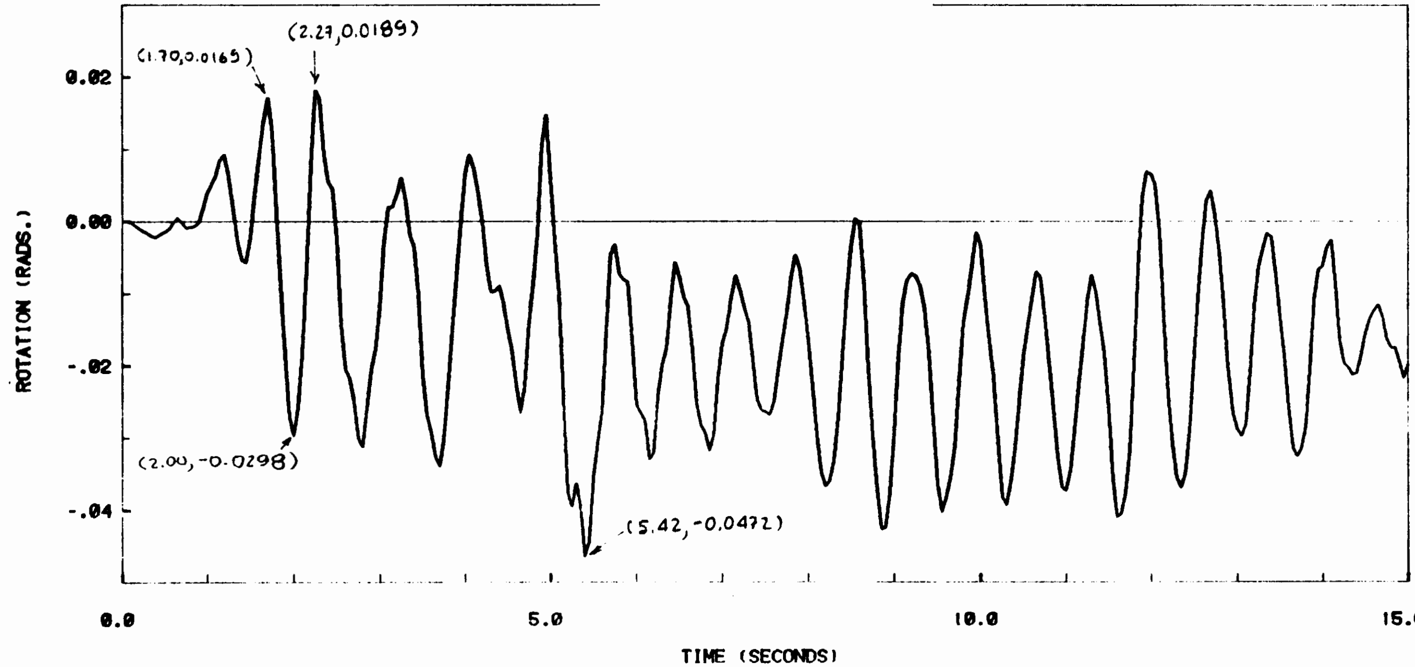

Fig. H.2D b)

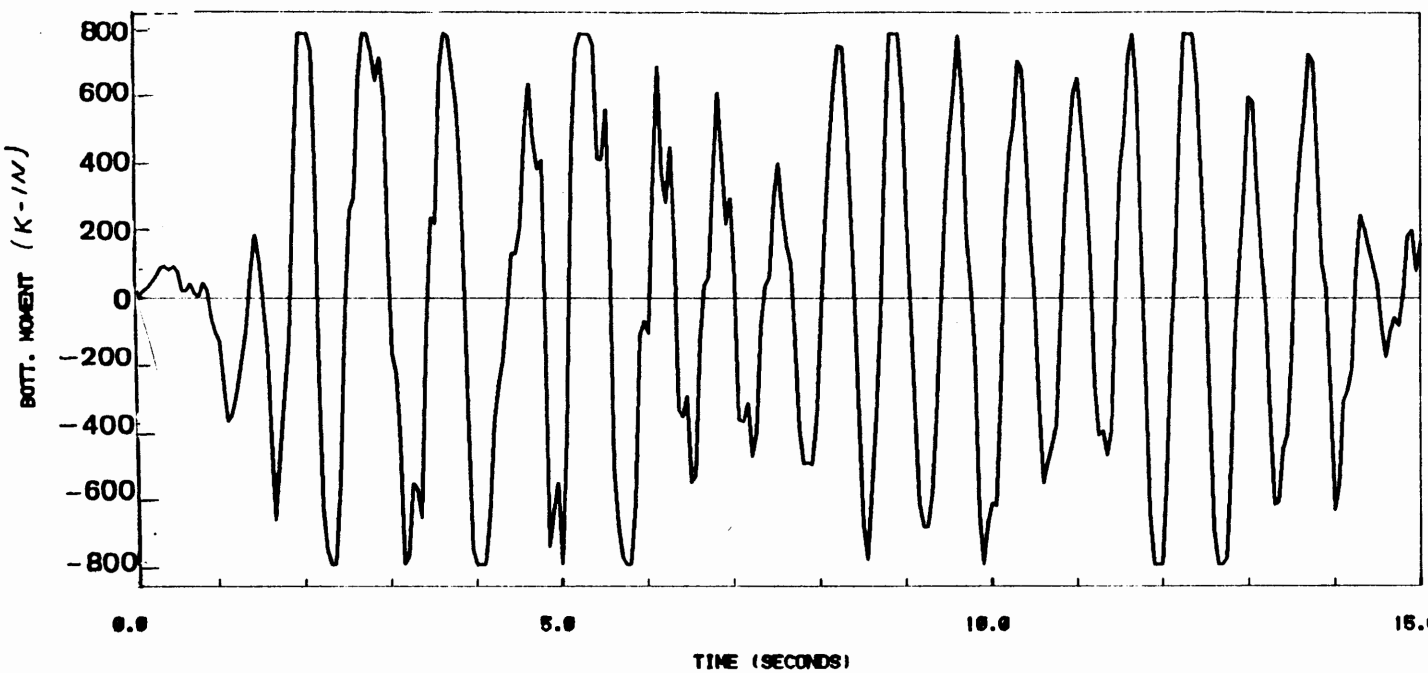

Fig. H.2D c)

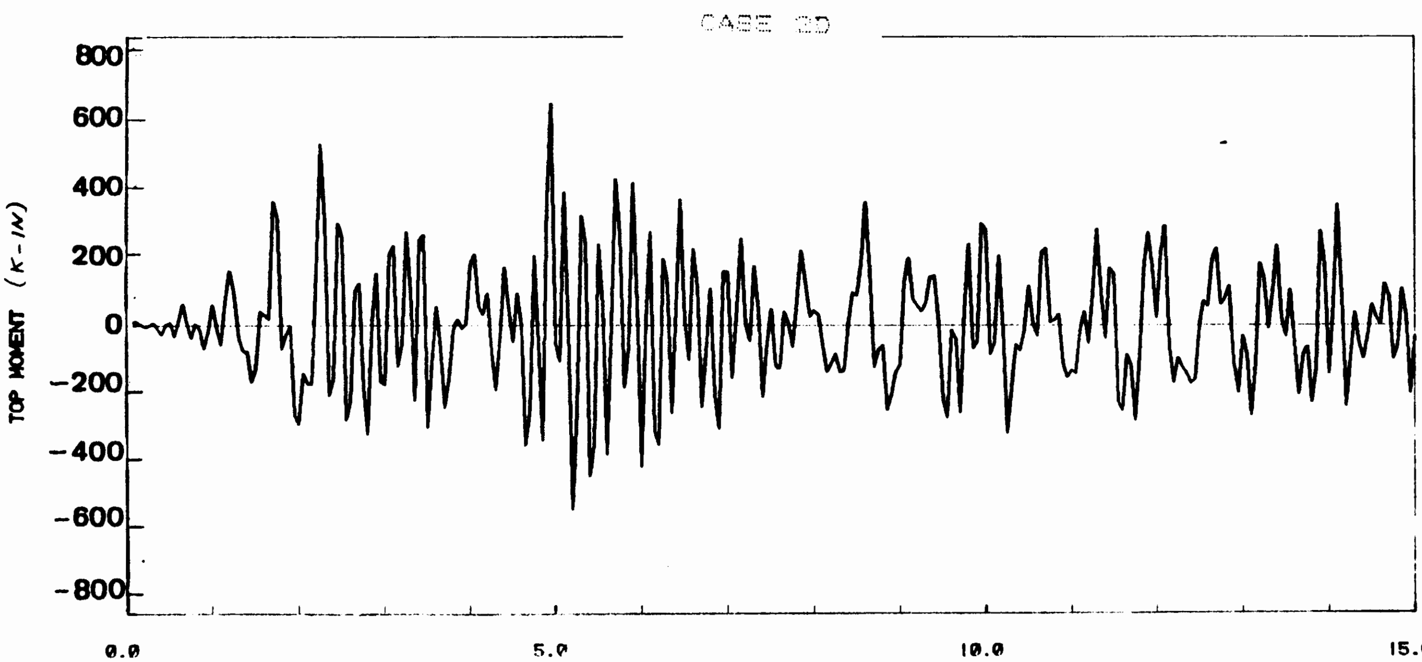

Fig. H.2D d)

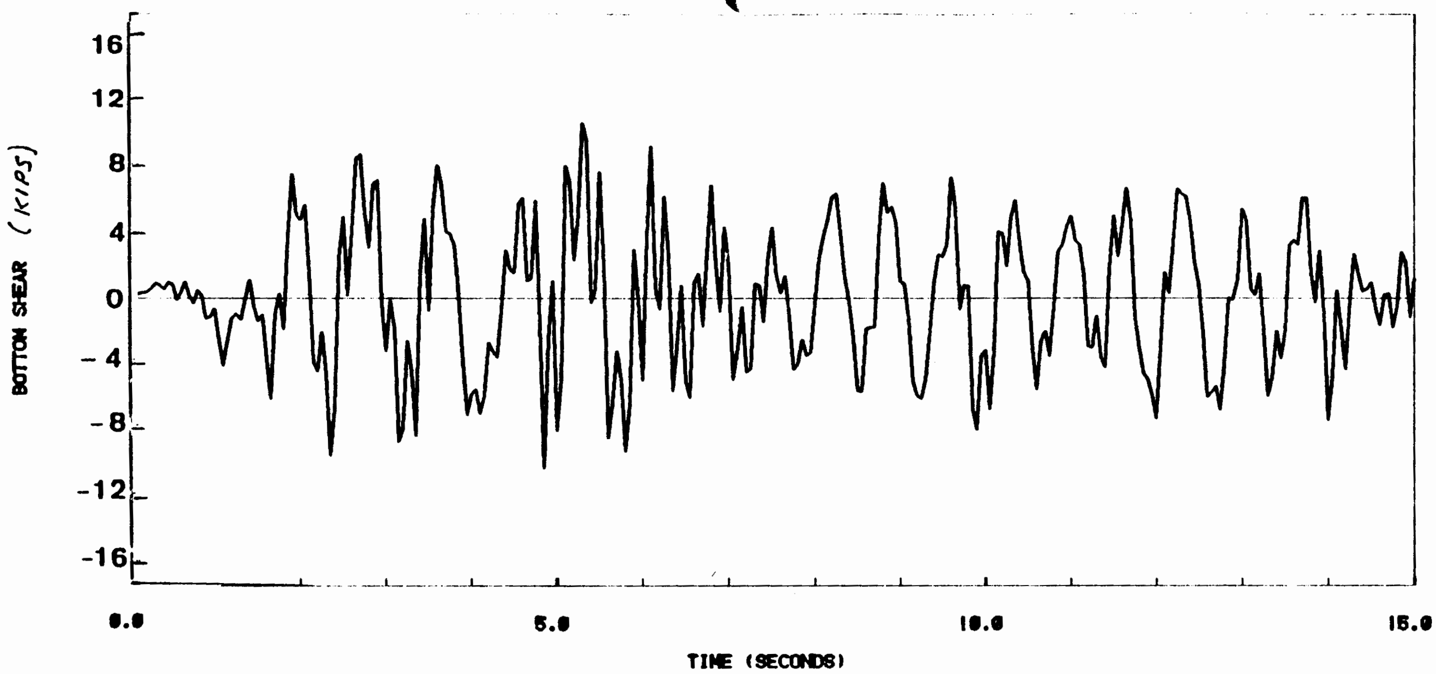

Fig. H.2D e)

CASE 2D

CASES 3:

INELASTIC RESPONSE OF 2DOF CANOPY MODEL TO DERIVED PACOIMA DAM NORMALIZED TO 0.35g

$EI = 6.28 \times 10^6 \ k\text{-}in^2$

$T_1 = 0.46$ sec ; $T_2 = 0.11$ sec

$M_y = 800^{k\text{-}in}$

CASE	PEAK CLIPPED ACCELERATION	FIGURE
3A	0.35g (unclipped)	H.3A
3B	0.30g	H.3B

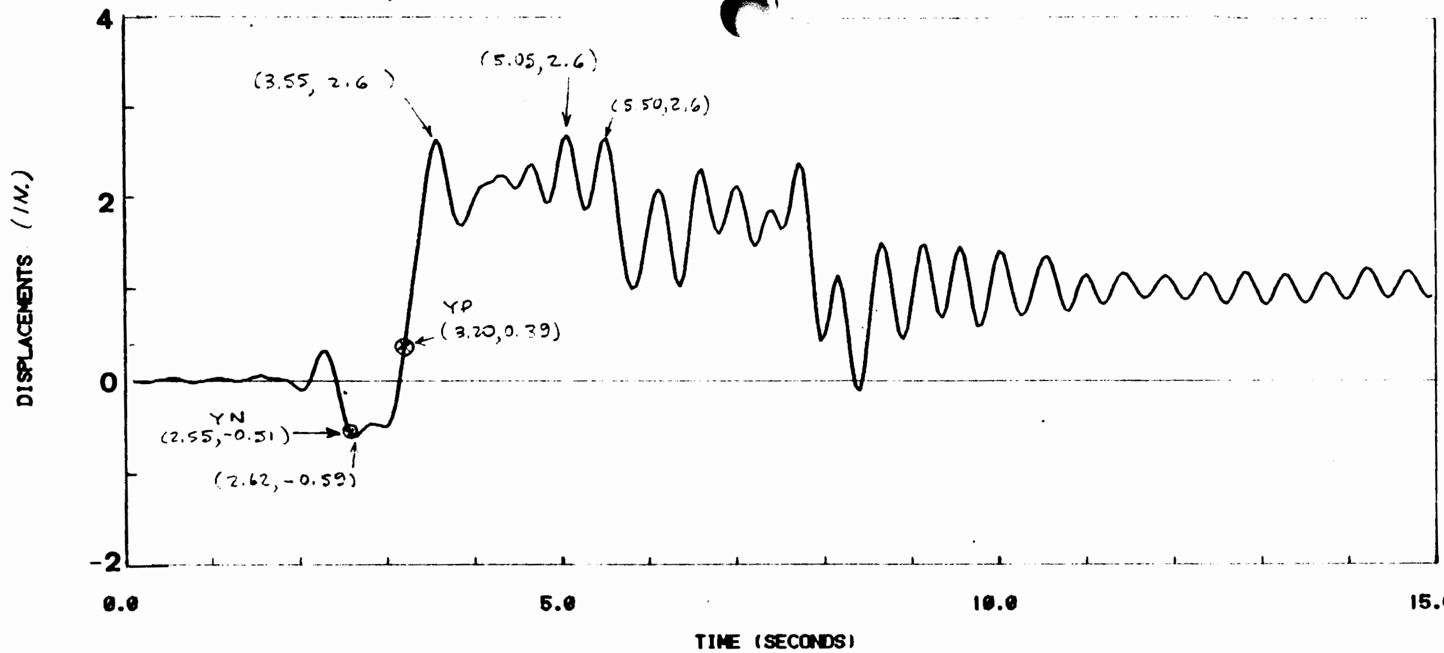

Fig. H.3A a)

CASE 3A

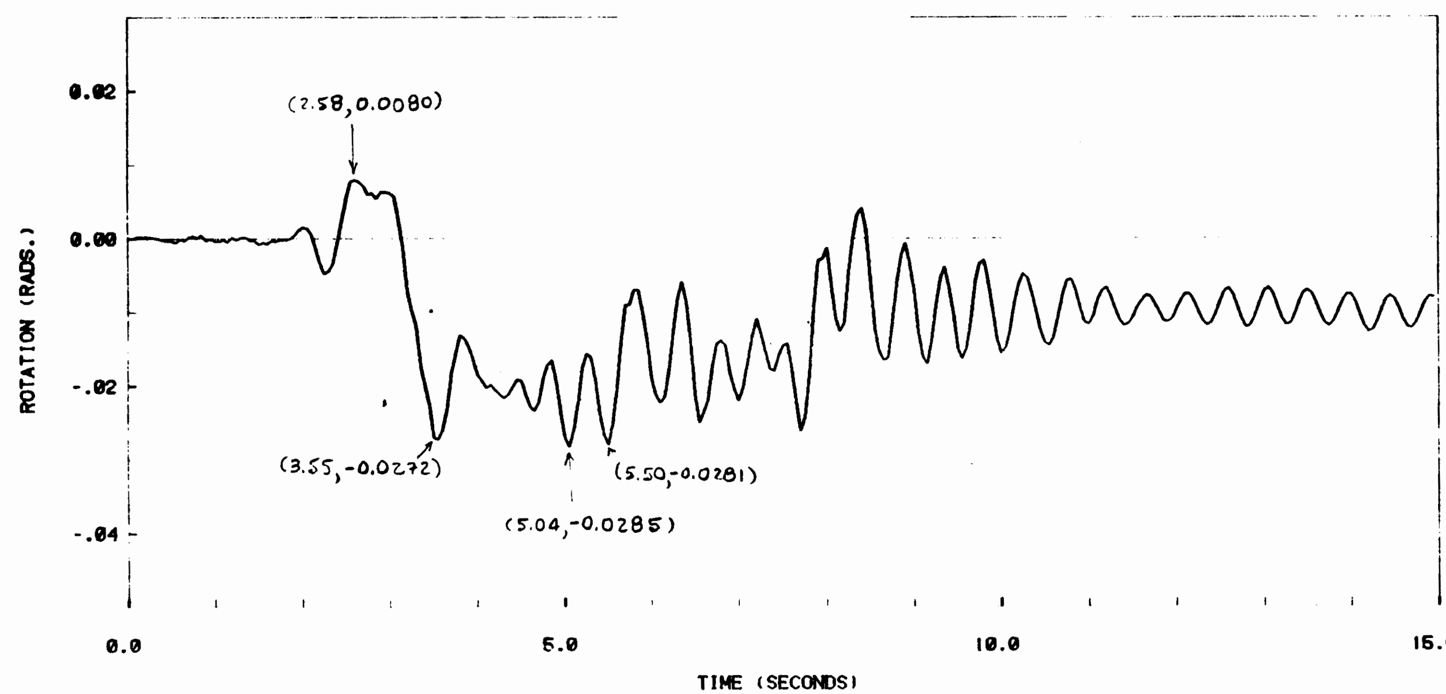

Fig. H.3A b)

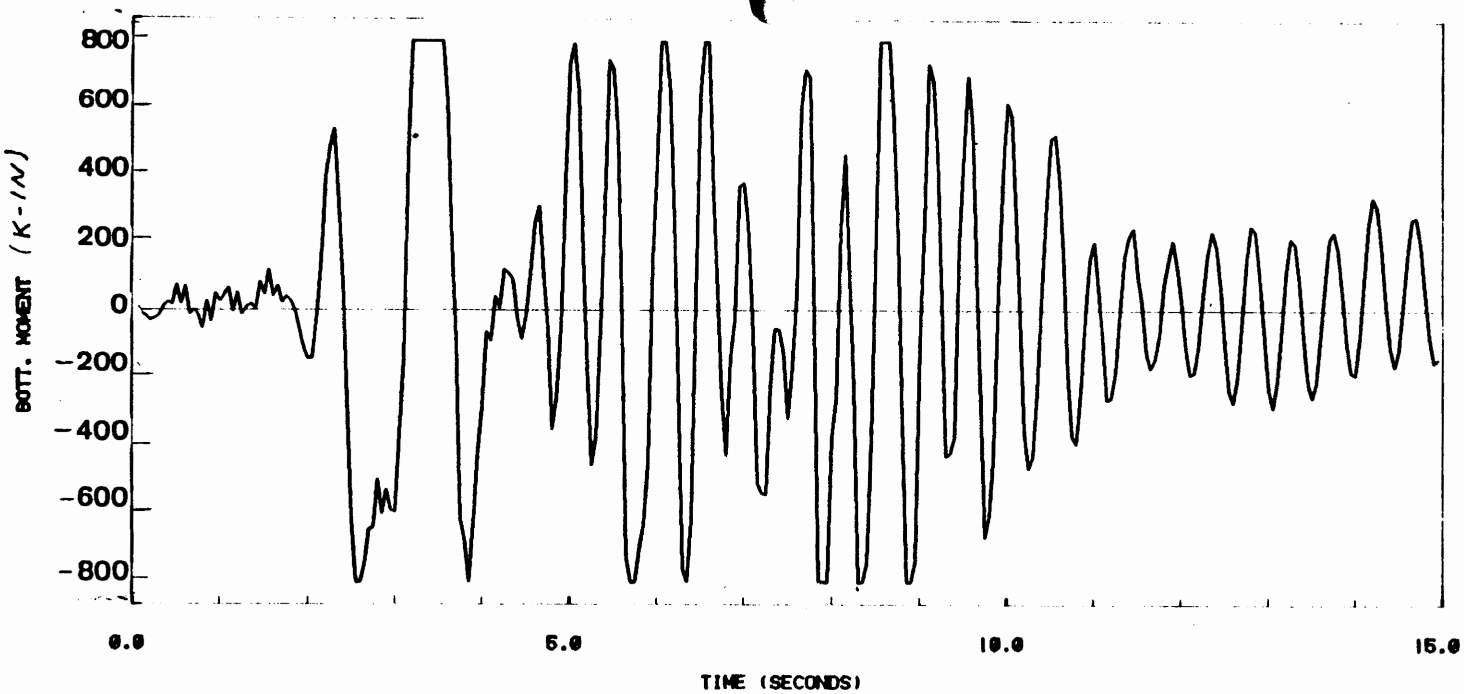

Fig. H.3A c)

CASE 3A

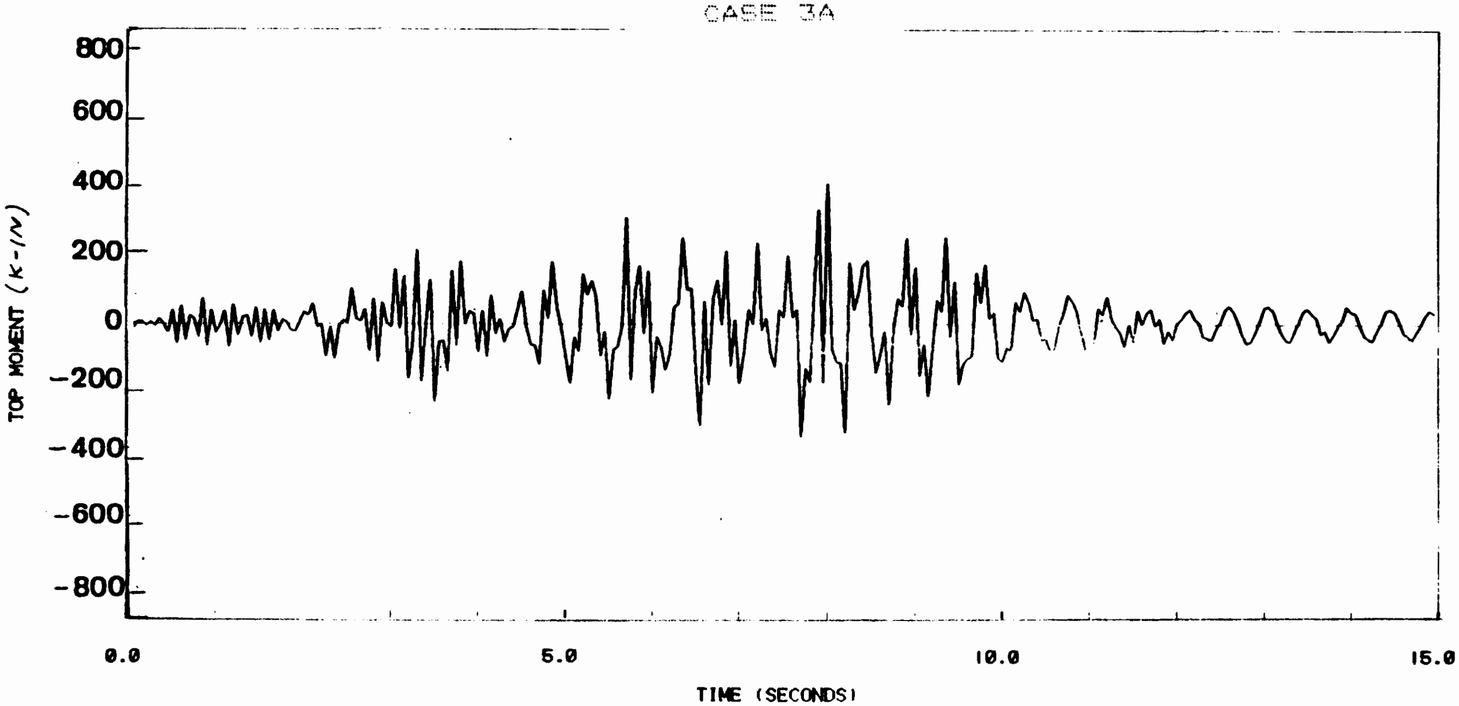

Fig. H.3A d)

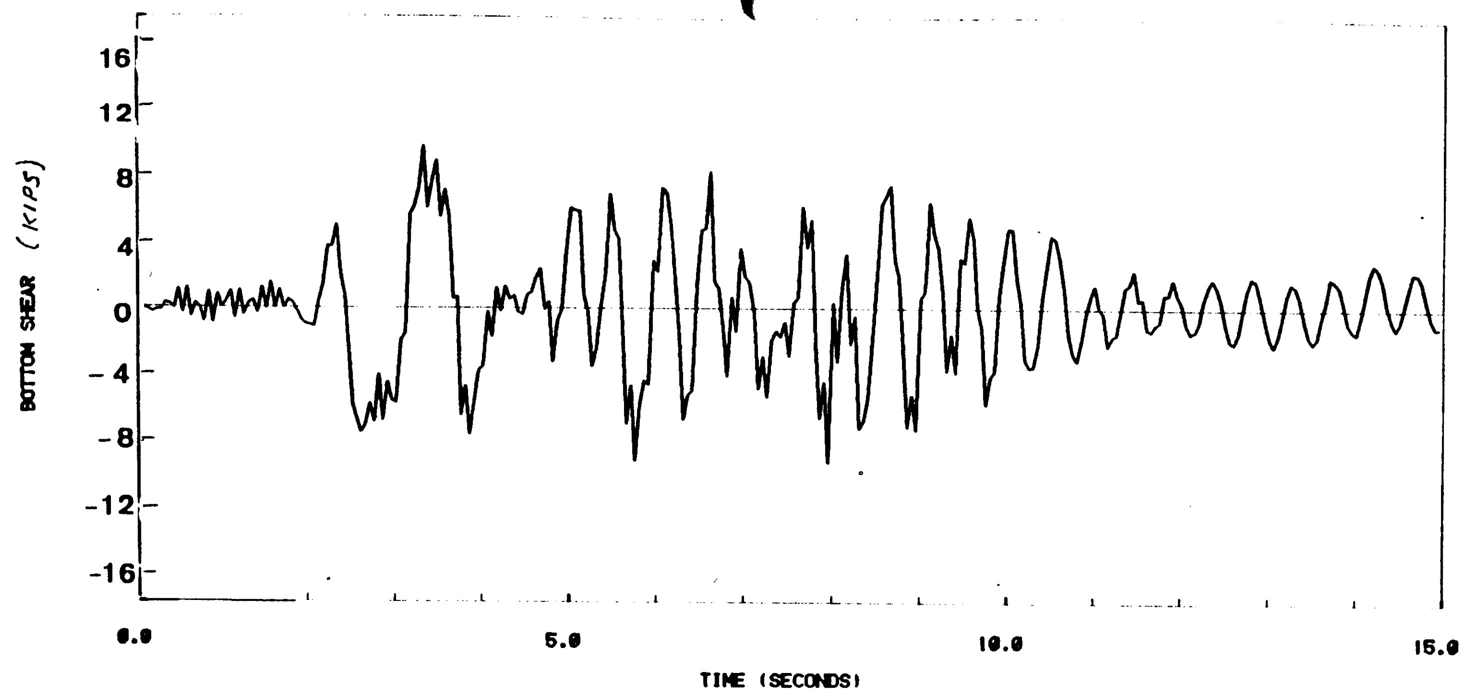

CASE 3A

Fig. H.3A e)

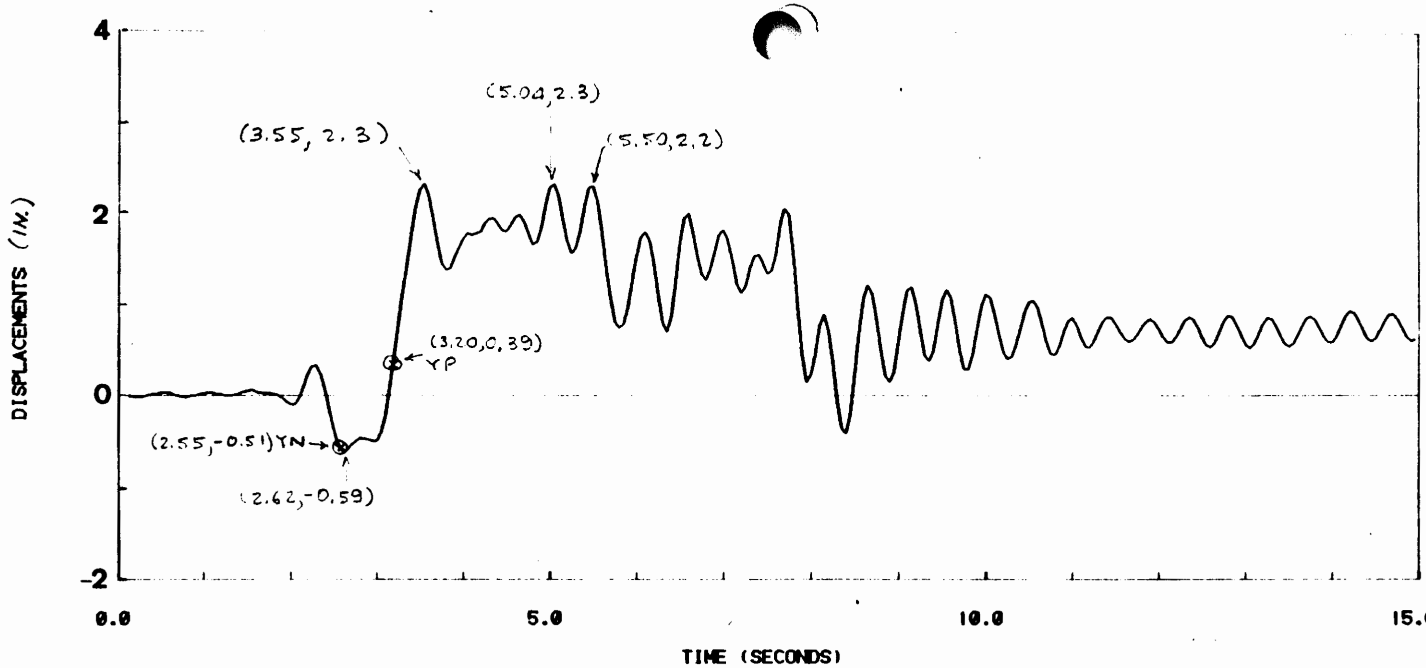

Fig. H.3B a)

CASE 33

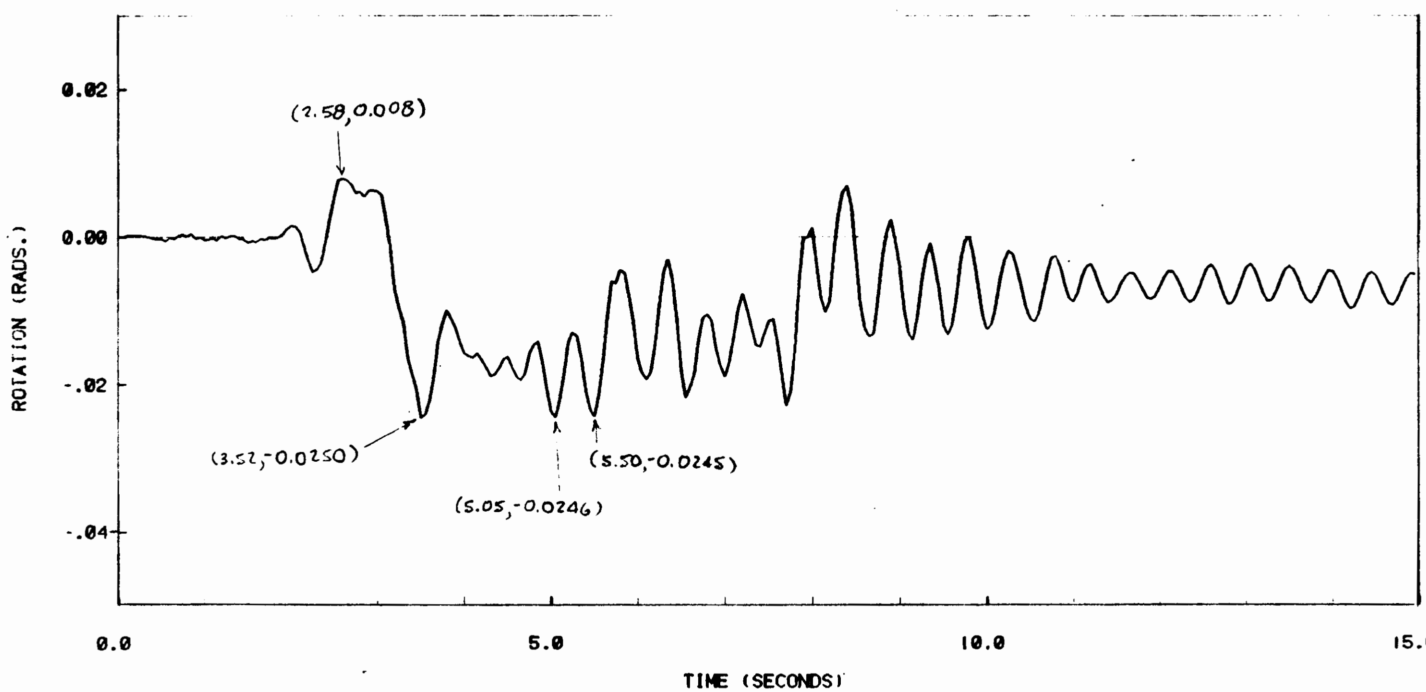

Fig. H.3B b)

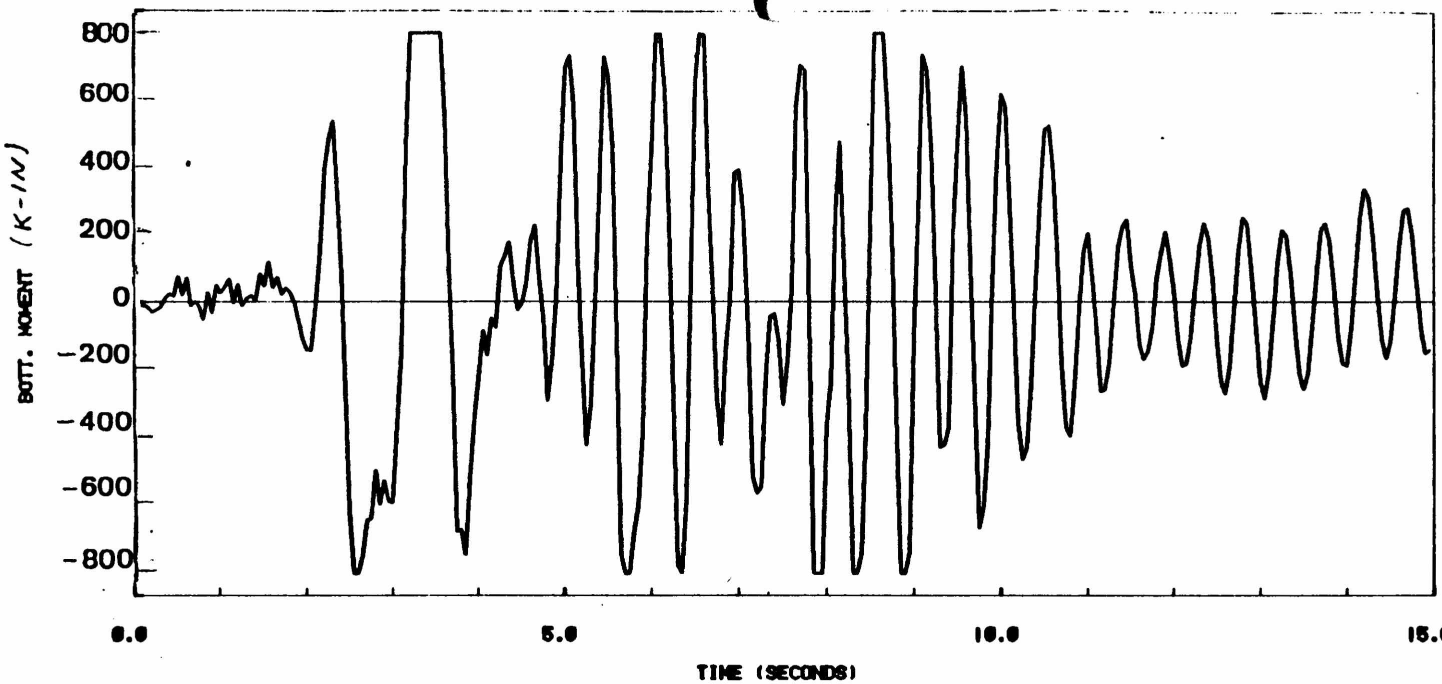

Fig. H.3B c)

CASE 3B

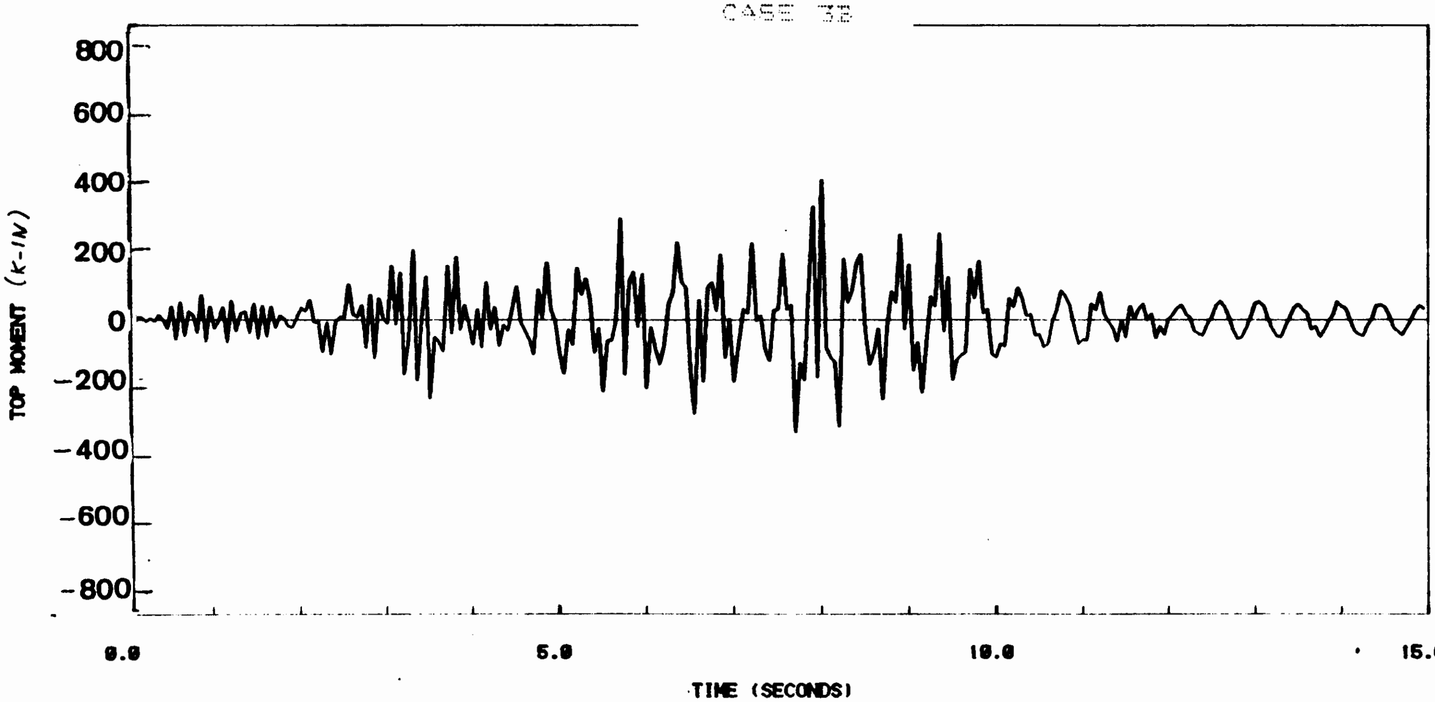

Fig. H.3B d)

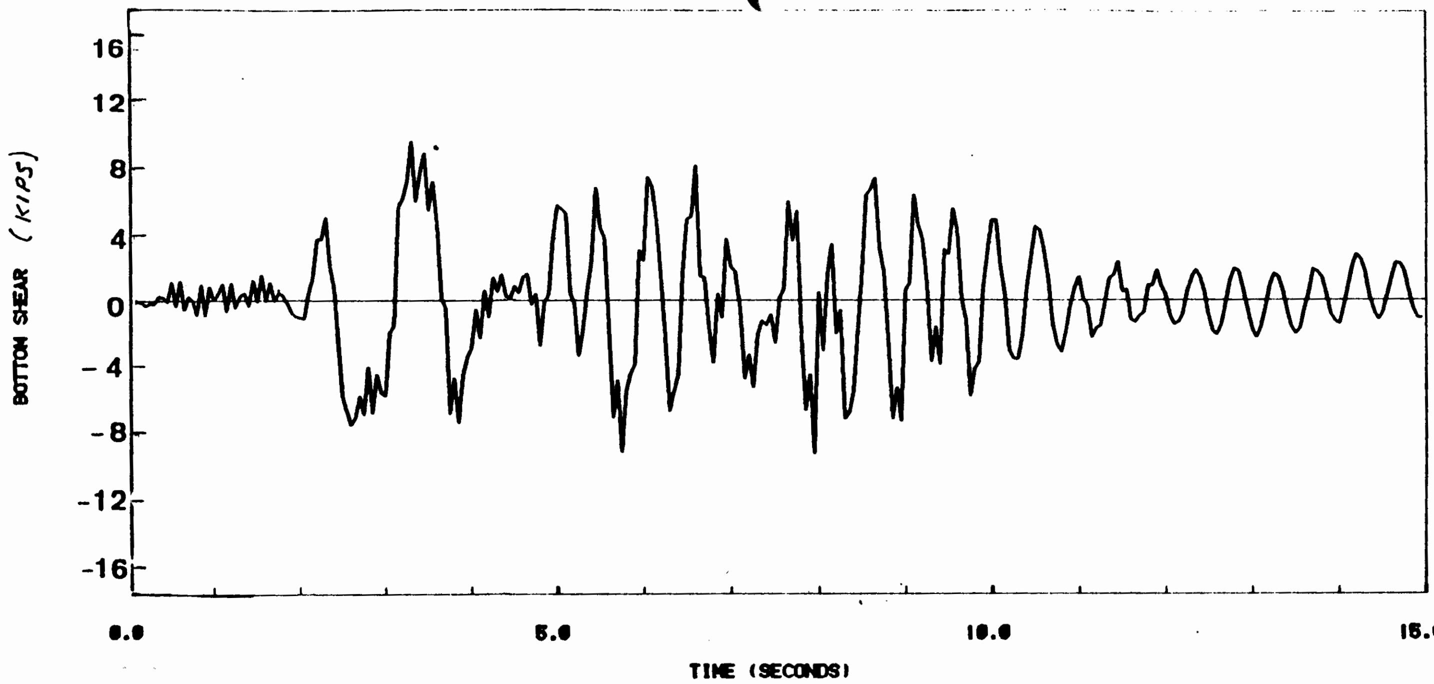

Fig. H.3B e)

CASE 3B

CASES 4 :

Inelastic Response of 2DOF Canopy Model to Derived Pacoima Dam Normalized to 0.35 g

$EI = 2.62 \times 10^6 \ k\text{-}in^2$

$T_1 = 0.72$ sec ; $T_2 = 0.18$ sec

$M_y = 800^{k\text{-}in}$

CASE	Peak Clipped Acceleration	Figure
4A	0.35 g (unclipped)	H.4A
4B	0.30g	H.4B

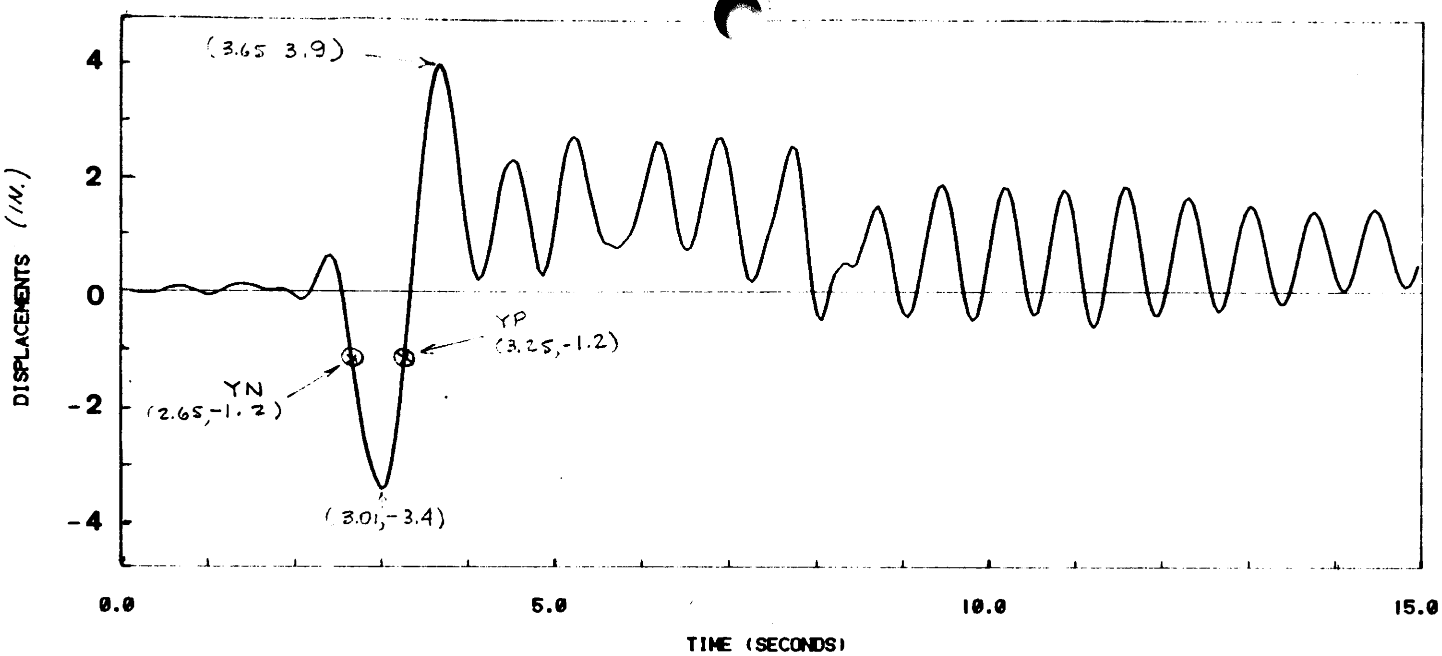

Fig. H.4A a)

CASE 4A

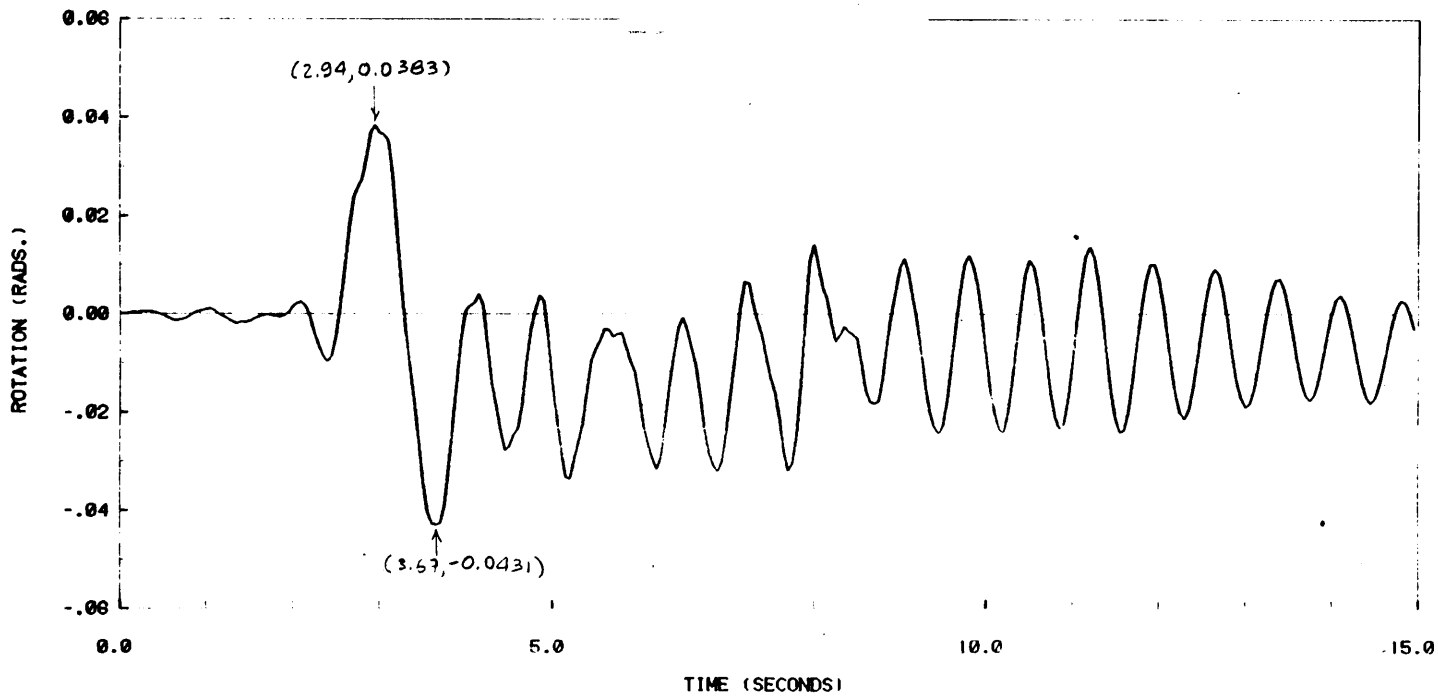

Fig. H.4A b)

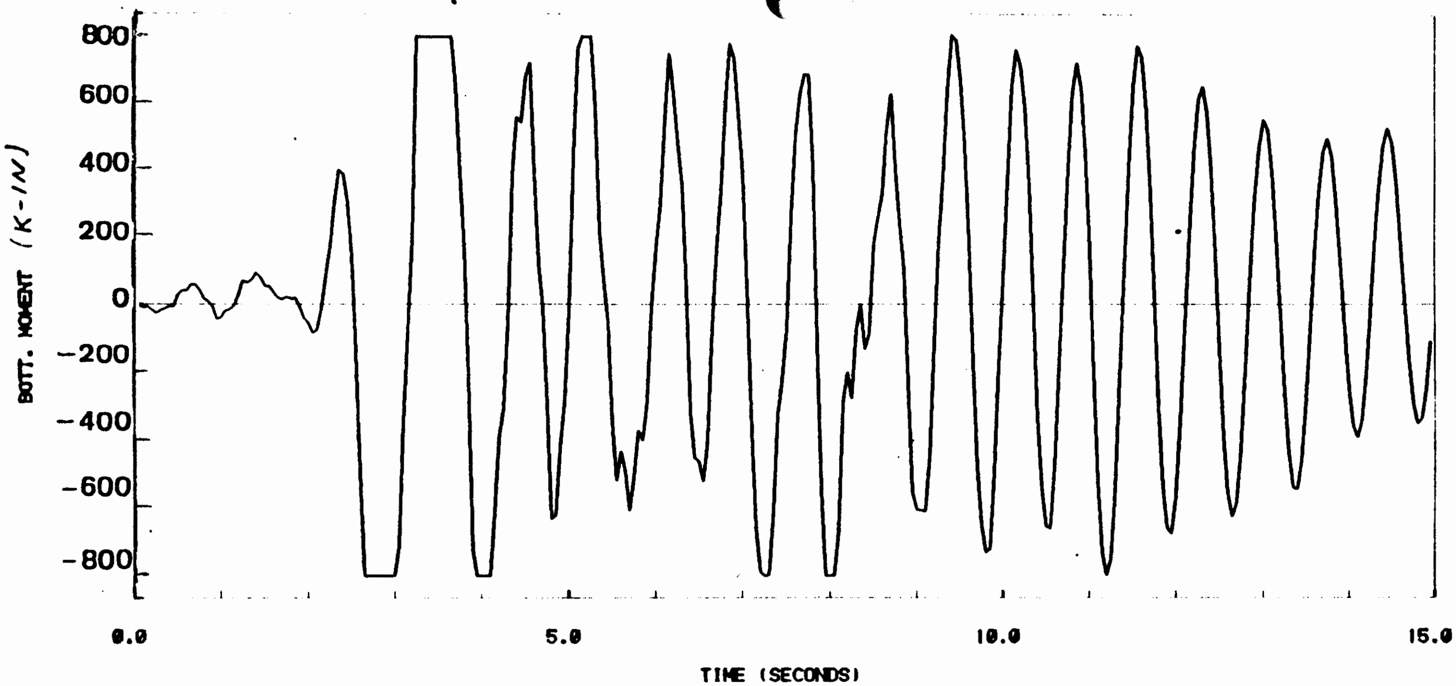

Fig. H.4A c)

CASE 4A

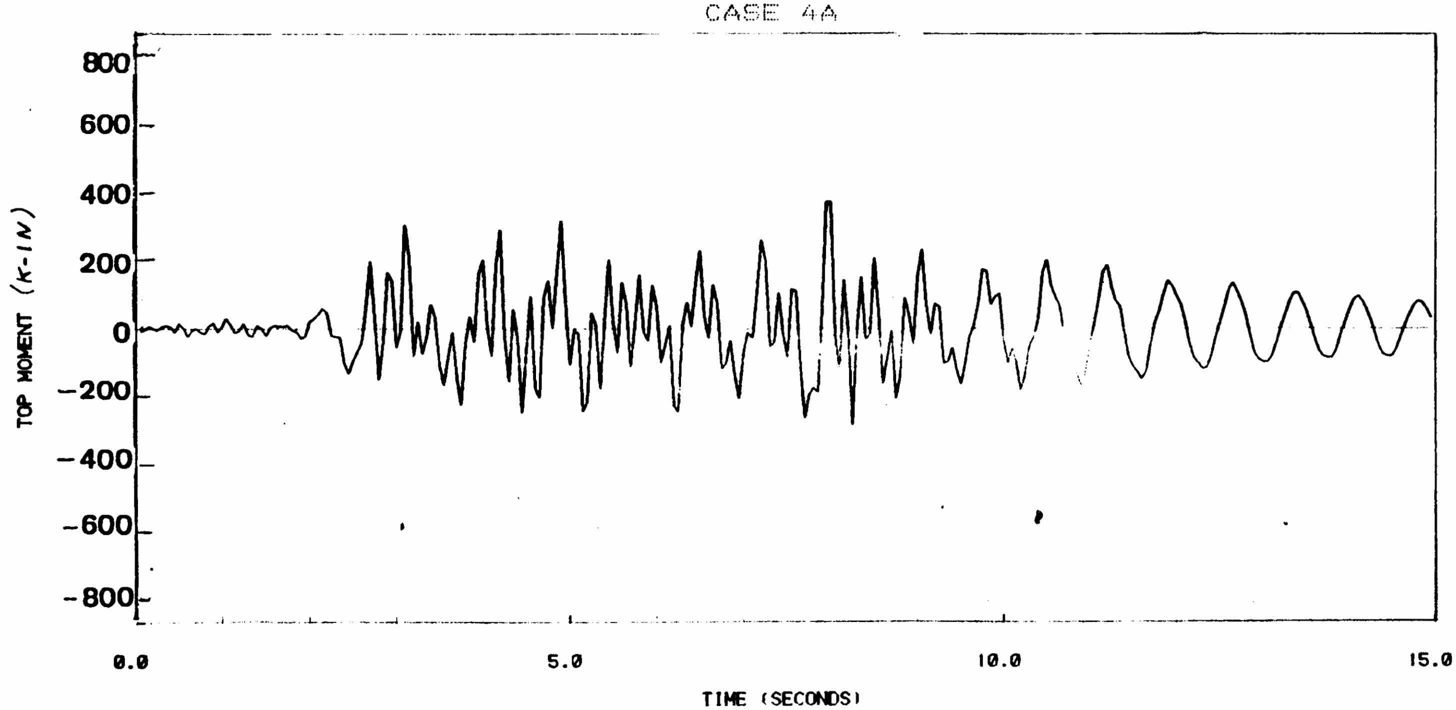

Fig. H.4A d)

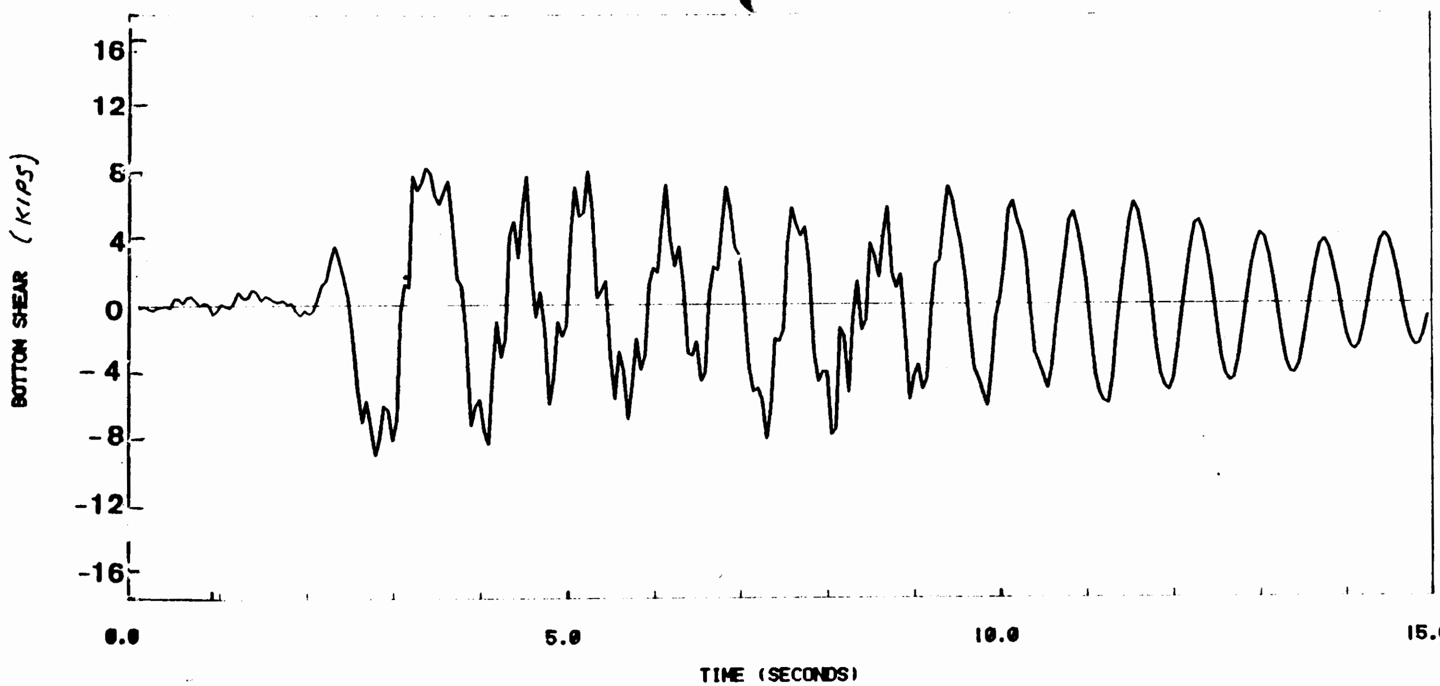

Fig. H. 4A e)

CASE 4A

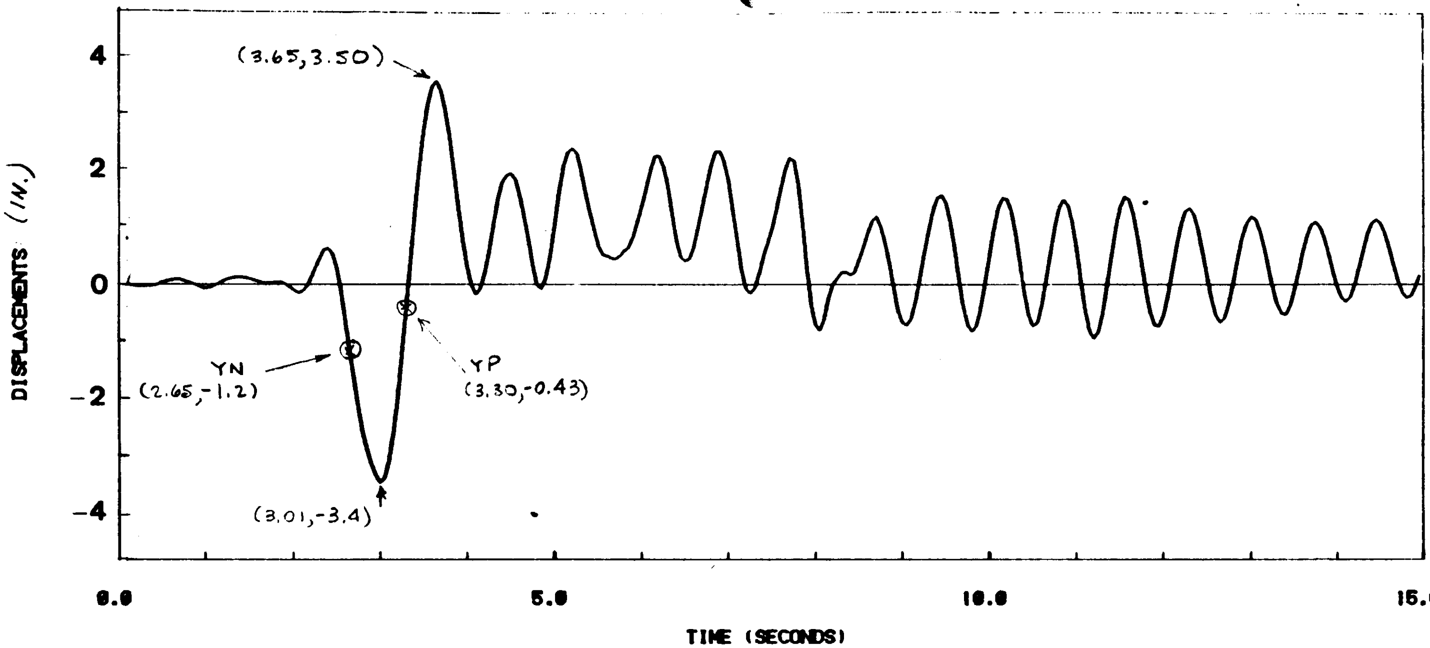

Fig. H.4B a)

CASE 4B

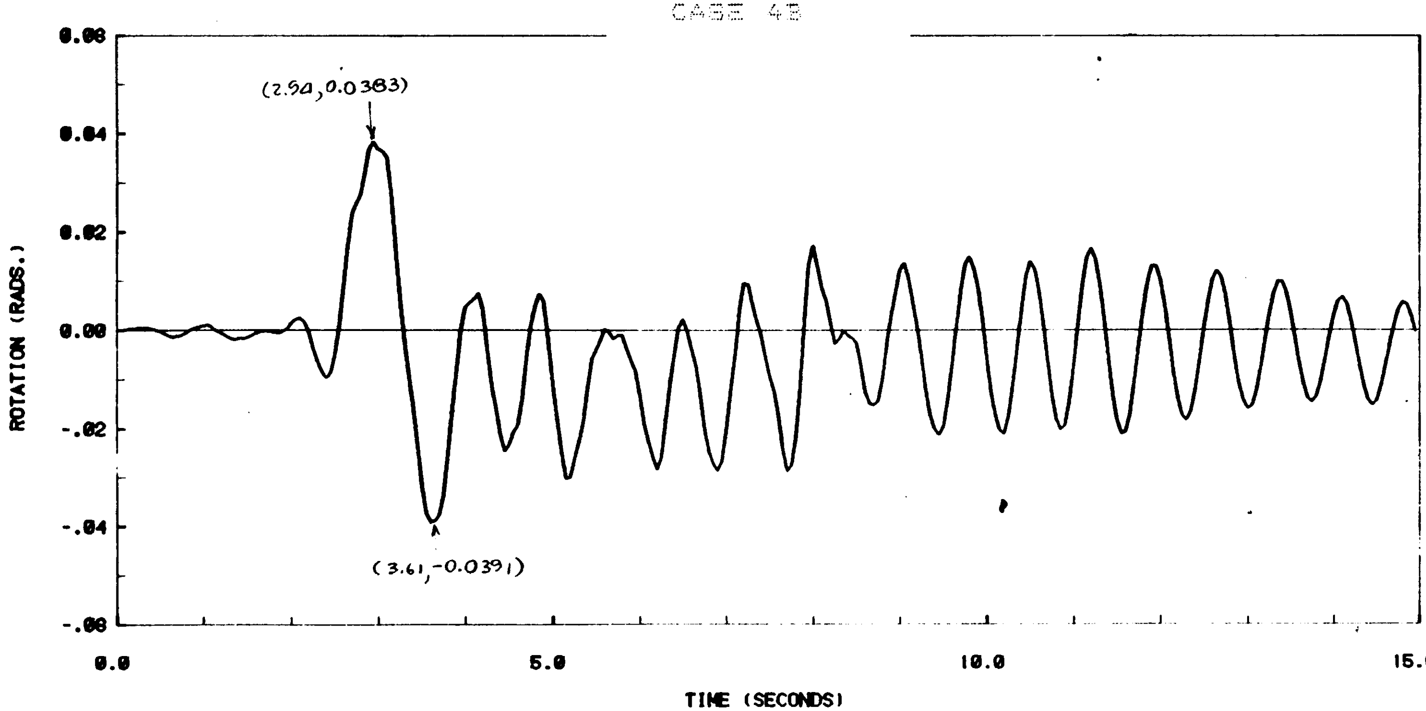

Fig. H.4B b)

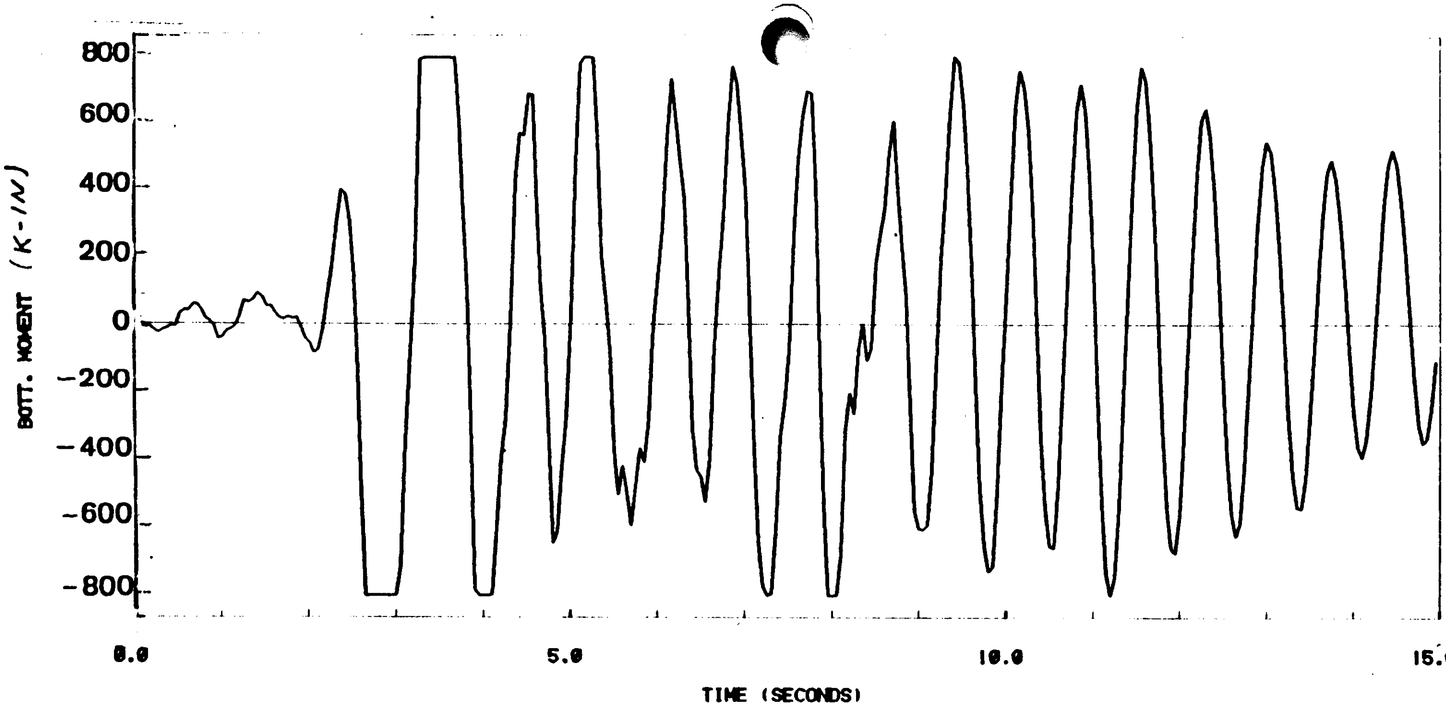

Fig. H.4B c)

CASE 43

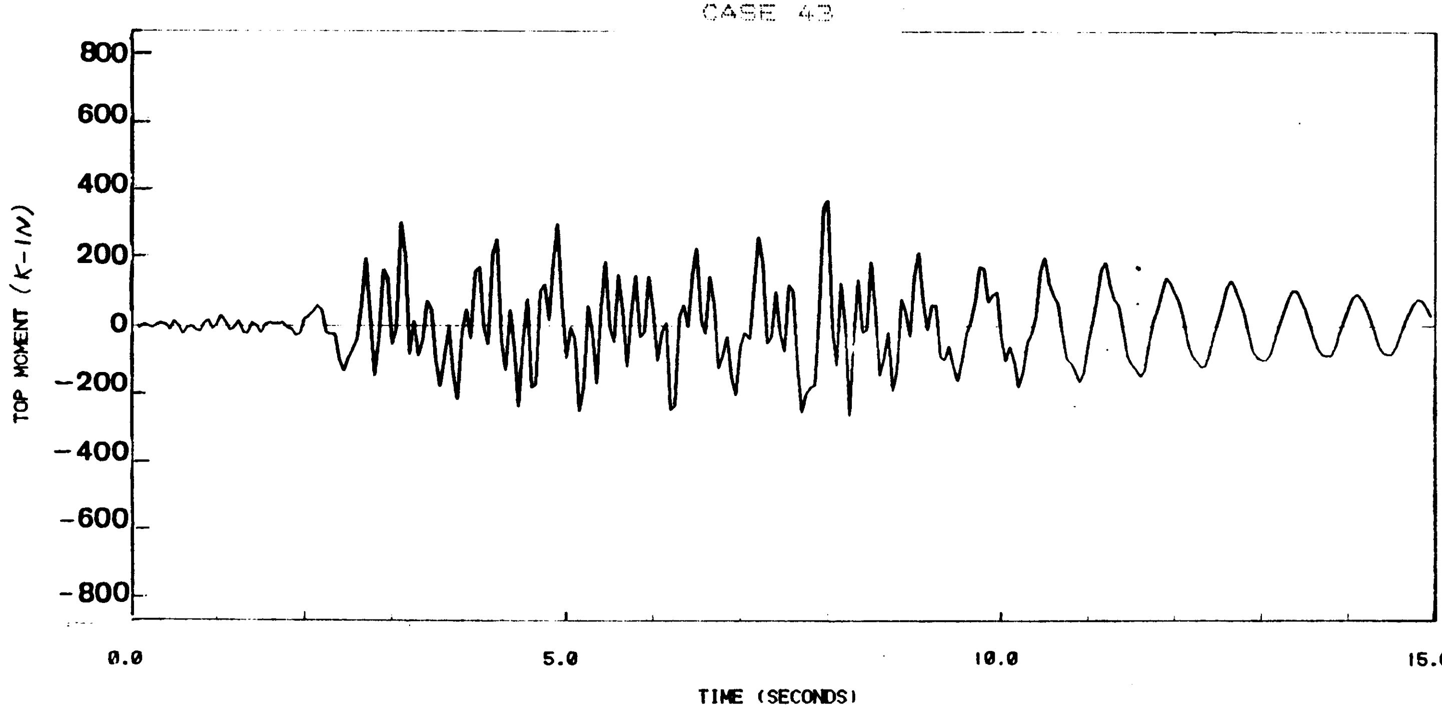

Fig. H.4B d)

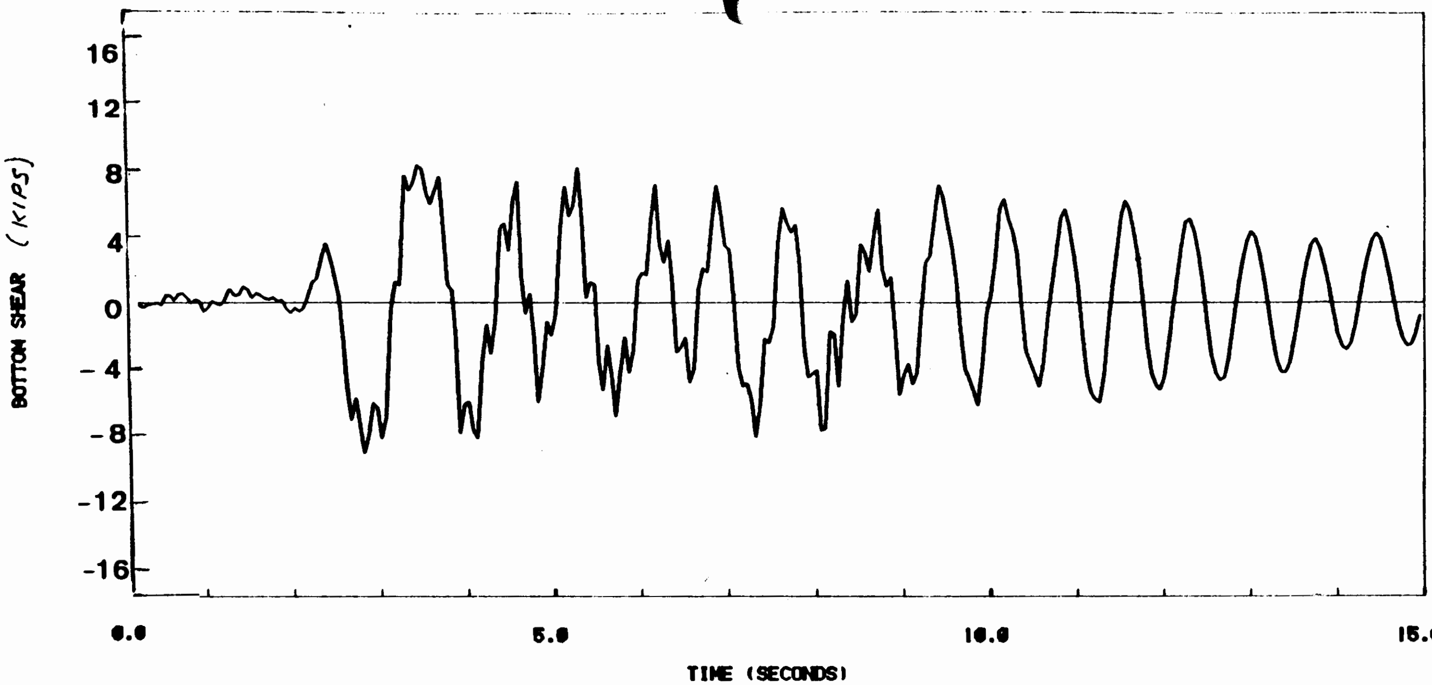

Fig. H.4B e)

CASE 4B

CASES 5:

INELASTIC RESPONSE OF 2DOF CANOPY MODEL TO EL CENTRO UNNORMALIZED (RECORDED), PGA = 0.348 g

$EI = 6.28 \times 10^6$ k-in^2

$T_1 = 0.46$ sec ; $T_2 = 0.11$ sec

$M_y = 800$ k-in.

CASE	PEAK CLIPPED ACCELERATION	FIGURE
5A	0.3485g (unclipped)	H.5A
5B	0.25 g	H.5B
5C	0.20 g	H.5C
5D	0.15 g	H.5D

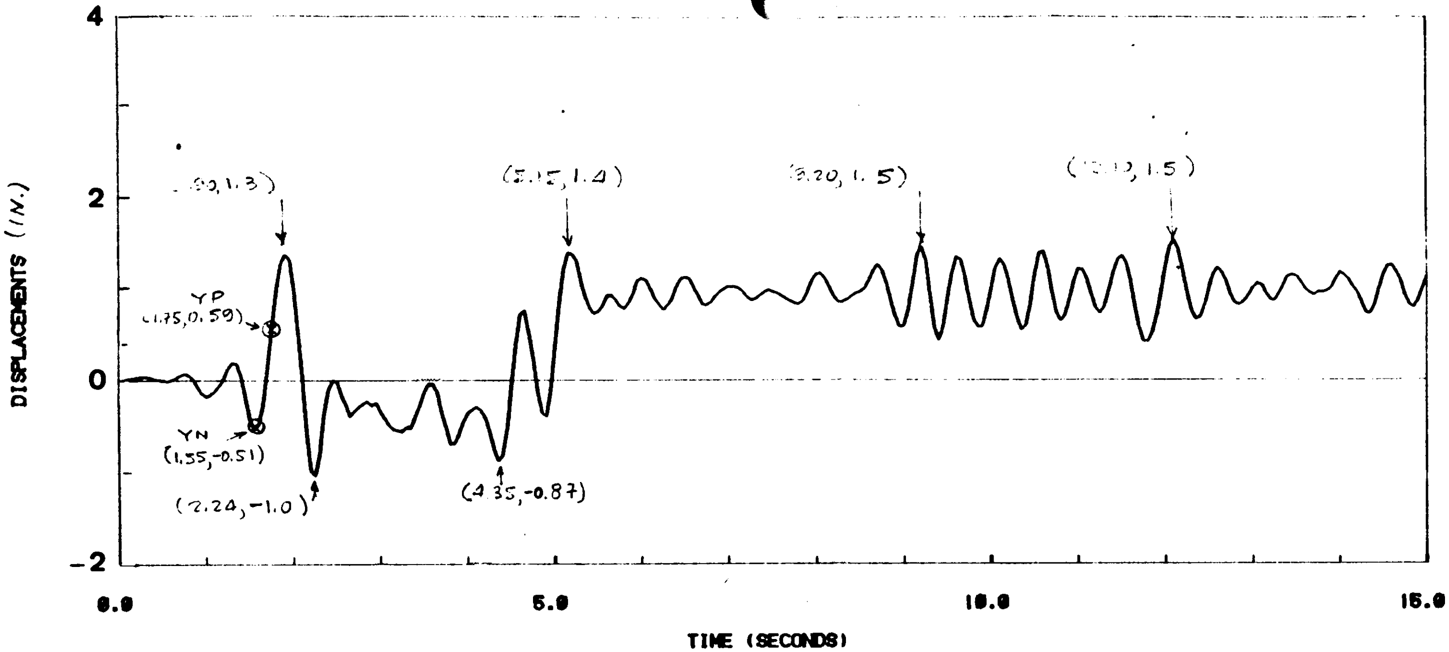

Fig. H.5A a)

CASE 5A

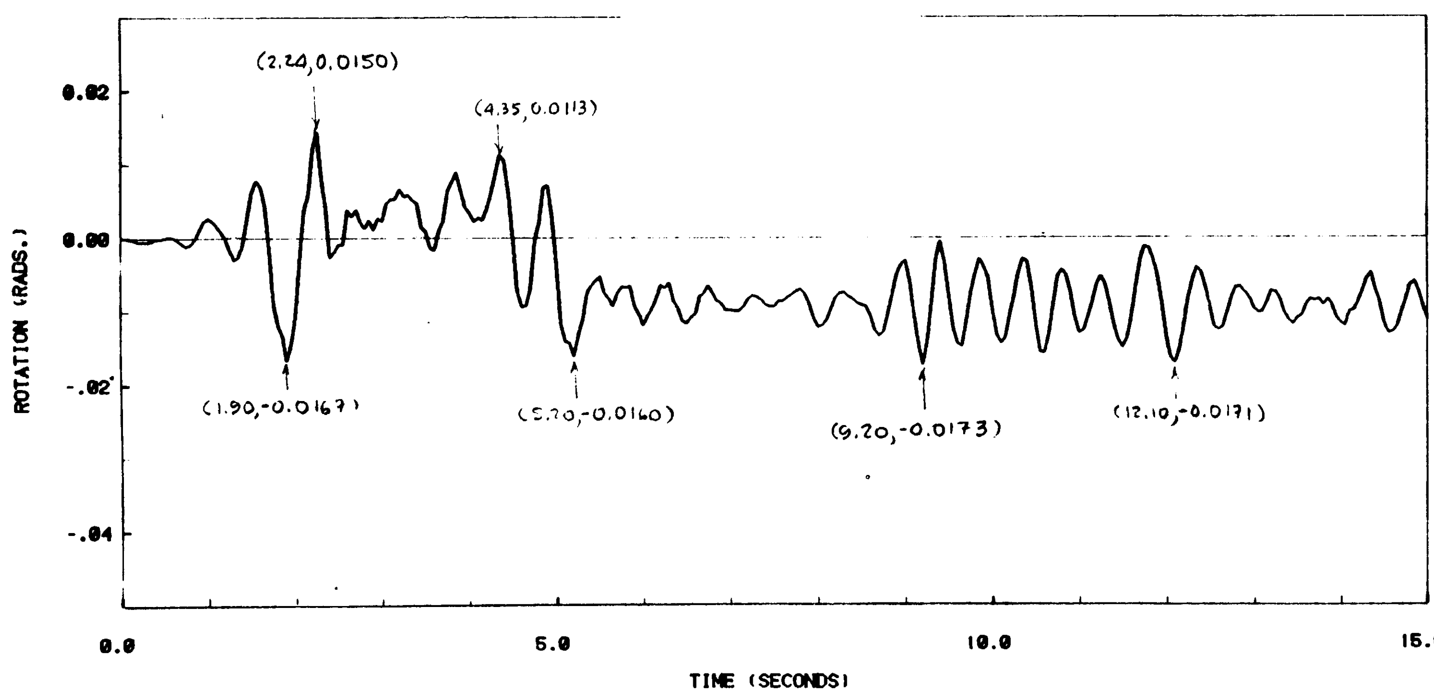

Fig. H.5A b)

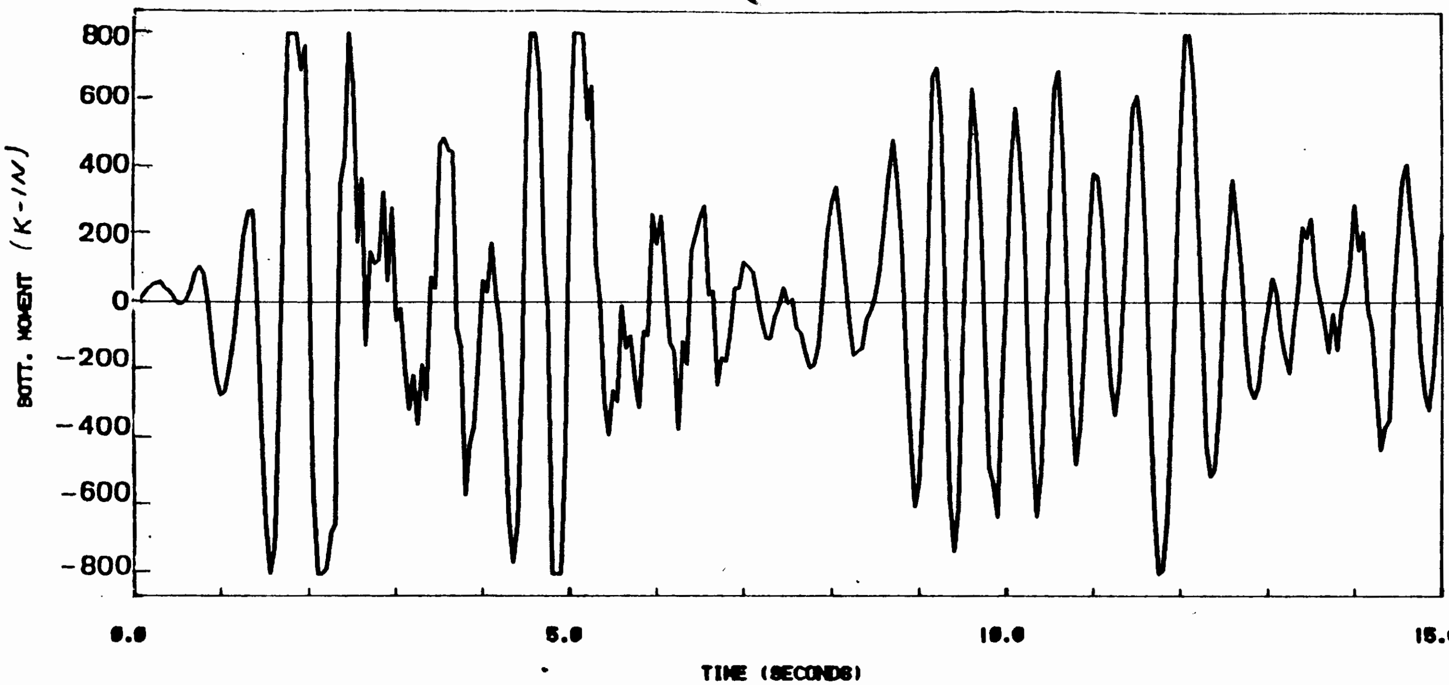

Fig. H. 5A c)

CASE 5A

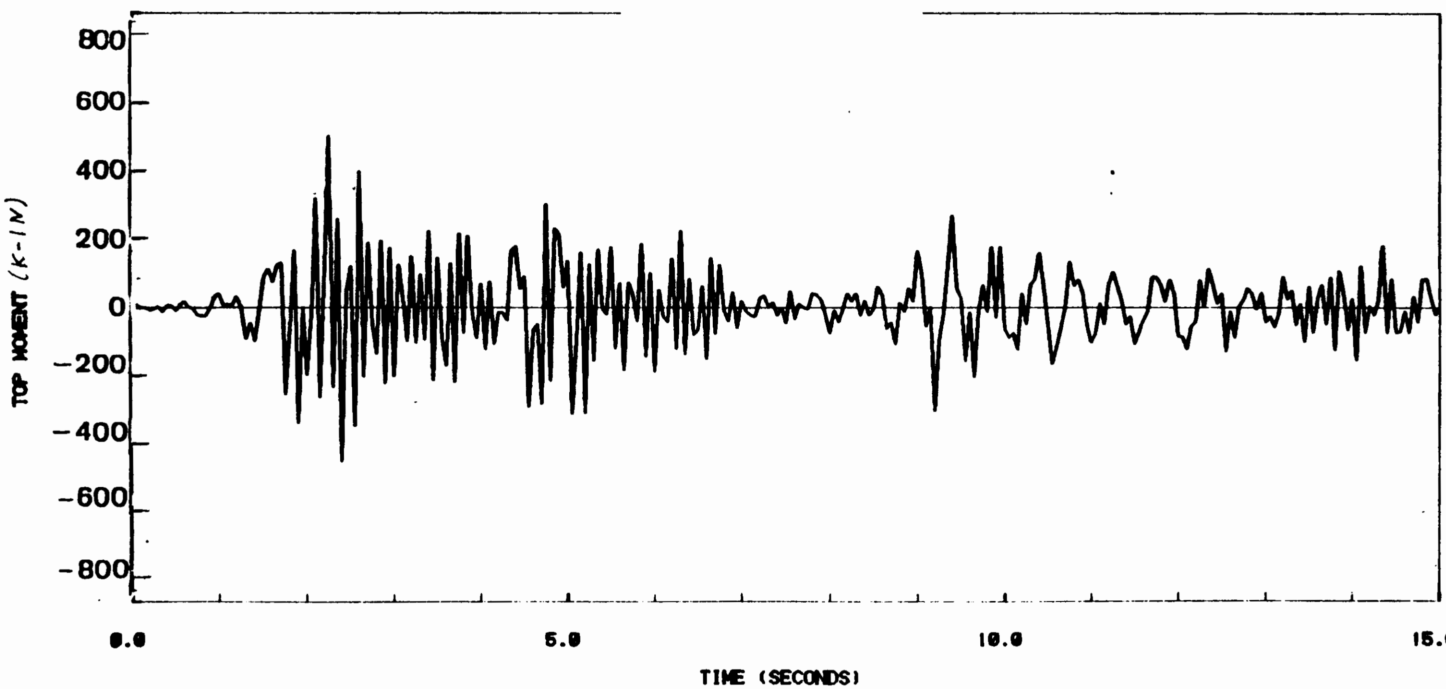

Fig. H. 5A d)

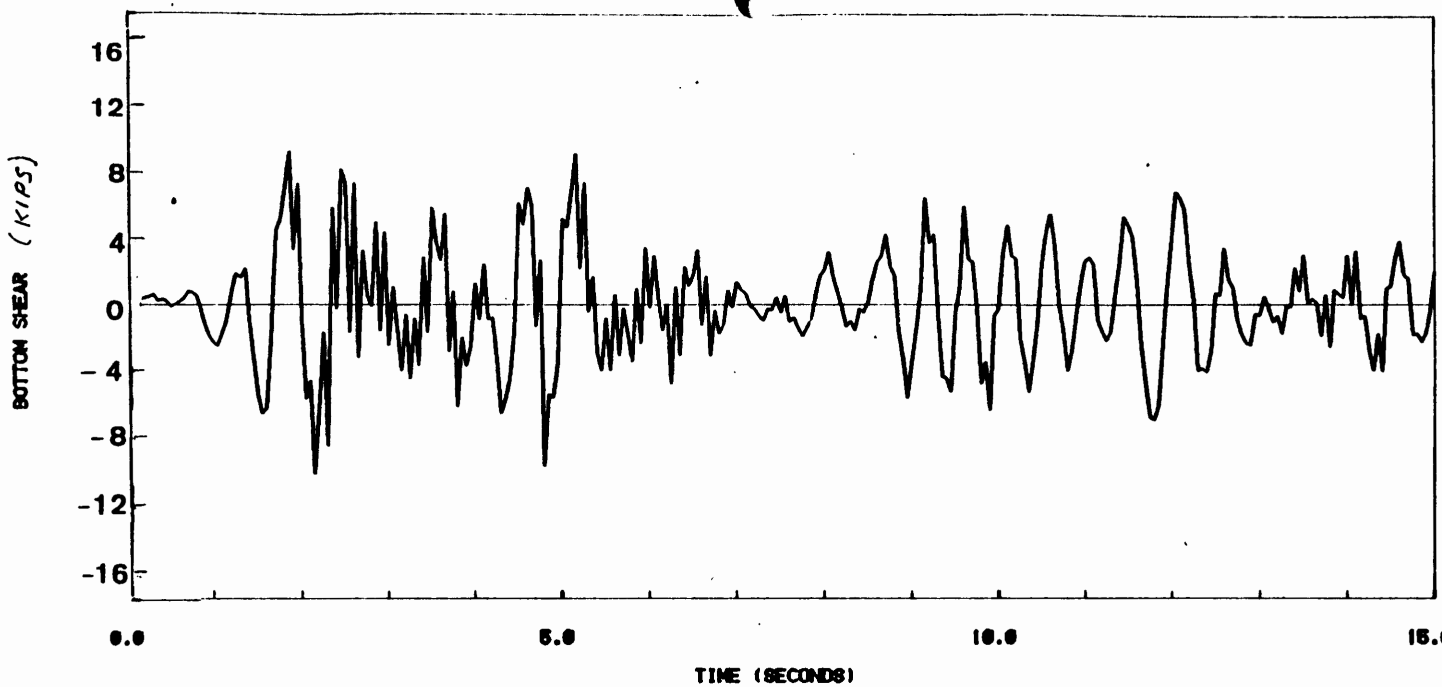

Fig. H.5A e)

CASE 5A

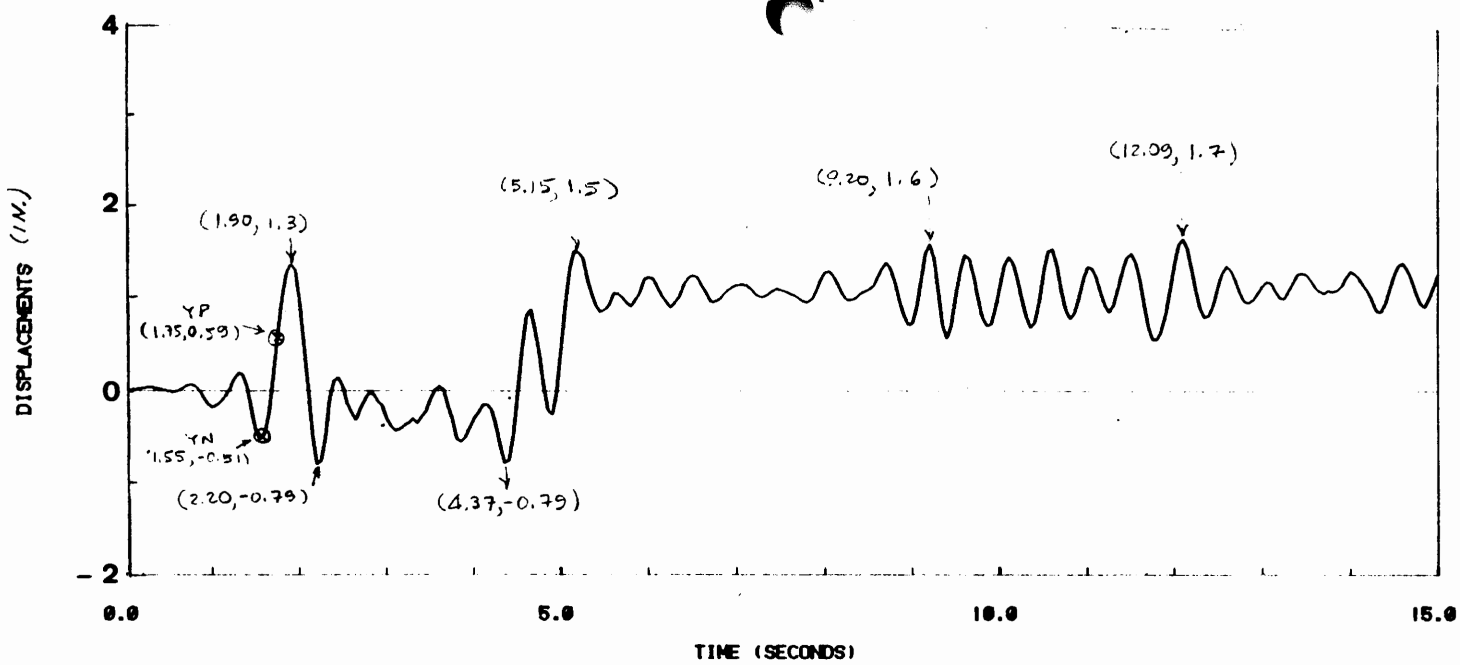

Fig. H.5B a)

CASE 53

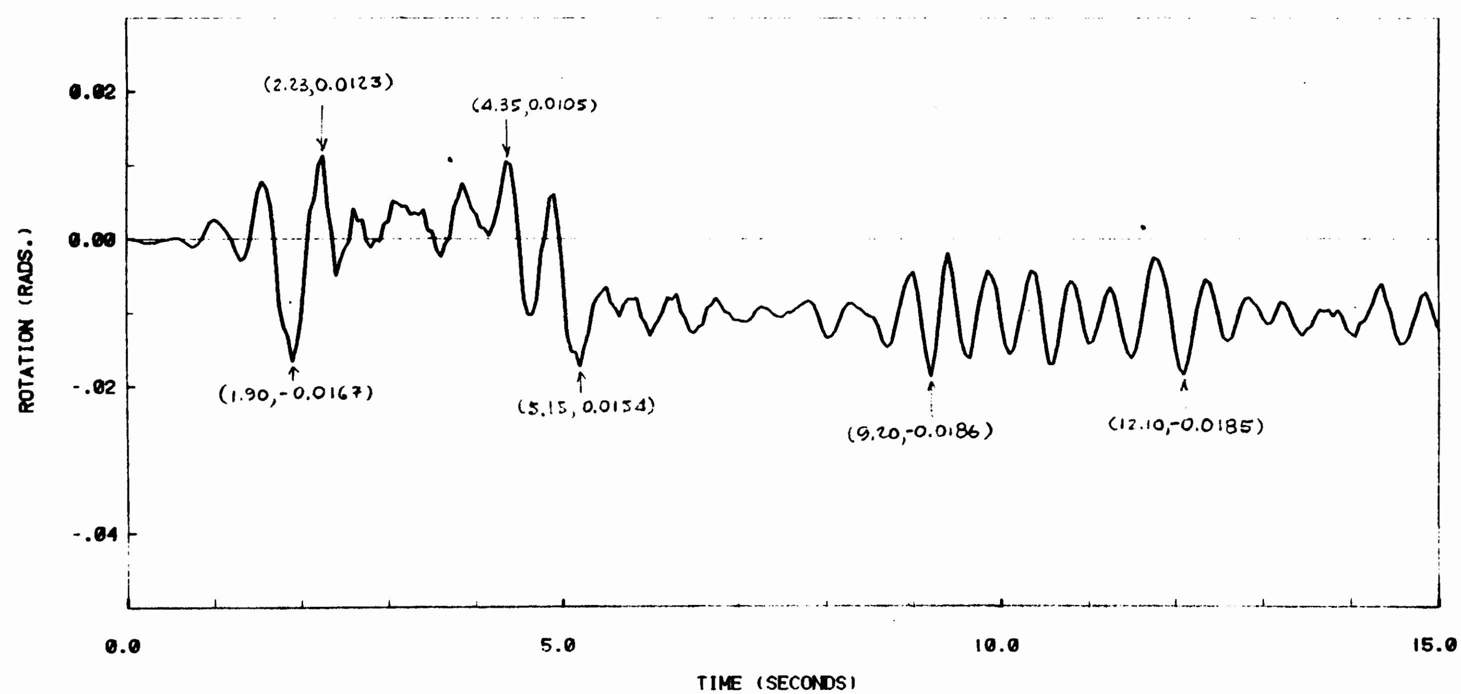

Fig. H.5B b)

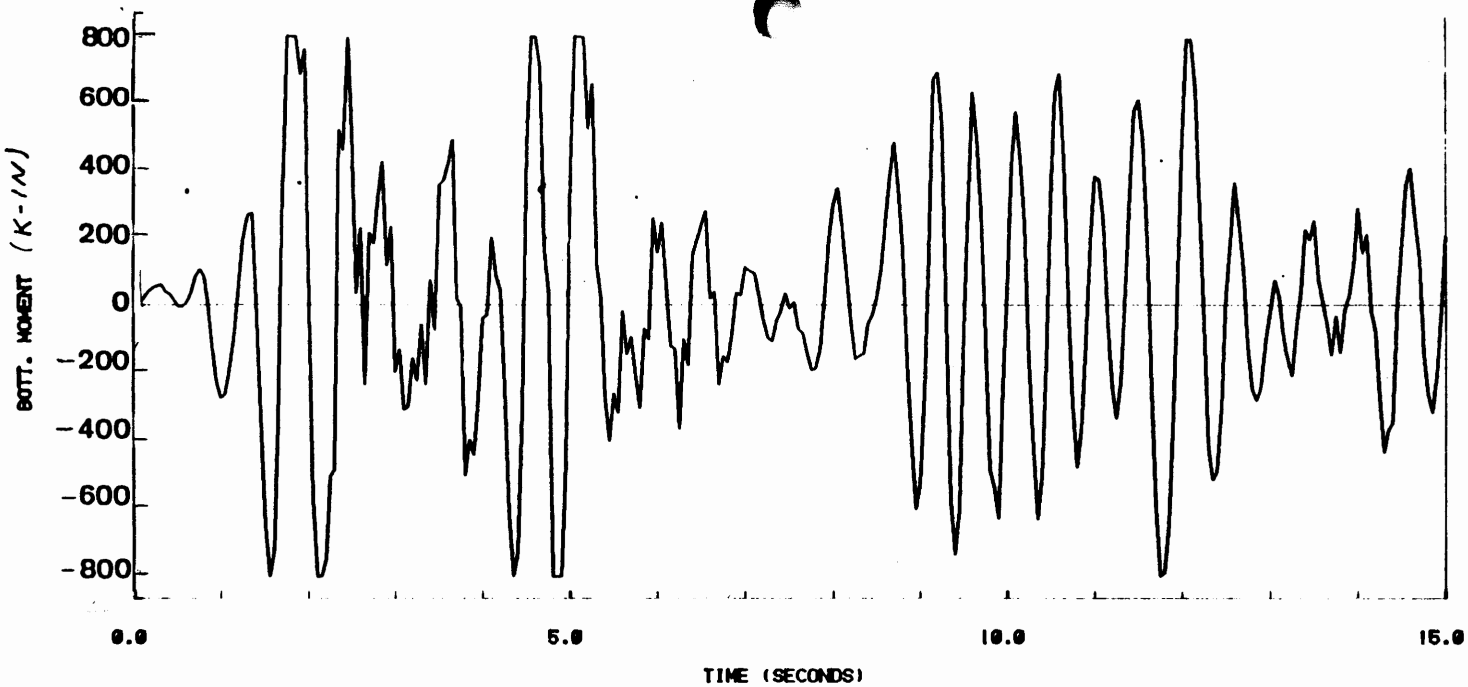

Fig. H.5B c)

CASE 5B

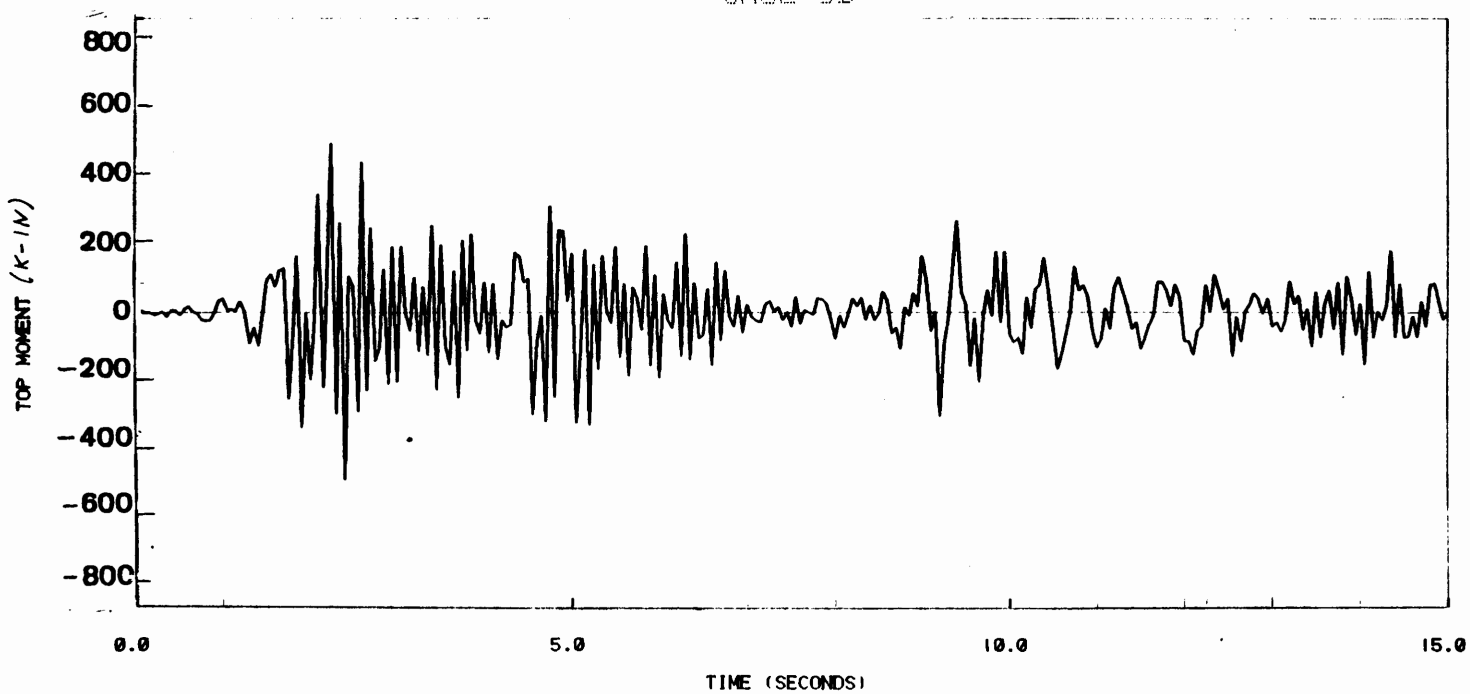

Fig. H.5B d)

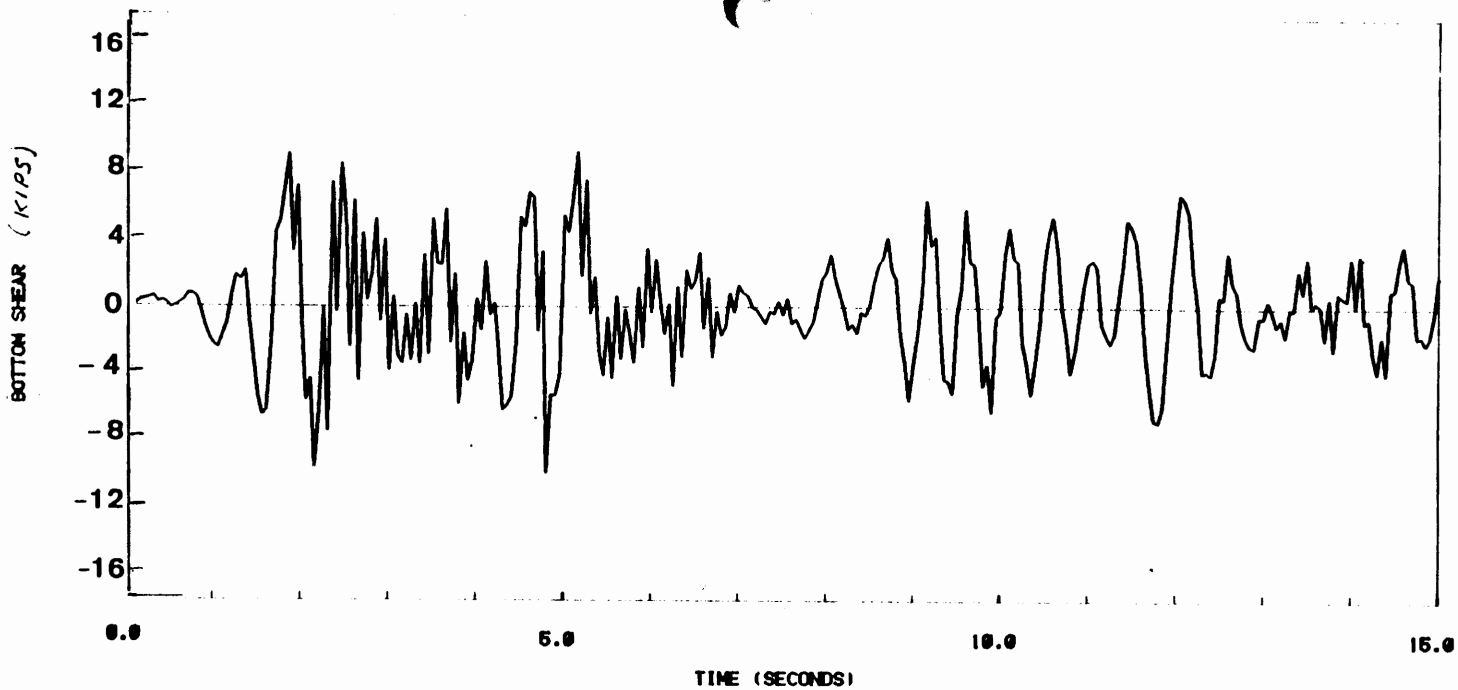

CASE 5B

Fig. H.5B e)

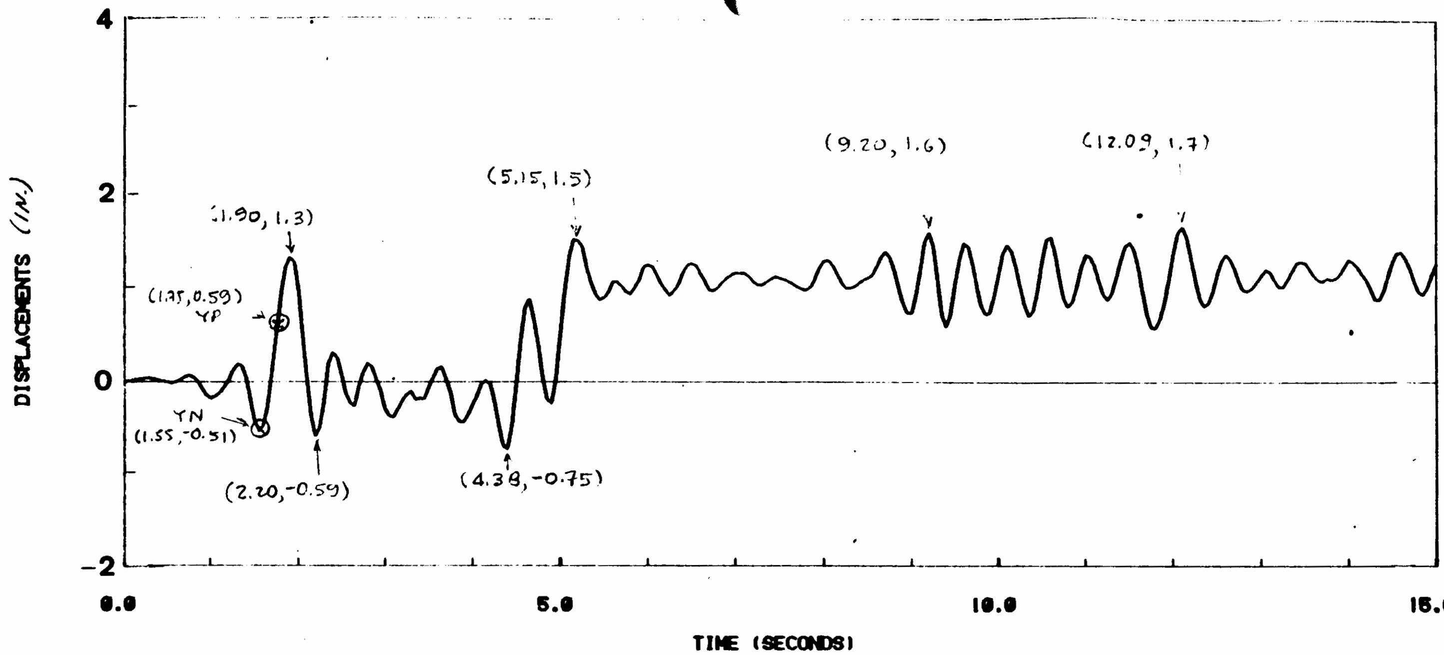

Fig. H. 5C a)

CASE 5C

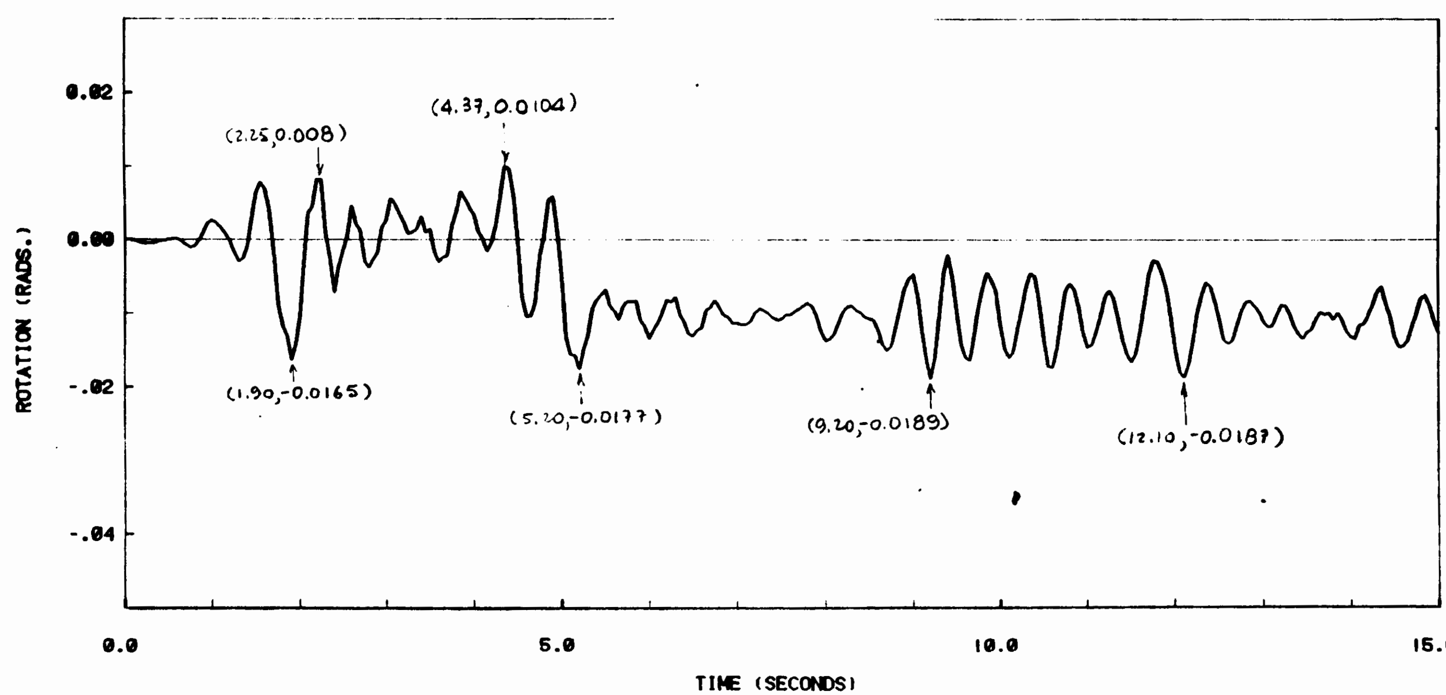

Fig. H. 5C b)

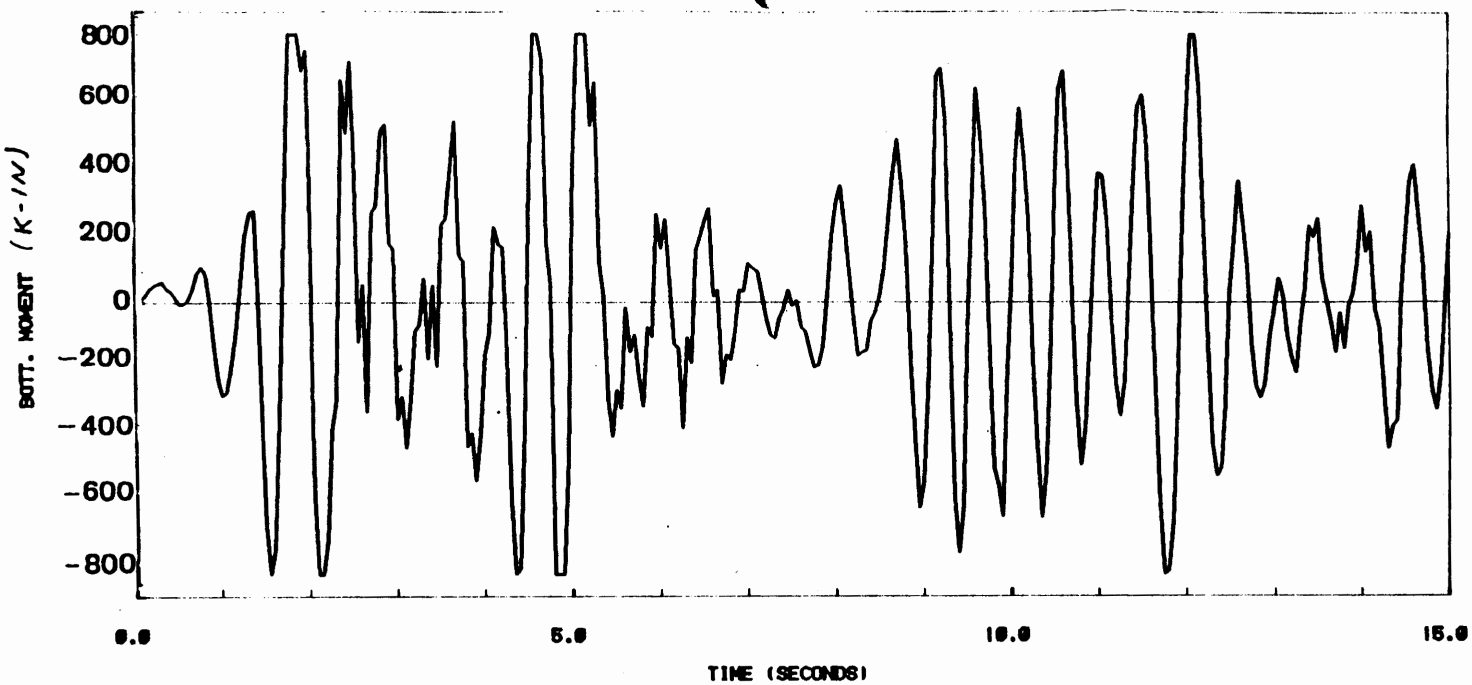

Fig. H.5C c)

CASE 5C

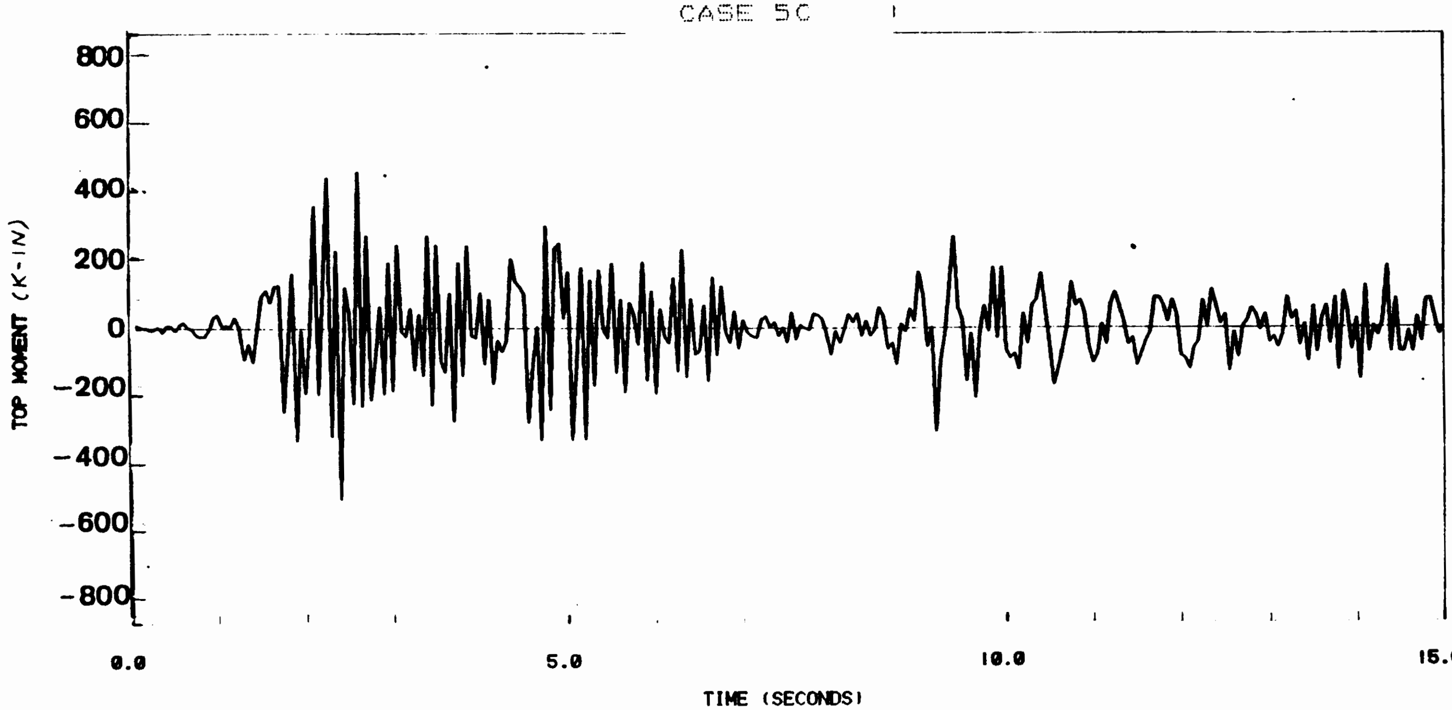

Fig. H.5C d)

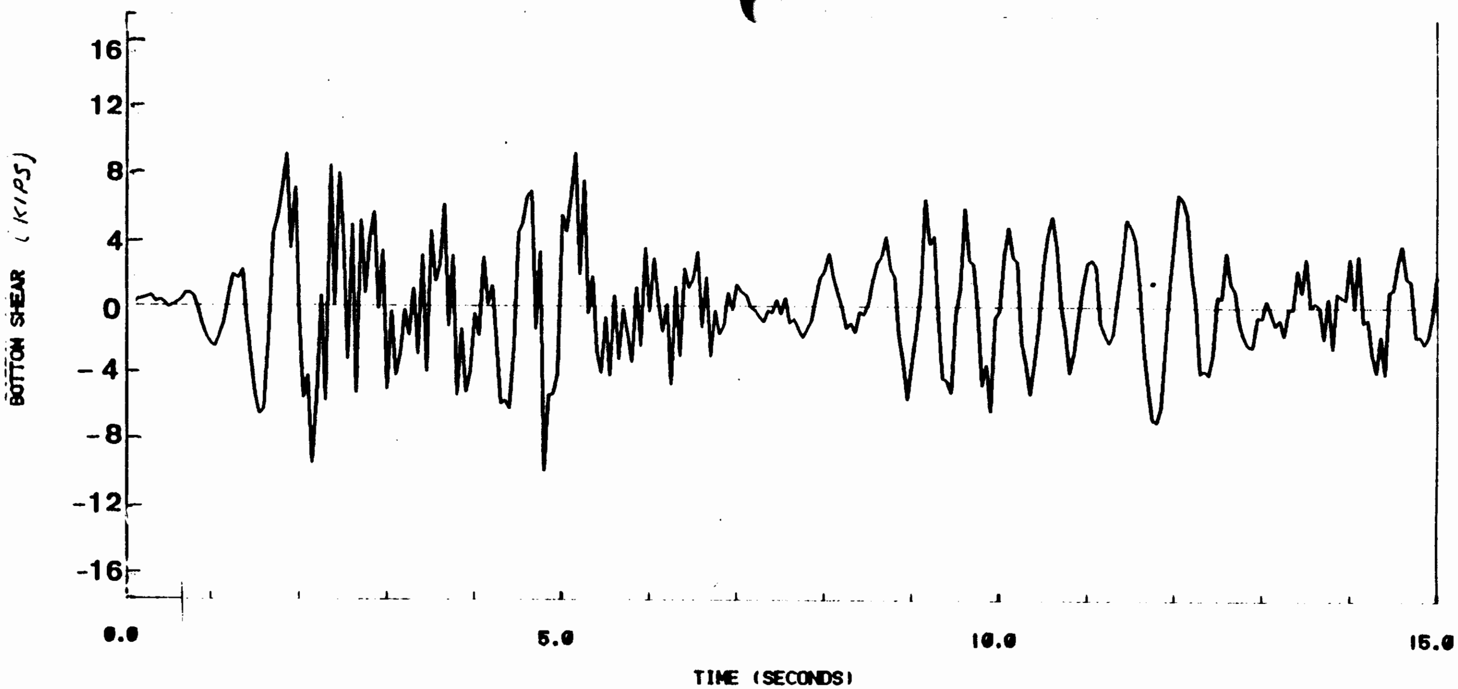

CASE 5C

Fig. H.5C e)

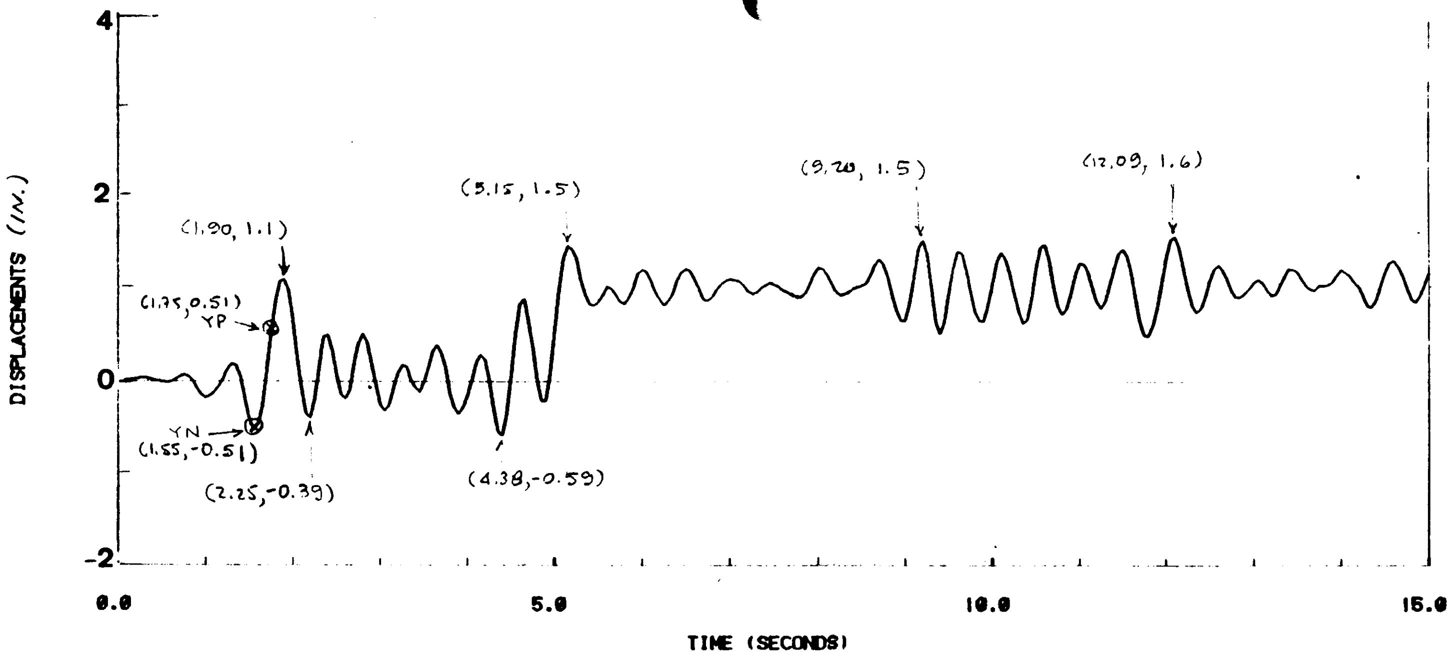

Fig. H.5D a)

CASE 5D

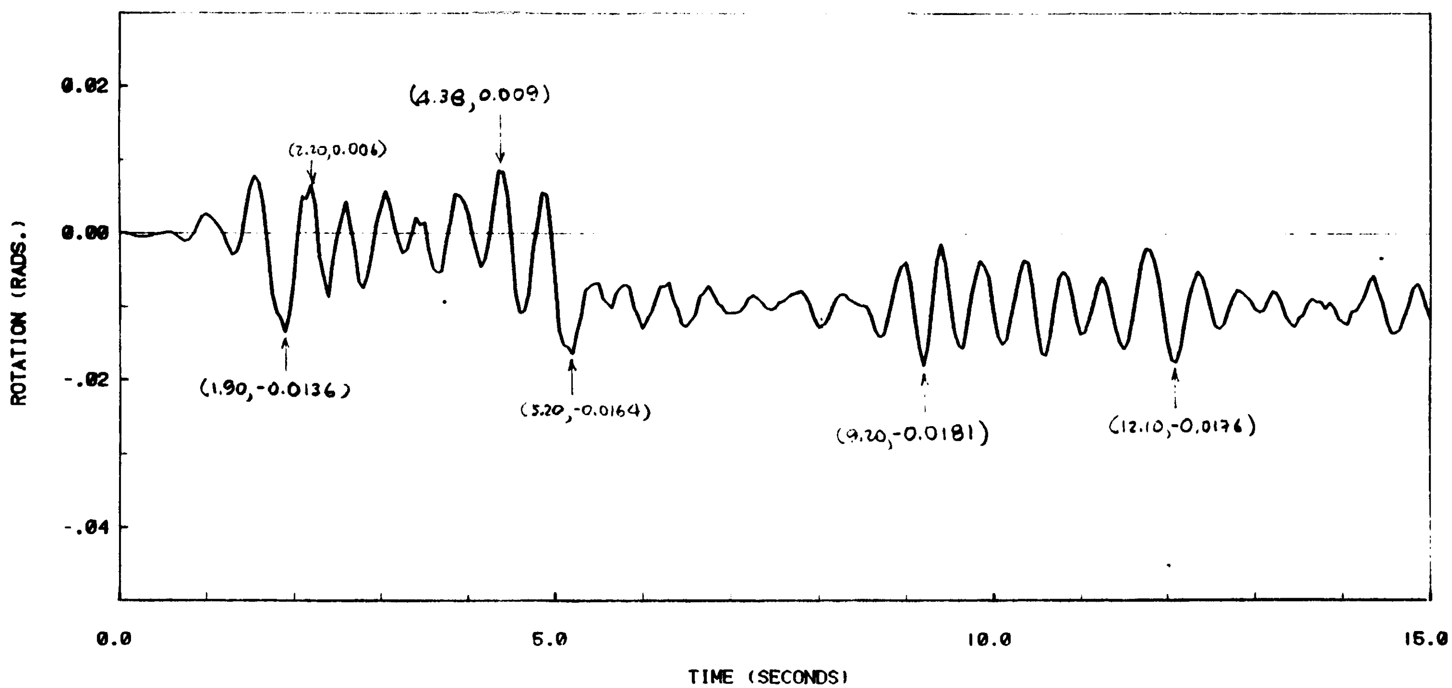

Fig. H.5D b)

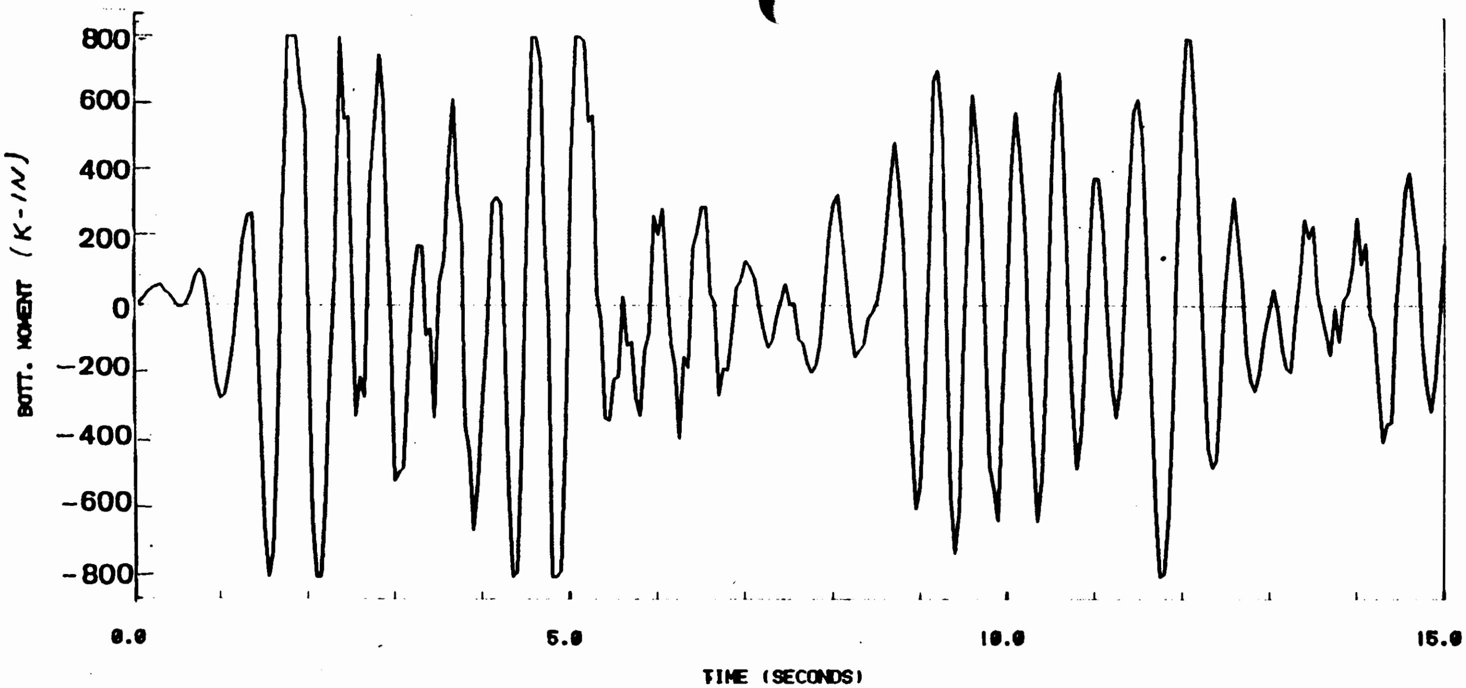

Fig. H.5D c)

CASE 5D

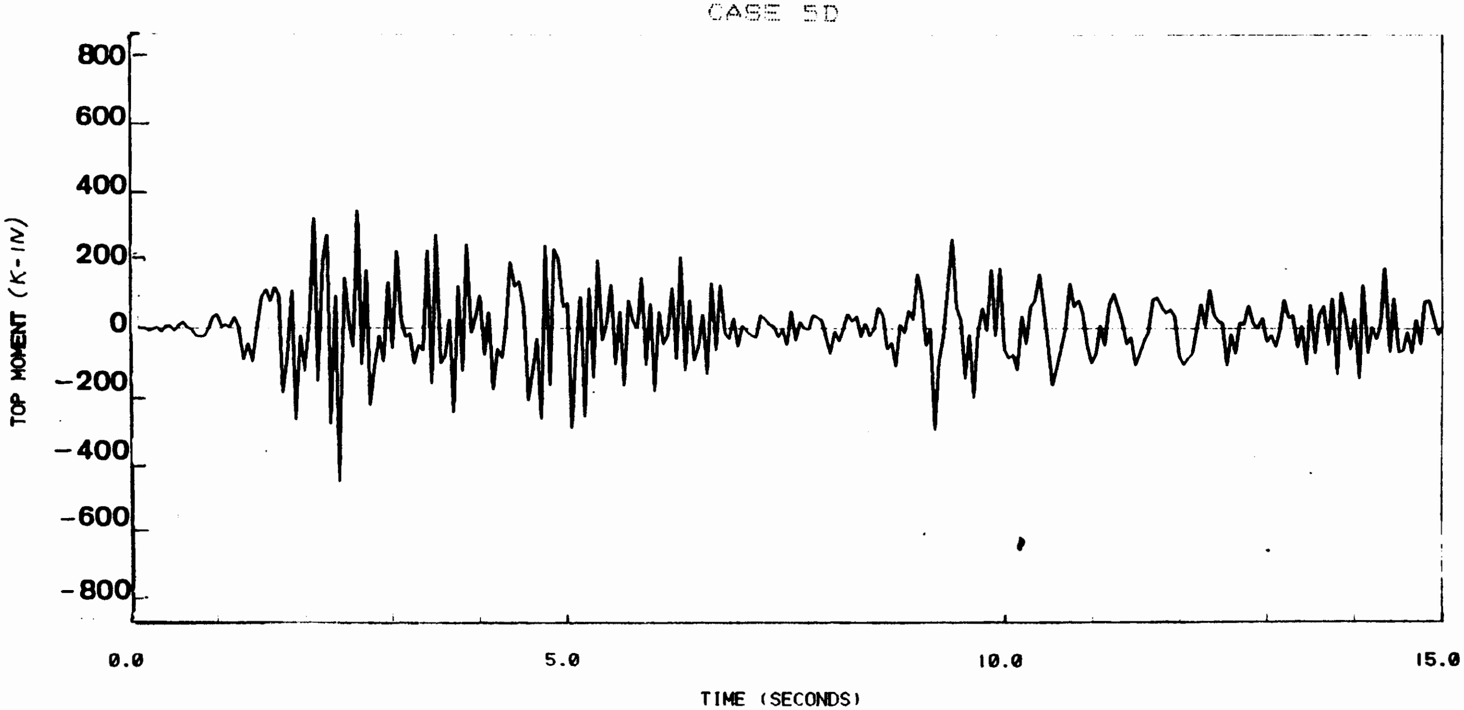

Fig. H.5D d)

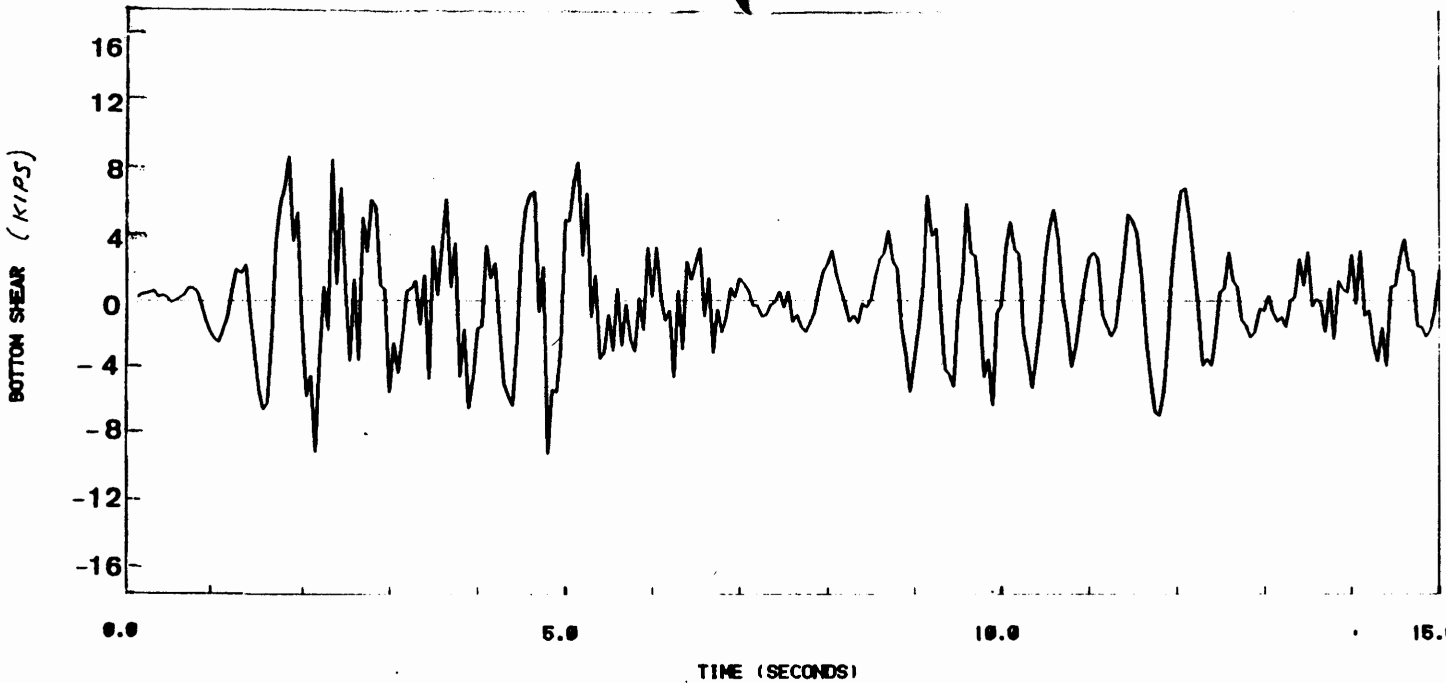

CASE 5D

Fig. H.5D e)

CASES 6:

INELASTIC RESPONSE OF 2DOF CANOPY MODEL TO EL CENTRO UNNORMALIZED (RECORDED), PGA = 0.348 g

$EI = 2.62 \times 10^{6}$ k-in.^{2}

$T_1 = 0.72$ sec ; $T_2 = 0.18$ sec

$M_y = 800$ k-in.

CASE	PEAK CLIPPED ACCELERATION	FIGURE
6A	0.3485g (unclipped)	H.6A
6B	0.30g	H.6B
6C	0.25g	H.6C

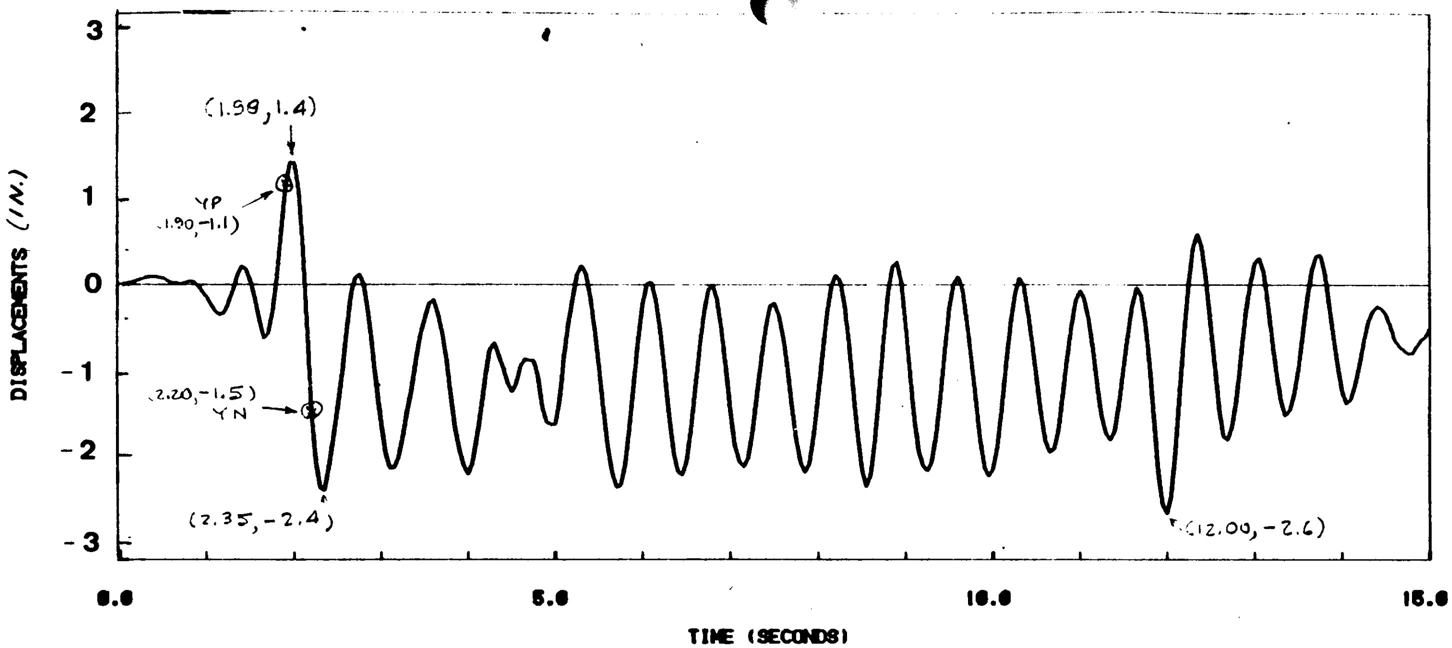

Fig. H. 6A a)

CASE 6A

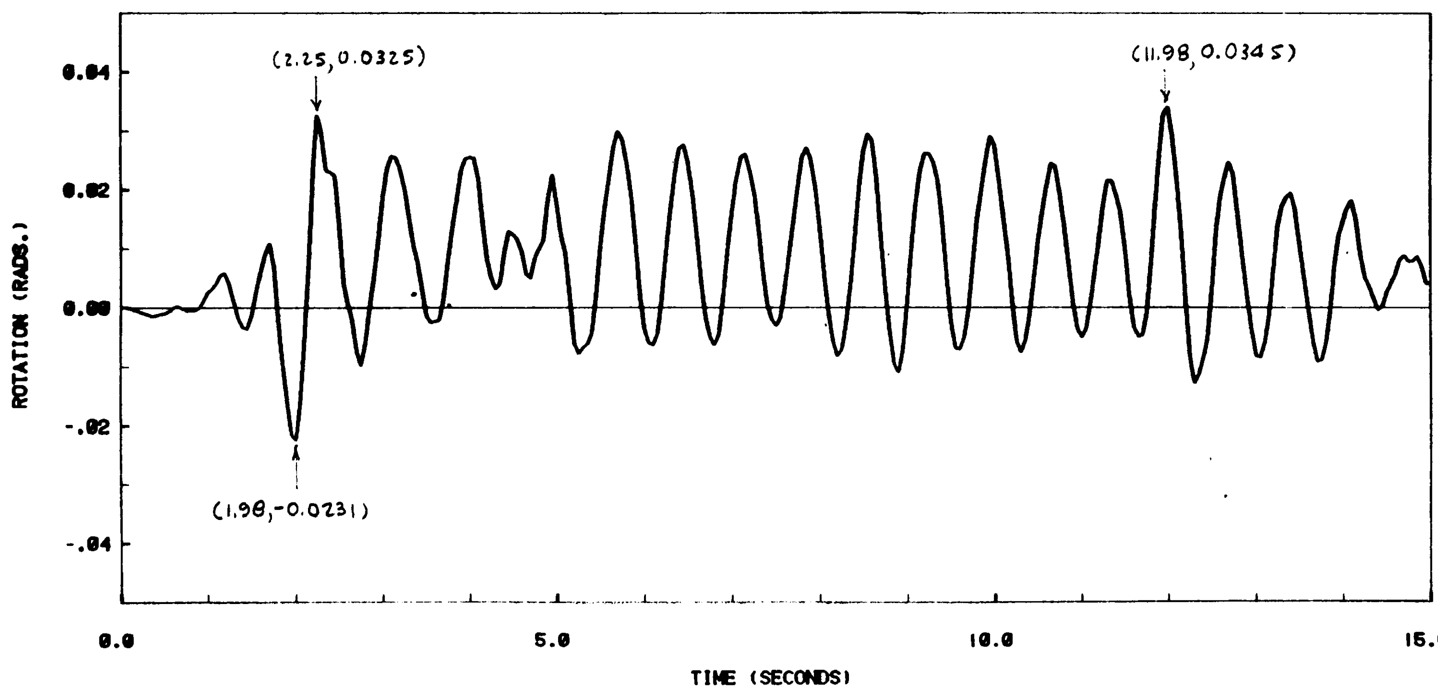

Fig. H. 6A b)

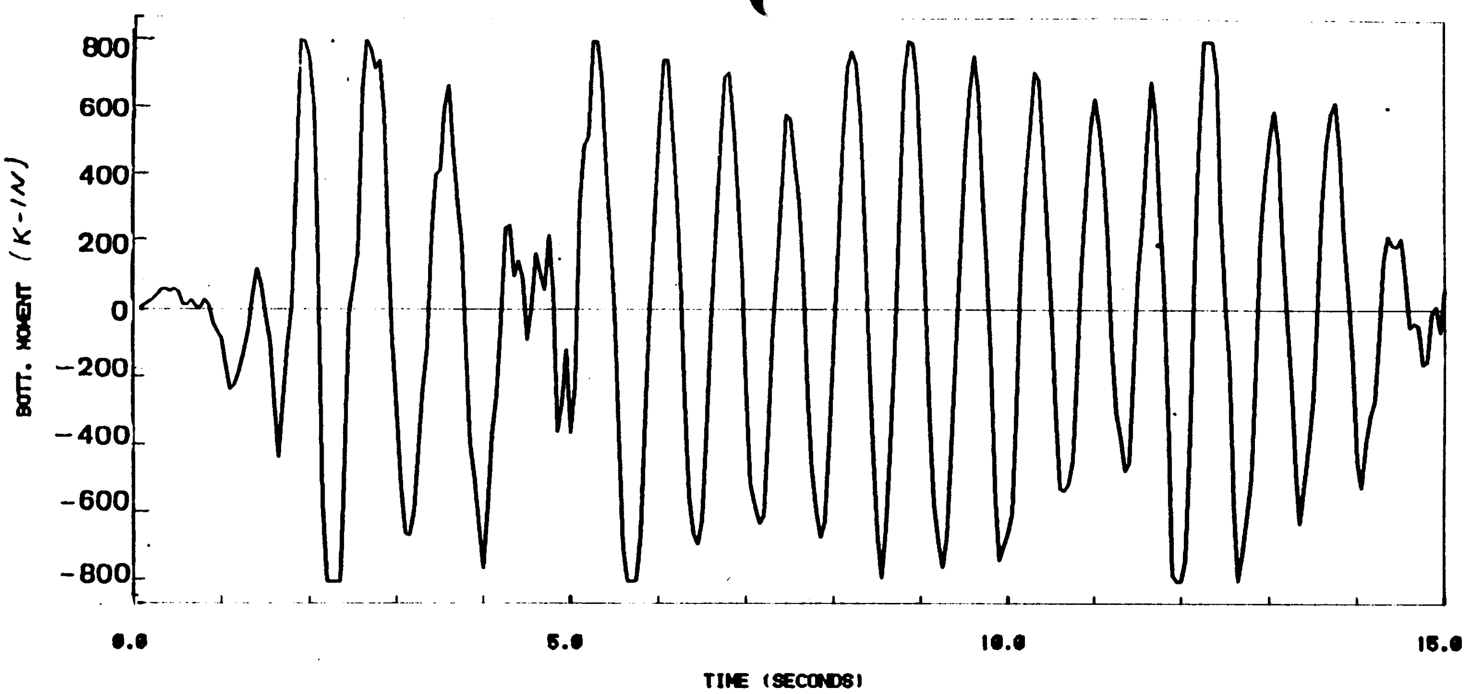

Fig. H.6A c)

CASE 6A

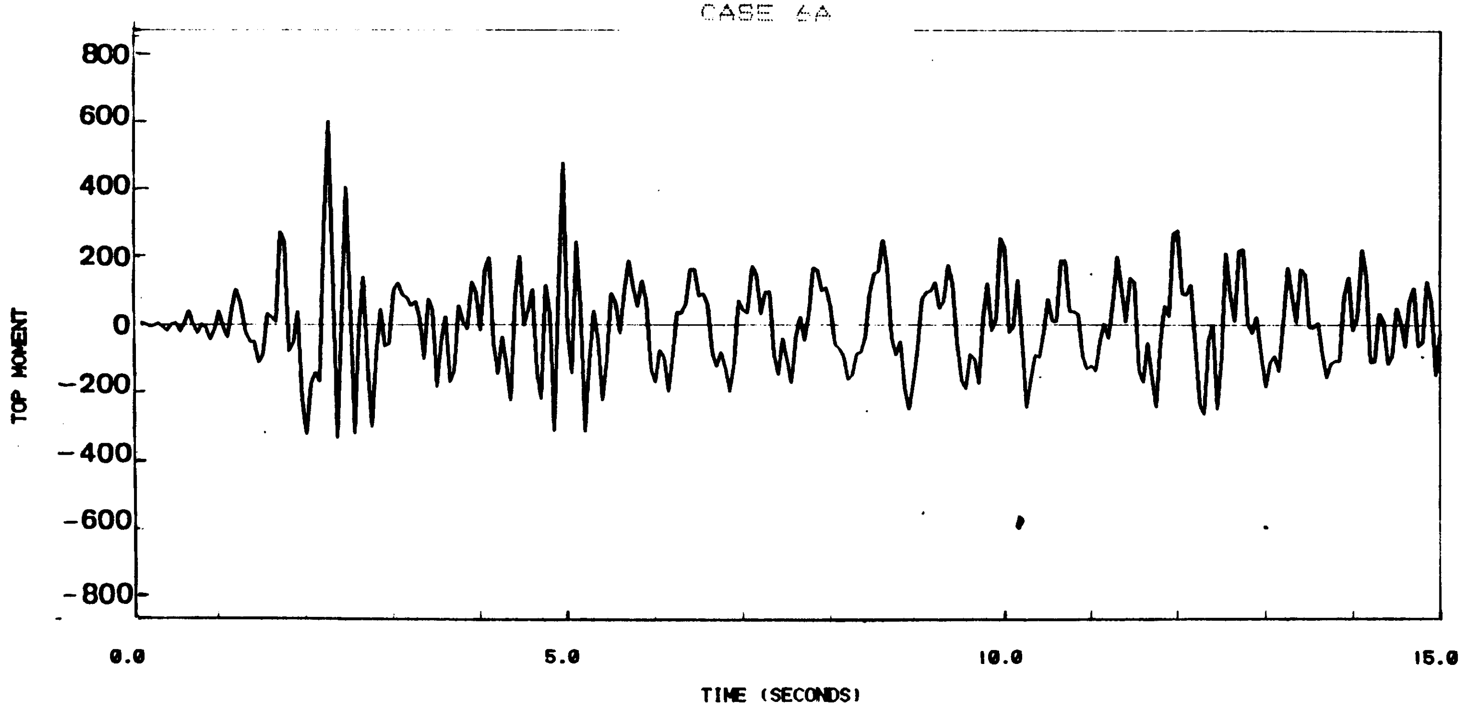

Fig. H.6A d)

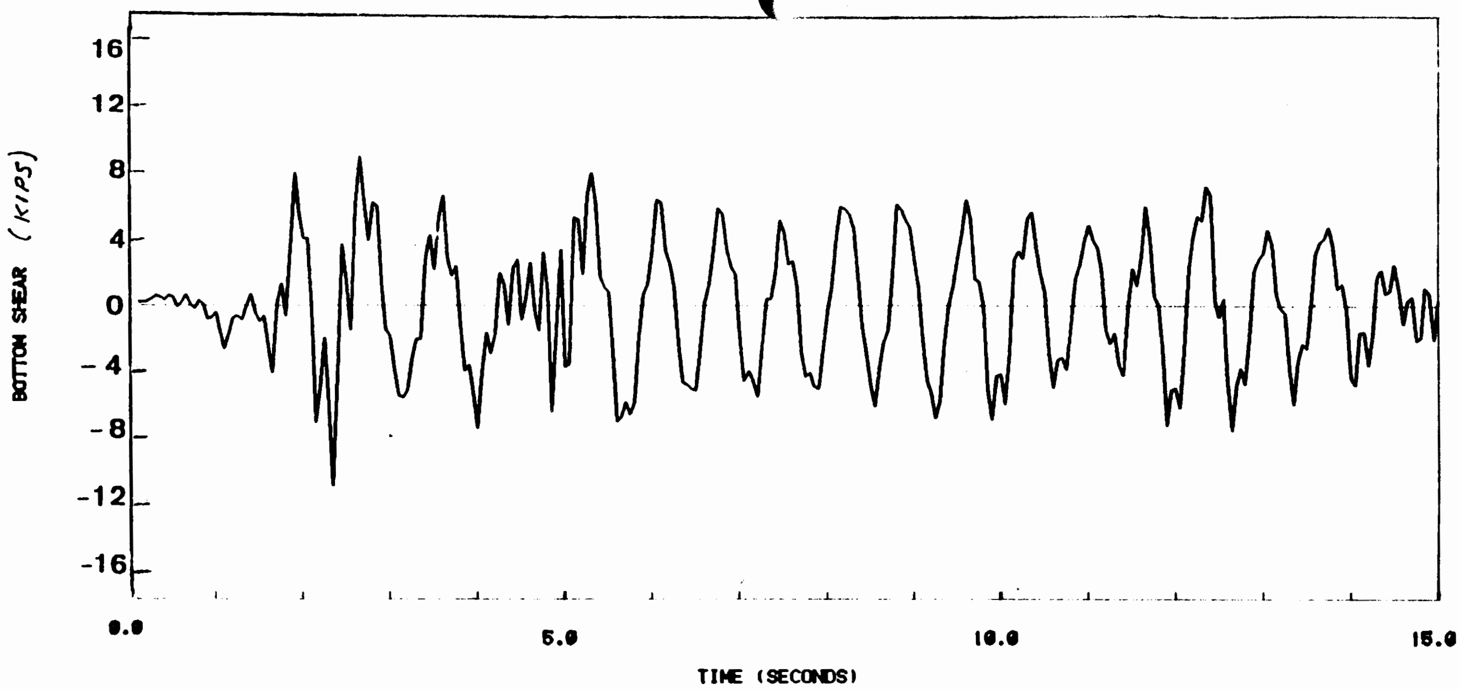

CASE 6A

Fig. H.6A e)

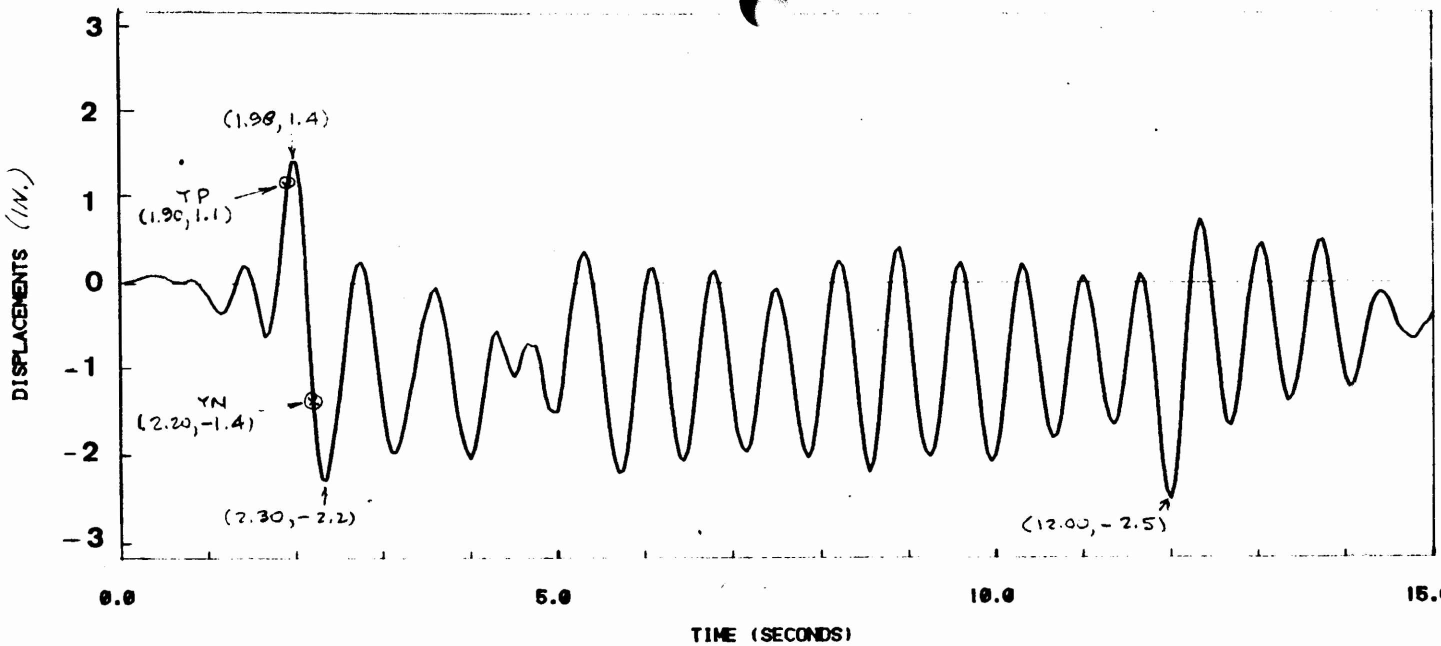

Fig. H.6B a)

CASE 6B

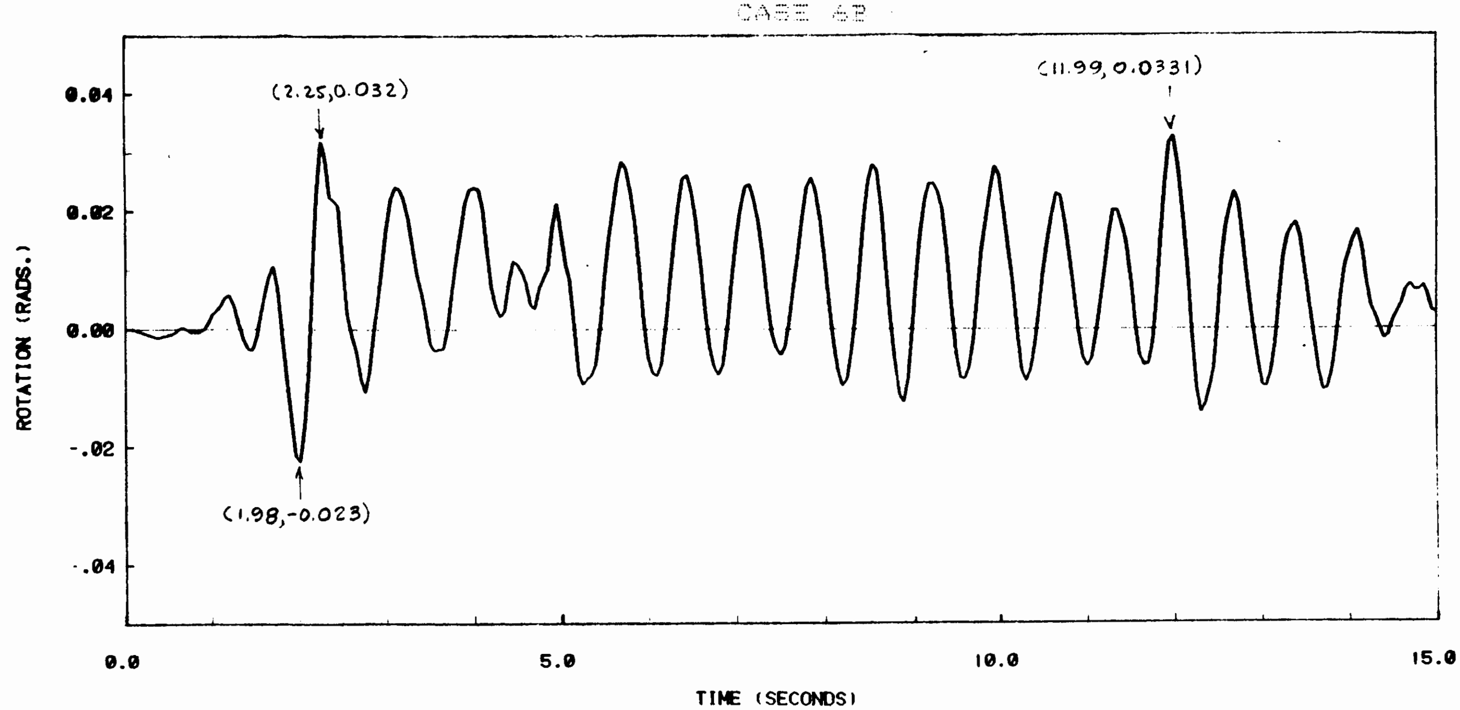

Fig. H.6B b)

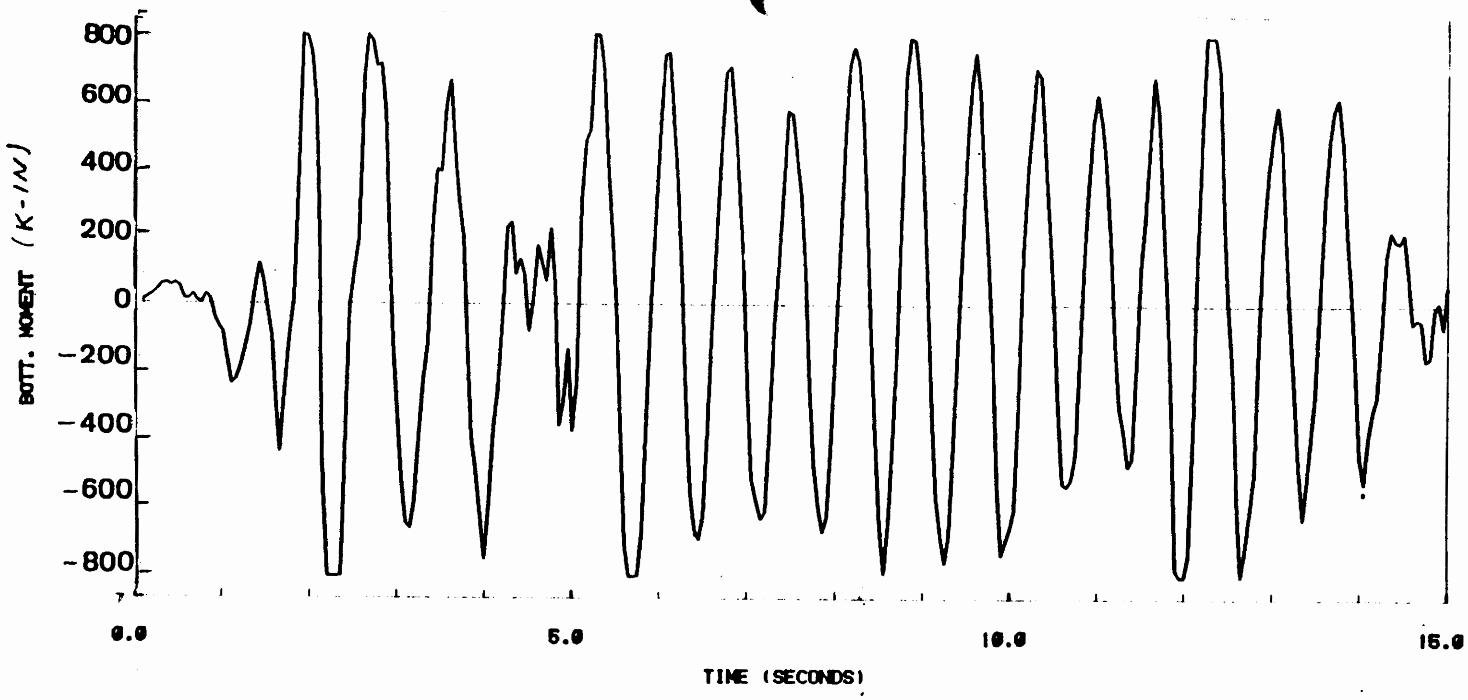

Fig. H.6B c)

CASE 6B

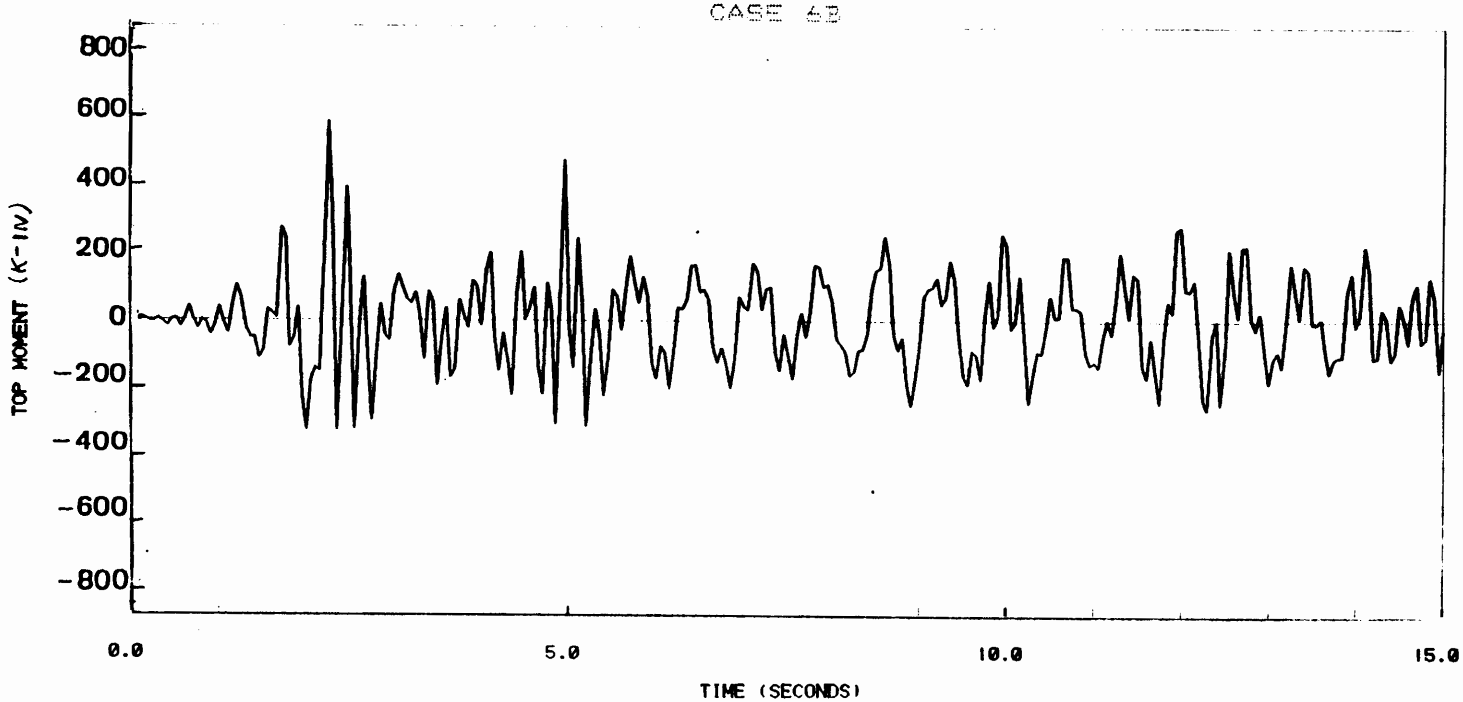

Fig. H.6B d)

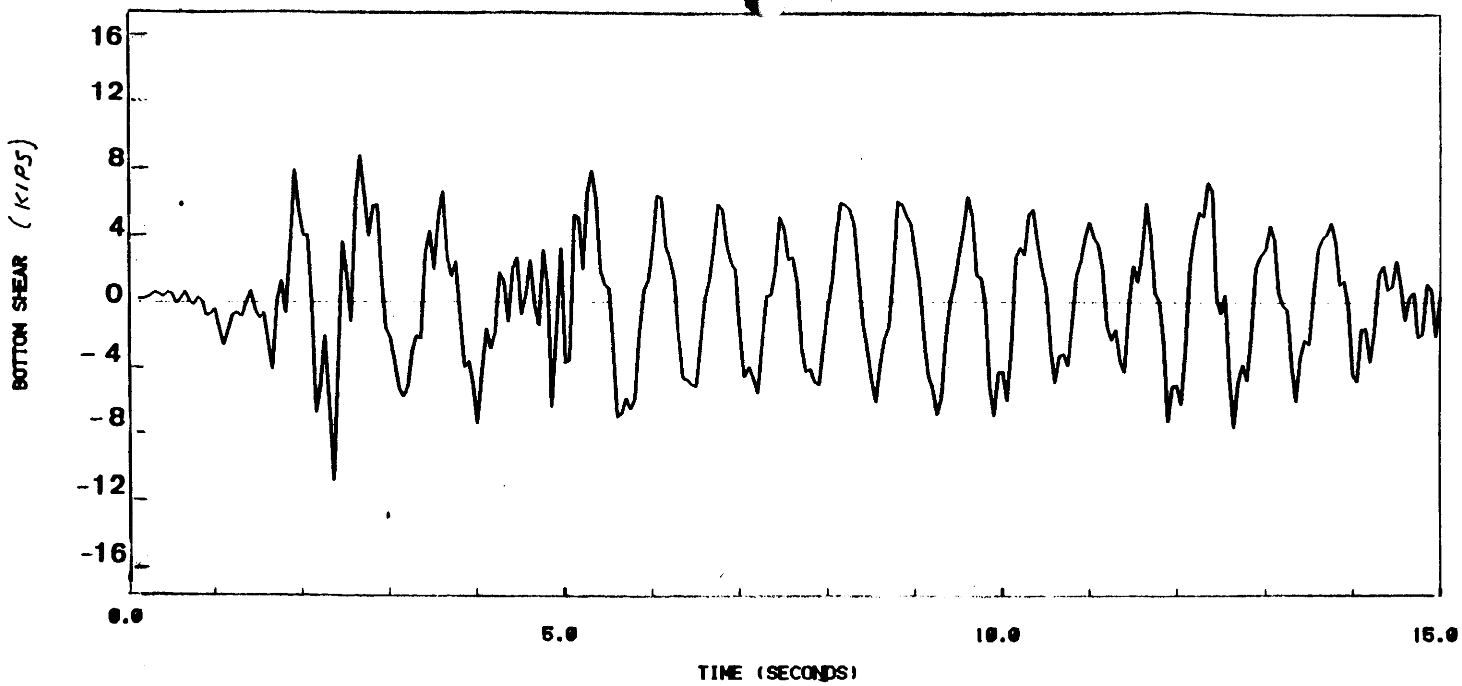

CASE 6B

Fig. H. 6B e)

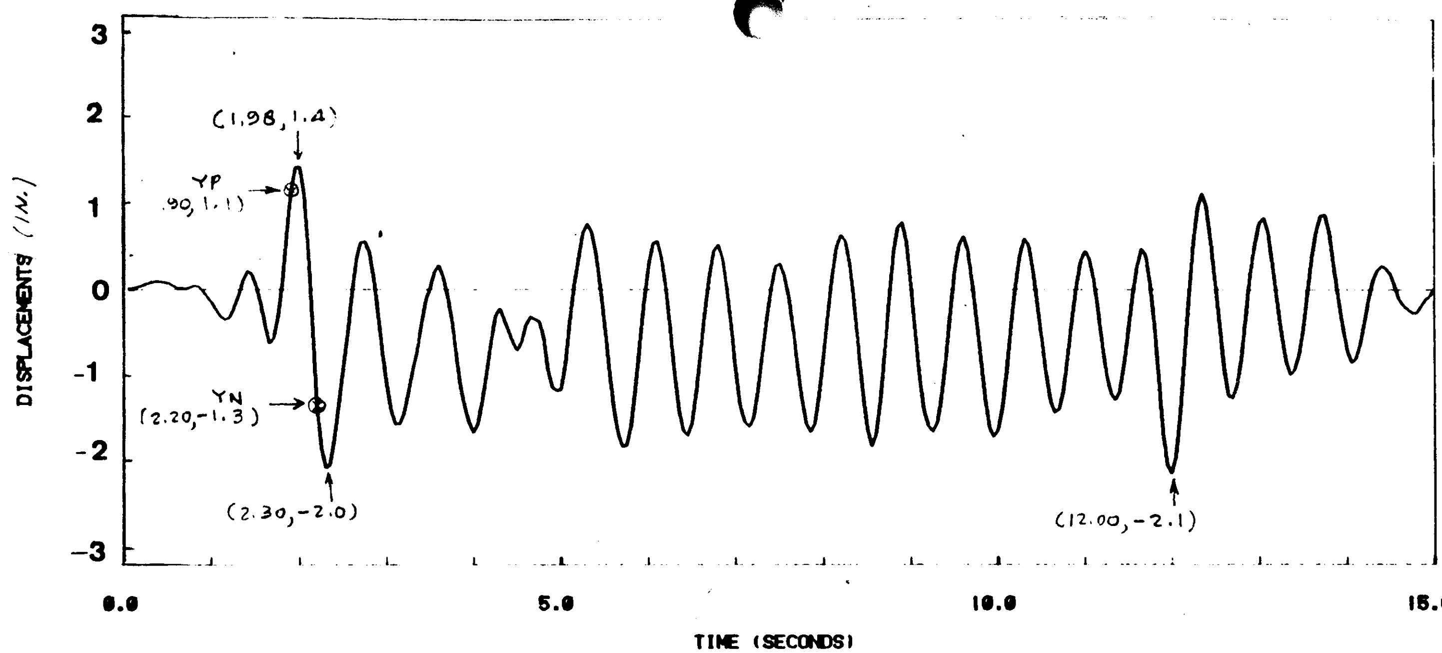

Fig. H.6C a)

CASE 6C

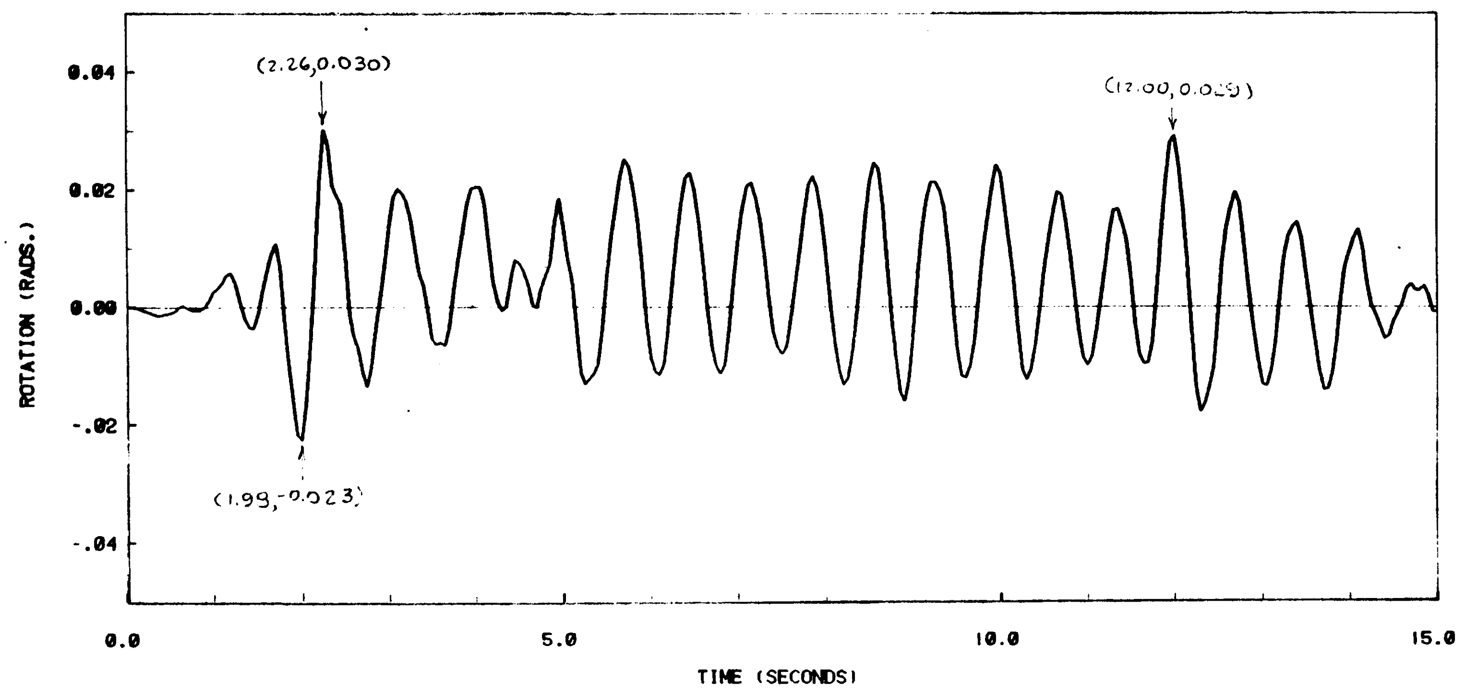

Fig. H.6C b)

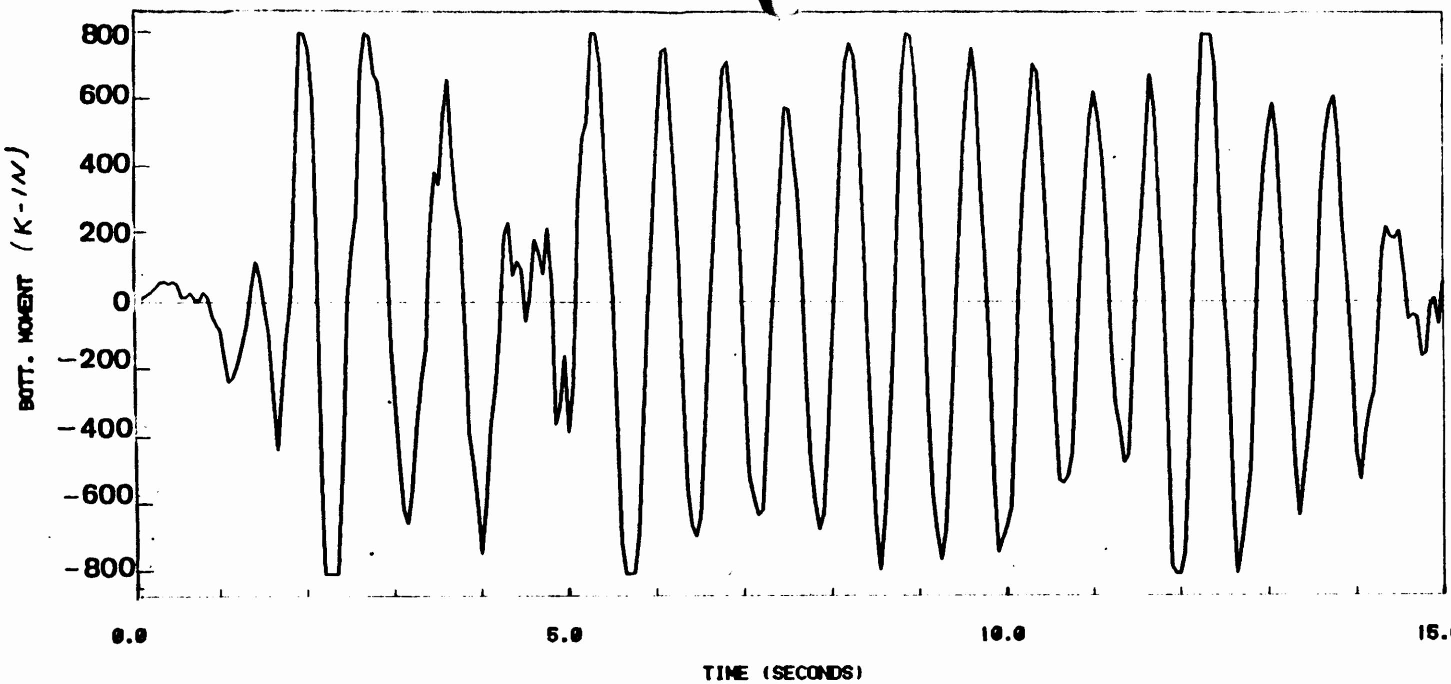

Fig. H. 6C c)

CASE 6C

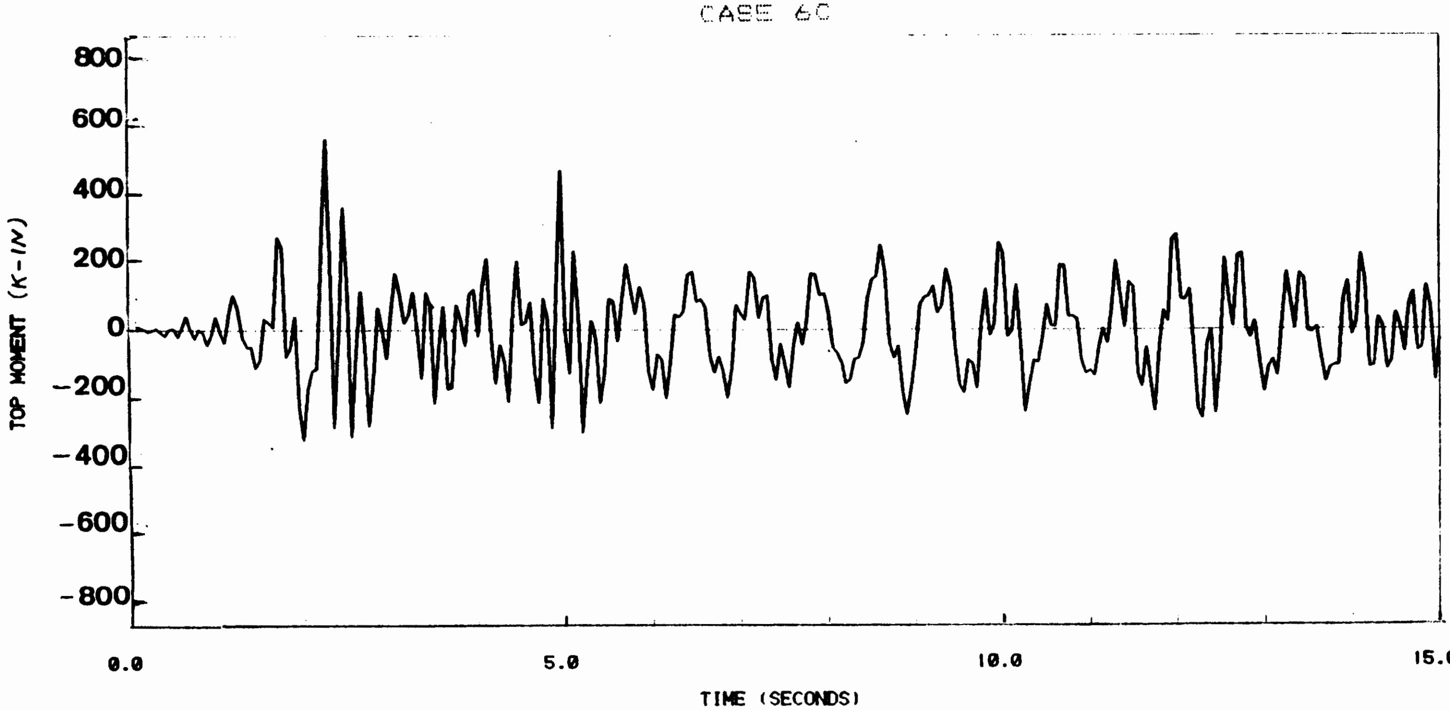

Fig. H. 6C d)

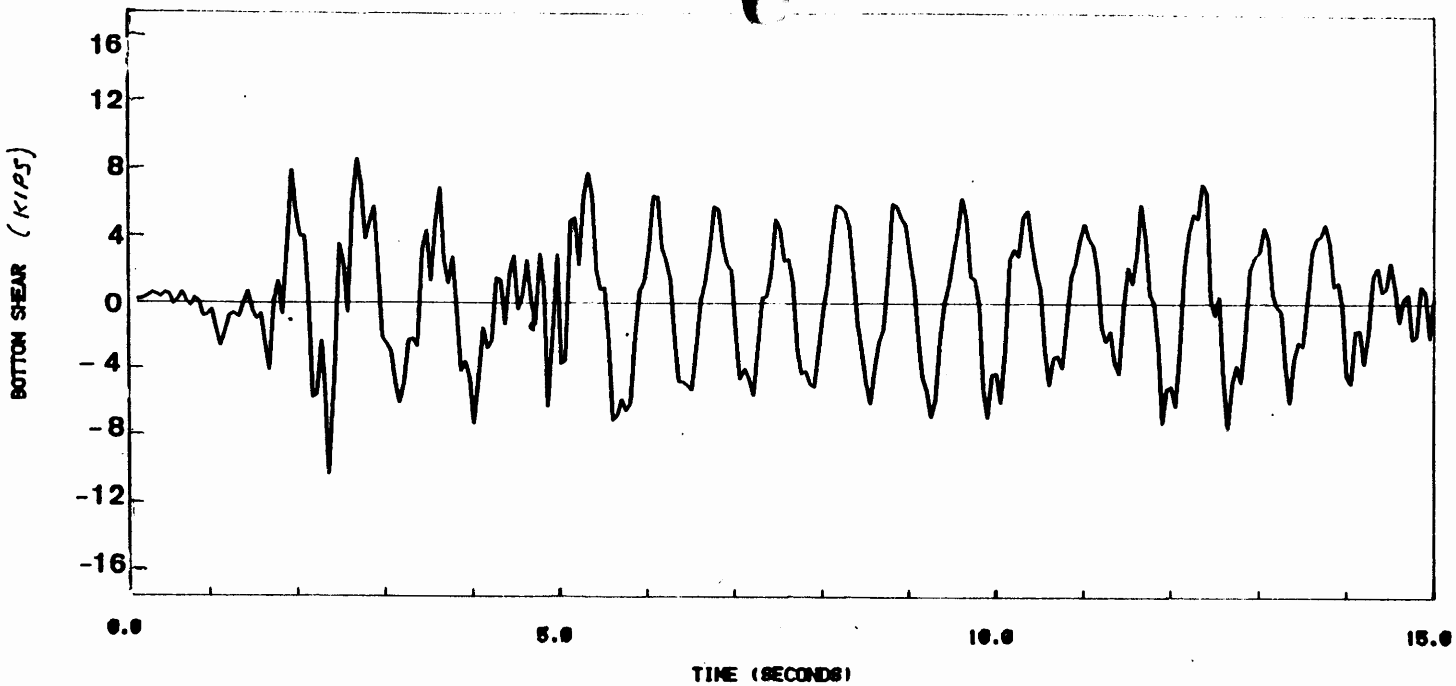

Fig. H.6C e

CASE 6C